ITER TECHNICAL REPORT

iter
china eu india japan korea russia usa

REPORT NO.
ITR-18-003

TITLE

ITER Research Plan within the Staged Approach (Level III – Provisional Version)

AUTHOR/AUTHORS
ITER Organization

AUTHOR EMAIL(S)
ITR.support@iter.org

DATE
17 September 2018

ITER Research Plan within the Staged Approach
(Level III – Provisional Version)

ITER Research Plan LIII – Provisional Version

Table of Contents

Acronyms

ACCC	Active Compensation and Correction Coils
AE	Alfvén Eigenmodes
Alcator C-Mod	*Tokamak operating between 1991 and 2016 at the Massachusetts Institute of Technology*
ASDEX-Upgrade	*Tokamak developed at the Max-Planck-Institute for Plasma Physics*
BES	Beam Emission Spectroscopy
BLV	Beam Line Vessel
BSV	Beam Source Vessel
CC	Correction Coils
CCB	Change Control Board
CCWS	Component Cooling Water System
CEA	Commissariat à l'énergie atomique
CI	Coherence Imaging
CIS	Central Interlock System
CODAC	Control, Data Access and Communication
CN-DA	China Domestic Agency
CQ	Current Quench
CS	Central Solenoid
CSs	Cooling Systems
CSS	Central Safety System
CTS	Collective Thomson Scattering
CX	Charge-Exchange
CXRS	Charge Exchange Recombination Spectroscopy
DA	Domestic Agency
DBC	Disruption Budget Consumption
DCLL	Dual-Coolant Lithium-Lead
DEFC	Dynamic Error Field Correction
DEMO	Demonstration Fusion Reactor (next step after ITER)
DIII-D	*Tokamak developed in the 1980s by General Atomics*
DIM	Divertor Impurity Monitor
DIP	Density Interferometer Polarimeter
DMS	Disruption Mitigation System
DNB	Diagnostic Neutral Beam
DT	Deuterium-Tritium
EAST	*Tokamak developed in Hefei, China*
EC	European Commission
EC	Electron Cyclotron
ECCD	Electron Cyclotron Current Drive
ECE	Electron Cyclotron Emission (Diagnostic)
ECH&CD	Electron Cyclotron for Heating & Current Drive
ECR	Electron Cyclotron Resonance
ECRH	Electron Cyclotron Resonance Heating

ECWC	Electron Cyclotron Wall Conditioning
EDA	Engineering Design Activities
EHF	Enhanced Heat Flux
EL	Equatorial Launcher
ELM	Edge Localized Mode
EM	Electro-Magnetic
EM-TBM	Electro Magnetic module
EPED	Name of model describing Edge Pedestal
EPM	Fast Particle Modes
ERM/KMS	Ecole Royale Militaire / Koninklijke Militaire School
EU-DA	European Union Domestic Agency
ETS	Edge Thomson Scattering
F4E	Fusion fur Energy
FC	Fission Chambers
FDR	Final Design Review
FI	Ferritic Inserts
FICX	Fast Ion Charge Exchange
FILD	Fast Ion Loss Detector
FIR	Fast Infrared
FOCS	Fibre Optic Current Sensor
FP	First Plasma
FPO	Fusion Power Operation Phase
FPPC	First Plasma Protection Component
FS	Faraday Screen
FW	First Wall
FWP	First Wall Panels
GDC	Glow discharge cleaning
GIM	Gas Injection Module
GIS	Gas Injection System
H&CD	Heating & Current Drive
HCCB	Helium-Cooled Ceramic Breeder
HCCR	Helium-Cooled Ceramic Breeder Graphite Reflector
HCLL	Helium-Cooled Lithium-Lead
HCPB	Helium-Cooled Pebble Beds
HFS	High Field Side
HNB	Heating Neutral Beam
HQ	ITER Headquarters
HRNS	High Resolution Neutron Spectrometer
HUST	Huazong University of Science and Technology
HV	High Voltage
HVPS	High Voltage Power Supply
I&C	Instrumentation and Control
IC	Ion Cyclotron
ICH&CD	Ion Cyclotron for Heating & Current Drive
ICRF	Ion Cyclotron Range of Frequencies

ICRH	Ion Cyclotron Resonance Heating
ICWC	Ion Cyclotron Wall Conditioning
IMAS	Integrated Modelling and Analysis Suite
INT-TBM	INTegral TBM
IO	ITER Organization
IO-CT	ITER Organization Central Team
IO-DA	ITER Organisation Domestic Agency
IPP	Max Planck Institute of Plasma Physics
IPR	Institute for Plasma Research
IR	Infrared
IRFM	Institut de la Recherche sur la Fusion par confinement Magnétique
IRP	ITER Research Plan
ISS	Isotope Separation System
ISS	Interspace Support Structure
ITB	Internal Transporter Barrier
ITPA	International Tokamak Physics Activity
IVT	In-Vessel Transporter
JA-DA	Japan Domestic Agency
JET	Joint European Torus
JET-ILW	JET ITER-Like Wall (material mix)
JT-60	*Tokamak developed in 1990s by the Japan Atomic Energy Research Institute*
KSTAR	*Tokamak developed in Korea by the National Fusion Research Institute*
LB	Liquid Breeders
LCFS	Last Closed Flux Surface
LFS	Low Field Side
LH	Lower Hybrid
LHCD	Lower Hybrid Current Drive
LHH&CD	Lower Hybrid Heating and Current Drive
LIF	Laser Induced Fluorescence
LLCB	Lithium-Lead Ceramic Breeder
LLNL	Lawrence Livermore National Laboratory
LM	Liquid Metal
LM	Locked Mode
LOS	Line-Of-Sight
LSM	Lower Steering Mirror
MAST	*Tokamak developed in the UK by the Culham Centre for Fusion Energy*
MD	Maintenance Detritiation
MGI	Massive gas injection
MHD	Magnetohydrodynamics
MIMO	Multiple-Input Multiple-Output
MOU	Matching Optics Unit
MPD	Multi-Purpose Deployer
MSE	Motional Stark Effect
NB	Neutral Beam

NBCD	Neutral Beam Current Drive
NBI	Neutral Beam Injection
NBTF	Neutral Beam Test Facility
NFRI	National Fusion Research Institute (KR)
NN	Neural Network
NRCKI	National Research Center "Kurchatov Institute"
NSTX	*National Spherical Torus Experiment magnetic fusion device developed by the Princeton Plasma Physics Laboratory*
NTM	Neoclassical Tearing Modes
NT/TM-TBM	Thermo-Mechanic module
NTV	Neoclassical Toroidal Viscosity
NWL	Neutron Wall Load
PA	Procurement Arrangement
PAM	Passive-Active Multi-Junction
PCR	Project Change Requests
PCS	Plasma Control System
PCSS	Port Cell Support Structure
PCSSP	Plasma Control System Simulation Platform
PF	Poloidal Field
PFC	Plasma Facing Component
PFPO-1	Pre-Fusion Power Operation 1
PFPO-2	Pre-Fusion Power Operation 2
PMS	Passive Magnetic Shield
PMT	Photomultiplier Tube
PID	Proportional-Integral-Derivative
PIS	Plant Interlock Systems
PP	Port Plug
PPEN	Pulsed Power Electrical Networks
PPPL	Princeton Plasma Physics Lab
PPTF	Port Plug Test Facility
PS	Power Supply
PVTc	Pressure-Volume-Temperature-composition
PWI	Plasma Wall Interaction
QST	National Institutes for Quantum and Radiological Science and Technology
R&D	Research and Development
RAFM	Reduced-Activation Ferritic/Martensitic
RAMI	Reliability, Availability, Maintainability & Inspectability
RE	Runaway Electrons
RES	RE Suppression
RF	Radio-Frequency
RF-DA	Russia Domestic Agency
RGA	Residual Gas Analyzers
RGRS	Radial Gamma-Ray Spectrometer
RH	Remote Handling

RMP	Resonant Magnetic Perturbations
RMS	Root Mean Square
RNC	Radial Neutron Camera
RSAE	Reversed Shear Alfvén Eigenmodes
RVTL	Removable Vacuum Transmission Line
RWM	Resistive Wall Mode
SB	Solid Breeders
SCM	Superconducting Magnet
SOL	Scrape-Off Layer
SPA	Single-Pass Absorption
SPI	Shattered Pellet Injection
SSEN	Steady State Electrical Networks
STAC	Science and Technology Advisory Committee
SWIP	Southwestern Institute of Physics
TAE	Toroidal Alfvén Eigenmodes
TBM	Test Blanket Module
TBMA	TBM Arrangement
TMB-PC	TBM Program Committee
TBS	Test Blanket Systems
TCV	Tokamak à Configuration Variable (Swiss Tokamak)
TCWS	Torus Cooling Water System
TF	Toroidal Field
TIP	Toroidal Interferometer Polarimeter
TL	Member Leader
TL	Transmission Line
TLM	Thermal Load Mitigation
TNS	Tangential Neutron Spectrometer
TQ	Thermal Quench
UKAEA	UK Atomic Energy Authority
UL	Upper Launcher
USM	Upper Steering Mirror
VDE	Vertical Displacement Events
VGRS	Vertical Gamma Ray Spectrometer
VNC	Vertical Neutron Camera
VS	Vertical Stabilisation
VSWR	Voltage Standing Wave Ratio
VUV	Vacuum Ultra Violet
VV	Vacuum Vessel
WCCB	Water-Cooled Ceramic Breeder
XRCS	X-ray Crystal Spectroscopy

Acknowledgements

The ITER Research Plan has been developed over a period of more than 10 years through an extensive collaboration between staff of the ITER Organization and experts from the Members' Domestic Agencies and fusion communities. Contributions from the following individuals to the preparation of the present version of the Plan are gratefully acknowledged:

P Andrew, IO
I Bandyopadhayay, IN DA (IN)
R Barnsley, IO
B Beaumont, IO
L Bertalot, IO
D Boilson, IO
X Bonnin, IO
C Bourdelle, CEA/IRFM (EU)
D Campbell, IO
A Chakraborty, IPR (IN)
D Chandra, IPR (IN)
M Clough, IO
C Darbos, IO
M De Bock, IO
G De Temmerman, IO
P de Vries, IO
D Douai, CEA/IRFM (EU)
X Duan, SWIP (CN)
J Elbez-Uzan, IO
M Fenstermacher, LLNL (US)
A Fossen, IO
L Giancarli, IO
J Graceffa, IO
M Graham, IO
Y Gribov, IO
J Gunn, CEA/IRFM (EU)
M Henderson, IO
S-H Hong, NFRI (KO)
G Huijsmans, EC (EU)
Y-K In, NFRI (KO)
A Isayama, QST (JA)
S Kaye, PPPL (US)
Y Kazakov, ERM/KMS (EU)
F Kazarian, IO
A Khan, IO
S-H Kim, IO
N Kirneva, NRCKI (RF)
M Kocan, IO
S Konovalov, NRCKI (RF)
Ph Lamalle, IO
M Lehnen, IO
V Leonov, NRCKI (RF)
E Lerche, ERM/KMS (EU)
S Lisgo, IO
X Litaudon, EUROfusion (EU)
A Loarte, IO
T Luce, IO&GA (US)
R Maingi, PPPL (US)
S Maruyama, IO
Y-S Na, Seoul Nat Uni (KO)
R Neu, IPP (EU)
I Nunes, IST (EU)
Y-K Oh, NFRI (KO)
S Pinches, IO
R Pitts, IO
A Polevoi, IO
R Reichle, IO
F Rimini, UKAEA (EU)
A Romannikov, NRCKI (RF)
R Rotella, IO
S Sabbagh, Columbia Uni (US)
V Safronov, RF DA (RF)
G Saibene, F4E (EU)
R Sartori, F4E (EU)
M Schneider, IO
K Schmid, IPP (EU)
B Schunke, IO
M Singh, IPR (IN)
G Sips, EC (EU)
A Sirinelli, IO
J Snipes, IO
J Stober, IPP (EU)
T Suzuki, QST (JA)
L Svensson, IO
Y Takase, Uni Tokyo (JA)
H Takenaga, QST (JA)
E Tsitrone, CEA/IRFM (EU)
V Udintsev, IO
H Urano, QST (JA)
J van der Laan, IO
D Van Eester, ERM/KMS (EU)
G Vayakis, IO
E Veshchev, IO
M Walsh, IO
C Watts, IO
S Willms, IO
S-W Yoon, NFRI (KO)
L Zabeo, IO
G Zhuang, HUST EDU (CN)

Executive Summary

The *ITER Research Plan* (IRP) has been developed to provide a guide to the overall research activities which should be undertaken within the framework of the ITER Project. When complete, the IRP should encompass both physics and technology research during ITER construction and operation (though technology R&D associated with the procurement packages formally falls within the *Project Plan and Resource Estimate*, rather than the Research Plan). The revised version presented here focusses on physics R&D and on the R&D and testing program of the (tritium breeding) Test Blanket Modules (TBM) adapted to the revised ITER project schedule developed during 2015 - 2016 within the Staged Approach. Ultimately, this document should aim to encompass activities such as operational R&D on heating and current drive and diagnostic systems, and operational R&D on the broader aspects of fusion technology associated with major ITER subsystems, such as superconducting magnets, remote handling, tritium handling technology etc. in order to provide a complete overview of the research scope and plans of the ITER project.

This version of the Research Plan is a provisional version of the baseline documentation that has been developed in response to the complete revision of the ITER project schedule within the framework of the Staged Approach, undertaken in 2015 – 2016 and reflects the ITER project strategy as of December 2017. The Staged Approach foresees First Plasma in December 2025, which is succeeded by a progressive upgrade of the capabilities of the ITER tokamak and facility interleaved with two periods of system 'commissioning with plasma' and experimental plasma studies in H and He plasmas. Completion of construction activities is scheduled for early 2035 and the transition to experiments in D/DT plasmas is planned for December 2035, with trace tritium experiments likely in early 2036 and a gradual transition to fusion power production over the next 12 – 15 months of experimental studies, leading to an initial demonstration of several hundred megawatts of fusion power production for several tens of seconds. In subsequent experimental campaigns in Deuterium Tritium (DT) plasmas, planned on a two-yearly cycle, the experimental basis for achieving the principal scientific mission goals of the ITER project are developed: a demonstration of $Q \geq 10$ for burn durations of 300 – 500 s and the development of long-pulse, non-inductive scenarios aiming at maintaining $Q \sim 5$ for periods of up to 3000 s. The plan incorporates elements detailed below to adapt the baseline version of the Research Plan (v2.2, November 2009) to the Staged Approach:

(i) Incorporation of a first divertor with all-tungsten plasma-facing components, installed during Assembly Phase II, following First Plasma;

(ii) Development of the Research Plan around a progressive increase in the installed Heating & Current Drive (H&CD) power towards the baseline capability of 73 MW and a staged installation of Diagnostics matching the measurement requirements of the Research Plan;

(iii) Exploration of options for studies of H-modes at lower toroidal magnetic field (1.8 T) and in H (as well as He), which was not previously considered feasible;

(iv) Strengthening of the development of a disruption management program to characterize disruption loads, and to implement effective disruption prediction, avoidance and mitigation;

(v) A significantly more extensive program of studies on plasma-wall interactions to characterize issues such as erosion, transport and redeposition of plasma-facing materials, fuel retention and removal, and degradation of plasma-facing materials under plasma exposure;

(vi) Start of commissioning of the Tritium Plant with tritium in 2033, during the second experimental campaign in H/He plasmas;

(vii) Transition to experiments in D/DT plasmas in December 2035, with the start of trace tritium experiments in early 2036, as a result of the accelerated commissioning of the Tritium Plant;

(viii) Progressive transition to full DT operation during 2036, with an expanding program of DT operation which aims to demonstrate fusion power production at a level of several hundred megawatts for several tens of seconds by the end of the first experimental campaign in D/DT plasmas in early 2037;

(ix) Development of the experimental program during the second and third DT campaigns towards the achievement of ITER's fusion power, fusion gain and long burn duration mission goals;

(x) Adaptation of the evolution of the Test Blanket Module testing program to the revised ITER schedule and experimental plan.

The structure of the Research Program has been analyzed within 4 broad areas: the experimental program during operations, the TBM development and testing program (as the first element of the Technology research program, still to be developed in detail), the possible upgrade program for the device's capabilities and the research program during construction. The issues which will be addressed within these areas can be summarized as follows:

Experimental Program during Operations

Within the framework of the Staged Approach, the ITER Research Plan has analyzed the physics research and plasma operation requirements from First Plasma, in December 2025, to the end of the 3rd experimental campaign in DT plasmas, expected to close (according to current assumptions about the cycle of ITER operations during the fusion power operation phase (FPO)) in spring 2041, at which time the long-pulse ($300 - 500$ s) $Q \geq 10$ goal of the ITER mission should have been achieved at power levels of ~500 MW, and significant progress made towards the achievement of $Q \sim 5$ for burn durations of ~3000 s in non-inductive plasmas. In this version, the IRP has developed an experimental program to fully commission plasma operation of the device, auxiliary and plant systems, and to achieve the level of DT plasma performance required satisfy the fusion performance goals of the project.

The principal aims and activities encompassed by the several operational phases spanning this period of ITER operation are summarized below.

Pre-Fusion Power Operation (PFPO)

- This operational phase will consist of two periods of plasma operation, a total of 37 months of experiments in H and He plasmas, interleaved with Assembly and Integrated Commissioning activities, to bring the tokamak, its auxiliary systems and facility plant systems up to their full performance level and capabilities;
- During this phase H and He plasma scenarios will be developed to allow the full commissioning of all tokamak sub-systems (except those involving the use of D or T) with plasma;
- It is planned that all baseline H&CD systems will be tested with plasma operation and brought up to the specified level of input power; options for dual-frequency operation of the

Electron Cyclotron Resonance Heating (ECRH) system and early operation of one Ion Cyclotron Rage of Frequencies (ICRF) antenna are being explored; Diagnostics, fuelling, control, protection and safety-related systems will also be commissioned;

- The Vertical Stability coils, Error Field Correction Coils and Edge Localized Mode (ELM) control coils will be commissioned and exploited routinely;
- The level of electromagnetic and thermal loads associated with disruptions and Vertical Displacement Event (VDEs) will be determined; disruption avoidance and mitigation techniques will be implemented and applied routinely;
- In-vessel components will be tested to the limits of the available thermal loads, and techniques for mitigation of heat loads will be developed;
- Methodologies for the characterization of fuel retention and dust production will be implemented and techniques for hydrogen and dust removal will be demonstrated; analysis indicates that a short campaign with low-level deuterium seeding of hydrogen plasmas could provide accurate measurements of fuel retention if any regulatory issues can be resolved;
- Initial H-mode operation will be established, H-mode behaviour characterized and ELM control techniques established; H-mode operation in He appears more accessible, but options for studying H-modes in H are being explored;
- A key milestone for the Pre-Fusion Power Operation phase (PFPO) will be the demonstration of L-mode plasmas at the full technical capability of the device (15 MA/5.3 T);
- Plasma pulse length, including that in plasmas at reduced parameters, will likely be limited by the operational time available to extend the pulse length for H&CD systems (and possibly also other auxiliary systems) to long-pulse operation; a minimal target of ~50 s has been established, but scenarios are available for plasma pulse lengths of 100 – 1000 s if sufficient experimental time is available;
- Initial studies of current drive efficiency and current profile formation will be performed;
- Diagnostic data will be validated and the consistency of the various measurements will be demonstrated;
- The interpretive software chain for the reconstruction of the plasma evolution will be refined and validated;
- During the PFPO-2 phase, the Test Blanket Module (TBM) program will test Electro Magnetic modules.

Deuterium Operation (Fusion Power Operation, Campaign 1)

- Certain ‘commissioning with plasma’ activities will be undertaken during initial deuterium operation, involving recommissioning of H&CD systems in deuterium (e.g. Neutral Beam (NB) injection with 1 MeV D^0), commissioning of any nuclear measurement systems (e.g. neutron detectors) and newly installed Diagnostics, commissioning of fuelling systems with deuterium (and eventually tritium); commissioning of additional control and interlock systems in preparation for nuclear operation;
- Disruption detection, avoidance and mitigation will be adapted to the highest parameters achievable in D plasmas;
- Plasma scenarios will be redeveloped up to the full technical parameters (15 MA/5.3 T) in D;

- Once commissioning of such systems is complete, a program of H-mode studies, including ELM control and divertor power load control, will be implemented, progressing to the highest parameters where robust H-mode operation can be sustained (possibly 7.5 MA/2.65 T);
- Development of reliable Neo-classical Tearing Mode (NTM) control in high confinement D H-mode plasmas, if not previously implemented in the PFPO program;
- The research program will then focus on characterizing the physics of D plasmas at the ITER scale in ohmic, L- and H-mode plasmas;
- Low concentration (trace) T experiments in D L- and H-mode plasmas will assess T transport and T fuelling requirements, and initiate the transition to DT experiments;
- Characterization of key aspects of plasma-wall interactions in the ITER environment in D plasmas will be performed;
- Preparatory studies of hybrid/non-inductive scenarios in D plasmas will be undertaken;
- Preparatory studies of 'burning plasma' issues (e.g. helium exhaust, fuel mixture control in trace T, etc.) will also be carried out to prepare control techniques for DT plasmas;
- In this operational phase (extending into the initial period of DT operation), the TBM program will test Thermal Neutronic modules.

Deuterium-Tritium Operation (Fusion Power Operation, Campaign 1)

- The initial DT experimental program will focus on developing the inductive ELMy H-mode scenario which provides the basis for achieving ITER's principal fusion power (500 MW) and fusion gain ($Q \geq 10$) mission;
- Additional experimental 'commissioning' will be required in order to develop all of the necessary measurement systems (e.g. fusion product measurements) and control techniques to support integrated scenarios at high fusion power; in addition, ICRF heating scenarios for DT plasmas will be commissioned;
- As the program progresses and the level of fusion power rises, disruption detection, avoidance and mitigation techniques will have to be adapted;
- DT H-modes are likely to be developed around 7.5 MA/2.65 T with durations of several tens of seconds (~50 s), incorporating reliable ELM control, NTM control and radiative divertor operation;
- The program will thereafter emphasize the rapid development of inductive operation, culminating in 12 - 15 MA/5.3 T DT H-mode operation with full feedback control at fusion powers of 200-300 MW for at least 50 s;
- Experiments would explore optimization of fuel mixture control, burn control, helium exhaust, plasma-facing component protection in DT plasmas;
- These plasmas would allow characterization of physics processes in DT ohmic and L-mode scenarios and initiate studies of burning plasma physics at $Q \geq 5$ in H-mode;
- If time permits, the development would continue towards optimization of plasma parameters to maximize Q, with the goal of reaching $Q = 10$ for ~50 s as rapidly as possible.

Deuterium-Tritium Operation (Fusion Power Operation, Campaigns 2 and 3)

- Inductive scenario development will focus on achieving ITER's primary fusion performance goal of $Q \geq 10$ at fusion power levels of 400 – 500 MW and at plasma burn durations of 300 - 500 s;
- Studies to characterize key aspects of PWI in the ITER environment in high fusion power/ high gain plasmas will be undertaken; in particular, demonstration of satisfactory tritium accounting, retention measurement and removal techniques will be an essential aspect of the program;
- Optimization of fusion power with $Q > 10$ during stationary or transient inductive conditions will be explored and plasma behaviour characterized in these conditions;
- Development of non-inductive current drive and current profile control in DT plasmas will support the exploration of both hybrid scenarios and fully non-inductive plasma regimes;
- It will be important to identify needs for upgrades to improve fusion performance or to improve the potential for non-inductive operation (e.g. ELM control coil power supplies for Resistive Wall Mode (RWM) control, if it has not been possible to do so at an earlier stage of the program);
- The program developed towards very long pulse, non-inductive operation foresees the establishment of DT plasma scenarios with current profile control and improved H-mode confinement having a burn duration of ~1000 s and several hundred megawatts of fusion power, based on the hybrid /improved H-mode scenario at $q_{95} \sim 4$;
- Non-inductive plasmas with the longest sustainable pulse duration (> 1000 s) and moderate fusion performance ($Q \sim 2$) would then be developed as a basis for meeting the non-inductive mission goal;
- In parallel, the program would aim to optimize fusion gain and pulse duration in the most promising long-pulse scenario(s) to establish plasmas with duration beyond 1000 s and $Q \geq 5$;
- This development would provide a plasma scenario allowing characterization of key aspects of Plasma-Wall-Interaction (PWI) in the ITER environment over very long durations (e.g. impact on fuelling, erosion/redeposition, fuel retention, etc.);
- The mission goal of demonstrating $Q \sim 5$ in fully non-inductive DT plasmas and extending this to the longest pulses which the ITER facility can support (nominally ~3000 s) would then be a major focus of a program which might require further experimental campaigns to realize fully;
- The establishment of plasma regimes in which α-particle heating is dominant, the key novel feature of ITER plasmas, will provide access to a wide range of burning plasma physics studies which will be integrated into the programs aimed at achieving the fusion performance milestones in both inductive and non-inductive plasmas;
- During the 2nd experimental campaign in DT, the TBM program will test a Neutronic-Tritium/Thermo-Mechanic module, while in the 3rd experimental period an INTegral module will be tested;
- The DT research program pursued during these initial FPO campaigns would also provide an opportunity to identify options for further upgrades to prepare longer-term Demo-targeted studies.

TBM Development and Testing Program

The TBM development program involves the design and construction of up to 6 TBM systems (TBMs plus all ancillary systems required for the operation and testing of the TBMs) by Members' teams, together with the design and construction, by the IO, of the required infrastructure to host the TBM systems within the ITER facility and to ensure all interfaces to ITER plant systems. The major elements of R&D required to support the development of the TBM systems have been identified. A testing program for the TBMs, to be implemented during operations, has also been developed and integrated into the experimental program. It is expected that the TBM testing program will be undertaken without interference to the physics research program during the major part of this period. As high fusion power, very long burn duration plasmas are developed in the 2nd and 3rd DT campaigns, it is likely that continuous, repetitive operation of ITER will be required for short periods (~6 days) to enable specific performance tests of TBMs and their associated systems. The structure of the TBM testing program foreseen at present is based on the successive installation and testing of 4 variants of each of the up to 6 TBM concepts being developed by the Members:

- During the PFPO-2 phase, the TBM program will test Electro Magnetic modules, which can allow the assessment of the overall functionality of the TBM systems, including their operation and control, and provide confirmation of the thermal behaviour of the TBM first walls in the tokamak environment; within the scientific program, studies of the impact of error fields and toroidal field ripple due to the TBM ferromagnetic materials will be undertaken and mitigation measures implemented where possible;
- During the FPO-1 campaign, encompassing both the D phase and the initial period of DT operation, the TBM program will test Thermal Neutronic modules, which are used to investigate neutronic response and to confirm the thermal behaviour of the TBMs;
- Neutronic-Tritium/Thermo-Mechanic modules will be tested during the 2nd experimental campaign in DT; this allows investigation of the thermo-mechanical behaviour at relevant temperatures and also permits the nuclear response to a Demo-relevant 14.1 MeV neutron flux to be determined, focussing on the actual tritium breeding and extraction functions;
- In the 3rd DT experimental period, an INTegral module will be tested in order to obtain information about tritium management and heat extraction in fully representative Demo breeding blanket conditions, including reproducible plasma performance; the experimental program will provide support to the testing of the INTegral module by preparing appropriate plasma pulses and pulse sequences.

The general objectives of the testing programs relating to each of the 4 stages outlined above and specific objectives of the R&D on different TBM concepts (liquid breeder/ ceramic breeder) have been identified. Guidelines for desirable modes of plasma operation to facilitate the TBM testing program have also been developed.

Upgrade Program

During the period of ITER construction and of initial plasma operation, it is anticipated that proposals for upgrades to the H&CD, diagnostic, fuelling and control systems will be developed and more concrete plans for changes to the ITER plasma-facing components will be put in place. As funding becomes available for the implementation of the highest priority upgrades, the operational program will need to be revised to accommodate the additional flexibility and capabilities which such upgrades will bring. This is likely to be even more relevant for the planning for the longer-term operation, focussing on optimization of fusion performance, extended pulse length, developing

a detailed understanding of burning plasma physics, and the investigation of Demo-relevant science and technology issues, which can be expected to benefit most from the upgrade program.

Research Program during Construction

The major focus of the physics research program accompanying construction will be to enhance the physics and technology basis for operation. The key activities which will need to be addressed in order to prepare for efficient experimental exploitation of the ITER facility have been identified as:

- H-mode access and characteristics, including core and pedestal transport in transient and stationary conditions, ELM mitigation, influence of 3-D fields;
- Plasma-wall interaction issues, including tritium retention and removal, dust production and removal, heat loads and power handling techniques, and the implications of these phenomena for Plasma Facing Component (PFC) lifetime;
- Magnetohydrodynamics (MHD) stability and control, including effective disruption/runaway electron mitigation measures, and control of sawteeth, neoclassical tearing modes, resistive wall modes and error field induced modes;
- Development of a comprehensive integrated modelling capability to support plasma operations and research;
- Scenario development, encompassing the development of all plasma scenario phases (ramp-up, entry and exit from burn and ramp-down) and the necessary control techniques for the range of reference scenarios foreseen.

Appendices

The ITER Research Plan also contains several Appendices which deal with aspects of physics, phasing of auxiliary systems within the Staged Approach, 'background' issues such as Tritium Availability and risks to the successful implementation of the research program:

- Appendix A: analysis of the case for deuterium seeding of hydrogen plasmas for improved characterization of fuel retention during the PFPO phase.
- Appendix B: discussion of H-mode power threshold and the influence of Toroidal Field (TF) ripple on H-mode performance as they impact the Research Plan.
- Appendix C: discussion of heat load management and the evolution of the expected heat loads to PFCs during the course of the Research Plan.
- Appendix D: definition of the requirements of a reference pulse which could be run regularly within the experimental program to characterize gradual changes in the plasma operating environment – of particular relevance to PWI studies.
- Appendix E: a review of modelling studies of the options for very long-pulse inductive and non-inductive scenarios in ITER and, in particular, the importance of Lower Hybrid Current Drive (LHCD) in such scenarios.
- Appendix F: discussion of the results of physics analysis undertaken in relation to the option for operation at 5 MA/1.8 T and of the physics risks associated with these plasma scenarios.
- Appendix G: discussion of the phasing of the H&CD systems during the Staged Approach and the current preparations for possible H&CD upgrades.
- Appendix H: discussion of the phasing of the plasma diagnostic systems during the Staged Approach and its impact on measurement requirements.

- Appendix I: brief analysis of expected availability of tritium from 'commercial' sources for the ITER DT program.
- Appendix J: Risk Register for the most significant physics risks to the successful implementation of the Research Plan.

Future Development of the Research Plan

It is intended that the ITER Research Plan should be subject to continuous development during the lifetime of the Project and, in time, should provide an instrument for managing and guiding the Project's scientific and technological research activities. Key analysis which should be pursued in the medium-term to expand the present document and integrate the scientific research program more completely with the overall Project development includes:

- Further detailing of the research program during construction with clear links to the ongoing fusion R&D programs in the Members' fusion communities;
- Detailing of elements of the Integrated Commissioning program to develop a more complete plan for the transition to plasma operation;
- Assimilation of more detailed analysis of plasma commissioning requirements for H&CD and diagnostic systems, including off-line commissioning requirements in preparation for commissioning with plasma;
- Elaboration of the program of burning plasma physics research, with a more detailed development of the major elements of this program;
- Development of a technology research program for the operations phase encompassing R&D activities on tokamak, auxiliary and plant systems (in addition to the TBM testing program discussed here) to provide an extensive technology basis for the design of future fusion power plants;
- Deeper analysis of the potential impact of possible upgrade paths on the first 10 years of the experimental program.

1 Introduction

1.1 Objectives

The *Project Specification* [ITER_D_2DY7NG, 2010] defines the overall programmatic objective of the ITER project as, 'to demonstrate the scientific and technological feasibility of fusion energy for peaceful purposes'. It also sets out a series of scientific and technical goals which should be satisfied to achieve this objective. The scientific goals, defined in terms of plasma fusion performance, are:

- The device should achieve extended burn in inductively driven plasmas with the ratio of fusion power to auxiliary heating power, Q, of at least 10 ($Q \geq 10$) for a range of operating scenarios and with a duration sufficient to achieve stationary conditions on the timescales characteristic of plasma processes.
- The device should aim at demonstrating steady-state operation using non-inductive current drive with the ratio of fusion power to input power for current drive of at least 5.
- In addition, the possibility of controlled ignition should not be precluded.

The technical goals, aiming to provide much of the technological basis for the design of future fusion power plants capable of generating electricity, are:

- The device should demonstrate the availability and integration of technologies essential for a fusion reactor (such as superconducting magnets and remote maintenance).
- The device should test components for a future reactor (such as systems to exhaust power and particles from the plasma).
- The device should test tritium breeding module concepts that would lead in a future reactor to tritium self-sufficiency, the extraction of high grade heat and electricity production.

The primary aim of the ITER Research Plan (IRP), therefore, is to define the plan of research and development and of facility exploitation necessary to meet these ITER mission goals. The research and development program includes activities directly related to specification of performance requirements for ITER components as well as R&D required from other facilities, so as to provide a solid physics and technology basis for the efficient exploitation of ITER. It should be expected that, in its final form, the IRP will define the full range of R&D activities to be implemented in pursuit of the detailed scientific and technical goals. The emphasis in this (as in previous) versions of the IRP is on the definition of the research program which will be implemented to satisfy the key scientific goals, while the discussion of technology activities is limited to the Test Blanket Module (TBM) testing program. While this latter element satisfies a key technical mission goal, future developments of the IRP should extend the discussion of technology R&D activities to encompass the wide-ranging research which will be undertaken on ITER tokamak, auxiliary and plant systems in pursuit of the full scope of the project's technical mission goals.

The IRP also aims to provide an analysis of the ITER facility's capability to meet its mission and considers possible upgrade paths which may be required to address science and technology issues supporting the achievement of specific mission goals. The current version discusses options for such upgrades and the potential impact of these upgrades on the project's scientific research program during the Operations Phase. In addition, a risk analysis has been carried out in which the likelihood and consequences of negative R&D or exploitation outcomes are assessed, identifying, where appropriate, possible risk mitigation and avoidance measures.

The Research Plan is organized around a series of key thematic research areas, which are integrated to form an exploitation plan for the facility. This exploitation plan has been embedded within the Staged Approach strategy developed during the revision of the ITER project schedule in 2015 – 2016. The implications of this schedule strategy for the overall structure of the IRP and for the scheduling of the key activities within the research program, including the transition to operation with deuterium-tritium fuel leading to significant fusion power production, are outlined in 1.3.

An attempt has been made to assign estimates of durations to the various elements of the experimental program within the IRP, but these are necessarily uncertain and become more so as the IRP progresses towards fusion power production, involving the study and optimization of burning plasmas, an entirely new regime of laboratory plasma research to which ITER will provide access. A perhaps more important output of the plan, at least at this stage of its development, is the logical sequence developed for the programmatic activities and the identification of the necessary prerequisites for the implementation of the major activities, in terms both of auxiliary hardware availability and of output from previous steps in the plan.

As the project moves towards the Operations Phase, it will be essential to maintain a regular review of the ITER Research Plan, as results from the accompanying R&D program and, later, from the experimental exploitation of ITER itself, become available. The IRP is thus to be viewed as a living document that evolves with the project. In addition, the IRP serves as a baseline from which the consequences of design or planning changes, or of unforeseen events, on the achievement of the ITER mission can be determined.

1.2 Methodology

The initial version of the Research Plan (IRP-v1.0), presented to the ITER Council Science and Technology Advisory Committee (STAC) in May 2008 [ITER_D_2FB8AC_v1.0, 2008], was developed during the 2007 - 2008 Design Review and was valuable in providing guidance to the capabilities required to support the implementation of a scientific research program which could address, and indeed fulfil, the project's key scientific mission goals. However, the subsequent evolution of the project schedule, involving in particular, a change in strategy for the hardware configuration at First Plasma and the installation of an all-tungsten divertor at the start of the nuclear phase, necessitated a significant revision of the IRP. Several updates were developed adapted to the changes in project strategy and schedule and presented to STAC during 2009. IRP-v2.1 was presented to STAC in October 2009 and, following minor modifications, was formally incorporated into the ITER Baseline at the Extraordinary ITER Council in July 2010 as IRP-v2.2 [ITER_D_2FB8AC_v2.2, 2009]. Although a further significant update (IRP-v2.3) was prepared and presented to STAC in May 2010 which was fully adapted to the subsequently approved ITER Project Schedule (IPS-2010), including a target date for First Plasma in late 2019 [ITER_D_346RPL, 2010], it did not complete the internal review procedure in time for incorporation into the ITER Baseline 2010, and so IRP-v2.2 has remained the reference Baseline version of the Research Plan until the present document.

While key elements of the Research Plan have been revised to incorporate changes in the project schedule and hardware configuration since 2010, perhaps most significantly the decision to initiate the experimental program with an all-tungsten divertor, uncertainties over delivery dates for 'deferred' components have prevented the development of a fully self-consistent revision of the Research Plan since 2010. The complete revision of the ITER project schedule within the framework of the Staged Approach, undertaken in 2015 – 2016, has provided the basis for the

preparation of an updated IRP which is consistent with the expected ITER tokamak and facility configuration during the period from First Plasma to full DT operation.

This revision of the IRP has been developed in collaboration with representatives of the Members' fusion communities nominated by the Domestic Agencies (DAs) who contributed wide-ranging expertise in fusion physics and tokamak operations to the analysis of the proposed experimental program during the ITER Operations Phase. Three dedicated workshops were organized at ITER Headquarters (HQ) involving ITER Organization Central Team (IO-CT) staff and the fusion community experts during the period July 2016 to March 2017:

- Workshop 1: 26 – 28 July, 2016
- Workshop 2: 14 – 17 February 2017
- Workshop 3: 14 – 17 March 2017

These workshops allowed a detailed discussion among the IO-CT staff and fusion community experts on the structure of the experimental program within the Research Plan, on the detailed experimental activities to be implemented, on the associated risks and the preparatory R&D which should be carried out, and also provided an opportunity to review the estimates of experimental time required to implement the foreseen program in the light of current operating experience on existing fusion facilities.

The workshop participants were provided with a summary of the output from the Configuration Workshop, held during 27 June – 1 July 2016, at which the facility hardware configuration during the Staged Approach was developed by the IO-CT and IO-DA management and staff. In addition, to provide background information on the key activities and issues within the existing Research Plan, the most recent report on the Research Plan, presented to STAC in 2014 [ITER_D_NSHUQ7, 2014], was made available to the participants prior to the workshop. This report was used as a point of reference for the analysis developed during the workshops. Complementary information on experimental risks identified by earlier analyses of the Research Plan was also provided for review by the Workshop participants [ITER_D_KTP2H5, 2013]. More detailed information on the hardware configuration of the principal ancillary systems and on key aspects of ITER physics were provided in a series of introductory presentations to the Workshop [ITER_D_TL5ACR, 2016]. To facilitate the analysis of major activities within the Research Plan, the Workshop participants were divided into several Working Groups each responsible for specific aspects of the experimental program.

The Working Groups were requested to analyze the key activities required to develop the research program following First Plasma, aligning the experimental activities with the planned hardware configuration within the Staged Approach (see Figure 1.2-1) so as: (i) to commission all required auxiliary systems with plasma to full performance (with pulse durations appropriate to the program requirements); (ii) to develop the experimental capability required to achieve initial DT fusion power production at levels of several hundred MW; and (iii) to propose a program of experiments in DT plasmas aimed at meeting the project's key mission goals in both inductive and non-inductive plasma scenarios, incorporating also the needs of the TBM testing program. Workshop participants were also requested to address:

- Whether requirements for system availability were consistent with the planned experimental program;
- Estimates of the experimental time required for the various experimental activities within the program;

- Experimental or operational issues which would require further analysis within the ITER R&D program to support the future development of the Research Plan;
- Risks to the Research Plan and possible mitigation measures.

The report presented here has been assembled from the analyses by the Working Groups of the elements outlined above.

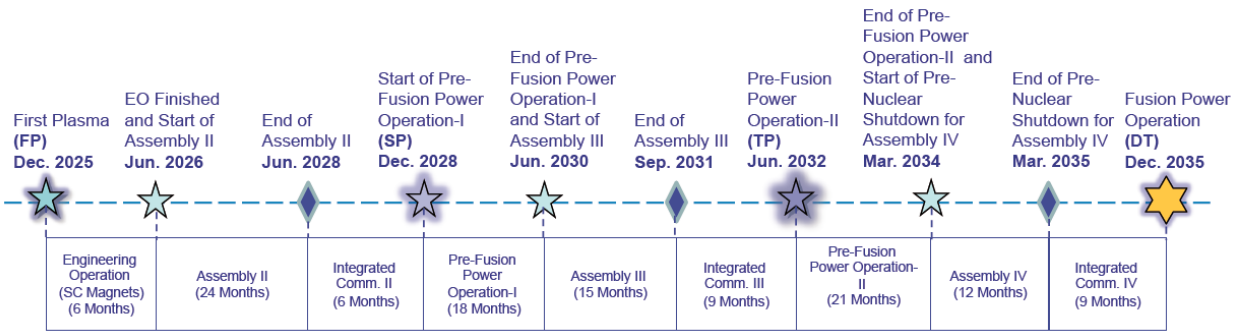

Figure 1.2-1: Schematic of the structure for the first 10 years of ITER operations within the Staged Approach.

The Research Plan presented in the current document addresses in detail the evolution of the scientific research program and of the TBM testing program during the 4 phases of the Staged Approach, but also extends the analysis beyond the initial phase of DT operation to the development of long-pulse, high fusion power plasmas satisfying the project's principal mission goals.

1.3 Overall Structure of the ITER Research Plan Present Version

1.3.1 ITER Research and Operational Phases

As noted in 1.2, the Research Plan has been adapted to the Staged Approach strategy within the revised ITER schedule with the overall aim of exploiting the available experimental capability to allow the transition to nuclear operation in late 2035, following First Plasma in late 2025. Furthermore, and as noted above, the development of the experimental program in DT plasmas is extended, on the basis of assumptions outlined in sections 2.6.4 and 2.6.5, to encompass the development of long-pulse plasmas at high fusion power and high fusion gain consistent with the project's mission goals.

Within the four stages of the revised operational schedule (including the longer-term extension of the final stage to an extensive development program of DT fusion power production in long-pulse DT scenarios and a research program in burning plasma studies), the principal goals are:

- **First Plasma:** achievement of the First Plasma milestone of plasma breakdown in hydrogen or helium with at least 100 kA of plasma current for at least 100 ms; during the subsequent Engineering Operation phase for commissioning of the Magnet systems to full current, circular limiter plasmas of up to 1 MA might be attempted.
- **Pre-Fusion Power Operation 1 (PFPO-1):** extensive 'commissioning with plasma' activities will be undertaken to establish diverted plasma operation in hydrogen/helium up to at least 7.5 MA/2.65 T, supported by a program of plasma control, diagnostics, ECRH and ICRF commissioning (assuming that one antenna providing 10 MW of ICRF heating is

available), as well as the systematic development of a disruption management/ mitigation capability to prepare for operation at higher currents; an option for operation at a toroidal field of 1.8 T has also been identified, which is under analysis and which could allow early access to H-mode operation with up to 30 MW of installed ECRH + ICRF power; this approach assumes that dual-frequency operation (104/170 GHz) of up to 1/3 of the gyrotrons could be implemented, or that up to 1/3 of the initial set of gyrotrons could be dedicated to low frequency (110 GHz) operation (both solutions would imply associated Electron Cyclotron (EC) transmission and launching system modifications), if needed for plasma start-up and/or heating.

- **Pre-Fusion Power Operation 2 (PFPO-2):** initial emphasis would be given to commissioning of the Heating Neutral Beam (HNB), Diagnostic Neutral Beam (DNB) and ICRF systems to full power, together with the necessary plasma control capability, to support the subsequent program; development of H-mode operation in hydrogen, with helium as back-up if this is not possible, reliable ELM control and divertor heat flux control would be a major thrust during this period of the research program; a further key goal would be the development of high power L-mode operation to demonstrate the full technical capability of the device; systematic studies of plasma-wall interactions and issues such as plasma-facing component erosion, redeposition, dust production, fuel retention and fuel removal would also be pursued in preparation for the nuclear phase. If the option for operation at 1.8 T were implemented, operation in H and in He H-modes would be possible at this stage, providing a physics basis to compare H-modes in H and He, which could be very important if H H-modes are not possible at higher fields in this phase. In addition, if H-mode operation at 1.8 T had been achieved in PFPO-1, this would allow the evaluation of the effects of the 3-D fields created by the TBMs in this phase, by comparing PFPO-1 (no TBMs) plasmas with those of PFPO-2 (with TBMs), and the development of mitigation schemes for such effects, if required.

- **Fusion Power Operation (FPO):** building on the experimental capabilities acquired during the previous operational phase, the initial aim of this campaign would be to demonstrate operation of high power H-modes in deuterium to prepare plasma scenarios for DT operation; beginning with trace tritium experiments, a gradual transition to full DT operation would be undertaken as the fuel reprocessing throughput of the Tritium Plant increased; the goal of the first campaign of DT operation would be to demonstrate fusion power production of several hundred MW for several tens of seconds at a Q value in the range of 5 – 10. In subsequent experimental campaigns, the fusion gain would be optimized to achieve $Q \geq 10$, the pulse duration in inductive plasma scenarios would be extended towards the goal of 300 – 500 s burn required by the *Project Specification*, and hybrid and fully non-inductive scenarios would be developed to achieve burn durations in the range 1000 – 3000 s with $Q \sim 5$.

The plan for each of the exploitation phases is based on a series of key research issues around which an experimental program has been developed to commission systems with plasma, to develop certain control capabilities, to establish specific plasma scenarios, to address uncertainties in the physics of plasmas at the ITER scale and in the burning plasma regime, and finally to perform detailed scientific studies of burning plasmas while optimizing their fusion performance. There is greater uncertainty, of course, in relation to the details of later phases of the Research Plan, since the results derived from earlier phases are expected to dominate the final planning of subsequent phases and, in addition, ITER is the first experiment which will provide access to the study of burning plasmas.

In addition to the development of the scientific research program during the Operations Phase, this document also presents, in 3.2, the research to be conducted within the Test Blanket Module (TBM) Testing Program from the first operational tests of TBMs in PFPO-2 to the completion of the first integrated tests of the operational behaviour of the blanket component for heat extraction and tritium breeding/ management, expected to take place during FPO campaign 3.

Section 4 of this report discusses a range of options for the implementation of upgrades to ITER operational systems and indicates, where possible, how the experimental results from the Research Plan can influence upgrade choices, as well as the implications of the upgrades for the subsequent research program. In section 5, the IRP discusses the key research activities foreseen to proceed in parallel to the construction phase. These activities are intended to complete the design basis for certain key auxiliary systems, to resolve issues impacting the efficiency of ITER operation, to prepare plasma scenarios to be used in ITER and to develop specific experimental techniques and tools required to achieve the foreseen scenarios. The discussion is focussed on key R&D issues, which are grouped into several areas of fusion physics research. The identification of these key R&D activities is closely linked to the resolution of physics and operational issues identified in the development of the Research Plan.

The present version of the IRP also presents several Appendices dealing with complementary discussions of several issues closely related to the implementation of the research program. Appendix A, Appendix C and Appendix D discuss specific issues associated with the plasma-wall interaction: Appendix A discusses the use of deuterium 'spiking' of hydrogen plasmas during PFPO-2 to provide an improved quantitative estimate of fuel retention, while Appendix C presents the considerations relating to the management of heat loads on the ITER divertor and Appendix D describes the establishment of a routine 'reference pulse' which would be of particular significance for characterizing the evolution of the condition of plasma-facing materials. Appendix B reviews the experimental implications of our understanding of the scaling of the H-mode power threshold to ITER and of the impact of TF ripple on H-mode performance, while the physics considerations related to H-mode operation at 1.8 T, an option for the research program which has emerged recently, are presented in Appendix F.

In view of the proposal within the revised ITER schedule to eliminate the option for a later inclusion of an LHCD system in ITER, Appendix E presents a brief review of results of modelling studies of long-pulse and non-inductive DT scenarios in ITER. In particular, the predicted plasma performance with and without inclusion of LHCD in the H&CD upgrade options are compared in terms of the Q-value achieved and of the proximity to the fully non-inductive state. An extensive discussion of the plans for the phased installation of the baseline H&CD systems, of options for modifications to the agreed baseline installation schedule and capabilities, and of the schedule implications of various upgrades to the baseline systems is presented in Appendix G. The strategy developed within the revised schedule for the phased installation of the baseline Diagnostic capability is presented in detail in Appendix H. A brief summary of considerations related to the availability of tritium from external sources to support the planned DT experimental program during the period from the late 2030's to the early 2050's is given in Appendix I. Appendix J provides an updated version of the Research Plan Risk Register, which deals with the most significant risks to the successful implementation of the planned experimental program and, in particular, to the timely achievement of significant fusion power production.

1.3.2 Assumptions on the Phasing of ITER Operational Capabilities

The central element of the revised ITER schedule within the Staged Approach is the phased installation of the operational capability of the ITER tokamak and of the ITER facility. A detailed

discussion of the Plant Configuration proposed for each phase of the Staged Approach was presented to the STAC in 2016, and the baseline 'Plant Configuration' within the revised schedule has been formalized in [ITER_D_TVG7YK, 2017]. Figure 1.3-1 provides a schematic overview of the evolution of the plant configuration during the Staged Approach, indicating in yellow options for PFPO-1 which are not yet in the baseline, but are currently under evaluation. The major elements impacting on the implementation of the Research Plan are summarized here for ease of reference. Further details relating to the phasing of the H&CD systems and to the sequence of Diagnostic installation are presented in Appendices Appendix G and Appendix H respectively. The following evolution of the auxiliary systems has been agreed to support the experimental program discussed in sections 2.4, 2.5 and 2.6:

(I) First Plasma (H/He) (FP):

- Initial set of PF/CS converters
- First Plasma Protection Components (FPPC) to provide required protection of in-vessel systems and vacuum vessel
- Central Control System fully operational
- H&CD installed power: P_{ECRH} = 8 MW from 1 upper launcher (6.7 MW coupled to the plasma)
- A limited subset of the baseline Diagnostic capability, essentially to characterize plasma breakdown and to provide limited plasma control and machine protection
- Fuelling: gas injection capability
- Vacuum: 6 cryopumps incorporating activated charcoal
- Vacuum Vessel baking and preliminary Glow Discharge Cleaning system

(II) Pre-Fusion Power Operation (H/He) 1 (PFPO-1):

- PF/CS converters upgraded to full performance
- Shielding blanket/beryllium first wall and all-tungsten divertor
- H&CD installed power: P_{ECRH} = 20 MW (all launchers)
- A subset of the baseline Diagnostic capability, with the emphasis on plasma control and machine protection
- Fuelling: full gas injection capability and at least 2 pellet injectors
- Disruption mitigation system: hardware commissioned
- Error field correction coils: hardware commissioned
- Vertical stabilization coils: hardware commissioned
- In-vessel viewing system; hardware commissioned
- An appropriate Be handling capability will be provided

All of the listed systems will be required to support the experimental program. In addition, the following options are being studied, with the aim of implementing these through later Project Change Requests (PCR) if their feasibility and benefit to the research program is confirmed:

- Up to 1/3 of the installed ECRH power to have a low frequency capability (104 or 110 GHz) either via a set of 8 dual-frequency gyrotrons (104 GHz), or a set of 8 dedicated low frequency gyrotrons (110 GHz), if needed for plasma start-up and/or heating.
- Acceleration of one ICRF antenna to provide up to 10 MW injected power capability at 40 – 55 MHz.

- A subset of 9 of the ELM coil power supplies to allow initial ELM control studies and an improved error field correction capability.

The experimental program detailed in 2.5.4 assumes that these additional capabilities will be available.

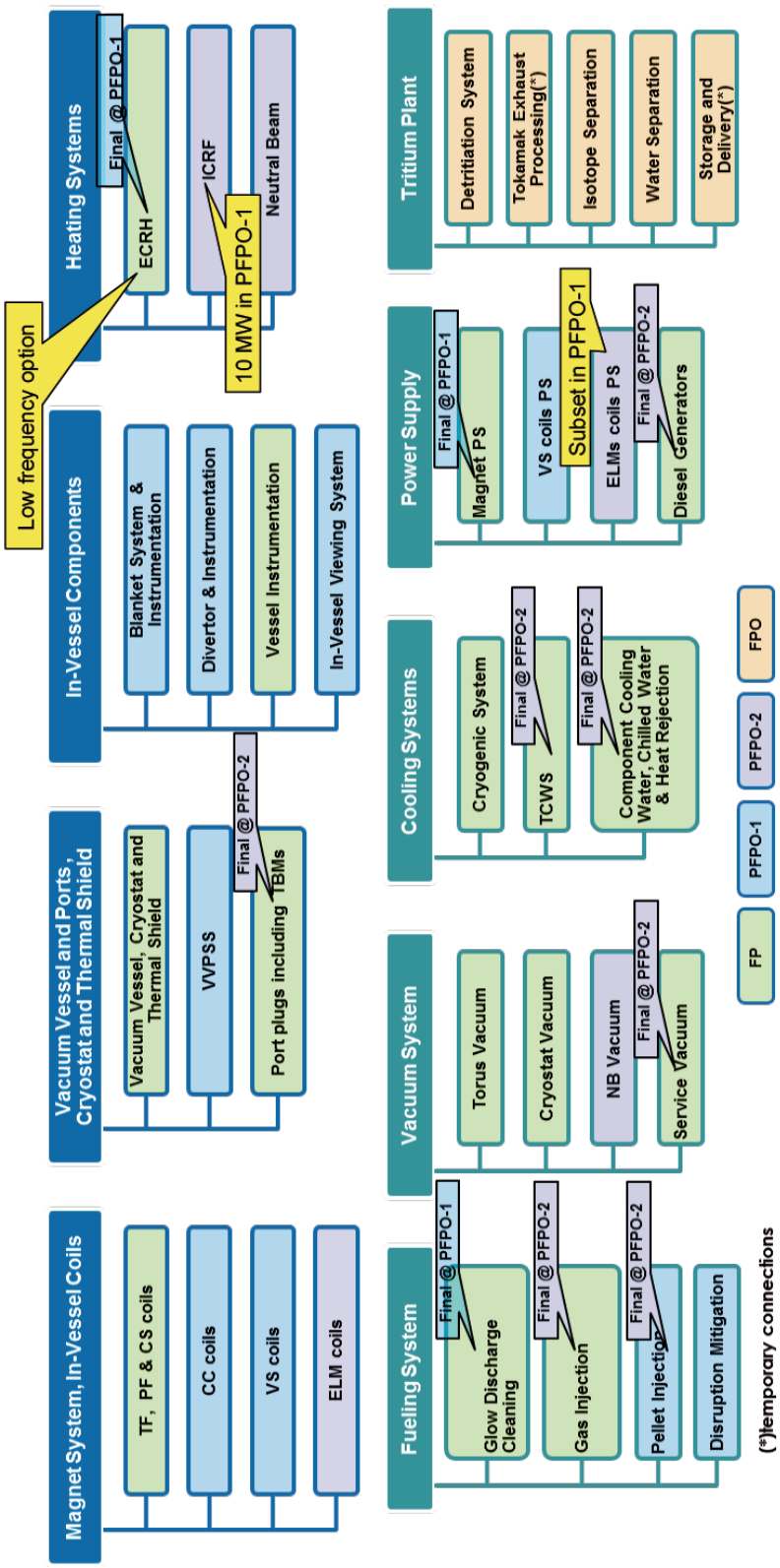

Figure 1.3-1: Schematic of the ITER 'Plant Configuration' at each phase of the Staged Approach, with the colour code indicating the stage at which each system becomes fully operational. (*) refers to temporary connections to delivery and exhaust of non-tritiated gases during PFPO phases.

(III) Pre-Fusion Power Operation (H/He) 2 (PFPO-2):

- H&CD installed power: P_{NB} = 33 MW, P_{ECRH} = 20 MW, P_{ICRF} = 20 MW (two antennas)
- Diagnostic Neutral Beam (DNB) system
- An extended set of Diagnostics for physics studies
- Fuelling: 2 additional pellet injectors
- ELM control coil system: hardware commissioned
- First set of TBM modules (EM-TBM) installed for initial phase of testing program
- Tritium Plant undergoing integrated non-active commissioning

(IV) Fusion Power Operation (D/DT) (FPO):

It should be expected that essentially all elements of the tokamak and its auxiliary systems will have been brought into operation during the PFPO phase in order to allow the efficient implementation of the D and DT phases of the program. Significant new capabilities that would be available for the nuclear phase include the measurement capability for 14 MeV neutrons; since this aspect of the neutron calibration will be scheduled just prior to the start of the nuclear phase of operations, and a range of fusion product diagnostics (see Appendix H). A principal goal of the PFPO phase is to ensure that all of the H&CD capability is commissioned to full power to at least ~ 50 s before the nuclear phase and that all elements of the fuelling systems are operational with all required gases except deuterium and tritium. As will be discussed in sections 2.4 and 2.5, key aims of the PFPO phase include commissioning of all aspects of magnetic control, several aspects of kinetic control (e.g. control of divertor heat exhaust), demonstration of reliable and effective disruption mitigation (including runaway electron mitigation), and demonstration of ELM suppression/ control. Thus, essentially all of the plant and ancillary systems should be in an advanced state of operation by the beginning of the nuclear phase. The major plant commissioning activity that would proceed in parallel with nuclear operation would be the expansion of the processing throughput of the Tritium Plant. This would rise gradually during the deuterium experiments and into the initial period of DT operation. In addition, if essential upgrades have been identified during PFPO to achieve the Q = 10 goal, it is likely that these will be implemented either before or in the early stages of FPO; this may require specific commissioning time to be dedicated to them.

1.3.3 Key Research Issues

1.3.3.1 Key Research Issues during Operation

The Research Plan for the exploitation phases is developed around a sequence of 'commissioning with plasma' activities and a series of key research issues. Some of these issues will be addressed in parallel so as to use experimental time efficiently, but many must be resolved before proceeding to address subsequent issues.

In the PFPO, the first physics objective will be to develop plasma scenarios suitable for system commissioning, particularly of the heating and current drive systems. This will necessarily involve extensive commissioning of the plasma control and protection systems (Central Interlock System, CIS; Central Safety System, CSS, Plasma Control System PCS) to ensure safe and reliable operation of the tokamak and investment protection. Such commissioning includes the use of the in-vessel coils for vertical stabilization of highly shaped plasmas and studies of the level of error field

in ITER, together with the determination of the impact of error fields on ITER plasmas, and of the use of the dedicated coil set to correct them routinely. In parallel with these commissioning activities, the characterization of disruptions, the development of reliable disruption prediction, and the commissioning and optimization of the disruption mitigation system (DMS) will be an essential research activity accompanying the gradual increase in plasma parameters during this period. Commissioning of diagnostic systems and data validation will be important early activities to provide the measurement capability for plasma control, disruption detection and more general machine protection: for example commissioning of a protection system for the all-metal plasma-facing components will be important in advance of the introduction of significant heating power and higher plasma thermal energies.

Once an adequate measurement, control and protection capability is in place, commissioning of the H&CD systems will be a priority to provide access to higher plasma parameters and, eventually, higher confinement. Initial physics studies carried out in this phase will also be the first opportunity to study tokamak plasma behaviour at the ITER scale. While there is still considerable uncertainty over the scaling of the H-mode power threshold to ITER (see, e.g. Appendix B) the experimental data indicates that it could be possible to obtain H-modes in helium plasmas with ECRH heating only. The option to operate ITER at 1.8 T, with an adapted H&CD capability (i.e. the possible additional 10 MW of ICRF) could open a path to early studies of hydrogenic H-modes, not previously considered possible during this early operational period. H-mode access would also permit an early assessment of crucial issues, such as ELM control, while potentially allowing a better definition of the requirements for future heating and current drive upgrades. As discussed in 2.2, there are many important plasma-wall interaction issues which will be of interest, even within the limited range of plasma parameters accessible during this period.

The additional H&CD and Diagnostics capabilities to be installed in advance of PFPO-2 will considerably expand the range of plasma scenarios and plasma parameters available for study, and will enrich the capability for physics studies at the ITER scale. ‘Commissioning with plasma’ activities will continue during this period, since it will be important to commission as many of the tokamak and plant systems as possible and test them thoroughly in advance of the transition to D/DT operation. Thus commissioning of plasma control, disruption management, machine protection, H&CD and Diagnostic systems will continue to feature extensively, but more sophisticated aspects of plasma control will be explored, including NTM suppression, sawtooth control, and possibly physics issues related to RWM control, and certainly divertor heat flux control. A more extensive program of H-mode studies and, in particular, of ELM control will be implemented, with the emphasis on studies of hydrogenic H-modes if access to H-mode in hydrogen plasmas proves possible. Extension of the plasma operating range to high current and to long pulses (at lower currents) will be key aims of the program during this experimental campaign: first operation at 15 MA/5.3 T should be demonstrated in L-mode, while the current drive capabilities of the HNB systems could allow pulse lengths of several hundreds of seconds in both L- and H-modes, if sufficient time for commissioning the H&CD systems to long-pulse operation is available. In addition, initial studies of current drive efficiency and formation of target q-profiles for hybrid and/or non-inductive scenarios could be launched during this phase in preparation for the development of these scenarios in DT plasmas. PWI studies will be of particular significance during PFPO-2, as quantitative studies of power deposition and of processes such as erosion, material migration, fuel retention (and removal) and dust generation are expanded with a view to developing a quantitative understanding of these issues in advance of DT operation. A wide-ranging program of PWI studies with a dedicated experimental program is therefore anticipated.

Following the transition to the FPO phase, plasma operation will initially focus on experiments in deuterium: the deuterium phase is likely to prove the first opportunity to perform detailed development of H-mode scenarios for later use in DT. Nevertheless, since the key goal of this phase is to transition to 50:50 DT plasmas and significant fusion production as rapidly as possible, the duration of the deuterium program will depend strongly on the pace of commissioning of the Tritium Plant, which is likely to begin the experimental campaign with a very limited throughput that will then grow over time. Therefore, while physics studies in deuterium L- and H-modes will provide extensive opportunities for the exploration of plasma behaviour at the ITER scale, once an adequate supply of tritium becomes available, it is favourable from the programmatic and mission perspectives to launch the development of plasma scenarios with increasing tritium fractions, though initial experiments with trace tritium in deuterium plasmas can provide a valuable tool for the investigation of physics processes governing tritium fuelling and transport. Alternatively, if the tritium throughput of the T-Plant rises more slowly than required, additional time could be allocated to scenario development in deuterium with the aim of minimizing development time required in DT. During this program, control of ELMs, core MHD and (simulated) plasma burn will be established and combined into fully integrated scenarios.

This phase will initially focus the experimental R&D on conventional inductive scenarios but also includes the initial development of advanced and hybrid scenarios. The extent to which the latter development is carried out will depend on the available experimental operational time until a significant tritium throughput is available. The aim of the present ITER Research Plan is to proceed to full DT operation as rapidly as allowed by progress in commissioning of required systems and in the experimental program. Thus priority is given to establishing an adequate basis for the demonstration of significant fusion power production and fusion gain for several tens of seconds in the most promising plasma scenario (currently assumed to be the inductive ELMy H-mode) and the extensive development of more advanced scenarios is deferred until later in the DT phase.

Once an adequate tritium throughput is established, the transition from deuterium towards full DT plasmas will follow a route of gradually increasing both plasma current and tritium fraction, allowing time for issues such as power handling, burn control, fuel mixture control and helium exhaust to be integrated into scenarios established initially in the deuterium phase. The first programmatic goal is to develop an integrated scenario capable of producing several hundred MW of fusion power for several tens of seconds. Achieving this goal during the first FPO campaign will be the striking demonstration of ITER and magnetic fusion capabilities and potential.

Once this level of fusion performance is achieved, the focus of the program will be on exploring optimization of DT scenarios, aiming to achieve the main mission goal of demonstrating $Q \geq 10$, which might firstly be accomplished in relatively short pulses of several 10s of seconds. In parallel a detailed study of burning plasma behaviour in the most performing scenario would be undertaken, the first steps into a new regime of fusion plasma studies. Thereafter, the development of plasma performance and the exploration of burning plasma physics would be intertwined in a program designed to optimize Q and extend the pulse duration towards several hundred seconds. Complementing the development of long-pulse burning plasma scenarios, experimental time would be devoted to the development of hybrid (or improved H-mode) scenarios and fully non-inductive scenarios. Achieving both long duration burns and a Q-value approaching 5 in the latter scenario is likely to involve a program of at least several years experimentation, while the hybrid mode may offer a quicker route to long-pulse operation if the physics observed in current experiments extrapolates sufficiently well to the ITER scale and to the burning plasma environment.

An important element of the Research Plan during DT operation is, of course, the study of a wide range of burning plasma physics issues:

- Waves and energetic particle physics;
- Fuel mixture control and helium exhaust;
- Self-heating and thermal stability;
- Macroscopic stability physics and control;
- Multi-scale transport physics;
- Physics of the plasma-boundary interface;
- Integrated burning plasma scenario development.

Additional key physics issues for advanced modes include current profile control and MHD control at pressures above the no-wall β-limit. These studies will not only address issues related to the ITER core mission but also leverage the unique capabilities that ITER provides within the worldwide fusion program. Examples of such capabilities include operation at low normalized gyroradius, operation with a low collisionality pedestal coupled with a high-density divertor, and operation with a large population of isotropic energetic particles.

These detailed physics studies will be complemented by a comprehensive technology program, in particular on the tritium breeding Test Blanket Modules, which are the subject of an extensive research program in the ITER Members and which will be a further significant contribution by the ITER Project to the development of fusion energy.

1.3.3.2 Key Research Issues during Construction

The key issues identified for the supporting Physics research program accompanying ITER construction have been grouped into four areas: H-mode issues; Plasma-wall interaction issues; MHD instability mitigation/control issues; and Scenario development issues. It is recognized that the four types of issues are linked. Indeed, one of the overall goals of the program is to develop the integrated modelling capability for ITER, within the Integrated Modelling and Analysis Suite (IMAS), to provide a 'flight simulator' that can be used as part of the preparation of experiments and that can be validated by the results in present fusion facilities, in advance of its application for the preparation of ITER plasma discharges. In addition, the R&D activities required to support the development and construction of the Test Blanket Modules are reviewed (see 3.2.1.2).

The key research issues during construction are discussed briefly in section 5 of the Research Plan. Resolution of these might have an impact on ITER in at least one of three ways: affecting the design of baseline components of the machine – though with the progress in the detailed design of ITER systems over the past 10 years and the transition to construction, the scope for influencing the baseline design is much reduced; influencing the choice or design of upgradeable components; or leading to improvements in the plasma scenarios and experimental plan foreseen for ITER, thereby improving the efficiency of ITER operation. Issues in the first category are obviously time-critical - their resolution must rely either on already existing capabilities or on modest extensions of those capabilities. The second category also has time constraints, but these are more difficult to define precisely: decisions on upgrades generally require long lead times that are a function of their complexity (i.e. for design, fabrication, and installation), and the supporting R&D may require additional time for new hardware as well as analysis. The last category encompasses a range of challenging issues whose outcomes impact the experimental time allocated in the ITER schedule to

the development of plasma scenarios which encompass adequate solutions at the ITER scale. Their resolution could also indicate that other upgrades need to be considered.

The list of key issues presented in the Research Plan is clearly not exhaustive. There are many other uncertainties in the physics and technology basis for ITER that can also impact performance and which are being addressed in the extensive research program being carried out in parallel to ITER construction. The items listed here, and discussed in more detail in section 5, are those currently considered to be the highest priority, in particular with regard to their perceived probability of leading to the need to modify or upgrade the facility.

2 Research Program during Operations

2.1 Overall Structure of the Experimental Program during Operations

The basic structure of the experimental program within the Research Plan has been maintained under the adaptation to the revised schedule within the Staged Approach. The program begins with 3 experimental phases (including First Plasma) in hydrogen/helium (i.e. non-activating fuels) in which all of the tokamak, plant and auxiliary systems are commissioned with plasma to high performance (not all aspects of system performance can be commissioned to the highest level in advance of fusion power production). Following the transition to the use of D/DT fuels, an initial campaign is designed to achieve significant fusion power production as rapidly as possible, and this is followed by a sequence of experimental campaigns on a two-yearly cycle. In these campaigns, in which the ITER scientific and technical mission goals are pursued (including the TBM testing program), burning plasma physics is studied in detail, and the physics basis for Demo design and operation is developed. The present Plan develops the exploration of the DT phase within the achievement of the principal scientific mission goals and so limits the time horizon of the program to the first 3 experimental campaigns in DT plasmas, as illustrated in Figure 2.2-1. The broad aims of each phase of this experimental program have been outlined in section 1.3.1, and these are expanded in some detail in sections 2.5.4.1, 2.5.5.1 and 2.6.1.

The structure on which the Staged Approach converged as a result of the schedule revision procedure implemented by the ITER project management during 2015 and 2016 is illustrated in Figure 1.2-1. This was developed on the basis of guidance from the Members on their anticipated budget constraints during the Construction Phase and the implications for the resources expected to be available to IO-CT and IO-DAs, but also on the understanding of ITER plasma operation and experimental R&D developed over the past 10 years. This understanding has been developed through the elaboration of previous versions of the Research Plan and additional experience gained through the fusion physics R&D programs in the Members' fusion communities, which have provided insight on the experimental time that will probably be required to progress from First Plasma to a level of plasma performance and operational efficiency in ITER which would: (i) confirm that the tokamak systems were performing satisfactorily, (ii) provide confidence that an adequate level of plasma performance had been achieved in ITER, and (iii) that the necessary level of experimental expertise (integration and control of plasma scenarios) had been demonstrated to justify the transition to DT operation and fusion power production. The resultant schedule towards DT operation incorporates both the project level and scientific/ technical considerations on the path towards DT operation.

The resultant structure of the experimental program, illustrated in Figure 2.2-1, therefore consists of:

- **First Plasma Campaign:** ~1 month, plus 6 months of Engineering Operation including, possibly, some plasma operation
- **Pre-Fusion Power Operation 1:** 18 months of hydrogen/helium plasmas
- **Pre-Fusion Power Operation 2:** 21 months of hydrogen/helium plasmas
- **Fusion Power Operation 1:** 16 months of initially D and subsequently DT plasmas
- **Fusion Power Operation 2:** 16 months of DT plasmas
- **Fusion Power Operation 3:** 16 months of DT plasmas

Beyond this period, which is the subject of the analysis presented in succeeding sections, the ITER experimental program would, of course, be expected to implement extensive scientific and technical

R&D in pursuit of its overall mission goal to demonstrate the scientific and technological feasibility of fusion energy for peaceful purposes and to provide key information for the further development of Demo. This longer-term development of the ITER program is beyond the scope of this version of the Research Plan.

2.1.1 Integration of the Research Plan into the Staged Approach

An essential element in the integration of the ITER Research Plan into the Staged Approach is the link between the hardware capabilities of the ITER facility (the 'Plant Configuration') at each stage of the Operation phase and the corresponding objectives. Once again, a balance has been struck between the project-level constraints on the procurement schedule and the operational requirements to fulfil overall objectives for the PFPO phase which would support a timely transition to DT operation, with a target date for this transition of late 2035. The evolution of the ITER facility hardware configuration has been outlined in section 1.3.2 and, as noted there, formalized in [ITER_D_TVG7YK, 2017], which defines the baseline configuration of the ITER facility at each phase of the Staged Approach. In addition, several options are being developed within the baseline configuration that are expected to be formally adopted through the project-level Project Change Procedure once their technical benefits and the technical/management feasibility of their implementation are confirmed. The key elements of these options, which influence the development of the Research Plan, and which have, therefore, been integrated into the analysis of the Plan (i.e. assumed to be available to the experimental program) are summarized in section 1.3.2.

In addition to the logical structure defining the steps necessary to progress from First Plasma to full performance in DT plasmas, the Research Plan makes estimates of the duration of each of the steps within the experimental program to obtain an overall estimate of the operational time required for successive phases of the program. This analysis is clearly subject to substantial uncertainties so far in advance of ITER exploitation. Nevertheless, in discussion with the fusion community experts participating in the Research Plan Workshops, a first estimate of the experimental time required by the principal activities was assembled, which forms the basis of the estimates given in the course of the discussions in later sub-sections of section 2.

As a point of reference, an estimate of the maximum number of experimental days available in PFPO-1, PFPO-2 and FPO is given in Table 2-1. The basis for this estimate is that applied in earlier analyses of the Research Plan, derived from the assumptions developed in the ITER RAMI analysis [ITER_D_28WBXD, 2012]: in 2-shift operation, which forms the basis of operational planning within the Staged Approach, it is assumed that the operational pattern is 12 days of experimental operation and 2 days of short-term maintenance within a 14-day cycle.

Table 2-1 – Overview of experimental days within the Research Plan campaigns

Campaign	Days
First Plasma Campaign (nominal 1 month)	25
Pre-Fusion Power Operation 1 (18 months)	470
Pre-Fusion Power Operation 2 (21 months)	545
Fusion Power Operation 1 (nominal 16 months)	415
Fusion Power Operation 2 (nominal 16 months)	415
Fusion Power Operation 3 (nominal 16 months)	415
Total	2285

Within a 2-shift operational day, a 30-minute pulse repetition time, for burn (or flat-top for non-active operation) durations of less than 450 s allows, in principle, 32 plasma pulses. When corrected for the 60% 'Inherent Availability' assumed for the RAMI analysis, and the loss of time associated with disruptions/disruption recovery, a total of 13 'good' plasma pulses per day results. Later in the FPO phase, as pulses with burn durations beyond 450 s are developed, the number of pulses per day will, of course, be reduced if a 25 % duty cycle is maintained. However, this reduction in 'good' pulses per day achieved within the constraint of a 25% duty cycle may be compensated, to some extent, by a reduction in the frequency of disruptions; this will necessarily be substantially lower in the FPO phase than in the PFPO phase as a result of the progress made in disruption management, as outlined in later sections, and of the need to avoid significant loss of experimental time due to the impact on in-vessel components of disruptions at high fusion power.

The estimates given in Table 2-1 are, of course, likely to be an upper bound to the number of days actually available to the experimental program, since the system performance assumed in the RAMI analysis relates to the operation of mature systems, but they nevertheless provide a basis for comparison with the estimates of the experimental time required for the main activities within the Research Plan presented in the following tables.

The transition from the PFPO phase, during which non-activating fuels are used, to the FPO phase, where deuterium and deuterium-tritium plasmas form the basis of the experimental program, is, of course, a key transition in the Research Plan. Within the Staged Approach, this is likely to occur following Integrated Commissioning IV, in the latter half of 2035. In preparation for supporting the experimental program following this transition, it is planned that the Tritium Plant will take the significant step of embarking on the commissioning of its operation with tritium in spring 2033 (see Figure 2.2-1). It is expected that early in FPO campaign 1 (2036), the T-Plant will be able to supply trace tritium amounts for the ITER experimental program. In the course of 2036, a fraction of the Isotope Separation System (ISS) will be operational and will be able to provide pure tritium for ITER operation, reaching a daily fuel throughput of the order of 10% of the final throughput during the FPO campaign 1 (the final throughput is specified as 200 Pam^3s^{-1} (~ 10^{23} D/T atoms s^{-1}) for a 300 – 500 s Q = 10 plasma with a duty cycle of 25%). The initial throughput will be sufficient to allow an expanding program of DT experiments to be developed during the latter half of the first FPO campaign, leading to significant fusion power production of several hundred megawatts during the campaign. This framework for the commissioning and operational start-up of the Tritium Plant forms the basis for the development of the FPO program presented in section 2.6.

2.2 Plasma-Wall Interaction (PWI) Issues for the Research Plan

2.2.1 Characteristics of Helium Operation

The effect of helium interactions with plasma-facing metals has received considerable attention in recent years due to the strong trapping exhibited by He in most metals and its tendency to cluster and form bubbles, which leads to strong morphology changes (Figure 2.2-2). The possible formation of a porous sub-surface structure (populated by a large fraction of voids/bubbles) and the observation of a strong reduction in the thermal conductivity of the surface in such cases [Cui, 2017] has raised concerns about possible reduction of the transient damage thresholds (especially for ELMs) after extended He plasma operations, as considered during the PFPO phases. Helium-induced embrittlement has indeed been observed after high-flux plasma exposure in linear devices showing that He plasma exposure of W leads to a reduced threshold for surface cracking.

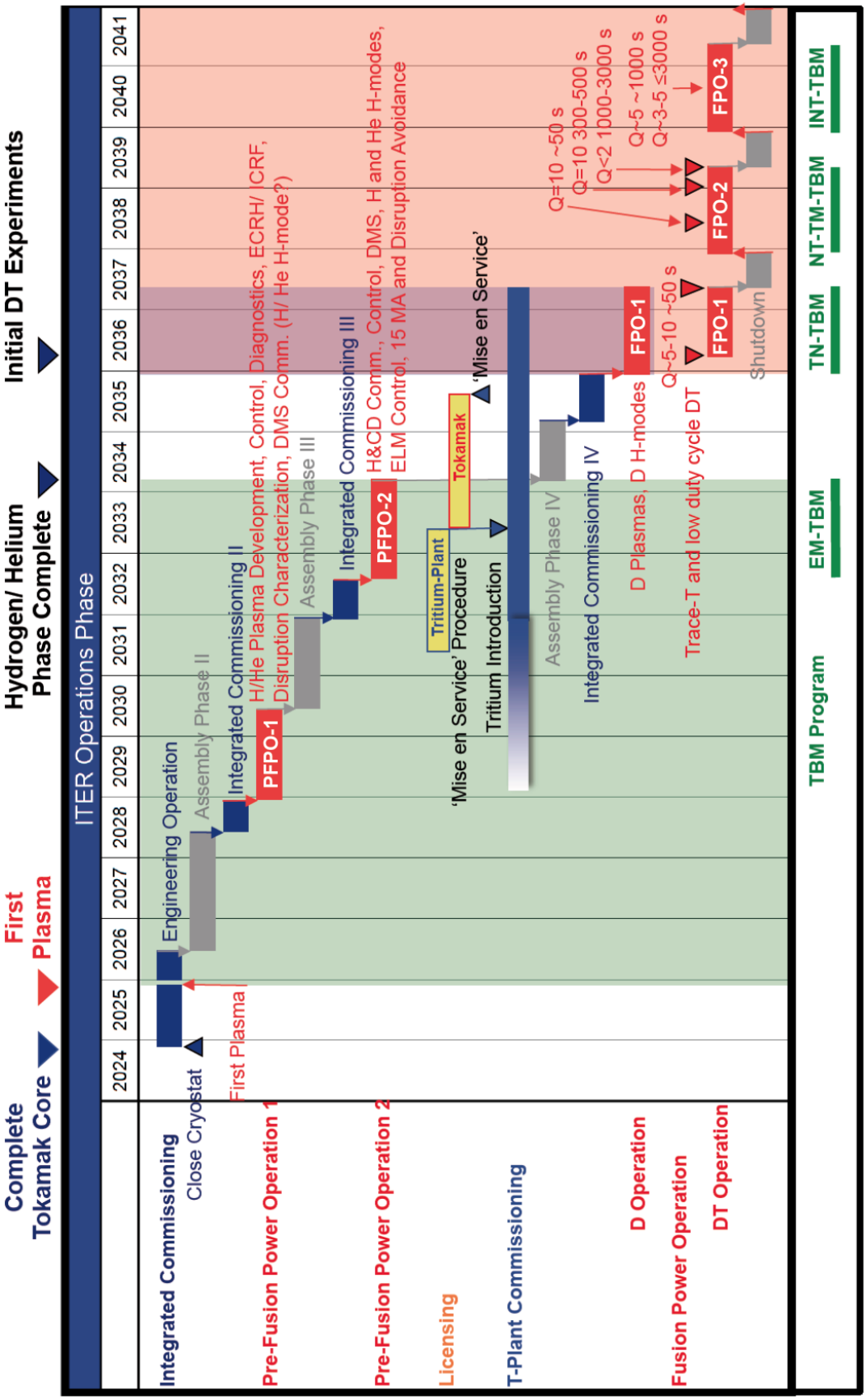

Figure 2.2-1: Operations Plan within the Staged Approach.

However, ELM-simulation experiments in electron-beam facilities have shown that for ITER-relevant high cycle number (~10^6), the cracking threshold of tungsten in terms of energy density is in any case very low [Wirtz, 2017]. This indicates that surface cracking might appear sooner if extensive He operations were performed, but that it would in any case be likely to occur whether or not Helium operation is performed, as He will be produced during DT operation.

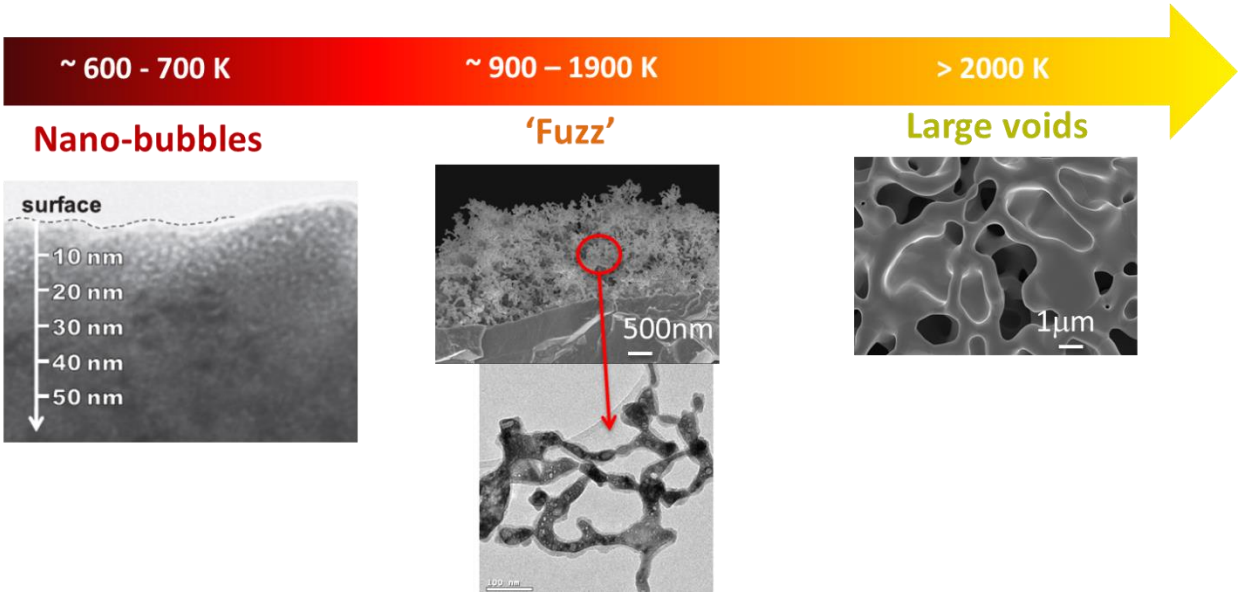

Figure 2.2-2: Illustration of the range of He-induced morphology changes on tungsten as a function of temperature. A dense network of nanobubbles is usually formed at temperatures below 600-700 K (left: image from [Miyamoto, 2011]), fuzz formation proceeds in the range 900-1900 K (centre: images from [De Temmerman, 2012]), large voids are typically formed at higher temperatures (right: image from [De Temmerman, 2012]).

The effects of He exposure on the mechanical properties of W have been studied using nano-indentation [Yoshida, 2005; Bernard, 2015] and revealed measureable increases in the hardness far from the implantation depth of the incident He particles. To date, however, the existing data is still insufficient to build a coherent picture of the effect of prolonged He (and plasma in general) exposure on the thermo-mechanical properties of W and how this might affect the power handling capabilities of the material in the long-term. It should be mentioned here that He effects on metals are strongly temperature-dependent. It is expected that the divertor heat fluxes, and hence surface temperatures, during pure He operations, as presently foreseen during PFPO-1 and 2, will be substantially lower than during high power DT operations where the He from fusion reactions will be present in the divertor exhaust. Any knowledge obtained on ITER regarding He-W interactions during non-active operations will therefore be difficult to extrapolate to burning plasma conditions.

A dedicated He campaign was performed in ASDEX-Upgrade in 2015 in part to study plasma-wall interactions in a full metal machine during He operations [Hakola, 2017]. A series of samples was installed on the ASDEX-Upgrade outer divertor target manipulator and exposed at the outer strike point location. The most noticeable result of this campaign was the observation that the outer strike point region was a deposition-dominated area during He operations, in sharp contrast to its status as an area of erosion during similar D discharges. More precisely, thick boron coatings (boronization is used for wall conditioning on ASDEX-Upgrade) were observed on the samples, implying an increase in wall erosion during He operation. The most likely cause for this observation is the higher average charge state of He ions impacting main wall surfaces (and higher mass) compared

with D, leading to enhanced boron sputter erosion of structures around the ICRF antenna and/or enhanced ELM-induced erosion of boron coatings and thus to the outer divertor becoming a net boron deposition zone for He plasmas. A confirmation of these results in JET would be very valuable. Translated to ITER, these results indicate that the material migration pattern during pure He operations could be very different from that expected during DT operations casting doubt on the usefulness of He operations for studies of beryllium co-deposition. In addition, given the difference in the retention mechanisms of H isotopes and He in plasma-facing materials, limited information is gained during He operations regarding fuel retention.

It may also be noted that divertor detachment physics in He plasmas differs significantly from that in hydrogenic plasmas [Loarte, 2000; Pitts, 2003; Wischmeier, 2003]. As a result of the higher ionization energy of He, the presence of a second ionization stage, and the lack of molecular chemistry, the loss processes which dominate plasma dissipation leading to detachment in a He plasma are distinct from those in hydrogenic fuel mixes. In hydrogen, plasma detachment proceeds first by means of momentum losses due to CX processes, whilst in helium, the main mechanism is radiative loss from electron-impact excitation and ionization events. Ionization mean-free paths are longer in He in comparison with hydrogenic plasma so that He neutrals may more readily escape from the target vicinity, radiating along the separatrix and above the X-point area, starving regions downstream of power. The net result is that the dynamics of plasma detachment are likely to be sufficiently different that power load control techniques developed in He plasmas may have limited applicability to operation at high power in D or DT and, thus, that H H-mode plasmas are preferable to develop such control techniques in this phase. On the other hand, the additional divertor radiation obtained in He means that operation is possible at higher input power before divertor detachment control is required (Appendix C) thus facilitating high power operation, if issues are identified in the control of power loads for H H-mode plasmas that require additional systems at this stage.

2.2.2 Steady-state near and far Scrape-Off Layer (SOL) power widths ($1/I_p$ scaling)

The radial profile of parallel power flow, and the extent to which main wall interactions will be important in ITER are still active areas of research throughout the fusion community and consensus has not yet been obtained. A particular concern is the very narrow near-SOL inter-ELM heat flux width ($\lambda_{q,near}$) now being predicted for ITER in the baseline burning plasma scenario (I_p = 15 MA) from a new scaling based on high resolution IR thermography measurements at the outer divertor target of several tokamaks [Eich, 2013]. As discussed in Appendix C, these new observations, unavailable at the time of writing of the previous ITER Research Plan, now extrapolate to $\lambda_{q,near}$ ~ 1.0 mm, a factor of ~3 lower than assumed in all plasma boundary modelling used to scope the operational window of the ITER divertor. The scaling, in which $\lambda_{q,near} \propto 1/I_p$ with little or no dependence on any other key SOL parameter previously found in similar scaling attempts (e.g. P_{SOL}, separatrix density, R) is strongly supported by analytic modelling based on neoclassical magnetic drift theory [Goldston, 2012]. However, very recent gyro-kinetic simulations at the ITER scale find a strong major radius dependence, giving $\lambda_{q,near}$ ~ 5-6 mm in 15 MA H-modes [Chang, 2017].

A simulation study [Kukushkin, 2013] using the SOLPS plasma boundary code of the consequences of a very small $\lambda_{q,near}$ showed, as expected, that the upstream density would have to rise significantly if extra dissipation is required in the divertor to reduce the peak heat flux density. This increase may be beyond what is tolerable from the operational density limit point of view or from the standpoint of maintaining adequate confinement. Moreover, the addition of divertor monoblock shaping in the high heat flux regions of the target exacerbates the situation and will require still higher dissipation if target heat flux densities are to remain below the 10 MWm^{-2} technology limit

for steady state power handing. The research community, recognizing the importance of this issue for ITER, is actively engaged in finding consensus as to what should be expected in ITER at high performance regarding $\lambda_{q,near}$. Further plasma boundary simulations, beyond those in [Kukushkin, 2013] are also required to study the extent to which impurity seeding could be used to provide the extra dissipation in the event of very narrow heat flux channels.

Ultimately, ITER operation will be required for the real $\lambda_{q,near}$ to be properly characterized. High spatial resolution IR diagnostics viewing a small toroidal region of the divertor vertical target are foreseen and will be operational for PFPO-1. Recent observations on ASDEX-Upgrade [Sieglin, 2016] have shown a similar parametric dependence for $\lambda_{q,near}$ in L-mode discharges to that previously found in H-mode, but with about twice the absolute magnitude. This is reassuring from the point of view of thermal load specifications, as this assumption was adopted for ITER. Moreover, the new measurements find a dependence of $\lambda_{q,near}$ on the edge plasma temperature, which is speculated as one explanation for the higher values in L-mode in comparison with H-mode. The implication is that measurements of divertor power widths in ITER L-modes can be used as guidance for the values to expect in H-mode. The ASDEX-Upgrade data also demonstrate a strong dependence of the divertor heat flux spreading parameter, S (due to perpendicular heat transport in the divertor) on divertor T_e and n_e and show that this parameter is a useful tool to characterize target heat loads.

A closely related issue is that of the SOL power width and divertor target wetting in the presence of magnetic perturbations for ELM control/mitigation. Dimensioning of the divertor targets and performance has been almost exclusively performed using the SOLPS code in 2-D and thus takes no account of 3-D fields. Some analysis for ITER has been performed [Schmitz, 2016], using the 3-D code EMC3-Eirene, showing how divertor fluxes are redirected into a 3-D pattern of helical magnetic footprints at the targets. At maximum perturbation strengths (maximum ELM control coil currents), these ‘fingers’ can extend well beyond the axisymmetric heat flux decay profile, even with plasma screening accounted for. These studies, however, have been extended to date only up to the high recycling regime. Further developments in EMC3-Eirene are required to access truly dissipative regimes (e.g. including strong seeding and recombination). Moreover, understanding of how the divertor heat flux patterns in the presence of 3-D fields are affected in highly dissipative regimes is hampered by the fact that ELM suppressed regimes on current devices are found to date only at low collisionality. Experiments in which higher density divertor plasmas have been run in the presence of 3-D fields generally find that the heat flux perturbation at the target introduced by the magnetic perturbations is removed in-between mitigated ELMs, when the plasma detaches and the profiles are very similar to those found in the absence of the perturbation. However, it is expected that the removal of ELMs during complete suppression, supposing such conditions can be found on current devices, will strongly modify the upstream outward particle and heat fluxes so that the divertor target profiles which would be found in this case are presently unknown.

The current status of this research was summarized by the ITER Organization in a report to STAC in 2016 and this issue has been given high priority in the International Tokamak Physics Activity (ITPA) Divertor and SOL and Pedestal Topical Groups, with joint experiments and modelling expected to provide substantially improved understanding in the coming years.

Concerning the far-SOL power and particle fluxes on ITER (expected to be dominated by filamentary, or blobby cross-field convective transport), this remains an area of uncertainty and is being actively studied, notably within the ITPA Divertor and SOL Topical Group. It has important implications for the magnitude of wall heat and particle fluxes and hence on power handling, material erosion/migration and ICRF coupling. Recent multi-machine efforts have identified a link

between the appearance of upstream density shoulders and the degree of divertor plasma collisionality in the L-mode [Carralero, 2015]. Similar behaviour has also been found inter-ELM in H-mode plasmas, but the results are less conclusive [Carralero, 2017], with divertor collisionality seemingly a necessary, but not sufficient condition for upstream density shoulder formation. No data are available for the case of perturbed magnetic fields for ELM control; measurements are difficult and rare under H-mode conditions.

Considerable progress has been made, however, in demonstrating the universal nature of far SOL turbulence in tokamaks and a model has been developed which successfully describes these statistics [Garcia, 2016]. It is also the case that SOL turbulence simulations are increasing considerably in sophistication, with several 3-D codes being developed capable of including sheared (X-point) geometries. It is likely that continuing R&D, both experimentally and theoretically, will lead to substantial improvements in the understanding of main chamber fluxes by the time ITER operation begins.

2.2.3 Edge localized mode (ELM) power width scaling

The issue of what constitutes a tolerable ELM energy loss (ΔW_{ELM}) with respect to erosion/damage of plasma-facing components is evolving and is a function, particularly in the divertor, of the choice of monoblock front surface shaping and of the response of W material to sustained operation at high temperatures in the presence of multiple, repetitive transients. The latter can be far away from melting, but still lead to surface cracking which may later seed the development of deeper macro-cracks.

The original specification adopted in the ITER *Heat and Nuclear Load Specifications* [ITER_D_2LULDH, 2009] for the allowed ELM energy loss, ΔW_{ELM}, was derived from plasma gun experiments in which melting of the edges of perfectly aligned, castellated tungsten targets was observed for energy densities above ~0.4 MJm^{-2} in plasma pulses with temporal envelopes characteristic of those expected during uncontrolled type-I ELMs in ITER [Klimov, 2009]. Together with the conservative assumption of no broadening on the divertor target during the ELM, and the specification (derived from sparse experimental data) of asymmetric energy sharing favouring the inner target, this led to a requirement for $\Delta W_{ELM} \lesssim 0.6$ MJ.

The above criterion was established on the basis of power flow to an axisymmetric, unshaped divertor target, before the fine details of the shaping required on the divertor monoblocks were addressed. Extensive studies of various shaping options have now been performed, accounting for 3-D ion Larmor orbits [Gunn, 2017]. During ELMs, when Larmor radii are on the mm scale, toroidal gap loading is predicted to occur which cannot be completely prevented, at both inner and outer targets, by surface shaping. The consequences of repeated flash melting or excursions well above the recrystallization temperature of these edges are unknown at present, but gradual erosion cannot be excluded. If this would eventually be considered intolerable for ITER operation, then it could be that, for example, divertor monoblock toroidal gap edge melting may set a limit on the allowable ELM size. Furthermore, the point at which this limit may have to be respected could occur earlier in the operational campaigns than previously thought.

It may even be the case that, if the simple theoretical model offered in support of the parallel ELM energy density scaling [Eich, 2017] (see Appendix C) applies to ITER, mitigating ELMs may not significantly reduce the peak ELM target energy densities (simply the area over which the energy is deposited on the target varies – this is observed experimentally), so that only full suppression would avoid the ELM-induced melting problem at the divertor. One should also bear in mind that monoblock shaping always increases the stationary power flux density onto the surface and the

increasingly recognized need to remain below tungsten recrystallization temperature, including ELM driven temperature excursions (see 2.2.6), may ultimately place tighter controls on the allowed power flux densities in the high performance phases.

ELM interactions with the main wall have not received the same level of scrutiny as the divertor interactions. On ITER, however, their effects on erosion can be significant under certain conditions, due notably to the much lower melting temperature of Be compared with W. Depending on the characteristics of the ELM filaments, SOL transport and the design of the magnetic equilibrium (e.g. [Kocan, 2015]), which determines the fraction of ELM energy reaching the walls, significant melting could occur in the secondary X-point region for large ΔW_{ELM}. This is not expected to be a problem until burning plasma operation [Loarte, 2008], though the detailed calculations of gap loading, which have been performed for the divertor, have not yet been attempted for castellations on the first wall. Even if some degree of Be tile gap melting does occur, it is expected to be less problematic, due both to the higher tolerance of the plasma to Be impurity and to the fact that stationary handling of power fluxes on the blanket first wall is not as critical as for the divertor.

2.2.4 Ammonia formation during N_2 seeding

Ammonia (NH_3) can be formed in tokamaks when nitrogen is seeded into the SOL/divertor plasma to reduce divertor heat fluxes. Experiments in the all-metal JET and ASDEX-Upgrade tokamaks have shown that a few percent (up to 8% in AUG [Neuwirth, 2012]) of the injected nitrogen is converted into ammonia. Tritiated ammonia is efficiently retained on the active charcoal used in the ITER cryopumps; it can only be recovered with full regeneration of the cryopumps. The tritium inventory on the cryopumps cannot exceed 180 g and regular regenerations (to ~100 K) will be performed during operations to recover the pumped hydrogenic species, a process which requires ~600 s, but which would not allow for ammonia recovery. Regenerations at higher temperature, whilst of course possible, are very time-consuming (about 6 hr per pump, 6 pumps in ITER) and therefore significant ammonia production could strongly affect the ITER duty cycle. The formation of tritiated ammonia also has an impact on the design of the tritium plant which needs to be able to decompose ammonia to recover tritium and at the same time avoid the formation of deleterious nitrogen oxides.

While it is clear that ammonia formation proceeds through surface reactions between nitrogen and hydrogenic radicals [ITER_D_QFF9XY, 2015], it is currently unclear whether these reactions proceed on plasma-exposed or plasma-shadowed areas and it is, therefore, currently not possible to predict the ammonia formation rates to be expected in ITER. Experimental activities are ongoing in tokamaks and laboratory devices to elucidate the formation process of ammonia under fusion-relevant conditions and to determine the reaction rates of the elementary steps involved. Continuation of this effort is required to allow the inclusion of the relevant nitrogen chemistry in fluid plasma-boundary codes.

2.2.5 Differences in medium-Z impurity seeding (N_2 vs Ne)

With the emergence of major tokamak experiments with all-metal walls in recent years (notably JET and ASDEX-Upgrade), it has become increasingly obvious that the plasma performance found in highly radiative scenarios with all-carbon PFCs is not always easy to reproduce when extrinsic seeding is used to replace the natural carbon impurity for divertor power flux control.

Nitrogen seeding provides the best performance with respect to older results in an all-carbon environment – not surprising considering the proximity of the radiation functions between C and N. As discussed in 2.2.4, however, the formation of tritiated ammonia during nitrogen injection is

likely to be an issue for ITER, mostly in the sense of a limitation on the achievable duty cycle. Neon would thus be a preferable alternative, with the added benefit that being a fully recycling gas naturally extends the timescales for avoidance of divertor monoblock overheating in the event of loss of seeding or other divertor reattachment events. This said, recent results from dedicated experiments on JET indicate that saturation of wall surfaces with nitrogen can result in rather long timescales for loss of detachment in the event that seeding gas is removed.

There is a fundamental difference between ITER and machines such as ASDEX-Upgrade and JET in the sense that machine size, magnetic field and achievable pedestal temperatures are insufficient to provide the combination of high divertor compression and low main chamber radiation for Ne in present devices. Experiments find in general [Bernert, 2017; Giroud, 2014] that radiation in N_2-seeded plasmas occurs preferentially in the divertor, whilst with Ne, for the same fuelling rates, main chamber radiation increases and there is little or no increase in divertor radiation. The increased main chamber radiation lowers the power crossing the separatrix and affects ELM frequencies. In addition, pedestal transport is modified by the presence of impurities. Nitrogen tends to increase pedestal top temperatures and hence confinement in both devices, whilst Ne injection increases the pedestal top density in ASDEX-Upgrade and reduces the pedestal pressure significantly on JET. In both devices, Ne injection beyond a certain level leads to an unstable situation.

In ASDEX-Upgrade, the decrease in ELM frequency reduces the effect of ELM impurity flushing and the increased pedestal density gradient enhances both Ne and W inward transport in-between ELMs, further enhancing core radiation losses [Bernert, 2017]. Both effects, together with the fact that Ne does not allow a reduction in divertor power loads by increased SOL/divertor radiation, mean that power exhaust with Ne appears difficult to study in ASDEX-Upgrade, even though the device is operating at values of P_{sep}/R close to those expected in burning plasmas on ITER. In JET, with values of P_{sep}/R currently about a factor of 2 lower than on ASDEX-Upgrade, Ne tends to reduce the power flow across the separatrix, provoking H-L back transitions, making a proper comparison between N and Ne difficult until more heating power is available [Bernert, 2017; Giroud, 2014].

These results may be contrasted with those found on radiative divertor experiments on Alcator C-Mod with molybdenum PFCs at high magnetic field [Loarte, 2011], in which for both N_2 and Ne seeding in EDA modes, partially detached divertor conditions were achieved at normalized confinement, H_{98} ~1 with edge power flows only marginally above the H-mode threshold power (by factors of 1 – 1.4), as in ITER. Here, as in the JET and ASDEX-Upgrade experiments, at high radiative fractions, the radiation is observed to occur mostly in the X-point region, with some incursion onto flux surfaces just inside the separatrix. Apparently, in C-Mod, this was insufficient to strongly affect the pedestal top, even in the case of Ne.

It is extremely difficult at present to confidently extrapolate the findings on current devices to ITER with respect to performance with low-Z impurity seeding. Simulations with SOLPS for burning plasma conditions [Pitts, 2015] show that for equivalent SOL power flow, ITER will compress both Ne and N strongly in the divertor, in the strike point regions, albeit with the Ne radiation distributed over a slightly more extended volume. Similar partially detached conditions are achieved, though different seeding rates are of course required in both cases. Integrated modelling using the boundary plasma scaling approach (see [Pacher, 2015] and Appendix C) has been applied to show that both N_2 and Ne provide adequate burning plasma operational windows, with N_2 marginally better due to slightly lower core radiation in comparison with Ne. However, more work is required here to

improve the integrated model and to extend the N_2 seeded boundary cases which are so far limited in scope (Ne seeding has traditionally been the favoured approach at ITER for power flux control).

In the end, it is likely that the large physical size of ITER and the much higher expected pedestal/separatrix temperatures in comparison with current machines mean that the differences being found today between N_2 and Ne will disappear at the ITER scale. Higher pedestal/separatrix temperature means lower Ne radiation in the core plasma. In the SOL/divertor, mean-free paths for ionization of neutral Ne are larger than for N and the relative importance of thermal and friction forces differ for the two species, with the net parallel force in the divertor being lower for Ne than N. Both effects drive lower divertor impurity enrichment for Ne, but the differences are likely to be much reduced with increasing device size.

Both experimentally and theoretically, the issue of low-Z impurity seeding is an area of very active research and significant advances can be expected in the coming years. It will be of particular importance to demonstrate, if possible, scenarios in which ELM control is properly integrated with extrinsic seeding for power flux control at high performance. Further experiments on JET, at the highest possible input power and current for which pedestal temperatures will be closest to those expected in ITER, have the best chance of reducing the gap to ITER in terms of operating conditions (size, performance) by the comparison of the efficiency of N_2 and Ne seeding with regard to divertor power flux control compatible with acceptable core plasma performance.

2.2.6 Tungsten-related material issues

One of the frequently mentioned advantages of tungsten as a plasma-facing material is its high melting point. Much lower temperatures are, however, required for recrystallization/grain growth to occur, resulting in strong changes in the material mechanical properties and, in particular, a reduction in strength/hardness, and shock resistance despite an increase in ductility. Appearance of macro-cracks on W during high heat flux testing at 20 MWm^{-2} is indeed attributed to exhaustion of ductility of the recrystallized W - the temperature being high enough for recrystallization to occur. To avoid the deleterious effects associated with recrystallization, an operational budget will need to be defined accounting for the time/temperature dependence of the recrystallization process (see Appendix C). Little is known about the recrystallization kinetics of the actual W to be used for the ITER divertor, and more information will be required to consolidate the actual operational budget.

Even if bulk recrystallization is avoided, significant surface damage can be caused by ELMs. Surface roughening/cracking/melting can occur depending on the ELM energy density. The evolution of the surface damage and its dependence on the base material temperature, the energy density and the pulse number has been extensively studied in electron-beam facilities and using powerful pulsed plasma and/or laser systems (see for example [Wirtz, 2017]). Most of these investigations have been performed on pristine material and in the absence of any particle irradiation.

Some studies have revealed the existence of synergetic effects for combined particle/heat loading where the general tendency shows a lower damage threshold for a plasma-exposed surface. A big unknown for ITER is whether and how these effects might affect the material compatibility with high performance plasmas. In particular, it is at present impossible to define a tolerable level of damage before deteriorated material properties would start to impact plasma performance due to enhanced tungsten release or reduced power handling capabilities. This is clearly an area where further research is needed before the start of ITER operations.

The effect of long-term stationary and transient plasma exposure (be it H, D or He) on the thermo-mechanical properties of W clearly remains an important topic where little information is available,

although indications exist for the modifications of material properties following plasma exposure. Extrapolation of these observations to the very high fluence expected in ITER is currently too uncertain. A proper assessment of the impact for ITER requires that these effects are accounted for in the modelling of the thermo-mechanical response of the material (as performed in [Panayotis, 2017] for example) and in turn would require knowledge of the evolution of material properties with plasma fluence (ultimate strength, toughness, thermal conductivity, etc.).

2.2.7 Castellation gap heat loads

Since the last major version of the IRP, a great deal of progress has been made on the divertor design, including the elimination, in 2011, of the first carbon/tungsten divertor from the ITER operational plans [Pitts, 2013]. This decision required an acceleration of the design work for the full-W version, which must now be in place for PFPO-1 and must guarantee operation well into the FPO phases (see 4.4 for more on the lifetime requirements and possible divertor upgrades).

One important design area that had not been addressed for the full-W divertor was the question of W monoblock shaping. Due to the high stationary power flux densities of which ITER will be capable, and the potential for significant transient energy densities, melting at leading edges across gaps between neighbouring monoblocks that arise from manufacturing and assembly tolerances becomes a real issue for component lifetime in the case of metal divertor targets. As a result of several years of design and physics studies (see e.g. [Pitts, 2017; Gunn, 2017; Gunn, 2016; Hirai, 2018]), the final PFC shaping is now essentially decided, for both the high heat flux and baffle regions of the vertical targets. What these physics studies have highlighted is the very complex nature of plasma interactions in the vicinity of gaps between PFCs; when the magnetic field and divertor geometries and ion Larmor orbits are properly accounted for, gap edges (running in both poloidal and toroidal directions) can be accessed by plasma ions when otherwise they would normally be magnetically shadowed under a pure optical approximation. This is particularly true during ELM transients, when energetic ions arrive at the divertor targets.

Sophisticated monoblock surface shaping; for example, the very complex, high precision machining applied to the individual components in the JET bulk W outer divertor target [Mertens, 2011] is not a realistic option for the ITER divertor design. The reference ITER design is a simple toroidal bevel to protect misalignment of toroidally adjacent monoblocks in the high heat flux areas [Pitts, 2017]. This will not protect loading of gaps running in the toroidal direction between poloidally neighbouring blocks. However, as discussed in Appendix C, any applied shaping reduces the allowed parallel power flux density which can be intercepted by the component; for the particular case of ITER, the current baseline toroidal bevel reduces the allowable stationary heat flux density by ~40% compared to a non-shaped solution and places strong limits on the allowed stored energy loss per ELM for the avoidance of toroidal gap edge melting. Toroidal gaps can be protected with the addition of a further poloidal bevel, but this only works at the outer target in ITER and will add a further penalty on the allowed stationary parallel heat flux densities.

The many thousands of gap edges in the ITER divertor mean that careful attention will have to be paid to power loading as performance improves during operations. Gap edge loading occurs on the Larmor radius scale, typically on the order of a few hundred microns, so that only the high resolution divertor IR systems viewing a small region of the vertical targets at single toroidal locations will be appropriate for the detection of these interactions. The lower resolution, machine protection IR systems will, however, be capable of detecting the stationary top surface loading on a substantial fraction of the individual monoblocks in the strike point areas. Although the ITER divertor design requirements have stimulated a good deal of recent R&D on current devices to study leading edge and gap interactions, this work should continue, in particular aiming to directly verify

the existence of ELM driven ion orbit loading. In this context, it is also important to continue theoretical studies of ELM evolution and transport to provide greater confidence in the specifications for particle energies and time envelopes used to derive the required ITER monoblock shaping.

2.2.8 Radio-Frequency-assisted wall conditioning techniques

The fact that the toroidal magnetic field, generated by superconducting magnets, will be continuously maintained during ITER operational periods, drastically reduces the efficiency of DC glow discharges. Ion Cyclotron Wall Conditioning (ICWC), operable in the presence of the toroidal field, is therefore foreseen for fuel and impurity removal between plasma pulses. This will also contribute to the mitigation of the tritium inventory build-up in the machine in the FPO campaigns. In case of unavailability of the ICRF system in PFPO-1, Electron Cyclotron Wall Conditioning (ECWC), also compatible with B_t, could be employed. Both methods use the conventional heating antennas to produce low temperature magnetized discharges. In ICWC, coupling of the power to the discharge results principally from collisional absorption of the radio-frequency (RF) energy by the electrons (non-resonant coupling), and the discharges can therefore be produced at any B_t. ICWC discharges present poloidal and radial non-uniformities inherent to RF wave absorption schemes. Operation in monopole phasing and/or mode conversion schemes [Lyssoivan, 2012] have improved discharge homogeneity and optimized wall coverage. ICWC is expected to require 1–5 MW of power in ITER with a duty cycle 1 s on/30 s off to make a He, H or D plasma with $n_e \sim 10^{17}$–10^{18} m^{-3} and $T_e \sim 5$–10 eV [Douai, 2011].

ECWC discharges can only be produced in the presence of the Electron Cyclotron Resonance layer (ECR) inside the vacuum vessel. As in ICWC, but to a greater extent, localized power absorption and high density in ECWC plasmas ($n_e \sim 10^{18}$-10^{19} m^{-3}) can affect discharge uniformity and cleaning efficiency, though pulsed operation is used to mitigate the latter effect. However, the technique suffers from low absorption per pass in the optically thin ECWC plasma, even at the fundamental of the ECR frequency, leading to the risk of exposing PFCs or diagnostics to excessive stray radiation. The ECWC operational parameters (pressure, power) should, however, be very similar to those of the ECRH-assisted breakdown foreseen in ITER. ECWC may require 1–10 MW at 170 GHz, with a duty cycle similar to that of ICWC.

In both techniques, using H or D as working gas the main flux to the wall is that of isotropic neutral hydrogenic species, either desorbed from wall surfaces [Douai, 2011] or resulting from molecular dissociation. The ion flux parallel to the magnetic field lines is largest on limiting surfaces, reaching typically 10^{21} ions $m^{-2}s^{-1}$, and decreases exponentially in the plasma edge until a few 10^{19} ions $m^{-2}s^{-1}$ [Lyssoivan, 2012]. For comparison, ion fluxes in a GDC plasma are typically 2-4 orders of magnitude lower (~10^{17} ions·$m^{-2}s^{-1}$) [Kogut, 2015]. In ICWC, fast charge exchange neutrals can in addition be produced, with temperatures above 1 keV and energies up to 50 keV. The large penetration depths of these particles into sub-surfaces (up to 200 nm in Be) makes them particularly attractive for T-removal.

ICWC is routinely applied between shots in the KSTAR tokamak for impurity removal [Kwon, 2011], but it is mainly considered for ITER as an efficient option to mitigate the T inventory build-up. Present extrapolations from current devices to ITER, in particular results from experiments in JET with ITER-like wall (JET-ILW) (operated with walls at 200°C), indicate that ICWC could remove up to ~0.35–0.6 g of T between plasma shots, i.e. an amount comparable to the estimated retention per pulse [Brezinsek, 2013-1; Shimada, 2011]. Experimental and modelling data [Kogut, 2016], however, show that surface temperature has a non-negligible impact on the isotopic

exchange efficiency. New experiments in the JET at lower wall temperatures (ICWC will be operated at 70°C in ITER) would therefore appear to be particularly relevant in this respect.

The efficiency of ECWC with metallic PFCs is less well documented. Recovery from disruptions with ECWC only has been successfully demonstrated on JT60-U [Itami, 2009]. Even in devices with carbon PFCs, the scarce published data on fuel removal in the literature indicates a lower efficiency than ICWC [Douai, 2016].

2.2.9 Divertor detachment control

The control of divertor power loading will be one of the most critical aspects of ITER operation and will need to be robust and reliable. Although the W divertor monoblock technology, which ITER will use on the vertical targets, is the most advanced currently available and can operate with steady state surface loads of ~10 MWm^{-2}, even relatively short durations above this value must be limited if recrystallization is to be avoided (see Appendix C and section 2.2.6). Stronger excursions, resulting in global surface melting in quasi steady state (namely on timescales significantly longer than ELM or disruption transients), will have severe consequences for surface topological deformation and must be absolutely prevented. The ultimate limit (defined by the achievement of the critical heat flux at the cooling interface [Escourbiac, 2016]), if sustained for long enough (of the order of a few seconds), can lead to a water leak requiring immediate and lengthy in-vessel intervention and the replacement of an entire divertor cassette. Although the heat flux densities required for this to occur can only be achieved during burning plasma operation at high current when SOL input powers are sufficiently high, Appendix C demonstrates that heat flux control may already be necessary during operation in PFPO-2, when P_{SOL} may attain values >40 MW. It will in any case be mandatory to develop and routinely deploy detachment control in the pre-nuclear operational phases before the introduction of D and T and the activation of components.

It is only relatively recently that power flux control has begun to be seriously developed in current devices, where the use of W divertor targets, invariably inertially cooled (e.g. ASDEX-Upgrade and JET), means that without it high power operation is not possible, even for relatively short pulse durations on the order of seconds. With several medium-sized superconducting divertor devices now in operation, of which two (EAST and WEST) use actively cooled W divertors and a third (KSTAR) has plans to upgrade to full-W actively cooled components by 2021, progress in controlling heat loads can be expected to become much more widespread.

To date, the most robust detachment controller has been that developed on ASDEX-Upgrade, where the current from an outer target shunt (with appropriate real time processing to remove ELM spikes) is used to measure the thermoelectric current into the outer divertor, which, because the inner target T_e is always very low between ELMs, is a good approximation to the outer target T_e and hence a measure of detachment state [Kallenbach, 2010]. The signal is used inside a PI controller to determine the impurity gas puffing rate required to achieve a given set divertor T_e. The system works routinely with nitrogen, which is well compressed in the ASDEX-Upgrade divertor (see 2.2.5) and is thus a direct actuator for divertor radiation. More recently, a real time double radiative feedback technique has been developed on ASDEX-Upgrade to simultaneously control injection of a main chamber radiator (Ar) and N in the divertor [Kallenbach, 2012]. Here a subset of 3 foil bolometer channels are used in the main chamber together with a fourth in the outer divertor leg, or in conjunction with the thermoelectric current controller. Other tokamaks have previously tried feedback on bolometer chords (e.g. [Goetz, 1999; Asakura, 2009]). A real time nitrogen feedback control technique has also been tested in JET using the degree of detachment obtained from ELM-filtered outer target Langmuir probe ion current densities [Guillemaut, 2017]. An earlier seeding control attempt on JET used a VUV nitrogen line [Maddison, 2011].

Unfortunately, owing to the complex structure of the water-cooled monoblock plasma-facing units, divertor shunts cannot be incorporated into the ITER divertor targets and thus power flux control methods must be developed based on the sensors which will be available. As well as an extensive array of bolometer channels in both main chamber and divertor, ITER will be equipped with comprehensive IR thermography, covering ~90% of the high heat flux areas of the divertor target. The spatial resolution will be rather coarse (for example on the scale of a single monoblock) in many regions, but since divertor target loading is rather toroidally symmetric in comparison with the first wall, the zones with highest spatial resolution can be preferentially chosen. However, IR surface power measurements have not to date been used for heat flux control in tokamaks, which means that the community has not yet developed a feedback scheme on the key parameter of interest for ITER: the surface heat flux density. There are issues associated with measuring power fluxes in detaching/recombining divertor plasmas (e.g. intense bremsstrahlung radiation in the IR band, strong reflections in metallic environments) and with the reliability of IR cameras operating in the 3-5 μm band. Research has typically focused on more robust, simpler and usually indirect techniques, such as the feedback on bolometer channels mentioned above. Nevertheless, the extensive IR coverage of the divertor being installed for ITER means that efforts should be intensified in the R&D Community to demonstrate that real time, IR-based target heat flux control is possible for metallic components in a highly dissipative (and hence radiative) regime, and to properly assess the limitations and/or find appropriate workarounds. Some effort on the development of a real time capable IR system has begun at ASDEX-Upgrade [Sieglin, 2015] and is expected to be tested in the near future.

Additional sensors with which ITER will be equipped and which may form part of detachment control loops are the arrays of divertor Langmuir probes and thermocouples attached to monoblocks in several toroidal locations. Since divertor neutral pressure is a key parameter in determining the degree of detachment, it is also possible that the ASDEX-type fast neutral pressure gauges that will be installed at various locations in several ITER divertor cassettes could eventually be used in a control loop. Nevertheless, issues of lifetime are important here: in-vessel diagnostics attached to divertor targets and requiring extensive electrical cabling to connect them with elements outside the vessel may not survive long enough to be considered as robust for heat flux control in the nuclear phases, when it will be needed routinely and during which operating conditions in the divertor will be the most severe.

2.2.10 PWI/plasma boundary code validation

In addition to the experimental efforts mentioned above, it is important that by the time ITER operation starts, the modelling tools in use within the community for plasma-wall interaction and plasma boundary physics studies in ITER-relevant regimes have reached a sufficient level of maturity and validation against experiments, including cross-benchmarking demonstrations [Wiesen, 2017]. Although it could be said that 2-D edge plasma fluid codes have, for the most part, already reached this level of maturity (e.g. [Kukushkin, 2011]), some questions remain about the difficulties that many such codes encounter when attempting to reproduce features such as electric fields [Chankin, 2007] and plasma flows in the SOL [Asakura, 2007], or the inclusion of drifts at the ITER scale. It is believed that many of these shortcomings are a result of the implicit Maxwellian fluid assumption used for the plasma description in these codes and could only be addressed by explicitly including plasma kinetic effects [Stacey, 2016]. Purely kinetic approaches [Takizuka, 2017], however, require enormous computer resources to provide results at the ITER scale.

Although it is expected that computing speeds will continue to increase in the coming years, it is often the case that any improvement in computer performance is balanced by further refinements of the physics model in the codes, keeping the run-times roughly constant. However, during ITER operation, there will be a strong need for a fast and reliable plasma edge solver, coupled to a suitable core model, which can be used for online analysis and preparation of ITER discharges. Fully consistent core-edge coupling models, however, are only now beginning to be established [Falchetto, 2014]. Moreover, the use, for example, of magnetic perturbations for ELM mitigation ultimately requires a 3-D description of the ITER boundary plasma. Current tools [Feng, 2017] still struggle to reach the highly dissipative regime present in the partially detached ITER divertor plasma, and significant effort will need to be devoted to overcome this hurdle. Conventional (i.e. non-turbulent) transport codes will also need to find a way to properly incorporate a turbulence ansatz [Rognlien, 2004] to obtain, for example, a more realistic description of the blobby intermittent transport which is experimentally known to dominate far SOL transport and, therefore, governs the particle and heat loads received by the main chamber walls. With a correct description of the fluxes reaching the walls, either through 2-D or 3-D models covering the entire vacuum vessel volume, more precise modelling of wall material migration, redeposition patterns and fuel retention in the plasma-facing components will become possible [Baelmans, 2011].

A great deal of development has taken place in the area of material migration modelling to understand erosion/deposition effects and to improve the accuracy of fuel retention estimates. Two types of approaches have been followed to study either local effects [Borodin, 2011] at the level of a given component or a given region of the machine, or global poloidally-resolved migration [Schmid, 2015]. The former approach allows the 3-D geometry of the ITER first wall panels (FWP) and, therefore the effect of component shaping on local material redistribution, to be accounted for. The latter approach has been shown to successfully reproduce the retention rates measured by gas balance in JET and the campaign averaged erosion/deposition pattern. The same modelling, when applied to ITER, shows that co-deposition of T with Be could occur predominantly either in the divertor or on the first wall itself, depending on the nature of the far-SOL plasma profiles. Three dimensional effects could play a strong role here given the highly shaped and conformal ITER first wall. The development of global 3-D material migration models would therefore allow a better description of erosion/deposition processes in ITER. This, in turn, clearly links to the development of 3-D boundary SOL codes mentioned above which can provide the plasma background used to study impurity generation and transport.

Migration modelling aims at describing where eroded particles deposit in the vessel and how much tritium is trapped in the resulting deposited layers, particularly in the case of ITER which will use a low-Z first wall with low erosion energy threshold for ion impact. One-dimensional diffusion/trapping models have been used [De Temmerman, 2017] to study the efficiency of tritium removal from co-deposits during PFC bake-out. The 1-D approach does not permit a consistent model describing the full outgassing process in which different regions of the machine are heated up to different temperatures (240^{o} C for the first wall and 350^{o} C for the divertor are considered for ITER) or the fact that the tritium retention in co-deposits will be strongly spatially dependent on the local co-deposition conditions [De Temmerman, 2008]. A possibility to tackle this issue is through the coupling of a diffusion/trapping model to the above-mentioned migration codes.

The area of plasma-material interactions represent a particular challenge for modelling because of the large span of temporal and spatial scales involved in the full process. Going from the atomistic scale of the ion/surface interaction processes (and resulting defect creation, trapping, diffusion, etc.) to the impact of these processes on the mechanical properties of the plasma-facing material, (i.e. being able to predict how the material thermal and mechanical properties will evolve with time

during operations), requires the development of multi-scale models which currently do not exist and are far out of reach. Some efforts are ongoing to bridge different scales and describe the interactions of hydrogen and helium isotopes with tungsten surfaces and the initial stages of morphology changes that they induce [Lu, 2014; Wirth, 2015], but a substantial expansion of these efforts will be required. The significant advances taking place in parallel on the experimental side such as the use of micro-mechanical measurements and the development of in-situ diagnostic systems will help by providing data to validate multi-scale models as they are being developed. All of these activities will need to be coupled together [Brooks, 2014] and embedded in the ITER integrated modelling framework, IMAS (Integrated Modelling and Analysis Suite [Imbeaux, 2015; Pinches, 2016]) in order to build reliable workflows able to provide a consistent picture of the ITER plasma and surrounding plasma facing components conditions.

2.3 Plasma Disruption Management

Plasma disruptions can cause substantial heat loads to the divertor and the first wall, high electro-magnetic loads on in-vessel components and on the vacuum vessel itself, and they may also lead to the formation of runaway electrons (REs) that can potentially cause water leaks due to the very localized deposition of energy on first wall panels or plasma-facing components (PFCs) of the divertor. Operation of ITER will have to strongly focus on avoiding disruptions with a high success rate and on mitigating those in which avoidance techniques fail [de Vries, 2016-02; Lehnen, 2016; Hollmann, 2015; Lehnen, 2015-1]. The Research Plan takes this requirement into account and significant operational time for commissioning and optimizing the disruption mitigation system and for establishing appropriate disruption forecasting and avoidance techniques and schemes, linked closely to basic and advanced control systems, is reserved in all three operational phases, PFPO-1/-2 and FPO. This research is explained in greater detail in the following sections. When possible, the Research Plan aims to commission each system one operational period before it will be needed. Figure 2.3-1 shows the various limits for melting of PFCs and for electro-magnetic loads during disruptions in ITER. It also indicates the potential maximum energy at various plasma currents that can be deposited by REs in case of full magnetic energy conversion, which is the most pessimistic scenario. The assessment of thresholds for PFC melting or for a possible failure of cooling channels after runaway impact is an ongoing R&D activity. Present predictions of these thresholds have large ranges due to uncertainties in the affected surface area. However, the foreseen energies at a plasma current I_p = 7.5 MA are presently expected to be sufficient to cause water leaks. It is important to note that within the green area in Figure 2.3-1, in which no PFC melting is predicted to occur, runaway electrons (RE) formation is not expected for unmitigated disruptions in the non-active phase of operation. In these conditions no influx of radiating impurities is expected to take place (moderate beryllium influxes are not expected to cool down the plasma significantly) so that high electric fields during the current quench will not develop and, in addition, no seed REs from tritium or Compton scattering are present in these plasmas. When mitigating disruptions, it is the role of the disruption mitigation system (DMS) to ensure RE avoidance by an appropriate choice of the injected species and quantity.

Given the high impact of disruptions on component lifetime and machine availability, an appropriate management scheme has to be in place to allow the timely achievement of the objectives of the ITER Research Plan. The disruption loads and their consequences determine the allowable disruption rates (and consequently the necessary avoidance rates) and mitigation success rates for the various phases of operation with increasing thermal and magnetic energies towards the Q=10 baseline scenario. To define these rates, a disruption budget consumption (DBC) that represents the ‘costs’ of a disruption at a specific magnetic and thermal energy is introduced

[Lehnen, 2016]. This DBC can be attributed to any disruption impact that is cumulative or for which an occurrence probability can be defined. Specifying the DBC values with a good physics basis is a prerequisite for establishing a reliable strategy for disruption management. Improving the physics basis for the definition of the DBC is a continuous process and, especially during operation, the forecast and the accounting of the DBC will have to be updated based both on the post-disruption assessment of the actual impact that occurred and on scalings for disruption loads that will be established. This careful accounting will allow identifying deviations from the planned budget consumption and – if required – to react accordingly by adjusting the operational plan. It is important to also note that mitigated disruptions can cause accumulation of the DBC for example through radiation flash heating of first wall components or through consumption of fatigue lifetime of in-vessel components. A main risk for the execution of the research plan is the accidental generation of runaway electrons during disruption mitigation. Since extrapolation from a certain plasma current level to the next has high uncertainties, runaway avoidance during disruption mitigation has to be carefully validated throughout the approach towards 15 MA operation.

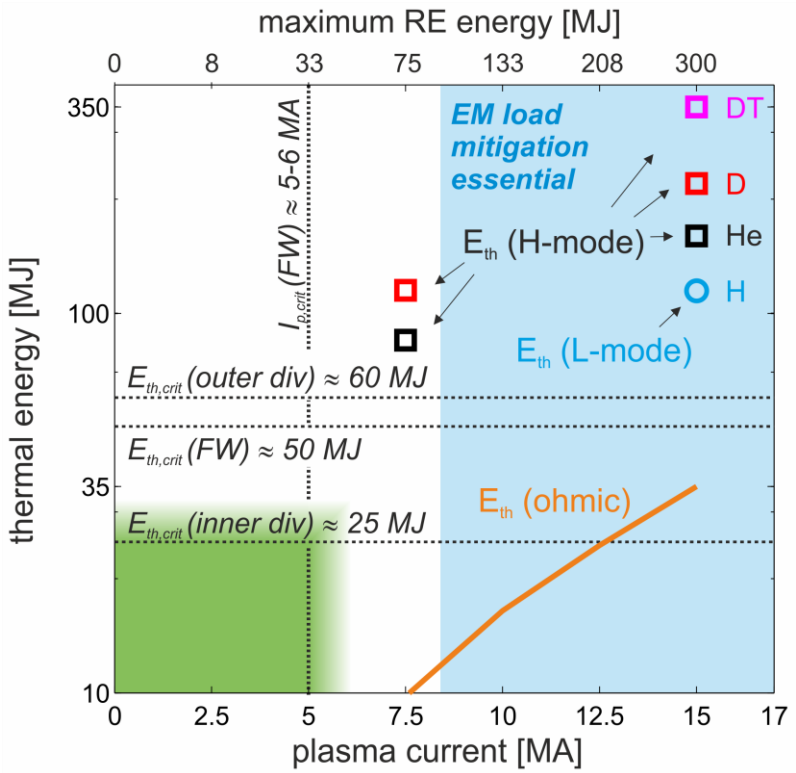

Figure 2.3-1: Operational range of ITER in terms of thermal energy and plasma current. Thermal load limits during the thermal quench are indicated by horizontal dotted lines and during the current quench by the vertical dotted line. At high plasma currents, it is at present assumed that cat. III halo currents will occur if electro magnetic (EM) load mitigation is not activated. The green area indicates the parameter range for which melt damage from unmitigated disruptions is not expected. The symbols indicate the target values for the planned operational scenarios. Operation at high current without auxiliary heating is not planned, but energies would already exceed melt limits under such conditions (orange line). The RE energy shown along the top axis is the maximum possible deposited energy for a given plasma current assuming full conversion of the magnetic energy to kinetic energy.

The maximum downtime after activation of the DMS is defined to be 3 hours. Although the highest priority is on mitigating the direct consequences of a disruption, the optimization of the DMS has also to take into account the impact of the mitigation action on the pulse rate and possibly also on

the performance of the subsequent pulse. Therefore disruption rates – and also mitigation rates in the early phase of operation – will have to be limited, but also the injected species and quantities have to be optimized to be not unnecessarily excessive, which would cause delays due to longer vessel pump-out times. Early verification of the impact of high material injection quantities on vacuum systems like cryopumps and gas handling systems is mandatory. This can be mainly done without plasma operation. Conditioning after DMS activation may be needed to remove residual impurities in the first wall, neutral beam injection (NBI) beam duct, etc. At present no quantitative analysis of this effect is available. In case of unmitigated disruptions, a robust conditioning pulse might be required in case of degradation of the first wall or divertor conditions to support high performance plasma operation through for example material splashing. These losses of operational time have to be taken into account and will also contribute to defining targets for disruption rates. This will also require reducing the number of mitigated disruptions in plasma parameter ranges for which no damage on PFCs is expected. Moreover, it will have to be considered when setting targets for the false alarm rates of the disruption predictor.

2.4 First Plasma

The operational activities surrounding the production of First Plasma in ITER, targeted within the Staged Approach for December 2025, consist of 3 main phases: Integrated Commissioning, First Plasma and Engineering Operation.

2.4.1 Integrated Commissioning

As installation of the various ITER plant and auxiliary systems is completed, each of the systems will undergo instrumentation and control (I&C) integration with ITER CODAC and system commissioning. This should ensure that each system satisfies those design requirements that can be tested in the absence of plasma in advance of their integration into the tokamak operations framework. Following completion of the construction of the tokamak core, scheduled for late 2024, a first period of Integrated Commissioning, lasting ~12 months, will occur, with the achievement of high vacuum conditions in the vacuum vessel, cooling of the superconducting magnets and demonstration of a significant level of performance, together with the commissioning of all major tokamak subsystems required to support plasma operation. A schematic of the sequence of events and estimates of time required for the various commissioning activities in shown in Figure 2.4-1.

Although a preliminary flow and planning for Integrated Commissioning have been prepared within the framework of earlier schedule exercises, a new activity has been launched to develop an up-to-date analysis of this phase of operations in order to develop improved estimates of the time required for completion of the various activities within this period and to confirm the detailed sequence of activities. The major activities determining the critical path through Integrated Commissioning are illustrated in the figure: the vacuum vessel and cryostat enclosures are evacuated and then leak detection is made at room temperature; after circulating, filtering and heating the water, the vacuum vessel and all in-vessel components are baked at high temperature and a second leak detection is performed; cooling of the superconducting coils to cryogenic temperatures and then energizing and charging of the coils are performed to approximately 50% of their maximum current – this involves extensive operation of the coils individually and then as an integrated system, together with commissioning of the protection systems. Finally glow discharge cleaning of the vacuum components is carried out to the extent necessary to achieve reliable plasma operation.

Integrated commissioning of control and auxiliary systems required for First Plasma is also performed during this period. The Gas Injection System (GIS) is likely to be the first auxiliary

system to undergo integrated commissioning, since it will be used during glow discharge cleaning of the vacuum vessel. Following offline commissioning of the ECRH power sources and transmission lines, the ECRH system will be integrated into the operational systems and short-pulse injection (up to 100 ms) will be used to condition one upper launcher. A subset of Diagnostics have been identified as essential for First Plasma (see Table H-1) and these must be fully commissioned to be ready to take data during the First Plasma campaign – the magnetics diagnostic will be critical to the implementation of this campaign and calibration and measurement consistency tests during this period will be an essential activity. The Plasma Control System, Central Interlock System and Central Safety System will also undergo integrated testing under CODAC during this period (PCS control of the poloidal field (PF) and central solenoid (CS) currents will be implemented during Magnet commissioning).

The culmination of the Integrated Commissioning activity would be a ‘dress rehearsal’ for plasma operation of the tokamak, in which all tokamak, plant and auxiliary systems are operated under CODAC control and satisfy the respective requirements for plasma operation.

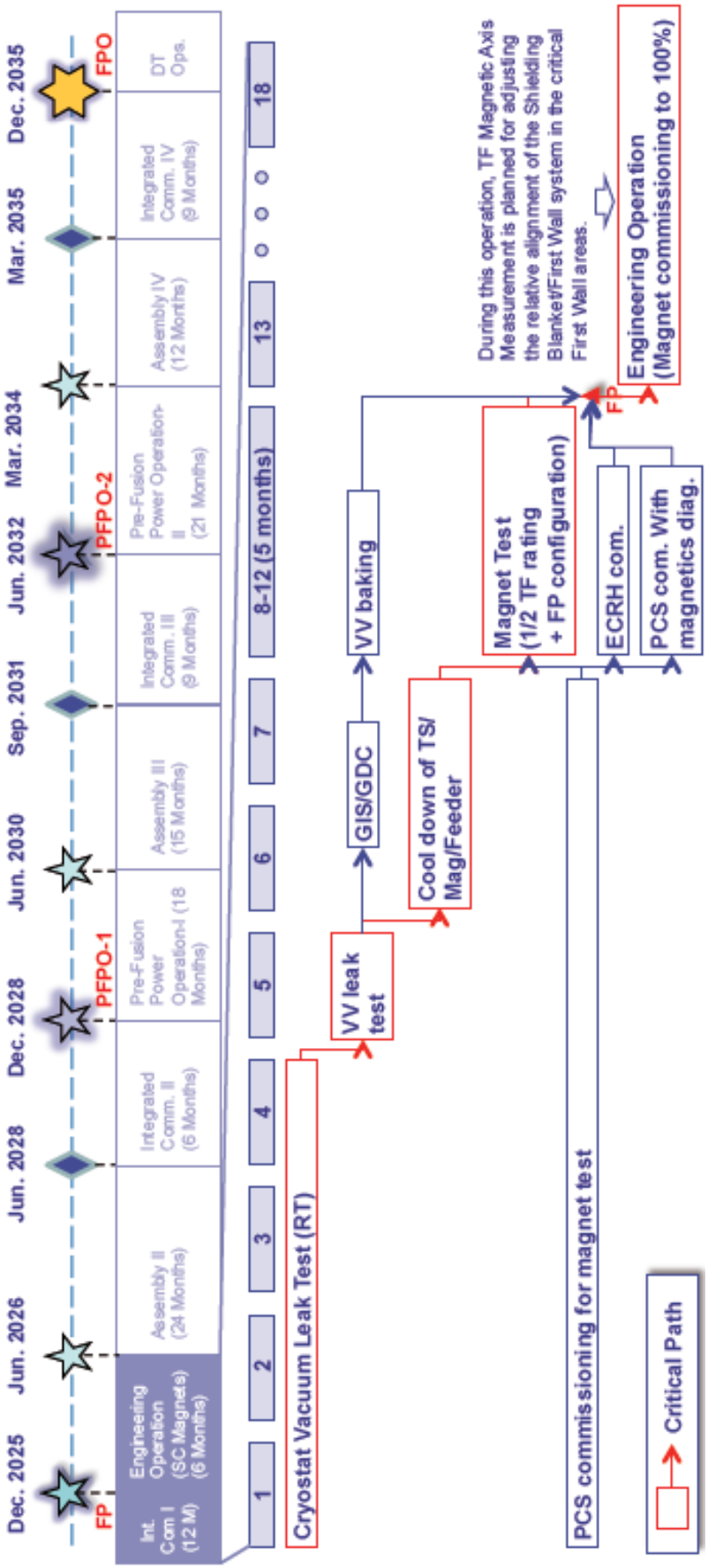

Figure 2.4-1: Schematic of the sequence of events during:

Integrated Commissioning

First Plasma

Engineering Operation

2.4.2 First Plasma

First Plasma remains, in essence, a demonstration of the successful integration of the tokamak core and principal plant systems (magnets, power supplies, cooling, cryogenics, vacuum, etc.) and is the conclusion of the first phase of integrated commissioning of the ITER facility. The achievement of First Plasma constitutes a demonstration that all core tokamak systems (i.e. excluding in-vessel components) have been commissioned successfully and that the device is capable of achieving plasma operation. During the First Plasma campaign, none of the main in-vessel components will be installed, in particular no blanket/first wall modules or divertor cassettes. Therefore, the vacuum vessel, in-vessel wiring, diagnostics and other installed in-vessel components will be protected by the First Plasma Protection Components (FPPC), consisting principally of 4 poloidal limiters, most likely with a stainless-steel PFC, capable of supporting 1 MA plasmas at 2.65 T (see, e.g., [ITER_D_T7KUNB, 2016]). The FPPC also include a divertor replacement structure that protects the bottom of the vessel, preventing plasma from reaching the divertor region.

Most of the Magnetic diagnostics will be installed for First Plasma, together with a subset of diagnostics required for the demonstration of plasma operation. This would include, in particular, H_α monitors, several IR camera lines of site, impurity monitors and hard X-ray monitor for detection of runaway electrons. Table 2-2 lists the minimum measurement requirements established for First Plasma and Engineering Operation together with the diagnostic systems that will be installed to meet these requirements (for further discussion, see section H.2 and Table H-1). Several MW of ECRH power will be available to assist the plasma breakdown. This will be launched from an upper port towards a mirror mounted on the inner wall of the vacuum vessel, which will reflect the EC radiation back through the centre of the poloidal field null into an opposite port where a beam dump will be mounted to limit the stray radiation in the torus. A total ECRH power of 6.7 MW at 170 GHz will be available for breakdown/ burn-through assist.

The essential parameters for First Plasma will be:

$I_p \sim 100$ kA
$t_{pulse} \sim 100$ ms
$P_{aux} < 6.7$ MW (for breakdown/burn-through assist)

Nevertheless, simulations indicate that if burn-through is achieved, a plasma current of > 0.5 MA might be reached lasting few seconds (see, e.g. [Kavin, 2016-2]).

2.4.3 Engineering Operation

Following First Plasma, a period of 6 months of Engineering Operation will be undertaken with the principal aim of commissioning the Magnet systems to full current operation. During this period, if time permits, the possibility of producing quasi-circular limiter plasmas of up to 1 MA for several seconds could be explored, since this would provide an opportunity to make initial observations of tokamak plasma operation in ITER prior to Assembly Phase II, and could also provide valuable information on the operation of the plasma control system in preparation for PFPO-1 operation.

A further key activity which will be implemented during this phase is a careful determination of the (toroidal) magnetic axis of the tokamak. This procedure, which is still under development, is aimed at obtaining a very precise mapping of the toroidal magnetic field within the vacuum vessel, from which the final position of the shielding blanket modules (to be installed on the vacuum vessel wall) can be determined to ensure that the individual first wall panels are well aligned toroidally/poloidally and, most important, radially with the last closed magnetic surface in ITER

limiter plasma configurations, to optimize their power handling capability during the limiter phase of the discharge.

Table 2-2 – Overview of minimum measurement requirements and installed diagnostic systems for the First Plasma and Engineering Operation campaign*

Measurement Requirement	Installed Diagnostic Systems
Magnetics for position, velocity, shape and MHD mode structure	• Magnetics System Electronics & Software • Continuous External Rogowski • Outer Vessel Coils • Steady State Sensors • Flux Loops • Inner Vessel Coils • Diamagnetic Sensors
Line averaged electron density (toroidal polarimeter/ interferometer)	• Density Interferometer (single channel)
Runaway electron detection (hard X-rays)	• Hard X-ray Monitor
Impurity identification and influxes (visible and near UV spectroscopy including $H_{\square}$ and visible bremsstrahlung), partial systems	• H_α/Visible in EPP12 • Vacuum Ultra-Violet Survey • Visible Spectroscopy Reference System (partial) - temporary • X-Ray Crystal Spectrometer
Visible/IR TV viewing (spectroscopically filtered), partial coverage	• Visible/IR Equatorial in EP16 (temporary) • Visible/IR Equatorial in EPP12 (partial)
Torus pressure and gas composition (torus pressure gauges, RGA)	• Pressure Gauges (temporary)
Toroidal Field (TF) Mapping	• Temporary set of magnetic pick-ups for TF mapping
Machine protection	• Tokamak Structural Monitoring System • Stray ECRH detector

** See Appendix H for further discussion of scope of systems labelled as 'temporary' or 'partial'.*

2.5 Pre-Fusion Power Operation Phase (PFPO)

The Pre-Fusion Operation Phase will be broken down into PFPO-1, which will exploit up to 20 MW of ECRH power plus an option for 10 MW of ICRF power, and PFPO-2, which will develop all three of the auxiliary H&CD systems to reach 20 MW of ECRH power, 20 MW of ICRF power, and 33 MW of NBI power, in preparation for the Fusion Power Operation (FPO) phase.

2.5.1 Objectives for the Pre-Fusion Power Operation Phase

In the Pre-Fusion Power Operation Phase, operation of the ITER tokamak with the majority of the systems required to achieve the Project's goals will be demonstrated. This includes commissioning of the H&CD systems, fuelling systems, plasma control, Diagnostics, etc., which are required to provide routine operation up to the nominal plasma current/toroidal field (15 MA/5.3 T) in L-mode and up to (approximately) 7.5 MA/2.65 T in H-mode. These aims will be pursued by developing

plasma scenarios that satisfy all the operational requirements in this phase, including those of core-edge plasma integration (ELM control, divertor power load control, etc.). In addition, development of control schemes and integration issues required to meet the needs of DT high-Q operation (including long-pulse/steady-state goals) will be investigated.

The PFPO Phase is divided into two sub-phases. In the first sub-phase (PFPO-1) a partial set of Diagnostics, H&CD systems (20 MW ECRH and 10 MW ICRF – the latter is a working assumption at present depending on whether the acceleration of 10 MW of ICRF is feasible or not), fuelling and ELM control power supplies, will be installed for commissioning and operation. In the second sub-phase (PFPO-2) the H&CD, fuelling, ELM control systems etc. will be completed to their baseline specifications.

The main objectives of PFPO-1 operation are:

- Commissioning of the plasma control, interlock and safety systems with plasma to levels supporting the experimental program (7.5 MA L-mode and 5 MA H-mode);
- Establishing error field correction and the characterization of error fields without TBMs;
- Commissioning of installed diagnostic systems, validation of data and integration into control/ interlock systems;
- Commissioning and establishing operation of divertor power load control schemes;
- Commissioning and routine operation of the available ECRH and ICRF, if available, systems to the installed power level for at least several tens of seconds;
- Commissioning of disruption prediction, avoidance and disruption/runaway electron mitigation systems and characterization of disruption loads;
- Establishment of routine and robust plasma operation in L-mode to at least 7.5 MA;
- Commissioning and exploitation of the Vertical Stability coils, Error Field Correction Coils and ELM control coils (with an initial set of power supplies);
- Exploration of H-mode operation in hydrogen and helium at 1.8T and investigation of ELM control;
- Initial physics characterization of ohmic, L-mode and H-mode plasmas;
- Initial characterization of plasma-wall interactions in the ITER environment.

The main objectives of PFPO-2 operation are:

- Commissioning and exploitation of the H&CD systems (HNB (33 MW), ICRF (20 MW), ECRH (20 MW), DNB) in plasma operation to their installed power level for at least 50 s;
- Commissioning of the additional Diagnostic systems, validation of data and integration into control/ interlock systems;
- Establishing routine error field correction with TBMs;
- Commissioning advanced plasma control capabilities required to execute the experimental program;
- Extension of the capability for disruption prediction, avoidance and mitigation up to 15 MA/5.3T L-mode plasmas
- Exploration of the capabilities of the ECRH system to control NTMs;
- Demonstration of divertor heat flux control capability in H-mode and L-mode to the highest P_{aux} = 73 MW;

- Establishing H-mode plasma operation up to 7.5 MA/2.65 T (in H/He, as the power threshold allows) and development of a reliable ELM control capability;
- Demonstration of 15 MA/5.3 T L-mode plasmas in H;
- Physics characterization of ohmic, L-mode and H-mode plasmas at the highest achievable parameters in terms of plasma current/magnetic field and input power in H/He plasmas;
- First characterization of the current drive capabilities of the ITER systems and development of key ingredients of the long-pulse scenarios (e.g. target-q formation and sustainment for ~10 s);
- Time allowing, initial attempt at long-pulse (< 1000 s) H-mode operation at 7.5 MA/2.65 T;
- Characterization of key aspects of plasma-wall interactions in the ITER environment (e.g. fuel retention/removal, dust production, PFC erosion/redeposition).

Together with these high-level objectives, the operational experience and experimental results are expected to provide key information regarding required upgrades to ITER systems, which might be needed to support the achievement of the high-Q goals in DT. These are described in section 4.

Regarding plasma-boundary physics, the main high-level objectives of the PFPO phases are:

- Determine quantitative characteristics of heat loads in quasi-stationary plasmas and during plasma transients (this strand of research would be closely linked to studies of disruption heat loads and their mitigation);
- Characterize processes determining material erosion, transport and redeposition;
- Quantify hydrogenic retention and demonstrate techniques to be used later for control of in-vessel tritium inventory (including need for routine wall conditioning/cleaning);
- Validate estimates of dust production and characterize dust generated;
- Validate the power handling performance of the Be first wall during limiter phases and characterize the power handling limits of the first wall during divertor operations;
- Characterize the operational domain of the tungsten divertor, including the establishment of reliable methods for divertor power load control.

The PFPO phases will allow the characterization of key aspects of plasma-wall interactions (PWI) in the ITER environment. Such measurements can begin as soon as plasma experiments are initiated in PFPO-1, but the higher powers and longer pulse lengths which can be achieved in PFPO-2 will be the first opportunity to access the new regime of PWI which ITER is expected to produce. In addition, most of the diagnostics for dust/tritium retention/erosion will only be installed prior to PFPO-2. Of primary importance is validation of the understanding of tritium retention, material migration and dust formation to provide input on these issues before nuclear operations begin. These analyses would also contribute to the refinement of the tritium/dust management strategy to be implemented during the various phases of DT operation; it is understood that this strategy will be fully validated during the DT phase.

Characterization of hydrogenic retention rates can be performed during both PFPO phases using gas balance during hydrogen operations, assuming that the required hardware is in place. Given the difference in the retention mechanisms of H isotopes and He in plasma-facing materials, gas balance measurements during pure He discharges bring limited information, with the possible exception of providing information on the background H level in the machine coming from the in-vessel PFCs. For as long as the beryllium first wall is in place, fuel retention in ITER is expected to be driven mainly by co-deposition of hydrogenic species with Be. Gas balance measurements

during PFPO-1 are made difficult by the low wall fluxes expected in this phase, given the low available input power. Measurements in pure H would therefore likely provide only an upper estimate of the hydrogenic retention and data for wall outgassing behaviour between discharges.

The tritium removal strategy in ITER foresees the use of thermal outgassing through the baking of PFCs to 240°C for the first wall and 350ºC for the divertor, respectively. In addition, conditioning discharges (GDC, ICWC) can be used for fuel removal by ion-induced desorption and isotopic exchange. The efficiency of these latter techniques should be studied early on, and, as for tritium retention, it can only be evaluated during operations with hydrogenic fuels. A full bake is therefore needed either during, or at the end of, PFPO-1 to provide a first indication of the wall release behaviour.

The pulse duration, and resultant divertor fluence, during these early phases will however be limited, so that a full validation of the baking efficiency can only be obtained when sufficient co-deposition has occurred in the machine, justifying the need for a dedicated campaign of repeated discharges in PFPO-2, with trace deuterium if possible. On the contrary, the efficiency of ICWC for wall conditioning can be studied in detail during PFPO phases. One limitation is that isotopic exchange of H and D can be performed only if D-trace experiments are possible, or if D-ICWC discharges are permitted.

Another critical aspect of the plasma boundary physics during PFPO phases is the characterization of PFC heat loads and the validation of models of power and energy deposition. Whilst the divertor heat loads during the PFPO phases should be well within the design limits for any reasonable divertor neutral pressure (Appendix C), wall heat loads may already reach their design limits during the limiter start-up phase of diverted discharges depending, for example, on the degree of first wall alignment to the magnetic axis or misalignments between adjacent panels. Careful characterization of the heat load pattern during limiter phases will therefore be required at the start of PFPO-1, and should be performed at the main value of toroidal field chosen during the campaign. First wall heat loads, in particular for the upper panels close to the secondary X-point, should also be characterized during divertor operations as a function of parameters such as primary-to-secondary X-point distance, triangularity, density, power, confinement mode (L- and H-mode). The same exercise will need to be repeated during PFPO-2 to help establish the limits on separatrix separation during FPO and to check if upper main chamber power handling will be adequate for burning plasma conditions.

Characterization of the near-SOL width in different operation regimes (L-mode, inter-ELM) will be a prime objective during PFPO phases to validate the divertor heat loads to be expected at higher performance. Commissioning of heat load control methodologies must also be extensively performed in the non-active operational phase since deuterium operation in the nuclear phase is expected to rapidly achieve conditions in which divertor detachment control will be mandatory for scenario development to high current and with tritium fuel. Early testing of power flux control, particularly in H-mode, is also advantageous in the sense that stationary heat loads will be far from technology limits and even uncontrolled ELM transient heat fluxes should be below damage thresholds for the tungsten monoblocks. Such testing must, however, be mostly conducted in H plasmas since detachment dynamics in He are very different and will not be representative of later operation in D and T.

2.5.2 Assumptions for Pre-Fusion Power Operation

The assumptions made in developing the ITER Research Plan have been broken down into the four operation stages to clarify what machine and system configuration is assumed to be available for

each stage. The systems and subsystems required at each stage are described in [ITER_D_SNE6G8, 2016] and [ITER_D_TVG7YK, 2017]. In the following analysis, it is assumed that the First Plasma campaign was successful in achieving full integrated commissioning of the operational ITER plant systems, including a plasma of at least 100 kA for at least 100 ms duration at 2.65 T in H and/or He and that the CS, PF, TF, and CC magnets were subsequently commissioned to their fully specified operating voltage and current values without plasma. It is also assumed that the first 8 gyrotrons of the ECRH system have been fully commissioned, at least for short pulse operation (> 100 ms duration) at 170 GHz through one upper launcher. The PCS, CIS, and CSS have all been fully commissioned for the functions required for First Plasma operation. Furthermore, it is assumed that all commissioning of plant systems and diagnostics required for the subsequent operation phase that can be performed without plasma has been carried out successfully during the integrated commissioning phase just prior to the restart of plasma operations.

It is planned to install the ELM and VS in-vessel coils prior to First Plasma, but it is assumed that they will be shorted with appropriate resistances to avoid arcing at the coil terminals and to avoid large induced currents in the coils during First Plasma (FP) operation. Since the in-vessel coil power supplies are not expected to be available for FP, full commissioning of these coils and their power supplies can only begin during the commissioning phase just prior to PFPO-1. It is assumed that the VS in-vessel coil power supplies will be installed and ready to commission the coils before the beryllium blanket modules are installed so that any issues found during coil commissioning can be resolved before the coils are trapped below the blanket modules. To allow initial H-mode operation during PFPO-1 and to begin to commission the ELM coils, it is assumed that at least nine of the ELM coil power supplies will be available and ready for commissioning of the ELM coils before the blanket modules are installed. Although a temporary glow discharge cleaning (GDC) system will be installed for FP, the permanent system will be installed and commissioned in preparation for PFPO-1 plasma operation. Following commissioning of the in-vessel coils, the shielding blanket modules, including the beryllium first wall, and the divertor with tungsten PFCs will be installed. The diagnostics required for the PFPO-1 phase (Table H-2 in Appendix H) will be installed during Assembly Phase II. The remainder of the gas injection system (GIS) will be installed through the lower ports, and one cask with two pellet injectors (PIS) will also be installed. The disruption mitigation system (DMS) will also be installed during Assembly Phase II. The three additional upper ECRH launchers and one equatorial launcher, together with the remaining 16 gyrotrons and their transmission lines will also be installed during Assembly Phase II to provide the full 20 MW ECRH power during PFPO-1. For the purposes of the Research Plan development, it is further assumed that the first ICRF antenna system will be installed in advance of PFPO-1 to provide an additional 10 MW of ICRF heating in PFPO-1, so that ICRF commissioning can begin early in the experimental program with the aim of providing a total of 30 MW auxiliary heating power for initial H-mode operation in this phase.

During Assembly Phase III, between the PFPO-1 and the PFPO-2 phases, a number of additional systems will be installed and these will be integrated into the operational environment during Integrated Commissioning III, prior to PFPO-2. This extended operational capability will include the second ICRF antenna system (assuming that the first one is installed for PFPO-1 operations) to provide a total of 20 MW ICRF heating, the diagnostic neutral beam (DNB) and two heating neutral beam (HNB) systems to provide 33 MW neutral beam power, additional diagnostics, a further pellet injector cask with 2 additional pellet injectors, and the first 6 Test Blanket Module (TBM) systems, incorporating ferromagnetic structural materials. During PFPO-2, it is planned to commission the three baseline auxiliary H&CD systems up to the full injected power capability of 73 MW. The additional diagnostics to be installed for operation in the PFPO-2 phase are listed in (Table H-3 in

Appendix H). With a total of 4 pellet injectors, high fuelling capabilities to full performance will be possible, as well as for ELM pellet pacing. The influence of the ferromagnetic TBMs on the required error field corrections to avoid low density locked modes, as well as their impact on H-mode performance, will form one component of the experimental activity in PFPO-2.

2.5.3 Plasma scenarios for hydrogen and helium operation

During the PFPO phase of operation, plasma fuelling will be limited to hydrogen or helium, though, as discussed in section 2.5.5.12.2.1 and Appendix A, a limited experiment with low deuterium concentration may be possible. It is expected that, whenever possible, preference will be given to hydrogen plasmas, since the overall fuelling, transport and recycling properties will be similar to those of deuterium and tritium and since there is some remaining uncertainty about the impact of helium plasmas on plasma-facing materials. Nevertheless, given that the H-mode power threshold is expected to be about 1.5-2.0 times lower in helium than in hydrogen, helium operation may be unavoidable in order to obtain a high quality H-mode enabling ELM control and mitigation tests to be undertaken during the PFPO phase. For these reasons, and given the uncertainties on the actual H-mode threshold in ITER, scenarios have been designed for both hydrogen and helium plasmas.

In subsequent sections details of the most relevant plasma scenarios are presented, including steps towards 15 MA operation, with an emphasis on H&CD conditions and on capabilities for long-pulse operation. In view of several operational options that have been identified in the Research Plan analysis following the development of the revised schedule within the Staged Approach, both baseline and optional scenarios are described.

The steps towards 15 MA operation described in the present document may be adjusted during the experimental campaigns according to actual observations and achievements. These steps will be progressive in magnetic field and plasma current, with some deviations from operation at $q_{95} \sim 3$ to allow the approach to the nominal 15 MA/5.3 T scenario to investigate carefully the issues and risks associated with disruptions. Figure 2.5-1 shows an estimate of the operational range for each H&CD system (EC, IC, NBI) for different values of magnetic field and plasma current. Due to the resonance conditions associated with the absorption of EC and IC waves, their operational ranges in toroidal magnetic field are constrained by the requirement that the power is absorbed sufficiently close to the plasma centre. The operational range of the HNB system is constrained by the minimum plasma density required to limit shine-through power losses to an acceptable level. Steps foreseen towards 15 MA operation are displayed as purple points on this figure.

The Staged Approach foresees the installation of the full ECRH system and a possible acceleration of the ICRF system installation, with one IC antenna installed in advance of the PFPO-1 campaign. The full baseline H&CD capability with, in particular, the full power ICRF and HNB systems will be installed in advance of PFPO-2.

Two principal areas on the installation of the H&CD systems required to meet the four-stage approach remain the subject of R&D studies:

- The available EC frequencies and the associated pulse duration: to enable successful EC-assisted breakdown and burn-through at third field (1.8 T), and a reliable path to H-mode for the heating phase, second harmonic frequency (X2), EC assistance may be required. However 170 GHz gyrotrons can only offer third harmonic (X3) EC assistance at this low field. Hence, low frequency gyrotrons are under investigation, though potentially the output power and pulse duration of the ECRH system will be more limited at the low frequencies under consideration, as documented in Appendix G. Three options are foreseen for the 24 gyrotrons of the ECRH system:

1) 24 single-frequency gyrotrons (SFG) at 170 GHz;
2) At least 16 SFGs at 170 GHz and up to 8 dual-frequency gyrotrons (DFG) at 104/170 GHz (UL);
3) At least 16 SFGs at 170 GHz and up to 8 SFGs at 110 GHz (UL).

- The acceleration of one IC antenna (~10 MW) for the PFPO-1 campaign, for which a preliminary analysis is described in Appendix G.

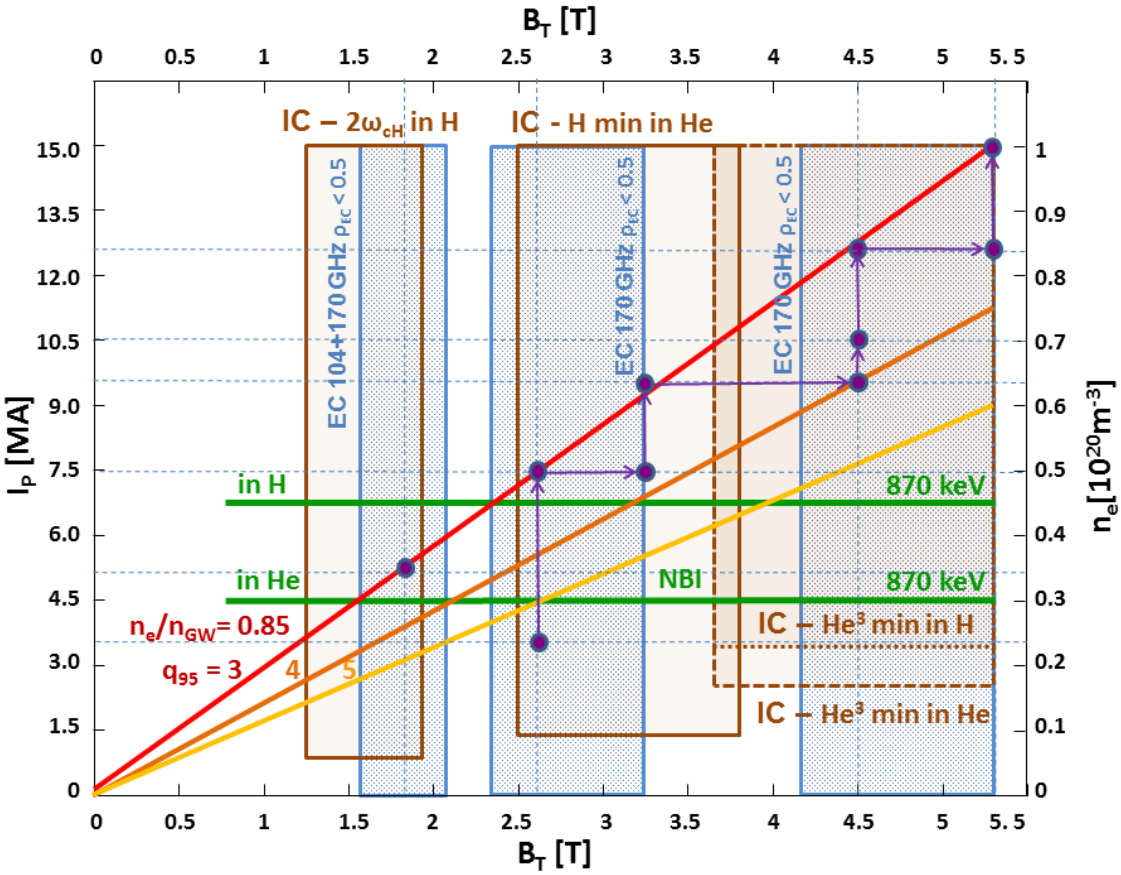

Figure 2.5-1: Operational range of H&CD systems over the relevant B_T, I_p and density range in ITER. The EC, IC, NBI operation ranges are in blue, brown and green respectively.

All these possibilities should be envisaged in the description of the scenarios foreseen at each operational step. The availability of H&CD systems is summarized in Table 2-3.

Scenarios in the non-active phase can be grouped in six main categories [Schneider, 2017-1]:

- First plasma: 100 kA/2.65 T
- First divertor plasma: 3.2 MA/2.65 T
- First $q_{95} = 3$ plasma: 7.5 MA/2.65 T
- First H-mode plasma: 5.0 MA/1.8 T
- Progressive steps: 7.5-9.5 MA/3.3 T, 9.5-10.5-12.5 MA/4.5 T, 12.5 MA/5.3 T
- First 15 MA plasma: 15 MA/5.3 T

For all these cases, it is likely that hydrogen plasmas will be developed first, followed by helium plasmas where operation in helium is necessary, e.g. only if a good H-mode cannot be achieved in

hydrogen plasmas with the available H&CD power. Details of these scenarios are described in the sub-sections below.

Table 2-3 – Availability and characteristics of H&CD systems in the four stages of the Research Plan (tbc = to be confirmed by future R&D studies)

Stage	First Plasma	PFPO-1	PFPO-2	FPO-1
ECRH system	Only UL (8 gyrotrons), 170 GHz, **6.7 MW**	Full system, 170 GHz (+104/170 or 110 GHz, tbc), **20 MW**	Full system, 170 GHz (+104/170 or 110 GHz, tbc), **20 MW**	Full system, 170 GHz, **20 MW**
ICRF system	None	1 antenna, **10 MW** (tbc)	Full system, 2 antennas, **20 MW**	Full system, 2 antennas, **20 MW**
HNB system	None	None	Full system, 2 injectors, 870 keV H beams, **33 MW**	Full system, 2 injectors, 1 MeV D beams, **33 MW**
Total	**6.7 MW**	**28-30 MW (**tbc)	**73 MW**	**73 MW**

2.5.3.1 First Plasma

The first plasma will be attempted initially in **hydrogen** at a magnetic field of **2.65 T** with a plasma current of at least **100 kA** for at least **100 ms**, with a possibility to go up to **~0.5-1 MA** for a few seconds **(~3s**) for first plasma observations and first PCS operation in view of PFPO-1 preparation [Gribov, 2016]. A CS coil current of **20 kA/turn** is planned as a target for magnet commissioning [Kavin, 2016-03] in preparation for attempting breakdown and burn-through [Kavin, 2016-11]. Complete burn-through could lead to a plasma current above 1 MA and steps will be taken to limit the plasma current below this value since the first plasma protection components are designed to handle disruptions up to 1 MA/2.65 T. In addition, currents approaching 1 MA may cause excessive impurity generation from the steel limiter surface [Pitts, 2016].

H&CD capabilities:

ECRH system: only one upper launcher (UL), i.e. 8 gyrotrons delivering **6.7 MW** at 170 GHz (X2).

2.5.3.2 First divertor plasma in PFPO-1

The first divertor plasma will be in **hydrogen** in L-mode at a magnetic field of **2.65 T** with a plasma current of **3.2 MA**. The goal is to establish initial divertor operation at the lowest possible plasma current, with a flat-top duration of at least 10 s, as a target for the commissioning of various systems, such as PCS, diagnostics, interlock systems, DMS [ITER_D_NSHUQ7, 2014]. The choice of 3.2 MA is based on an analysis indicating that this is the minimum current allowing reliable magnetic control with a full bore divertor configuration. The currents in the CS coils can be varied **from 12 kA/turn to 30 kA/turn**, leading to a flat-top duration **between 10 s and 200 s** [Kavin, 2015-08].

H&CD capabilities:

ECRH system: EL+UL launchers, 24 gyrotrons delivering a total EC power of **18-20 MW**, with the following possibilities:

- *Option 1*: 24 gyrotrons delivering 20 MW at 170 GHz (X2).
- *Options 2 and 3*: at least 16 gyrotrons delivering 13.3 MW at 170 GHz (X2) and up to 8 gyrotrons delivering 6.7 MW at 104 or 110 GHz (O1) from the UL[1].

2.5.3.3 First q_{95} = 3 plasma in PFPO-1 and PFPO-2

The first $q_{95} = 3$ scenarios will use **hydrogen** and **helium** plasmas at a magnetic field of **2.65 T** with a plasma current of **7.5 MA**. At this combination of parameters, hydrogen plasmas are likely to remain in L-mode, while current expectations in the H-mode threshold scaling for helium plasmas indicate that H-mode operation should be achieved with the H&CD power available in PFPO-2 and there is some possibility of achieving helium H-mode operation at 2.65 T in PFPO-1 if sufficient ECRH and ICRF power can be injected. The maximum flat-top duration will typically be of the order of **a few 100 s** with a CS coil current varying **from 30 kA/turn to 45 kA/turn** [Kavin, 2016-02; Kavin, 2016-03]. Operation above 40 kA/turn will consume the CS coil fatigue lifetime, and hence long-pulse operation will be addressed during the PFPO phase only if operational time permits and long pulses of interest can be produced without significant consumption of the CS fatigue life.

H&CD capabilities:

- **ECRH system:**
  PFPO-1 and PFPO-2: EL+UL launchers, 24 gyrotrons delivering a total EC power of 20 MW with 170 GHz gyrotrons (X2) and possible 104 or 110 GHz gyrotrons (O1).
- **ICRF system:**
  PFPO-1: one antenna delivering 10 MW to the plasma.
  PFPO-2: two antennas delivering 20 MW to the plasma.
  Scenarios [Schneider, 2016]*:*
  - ***Hydrogen plasmas:*** there is no good heating scheme. The best scheme is 2nd harmonic He^4 heating ($f_{IC} = 40\ MHz$) with an He^4 concentration of ~20% leading to ~50% of single-pass absorption (SPA) dominantly on electrons, hence very broad.
  - ***Helium plasmas:*** the best heating scheme is fundamental minority H heating ($f_{IC} = 40\ MHz$) with an H concentration of ~2-8% leading to a SPA of almost 100%.
- **HNB system:**
  PFPO-1: no NBI power.
  PFPO-2: two injectors of 870 keV hydrogen beams delivering a total of 33 MW to the plasma; however the actual power and energy that can be applied will be limited by shine-through power levels, leading to an NB injected power varying from ~10 MW (in H plasmas), to ~20 MW (in He plasmas) and to 33 MW at higher densities [Kim, 2016].

In order to compensate for the lack of a good ICRF heating scheme in hydrogen plasmas at 2.65 T, one option is to heat small amount of He^3 (<1%) at its fundamental resonance ($f_{IC} = 40\ MHz$) at 3 T and/or 3.3 T in a H:He^4 mixture with ~15% of He^4 using the 3-ion heating scheme [Kazakov, 2015]. These scenarios could be applied both in PFPO-1 and PFPO-2. Under these conditions, the SPA is estimated to be of the order of 80-90% shared between central electron heating and off-axis ion heating on the high field side (HFS). These optional scenarios offer the possibility to reach H-mode in hydrogen plasmas when operating close to half field, thus enabling long-pulse operation

[1] Feasibility studies for SFGs at 110 GHz have not yet been performed and hence there is an uncertainty on the EC capabilities in terms of power and pulse length at low frequency.

and ELM control at $q_{95} = 3$, and limiting the need for helium plasma operation at half field. However, establishing a basis for the exploitation of this scenario in ITER requires further experimental R&D to demonstrate efficient heating under analogous conditions to ITER plasmas. In addition, adding 10-15% of He^4 reduces the minimum allowable operational density with respect to NBI shine-through. If observations from recent JET experiments [Hillesheim, 2016] are confirmed, such a fuel mixture could also allow access to hydrogenic H-mode operation at lower input power. However, W accumulation needs to be further investigated due to a possible increase of W concentration with the dominant off-axis and reduced central heating. Furthermore, controlling He^3 concentration in the presence of He^4 may be challenging [Hellerman, 2017]. Finally, ion losses are still to be assessed since they can be significant due to off-axis fast trapped ion acceleration and plasma response to 3-D magnetic fields (intrinsic and corrected by error field correction coils or to applied fields for ELM control).

2.5.3.4 5 MA/1.8 T scenarios in PFPO-1 and PFPO-2

5 MA/1.8 T scenarios are designated as *first H-mode plasmas* in the context of the PFPO-1 phase since they are aimed to enable H-mode operation in this phase with very limited auxiliary heating (between 20 and 30 MW depending on hypotheses on ECRH frequencies and ICRF acceleration plan). However these scenarios will be investigated both in PFPO-1 and PFPO-2, and both in **hydrogen** and **helium** plasmas. Maximum sustainable flat-top durations for these scenarios extend **from ~200 s to ~1400 s** for CS coil current values varying **from 20 kA/turn to 45 kA/turn** [Kavin, 2016-09]. Again, operation at CS coil currents above 40 kA/turn should be limited in order to reduce the consumption of the CS coil lifetime before the FPO phase. Operation at such low field leads to an overcompensation of the magnetic field ripple by ferromagnetic inserts, inducing a ripple at the plasma separatrix of -1.3%, as described in detail in Appendix F. Ripple-induced fast ion losses still need to be assessed in these scenario conditions. If this ripple level is found to be critical, it can be reduced to -0.55% by increasing the plasma-wall distance [Kavin, 2017-01], but doing so risks a significant degradation in the ICRF coupling performance.

H&CD capabilities:

- **ECRH system:**
  PFPO-1 and PFPO-2: EL+UL launchers, 24 gyrotrons delivering a total EC power of 20 MW. For 1.8 T scenarios, the options 2 and 3 with up to 8 low frequency (104 or 110 GHz) gyrotrons may be required to ensure X2 breakdown and burn-through. X2 absorption can be provided by either 104 or 110 GHz gyrotrons; this also provides preheating of the plasma such that the X3 absorption by 170 GHz gyrotrons becomes more efficient [Snipes, 2016-01]. This mode of operation is possible due to the fact that the absorption of the EC waves is central for both frequencies at 1.8 T, leading to a synergetic effect, as shown in Figure G1-1[2].

- **ICRF system:**
  PFPO-1: one antenna delivering 10 MW to the plasma is assumed.
  PFPO-2: two antennas delivering 20 MW to the plasma.
  Scenarios:
  - ***Hydrogen plasmas:*** the best heating scheme is 2nd harmonic H majority ($f_{IC} = 53\ MHz$) leading to a SPA of almost 100%.

[2] This needs to be confirmed by further modelling of ECRH scenarios with a combination of 104 or 110 GHz and 170 GHz frequencies at 5 MA / 1.8 T in a time-dependent transport simulation.

- ***Helium plasmas:*** the best heating scheme is 2nd harmonic H minority ($f_{IC} = 53\ MHz$). Preliminary analysis shows that this scheme leads to an SPA of almost 100%, which is counter-intuitive, given that 2nd harmonic minority schemes are not expected to be very efficient. The good absorption is associated with the fact that the absorbed power is inversely proportional to the square of the magnetic field, leading to a factor of ~ 10 increase in absorption at one-third field compared to that at full field.

- **HNB system:**
  PFPO-1: no NB power.
  PFPO-2: two injectors of 870 keV hydrogen beams delivering a total of 33 MW to the plasma; however, the total power and the injection energy that can be applied in such scenarios will be limited by the shine-through power level: injection should be possible at roughly 8 MW/500 keV in H plasmas and 16.5 MW/650 keV in He plasmas [Singh, 2017].

2.5.3.5 Progressive steps towards full current in PFPO-1 and PFPO-2

Steps in magnetic field and plasma current are illustrated in Figure 2.5-1 [Kim, 2016]. They have not been modelled in detail yet, and hence their description is still at a preliminary stage. These steps are foreseen both in **hydrogen** and **helium** plasmas. They will likely be in L-mode since H&CD capabilities are reduced at intermediate values of field and current, as shown in the operational ranges of Figure 2.5-1.

Foreseen ECRH heating characteristics are given below, cf. Figure G-1:

- 3.3T: At least 13.3 MW at 170 GHz (X3/X2) and up to 6.7 MW at 104 or 110 GHz (X2/X1).
- 4.5T: At least 13.3 MW at 170 GHz (X2/X1), no resonance for 104 or 110 GHz.
- 5.3T: At least 13.3 MW at 170 GHz (X1), no resonance for 104 or 110 GHz.

ICRF heating schemes are likely to use fundamental He^3 minority in hydrogen plasmas (for an ICRF frequency varying from 40 to 53 MHz for fields from 3 T to 5.3 T). In helium plasmas, the best ICRF heating scheme is likely be fundamental H minority at 3.3 T and fundamental He^3 minority at 4.5 T and 5.3 T, though this is to be confirmed by further modelling.

The applicable NBI power and energy is directly correlated to the density and the possible combinations need to be accurately assessed for the different plasma currents/ densities foreseen in these scenarios. The NB shine-through power depends on the fraction of the Greenwald density at which it is chosen to operate, and this will be adjusted according to actual experimental conditions and observations.

2.5.3.6 First full current plasma in PFPO-1 and PFPO-2

The first **15 MA/5.3 T (L-mode)** plasmas will be developed in PFPO-2, since it is not considered likely that there will be sufficient operational time available in PFPO-1 to develop the scenario and to commission reliable operation of the disruption detection and mitigation systems to this level of plasma performance. However, performing full field/low current discharges, typically 3.5MA/5.3 T, is foreseen during PFPO-1 in limiter configuration to develop disruption mitigation capabilities with respect to runaway avoidance before applying the DMS at currents above 3.5 MA.

For the 15 MA/5.3 T scenario, the H-mode power threshold in hydrogen is expected to be well beyond the level of installed heating power, while it might just allow H-mode access in helium at densities of around 50% of the Greenwald density. Nevertheless, the risks associated with operating such high current plasmas just above the H-mode threshold are such that it is more likely that the

development and demonstration of 15 MA plasmas during the PFPO-2 phase will be carried out in the hydrogen L-mode regime. The flat-top duration can vary from **~10 s** in ohmic plasmas to **~100 s** with full auxiliary power (73 MW), for a CS coil current of **45 kA/turn**.

H&CD capabilities:

- **ECRH system:** EL+UL launchers, 24 gyrotrons delivering a total EC power of **20 MW**, with following possibilities:
  - *Option 1*: 24 gyrotrons delivering 20 MW at 170 GHz (O1)
  - *Options 2 and 3*: At least 16 gyrotrons delivering 13.3 MW at 170 GHz (O1); the up to 8 low frequency gyrotrons (104 or 110 GHz) have no resonance inside the plasma for fields above 4 T.

- **ICRF system:**
  PFPO-1: one antenna delivering 10 MW to the plasma is assumed.
  PFPO-2: two antennas delivering 20 MW to the plasma.
  Scenarios [Schneider, 2016]*:*
  - ***Hydrogen plasmas:*** the best heating scheme is fundamental He^3 minority (with a concentration <1%) in a H:He^4 mixture ($f_{IC} = 53\ MHz$) leading to a SPA of ~95%.
  - ***Helium plasmas:*** the best heating scheme is also fundamental He^3 minority ($f_{IC} = 53\ MHz$), with a He^3 concentration of ~4-5%.

- **HNB system:**
  PFPO-1: no NB power.
  PFPO-2: two injectors of 870 keV hydrogen beams delivering a total of 33 MW to the plasma.

2.5.4 Operations plan for PFPO-1

2.5.4.1 PFPO-1 Objectives

The PFPO-1 phase is the first plasma operations phase with the beryllium blanket and tungsten divertor installed, allowing plasma currents greater than 1 MA and plasma durations beyond several seconds. Initially, plasma initiation will need to be re-established in hydrogen at 2.65 T with the new first wall conditions. This will be followed by the development of limited low elongation plasmas at currents of up to 2 – 3 MA, together with the development of disruption and runaway electron (RE) mitigation. Plasma magnetic control of the current, position, and shape, including vertical stability control of elongated plasmas will lead up to 3.5 MA diverted plasma operation. Routine operation will then be developed up to 7.5 MA to provide a suitable plasma configuration for the commissioning of diagnostics and the ECRH power up to the full 20 MW and the first ICRF antenna, which is assumed to be available for operation, up to 10 MW for at least 50 s duration. Effective disruption and RE mitigation will have to be progressively established as the plasma current is gradually increased. The toroidal field and plasma current will increase in steps beyond 7.5 MA/2.65 T up to 7.5 MA/5.3 T and, if time allows, possibly up to 10 MA. Time permitting, and depending on the progress of the experimental program, the pulse duration may be extended to beyond 100 s at lower plasma currents to qualify the H&CD systems for longer pulse operation in PFPO-2.

A significant part of the initial operation program will be devoted to the commissioning of H&CD, fuelling, control and diagnostic systems with plasma. For the last, in particular, the calibration and determination of the measurement capabilities of the installed diagnostics, as well as the resolution of possible inconsistencies among the measurements of plasma parameters, are essential to allow an efficient progress of the experimental program. Table 2-4 lists the additional measurement

requirements beyond those specified for FP established for the PFPO-1 campaign together with the additional diagnostic systems which are planned to be installed in Assembly Phase II to meet these requirements, when integrated with diagnostic systems already installed for FP. The requirements focus on the need for basic characterization of essential plasma parameters, plasma control capability and machine protection. There is typically more than one diagnostic system satisfying each requirement, in part because the required parameter involves the integration of

Table 2-4 – Overview of <u>additional</u> measurement requirements and <u>additional</u> diagnostic systems installed for the PFPO-1 campaign*

Measurement Requirement	Installed Diagnostic Systems
Magnetics for position, velocity, shape, MHD mode structure and halo currents	• High Frequency Sensors • Divertor Coils • Divertor & Blanket Rogowski Coils • Divertor Shunts
Core profiles of n_e and T_e (TS, ECE)	• Core Plasma Thomson Scattering (1 laser) • Electron Cyclotron Emission • Toroidal Interferometer Polarimeter (TIP measures line integrated density in EQ9) • Density Interferometer Polarimeter (DIP measures line integrated density in EQ8)
T_i and High-Z impurity content (XRCS and Radial Soft X-ray Cameras)	• X-Ray Crystal Spectrometer • Radial X-Ray Camera
Impurity identification and influxes, Z_{eff} (visible and near UV spectroscopy, including H_α and visible bremsstrahlung, He, Be, Ne, Kr, Ar, W emission)	• H_α Visible (partial) • Core Imaging X-ray Spectrometer • X-Ray Crystal Spectroscopy Edge • Visible Spectroscopy Reference System • Vacuum Ultra-Violet Edge • Divertor Impurity Monitor (partial) • VUV Divertor
Radiated power distribution (Bolometry)	• Bolometry System
Neutrons (Micro Fission Chambers, Neutron Flux Monitors, Divertor Neutron Flux Monitors, Neutron Activation System)**	• Microfission Chambers • Neutron Flux Monitor Systems • Neutron Activation System • Divertor Neutron Flux Monitors • Neutron Calibration (2.5 MeV) (partial) • Neutron Facility Area
Divertor plasma characterization (incl. divertor duct pressure and gas composition)	• Langmuir Probes • Pressure Gauges (cassette) • Residual Gas Analyzers (2 channels)
Visible/IR TV viewing (full coverage)	• Visible/IR Equatorial Ports • Visible/IR Upper Ports
PWI/Heat Load characterization	• First Wall Samples • Divertor IR Thermography

	• Thermocouples (Divertor) • Calorimetry (for testing with aux. heating)
Data for gas balance measurements	• Pressure Gauges
In-vessel viewing system	• In-vessel viewing system

* *The table lists the additional diagnostic systems planned for installation prior to PFPO-1 to meet the additional measurement requirements (when integrated with the systems installed for FP). See Appendix H for a discussion of the scope of systems labelled as 'temporary' or 'partial'.*

*** Neutron measurements are required to monitor neutron production during the non-active phase.*

measurements from two (or more) diagnostics and in part to provide an element of redundancy (risk reduction) in the installed measurement capability.

Routine operation at 7.5 MA/2.65 T will be performed and is essential to support the experimental program envisioned for this and later operation phases. This task includes qualification of the plasma shape and current control, development of robust scenarios for current ramp-up and ramp-down, basic control of the plasma density, and robust plasma initiation. It requires that the first wall protection and disruption protection have been successfully completed. It is expected that this development will be performed in L-mode plasmas in H with He, a scenario required for commissioning of the ICRF to highest powers (with the first harmonic hydrogen minority scheme). He plasmas at 2.65 T will also be required to determine the scaling of the H-mode threshold with toroidal field by comparing the requirements for 1.8 and 2.65 T plasmas.

Routine operation of the ECRH system at full power (note: this may not achieve 20 MW, depending on the option chosen to provide breakdown/heating capability at 1.8 T) for several tens of seconds is also necessary to support the physics program envisioned for this and later operation phases. Operation at both 2.65 T and 5.3 T is expected. Proper aiming and localization must be verified. At 5.3 T, optimization of the polarization will be required.

Routine operation of the ICRF system at 10 MW for several tens of seconds, if available in this phase, is necessary to support the physics program planned for this and later operation phases. This includes integration of the PCS control of gas and antenna-plasma gap to optimize coupling, qualification of the wall protection systems to handle antenna and fast particle loss issues, and ensuring compatibility of the ICRF coupling with levels of non-axisymmetric fields from the ELM control coils expected during ELM mitigation. While commissioning at low power can be developed at 2.65 T in H plasmas, high power ICRF commissioning will require 2.65 T He plasmas (H minority first harmonic) and 1.8 T H plasmas (majority second harmonic).

Demonstration of a robust first wall protection system is required to progress beyond the basic 3.5 MA limiter operation. This includes interpretation of the signals from the protection cameras and development of appropriate avoidance and response functions in the PCS, including termination protocols.

Qualification of operation at 5.3 T is also necessary in the PFPO-1 phase, since the risk of runaway generation is higher during full field operation, and this should be assessed at low plasma current as soon as possible. The commissioning of the ECRH system at 5.3 T is also important to assess the risk of stray radiation arising from reflection at the X-mode cut-off layer.

Routine disruption management must be established in this phase. The quantification of forces and runaway generation and the effectiveness of the DMS to mitigate these should be performed as early as possible to assess the need for upgrades to the DMS. Disruption management also includes

development of the capability to predict conditions which are more likely to lead to disruption, implementation of avoidance strategies, and a robust triggering algorithm for the DMS.

Assessment of intrinsic error fields and of the efficacy of the external correction coils to mitigate their effects are essential in this operation phase. It is important to characterize the magnetic geometry prior to the introduction of the TBMs in PFPO-2 to understand any effects that the TBMs may introduce and to develop mitigation strategies.

It would also be desirable within the PFPO-1 phase to achieve:

- Plasma current operation above 7.5 MA, particularly to qualify disruption protection;
- Plasma operation for > 100 s duration to qualify H&CD systems.

Operation above 7.5 MA is highly desirable in PFPO-1 to accelerate the approach to operation at full technical parameters (15 MA/5.3 T) in PFPO-2. The DMS will be qualified for 7.5 MA/5.3 T and it would be desirable to increase the plasma current up to 10 MA to demonstrate its effectiveness in these conditions.

Operation of the ECRH and ICRF systems for > 100 s is important to test the in-vessel components of these systems as early as possible in the program to mitigate risk. Long-pulse operation will also allow more effective use of machine time for the retention experiments if they are performed in this phase (i.e. if the required hardware is installed).

The H-mode power threshold will be determined at 1.8 T (in H and He) and 2.5 T (He). If the measured power threshold turns out to be consistent with predictions of the standard scaling (see Appendix B), H-mode operation in 5 MA/1.8 T plasmas in H and He will be demonstrated; these will be the first ITER H-mode plasmas. Plasma parameters in these H-mode plasmas, uncontrolled ELM losses, stationary divertor power loads, etc., will be characterized. ELM control will be demonstrated with an initial set of power supplies for the ELM control coils and initial experiments on divertor power load control in H-modes will be carried out at this stage. These H-mode plasmas will provide reference conditions in preparation for studies of the possible influence of TBMs on H-mode performance and to develop mitigation schemes in PFPO-2.

In addition to the physics interests, it is expected that several control issues for H-mode plasmas will be addressed during initial H-mode operation. These include shape control across the L-H and H-L transitions, fuelling strategies for L-mode and H-mode, gap and gas control for maintaining ICRF coupling, and early indication of the need for mitigation of impurity accumulation in the plasma centre. Addressing these in PFPO-1 would accelerate the PFPO-2 research program significantly.

The need to reduce the field to 1.8 T introduces a set of additional objectives:

- Commission the ECRH system at two frequencies (104 GHz/110GHz and 170 GHz), if lower frequency gyrotrons are installed (options 2 and 3);
- Develop plasma scenarios at 1.8 T;
- Commission the ICRF system to heat at 1.8 T;
- Commission the ELM control coils with the initial set of power supplies.

The option to operate at 1.8 T may require dedicated commissioning of the ECRH system (two frequencies) and demonstration of its application to ITER scenarios. This may require the use of the lower frequency gyrotrons for plasma initiation and plasma preheating, and of the higher frequency gyrotrons (170 GHz) for plasma heating in third harmonic. Similarly, the ICRF system would need to be commissioned to allow H-mode operation in hydrogen plasmas at 1.8 T. It would be of

particular interest to commissioning the ICRF antenna at the highest voltage stand-off capability in order to allow a larger distance between plasma and antenna, since this may be required to minimize the TF ripple effects on these 1.8 T H-modes.

2.5.4.2 Establishing routine operation with plasma to 3.5 MA divertor configuration

PFPO-1 follows Assembly Phase II with the installation of the first wall panels and divertor. During PFPO-1, the ITER Research Plan aims for a progressive commissioning of plasma operation and control capabilities towards 7.5 MA at 2.65 T. For the initial phase of operation up to 3.5 MA/2.65 T in hydrogen, the intermediate milestones are:

- Commission robust plasma initiation;
- Limiter operation at 2 MA, then at 3.5 MA;
- Divertor operation at 3.5 MA.

The main commissioning items during this period are (i) the magnetic control, including vertical stability (VS), (2) documentation of disruption loads and effectiveness of mitigation methods (3) density control using gas and pellet fuelling, (4) the assessment of heat loads to the blanket and divertor modules and (5) initial operation of ECRH and ICRF H&CD systems.

2.5.4.2.1 Commissioning of robust plasma initiation

PFPO-1 will start with commissioning and optimization of the plasma initiation and burn-through. A robust operating space needs to be determined and the control of the plasma formation needs to be commissioned. Overheating of in-vessel components or arcing due to stray EC radiation before and during breakdown is potentially an issue and, if a robust breakdown/ burn-through strategy without EC assist can be established, the routine use of ohmic breakdown would be the preferable approach.

For operation up to 3.5 MA a precharge of the central solenoid (CS) of 20 kA is sufficient. The plan envisages a start of operations at 2.65 T at maximum loop voltage using ohmic breakdown with prefill scans and PF coil bias scans for a first optimization of the timing of the plasma formation. This will give the basis for the application of the EC breakdown assist, to obtain plasma formation (in case ohmic breakdown is not successful) and to expand the operation window for reliable breakdown. Using EC assist requires that the injection of EC waves into vacuum is commissioned due to high stray radiation (interlocks).

The operational domain for plasma formation should be documented in terms of gas dosing range (prefill), PF coil bias, timing of the gas and bias with respect to the loop voltage evolution and the timing of the EC power waveform. Ideally the plasma formation should be commissioned at different CS precharge currents (10 - 30 kA).

Ideally EC should only be applied with significant single pass absorption, i.e. electron temperatures around 100 - 200 eV. Absorption may be judged observing the area of first reflection with an infrared system comparing to a short pulse in the empty vessel.

Optional for this first phase are the commissioning of plasma initiation at 5.3T and using helium. Both can be commissioned when required by the research program. Helium operation of ITER could in principle also be achieved with plasma formation in hydrogen. This requires EC operation in O-mode. Experiments in present day devices show that break down assist is more effective in helium and, therefore, faster with a shorter phase of high stray radiation. The effects during burn-through are not too different in both gases.

2.5.4.2.2 Limiter operation up to 2MA

The first demonstration of plasma magnetic control is planned at low currents of $I_p \sim 2$ MA and in limiter configuration, with a flat-top phase of several seconds. For the shape measurement, the computed plasma boundary from magnetic data needs to be validated against other diagnostics such as (infra-red) camera images of the blanket modules and probe measurements. Magnetic control commissioning will go in several stages, from mainly preprogrammed plasma formation, I_p control, boundary flux control (or centroid control), tests of VS at low elongation (natural elongation, $\kappa \sim 1.5$) and verifying control gaps in limiter operation.

A first assessment of heat loads on the blanket first wall panels will be performed, although estimates of the PFC power loads during PFPO-1 indicate that during this period power loads on PFCs should be well within their design limits. Additional time will be required for validating the wall protection techniques. Corrective actions need to be identified and tested on real pulses, in case limiting conditions are reached, as part of the event handling development (see section 2.5.4.4).

Correction of error fields with toroidal mode number n = 1 will be performed by the external Error Field Correction Coils. During the initial operation phase, algorithms for error field reduction will be developed. The in-vessel (ELM control) coils could be used for an improved assessment and correction of the error field structure.

The DMS needs to be commissioned during early plasma operation, to start the documentation of initial disruption forces (unmitigated, mitigated) and RE assessment in limiter plasmas as outlined in section 2.5.4.6.1.

Initial technical commissioning and characterization of the fuelling system can be performed without plasma. The commissioning of the plasma density control consists of two stages; the first with only the gas valves and a second stage with both the gas valves and pellet injectors. Both basic, simple control and model-based control need to be commissioned. Density control with gas injection in limiter (2 MA) and different phases of the discharges such as the current rise and ramp-down will be commissioned, initially with hydrogen gas fuelling alone. Density limits and fuelling limits will need to be documented. The interferometer is essential for line-averaged electron density measurements, associated with boundary reconstruction for the calculation of the average density. For helium operation, planned later in PFPO-1, density control will need to be re-optimized and the density achievable in helium needs to be assessed.

2.5.4.2.3 Limiter operation up to 3.5 MA

After completion of the initial commissioning at 2 MA and assessment of the disruption forces, operation will be expanded to 3.5 MA in limiter configuration with low natural elongation. VS control will be commissioned with and without in-vessel VS coils, by gradually increasing the plasma elongation to nearly diverted plasmas. Tuning and optimization would include, if possible, reduction of low frequency noise in the dz/dt diagnostic signal used in the feedback stabilizing loop.

As soon as plasmas with an electron temperature of several hundred eV are achieved, EC commissioning can start. The principal issues to be checked are the beam polarization and the launcher angles. Operation of EC at 2.65 T is planned, injecting X-mode and heating at the second harmonic resonance. For the equatorial launcher (EL), in particular, this approach is potentially hampered by strong absorption at the 3rd harmonic (X3 heating) towards the plasma edge on the low field side (LFS). Potential cross polarization (O-mode) may be strongly absorbed at the 2nd harmonic resonance (O2-heating). These additional absorptions may complicate the verification of polarization and location of deposition. X3 and O2 heating significantly contribute at higher

temperatures and densities. It may therefore be necessary to perform the polarization tests at the lowest currents for which a diverted plasma can be achieved. This needs further analysis using beam tracing codes. It is noted already here that X3 heating can be avoided by increasing the toroidal field for this intermediate operational point from 2.65 T to 2.75 T.

In parallel, a further assessment of the DMS system will be carried out for limiter operation up to 3.5 MA, together with the documentation of the disruption loads and the potential for creating RE (see section 2.5.4.6.1 for details).

Also heat loads to blanket modules, error field correction and density control may need further assessment and optimization at 3.5 MA.

2.5.4.2.4 Divertor operation at 3.5 MA

It should be noted that operation in a divertor configuration at low plasma current (3.5MA) is challenging from the point of view of control of the magnetic configuration. However disruptions at low current have lower risk of localized damage to PFCs, allowing optimization of the plasma magnetic control, optimization of the plasma-wall gaps, strike point control and stabilization of plasma vertical displacements in the divertor configuration both with and without the VS in-vessel coils. For divertor operation, additional validation with other diagnostics is required, e.g. to confirm the location of strike points, plasma/wall separation etc.

First diverted plasmas at 3.5 MA will be at lower elongation ($\kappa \sim 1.5$) to allow tests with and without VS coils. Operation will be extended to full bore at full elongation, once the control of the plasma boundary, the control of the strike points and VS have been commissioned.

A plasma scenario needs to be developed with current ramp-up, X-point formation and ramp-down in divertor configuration using feedback control of plasma current, plasma-wall ‘gaps’ and strike point positions. In addition, scenarios with different rates of current ramp-up (with/without ECRH) and ramp-down will be explored. This will also allow validation/adaptation of the plasma transport models used in simulations describing these phases of the scenario.

Commissioning of event handling and ramp-down or shut down strategy/logic is important during the initial divertor operation phase, laying the basis for routine divertor operation in ITER. Commissioning of basic wall protection could be performed at much lower limits or by means of artificially triggered events to commission the PCS response.

The density control needs to be tuned for divertor operation using both gas dosing and pellet fuelling. Once pellets are actually being produced and injected, plasma operation will be required to validate the quality of the pellets entering the chamber. Tests will be necessary for pellets of different sizes.

Substantial commissioning of the DMS system will be performed at 3.5MA divertor operation, as outlined in section 2.5.4.6.1. Commissioning of the H&CD systems (ECRH and ICRF) will also be launched; ECRH having been restricted to plasma initiation and burn-through in the early phase of operation. ECRH will be used in the optimization of the plasma initiation and current rise, while ICRF will initiate the first coupling studies (short pulse). Commissioning of the H&CD systems with plasma is outlined in section 2.5.4.5.

2.5.4.2.5 Time required for obtaining routine divertor operation at 3.5 MA/2.65 T (hydrogen)

During this first period of operation, in particular, the main activities relate to the commissioning of systems. Table 2-5 provides estimates of the time required to implement the main tasks at 2.65 T in hydrogen.

Table 2-5 – Estimates of experimental time required for initial activities at 2.65 T

Deliverable	Description	Time required (days)
Plasma initiation	At 2.65 T, hydrogen: optimize gas, PF coil bias, and timing; EC power scan: start with ohmic breakdown, and then add EC; document robust operational range; optional: optimization for 5.3 T or helium.	7
2 MA limiter	The first demonstration of plasma magnetic control together with an assessment of heat loads to first wall; error field correction.	11
3.5 MA limiter	Optimization of VS control at higher elongation; check gap control.	11
3.5 MA divertor	Optimize shape control to full bore plasma operation; optimize current rise and current ramp-down; commission event handling; commission basic wall protection.	28
		57
Parasitic to the main deliverables		
Density control and fuelling	Optimize density control in limiter configuration using gas dosing; commission density control for divertor plasmas including pellets.	(9)*
1st DMS tests	Disruption studies in limiter plasmas at 2 MA and 3.5 MA, including RE studies; disruption forces and their mitigation in divertor plasmas at 3.5 MA; document disruption forces (mitigated and unmitigated).	(15)**
Heating	ECRH for plasma initiation, short pulses (<1 s) of ECRH in limiter and divertor plasmas; start of ICRF coupling and voltage stand-off studies.	(15)**

** Included in time required for limiter and divertor commissioning.*

*** Detailed (and counted) in other sections of the IRP.*

2.5.4.3 Validation of diagnostic data and demonstration of measurement consistency

As discussed in section 2.4, diagnostic calibration and validation activities will be initiated during Integrated Commissioning (e.g. magnetic measurements, neutral pressure measurements etc.). Subsequently, following FP, but before the blanket modules are installed, extensive measurements will be made of the (toroidal) magnetic axis of the toroidal field to align the blanket modules (see section 2.4.3), which will already require validation and demonstration of measurement consistency of the magnetic field measurements with modelling of the field in the absence of eddy currents. With FP, there will also be the opportunity to validate and demonstrate the measurement consistency between the magnetic diagnostics and modelling, including eddy currents in the conducting structures. From early in PFPO-1, as each of the diagnostics is commissioned, their measurements will need to be validated and the consistency between various measurements will need to be demonstrated, particularly for control and investment protection functions. This validation and consistency process will continue throughout all the operational phases as the installed diagnostic capability expands.

Once routine operation is underway, the process for the data validation will not require dedicated plasma time for the majority of the cases. Detailed commissioning and validation plans for the diagnostic systems are not yet fully developed, but it is expected that many systems can be commissioned, and their data validated and cross-checked, under the standard plasma scenarios which will be operated as the experimental program develops.

Nonetheless, dedicated pulses for diagnostic commissioning are included in the planned run-time estimates and progress to the target plasma scenario will be performed in steps after diagnostic validation. For example, plasma boundary and equilibrium reconstructions will be used to check the consistency of magnetic measurements from different poloidal and toroidal locations once the plasma current exceeds several MA, to ensure adequate signal-to-noise ratios in the magnetic measurements. Plasma shape and position control require verification that the accuracy of the plasma boundary calculation is within the expected uncertainties. Plasmas with sufficiently large plasma-wall gaps for limiter plasmas will be established before operation of configurations with the full bore reference shape is undertaken. Similarly, before achieving an acceptable plasma control, the full equilibrium reconstruction is required to allow isoflux control. Transitions from limiter to diverted plasma will then be designed to guarantee the protection of the in-vessel components against uncertainties in plasma shape.

After achieving sufficient levels of plasma current and density, comparisons of Thomson scattering and interferometer density measurements, for example, will be used to cross-calibrate the various density measurements and ensure consistent densities, including synthetic diagnostic modelling to simulate the expected signals within the estimated inversion errors of chord-averaged measurements compared to local measurements. Similarly, comparisons of kinetic pressure derived from measurements of electron and ion temperatures and densities will be made with magnetic measurements of the plasma stored energy to check diagnostic consistency. With the beginning of plasma heating, measurements of the ion temperature and of the current profile will assume increasing importance, though the measurement capability in this area will be limited (see Appendix H, section H.3) until PFPO-2, when the HNB, DNB, Charge Exchange Recombination Spectroscopy (CXRS) and Motional Stark Effect (MSE) systems will be operational. Diagnostic cross-calibrations and absolute calibration certainly will also require some time.

Overall, diagnostics required for investment protection will also have to be rigorously validated and checked for consistency across multiple measurements. Plasmas with reduced risk for investment protection will be used until accurate data validation and consistency have been obtained. For example, the plasma shape will be cross-checked with visible camera images that will provide the contact point during the limiter phase and the strike-point locations during diverted operation.

During the PFPO-1 phase, as additional diagnostics come on line and plasma conditions and durations improve, diagnostic data validation will work towards applying automatic procedures to compare different measurements of the same parameter, using data from different locations or derived from different methods of measuring the same or similar parameters, or using comparisons of synthetic diagnostic models. Automatic routines will check measurement consistency among different diagnostic signals and provide firstly off-line, and eventually real-time, validation of signals within the plasma control system simulation platform (PCSSP), to allow the replacement of signals that are inconsistent and to ensure valid signals, particularly for plasma control and investment protection functions.

More sophisticated models of the plasma behaviour will also be used within the Integrated Modelling and Analysis Suite (IMAS) to check measurement consistency with the expectations from modelling. Any discrepancies will be used to help validate measurements from different

diagnostics or to improve synthetic diagnostic modules and theoretical models. As more diagnostics are brought into full operation and increasing levels of additional heating power are commissioned throughout the PFPO-1 phase, it will be possible to check the consistency of more sophisticated measurements and the associated models of plasma behaviour, including particle and energy transport models, whose validation and consistency are required both to ensure reliable operation in later operational phases and to provide a detailed understanding of physics processes in burning plasmas. This activity will therefore be essential preparation for subsequent high plasma performance operation and fusion power experiments.

Based on experience in current devices, 10 run days have been allocated in PFPO-1 for dedicated diagnostic commissioning, but, as noted above, the diagnostic commissioning and validation activities will be considerably more extensive than implied by this figure.

2.5.4.4 Commission control, interlock and safety systems

2.5.4.4.1 Plasma Control (Conventional control)

During initial operation in PFPO-1, all of the basic control functions will be commissioned as well as commissioning/verification of the PCS supervisory monitoring functions, event handling logic, and the interaction with the CIS. All technical commissioning that can be carried out without plasma for PCS control of the actuators, the communications among plant systems, supervisory systems, and the PCS failure monitoring will be performed before plasma operation.

The strategy for PCS commissioning in PFPO-1 will be aligned with the overall logic of the Research Plan, consisting of three stages with two options for further development:

1) commissioning of magnetic control up to robust diverted operation at 3.5 MA/2.65 T;

2) commissioning of magnetic control up to 5 MA/2.65 T;

3) commissioning of magnetic control up to 7.5 MA/2.65 T;

further development option 1) H-mode operation at 5 MA/1.8 T to commission initial ELM control techniques; and option 2) commissioning of magnetic control up to ~10 MA/5.3 T, initiating the development towards 15 MA L-mode operation, which depends on progress in the development of disruption and runaway mitigation. This phase will first commission initial plasma current, position and shape control with limited plasmas, followed by diverted plasma operation and the commissioning of reliable vertical stability control at high elongation. Equilibrium reconstruction will be required in the first phase as well as error field control, particularly to correct for n = 1 error fields. Density control will be commissioned for both gas and pellet fuelling. ECRH breakdown assist will need to be recommissioned with the beryllium first wall and divertor, and ECRH control will also need to be commissioned for burn-through, heating during the plasma current flattop and during the ramp-down. ICRF commissioning of the first antenna will include plasma position, shape, and localized edge density control to optimize ICRF coupling. Further commissioning will bring the ECRH power up to 20 MW and the ICRF up to 10 MW. If the H-mode threshold is within the available power of $\leq$ 30 MW, first H-mode operation may be developed at 5 MA/1.8 T, allowing first tests of ELM control with pellet pacing and with a subset of the ELM control power supplies. Initial forecasting and event handling schemes will be developed to anticipate controllability boundaries and to allow evasive actions, to optimize plasma operation and avoid disruptions. Depending on the development of disruption and runaway electron mitigation techniques, magnetic control commissioning could be extended up to ~10 MA at 5.3 T toward the end of the PFPO-1 campaign.

Magnetic control

Control functions:

- Plasma initiation with feedback control on the prefill neutral pressure;
- Current, shape, and position control (including current saturation avoidance techniques);
- Vertical stability control (with and without in-vessel coils);
- Plasma boundary control through L-H and H-L transitions for H-mode operation;
- Commissioning of error field correction with the dedicated error field correction coils.

A primary objective will be to develop the capability to properly control the shape of the plasma through all the plasma pulse phases including transitions and to guarantee the required plasma-wall gap clearances.

At the outset, real-time plasma boundary reconstruction and the vertical stabilization system will be commissioned and validated using real-time plasma simulation techniques in PCSSP so that their operational commissioning can begin with the pulses foreseen from the FP campaign. It will be prudent to use larger plasma-wall clearances and a substantial margin on vertical stability until the necessary control techniques can be fully validated and optimized.

Density control

Control functions:

- Gas injection system commissioning including calibration and validation of the models used in control simulations;
- Pellet injection technical commissioning with plasma (availability of a measurement of the pellet entering the vessel is not confirmed at the time of writing this document);
- Validation of the feedback control loop: multiple scenarios by means of single to multiple valves; the use of the pellet injection for density control should be commissioned as well (reduced configuration of the system);
- Validation of the density control schemes by using different diagnostics inputs.

H&CD system control

Starting with technical commissioning:

- Technical commissioning with plasma (i.e. 20 MW EC power injected for a short time);
- ECRH technical commissioning: commissioning and validation at low power of the control of the local deposition;
- ICRF (one antenna): technical control for power, antenna phasing and frequency sweeping; initial power coupling control development; IC for wall conditioning.

Initially, the ECRH control system will be tested without plasma, i.e. launcher setting, polarization setting, polarization adaption as launchers move. This should be tested with a low power source up-stream of the polarizers. This also includes an experimental verification of the assumed propagation of the polarizations through the network of waveguide switches. The interaction of PCS with the lower-level EC-launcher and polarizer control can (in principle, though not necessarily in practice) also be tested with the vessel open (safety measures around the moving launchers should be implemented). Testing power switching by the PCS may be possible into dummy loads.

With plasma, polarization shall be optimized by minimizing the non-absorbed power as detected by the infrared view of the respective HFS area. This may have to happen already at low plasma current. The deposition is verified by power modulation and comparison to Fourier-transformed

Electron Cyclotron Emission (ECE) measurements. If X3-heating is significant, this is the point to decide if the toroidal field shall be raised by 0.1 T or if the equatorial launcher shall be used in O-mode at 2.65 T (weak Electron Cyclotron Current Drive (ECCD)). Interlocks will have to be tested with plasma; these may include interlocks to impose lower limits on plasma current, density, electron temperature (in case of X3 or O2 heating). Stray radiation monitoring with a large number of ECRH sniffer probes at various poloidal and toroidal locations is planned. The in-vessel elements of the ITER ECRH system will be, in many respects, similar to those of the new W7-X system, which has started operation (10 MW, 2000 s). It is strongly recommended to take advantage of the experiments that will be undertaken at W7-X during the next five years to gain experience for ITER. A potential safety issue relates to possible damage to the vacuum window, which requires a priori testing of the respective safety system (close fast valve, switch off beam).

Exception handling

Requires:

- Commissioning of the event handling system logic (this phase requires commissioning/validation each time a new logic implemented);
- Commissioning of the algorithms/data processing for event detections (i.e. vertical stability margin for VDE avoidance, island tracking technique and diagnostics required later for NTM suppression, etc.).

Note that each new exception handling event and algorithm will require commissioning to implement it in the system.

Real-time recognition of off-normal events, such as the development of a significant population of runaway electrons or approaching the predicted boundary for vertical stability, and the automated initiation of counter measures, including discharge termination, should be validated and introduced into operation as soon as practical. Real-time protection for critical PFCs will need to be commissioned as a prerequisite for sustaining reliable operation in the next phase in which the power and energy input will increase. These functions will be included in the plasma control system functionality but an additional level of protection will be included in the central interlock system, to protect against plasma events, with a high level of integrity.

Since the ITER Plasma Control System (PCS) will have an unprecedented level of sophistication, it is clear that commissioning of its more complex functions will continue in parallel with plasma operation throughout much of the experimental program. The PFPO-1 phase will lay the foundation for an extensive program in plasma control, complementing progress in the science program as the required level of fusion plasma performance is developed to achieve ITER's goals.

2.5.4.4.2 Commissioning of the interlock system

The investment protection system is a collection of dedicated Plant Interlock Systems (PIS) and a Central Interlock System (CIS) to protect against exceeding operational limits, to ensure that the systems and components are protected against self-induced faults, faults generated by other systems and unintended consequences of plasma operation.

The following steps will be taken to validate the interlock system:

- Technical commissioning (communication);
- Commissioning of the interlock trigger from each of the plant systems;
- Commissioning of the diagnostics used for operations (i.e. cameras);
- Commissioning of the PCS-CIS interface;

- Commissioning of the avoidance/mitigation activities in coordination with the PCS (i.e. plasma stop and termination by means of CIS trigger);
- Commissioning of the dedicated diagnostics including links with the CIS.

The operation of DMS via CIS for PFPO-1 is discussed in detail in section 2.5.4.6.

While the PCS will act as the first line of defence for investment protection, the CIS will always back up the PCS for ultimate investment protection even for complex functions during plasma operation, including first wall and divertor heat load protection. With each step up in plasma current and heating power, at least one day of run-time dedicated to commissioning first wall and divertor protection is included in the estimated run-time.

2.5.4.4.3 Safety System commissioning

For ITER, a set of use cases has been identified where the plasma is either involved in or affected by safety functions. It is then mandatory to demonstrate that the safety events are detected and the corresponding actions are performed. At present the only action associated with a Safety event during operation is the activation of the Fusion Power Shutdown System (FPSS). The system has to be tested eventually during dedicated plasma operation, probably with reduced performance to avoid the risk of damage to internal components. Additionally all the critical event detection has to be validated and tested similarly to the approach expected for the investment protection functions.

At present the only Protection-related (i.e. safety-related) plasma parameter is the plasma current. No formal decision has been made on the functionality of this parameter but commissioning and validation for the plasma current measurement is expected as well as for the associated safety system function.

2.5.4.4.4 Control commissioning deliverables

For PFPO-1, the control commissioning deliverables include:

- Plasma initiation with the beryllium first wall and tungsten divertor at 2.65 T in hydrogen; including neutral prefill feedback and ECRH breakdown control;
- Initial CIS plasma operations related functions;
- Plasma current, position, and shape control for limited plasmas to 3 MA;
- Real-time equilibrium reconstruction;
- ECRH control for burn-through and heating during the plasma current flat-top and ramp-down;
- Plasma current, position, and shape control for 3.5 MA/2.65 T diverted plasma;
- Vertical stability control to 3.5 MA/2.65 T;
- Density control with gas and pellet injection;
- Error field control, particularly to correct for n=1 error fields;
- Further commission CIS plasma operations related functions;
- Plasma current, position, and shape control up to 5 MA/2.65 T;
- ECRH operation at powers of up to 20 MW;
- First ICRF antenna, including plasma position, shape, and localized edge density control for ICRF coupling;
- ICRF operation at powers of up to 10 MW.

2.5.4.5 Heating & Current Drive (H&CD) commissioning (ECRH, ICRF) in plasmas up to 7.5 MA/2.65 T

The four-stage approach foresees the installation of the full ECRH system and a possible acceleration of the ICRF system implying the installation of one IC antenna, in advance of the PFPO-1 campaign, presently under study. The full ICRF system, the HNB and DNB will be installed in advance of PFPO-2. The H&CD commissioning schedule is directly linked to this plan. Each H&CD system requires a commissioning period without and with the plasma. The present analysis focusses, for the most part, on the H&CD commissioning with the plasma, together with the risk assessments and necessary diagnostics and control.

ECRH commissioning:

The early ECRH commissioning has to be undertaken prior to FP and is described in 2.4. The PFPO-1 phase will benefit from the full ECRH power capabilities, i.e. the set of 24 gyrotrons delivering a total EC power of 20 MW. As described in Appendix G, three options are considered: 1) 24 single-frequency gyrotrons at 170 GHz; 2) At least 16 single-frequency gyrotrons at 170 GHz and up to 8 dual-frequency gyrotrons at 104-170 GHz; 3) At least 16 single-frequency gyrotrons at 170 GHz and up to 8 single-frequency gyrotrons at 110 GHz. The two last options are foreseen to enable second harmonic assisted breakdown (X2) and plasma pre-heating in case of operation at 1.8T. At this stage where these options are still under investigation, the three of them have to be considered in the commissioning plans. All gyrotrons are assumed to be conditioned up to the torus windows ahead of the operation with plasma. The ECRH commissioning should demonstrate the following capabilities:

- Demonstration of local deposition (correct polarization, separately for each gyrotron and frequency) with an appropriate launcher control. If the deposition initially occurs at an unexpected location, reasons may be manifold (launcher angles, X3 parasitic absorption, ray tracing parameters, equilibrium, mapping routines, analysis of ECE data, …).
- Launching 20 MW at short pulse via the equatorial launcher (EL) and/or the upper launchers (ULs).
  Short pulse conditioning of all beam lines and parallel operation of all gyrotrons (screening of interference of magnetic fields) and power supplies shall be demonstrated, along with the full power capacity of launchers. It is important to use all beams of one launcher since internal stray radiation adds up. These launchers will not have operated with more than one beam at a time before they are installed. Sufficient time needs to be allocated for this conditioning.
- The effect of X3 heating at 2.65T for the equatorial launcher shall be checked. If crucial, the magnetic field may need to be increased by 2-4% or the EL polarization to be changed from X- to O-Mode.
- The X1 reflection for O1 heating scheme at 5.3 T has to be proven to be lower than 1%.
  If the 1st harmonic is used for heating (high fields in ITER) then O-mode is required. Any cross-polarized fraction will be reflected back at the X-Mode cut-off focussed on the LFS-vessel-wall. ITER assumes 1% cross polarization corresponding roughly to a power density of 1-10 MWm^{-2} at the location of the first reflection on the outer wall. Such an optimistic estimate is the basis for the window design. Windows are typical components endangered by incompletely absorbed EC-beams. ITER has to demonstrate here that these design values for cross polarization can be matched (or that no window is hit by one of the reflected

beams). A proper detection of the absolute amount of cross polarization needs to be developed. In present day devices cross polarization has been demonstrated to be below 3 % close to the resolution limit. Since ITER will use stray radiation bolometers, it may be possible to sweep the reflection toroidally across such a device ramping the density in the plasma, but this scheme needs further assessment.

- Long-pulse heating above 50 s shall be achieved. At this stage, the whole ECRH system and the ITER vessel are cooled. The cooling is designed on the basis of predefined heat-fluxes. On thin metal surfaces directly on top of the cooling channels (beam scrapers, etc.) no problems are assumed, since those loads are well defined. There are usually regions more distant from the next cooling channel for which a certain temperature gradient is allowed to remove a typical average energy input. Any anisotropy of the surface heating of a substantial fraction of 1 MWm^{-2}, which is the average neutron energy absorption in the wall, may increase these gradients on long time scales finally leading to hot spots. These possible issues need to be detected and ameliorated before the nuclear phase. Spill-over losses due to a large asymmetric mode content also need to be addressed (5% are allowed, which allows for example beam shapes with 2 maxima).

As stated above, for the PFPO-1 campaign the full ECRH system will be commissioned with the plasma, i.e. the 24 gyrotrons, delivering a maximum power of 20 MW, using both the ULs and EL. This commissioning duration is expected to be around 75 days. It will mostly be carried out in 7.5 MA/2.65 T scenarios, with 2nd harmonic X-mode ECRH absorption, requiring a low density and modest temperature ($n \sim 10^{19}$ m^{-3} and $T \sim 1$ keV) to achieve full absorption of the ECRH power. This commissioning period does not need to be exclusive and could be associated with other plasma operations. The ECRH commissioning plan will consist of the following steps:

- Progressive increase of the ECRH power from 1 to 20 MW;
- Progressive increase in the pulse length from 10 ms to 10 s;
- Commissioning of the beam polarization sweeping by steering the mirrors to their full range; this requires around 5 sweeps per beam (8 beams for each of the 4 UL and 24 beams for the EL), requiring 3 s for one mirror sweep – the operational constraint is the necessity of constant plasma parameters during a 3 s sweeping period;
- Launchers are slowly conditioned to long pulses, with a growing factor of 1.4 for the pulse duration, up to a duration of ~ 50 s; multiple launcher commissioning is possible in the same pulse;
- Power modulation capability needs to be tested during this commissioning period.

Further ECRH commissioning time will probably be necessary as the toroidal field is raised towards 5.3 T, for which the heating scheme would be fundamental O-mode absorption. As the plasma scenarios are developed towards higher current and field, it will be necessary to switch from the 2nd harmonic X-mode heating scheme to the fundamental O-mode scheme. In addition, the option for operating at a toroidal field of 1.8 T would require an allocation of further commissioning time to the ECRH system.

The ECRH commissioning requires the measurement of electron temperature profiles, and density profiles, the latter associated with real-time ray-tracing modelling needed to predict the wave propagation properties during the discharge and, if necessary, to trigger a controlled shutdown of the ECRH to avoid wall damage. Clearly magnetic reconstruction is also needed – at some point an accurate determination of the radial localization of the principal rational q-surfaces will also be required to deal with the growth of NTMs (a more detailed assessment of the stage of the experimental program at which NTMs are likely to appear is necessary).

Risks associated with ECRH system commissioning are mostly due to stray radiation emitted during breakdown and burn-through phases. Errors in the polarization setting and localized density fluctuations at the separatrix (e.g. due to ELMs) could induce extra radiation losses within the main chamber, possibly leading to some PFC damage.

ICRF commissioning:

Feasibility studies on accelerating the ICRF system to provide an antenna delivering 10 MW of power during PFPO-1 are underway, as described in Appendix G. Nevertheless, the present assumption for the development of the IRP (agreed by ITER management) is that one ICRF antenna will be operational in PFPO-1 and two antennas will be operational for PFPO-2. The commissioning of the ICRF system must therefore begin during PFPO-1. Further commissioning is, of course, required during PFPO-2 in order to test the cross-talk of the two antennas and to adjust the matching for H-mode operation.

Some ICRF commissioning will be carried out in vacuum prior plasma operation; antenna conditioning at high voltage in vacuum is necessary: (i) to confirm the operational strategy for avoidance of multipactoring conditions and (ii) to condition the system progressively to high RF voltage, using trains of short pulses of increasing voltage, in order to establish the reliable maximum operating voltage, for all foreseen operating frequencies.

The start of the commissioning of the ICRF system with the plasma will take place at half-field. Part of this commissioning does not need a particularly efficient ICRF heating scheme, hence it can be started in hydrogen and carried on in helium plasmas[3]. The commissioning period with the plasma is estimated to be around 2 to 4 weeks, and can be supplemented by commissioning during plasmas targeted at other goals. The commissioning of the ICRF system will be mostly carried out in L-mode, but extra commissioning time will be required in H-mode plasmas (hence mostly in PFPO-2), as described in section 2.5.5.2. The commissioning can be split into two different categories, early and advanced commissioning. Early ICRF commissioning is discussed here while advanced commissioning is split between this section and section 2.5.5.2, since some of the activities imply the presence of the two antennas and L-H transition capabilities.

ICRF early commissioning (requires 5 to 20 s pulse dedicated time):

- Assessment of the antenna coupling and behaviour of the automatic matching system on plasma completing the commissioning of the relevant algorithms with CODAC, at low power;
- Dedicated tests of the arc detection system, an essential component of the ICRF system protections, to be validated both in L- and H-mode plasmas;
- Test of the common antenna phasing, i.e. dipole, current drive and 00ππ phasing;
- Test of the real-time frequency sweeping capability (± 1 MHz);
- Test of the power modulation capabilities.

ICRF advanced commissioning (requires ~ 60 s pulse dedicated time and thus will be addressed as the development of long pulses allows):

- Progressive increase of the coupled power;

[3] In H plasmas at 2.65 T, the envisaged ICRF heating scheme relies on direct electron heating by the fast magnetosonic wave, for which wave absorption is less efficient than with the minority heating schemes available in other plasmas or at higher magnetic fields. In He plasmas at 2.65 T, the envisaged ICRF scenario is fundamental minority H heating, which is an efficient heating scheme.

- Progressive increase in pulse length: test of long-pulse operation at high power;
- Demonstration of RF coupling control via gas puffing and control of the gap between the separatrix and the antenna in L-mode;
- Assessment of the production of impurities by ICRF;
- Assessment of the compatibility of impurity gas puffing, used for divertor protection, with the ICRF coupling performance in L-mode;
- Test of the effect of 3-D fields (ELM coils) on the RF coupling and heat loads; first wall and divertor protection with ICRF heating, i.e. localized loads due to fast particles, must be verified.

Additional commissioning time could be required for 1.8 T scenarios where the ICRF heating scheme would be 2nd harmonic fundamental H heating (primarily in H plasmas, but possibly also in He plasmas, although the efficiency of ICRF schemes in He plasmas at 1.8 T has not yet been fully assessed).

Several risks are associated with this commissioning. There is a possible antenna multipactoring issue that could pose a risk to the ICRF system. Uncertainties on RF-sheaths for a given strap configuration are large and this effect could lead to further localized wall erosion damage via impurity acceleration. Uncertainties on the SOL density and on the distance between the separatrix and the antenna lead to uncertainties on the RF coupling performance. Successful commissioning will require the monitoring of the antenna front face by the visible and infrared cameras, and availability of the RF arc-detection system. Finally, control of the minority ion concentration will be desirable to adequately implement the desired heating scenarios. The overall operational range of the H&CD systems is summarized in Figure 2.5-1 where low toroidal magnetic field (1.8 T) scenarios are also included.

2.5.4.6 Disruption management program in PFPO-1

This section describes the experimental program required with respect to disruption prediction, avoidance, mitigation and loads. It is important to note that the program elements described here are strongly interlinked with each other and with other elements of the Research Plan. Especially, scenario development and the gradual increase in plasma current will have to go hand in hand with the disruption alleviation activities listed here. Capabilities for disruption forecasting and avoidance and their commissioning in PFPO-1 will be covered in section 2.5.4.8.

2.5.4.6.1 Disruption Mitigation System (DMS) commissioning/optimization

The present design of the DMS results in a multi-dimensional parameter space for the mitigation scheme. Multiple injectors in several locations with different injection quantities and species compositions for thermal load mitigation and for runaway electron suppression will be available [Baylor, 2015; Maruyama, 2015]. It is expected that by the time the commissioning work with plasma will start, the parameter space will be narrowed down with the experience gained from present devices. Nevertheless, it is highly likely that achieving all disruption mitigation goals will only be possible with fine adjustments of the injection parameters during ITER operations and therefore a substantial number of dedicated pulses to disruption studies will be required in PFPO-1 and PFPO-2. Also, the risk involved if mitigation is not complete during the optimization activities requires a careful and thus pulse intensive approach. Note that due to uncertainties in the DMS design and the most optimal injector set, the final configuration of the injectors may still evolve over the next few years.

Commissioning and optimization of the DMS aims at: *(a) Thermal load mitigation, (b) Electro-magnetic (EM) load mitigation*, and (*c) RE avoidance validation.* The commissioning work in PFPO-1 will start at low current and 2.65 T to reduce risks during the initial phase of DMS usage. The commissioning program will be strongly interlinked with the gradual increase in plasma current when developing plasma scenarios. For validation of runaway suppression it will also be important to run at toroidal field of 5.3T and low plasma current early in PFPO-1.

(a) Thermal load mitigation

Thermal loads are caused by both the plasma thermal energy loss during the thermal quench and by conductive losses of the magnetic energy in weakly radiating current quenches. In both cases, the mitigation strategy aims at radiating a large fraction of these energies. Whereas the high-Z quantities required to radiate the magnetic energy on the timescale of the current quench is expected to be low and compatible with EM load limits, the number of particles required for the thermal quench is uncertain and might be in conflict with allowable current decay times (see also 2.5.4.6.2). In both cases, the quantities have to be validated and the injection scheme has to be adapted if required. The compatibility of the thermal load mitigation scheme with the runaway avoidance scheme is mandatory. The margin to runaway formation has to be kept large enough while optimizing thermal load mitigation.

The following Milestones have to be achieved in PFPO-1:

2.5.4.6.1.1 Confirmation of current quench heat load mitigation for 7.5 MA operation

Prerequisite to run 7.5 MA scenarios.

Experimental strategy:

- Confirm mitigation in target plasmas of varying magnetic energy, starting at low plasma currents;
- Confirm required quantities and injection scheme to achieve 100% radiated power fraction during the CQ;
- Validate compatibility of heat load mitigation with RE avoidance scheme.

2.5.4.6.1.2 Confirmation of thermal quench heat load mitigation in L-mode

Prerequisite to run at thermal energies above melt thresholds.

Experimental strategy:

- Confirm mitigation in target plasmas of varying thermal energy in L-mode;
- Confirm required quantities and injection scheme to achieve high radiation fractions during the thermal quench;
- Validate compatibility of heat load mitigation with RE avoidance scheme and EM load mitigation scheme.

(b) EM load mitigation

EM load mitigation aims at reducing the halo current amplitude and asymmetry during VDEs while keeping the current quench slow enough to not exceed limits on eddy current forces on in-vessel components. Model predictions have to be validated to allow projecting requirements towards higher energies.

The following Milestones have to be achieved in PFPO-1:

2.5.4.6.1.3 Confirmation of EM load mitigation scheme for 7.5MA operation

Prerequisite to run 7.5 MA scenarios.

Experimental strategy:

- Confirm mitigation in target plasmas with varying magnetic energy vertically stable and in deliberate VDEs;
- Confirm dependency of current quench rates on injected quantities, species and on the injection scheme;
- Validate halo current mitigation goals;
- Validate compatibility with RE avoidance scheme.

The DMS commissioning activities, as well as the validation of EM loads during disruptions, will require operation at 5.3 T as early as possible and preferably in the early phase of PFPO-1, during limiter operation with currents up to 3.5 MA and during x-point operation with up to 7.5 MA.

(c) RE avoidance validation

Of high priority during DMS commissioning is to establish a mass injection scheme that guarantees the suppression of runaways to acceptable limits. Due to the severe energy loads that can be caused in case of substantial runaway formation, the initial tests of the operational space of the DMS with respect to runaway generation have to be performed at currents of the order of 2-3 MA. The limiter configuration and a high B_t will provide the most favourable conditions for runaway formation and are thus the worst case testbed [Reux, 2015]. As extrapolation from these conditions to higher currents has non-negligible uncertainties, further tests to validate the mitigation scheme with respect to runaways have to be done at higher currents. These tests will require proceeding in small current steps, which has been taken into account in the required number of pulses for DMS commissioning.

The following Milestones have to be achieved in PFPO-1:

2.5.4.6.1.4 Confirmation of the injection scheme with maximum margin to RE formation

Prerequisite for using the DMS in closed-loop operation.

Experimental strategy:

- Gradual increase of B_t to 5.3T at 3.5 MA in limiter configuration;
- Variation of injection species and injection scheme towards thresholds for RE formation.

2.5.4.6.1.5 Confirmation of the margin to RE generation in diverted configuration

Prerequisite to use DMS in closed-loop operation above 3.5 MA in divertor configuration.

Experimental strategy:

- Target plasma of 3.5 MA at 2.65 T in divertor configuration;
- Variation of injection species and injection scheme towards thresholds for RE formation starting from confirmed scheme for limiter configuration.

The estimated number of pulses/days required for DMS commissioning/optimization in PFPO-1 is 560/43.

2.5.4.6.2 Disruption Load Validation

Validation of the heat loads and their scaling with plasma parameters is essential to define the requirements for mitigation in terms of mitigation efficiency, but also in terms of the prediction success rates and false alarm rates of the disruption prediction and detection system which will be part of the PCS with the aim of triggering the DMS. Establishing scalings of VV and BM electromagnetic loads is a prerequisite in order to go to higher plasma currents within the progressive start-up approach. Disruption models will help to achieve a high accuracy towards higher currents and to reduce the number of experimental data points needed to establish the scaling. Model validation will be therefore an integral part of this work. These models will be especially important if thermal and electromagnetic loads make it necessary to limit the maximum current for unmitigated disruptions in order to avoid unacceptable damage to the first wall or the divertor and to avoid the occurrence of category III electro-magnetic loads on the VV.

The following Milestones have to be achieved in PFPO-1:

2.5.4.6.2.1 Confirmation of EM load scaling models

Prerequisite to increase current beyond 7.5 MA.

Experimental strategy:

- Variation of plasma current at 2.65T over a range sufficient for projecting to 15 MA, but considering possible melt damage at higher current levels;
- Measurements of halo currents and forces/displacements on components including the VV during deliberate VDEs;
- Confirm predicted asymmetry and dynamic amplification;
- Confirm impact of plasma parameters e.g. internal inductance, elongation, current.

2.5.4.6.2.2 Confirmation of melt thresholds for thermal loads during the current quench

Prerequisite to increase the plasma current above the predicted critical current of about 6 MA.

Experimental strategy:

- Monitoring of first wall heat fluxes during upward and downward deliberate VDEs with gradually increasing plasma current.

2.5.4.6.2.3 Confirmation of melt thresholds for the divertor

Prerequisite to increase the thermal energy beyond the predicted critical energy of 25 MJ.

Experimental strategy:

- Deliberate major disruptions and downward VDEs with gradually increasing thermal energy.

2.5.4.6.2.4 Confirmation of melt thresholds for the first wall

Prerequisite to increase the thermal energy beyond the predicted critical energy of 50 MJ.

Experimental strategy:

- Deliberate upward and downward VDEs with gradually increasing thermal energy;
- Possibly conduct post-thermal quench mitigation if higher currents are required to prevent excessive current quench heat loads.

The estimated number of pulses/days required for Disruption Load Validation in PFPO-1 is 130/10.

2.5.4.6.3 Disruption Mitigation System (DMS) trigger generation

Achievement of the target disruption rates requires the development of avoidance and prevention strategies, whilst the ability to attain the target mitigation rates depends on the development of reliable prediction schemes. In early operation, disruption prediction will start with basic threshold-based indicators such as mode amplitudes. As operation moves to more complex scenarios, the predictor will have to be adapted and more input signals will need to be added. As mentioned above, the requirements on the mitigation success rate for the loads during the current quench are extremely demanding when 15 MA operation is approached. These rates will be achieved by adding also indicators that a disruption is ongoing, such as the vertical plasma position or the current spike at the thermal quench [Pautasso, 2016]. Statistical methods such as SVM require training, but present developments are focussing on reducing the size of the training set and to improve portability. Such schemes can complement threshold-based approaches. Approaches using physics-based models including real-time modelling and automated disruption event characterization are presently under development to further improve disruption prediction capability while minimizing false positive predictions for these new schemes. Such schemes will be fully-developed by PFPO-1 and will be exploited.

The disruption predictor within the PCS is a module that solely aims on deciding to trigger the DMS. Different injection schemes may be chosen to optimize the mitigation action for various disruption situations. The PCS will also be responsible to decide about the injection scheme based on plasma parameters, plant system status and DMS status. Note that the Central Interlock System (CIS) can, upon input from plant systems or from the plasma current measurement, also initiate a mitigated disruption by triggering the DMS. In that case the injection sequence will either be the latest issued by PCS or a default sequence. Testing and defining the injection sequences are part of the DMS commissioning work.

Targets for disruption rates and mitigation success rates have to be defined as mentioned in 2.3 when taking steps in plasma current or thermal energy. However, confirming that these targets are achieved before taking the next step in performance cannot be done by a statistical approach since this would require too many pulses or disruptions. Therefore, it will be mandatory to assess the effectiveness of the chosen prediction algorithms by dedicated tests accompanied by modelling validation. Within the threshold-based approach, it is expected that the database from present experiments allows knowing the relevant parameters to consider in the threshold tests and to narrow down threshold values based on validated scalings, physics-based modelling, and event characterization analysis. Sufficient operational time has been planned to establish and test the algorithms in ITER.

The following Milestones have to be achieved in PFPO-1:

2.5.4.6.3.1 Disruption detection ready for high current operation

Prerequisite to increase current beyond the cat. III threshold. The required reliability depends on the expected loads and might vary for different plasma currents (c.f. sections 2.3 and 2.5.4.6.2).

Experimental strategy:

- Establish algorithms for detecting the thermal quench, the start of the current quench and a vertical displacement;

- Test the algorithms during low current operation and deliberate disruptions, if necessary.

2.5.4.6.3.2 Thermal quench prediction sufficient for L-mode operation

Prerequisite to run high energy L-mode beyond the melt threshold. The required reliability depends on the expected loads and might vary for different thermal energies (c.f. sections 2.3 and 2.5.4.6.2).

Experimental strategy:

- Establish threshold-based algorithm for predicting the thermal quench;
- Implement statistical methods and physics model-based methods in parallel;
- Perform dedicated disruptions to optimize the predictor if necessary;
- Implement and test decision schemes in the PCS for the injection sequence;
- Test the algorithms during low current operation and deliberate disruptions, if necessary.

2.5.4.6.3.3 Injection sequences ready for high current operation

Prerequisite to increase current beyond the category III threshold.

Experimental strategy:

- Establish injection sequences for early injection before the thermal quench (TQ) and for late injection into the CQ;
- Verify RE avoidance and current quench (CQ) mitigation efficiency.

2.5.4.6.3.4 Injection sequences ready for elevated thermal energies

Prerequisite to run high energy L-mode beyond the melt threshold.

Experimental strategy:

- Establish injection sequences for pre-TQ injection;
- Verify RE avoidance, TQ and CQ mitigation efficiency.

The estimated number of pulses/days required to establish the DMS trigger function in PFPO-1 is 135/11.

2.5.4.7 Development of reliable operation at 7.5 MA/2.65 T

2.5.4.7.1 Establishing 7.5 MA/2.65 T divertor plasmas with heating

Following the development of routine diverted plasma operation up to 3.5 MA and 2.65 T and the commissioning of disruption and RE mitigation, diagnostics, plasma control, interlock, and safety systems and initial commissioning of the ECRH and ICRF H&CD systems at relatively modest plasma current levels, plasma scenarios will be developed up to 7.5 MA at 2.65 T. The plasma scenarios will be initially developed in hydrogen, but a significant amount of operation in helium will also be required to commission and develop ICRF heating schemes, which may allow H-mode operation if the H-mode threshold is within the available power limit.

The first step will be to increase the plasma current to 4 MA at 2.65 T and further develop plasma current, shape, and position control in hydrogen. This is a small increase in current so that the development should be straightforward to quickly ensure robust magnetic and density control as well as improved disruption and RE mitigation. Depending on the level of error fields found due to coil manufacturing and installation tolerances, error field correction may also require further

development. Although it is a modest increase in current, routine operation at 4 MA is considered the next deliverable milestone.

The development of 5 MA, 2.65 T discharges will be a significant increase in plasma current that will approach the upper limits for which melt damage from unmitigated disruptions is not expected. Thus, at this stage, care will have to be taken assessing first wall heat loads following disruptions to ensure investment protection. Further development of plasma current, position, and shape control will be required including robust vertical stability control. Full commissioning of the ECRH and ICRF heating systems at this current level in helium plasmas would help to assess disruption heat loads at still relatively low plasma current. Plasma termination scenarios for both standard ramp-down and for emergency terminations will need to be developed at this stage to prepare for higher current operation. Routine operation of 5 MA plasmas is the next deliverable milestone.

A further increase in plasma current to 6 MA will require more development of plasma current, position, and shape control emphasizing robust vertical stability control at higher plasma current to minimize possible VDEs. Melt damage from unmitigated disruptions is expected at this current level and there is increased risk of damage from RE. Thus, particular attention will need to be paid to develop robust disruption and RE mitigation techniques. Further development of termination scenarios controlling impurity accumulation and vertical stability in the ramp-down will also be required. Routine operation of 6 MA plasmas is the next deliverable milestone.

Depending on the observed scaling of disruption forces and heat loads, it may be feasible to then develop 7.5 MA, 2.65 T scenarios, which will be the first scenarios at $q_{95} = 3$; care will be required in the development as such plasmas are expected to be more susceptible to disruption-inducing MHD phenomena. Plasma current, position, and shape control emphasizing robust vertical stability control will require further development. Core fuelling with pellet injection may be required at this current level. Central electron heating with ECRH and ICRF should be developed to control impurity accumulation in the core. Sawtooth control should also be developed as large sawteeth are expected at low q. Additional first wall and initial divertor heat flux control should also be developed at this stage. Advanced control commissioning that will include capabilities for disruption avoidance in PFPO-1 will be discussed further in section 2.5.4.8. Further development of plasma termination scenarios is required to avoid impurity accumulation and ensure vertical stability in the ramp-down. Routine operation of 7.5 MA, 2.65 T plasmas is the next deliverable milestone. The pulse duration of these scenarios should then be extended out to ~50 s in helium to provide a standard ITER scenario for development of the heating schemes. Since this scenario is the half current, half field equivalent of the baseline 15 MA, 5.3 T scenario, development of robust operation at 7.5 MA, 2.65 T is required to commission all systems in PFPO-1, particularly if the H-mode threshold were low enough in helium plasmas to fully develop H-mode operation and ELM control at $q_{95} = 3$.

2.5.4.7.2 Studies of off-axis ECRH at 7.5 MA/2.65 T

As discussed later in section 2.5.5.11, the plan to expand L-mode operation from 7.5 MA/2.65T to 15 MA/5.3T in hydrogen plasmas in PFPO-2 relies on several intermediate I_p/B_t steps with q_{95} = 3-4. This is also the basis for the development of L- and H-mode plasmas in FPO, as described in sections 2.6.3.4, 2.6.3.5 and 2.6.4. For several of the scenarios in the development sequence it will not be possible to ensure that the ECRH power will be deposited centrally and, for some extreme cases in this step ladder, $\rho_{ECRH} \sim 0.5$ (peak of the power deposition profile). This raises the question as to whether W accumulation may occur in such L-mode plasmas or not, thus potentially

increasing disruptivity. If this is the case, some steps in the initially proposed step-ladder will be omitted at the cost of larger changes of I_p/B_t between consecutive steps.

Due to the significant implications of this issue on the further development of scenarios in the IRP, an assessment is included in PFPO-1. In general the problem of W accumulation with off-axis heating is found to be more serious for H-mode conditions (including exit phases) than in stationary L-modes in present experiments, given the reduced edge transport in the former. It is, therefore, possible that by ensuring that the W divertor influx remains low in ITER (low sputtering and high prompt redeposition as discussed in Appendix C) W accumulation may not occur in L-mode plasmas even when ECRH heating is not fully on-axis.

The assessment will consist of a series of L-mode discharges at 7.5MA/2.65T with ECRH heating at a level of ~ 14-20 MW and a range of plasma densities ($<n_e> = 0.2 – 0.8 \times n_{GW}$) with pellet fuelling and gas fuelling. In these conditions the injection angle of the ECRH equatorial launcher will be adjusted from providing dominant central heating ($\rho_{ECRH} \sim 0.2$) to off-axis heating $\rho_{ECRH} \sim 0.5$ and W density and divertor plasma parameters/W influxes will be measured. The aims of the experiments are:

a) to determine which is the level of off-axis ECRH heating that, if exceeded, causes W accumulation, and

b) to determine if this level depends on divertor plasma conditions (influenced by the separatrix density) and/or core density profiles (modified by pellet fuelling compared to gas fuelling).

The total number of experimental days estimated to be required for this assessment is 3.

2.5.4.8 Advanced control commissioning in PFPO-1

Several control systems will need to be commissioned to support ITER physics research in the three primary research phases of the Staged Approach. These systems should aim to fulfil all commissioning tasks well before their intended use, and preferably one operational phase earlier than required to allow full system checkout under normal ITER operations. This will best reveal the practical requirements of each system beyond what is envisioned and planned for prior to their use in operation.

Once routine plasma operation is achieved and robust basic magnetic and kinetic control schemes allow standard plasma pulses to be easily reproduced, more advanced control functions can be commissioned. Advanced control here refers to control functions that go beyond basic plasma current, position, and shape control, beyond basic density control, and beyond basic heating system control. The more advanced control functions include kinetic control functions such as: first wall and divertor protection, β and stored energy control, rotation profile control, and minority species control; MHD and error field control functions such as: ELM, NTM, dynamic error field and RWM, and sawtooth control; and supervisory control functions including exception handling and more advanced actuator management functions. The physics requirements for all control functions of the PCS are described in the *PCS Physics Requirements Document for the Preliminary Design* [ITER_D_TVUZP2, 2016], and the detailed interface requirements between the PCS and each of the plant systems and diagnostics can be found in the PBS-47 interface sheets that are listed in the *PCS Document Production Plan* [ITER_D_RD59AJ, 2016]. Note that all disruption related control in PFPO-1 is described in section 2.5.4.5. The run-time estimates given here are for commissioning of advanced control schemes, but further development of the physics R&D needed to develop robust control is likely to require significantly more run-time as part of the physics program.

2.5.4.8.1 Plasma kinetic control

First wall protection is one of the first advanced control functions that will need to be commissioned before plasma heat loads on the first wall are sufficient to exceed the power handling capability of the beryllium first wall panels. The first wall shaping has been designed based on the heat flux e-folding length presently scaled to ITER from current experiments to withstand steady-state limiter plasma operation up to about 7.5 MA with additional ECRH power in MW $\leq$ the plasma current level in MA (see Appendix C for more details). Because of uncertainties in the extrapolation of that scaling to ITER, however, it is prudent to avoid limiter plasma operation beyond about 3.5 MA, when diverted plasmas should be achievable. A few discharges with special shapes with plasma currents between 3.5 and 7.5 MA will be needed to fully commission first wall heat flux control, to investigate heat loads from plasma contact at different points along the first wall, in particular to compare the protection of the high heat flux panels and the normal heat flux panels. An estimate of 10 days of commissioning discharges for first wall heat flux control are expected to be required to ensure adequate control as the plasma current is gradually increased. Note that if the plasma current is raised beyond 7.5 MA in PFPO-1, robust first wall protection must be demonstrated in both the PCS and the CIS to ensure investment protection of the first wall.

Divertor protection will not be required in the PFPO-1 phase since there will be at most 30 MW of auxiliary heating power and the divertor is not expected to be overloaded for auxiliary heating levels under 40 MW (see Appendix C for more details). However, it will be important to begin to develop divertor protection during the PFPO-1 phase before it becomes essential for investment protection. Initial tests of divertor heat flux control algorithms can begin once routine diverted plasma operation is achieved. With the limited auxiliary heating power available in PFPO-1, it may not be possible to fully demonstrate effective divertor heat flux control, but it may still be possible to control the limited heat flux reaching the divertor target. An estimate of 5 days commissioning is expected to develop initial divertor heat flux control in PFPO-1.

Once the ECRH and ICRF systems are nearly fully commissioned, initial tests of β and plasma stored energy control will be possible. While these control schemes are not required during PFPO-1, development of effective β and stored energy control should begin in this phase to prepare for PFPO-2. Before plasma parameters approach $q_{95} = 3$ at 7.5 MA, 2.65 T, it will be valuable to develop β and stored energy control to better control MHD stability, particularly to achieve longer pulse durations at nearly full auxiliary heating power. This can be attained by relatively simple proportional-integral-derivative (PID) control algorithms, or more sophisticated physics model-based controllers [Goumiri, 2017]. Various sensors could be used for this real-time control. The simplest and less accurate approach would be to use a diamagnetic flux measurement and a simplified-yet-established equilibrium model to compute the stored energy in real-time. A more accurate approach would be to utilize the computed plasma stored energy produced by the real-time equilibrium control in the PCS. The timescale of interest for plasma stored energy or β is the plasma energy confinement time, τ_E, which is expected to be far longer than the control system latency. The τ_E can be occasionally altered in a non-predictable way by plasma physics phenomena such as microinstabilities, which make such control necessary to maintain steady-state conditions. Control of the plasma stored energy or β has already been performed in many tokamak devices, and such control is well understood. An estimate of 2 days commissioning is allocated to begin to develop β and stored energy control in PFPO-1.

Another advanced control technique worth attempting during the PFPO-1 phase is rotation profile control. While intrinsic plasma rotation is likely to be difficult to control, there may be some limited control with ECRH or ICRF heating. In addition, even with the limited set of available

ELM control coil power supplies in the PFPO-1 phase, the application of 3-D fields from the ELM control coils could also be attempted for rotation profile control as observed in some experiments [Garofalo, 2008; Sabbagh, 2016]. While rotation profile control is not required in the PFPO-1 phase, initial attempts to develop rotation profile control in this phase will provide valuable opportunities to assess different techniques that will become more important in later operational phases to stabilize MHD instabilities and improve plasma performance. Rotation profile measurements of both the core and edge should be available from X-ray crystal spectroscopy systems 55.ED and 55.EI.

For more than a decade, the physical phenomenon of neoclassical toroidal viscosity (NTV) [Shaing, 2015] has been established as a technique to alter the plasma rotation in a tokamak in a controlled fashion when a largely non-resonant, weak three-dimensional (3-D) magnetic field is applied [Zhu, 2006]. The effect has been used routinely in tokamak devices primarily to slow the plasma rotation by providing drag. However, the effect can also accelerate the plasma from near-zero values, originally found to provide rotation in the direction counter to the plasma current [Garofalo, 2008]. More recent experiments have examined a generalization of NTV physics and have demonstrated plasma acceleration in the same direction as the plasma current as well, while producing large, favourable plasma rotation shear and rotation speeds far exceeding ITER simulations of plasma rotation in the pedestal region [Sabbagh, 2016]. In this case, the plasma velocity is altered toward the so-called NTV offset rotation value, which changes with plasma minor radial position.

This 3-D field actuator can then be used either under open or closed-loop control to alter the plasma rotation. Note that the initial toroidal plasma rotation profile at any time before the application of the 3-D field will not be zero, but rather the so-called, but well-established ‘intrinsic rotation’ of the plasma, which depends on several plasma parameters but for which a first-principles plasma physics model is not yet available. However, the NTV effect can effectively slow the local value of the plasma rotation when it is larger than the NTV offset rotation, and speed up the rotation when it is slower than the NTV offset rotation value. The effect of slowing the plasma rotation using a predominantly non-resonant 3-D magnetic field spectrum is robust and well-established. The ability of increasing the plasma velocity by NTV has also been demonstrated in tokamaks, but with less experimental experience. Present experiments (2016+) are being conducted to gain further experience with the generalized NTV offset rotation effect. Note that while the NTV offset rotation effect has been shown to produce plasma rotation well above ITER simulations in the pedestal region, based on present research it is expected that the effect will be limited to producing rotation values near plasma diamagnetic drift values, which may still be adequate for ITER needs.

The key timescale for rotation control active feedback is the plasma momentum diffusion time, which is far slower than the expected system latency. Real-time measurement of the plasma rotation will be required if closed-loop feedback is desired. Note that open-loop control might be sufficient for plasma operation during PFPO-1. An estimate of 2 run days has been allocated to initial tests of rotation profile control in the PFPO-1 phase.

Another more advanced control that should be commissioned in the PFPO-1 phase is the control of minority species for ICRF heating schemes and the mixture ratio of different plasma fuelling species. To commission ICRF heating from the first antenna, the control of minority species density within a majority background fuelling species will be required in PFPO-1. The diagnostics available in PFPO-1 that can at least provide some information on the minority content and species mixture include the visible H_α system (55.E2) and the vacuum ultraviolet system (55.E3). The commissioning of minority species control will be included in the overall run day allocation for ICRF commissioning. With only hydrogen and helium fuel available in PFPO-1, fuel mixture

control may not be required in this phase, except possibly for some H-mode experiments. Still, it would be valuable to begin to develop fuel mixture control experiments even in this phase as part of changeover experiments between hydrogen and helium.

2.5.4.8.2 Magnetohydrodynamics (MHD) and Error Field control

With a limited set of ELM coil power supplies and both the ECRH and ICRF H&CD systems commissioned in PFPO-1, it will be possible to begin to develop advanced control schemes for several MHD instabilities and for error field correction. Depending on the level of error fields found in ITER due to coil manufacturing and installation tolerances, it may already be necessary to correct for error fields with the external correction coils at low plasma current to avoid low density locked modes in the current rise [Buttery, 2000; Luxon, 2003]. The correction of small, non-axisymmetric magnetic fields in a tokamak generated by the real three-dimensional, non-toroidally-continuous nature of device components is important to maximize plasma performance and yield superior plasma stability. These 'error fields' can change in time throughout the plasma pulse duration. The plasma itself can amplify such fields, and such amplification can itself be dynamic in nature (time varying in amplitude and toroidal phase). Typically, the most deleterious error fields have toroidal mode number n = 1, with varied poloidal field spectra.

The correction of device-generated error fields, called 'dynamic error field correction' (DEFC), or those caused by plasma amplification of these fields, or due to global plasma modes, such as the RWM (whether it be stable, or unstable), has been well-established in tokamak experiments using both PID and model-based control techniques [Sabbagh, 2006; Sabbagh, 2013]. As the typical unstable, global MHD mode that appears in this situation is the RWM, the approach is typically named RWM control. Unstable RWMs are not expected in ITER until high performance plasmas are produced, most likely in the FPO phase of operation. However, the control algorithms, sensors, and actuators used for DEFC and RWM control are the same, so that commissioning of the control system for these tasks can be performed at the same time. The only difference that may occur for RWM control is that control of faster growing unstable RWMs may require faster power supplies than will be available in PFPO-1 for the ELM control coils.

The sensors for DEFC and RWM control are relatively low frequency (< 1 kHz) magnetic sensors, typically partial saddle loops, that are positioned toroidally to allow real-time discrimination of n = 1 magnetic field perturbations. Discrimination or higher-n numbers will be required to correct higher-n error fields and modes as desired (or determined to be needed after the initial operation of ITER), but correction of fields with n > 3 may not be important. Many such sensors will be available for PFPO-1 and later operational periods. The actuators to be used for DEFC are the external error field correction coils (for nearly static error field components) and the ELM control coils (for dynamic error field components, plasma amplification of the error field, or plasma mode activity toroidally rotating faster than the external error field correction coils can track). The key timescale for active feedback is the time rate of change of the error field for DEFC, and the time rate of change of the plasma amplification of such fields. When due to an unstable RWM, this timescale is determined by the inverse of the mode growth rate. These timescales will be significantly slower than the latency of the feedback system. However, the timescales will bridge across the capability of the slower external coils, to the faster ELM coils.

As part of the previously mentioned initial rotation profile control development it will also be possible to begin to develop dynamic error field correction (DEFC) [Garofalo, 2002; Sabbagh, 2010; Paz-Soldan, 2014] using the ELM control coils with a limited set of power supplies available in this phase. This also provides an opportunity to develop initial RWM control schemes [Boozer, 1995; Garofalo, 1999; Bialek, 2001; Fitzpatrick, 2002; Okabayashi, 2005; Sabbagh, 2006;

Reimerdes, 2007] with the limited ELM control coil power supply set, even though such control will not be required until high performance operation is achieved.

With at least two pellet injectors and a limited set of ELM control coil power supplies, it will be possible to begin to develop ELM control techniques in PFPO-1. While ELM control is not expected to be required in the PFPO-1 phase because the expected heat loads for these lower plasma current and lower auxiliary power conditions are not expected to be severe, it is important to begin to develop ELM control techniques as soon as H-mode operation will be obtained to prepare for higher performance operation. After the ECRH system, one ICRF antenna, and the pellet injection systems are fully commissioned in PFPO-1, H-mode operation will be attempted as described in section 2.5.4.9. If ELMy H-modes are achieved, then ELM control techniques with both pellet pacing [Lang, 2004; Baylor, 2013] and application of 3-D fields [Evans, 2004; Suttrop, 2011] with the ELM control coils will be tested. An estimate of 6 run days is allocated to initial ELM control experiments in PFPO-1.

Once the ECRH system is fully commissioned, initial tests of NTM control should be attempted already in PFPO-1 well before it will be required to avoid disruptions at higher plasma performance. At 7.5 MA, 2.65 T with the full 30 MW of auxiliary heating power available in PFPO-1, it may be possible to drive NTMs unstable, particularly if relatively high plasma performance H-mode operation were achieved. Even at lower plasma performance, classical tearing modes are likely to be driven under some conditions and their control with the ECRH system could be attempted. Much previous work has been done to understand and develop NTM control on existing devices and for ITER [La Haye, 2006; Maraschek, 2007; La Haye, 2009; Sauter, 2010; Austin, 2011; Reich, 2012; van den Brand, 2012; van den Brand, 2013; Rapson, 2014] that give some confidence that NTM control will be effective on ITER. The specific conditions in ITER, however, will require significant run-time to fully develop NTM control on ITER. For the initial commissioning of NTM control, 6 run days have been allocated in PFPO-1.

Once the ECRH and ICRF H&CD systems are fully commissioned, it will be possible to also begin to develop sawtooth control techniques in PFPO-1 before they will be required for high plasma current and low-q operation in PFPO-2. At 7.5 MA, 2.65 T with the full 30 MW of auxiliary heating available in PFPO-1, since $q_{95} \sim 3$, these scenarios are likely to have relatively large sawteeth, which would provide a good plasma scenario for initial sawtooth control commissioning. A great deal of work has been done previously to develop an understanding of sawtooth control, to demonstrate it on existing devices with both ECRH and ICRF heating, and model sawtooth control on ITER [Muck, 2005; Graves, 2005; Chapman, 2007; Graves, 2009; Chapman, 2009-1; Goodman, 2011; Kim, 2014]. Initial sawtooth control commissioning has been allocated 2 run days in PFPO-1.

2.5.4.8.3 Supervisory control

A key feature of the ITER PCS is advanced supervisory control, which includes exception handling when a plant system or plasma event occurs that requires a real-time change in control as well as shared actuator management that attempts to optimize a limited number of actuators for multiple simultaneous or consecutive control functions. Some initial exception handling is already required from FP to monitor operation limits and take action if prescribed thresholds are approached such as for coil protection. Exception handling is also used to perform real-time tuning or changes of controllers through comparison with expected performance based on prior modelling. Exception handling is an essential part of the PCS as the first line of defence for investment protection. As plasma performance increases, so do the requirements for exception handling to optimize the available run-time. Some aspects of exception handling are already performed on JET and ASDEX Upgrade. The PCS design team has published references to the ITER PCS design including

exception handling [Humphreys, 2015; Raupp, 2017]. An estimate of 12 run days has been allocated to commission and develop exception handling in PFPO-1.

Once the ECRH system is fully commissioned to deliver 20 MW of power to the plasma routinely, the initial actuator management commissioning can begin. This will include automatic switching of power from the equatorial to one of the upper launchers as well as switching power between the upper and lower steering mirrors (USM, LSM) of each upper launcher. The control is straightforward, but the timescales for switching (~3 s) need to be included in the algorithms and the consequent dead time needs to be taken into account in the impact on the shared actuator control schemes such as sawtooth and NTM control. Descriptions of the PCS architecture requirements and of how shared actuator management will work have been published [Treutterer, 2017; Humphreys, 2015]. An estimate of 7 run days has been allocated for commissioning shared actuator management in PFPO-1.

2.5.4.8.4 Advanced control commissioning deliverables for PFPO-1

For PFPO-1, the advanced control commissioning deliverables include:

- H-mode operation in plasmas at 5 MA/1.8 T including handling of L-H and H-L transitions;
- Initial ELM control with pellet pacing and with a subset of the ELM control power supplies;
- Initial first wall and divertor heat load protection;
- Initial β and stored energy control;
- Initial rotation profile control;
- Minority species control for ICRF heating schemes;
- Initial NTM, dynamic error field and RWM, and sawtooth control as plasmas parameters allow;
- Development of more advanced actuator management functions;
- Initial forecasting and event handling schemes to anticipate controllability boundaries and to take evasive action to optimize plasma operation and avoid disruptions;
- Magnetic control at plasma parameters of up to ~10 MA/5.3 T, depending on the development of disruption and runaway mitigation.

2.5.4.9 Options for H-mode operation in PFPO-1

2.5.4.9.1 Summary of scenarios

Experience operating ITER with H-mode plasmas in the first pre-nuclear phase (PFPO-1) would provide critical information to optimize the exploitation of H-mode operation more than 2 years later in the second pre-nuclear phase (PFPO-2), when the full complement of the H&CD systems is available. The primary goals of the H-mode operation campaign in PFPO-1 are to: 1) Validate the predictions of the L-H threshold power and its scaling with density and, as far as possible, with toroidal field, 2) Provide the first assessment of the energy and particle confinement properties of (dominant electron heated) H-mode plasmas in ITER, 3) Perform initial tests of ELM control using a reduced set of in-vessel ELM control coils in plasma conditions for which unmitigated type-I ELMs are not expected to cause melting of the W divertor monoblocks, 4) Validate projections of the H-mode SOL power flux width in preparation for higher power H-mode operation in later phases, and 5) Provide reference ITER H-mode plasma conditions to evaluate the possible effects of TBMs on H-mode performance at 1.8 T. This will be explored in PFPO-2 together with the optimization of the mitigation of the TBM effects with the ex-vessel error field correction coils and

the in-vessel ELM control coils, for which the reference of H-mode conditions in PFPO-1 are crucial.

With this motivation, the plan for H-mode operation in the PFPO-1 phase can be summarized as follows:

- **Highest priority and first H-mode attempts (31 days, if hydrogen H-mode operation is successful):** H-mode operation in hydrogen-dominated plasmas at 5 MA/1.8 T
- **Operation to assess ripple effects on H-mode and to provide conditions for H-mode exploration if H-mode in hydrogen is unsuccessful (10 days):** H-mode operation in helium plasma at 5 MA/1.8 T
- **Assessment of the L-H power threshold dependence on B_t (3 days):** H-mode operation in helium plasma at 7.5 MA/2.65 T

Consistent with the Staged Approach plan, the H&CD systems available in PFPO-1 are assumed to be 20 MW of ECRH with up to 8 gyrotrons at 104 GHz or 110 GHz, depending on the technical solution chosen, and the remainder of, at least, 16 gyrotrons at 170 GHz, and a single ICRF antenna/system capable of providing up to 10 MW of heating power to the plasma. To achieve H-mode at these power levels requires a scenario for which the L-H power threshold is less than 30 MW. Projections of the L-H threshold powers for ITER plasmas operated at one-third of the maximum current and field (5 MA and 1.8 T) indicate that 30 MW could be up to a factor of 2-3 above the threshold for Helium plasmas and up to a factor of 1.5 above the threshold for hydrogen plasmas, if all the available heating power can be coupled to these plasmas and the plasma density is set to the value needed to minimize the threshold power, as discussed in more detail in Appendix B. At half current and field (7.5 MA and 2.65T) the 30 MW available in PFPO-1 is marginal to exceed the threshold power in helium plasma (a factor ~ 1.1-1.5), and below the threshold for hydrogen. In addition to the additional heating it is assumed that there will be a set of power supplies connected to the ELM control coils so that n = 3 operation with coil current up to ~30 kAt will be possible.

The total operational time for H-mode plasmas in PFPO-1 is in the range of 34 – 44 days, depending on whether the 5 MA/1.8T hydrogen plasmas provide appropriate H-mode performance to meet the main required goals of the experiments (H-mode characterization and exploration of ELM control) or helium plasmas are required. Details of the expected deliverables from this initial H-mode exploration phase in PFPO-1, the rationale for the prioritization of these first H-mode attempts are given below. The associated R&D that could be undertaken during ITER construction to address the outstanding issues for H-mode operation is described in section 5.1 while the technical issues and detailed physics risks associated with 5 MA/1.8 T operation in ITER are described in Appendix F.

Note that a transition from L- to H-mode will change the plasma inductance and β. These changes will require adjustments to poloidal field currents in gap control to preserve the plasma boundary shape and strike point positions. The response of the control system needs to be commissioned for L-H and H-L transitions in flat-top or during current ramp-up and ramp-down phases. Limitations on CS and PF coil currents for shape control in H-mode need to be commissioned and PCS needs to be further optimized to cope with a sudden loss of heating to the plasma. Standard plasma ramp-down scenarios following H-mode need to be developed and plasma termination scenarios for fault conditions during H-modes need to be commissioned. The response of the plasma control system to H-modes and ELMs, in particular VS, needs to be optimized and the limitations documented at as

low a plasma current as possible, to ensure that disruptions due to loss of vertical stability of the plasma do not cause melting of PFCs.

2.5.4.9.2 Motivation for low field (1.8 T) operation in PFPO-1

There are several positive aspects of operating the first H-modes in ITER at low toroidal field:

- *Lower power threshold for H-mode access:* as mentioned in section 2.5.4.9.1 and discussed in more detail below and in Appendices Appendix B and Appendix F, operation at one-third field should allow H-mode operation early in the experimental program, even for the relatively low 20 MW of ECRH and 10 MW of ICRF assumed to be available in PFPO-1, which is not possible at higher fields in this phase. This is particularly true for helium plasmas, where P_{LH} from the reference scaling is in the range of 10-15 MW.
- *Investment protection during commissioning:* For events that can lead to melting of plasma-facing components, such as ELMs, disruptions, and runaway electrons, the commissioning of control and mitigation systems should start in plasma operating regimes where unmitigated events pose a low risk for melting. This is achieved by keeping the plasma current, toroidal field, and stored energy in the system as low as possible, while still matching key plasma parameters, such as q_{95}, to those at high performance operation and approaching as much as possible others that are known to affect ELM behaviour (e.g. plasma collisionality). Evaluation of the expected ELM energy densities for these plasma current levels in ITER [Polevoi, 2016] based on the EPED pedestal pressure predictions and empirical scalings from experiment (mostly based on ASDEX-Upgrade and JET [Eich, 2017]) show that uncontrolled ELMs at 5 MA/1.8 T in ITER will not cause melting of the top surface of the divertor W monoblocks in the high heat flux areas of the vertical targets, even for the most conservative assumptions for the pedestal plasma pressure (same pressure for H and He H-modes as for DT plasmas) and divertor ELM energy density (largest value within experimental scatter and considering largest in/out ELM deposition asymmetries). There will also be some margin against overheating of divertor monoblock toroidal gap edges, which has recently been identified as more problematic than previously thought, even with the toroidal bevelling of the monoblock front surfaces, designed to avoid heavy stationary loading on misaligned poloidal gap edges [Gunn, 2017]. This is discussed further in Appendix C. In addition, 5 MA H-mode plasmas are inside the zone of acceptable operation with respect the avoidance of melting during unmitigated disruptions, as described in section 2.3.
- *Operation at q_{95}=3:* The ratio of plasma current to toroidal magnetic field near the edge of the plasma core (~q_{95}) is a key operating parameter for ELM control via 3-D fields, since the currents in the control coils need to be carefully tuned for a particular value of q_{95}. q_{95} = 3 is the reference value of the baseline Q=10 inductive scenario H-mode at 15 MA/5.3 T and this can be matched by operating at 5 MA/1.8 T. The level of 5 MA is comfortably above the 3.5 MA lower limit for good plasma position control in diverted operation in ITER, as discussed in section 2.5.4.2.
- *H-mode operation at 1.8 T in the PFPO-2 campaign:* if H-mode experiments at 1.8 T in the PFPO-1 campaign proves successful, this would open the possibility of robust hydrogen H-modes in the PFPO-2 campaign (if this is marginal in PFPO-1 for H) as the ICRF heating will be increased to 20 MW and thus allow the possibility of comparing hydrogen and helium H-modes for the same I_p/B_t in ITER. This would also allow the evaluation of the possible effects of TBMs on H-mode performance by comparing similar

H-mode plasmas in PFPO-1 (no TBMs) and in PFPO-2 (with TBMs) at 1.8 T. This is an important ingredient to guide the optimization of the mitigation of the possible effects of TBM effects on H-mode plasmas with the ex-vessel error field correction coils and the in-vessel ELM control coils in ITER.

2.5.4.9.3 Details of the experimental plan for H-mode operation in PFPO-1

Assuming that the evaluation of all aspects of 1.8 T operation described in Appendix F is satisfactorily resolved, the program foreseen for PFPO-1 would amount to 44 days of operation. This will be preceded by the completion of commissioning of the available H&CD systems in hydrogen L-mode plasmas at 3.5-5 MA/1.8 T (at least 13.4 MW of ECRH at 170 GHz, up to 6.7 MW of ECRH at 104-110 GHz and 10 MW of ICRF with heating pulse lengths of up to ~ 30 s). Details of each of the experimental plans for each of the H-mode scenario considered are given below.

2.5.4.9.3.1 First H-mode studies: initial H-mode operation in hydrogen plasma at 5 MA/1.8 T (17 days)

H-mode plasmas will be produced by applying the maximum available power (20 MW of ECRH and 10 MW of ICRF) to 5 MA/1.8 T plasmas – this will already have been commissioned to pulse lengths of ~ 30 s in L-mode plasmas. The first magnetic configuration to be explored will have the standard ITER shape and a (separatrix) TF ripple of ~ -1.3%. Initial focus of these experiments will be the achievement of an L-H transition at $n_e \sim 0.4 \times n_{GW}$, the assessment of the issues related to the coupling of ICRF in these conditions and an exploration of the density dependence of the H-mode threshold to determine the minimum density for H-mode access. An assessment of the required antenna-plasma distance to achieve the required coupling, including the changes of the edge density profile following the H-mode transitions, which may require optimization of gas fuelling, and of the resulting first wall deposited power by (ICRF-accelerated) fast particles trapped in the ripple wells will be performed for several values of target L-mode density. These experiments will involve RF power ramps to maximum power on timescales of ~20 s followed by a constant power phase of ~10 s to determine if type-I ELMy H-mode conditions can be sustained. These experiments will provide the first H-mode plasmas in ITER, as well as first measurements of the evolution of plasma parameters, following the L-H transition (important to define the details of H-mode experiments in PFPO-2).

Assuming that appropriate ICRF coupling can be kept with a significant distance between the antenna and the plasma, the plasma-wall gap will be increased in several steps until a ripple level of 0.55% at the separatrix is achieved, with the corresponding changes in plasma shape to maintain $q_{95} \sim 3$ (this requires an inwards displacement of 0.4 m with respect to the reference shape, as discussed in Appendix F). This will allow an evaluation of the optimum distance for hydrogen H-mode access in this phase, which will be a compromise between ICRF coupling and power fluxes of ripple-trapped particles to the first wall. From the perspective of later ELM control studies, it is preferable to maintain the plasma as close to the first wall and ELM control coils as possible, as the intensity of the applied field decreases strongly with the plasma-wall distance. The time required to complete this initial H-mode access assessment in hydrogen plasmas is estimated as 10 days.

It is expected that by this time some evidence of H-mode access in hydrogen plasmas will be obtained and the required power for this access versus antenna-wall distance (or separatrix TF ripple value) and plasma density will have been characterized. If H-mode access in hydrogen is not achieved at this stage, the rest of the research on H-mode and ELM control in PFPO-1 (section

2.5.4.9.3.2) will be performed with helium plasmas, which will require the research in section 2.5.4.9.3.3 to be performed at this stage.

Even if H-mode access in hydrogen plasmas is achieved, stationary type-I ELMy H-modes might not be sustained due to the low margin of power over threshold in hydrogen plasmas and/or to the specific ICRF heating issues at 1.8 T. If so, helium will be introduced by the gas introduction system (targeting small concentrations ~10%) to see if this can provide additional margin for stationary type-I ELMy H-mode operation via the reduction of the H-mode threshold, as observed in JET [Hillesheim, 2016]. Besides helium concentration scans, this will require a series of density scans and antenna-wall scans analogous to those performed for hydrogen. The total time required to complete this assessment of mixed He-H H-mode plasmas is estimated to be 3 days.

Assuming that either pure hydrogen plasmas or mixed H-He plasmas provide stationary type-I ELMy H-mode plasmas, the rest of the studies on type-I ELMy H-mode characterization and control will continue with hydrogen-dominated plasmas. If this is not successful the research will shift to helium H-modes and the studies under section 2.5.4.9.3.2 will be performed in helium, following the studies in section 2.5.4.9.3.3 that would start at this stage.

This phase will conclude with the assessment of stationary type-I ELMy H-mode characteristics of 1.8 T H-modes with RF heating pulses of up to ~30 s, including a range of currents from 3.5 to 5.0 MA, approximately covering the range, q_{95} = 3.0-4.3, which is relevant for ITER high-Q reference scenarios. It is expected that some properties of these H-modes will have been assessed during the initial experiments to determine H-mode access, as described above. These dedicated experiments will prioritize power and density scans (ideally over $n_e \sim 0.2\text{-}0.9 \times n_{GW}$) to determine the operational range of type-I ELMy H-modes, their confinement properties, ELM behaviour and associated power/particle fluxes to PFCs. An initial assessment of the effects of plasma fuelling schemes on type-I ELMy H-modes will also be performed by comparing gas fuelled hydrogen H-modes with pellet fuelled ones (two pellet injectors will be available in PFPO-1) at several plasma density levels. This is expected to require at most 4 days of operation during which verification of the functionality of the systems needed for gas balance will take place, in preparation for dedicated gas balance experiments in PFPO-2. Due to the low margin of the available heating power above the L-H transition, the ranges of these scans are expected to be limited. However, it is important to perform this stationary type-I ELMy H-mode characterization at this stage because these 1.8 T H-modes will be the reference plasmas on which the effects of TBMs will be evaluated and mitigated during PFPO-2. The experimental measurements in these scans will provide the first indication of the scaling with plasma current of the divertor power fluxes in type-I ELMy H-modes between ELMs and during ELMs and of the pedestal plasma parameters and overall energy confinement of H-modes in ITER, which is important for the detailed planning of H-mode experiments in PFPO-2.

As discussed in detail in Appendix C, for this level of additional heating ($P_{input} \leq 30$ MW) no active measures to mitigate the divertor power loads are expected to be required for 5 MA/1.8 T plasmas. However, some degree of control of the divertor plasma temperature may be required not to have excessive W sputtering; this could limit the low range of plasma densities to be explored and/or may require the use of impurity seeding in these conditions. The precise value of the divertor plasma temperature with acceptable W net influx will be determined by the effectiveness of W prompt redeposition in these ITER H-mode and thus will be an issue to assess in these experiments.

2.5.4.9.3.2 First ELM control experiments 5 MA/1.8 T (14 days)

Assuming that experiments in section 2.5.4.9.3.1 deliver stationary type-I ELMy H-modes in hydrogen dominated plasmas, the next step will be to investigate ELM control in these conditions.

Otherwise, the experiments in helium plasmas under section 2.5.4.9.3.3 will take place first and then the ELM control experiments in this section will follow but in helium plasmas.

ELM control experiments will be performed in plasma conditions which are optimum for the achievement of stationary type-I ELMy H-modes at 5 MA/1.8 T (e.g. optimum plasma density and separatrix-wall distance). The focus will be on the application of resonant magnetic perturbations (RMPs) with the ELM control coils, but also on the assessment of the potential of back-up ELM triggering techniques, i.e. vertical plasma oscillations and pellet injection. This study is important at this stage because these techniques are expected to be applied when expanding the operational range of type-I ELMy H-modes to higher currents and fields to avoid melting of the W divertor (see section 2.5.5.7). In fact, from preliminary estimates (to be refined in the near future), the requirements for the back-up ELM triggering techniques are not expected to be very demanding for 5 MA/1.8 T H-modes. For the vertical plasma oscillations it is estimated that the current required in each of the in-vessel vertical stability coils to provide a 20 Hz vertical oscillation of the plasma position by ±4 cm, which is expected to be sufficient to trigger ELMs in ITER [Gribov, 2015], is ±27 kA, i.e. less than 50% of their design limit of 60 kA. Similarly, the pellet size required for ELM triggering at this level of plasma current is expected to be 1/3 of that required to trigger ELMs for 15 MA/5.3 T Q =10 plasmas (2.0×10^{21} D atoms/pellet [Futatani, 2014]) and, thus, about an order of magnitude lower than the maximum pellet size that can be provided by the pellet injectors (6.2×10^{21} D atoms/pellet). The two pellet injectors available in PFPO-1 provide a combined pellet injection frequency of up to 32 Hz, allowing a controlled increase of the ELM frequency by more than an order of magnitude compared to that of uncontrolled ELMs [Loarte, 2014].

The assessment of the potential of the back-up ELM triggering techniques in ITER is not expected to require a very substantial experimental time and can be possibly done in parallel with the development of ELM control by RMPs by dedicating few seconds of the stationary H-mode phase to them. On the other hand, the development of ELM control by RMPs is foreseen to be much more time consuming. The Staged Approach foresees a reduced set of power supplies to be connected to the ELM control coils in PFPO-1. These will be capable of creating an n=3 magnetic field perturbation with a similar pitch to that of the edge magnetic field for q_{95} = 3 as, shown in Figure 2.5-2, by connecting up to 3 coils to each power supply. This will allow a maximum current level of up to ~ 30 kAt in the active ELM control coils which can produce a B_r/B_t perturbation for 5 MA/1.8 T plasmas similar to that for 15 MA/5.3T with the maximum baseline current level of 90 kAt. The connection of the power supplies to the ELM control coils will be configured so that the current level can be adjusted independently for each row of coils thus providing some capability to vary the poloidal spectrum of the perturbation applied by choosing appropriate current levels in the three rows of coils.

The ELM control experiments with RMPs will characterize the effects of the applied fields on the access and sustainment of stationary type-I ELMy H-modes at 5 MA/1.8 T, in particular: on the power required for H-mode access and the stationary pedestal plasma parameters, ELM energy losses and frequency, overall energy, momentum, particle and impurity confinement and power fluxes to plasma-facing components (including divertor and first wall). This will be performed by systematic scans of the coil current levels in the three rows of the ELM control coils and q_{95} scans, by variation of the plasma current, with the ultimate goal of achieving ELM suppression. For the H-mode access phase, this will include the optimization of the timing between the applied RMP fields and the additional heating power ramp to ensure a robust transition to H-mode while avoiding long ELM-free periods. For the stationary type-I ELMy H-mode phase, and to the extent possible with the reduced set of power supplies, the optimization of the RMP field applied to minimize the effects on H-mode confinement while maintaining a given level of ELM control (including

suppression, if possible) will be studied and the consequences for localized power fluxes to PFCs and impurity exhaust evaluated. This will provide the first evidence of potential issues related to localized power fluxes to PFCs, although at this plasma current level and additional heating levels it is expected that active mitigation (e.g. time variation of the magnetic perturbation applied) [Loarte, 2014] will not be required.

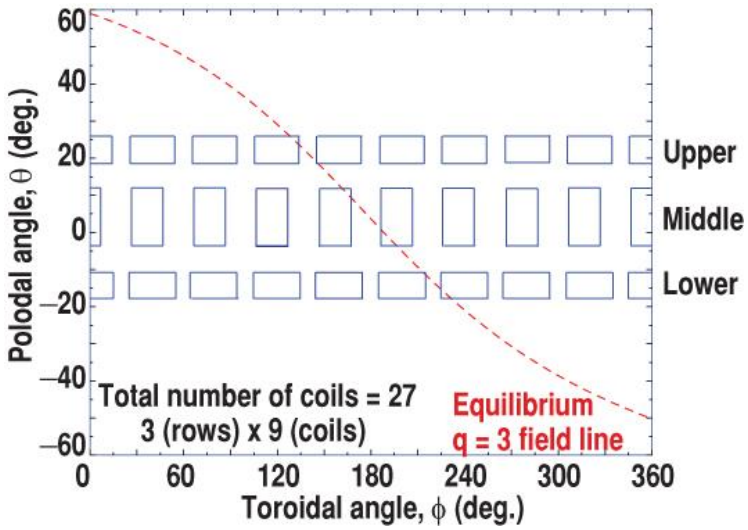

Sector	1	2	3	4	5	6	7	8	9
Upper	$-I_U$	0	$+I_U$	$-I_U$	0	$+I_U$	$-I_U$	0	$+I_U$
Equ.	$+I_E$	$-I_E$	0	$+I_E$	$-I_F$	0	$+I_F$	$-I_F$	0
Lower	0	$+I_L$	$-I_L$	0	$+I_L$	$-I_L$	0	$+I_L$	$-I_L$

Figure 2.5-2: (Top) Projection of individual in-vessel ELM control coils on the poloidal and toroidal planes. (Bottom) Connection of the ELM control coils to produce an n = 3 perturbation for ELM control in PFPO-1 with 3 levels of current (if required) in the Upper, Equatorial and Lower row (I_U, I_E, I_L < 30 kAt).

As far as possible, the plasma parameters of the stationary type-I ELMy H-modes will be scanned by varying input power, plasma density and fuelling scheme (gas versus pellets) and the characteristics of the RMP fields applied will be retuned to maintain the same level of ELM control (including suppression, if possible). This will include an evaluation of the changes to RMP required to avoid ELM triggering by the injection of fuelling pellets, with a similar deposition profile to that expected for 15 MA/5.3 T Q = 10 plasmas, if ELM suppression is achieved. The total time required to perform these experiments is estimated to be 14 days. The results obtained during this phase will be essential for the validation of models for ELM control and for the detailed planning of H-mode experiments in PFPO-2, where ELM control may already be required to avoid divertor melting and W accumulation in higher current H-modes.

2.5.4.9.3.3 H-mode in helium at 1.8 T and 5.0 MA (10 days)

The extent of H-mode operation in helium plasmas in this phase of PFPO-1 will depend to which level the experiments in section 2.5.4.9.3.1 deliver reliable stationary type-I ELMy H-mode plasmas in hydrogen. If this is not possible, either due to the higher H-mode threshold of hydrogen plasmas or because of issues limiting ICRF heating at 1.8 T in hydrogen plasmas (e.g. compatibility with high TF ripple, etc.), the experiments to characterize type-I ELMy H-modes in 5 MA/1.8 T in section 2.5.4.9.3.1 and the ELM control experiments in section 2.5.4.9.3.2 will be performed in helium plasmas.

Operation in helium plasmas in PFPO-1 will require additional operational time to determine the H-mode threshold in 5 MA/1.8 T H-modes and its scaling with density as well as to determine the effect of TF ripple in helium H-mode access and on the sustainment of type-I ELMy H-mode conditions. The experiments would be analogous to those in the first part of section 2.5.4.9.3.1 and are thus expected to require 10 operational days. For helium plasmas the main heating scheme to be used is ECRH and, thus, the investigation of ripple effects on H-modes is much more straightforward than when ICRF is required. On the other hand, if the proposed ICRF scheme based on second harmonic hydrogen minority in helium plasmas proves viable to provide 10 MW of heating in ITER (see Appendix F), this would allow operation in H-mode with $P_{inp}/P_{L-H} \sim 2.0$-3.0. This would provide a much better way to characterize the scaling of H-modes with additional heating power level in PFPO-1 than with hydrogenic plasmas and experimental time needs to be considered for such studies. In addition, operating with helium plasmas in PFPO-1 gives the possibility to evaluate the scaling of the H-mode threshold power already in PFPO-1 by comparing results of the power required to access the H-mode with 1.8 T and 2.65 T plasmas (see section 2.5.4.9.3.4).

In view of the arguments above and the likely need to perform the type-I ELMy H-mode characterization in helium plasmas for 7.5 MA/2.65 T (see section 2.5.5.7), for which reference scenarios at 5 MA/1.8 T are required, 10 days of helium H-mode operation at 5 MA/1.8 T are included in PFPO-1. It should be noted that the final number of days of helium H-mode operation in PFPO-1 may end up being significantly longer (up to 28 days) if the initial hydrogen H-mode development in section 2.5.4.9.3.1 is not successful. In that case the type-I ELMy H-mode characterization (4 days in section 2.5.4.9.3.1) and the ELM control experiments (14 days in section 2.5.4.9.3.2) will be performed in helium.

2.5.4.9.3.4 Determination of the H-mode threshold in helium plasmas at ~ 2.65 T (3 days)

The H-mode threshold for helium plasmas at 7.5 MA/2.65 T is predicted to be in the range of 19-28 MW (at $n_e = 0.4 \times n_{GW}$) while it is 37 MW for hydrogen plasmas. Therefore, the available heating power (10 MW of ICRF and 20 MW of ECRH) is sufficient to attempt the determination of the H-mode threshold scaling in helium plasmas at ~2.65 T. In this case, the ICRF scheme to be used is hydrogen minority in helium plasmas, which can provide central heating at this field value. The ECRH heating power, on the other hand will be on-axis for the 170 GHz operating in O-mode providing at least 13.3 MW (off-axis for X-mode) and the remaining up to 6.7 MW of the 104-110 GHz gyrotrons will be off-axis. The ripple at the plasma separatrix is 0.55% at this level of toroidal field and, thus, ripple-related issues are not expected to be important in these conditions (see Appendix B).

These experiments will involve RF power ramps to maximum power in timescales of ~ 20 s followed by ~ 10 s constant power phase (to determine if type-I ELMy H-mode conditions can be sustained) for a range of L-mode target densities (ideally $n_e \sim 0.2$-$0.9 \times n_{GW}$, or the highest

achievable by gas puffing) and restricted scans of the toroidal field (~ 15%), to reduce the H-mode power threshold if this is found to be marginal, while maintaining dominant central heating.

As these experiments will necessarily operate near the H-mode threshold, long ELM-free periods may occur that can cause W accumulation and sudden disruption-prone H-mode terminations [de Vries, 2016; Köchl, 2016]. To avoid this, the ELM back-up triggering schemes discussed in section 2.5.4.9.3.2 (vertical plasma oscillations and pellet hydrogen injection) will be applied. Both of them are expected to be effective in triggering ELMs at this level of current and field [Gribov, 2015; Loarte, 2014] within the design specifications of both the vertical stability coils/power supplies and of the pellet injector. This will be further verified by the demonstration of these schemes with 5 MA/1.8 T H-modes in section 2.5.4.9.3.2. It is not expected that stationary type-I ELMy H-modes will be achieved in this phase even if the ELM back-up triggering schemes are applied. In particular, the continuous injection of hydrogen pellets to trigger ELMs in helium plasmas will increase the H-mode threshold towards that of hydrogen and will eventually lead to a H-L transition. However, the quantitative percentage of hydrogen in helium at which this will actually occur in ITER remains uncertain [Ryter, 2013; Hillesheim, 2016].

2.5.4.9.4 Deliverables for the H-mode operation campaign in PFPO-1

The key deliverables expected from operation of ITER in H-mode during PFPO-1 are:

- *Quantification of the power required for H-mode access:* The operating scenarios and planned experiments are designed to assess the L-H transition threshold power (P_{LH}) as soon as possible in the experimental program. This will provide an initial assessment of H-mode access in ITER over a range of species (H and He and H-He mixtures), densities and fields (1.8 T and 2.65 T). This is essential both for the detailed planning of H-mode operation in PFPO-2 and to determine if an upgrade of the baseline heating power level of 73 MW will be required to ensure successful DT operation. There are significant differences between ITER operation and the data from present tokamaks, from which P_{LH} predictions for are made for ITER, that are known to affect the required power to access the H-mode. Therefore, a confirmation of the actual level of power required to access the H-mode in ITER is essential for the rest of the experimental program and to plan power upgrades. These would mitigate the effects of a larger than expected H-mode threshold that could otherwise impact the start of FPO operation in ITER.
- *Determination of the confinement properties of H-mode plasmas and pedestal plasma characteristics:* This initial plasma operation will provide the first experimental evidence for the performance of type-I ELMy H-mode plasmas in ITER and of the limits to the edge plasma parameters imposed by MHD stability in ITER. The specific aspects of ITER plasmas that will be characterized concern: stiffness of the core temperature profiles in electron heated H-modes with no torque input (albeit at high T_e/T_i), particle transport with low core sources and gas versus pellet fuelling of ITER H-modes, edge MHD stability of collisionless pedestal plasmas in ITER (the expected pedestal collisionality of 5 MA/1.8 T H-modes ne = $0.4\times n_{GW}$ in ITER is a factor of 2.5 times lower than for 15 MA/5.3 T Q = 10 plasmas).
- *Characterization of ELMs (energy-particle losses and power fluxes to PFCs) and demonstration of their control:* The initial H-mode plasmas in PFPO-1 will produce the first type-I ELMs in ITER and their features will be investigated over a restricted range of plasma currents, input powers and plasma densities. These experiments will be used to validate the predictions for the uncontrolled ELM energy losses, ELM power fluxes, and

impurity exhaust (including W). These are key to determine the range of plasma currents in which uncontrolled ELMs will be acceptable in ITER and thus for the strategy to expand the range of type-I ELMy H-modes towards higher plasma currents in PFPO-2.

- *Investigation of the ELM control capabilities and of the effects of RMP fields on H-mode access and confinement:* The initial set of ELM control coil power supplies will provide n = 3 magnetic field perturbations with a reduced set of poloidal spectra that allow the first optimization studies for the application of RMP fields to H-mode plasmas in ITER to be performed. The experiments planned in PFPO-1 will provide first evidence of the effect of 3-D fields on the power/density required for H-mode access, ELM control (with the goal of achieving ELM suppression in 5 MA/1.8 T plasmas), power/particle fluxes to the divertor/first wall, pedestal plasma characteristics and energy, particle and momentum transport in controlled/suppressed type-I ELM H-modes. In addition, the demonstration of ELM triggering back-up schemes (vertical plasma oscillations and pellet pacing) will be performed and their effect on ELMs and on the H-mode plasmas will be investigated. ELM control validation of the reference scheme based on RMPs and of back-up schemes is very important for the detailed planning of H-mode operation in PFPO-2 at higher field and current, for which uncontrolled ELMs could lead to melting of the W divertor monoblocks.
- *Provide first operational experience of ICRF heating of H-mode plasmas:* The application of ICRF for the heating of 5 MA/1.8 T H-modes will provide the first operational experience of this heating scheme in H-mode conditions in ITER, including during the H-mode access phase. This will allow the demonstration of the capabilities of ICRF to couple power for the typical edge plasma conditions of H-modes in ITER, including a scan of separatrix-wall distance, both for stationary phases (possible steep density gradients in the SOL and pedestal between ELMs) and during ELM transients, and for a range of conditions (e.g. with uncontrolled and controlled ELMs) as well as in suppressed-ELM H-modes. This will allow the tuning of the ICRF systems to provide efficient heating for H-modes in ITER which will be further exploited in PFPO-2 and later phases.
- *Establish reference H-mode performance without effects of TBMs:* The experimental program in PFPO-1 will provide reference conditions regarding H-mode access and type-I ELMy H-mode performance without the TBMs at 1.8 T, as they are not installed in this phase. This information is key to evaluate the effect of the TBMs on H-mode access and performance in PFPO-2, which, if sizeable, will then be followed by the development of mitigation schemes utilizing the error field correction coils and the ELM control coils within the PFPO-2 program. The potential issue with this strategy is that given the available power in PFPO-1, the assessment of the TBM effects will have to be done at 1.8 T in PFPO-2, as the reference plasmas will be at this field. As discussed above and in more detail in Appendix F, 1.8 T operation in ITER has a level of ripple much higher than at 2.65 T or 5.3 T (factors of 2.5 - 4) and the TBM themselves also create a ripple which varies with the toroidal field. Therefore, specific experiments and analysis will be required to separate the effect of both ripple effects when comparing plasmas at 1.8 T in PFPO-1 without the TBMs and in PFPO-2 with the TBMs. To allow this, the assessment of the effect of TF ripple on H-mode plasmas is included in PFPO-1 (possibly in helium plasmas that do not rely on ICRF heating, if ICRF coupling with large separatrix-wall gaps turns out to be problematic).

- *Initial validation of predictions of power fluxes in ITER H-modes:* The H-mode experiments in PFPO-1 are planned to cover a range of currents from 3.5 – 5.0 MA. This will provide the first evidence for the magnitude of the divertor power fluxes in ITER type-I ELMy H-modes and of the scaling of their fall-off length with current, expected to scale inversely proportional to plasma current [Goldston, 2011; Eich, 2013]. Operation with 3-D fields applied for ELM control will provide first experimental evidence of the effect of these fields on power fluxes to plasma-facing components (first wall and divertor) between ELMs and in suppressed ELM regimes (if achieved) and on their dependence of plasma parameters (chiefly density) [Schmitz, 2016]. This validation is important to confirm and improve the physics basis for the prediction of power fluxes to PFCs in ITER H-mode plasmas, which is required for the planning of experiments during PFPO-2 and FPO where higher levels of additional heating will be used and schemes to control the divertor power fluxes will have to be developed.

2.5.4.9.5 Assessment of diagnostic capabilities to perform H-mode research during PFPO-1

The main objective of the PFPO-1 H-mode research program is the determination of the access conditions (heating power, density etc.) to H-mode and the characterization of the properties of uncontrolled and controlled/suppressed type-I ELMy H-modes. The diagnostic set considered for PFPO-1 (see Appendix H) can provide an appropriate set of measurements to determine:

- Key core plasma parameters in these experiments such as n_e, T_e, T_i, toroidal plasma rotation and impurity levels (including W);
- Power and particle fluxes to plasma-facing components as well as the influxes of recycled species and impurity influxes.

It is likely that the time resolution of these diagnostics will not meet the requirements for 15 MA/5.3 T operation, as discussed in Appendix H, but the expected time resolution is considered to be adequate to the objectives of this phase. Regarding edge plasma characterization the situation is less clear. For electron parameters it depends on whether or not some of the diagnostics foreseen to be available to provide experimental measurements in PFPO-2 will already be functional towards the end of PFPO-1, when the H-mode experiments will be performed. Of particular interest, as discussed in Appendix H, is the early availability towards the end of PFPO-1 of the edge Thomson scattering system, as this allows the measurements of both electron temperature and density in the edge and the determination of edge pressure gradients. In addition to this, and as a risk mitigation measure, the ECE system could be used to determine the pedestal temperature in PFPO-1 but this is expected to require a new radiometer to measure 2^{nd} harmonic ECE to be added to the baseline configuration. This, together with a peripheral density measurement from the interferometer, could provide a measurement of the electron pressure at the pedestal, although not of its gradient at the plasma edge. Given the unavailability of the HNB and DNB systems in PFPO-1, all ion temperature measurements will rely on the X-ray spectrometer for the core and on the X-ray crystal spectrometer for the edge, which are expected to provide good quality measurements given the high electron temperatures (core and edge) expected in these 5 MA/1.8T H-mode plasmas (see Appendix F).

2.5.4.10 Edge physics and PWI studies in PFPO-1

2.5.4.10.1 Wall Conditioning and cleaning

2.5.4.10.1.1 Glow Discharge Cleaning

Glow discharge cleaning (GDC), is one of the primary conditioning techniques, along with baking of the vacuum vessel and blanket/first wall at 200°C and 240°C respectively, which ITER will use to prepare in-vessel component surfaces prior to machine start-up and thereafter for plasma operations following maintenance procedures requiring in-vessel access. The efficiency of GDC, i.e. its ability to efficiently desaturate wall surfaces and remove medium Z impurities (adsorbed oxygen, water or carbon) must be assessed either in H_2 or in He in PFPO-1. It should be noted that the impact on subsequent plasmas of He-GDC (or any He-based plasmas) operated on Be PFCs has never been assessed in a tokamak since JET with the ITER-Like Wall (ILW) has never operated in He.

Careful tuning of GDC discharge parameters (pressure, current) will allow the optimization of cleaning efficiency. Qualitative and quantitative assessment of the exhaust gas will be performed using Residual Gas Analyzers (RGA), and their proper calibration beforehand is mandatory. Spectroscopy on selected impurities (e.g. oxygen, carbon, beryllium) could also eventually be foreseen as a monitoring tool during later GDC phases when the diagnostics become fully available. Eventually, as for all major tokamaks, routine GDC protocols will be developed, in combination with bake-out cycles, such that conditioning is performed until designated vacuum conditions are obtained.

The continuous follow-up of wall conditions after the first plasma, by means of optical emission spectroscopy and mass spectrometry, and the impact of impurity levels on plasma operation and performance during PFPO-1 will not require dedicated machine time but will be particularly important to define further conditioning needs. This should include routine monitoring of impurity sources in reference pulses (see Appendix D).

2.5.4.10.1.2 Ion Cyclotron Wall Conditioning/Electron Cyclotron Wall Conditioning

Ion Cyclotron Wall Conditioning (ICWC) and Electron Cyclotron Wall Conditioning (ECWC) need to be developed for the conditioning of the first wall surfaces between pulses, i.e. when the toroidal magnetic field is on. As stated in section 2.2.8, ICWC is preferable to ECWC, but the latter option should be maintained in case of unavailability of the ICRF system in PFPO-1. Among the questions to be addressed in PFPO-1, but which are common to all operation phases, is the ability of such magnetized low temperature plasmas to efficiently remove intrinsic (oxygen, water or carbon) and extrinsic (nitrogen, argon) impurities thus allowing/easing plasma initiation (burn-through), to recover from disruptions, and to control density in long-pulse discharges ($t \geq 200$ s) with the ITER material mix. The control of hydrogen wall content by ICWC or ECWC discharges and thereafter in ensuing plasmas may turn out to be mandatory to achieve PFPO-1 and PFPO-2 targets. It is therefore preferable to develop ICWC or ECWC scenarios for each of the main toroidal field values that are expected to be used routinely in PFPO-1. For $1.8 \leq B_t \leq 3.3$ T and f = 170 GHz, ECWC plasmas will be produced at the 2^{nd} or the 3^{rd} harmonic of the ECR frequency, and it is unclear what the single pass absorption will be in these discharges. Since coupling of the power in ICWC is mainly non-resonant, discharges can be produced at very low B_t. The so-called high harmonic (n~10) ICWC scenario, successfully operated in ASDEX-Upgrade and in the JET-ILW, may even therefore be envisioned in the case of failure or unavailability of GDC in ITER.

Schemes for optimization of the cleaning efficiency are common to both techniques, proceeding first with variations of pressure and power. Due to the relatively high densities of ICWC/ECWC plasmas (in comparison with GDC), a very large fraction of the desorbed flux is immediately re-ionized and re-implanted into wall surfaces and only a small fraction is exhausted through the pumping system. The discharge duty cycle must therefore be adapted to mitigate this. Finally, the poloidal field patterns need to be optimized in both discharges at each frequency/toroidal field combination (f/B_t) in order to increase uniformity, wall coverage and efficiency. As for GDC, qualitative and quantitative assessment of the exhaust gas will require the use of the tokamak pressure measurement RGAs. Spectroscopy and visible cameras can be used to assess the areas wetted by the discharge, whereas interferometry and ECE will permit the evaluation of basic plasma parameters and discharge uniformity.

2.5.4.10.2 Fuel retention management

Most of the dust/tritium retention/erosion diagnostics will become available during PFPO-2. The focus of PFPO-1 will therefore be on commissioning and testing fuel management related systems, as well as obtaining first estimates of fuel retention and removal efficiency in hydrogen plasmas. These may be later refined and validated during PFPO-2 through a dedicated migration/retention experiment, including, if possible, hydrogen discharges with trace deuterium (section 2.5.5.12.2.1).

2.5.4.10.3 Gas balance in hydrogen

The most widely used technique for the evaluation of in-vessel fuel retention is the so-called 'gas balance' technique, which consists of a precise accounting of the amount of injected and exhausted fuel species. Based on measurements from all metal devices, and in particular from the JET-ILW, the expected retention rate will be lower than 1% of the injected fuel, so that careful calibrations of the gas injection system and of the pumping speeds of the different sub-systems will be required.

The most accurate method is to perform PVTc (Pressure-Volume-Temperature-composition) measurements on gas tanks connected to both the gas injection system and the tokamak exhaust. Part of the required hardware will be available for PFPO-2 to allow for He^3 recycling (ICRF minority). A small upgrade is required to enable gas balance analyses, consisting mainly of the installation of a dedicated gas container connected to the gas injection. Making this system available for PFPO-1 is technically possible and there appears to be no showstopper in terms of schedule. Resources will, however, have to be identified to purchase the required hardware and ensure timely installation before PFPO-1.

No dedicated operation time will be required for gas balances in PFPO-1 and measurements will be performed parasitically when hydrogen discharges are performed requiring regeneration of the divertor cryopumps to recover the pumped hydrogen. For the reasons mentioned in section 2.2.1, gas balance in He is not relevant for fuel retention studies, but monitoring of the exhaust gas composition during He discharges will provide indications on the background H sources and their evolution with time over a campaign. Note that gas balance analysis should, if possible, be performed at least each time a reference discharge is performed (see Appendix D) providing information on the evolution of the wall conditions and the retention rates. Time will be required to determine the pumping speeds of the different systems, and perform a calibration of the gas injection system, but this can probably be done during short-term maintenance periods.

2.5.4.10.3.1 Ammonia formation during nitrogen-seeded discharges

Although power flux densities will be too low in PFPO-1 to require impurity seeding (see Appendix C), the development and commissioning of divertor detachment control will make use of seeded impurities to characterize and validate the required diagnostics and actuators and the plasma response. First studies of ammonia formation can therefore be performed during this phase whenever nitrogen injection is performed. Recent results from ASDEX-Upgrade and laboratory studies indicate that ammonia formation might proceed mainly from shaded areas in the divertor region not in direct contact with the plasma, so that the ammonia formation rate might only depend on the relative fluxes of hydrogenic and nitrogen radicals to those surfaces and not too much on the actual divertor plasma conditions. In this case, a first estimate of ammonia formation rates could be obtained already during PFPO-1. This will require analysis of the exhaust gas composition using RGAs. Calibration of these RGAs might require the injection of known amounts of ammonia into the empty vacuum vessel. In addition, complete regeneration of the cryopumps will be necessary to recover the ammonia trapped on the active charcoal, the amount of which can be determined by chromatography of the exhaust gas. One unknown at this time, is that it has been observed in both JET and ASDEX-Upgrade that a certain plasma operation time is required to reach a stationary ammonia formation rate and at present it is not clear what typical discharge durations will be required on ITER.

2.5.4.10.3.2 Baking studies

Relatively low Be erosion and co-deposition rates are predicted during the low power discharges of PFPO-1. To first order these rates depend on the wall particle flux, itself related to the edge plasma density/temperature. The thickness of the hydrogen containing co-deposits formed during PFPO-1 will therefore be much lower than that expected during later high-power operations. First indications of the hydrogenic release behaviour during a bake-out of the PFCs can, however, be obtained if a bake is executed at the end of PFPO-1 (assuming that it ends with hydrogen plasmas). In addition to providing data on the release kinetics of retained gases as the PFC temperature is increased, such baking will allow a first validation of the global migration (including diffusion/trapping) models used to predict T-retention in later nuclear operations. Since baking is a time-consuming activity, possible only when the magnetic field is off, these studies are best executed at the end of PFPO-1, before the start of the subsequent assembly phase.

2.5.4.10.3.3 Development of a 'raised strike points' scenario

Current predictions indicate that co-deposition of Be and T in the divertor will mainly occur on the upper part of the vertical targets and on the baffle area. Given the possible limitations in the efficiency of the divertor bake for tritium removal from thick co-deposits [De Temmerman, 2017], and the fact that divertor baking is a time-consuming activity, which can probably not be executed too often during a campaign, it is of interest to explore techniques capable of accessing the fuel trapped in these co-deposits. Besides inter-pulse ICWC/ECWC, one possibility is to run a plasma discharge with strike points located further up the vertical targets or even on the baffle region. This would allow a local heating of the co-deposits, together with isotopic exchange and, possibly, some physical sputtering of the co-deposits if the local T_e is high enough.

The possibility of running ITER plasmas with raised strike-points was examined in [Kolesnikov, 2013] in the context of the old divertor strategy with carbon in the strike point regions – the idea was to position strike points on a W region extending down from the baffle region to gain early experience operating on W targets. Since then the CFC/W divertor was eliminated in favour of the full-W variant. The study found that for strike points raised to just below the current transition

region from the straight to curved parts of the vertical W divertor targets, L-mode plasmas up to 14 MA would be controllable in terms of vertical stability, well above the maximum plasma currents envisaged to be attempted in PFPO-1. No analysis of the divertor pumping efficiency in these configurations has yet been made. For detritiation studies, strike point locations on the baffle area may even be required (providing proper attention is paid to monoblock edge overheating given the lower tolerances on block to block alignment in the baffle area). Dedicated time will be required to develop such equilibria and to assess the maximum allowable input power etc.

2.5.4.10.4 Material migration studies

Initial studies of material (mainly Be) migration in ITER can be performed during PFPO-1. Visible spectroscopy in the main chamber and the divertor will be available during this phase. Monitoring the evolution of the main chamber and impurity sources requires that a standard (or reference) monitoring discharge is executed regularly during the campaign so as to provide reproducible and identical plasma conditions. Such a reference pulse would also be useful other purposes such as diagnostic calibration, verification of the thermal response of the plasma-facing components, verification of the wall conditions, etc. (see Appendix D). The pulse will consist of several phases such as limiter, L-mode, H-mode, with scans of the separatrix location and outer wall gap distance, allowing the study of Be transport in different plasma configurations. The discharge will evolve with the machine capabilities, and during PFPO-1 will probably consist only of the limiter and L-mode phases. Absolute calibration of the spectroscopic diagnostics will be required, together with a regular monitoring of the transmission of the optical path, to be able to convert the measured signal into photon fluxes which can then be compared to the signals calculated by synthetic diagnostics of edge plasma codes.

In addition, a set of first wall samples will be installed during the assembly/maintenance phase prior to each operation phase. They will be installed in slots between First Wall Panels (FWP) at different toroidal and poloidal locations and will be shadowed from direct plasma impact. The aim is to evaluate the first wall erosion caused by fast charge-exchange (CX) neutrals. The sample surface will be made of Be with marker layers to provide high resolution erosion measurements. After PFPO-1, some (or all) of the samples will be retrieved and analyzed in a dedicated laboratories. The data from these samples will provide useful information to validate the edge plasma/migration models used to predict material migration.

2.5.4.10.5 Limiter heat load characterization

As in many tokamaks, plasma current ramp-up in ITER will begin in limiter configuration on the Be first wall. This will be the case for all plasmas, in all operational phases, with the only difference being the range of B_t which will be explored in each phase. The FWP are designed such that start-up can be on either the outboard or inboard equatorial regions, with enhanced heat flux (EHF) panels installed there to handle perpendicular heat loads up to ~4.5 MWm^{-2} [Mitteau, 2011]. For a number of reasons [Kocan, 2015], inboard start-up is preferred and the majority of start-up scenarios developed for ITER favour this route. So far, all ramp-down scenarios bring the plasma down into a limiter configuration on EHF outboard panels, first at the equatorial midplane then later, in the very final stages, mostly on panels in the lower part of the poloidal cross-section at low I_p.

In recent years, a great deal of work has been invested in the R&D community, led through the ITPA Divertor and SOL Topical Group, to properly characterize start-up limiter heat loads. This was stimulated by the first measurements on the JET ILW Be main chamber protection limiters [Nunes, 2012; Arnoux, 2013] which found strong evidence for a very narrow feature in the SOL

parallel heat flux at the last closed flux surface (LCFS) of inboard limiter plasmas, followed by the normal 'broader SOL' (of width $\lambda_{q,main}$), which had previously been assumed for the design of the ITER FWPs to be the only structure of limiter SOLs. In fact, multi-device studies [Kocan, 2015] have revealed that the width, $\lambda_{q,near}$, of this narrow feature scales with $1/I_p$ in the same way as for the near-SOL in diverted H-modes (see Appendix C). It has also been shown [Goldston, 2015] to be reasonably well matched by the heuristic drift model developed for the H-mode [Goldston, 2012].

In the light of the JET findings, a very extensive multi-machine database has been constructed for the inboard limiter $\lambda_{q,main}$ [Horacek, 2016] to try and confirm the original assumptions for the broad SOL width made for the ITER wall design which were based on very sparse data. The new scalings derived from these databases for both $\lambda_{q,near}$ and $\lambda_{q,main}$ have been used to redefine the toroidal shape of the ITER inner wall FWPs [Kocan, 2015] since the previous major release of the ITER Research Plan (the outer wall panel shape remains unchanged). This new shape takes into account the presence of a double exponential structure in the SOL parallel heat flow.

A great deal more information is now also available regarding the accuracy with which the blanket can be mechanically aligned (see *Final report from the Magnetic Axis Working Group* [ITER_D_SSKMMC, 2016]) and it is now even more important than before that the Research Plan foresees adequate operational time for limiter heat load verification to carefully validate FWP heat loads, given the penalties that must be introduced to account for blanket misalignments and the fact that the real design of the FWP contour is only an approximation to the ideal shape defined by physics [Mitteau, 2015].

Dedicated limiter heat load studies will be required in PFPO-1 at all major toroidal field values to be used for scenario design and DMS commissioning. Part of these experiments can be conducted during the commissioning phases that must be performed to establish routine limiter operation, as detailed in section 2.5.4.2. The first stages will be at lower I_p (2 MA), followed by a step to near 3.5 MA, which is the approximate plasma current at which a divertor configuration can be formed according to current scenario design. This commissioning will also include development of ECRH heating scenarios; this is important for limiter heat load testing which requires additional power. The early tests, probably starting at lower B_t, will permit a first crude look at the influence of FWP misalignment on the power distribution (using the wide angle main chamber IR viewing diagnostics) and a cross check of the magnetic axis measurements which will have been performed following the first plasma attempts and prior to full blanket installation.

The FWP shape design has been optimized for $\lambda_{q,main}$ = 15 mm and 50 mm for outboard and inboard limiter plasmas respectively and $\lambda_{q,near}$ = 4 mm for inboard limiter configurations (the narrow feature is not present for plasmas limited on the outboard). The chosen values for $\lambda_{q,main}$ fall within the inner wall limiter multi-machine database scatter at for I_p up to 7.5 MA, the highest plasma current considered in the FWP design (see *Heat and Nuclear Load Specifications* [ITER_D_2LULDH, 2009]). Regression analysis of the database finds a best fit engineering parameter scaling for inboard limiter plasmas of $\lambda_{q,main} \propto (P_{IN}/V)^{-0.4}\kappa^{-1.3}$ with P_{IN} the total input power, and V the plasma volume. For inner wall limiter configurations, a second parameter also plays an important role in the new shape design: the effective ratio of power transported in the near and main SOL regions of the profile. This has been fixed at R_q = 4 for the ITER inner FWP [Kocan, 2015], but is uncertain since the data from the multi-machine experiments are more scattered and a scaling cannot yet be defined. There is, however, some flexibility here since the chosen toroidal shaping allows for a range of possible R_q before power overload, although this will be sensitively dependent on the degree of FWP misalignment and must be carefully checked.

Thus, according to current best scalings, there is no explicit B_t dependence in either $\lambda_{q,main}$, or $\lambda_{q,near}$, a relatively clear $\lambda_{q,near} \propto 1/I_p$ dependence and uncertainty in the variation of R_q, though there is some evidence for a direct scaling with P_{IN} [Horacek, 2015], so that both $\lambda_{q,main}$ and R_q are likely to be input power dependent. Detailed assessment of the FWP power handling during design phases was conducted assuming B_t = 5.3 T, so that the safety factor at the Last Closed Flux Surface (q_{LCFS}) will be lower at a given I_p for ramp-ups with 1.8 T and 2.65 T (e.g. for near full bore limiter plasmas at κ ~1.5 at 3.0 MA, q_{LCFS} ~ 10 (5.3 T), 5 (2.65 T) and 3.5 (1.8 T)). For a given plasma shape, this is unfavourable for FWP loading since higher pitch angles at lower field mean that field line penetration may occur in regions not anticipated in the original design. Detailed field line mapping for all configurations to be tested, incorporating basic SOL heat flow models, will need to be performed before any dedicated power loading experiments. The very first attempts at low I_p can be used to calibrate the models and tools now being put in place to perform these assessments. It should be noted, however, that the main chamber IR systems, which are the primary diagnostics for this experiment, will not be sensitive to very low surface temperatures and so at very low input power, limiter heat flux patterns may not be easy to measure.

Once limiter plasma and EC power commissioning are satisfactorily completed at each given B_t, dedicated limiter heat load characterization in PFPO-1 should include the following main elements, conducted for both inboard and outboard limiter configurations:

- Elongation scan at fixed I_p and P_{IN};
- Power scan at fixed shape (elongation) and I_p;
- I_p scan at fixed elongation and P_{IN};
- Density scan over the range possible at fixed I_p, P_{IN} and elongation.

The experiments should be performed in hydrogen plasmas since helium sputtering will be higher and impurity distributions different to those in hydrogenic plasmas. Moreover, if the narrow feature width scales with ion orbit width, this will be different in H and He. Similar experiments could be run, if required, in He plasmas to expand the limiter loading database, but this should not be a priority in the Research Plan.

A simple criterion was adopted for the FWP shape design to define the maximum power fluxes during limiter phases: $P_{limiter}$ [MW] < I_p [MA], so that at the highest specified I_p (7.5 MA), a total of 7.5 MW of heating power (ohmic plus additional heating) is assumed. This allows for a reasonable margin for ECRH heating, though as mentioned above, detailed wetted area and power flux density calculations will be required prior to any limiter plasma work at higher input powers. The lower power commissioning stages will have permitted any gross FWP panel misalignments to be quantified and this will also set the limits to what can be done during the full heat load characterization, both with respect to input power and plasma shape variation. The maximum values of P_{IN} and, in particular I_p, will need to be chosen for these experiments once the first commissioning results are available and will be dependent on progress with disruption mitigation (see section 2.5.4.6).

Experiments on JET with Be limiters performed long before the ITER-Like Wall installation found no runaway generation during unmitigated disruptions up to 5 MA at high toroidal magnetic field [Harris, 1990], but the limiter configuration is more favourable for runaway appearance when mitigation is deployed [Reux, 2015]. However, thermal loads during the current quench of unmitigated disruptions at higher currents can be prohibitive due to conversion of magnetic energy into thermal power flux and subsequent melt damage to the first wall [Matthews, 2016]. The choice of maximum I_p for the limiter heat load characterization will therefore primarily be determined by

the status of DMS testing. If feasible, maximum target values would be ~4 MA at 1.8 T and ~6 MA at 2.65 T. Nearly circular plasmas will likely be restricted at the higher current and powers due to unacceptable field line penetration. These are in any case of lower interest, other than to test the shaping design, since nearly circular plasmas will only ever occur at very low I_p (hence low power) in the very early ramp-up phases.

The aim of these limiter heat load validation experiments is to set the limits on what is acceptable with regard to first wall power loading, to check if the input physics assumptions defining the wall shape are applicable at the ITER scale, to benchmark field line tracing and wall shape parameters and to test wall protection algorithms. The full main chamber IR diagnostic (WAVS: Visible/IR) system must be in place to conduct this validation – experience from JET [Nunes, 2012] demonstrated how important it is to be able to see as much of the limiter surface as possible. For the actively cooled FWPs, steady state power handling is achieved in several seconds, so that the experiments should guarantee phases of this duration for each of the chosen scenarios. The active cooling is advantageous in the sense that several experimental points can in principle be obtained in a single discharge, depending on the maturity of plasma shape control. Once experiments have been performed at the first chosen value of B_t, it should be relatively straightforward to repeat the scans, or a subset, at higher toroidal field and less dedicated experimental time should be required.

2.5.4.10.6 Heat loads and detachment control during divertor operations

A proper determination of heat loads to main chamber and first wall PFCs during diverted operation and demonstration of their control, particularly in the divertor, is a key element of the PFPO phases, in preparation for nuclear operation, when robust power flux control will be mandatory for ITER to achieve its mission goals. Providing as comprehensive a database as possible in the early operational phases will also allow years of model development to be validated, hopefully improving confidence that the physics of divertor power dissipation and SOL transport in ITER is well understood. The main elements to be addressed are (see also section 2.2.2):

- Scaling of the near SOL L-mode and inter-ELM H-mode heat flux width;
- Characterization of the far-SOL width for power and particles (main chamber interactions) in L-mode and inter-ELM H-mode;
- Assessment of upper FWP power handling;
- Understanding divertor detachment behaviour;
- Effects of 3-D magnetic fields for ELM control on divertor target power distribution;
- Assessment of ELM transient divertor and main wall power loading.

Many of the required measurements will be naturally obtained during commissioning and development of scenarios in the early phases and only a relatively small number of dedicated plasmas are likely to be required, particularly in PFPO-1, when power levels will be low. As shown in Appendix C, steady state power loads at the divertor do not challenge the heat handling capacity of the divertor monoblocks for $P_{SOL} \lesssim 40$ MW, which cannot be achieved until PFPO-2, and even then the heat load is only problematic at low divertor neutral pressure (high divertor plasma temperature), at which W ingress may in any case be prohibitive. It is also the case that for the maximum input power available in PFPO-1, L-mode and ELMy H-mode loads to the upper FWP in the secondary X-point point region for the baseline equilibrium at $q_{95} = 3$ are also far below (at least a factor 3) the maximum power handling capability of the EHF FWP #8,9 located in this area, even for $\Delta r_{sep} = 4$ cm, the lowest primary to secondary separatrix separation allowed during the burning plasma phase [ITER_D_TF3RCZ, 2016].

In PFPO-1, therefore, PFC power loads will be well within their design limits, so that active control is not required beyond the usual (accurate) control of the plasma shape (wall gaps, strike point positions, etc.) and the respect of operational limits (see e.g. section 2.5.4.6). Specific heat load studies in this phase can therefore be pursued without concern for PFC damage, provided the DMS has been adequately commissioned. Experiments will rely heavily on main chamber and divertor IR cameras, including the high resolution divertor systems viewing the inner and outer targets at single toroidal locations.

The following studies are to be performed, if possible, in this phase:

- L-mode divertor heat load characterization in H and He at the different toroidal fields to be used, including:
  - Power and density scans;
  - Current scans from the minimum (~3.5 MA) to the maximum foreseen at each B_t (e.g. 5 MA at 1.8 T, 7.5 MA at 2.65 T).

  In reality, there will be a limit to the lowest input power or highest density which can be explored since the ITER divertor is highly dissipative and too low a power or too high a density will result in strong detachment and operation too close to disruption boundaries. The best power load measurements will be obtained with low density/high power and with the divertor more attached. The aim is to obtain the L-mode scaling of $\lambda_{q,near}$ and estimates of the divertor power flux spreading parameter. Different combinations of B_t and I_p will also allow characterization of the divertor wetting as a function of total incidence angle.

- H-mode divertor heat load characterization at 1.8 T: a first look at the inter-ELM $\lambda_{q,near}$ and fast IR measurements of unmitigated ELM heat loads, hopefully providing information on potential issues of castellation gap edge loading and first data for comparison with ELM energy density scalings (Appendix C).

- Assessment of upper FWP heat loads and far-SOL power and particle widths using the upper chamber viewing IR and main chamber visible spectroscopy, including:
  - Scans in Δr_{sep} up to double null in L-mode and to Δr_{sep} ~4 cm in H-mode for primary combinations of I_p, B_t;
  - Density scans up to close to the density limit at fixed power in hydrogen L-modes to investigate SOL density profile broadening and its possible link to divertor detachment. Similar observations also of value in H-mode, but the available parameter range is likely to be restricted in PFPO-1.

Power levels will, in general, be too low in PFPO-1 to provide serious tests of divertor heat flux control using extrinsic seeding, except at the lowest densities (and thus high divertor plasma temperatures) when the relevance of such seeding is questionable. At more reasonable densities, the addition of even small quantities of impurities is likely to result in strong detachment. Prior to any detachment control tests, an important first goal will be to characterize as best as possible the divertor plasma itself, even in simple L-modes, to provide a database for model benchmarking to ensure that the basic detachment behaviour in simple situations is properly understood. The diagnostic tools necessary to constitute this database should be mostly available in PFPO-1 (e.g. divertor target Langmuir probes, fast in-vessel pressure gauges, divertor target IR, divertor bolometry and spectroscopy).

Some aspects of the divertor heat flux control methods developed at this stage can nevertheless certainly be trialled in PFPO-1, in addition to tests, for example, of divertor reattachment provoked by local modifications to divertor gas fuelling and due to the effect of asymmetric toroidal gas

injection. In this respect, hydrogen plasmas are more appropriate since detachment behaviour in He is very different (see section 2.2.1) and, depending on the control sensors used, He plasmas would not be a good testbed for later operation at high power with hydrogen isotopes as fuel. If impurity seeding is to be tried, then it should be focused on N_2, which radiates more readily in the divertor and which has the added benefit of providing an early assessment, in PFPO-1, of potential ammonia formation rates (sections 2.2.4, 2.5.4.10.3.1 and 2.5.5.12.2.2).

Depending on the availability of power supplies for the ELM control coils, some first measurements of perturbed divertor heat flux footprints may also be possible in PFPO-1. Experiments in hydrogen L-modes can already be extremely informative and can be used as benchmarks for modelling of divertor response to 3-D fields, which is a routine methodology in current devices. Experiments with 3-D fields in H-modes (H or He) at 5MA/1.8 T, if possible, would provide a first chance to study divertor heat load patterns under conditions of ELM mitigation, but would probably not allow relevant dissipative conditions to be accessed owing to the very low input powers.

2.5.5 Operations plan for PFPO-2

2.5.5.1 PFPO-2 Objectives

Operation at the full design parameters of 15 MA/5.3 T is essential in this phase. This ensures that all critical systems have been commissioned prior to nuclear operation. In addition, operation in H-mode at 7.5 MA/2.65 T ensures that key physics and control issues related to H-mode operation in DT are addressed at this stage, reducing the risk for D and DT operation in FPO. On the other hand, H-mode operation at 5 MA/1.8 T allows the identification of TBM effects on H-modes and the development of mitigation schemes, if required.

Routine operation of the HNB system at 33 MW for at least 50 s is necessary to support the physics program envisioned for this and later operational phases. This includes commissioning of the magnetic field reduction system and the protection systems specific to shine-through (first wall) and fast ion loss (first wall and divertor). Both of these issues are especially important for H-mode operation because they are the most likely factors to limit the use of the HNBs in hydrogen (and to a lesser degree, helium) H-mode plasmas. Due to the high shine-through power fraction in H plasmas, operation in H H-modes will most likely be restricted to short periods (~10 s) and to a very narrow density range. Thus a proper evaluation and protection of the first wall against excessive shine-through loads is essential to carry out the H-mode research program. On the other hand, both MHD instabilities and the application of 3-D fields for ELM control can potentially increase the fast ion losses from NBI and lead to localized power fluxes on the PFCs. Therefore, it is essential that together with the increase in NBI power injected into the ITER plasmas and the development of H-mode operation, fast ion losses are measured and the corresponding power fluxes are maintained under control.

Routine operation of the ICRF system at 20 MW for at least 50 s is necessary to support the physics program envisioned for this and later operational phases. In addition to the tasks in PFPO-1, this requires commissioning operation of both antennas simultaneously and at high power at 1.8 T in H plasmas and at 2.65T in He plasmas.

For this operational phase, the ECRH system will have already been commissioned and will be applied to the development of scenarios. Specific commissioning activities will be required for the application of the system to NTM control in H-modes, if NTMs are found to be unstable in the PFPO-2 scenarios.

During PFPO-2, the installed diagnostic set will be very close to its final configuration for DT operation; the additional measurement requirements for the PFPO-2 campaign and associated diagnostic systems to be installed prior to PFPO-2 are listed in Table 2-6. These additional requirements expand considerably the range of physics studies that will be possible and also provide access to expanded control capabilities, for example in relation to current drive and current profile control. Therefore, significant effort will be dedicated to the commissioning with plasma of the newly available diagnostics, as well as to their calibration and to the resolution of possible inconsistencies among plasma measurements. In this phase, plasma parameters are expected to approach comparable values to those in DT plasmas and, therefore, the demonstration of the diagnostic capabilities to support the operational program, as well as the accompanying research program, at this stage of operation is a major objective of PFPO-2.

Since this is the last operational phase before the machine will become activated, it is important to commission all systems required for DT operation as thoroughly as possible, so that any required changes can be performed during the pre-nuclear shutdown between the PFPO-2 and the FPO phases. This includes commissioning all required control, interlock, and safety functions.

The TBMs will be introduced during this operational phase and, therefore, specific experiments will be performed to characterize the resultant error fields, to evaluate the effects on L-mode and

Table 2-6 – Overview of <u>additional</u> measurement requirements and <u>additional</u> diagnostic systems installed for the PFPO-2 campaign[*]

Measurement Requirement	Installed Diagnostic Systems
Core profiles of n_e and T_e	• Core Plasma Thomson Scattering (full) • Reflectometry Low Field Side • Poloidal Polarimeter (10 channels) • Reflectometry High Field Side
Core T_i, impurity measurements (CXRS)	• Charge Exchange Resonant Spec. Core
Edge profiles of n_e, T_e and T_i (TS, ECE, Reflectometry, CXRS)	• Edge Thomson Scattering ($0.85 < r/a < 1$) • Charge Exchange Resonant Spec. Edge • Charge Exchange Resonant Spec. Pedestal • Reflectometry Low Field Side • Reflectometry High Field Side
Current profile measurements	• Poloidal Polarimeter (10 channels) • Motional Stark Effect (baseline)
Divertor plasma characterization	• Divertor Thomson Scattering
Fuel species	• Charge Exchange Resonant Spec. Core • Neutral Particle Analyzers
PWI/ Heat Load characterization	• Dust Monitor • Erosion Monitor • Tritium Monitor (commissioning) • Calorimetry

[*] *The table illustrates the additional diagnostics systems planned for installation prior to PFPO-2 to meet the additional measurement requirements (when combined with the FP and PFPO-1 systems). Certain systems partially installed prior to PFPO-1, as shown in Table 2-4, will be extended or completed in advance of PFPO-2 - see Appendix H for a full list of diagnostic systems planned for installation prior to PFPO-2.*

H-mode plasmas, and to develop mitigation schemes. It is essential, if sizeable effects are found, that effective mitigation schemes are developed at this stage to ensure low disruptivity and high energy confinement of H-mode plasmas before the plasma current, toroidal field and input powers are increased to their nominal baseline values later in PFPO-2. This will require the re-optimization of error field correction with the external correction coils and, possibly, additional support from the ELM control coils for L-mode plasmas. Similarly, to characterize the effect of error fields on H-modes, specific experiments to compare H-mode performance at 5 MA/1.8 T in PFPO-1 (no TBMs) with that obtained in PFPO-2 (with TBMs) are included in this phase, together with the development of mitigation schemes (minimization of error fields with external correction coils and ELM control coils), if required. The magnetic field reduction systems for the NBIs will produce additional sources of error fields, which may also require a re-optimization of the error field correction to be carried out in this phase to mitigate their effects.

The H-mode research program in PFPO-2 will provide the physics basis and control schemes on which to base H-mode scenario operation in FPO. By the exploration of H-modes at two toroidal fields (1.8 T and 2.65 T) and over the range $q_{95} \approx 3$ - 5 (I_p = 3.5 - 5 MA for 1.8 T and 5.0 - 7.5 MA for 2.65 T) in hydrogen/ helium plasmas, the following objectives will be fulfilled:

- Determination of the H-mode threshold in H and He over a density, toroidal field and q_{95} range allowing the evaluation of the power required for H-mode access in DT operation;
- Demonstration of fully integrated H-mode scenarios including power load control, ELM control, fuelling, core W control, which are key to the development of similar scenarios in FPO;
- Optimization of ELM control, divertor power load control and heating power mix for H-mode plasma performance;
- Demonstration of shape, ELM control and power load control on entry to and exit from H mode phases;
- Development of robust current ramp-up/down scenarios, including response to off-normal events.

On the other hand, the L-mode program in H plasmas to 15 MA/5.3 T will demonstrate the capabilities of the ITER tokamak and its ancillary systems to operate at their nominal design parameters, including heating, fuelling and the capability of the diagnostic and control systems to provide robust (disruption-free) plasma operation. Expanding the current range beyond 7.5 MA will require qualification of the DMS in a careful step-wise fashion. Commissioning of predictive systems for disruptions with avoidance strategies, development of an algorithm to trigger the mitigation system, and qualification of the mitigation system at each specific current step will be performed. The proposed step-ladder approach from 7.5 MA/2.65 T to 15 MA/5.3 T follows a q_{95} = 3-4 band with changes of both I_p and B_t. This implies some variation in the heat deposition profile that can move off-axis (up to $\rho = 0.5$) for some steps, if NBI is not used (which is likely at the lower currents due to the high shine-through density limit in H plasmas). Therefore, W accumulation will have to be carefully monitored and controlled; specifically the interplay between divertor conditions (W sputtering source) and core W control will need to be assessed. If the installed heating systems (chiefly ECRH and ICRF) are shown to be insufficient to provide W accumulation control, some of the specific values of the I_p/B_t step-ladder will have to be adjusted or, eventually, a constant 5.3 T route may have to be chosen for this development. This is less desirable because q_{95} changes from 6 to 3 along this route, so that MHD stability can change significantly at each step in I_p, and it can become more complicated to ensure stability as I_p approaches 15 MA. In addition to the operational experience, the L-mode plasmas obtained through

this development will provide first experimental evidence of core transport physics of plasmas with parameters not far from those at Q = 10, which are essential to validate the understanding of transport physics at the ITER scale and to plan D and DT operation in FPO.

If experimental time allows (in the plan an operational period of 6 days is put aside for an initial attempt), it would be desirable to extend the operation of the H&CD systems to several hundred seconds, allowing long-pulse H-mode operation to be developed. This would provide initial experimental evidence of long time-scale behaviour of ITER H-mode plasmas in preparation for DT operation.

In addition to this long pulse demonstration, specific issues related to long-pulse operation in DT will already be assessed at this stage. This includes target-q profile development in the current ramp-up and sustainment for ~10 s in the flat-top, and assessment of the current drive capabilities of the ITER H&CD systems, particularly NBI and ECRH, in H-mode plasmas that can provide an initial assessment of possible issues related to the application of these schemes in FPO long-pulse operation (e.g. triggering of Alfvén Eigenmode instabilities which could reduce NB current drive) and allow the development of schemes to mitigate them, if required.

It would also be desirable to demonstrate core MHD instability control, even if this may not be required at this stage in the development of the ITER Research Plan, to ensure that the required schemes are developed in advance of their application in FPO and to ensure that the necessary upgrades are launched at this stage, if the baseline capabilities are found to be insufficient. Such studies would focus on the control of sawteeth and tearing modes primarily by the application of focussed ECRH/ECCD.

Finally, as discussed in section 2.5.1, the wide range of experimental conditions and plasma parameters expected in PFPO-2, in particular the high power and long-pulse operation aspects, will provide access to studies of key PWI and heat load management issues in preparation for the significantly more challenging edge and divertor parameters expected at high fusion power during FPO.

2.5.5.2 Plasma restart in PFPO-2 (including influence of Test Blanket Modules)

The plasma restart in PFPO-2 should aim to re-establish routine plasma operation at 7.5 MA/2.65 T as rapidly as possible. The restart will be in hydrogen and should re-establish plasma initiation at 2.65 T with further optimization when required. It should include plasma initiation at full CS precharge of 40 kA at 5.3 T, for the preparation of operation at 15MA/5.3T later in PFPO-2.

PCS should demonstrate routine operation at 7.5 MA/2.65 T during this restart phase by recommissioning plasma shape control, VS control, density control with gas and pellets and event handling. In parallel, the DMS system should be recommissioned using reference pulses from PFPO-1, and any changes to DMS hardware or control implemented during Assembly Phase III should be commissioned.

The interlocks for the H&CD systems should be retested and the ECRH systems and ICRF systems that were previously commissioned in PFPO-1 should re-establish heating power at >50% of maximum power for > 5s. The restart targets for systems that were already available in PFPO-1 will have to be defined to show readiness for commissioning of new systems. The main target for the restart in PFPO-2 is to re-establish routine operation at 7.5MA/2.65T to allow for commissioning of the additional H&CD installed during Assembly Phase III to be performed with plasma as early as possible, since the further development of the research program relies heavily on the availability of a reliable H&CD capability at a significant power level.

2.5.5.2.1 Documenting the effect of the Test Blanket Modules (TBMs) during plasma restart

The newly installed TBMs may have an effect on magnetic measurements, plasma rotation, the plasma response to error fields and overall plasma performance, particularly in H-mode. The effect on magnetic measurements can be documented without plasma operation in the machine commissioning before plasma operation. However, the effect of the TBMs on error fields and their control requirements will have to be measured by assessing the lower density limit for plasma operation (error field locked modes) and the effect on plasma rotation. The error field correction (commissioned in PFPO-1) will almost certainly have to be re-optimized to include the effect of the TBMs at an early stage of operation. This error field correction re-optimization should also consider the possible additional error fields produced by the Magnetic Field Reduction system for the NBIs. The effect the TBMs on overall plasma performance can probably be assessed most readily by repeating H-mode pulses from PFPO-1. Although these will be H-modes at low performance (up to 30 MW input power and 1.8T magnetic field only), the effect on pedestal parameters or plasma rotation could be uniquely documented from these experiments.

2.5.5.3 Heating & Current Drive (H&CD) commissioning (HNB, DNB, ICRF)

The commissioning of the H&CD systems to full power and pulse lengths of at least several tens of seconds (longer as experimental time and priorities permit) is a key goal for the PFPO-2 campaign of operation to allow access to H-mode operation and to demonstrate the operational capability of the H&CD systems before the transition to fusion power production. For the neutral beams, operating at 870 keV in hydrogen during the PFPO phase, extensive commissioning of the beamline components without plasma is foreseen during Integrated Commissioning III. Commissioning with injection into the ITER plasmas can start after pre-commissioning of the NB Magnetic Field Reduction system (Active Compensation and Correction Coils), to decrease the residual magnetic fields to acceptable limits (~0.1 mT in the region between the grounded grid and the neutralizer) in order to limit the beam deflection and to ensure maximum beam transmission with minimal losses due to direct interception. In addition, stable operation of a standard full-bore plasma with a flat-top diverted phase having a density above the minimum shine-through density limit must be well established and the critical diagnostics for protection against unacceptable shine-through heat load on the blanket first wall panels confirmed to operate routinely as real-time monitors (i.e. density, impurity, and IRTV viewing the relevant first wall panels). This capability will therefore need to be integrated into PCS and the beam interlock system. The error field correction (commissioned in PFPO-1) will then have to be re-optimized taking into account the error field produced by the NB Magnetic Field Reduction system, as already mentioned in section 2.5.5.2.1 above.

Most of the ECRH commissioning will have been undertaken prior first plasma and during PFPO-1. All beamlines must be reconditioned to full power for a duration of ~50-100 s in PFPO-2. The ECRH heating interlocks will also need to be re-established: all gyrotrons and launchers should be reconditioned at 90% of previous power levels.

ICRF commissioning:

As described in section 2.5.4.5, the ITER Research Plan assumes that the ICRF acceleration program allows one ICRF antenna to be commissioned during PFPO-1, while the second antenna will be commissioned during PFPO-2. Additional ICRF commissioning of both antennas will be required during PFPO-2 due to the mutual interaction of the 2 antennas and, if H-mode operation at 1.8 T is not successful in PFPO-1, due the need to adapt the antenna coupling to the different edge and SOL conditions in H-mode, as well as to the dynamic matching of properties and power coupling during the L-H transition. Advanced commissioning steps described in section 2.5.4.5

must be briefly repeated during PFPO-2 to verify that the performance is the same with different plasma conditions. The additional ICRF commissioning steps are described below.

Additional ICRF advanced commissioning (requires ~ 60 s pulse dedicated time and thus will be addressed as the development of long pulses allows):

- Demonstration of RF coupling control via gas puffing and control of the gap between the separatrix and the antenna, to be performed both in L-mode and H-mode[4];
- Assessment of the compatibility of impurity gas puffing, used for divertor protection, with the ICRF coupling performance, to be carried out both in L- and H-mode plasmas;
- Operation with the two antennas simultaneously in order to test the cross-talk limits, i.e. the reciprocal effect of the antennas due to their receivers/transmitters behaviour (frequencies are required to be different by typically 100 kHz in order to avoid interference between the two antenna control and data acquisition systems);
- Commission ICRF for wall cleaning (ICWC).

An additional risk to those listed in section 2.5.4.5 is the possible parasitic edge resonances with He^3, if this is injected for alternative heating schemes, leading to additional wall loads. Such an eventuality would need to be prevented by adequate operating instructions.

NB commissioning:

Commissioning of the HNB and DNB systems will be carried out at half-field in H or He plasmas, using H beams with energies of up to 870 keV and 100 keV for the HNB and DNB respectively. The density above the minimum shine-through density limit must be well established. The initial shine-through assessment is illustrated in Figure 2.5-3 for various densities and plasma current levels in H and He plasmas. The commissioning time is estimated to be around 50 days and does not need to be exclusively allocated to this activity. The NB commissioning with the plasma will be carried out following these steps:

- First pulses would be dedicated to duct conditioning with pulse lengths ~ 0.1 s, and will be progressively extended in steps to a maximum of 1 s, with continuous monitoring of the heat loads and pressure rise in the duct region due to beam duct degassing. A total of 50 beam pulses is estimated and could be combined in a long-pulse plasma discharge with a flat-top of 100 s depending on the progress of the conditioning and the gap required between the beam pulses to restore the conditions to acceptable limits before the next beam pulse.
- The beams ducts for each of the three beam lines, HNB-1, HNB-2 and the DNB will initially be individually conditioned. When the HNB-1 and DNB systems are operated in parallel, several extra conditioning pulses may be required to condition the cross over region in the duct. This may also be the case for the shared vacuum vessel pressure suppression system (VVPSS) region between the HNB-1 and HNB-2.
- The pulse length will be progressively extended from 1 s to 2 s, 3 s, 5 s and 10 s, once the duct is conditioned.

[4] The RF coupling is usually better in L-mode than in H-mode plasmas, due to smaller density gradients. Optimizing the matching algorithm settings for the L- to H-mode transition, during which the coupling varies rapidly, will require due attention, since the H-mode access is bound to depend on the coupled ICRF power. The acquisition of sufficient experimental data will allow optimization of the algorithm by better anticipation of the transition. The fine-tuning of the matching will be carried out during the commissioning. A database of matched configurations should be established based on this commissioning phase.

- A range of different tilted beam angles need to be tested in case that it is required to change them for different scenarios, checking the associated shine-through and power density limits, but this implies only a small number of additional pulses.
- Various beam energies need to be commissioned, since the beam energy affects the re-ionization power on the beamline components.

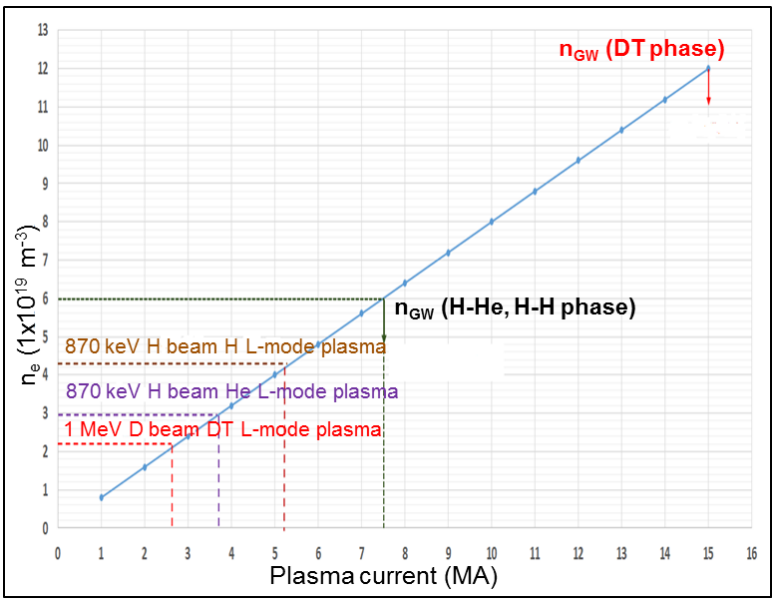

Figure 2.5-3: Shine-through limits for a range of densities/ plasma currents and various HNB beam energies and species (870 keV H beams for H/He plasmas and 1 MeV D beams for D/DT plasmas).

- The power modulation capabilities of the HNB system need to be tested during this commissioning period.

A similar conditioning process will be repeated for deuterium plasmas in the FPO phase, but with D beams at energies of up to 1 MeV.
The main risk during the HNB commissioning activity arises from the shine-through losses, which are greatest at low density, but losses to the blanket first wall can also be increased by prompt orbit losses, enhanced at low plasma current due to the reduced confinement. Therefore, as noted above, HNB commissioning requires real-time heat load measurements on the first wall, together with the density profile, impurity concentration and (if possible) fast ion loss measurements.

2.5.5.4 Diagnostics commissioning and validation

Many more core and edge diagnostics will be available in PFPO-2 (see Table 2-6 and Table H-3 in Appendix H), as well as the HNB and DNB, which will allow MSE and CXRS measurements to be implemented. This will allow significantly improved measurements to be made of the higher performance plasmas that will be performed in this phase and require substantial commissioning and validation of the measurements.

A number of dedicated plasma sessions will be required not only for the commissioning of the new diagnostics but also for the calibration of some of the previously installed set due to new plasma conditions.

2.5.5.5 Disruption management program in PFPO-2

The disruption program in PFPO-2 will mainly focus on adapting disruption prediction, avoidance and forecasting capabilities, and optimizing the mitigation schemes for high current operation and for H-mode operation.

2.5.5.5.1 Disruption Mitigation System (DMS) commissioning/optimization

The DMS will be optimized towards higher currents and higher thermal energies, including assessment of eddy current forces during fast current quenches. The latter will aim at maximizing – within the load limits – the radiated power fraction during the thermal quench in preparation to thermal load mitigation and runaway suppression. Thermal load mitigation has to be confirmed for VDEs and MDs and scalings on thermal energy, impurity species and quantity need to be established. Radiation peaking has to be reduced to stay below melting thresholds when extrapolating towards full performance pulses. This will require amongst others to optimize the sequence of all injectors.

RE avoidance has highest priority when approaching high current operation and the injection schemes have to ensure sufficient margin to RE seed formation during the thermal quench. However, testing this margin bears significant risks at high currents. Therefore, the constraints on the injection quantities and sequences will have to rely to a great extent on modelling that was already validated at lower current levels. Nevertheless, uncertainties will be high due to the exponential growth in avalanche multiplication when increasing the plasma current.

DMS reliability needs will increase with current and energy. This will require more focus on robust injection schemes that also consider failure of an injector during the injection sequence and possible recovery scenarios. The PCS algorithms also will have to be updated to react on any loss of DMS injectors during the plasma pulse, either by changing the pulse schedule or by choosing back-up injectors.

The following Milestones have to be achieved in PFPO-2:

2.5.5.5.1.1 Confirmation of EM load mitigation at 15 MA

Prerequisite for operating at 15 MA.

Experimental strategy:

- Monitor mitigation performance during ‘natural’ mitigated disruptions, possibly hold points if data is insufficient
- Possibly, perform deliberate mitigated disruptions at currents above 7.5 MA if database is not sufficient to allow scaling to the next current level

2.5.5.5.1.2 Confirmation of thermal quench heat load mitigation in H-mode

Prerequisite to run routinely at H-mode thermal energy levels.

Experimental strategy:

- Produce target plasmas with varying thermal energy in H-mode
- Confirm or adapt required quantities and injection scheme to achieve high radiation fractions during the thermal quench
- Validate compatibility with RE avoidance scheme and EM load mitigation scheme

The estimated number of pulses/days required for DMS commissioning/optimization in PFPO-2 is 260/20.

2.5.5.5.2 Disruption Load Validation

Most of the work on load validation is expected to be carried out in PFPO-1. However, certain heat load validation may require operating in H-mode or at higher currents. Further unmitigated disruptions may have to be performed if the accuracy of the electromagnetic load scalings derived from up to 7.5 MA operation is not sufficient. Establishing reliable scaling for thermal loads occurring during the thermal quench at higher stored thermal energies in L-mode during VDEs and MDs may also require operation at higher currents. The load scalings are important for defining target values for disruption rate and mitigation rate.

The estimated number of pulses/days required for Disruption Load Validation in PFPO-2 is 10/1.

2.5.5.5.3 Disruption Mitigation System (DMS) trigger generation

Start of H-mode operation will require adapting disruption prediction and possibly also detection schemes. Also the algorithms within the PCS determining the appropriate injection sequence in each phase during a pulse will have to be adapted to the new plasma scenarios. Any tests of prediction or detection schemes that include deliberate disruptions have to be performed using the disruption mitigation system. Extended diagnostic capabilities will have to be taken into account and exploited for the prediction algorithms. Note that the required mitigation rates will also depend on the tendency of unmitigated disruptions to form runaway electrons. For higher thermal energies, the impurity influx especially from the divertor can lead to faster thermal and current quenches, facilitating RE formation.

The following Milestones have to be achieved in PFPO-2:

2.5.5.5.3.1 Thermal quench prediction ready for FPO

Prerequisite for FPO. The required reliability depends on the expected loads and might vary for different thermal energies (c.f. sections 2.3 and 2.5.4.6.2).

Experimental strategy:

- Monitor the performance of disruption prediction algorithms;
- If required expand threshold and physics model-based algorithms for predicting the thermal quench during H-mode operation, implement statistical methods in parallel;
- Perform dedicated mitigated disruptions if required to optimize the disruption predictor;
- Implement and test decision schemes in the PCS for the injection sequence.

2.5.5.5.3.2 Injection sequences ready for FPO

Prerequisite for FPO.

Experimental strategy:

- Optimize injection sequences for pre-TQ injection;
- Verify RE avoidance, TQ and CQ mitigation efficiency.

The estimated number of pulses/days required to establish the DMS trigger function in PFPO-2 is 75/6.

2.5.5.6 Advanced control commissioning in PFPO-2

With the additional systems that will be available in PFPO-2, many advanced control schemes will need to be commissioned as soon as the associated actuator and diagnostic systems required for their implementation are commissioned. Since this is the last operational phase before the tokamak structures will become activated in the FPO phase, it is important to commission as many advanced control schemes as possible so that any changes in the hardware and software can be carried out prior to the FPO phase. Note that all disruption related control in PFPO-2 is described in section 2.5.5.5. The run-time estimates given here are for commissioning of advanced control schemes, but further development of the physics R&D needed to develop robust control is likely to require significantly more run-time as part of the physics program. The main new actuators in this phase include additional pellet injectors both for fuelling and pellet pacing, the second ICRF antenna to inject 20 MW of ICRF power, and two HNB systems to provide 33 MW of NB power, as well as the remainder of the ELM coil power supplies to provide full independent control of the ELM coils. The installation of the first six ferromagnetic TBMs will also require recommissioning of error field correction. The development of more sophisticated actuator sharing, event handling, integrated control, and forecasting techniques will also be required in this phase.

2.5.5.6.1 Magnetic control

The development of plasma current, position, shape, and vertical stability control will have to be extended during the PFPO-2 phase up to 15 MA and 5.3 T. While this will build on the magnetic control that was developed during PFPO-1 at currents of perhaps 10 MA, because of the increased risk of damage to in-vessel components at higher plasma current, great care will have to be taken to raise the plasma current gradually to 15 MA while ensuring the effectiveness of disruption and runaway mitigation techniques. Increased attention will also need to be paid to plasma shape and position control at higher plasma current.

2.5.5.6.2 Plasma kinetic control

While first wall protection will have already been developed in PFPO-1 at auxiliary heating powers of up to 30 MW and to plasma currents of at least 7.5 MA, in the PFPO-2 phase it will need to be developed further for total auxiliary heating powers of up to 73 MW and plasma currents of up to 15 MA. As part of HNB commissioning in this phase, first wall protection against NB shine-through will need to be developed. This will be carried out by gradually increasing NB energy (and power) and pulse length. The plasma current will be gradually raised to 15 MA and the first wall protection must include this additional ohmic heat flux at low q_{95}. An additional 8 days of first wall protection commissioning is estimated in PFPO-2 as the H&CD systems are commissioned to full power and the plasma current is raised to 15 MA.

Initial divertor protection commissioning was carried out in PFPO-1, but the relatively low auxiliary heating power in that phase is not expected to challenge the divertor. Only above 40 MW of auxiliary heating power is the divertor heat flux protection expected to be required. As the H&CD systems are commissioned to full power in PFPO-2, divertor protection will become essential. See sections 2.5.5.12.3, 2.5.5.11.4, and Appendix C for more details. An additional 7 days of divertor protection commissioning are estimated for PFPO-2.

The sensors used for plasma stored energy and β control in PFPO-2 are expected to remain the same as those commissioned in the PFPO-1 period. However, the actuators will change substantially since HNB and additional ICRF will be added providing a total of 73 MW of auxiliary heating power. Algorithms that divide the mix of the H&CD systems used (e.g. ECRH, ICRF, and HNB) will need to be formulated, implemented, and tested. Any model-based algorithms implemented in the PFPO-1 period will need to be upgraded to include all three H&CD system actuators and commission H&CD system actuator sharing. An estimate of 4 run days has been allocated to β and stored energy control in PFPO-2.

Initial temperature and pressure profile control will be commissioned in the PFPO-2 phase since the profile diagnostics and full H&CD systems will then be available. A real-time evaluation of the plasma pressure profile can more sensitively determine instability thresholds for MHD modes such as ELMs, NTMs, kinks, or RWMs when compared to using plasma β (the volume integral of the plasma pressure profile) alone. The sensors used in such a control system will be direct real-time measurements of the plasma temperature profile or the plasma pressure profile based on measurements of plasma temperature, density, and the profile of the effective plasma charge state, Z_{eff}. The real-time evaluation of the pressure profile peaking factor p(0)/<p>, together with a model of the direct measurement, might be sufficient initially. Actuators for plasma temperature and pressure profile control would include the heating system actuators mentioned earlier, but now the localization of the heating would be changed to provide the profile alteration. The control algorithms are expected to range from simple limits to temperature and pressure gradients, suitably normalized to yield improved estimates of instability limits, to more comprehensive stability physics models that are still computable in real-time, or precomputed ‘stability maps’ that can be evaluated simply, or via real-time application of neural networks in the PCS. An estimate of 2 run days has been allocated for initial temperature and pressure profile control commissioning in PFPO-2.

Rotation profile control will be upgraded from the system commissioned in PFPO-1, now including new capabilities. Sensors will include real-time evaluation of the plasma rotation profile from the charge exchange diagnostic which will be possible with the availability of the NB systems. Inclusion of new sensors will require their implementation into the PCS and further system commissioning time. ITER NBI modelling does not predict that this system will provide sufficient torque on the plasma to be used as an actuator. Instead, the plasmas operated at higher plasma current and toroidal field in PFPO-2 are expected to have increased intrinsic rotation. The physics understanding of intrinsic rotation based on the data taken in ITER in both PFPO-1 and PFPO-2 may produce a more accurate real-time model of this effect that could be used to upgrade the controller during PFPO-2 if deemed necessary. An estimate of 2 run days has been allocated for additional rotation profile control commissioning in PFPO-2.

Initial current density profile control will be commissioned in PFPO-2 with the additional Neutral Beam Current Drive (NBCD) available and the current density profile measurements that will also be available with the HNB and associated diagnostics. This will allow tailoring of the current density profile late in the current rise once NB shine-through can be avoided as well as some control of the radial locations of the q=1.5 and q=2 surfaces for improved NTM control. An estimate of 2 run days has been allocated for initial current density profile control commissioning in PFPO-2.

Once all three heating systems have been commissioned, it will be possible to simulate fusion burn control by using one heating system as an actuator to simulate fusion power. Such experiments have been carried out on a number of existing tokamaks [Jones, 2001; Noterdaeme, 2003; Mayoral,

2004; Shimomura, 2007; Hawryluk, 2014], providing a strong basis for these initial burn control simulation experiments on ITER. An estimate of 2 run days has been allocated for initial burn control commissioning in PFPO-2.

2.5.5.6.3 Magnetohydrodynamics (MHD) and error field control

With a second pellet injector cask with two additional pellet injectors, the full set of ELM control coil power supplies, and the full 73 MW heating power, as well as additional diagnostics to measure ELMs, it will be possible to further commission ELM control techniques in PFPO-2. Having 4 pellet injectors will allow pellet pacing with two injectors while fuelling with the other two injectors. The full ELM control coil power supply set will allow n=3 and n=4 configurations of the ELM control coils and allow rotating the ELM coil perturbations to spread out the ELM heat flux. With the full 73 MW auxiliary heating power, it should be possible to obtain type-I ELMy H-modes in helium in PFPO-2. An additional 6 run days have been allocated to commission ELM control in PFPO-2.

The DEFC and RWM control system initially commissioned during PFPO-1 will provide important practical operational experience for upgrading and recommissioning the system for PFPO-2. The ferromagnetic TBMs added during this phase may significantly change the intrinsic and dynamic error fields of the device. Also, the additional heating systems will produce greater plasma stored energy and β, which will increase plasma amplification of error fields and may begin to approach MHD stability limits. Sensor changes during this period include the acquisition and real-time analysis of existing magnetic sensors for detection of $n > 1$ error fields and possible plasma amplification of these fields. Additional power supplies for the ELM coils will extend the capabilities of the actuators for this task, making the control system more effective. A model-based control system should be upgraded to include the added TBM modules, NB Magnetic Field Reduction system, sensors, and actuator capabilities. An additional 5 run days have been allocated to commission DEFC and RWM control in PFPO-2.

With the full 73 MW additional heating available in PFPO-2, it will be possible to use the HNB and ICRF systems to increase the plasma β while using the ECRH system for NTM control. While the expected β values of around unity may still be too low to demonstrate full NTM control in PFPO-2, it is likely that classical tearing modes will appear in the current rise as well as in the flattop, which will allow additional commissioning of NTM control techniques. NTM control is not yet a routine tool for disruption prevention/delay in present tokamaks and may require significant further development on ITER, depending on how effective NTM control schemes developed on existing devices prove to be on ITER. This is partially due to its complexity, but also to the over-subscription of the ECRH systems in present devices. Additionally, the temperature at the q=2 surface on existing devices is rather low compared to that expected in ITER, requiring large power levels to drive the necessary current. The concepts for control have been successfully demonstrated, but there remains room for significant optimization; in addition, existing schemes are, to some extent, specific to the launcher geometry of each machine. An additional 5 run days have been allocated to commission NTM control in PFPO-2, but further run-time is likely to be required as part of the physics program.

Having the full 73 MW of additional heating and, in particular, the ability to drive fast ions with both ICRF and NBI, it will be possible to begin to excite Alfvén Eigenmodes both in the current rise and in the flattop. While Alfvén Eigenmode control techniques are still the subject of R&D on existing devices, it is expected that current density and pressure profile control techniques will also allow some control of Alfvén Eigenmodes. Some control or influence of ECRH on Reversed Shear

Alfvén Eigenmodes (RSAEs) and Toroidal Alfvén Eigenmodes (TAEs) has been observed on existing devices [Van Zeeland, 2009; Garcia-Munoz, 2015; Van Zeeland, 2009] and should be further developed for future use on ITER. It is not expected that the fast ion population will be so large in PFPO-2 that Alfvén Eigenmode control will be required in this phase, but it will be important to begin to commission Alfvén Eigenmode control techniques before such control is required in the FPO phase. While no dedicated run days have been allocated to Alfvén Eigenmode control in the present plan, it is expected that such experiments could be carried out during the current density and pressure profile control experiments in PFPO-2.

2.5.5.6.4 Supervisory control

As the actuator and diagnostic systems and plasma performance increase in PFPO-2, additional commissioning of advanced supervisory control within the PCS will be required for the first line of defence for investment protection as well as for managing shared actuators across multiple control functions.

Additional exception handling commissioning will be required to deal with potential plant system faults and plasma events as the number of plant systems and plasma performance increase. With the full 73 MW available from all three H&CD systems, a fault in one H&CD system could be mitigated by using another system, under certain conditions, for some control functions. Similarly, a fault in one diagnostic channel or system could be mitigated by using a redundant channel or another diagnostic system. Anticipating plasma events such as an H-L transition to prepare for the resulting drop in plasma β and radial shift in plasma position need to be commissioned as part of exception handling [Raupp, 2017]. An additional 5 run days have been allocated to PCS commissioning in PFPO-2 that will include exception handling.

With the full 73 MW additional heating available from all three H&CD systems, more sophisticated actuator sharing techniques will need to be commissioned in PFPO-2. As the plasma performance increases, more instabilities are likely to appear and more simultaneous control schemes with multiple actuators will be developed. Preparation for simultaneous control of NTMs at q=1.5 and q=2, as well as sawtooth control and central electron heating for impurity control will need to be demonstrated in PFPO-2. As each of these control schemes is commissioned, it will become necessary to also develop shared actuator control with priorities adjusted in real-time for each control function.

2.5.5.6.5 Advanced control commissioning deliverables

The deliverables for advanced control commissioning during the PFPO-2 phase include:

- Plasma current, position, shape, and vertical stability control to 15 MA/5.3 T;
- Density control with gas and pellet injection up to 15 MA/5.3 T;
- Disruption avoidance, detection, and prediction schemes to 15 MA;
- HNB system operation (2 beamlines) at powers of up to 33 MW for at least several tens of seconds;
- ICRF system (2 antennas) operation at powers of up to 20 MW for at least several tens of seconds;
- First wall and divertor heat flux control to full auxiliary heating power;
- All H&CD systems operating simultaneously at injected powers of up to 73 MW;
- Actuator sharing, event handling, and forecasting systems;
- H-mode operation with L-H and H-L transition control;
- ELM control coils and pellet pacing for ELM control;

- Error field correction in the presence of the TBMs;
- Error field correction in the presence of the NB Magnetic Field Reduction system;
- Sawtooth and NTM control;
- β and pressure profile control;
- Temperature, density, impurity, rotation, and current density profile control.

2.5.5.7 H-mode Studies in PFPO-2

2.5.5.7.1 Summary of scenarios

The development of the remaining aspects of H-mode operation in the non-active phase will be completed during PFPO-2. This will be a more extensive experimental program (a factor of ~3 times longer) than in PFPO-1 because of the substantial improvement of the capabilities of ITER for H-mode operation and improved diagnostics. These include the full complement of the baseline heating systems and power supplies for the ELM control coils and improved diagnostics for edge plasma parameters (e.g. reflectometers and edge Thomson scattering, if not operational towards the end of PFPO-1) and ion temperature (e.g. charge-exchange spectroscopy), as detailed in Appendix H. To minimize the risks of initial H-mode operation in FPO, it is important that both operational and physics issues of H-mode operation in ITER are addressed up to a plasma current level of 7.5 MA. This would allow H-mode operation in FPO to start at this level of current and proceed upwards in DD and then DT. The main goals of the PFPO-2 phase are:

1. confirm the predictions of the H-mode power threshold and power required for sustainment of high confinement type-I ELMy H-modes over a range of I_p, B_t, plasma densities and species (hydrogen and, most likely, helium);
2. establish stationary type-I ELMy H-modes over a range of I_p, B_t, plasma densities and powers in order to: a) characterize the scaling of H-mode energy and particle confinement in ITER, b) characterize ELM power fluxes to plasma-facing components, c) characterize effects of ELMs on W production and impurity exhaust that may establish limitations to the uncontrolled ELM energy loss/frequency, d) to complete the initial assessment of the scaling of the SOL power flux with a wider range of toroidal fields, plasma currents, densities and input powers and e) to extend their duration to identify possible issues related to long-pulse operation such as long timescale recycling issues or transport changes due to the global relaxation of the current profile;
3. demonstrate ELM control over a range of $q_{95} > 3$ (possibly up to 4.5) with 3-D magnetic fields for both ELM transient power exhaust and impurity exhaust and to assess the potential of the back-up ELM triggering schemes for $I_p > 5$ MA H-mode operation;
4. determine the effects of the TBMs on H-mode plasma and performance by comparison with PFPO-1 experiments and, if sizeable, to mitigate their effects by the application of correcting fields with the error field correction coils and the ELM control coils first at 1.8 T and then at 2.65 T.

The total operational time for H-mode experiments in PFPO-2 is 126 days; the experimental plan for H-mode plasmas in PFPO-2 can be summarized as follows:

- **H-mode operation to connect with PFPO-1, evaluate/mitigate TBM effects and extend H-mode operation at 1.8 T (40 days)**: This will require the use of the same species as in PFPO-1 (hydrogen or helium) and currents (mostly 5 MA) plus additional experiments to exploit the increased additional heating, enhanced ELM control capabilities and improved diagnostic of the plasma.

- **Expansion of H-mode operation towards 7.5 MA/2.65 T (65-80 days)**: This will include an exploration of H-mode hydrogen plasma operational range at 2.65 T and up to 7.5 MA, including the use of small proportions of helium and impurities to expand this range, followed by the characterization of H-mode plasmas and optimization of ELM control. The latter will be performed in helium plasmas if the hydrogen stationary H-mode development proves unsuccessful. Alternatively, assuming that R&D in present experiments confirms that this is a viable solution for ITER, other options for hydrogen operation at 3.0-3.3 T with ICRF three ion heating (He^3 + He^4) maybe considered to replace helium plasmas.
- **Development of long-pulse H-modes (6 days)**: this will require H-mode plasmas in hydrogen at 1.8 T or 2.65 T depending on the outcome of the research in PFPO-2.

Consistent with the Staged Approach plan, the H&CD systems available in PFPO-1 will be: 20 MW ECRH (with, at most, 6.7 MW at 104-110 GHz and, at least, 13.3 GHz at 170 GHz), 20 MW ICRF, and 33 MW of neutral beams (HNB) with hydrogen neutrals at 870 keV. To a large degree, the plasma conditions to be explored in PFPO-2 will be determined by the power that can be coupled to the plasma in the range of fields that will be investigated in H-mode and by the H-mode threshold of the plasmas to be explored.

For ICRF heating of hydrogen plasmas there is a good scenario with strong SPA for 1.8 T (second harmonic majority hydrogen) but not for 2.65 T, while for helium plasmas there is a good scenario with strong SPA at 2.65 T (first harmonic minority hydrogen) and, possibly (this will be assessed in PFPO-1), at 1.8 T (second harmonic minority hydrogen). As mentioned above, other ICRF schemes with strong SPA in hydrogen plasmas are possible by using the newly demonstrated three-ion [Kazakov, 2015] scheme demonstrated in JET and Alcator C-Mod [Kazakov, 2016]. This may be viable at 3.0 or 3.3 T in ITER, although its demonstration for the specific ions to be used in ITER remains outstanding and will imply strongly off-axis ICRF power deposition profiles, as discussed in section 2.5.5.7.4.6. For these reasons, this possibility is considered as an option at present and, if found viable for ITER, may be explored within PFPO-2 instead of the 2.65 T hydrogen and helium plasmas considered in the reference operational plan below.

Similarly, the application of NB heating to low density H-modes in this phase will be limited by shine-through loads on the blanket shield module that intersects the beams at the outer first wall, which is required to have a lifetime of at least 30,000 pulses. Two approaches can be taken to circumvent this issue: one is to shorten the HNB pulse and the other to decrease the HNB energy, although this implies a reduction of the HNB power with $E_{HNB}^{2.5}$ due to the perveance matching constraint [Singh, 2017]. Detailed studies have been carried out to determine the power levels that can be applied in long pulses (> 100s) with acceptable shine-through loads for a range of plasma densities and of the NB pulse duration at maximum power when operating under these densities for hydrogen and helium plasmas [Singh, 2017; Kim, 2016] and the key results are shown in Figure 2.5-4 and Figure 2.5-5, together with the expected H-mode thresholds for 5 MA/1.8 T and 7.5 MA/2.65 T in hydrogen and helium plasmas. As shown in these figures, for both toroidal field values, significant power in addition to that from the HNB is required to access H-mode plasmas in hydrogen, while the required additional power is much lower for helium. Access to H-mode for 7.5 MA/2.65 T in hydrogen will be possible with HNB and ECRH alone, but only by operating at relatively low densities and, thus, for NB power durations of less than 40 s.

Within the commissioning activities at the start of PFPO-2 the shine-through power deposition will be assessed with L-mode plasmas first in hydrogen and then in helium, as described in section 2.5.5.3. If this assessment were to show that the predictions substantially overestimate the shine-through power deposition levels, this would enlarge the hydrogen H-mode operational space at

1.8 T and 2.65 T in ITER. On the other hand, if the predictions would underestimate the real level of shine-through loads this would eliminate the possibility of H-mode operation at 2.65 T in ITER for hydrogen plasmas. The experimental plan for PFPO-2 described below is developed according to the shine-through load levels as predicted and to the H-mode threshold levels described in Appendix B. The plan would, therefore, need to be adjusted depending on the experimental results concerning the H-mode access powers and the shine-through power loads determined by experiments in ITER itself.

The total operational time for H-mode experiments in PFPO-2 is 126 days. Details of the deliverables from these plasmas, the rationale for the prioritization of the H-mode mode research and the risks associated with each phase are discussed below. The associated R&D that could be performed during ITER construction to refine the H-mode plans during PFPO-2 is discussed in section 5.1.

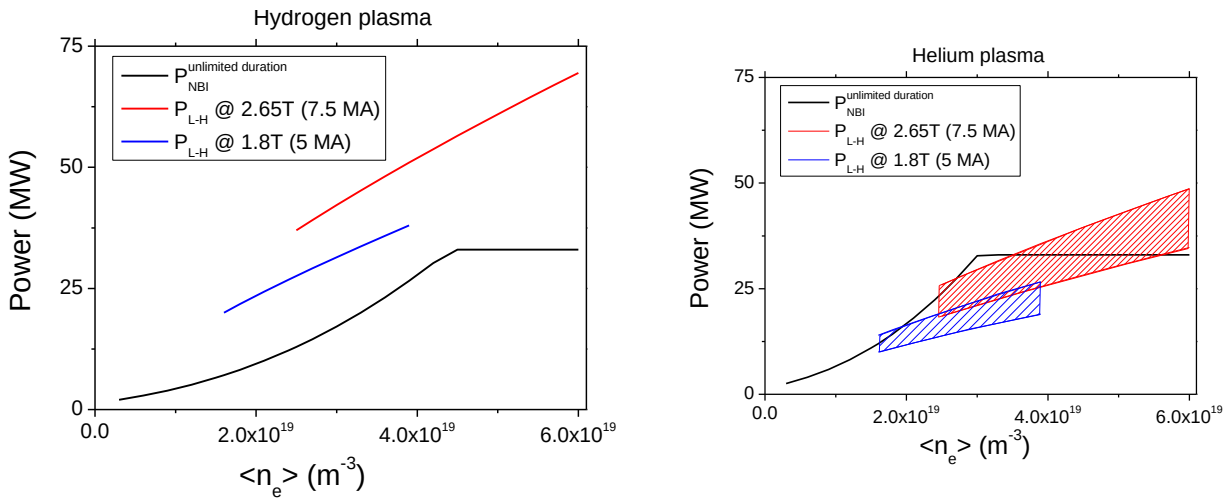

Figure 2.5-4: Maximum heating power which can be applied with unlimited duration versus plasma density with acceptable are shine-through loads for plasmas at 5 MA/1.8 T and 7.5 MA/2.65 T in (left) hydrogen and (right) helium. The red and blue lines (or shaded areas) show the expected H-mode threshold power for these plasma conditions and the density range of $n_e = 0.4 - 1.0 \times n_{GW}$, where n_{GW} (5 MA) = 4.0×10^{19} m^{-3} and n_{GW} (7.5 MA) = 6.0×10^{19} m^{-3}.

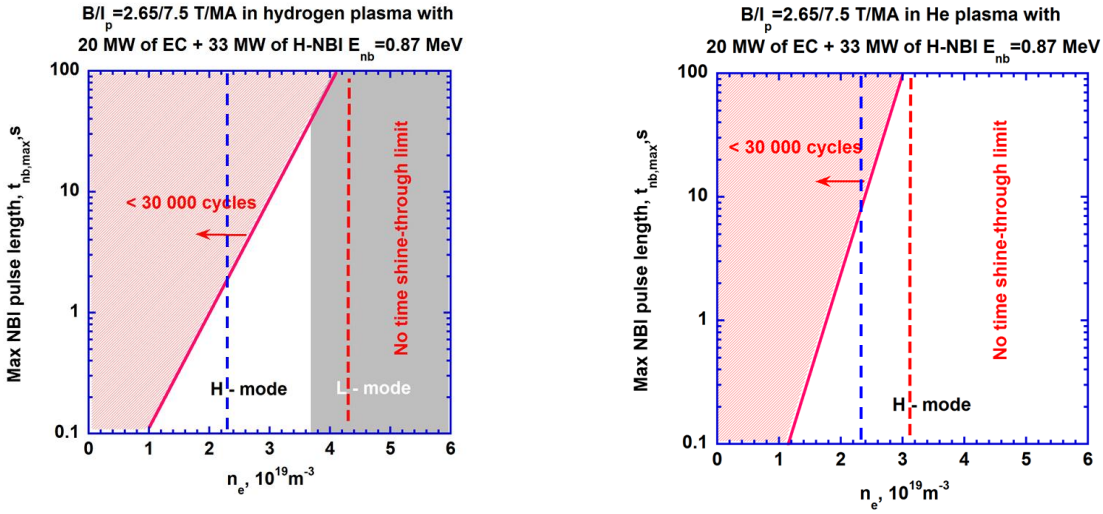

Figure 2.5-5: Duration of the NBI heating pulse at maximum power (33 MW at 870 keV) versus plasma density with acceptable shine-through loads for (left) hydrogen and (right) helium plasmas at 7.5 MA/2.65 T. The vertical red dashed line corresponds to the density for which NBI at full power can be applied without any limitation in heating pulse length and the vertical blue line to $n_e = 0.4 \times n_{GW}$; for densities lower than these the scaling providing the H-mode threshold power in ITER is not expected to be valid.

2.5.5.7.2 Motivation for H-mode scenarios in PFPO-2

H-mode operation during PFPO-2 aims at characterizing this scenario and developing the control schemes that will be required up to currents of ~7.5 MA, which are foreseen for the start of H-mode operation in FPO. During PFPO-2 all systems required to perform this research will be available in ITER in the final baseline configuration including heating and current drive, pellet fuelling, diagnostics (except most of the fast particle and some neutron diagnostics) and ELM control coils. In elaborating the PFPO-2 plan, it is assumed that in PFPO-1: an initial assessment of the additional heating power level to access H-mode in ITER will be performed, H-mode operation at 1.8 T will be demonstrated in a reduced operational range, and initial studies of ELM control with RMP fields will be performed. The availability of all the required systems in PFPO-2 will allow a wider exploration of H-mode plasmas in hydrogen and helium to be performed in conditions closer to those in FPO, to perform a first systematic study of H-mode performance in ITER plasmas with $T_e \sim T_i$ and of the integration of core confinement and edge compatibility issues including radiative divertor operation and ELM control. These studies are essential to minimize the risks during initial FPO operation and are not possible during PFPO-1. The integration of core confinement and edge compatibility is particularly critical for the ITER mission since, for the conditions required for high Q operation, unmitigated power fluxes are expected to exceed the power flux capability of the W divertor, excessive W production and core plasma contamination can lead to the loss of the H-mode and type-I ELMs are expected to cause melting of the plasma-facing components and cause significant W influxes that may also lead to the loss of the H-mode. Given the importance of demonstrating the compatibility of H-mode operation (with the required confinement level for high-Q operation) with acceptable edge plasma conditions (i.e. acceptable stationary and transient power fluxes and impurity sources), it is essential that this issue is addressed thoroughly and as soon as possible in the ITER Research Plan and thus in PFPO-2. This will allow the development of mitigation strategies to be formulated and refined (e.g. development

of other high confinement plasma scenarios in ITER alternative to the controlled-ELM H-mode, etc.) in advance of FPO should major issues be identified in the development of the plan described below.

2.5.5.7.3 Risk to the success of the H-mode studies in PFPO-2

There are five principal issues related to H-mode operation in PFPO-2:

- *H-mode access:* The basic considerations related to this issue have been outlined in already in section 2.5.4.9 and are further discussed in Appendix B, and an initial assessment of the power required for H-mode access will have been performed at 1.8 T (for hydrogen and helium) and at 2.65 T for helium in PFPO-1. Nevertheless, due to the large ripple at the separatrix for 1.8 T, the low margin for 2.65 T H-mode access in helium plasmas in PFPO-1 and the presence of the TBMs, it is possible that deviations on the expected H-mode threshold power are identified at this stage that would require a modification of the plan below. It should also be noted that the application of 3-D fields (particularly, with the alignment required for strong ELM mitigation or suppression) can affect significantly the H-mode threshold, as originally observed in DIII-D, MAST [Fenstermacher, 2010] and later in ASDEX-Upgrade [Ryter, 2013]. While an initial assessment of this effect should already have been performed in PFPO-1, the new flexibility regarding ELM control in PFPO-2 (all power supplies available allowing a large range of toroidal/poloidal spectra to be applied up to a maximum current of 90 kAt) may lead to new findings in this area that would require a modification of the plan below.
- *Plasma performance at Q ~ 10 relevant P_{inp}/P_{L-H}:* It is frequently observed that in order to achieve high energy confinement the edge power flow has to exceed the H-mode threshold by a given margin [Martin, 2008]. Two factors are thought to be at play in determining this behaviour one is related to changes in ELM behaviour (type-III to type-I and the need to avoid long ELM-free periods in devices with high-Z PFCs) and the other to the positive interaction between core confinement and edge MHD stability leading to an increase of the overall plasma energy [Garcia, 2015; Urano, 2016] but the details of both remains to be understood. Typically, for ITER operation it is assumed that $P_{sep} > 1.2 - 1.5 \times P_{L-H}$ is required to achieve the energy confinement time corresponding to the ITER-H98(y,2) scaling, although the confinement that will be achieved in hydrogen and helium plasmas is expected to be lower than in DD/DT. During PFPO-2 the level of available heating will allow addressing the changes to H-mode plasma confinement at a relevant margin of the edge power flow over the L-H transition at 1.8T for hydrogen and helium plasmas and at 2.65 T, most likely only for helium plasmas. If the assessment in PFPO-2 reveals that a significant margin over the H-mode transition is required to achieve high confinement H-modes in ITER, this may affect the level to which the characterization of H-modes and the demonstration of edge–core integration will be performed thus postponing the studies until FPO and increasing the risk of later operation. In addition, an upgrade of the additional heating systems should be launched at this stage in order to minimize the risk that ITER will not achieve the required performance for high-Q operation in DT.
- *Conflicting requirements for stationary and ELM power load control and W control:* Although an initial assessment of this issue may already result from experiments during PFPO-1, it is only during PFPO-2 that the edge plasma parameters during H-modes will have sufficiently high values to provide the key features of H-mode operation in FPO. These features include the low core plasma neutral source due to efficient ionization of neutrals in

the divertor, SOL power e-folding lengths in the mm scale and edge power flows of up to 50-60 MW. The control of stationary power fluxes in ITER at these power levels is expected to require operation with high separatrix densities and, possibly, radiative power dissipation at the divertor, as discussed in Appendix C. This, in turn, is expected to prevent impurity penetration through the pedestal by providing impurity exhaust between ELMs [Dux, 2014], but may also reduce the efficiency of impurity exhaust during ELMs. This, together with the transient W influxes from the divertor following the ELMs may restrict the range over which the integration of all requirements can be achieved at this stage [Dux, 2017]. Depending on the results obtained, this may imply that only suppressed ELM regimes (i.e. no transient W influxes) are viable to achieve high-Q operation in ITER, or that alternative ELM-less plasma scenarios to the controlled/suppressed ELMy H-mode need to be explored at this stage (QH-mode, I-mode, etc.). Performing this assessment as soon as possible in the ITER experimental program (i.e. in PFPO-2 as considered here) will allow the early mitigation strategies to prevent this risk materializing in FPO.

- *Development of ELM control schemes and plasma-facing component melting avoidance:* It is important that, as ELM control schemes are developed, substantial melting of plasma-facing components is avoided. The strategy developed in PFPO-1 and PFPO-2 is based on predictions that melting of W divertor monoblock will not occur during uncontrolled ELMs at 5 MA/1.8 T (including edges) but this may then occur at 7.5 MA/2.65 T (at least for toroidal edges), as discussed in Appendix C. In view of this, and the considerations on post-ELM W influxes above, it is important that ELM control is maintained to avoid melting as the ELM control schemes are developed, particularly because of the fine tuning issues related to the alignment between the applied 3-D field magnetic perturbation and the edge magnetic field. This risk is already significantly reduced within the proposed staged operation plan by the application of vertical plasma position oscillations, which are expected to be effective to trigger ELMs up to currents of at least 7.5 MA [Gribov, 2015] and by the use of the four available fuelling pellet injectors as back-up for ELM control by injecting pellets from the LFS and HFS. In this application the expected pellet frequency that can be achieved is up to 64 Hz and should allow $\Delta W_{ELM} \leq 0.375$ MJ over the range of H-modes explored, if this does not cause excessive fuelling of hydrogen plasmas or dilution of helium plasmas. If issues are identified at this stage regarding ELM control that would make it questionable for high-Q plasmas in DT, possible mitigation actions would involve the addition of two further pellet injector for ELM triggering before FPO operation and or the above mentioned exploration of alternative plasma scenarios to the controlled/suppressed ELMy H-mode at this stage.

- *Fuelling of He plasmas at 7.5 MA/2.65 T*: Fuelling of He plasmas can only be performed by gas fuelling and this is not efficient in ITER to fuel the plasma because of the high ionization efficiency of neutrals in the SOL/divertor plasma; pellet fuelling is not possible due to H contamination of the He H-modes. Integrated simulations that take into account the limits that divertor detachment imposes to the separatrix density (see Appendix C) and anomalous core particle transport in ITER [Militello-Asp, 2016; Polevoi, 2013], show that H-mode scenarios exist which allow unrestricted application of NBI both in the access phase and the stationary phases. If experiments did not reproduce the modelled separatrix density and core density profiles in these simulations and lower density values were to be achieved (particularly in L-mode), the application of NBI in He plasmas would be more complex and the He H-mode scenarios more difficult to develop. Possible mitigation strategies consist on: a) reducing the NBI energy and thus power injected, to cope with a lower plasma density

with acceptable shine-through loads, and b) triggering the L-H transition with ECRH+ICRF and then applying the NBI to full power once the density has increased in H-mode.

2.5.5.7.4 Details of experimental plan and deliverables for H-mode scenarios in PFPO-2

The PFPO-2 experimental plan starts with similar H-mode plasmas to those that should be obtained before the end of PFPO-1 and then expands the H-mode operational range towards 7.5 MA/2.65 T. Due to the high H-mode threshold of hydrogen plasmas at 2.65 T and the lack of a suitable heating scheme (for ICRF) or restrictions (NBI shine-through loads) in the application of the baseline heating systems, the reference research plan in PFPO-2 is to perform comparisons of hydrogen and helium H-mode plasma behaviour at 1.8 T and the main H-mode scenario development in helium plasmas at 7.5 MA/2.65 T. Despite this, the plan includes an early assessment of the H-mode operational range that can be achieved in hydrogen plasmas at 7.5 MA/2.65 T so that the limitations expected for these plasmas can be corroborated experimentally (high shine-through power loads requiring high density for NBI and high H-mode threshold) and includes dedicated studies to enlarge this operational range. Following this assessment and studies, it will be possible to decide whether to conduct the main H-mode scenario development in helium plasmas at 7.5 MA/2.65 T or if hydrogen plasmas would be a possibility. The latter would obviously advantageous for the extrapolation of the results obtained in PFPO-2 to FPO but, for the reasons explained above, is not considered feasible with the experimental evidence at this stage and the modelling performed for ITER so far.

2.5.5.7.4.1 H-mode operation to connect with PFPO-1, evaluate/mitigate TBM effects and to extend H-mode operation at 1.8T (40 days)

The main objective of this phase is first to assess the effects of the TBMs on H-mode plasma in the same plasma conditions as obtained in PFPO-1 at 5 MA/1.8 T, mitigate these effects if sizeable, and then expand the operational range of 1.8T plasmas, predominantly in hydrogen plasmas to take advantage of the increased additional heating power level in this phase.

Based on the results from operation at 1.8T in PFPO-1, the experiments in PFPO-2 will start in the conditions that provide type-I ELMy H-modes with high energy confinement. In principle, in order to provide a better assessment of the effect of the TBMs on H-mode plasmas, it is preferable to select plasma shapes whose separatrix-wall distance is as close to the reference ITER shape as possible while ensuring high energy confinement (if the -1.28% ripple level at the reference separatrix position turns out to degrade confinement unacceptably) and in hydrogen, if possible (if not in helium). The H-mode access experiments with power ramps (20s ramp-up followed by 10 s stationary) would be repeated in PFPO-2 applying the same heating levels and schemes as in PFPO-1. The possible differences regarding H-mode access and sustainment due to the presence of the TBMs will be documented and, if significant, schemes to mitigate these effects will be developed. This will be based on the optimization of n = 1 error field correction for H-mode plasmas with the external coils and the use of the ELM control coils (now with the full baseline capabilities) to fine tune static low-n error field correction and, possibly, to develop active correction schemes.

Once the schemes to mitigate the effect of TBMs have been developed, the program will continue by expanding the H-mode operational range of 1.8 T H-modes taking advantage of the increased additional heating power level in this phase and of the full ELM control capabilities with 3-D fields for both hydrogen and helium plasmas. This will include experiments similar those already performed in PFPO-1 over a range of currents of 3.5-5.0 MA and will address the scaling of H-mode confinement, pedestal/SOL plasma parameters with increasing input power and margin above the H-mode threshold power. The increased input power will also allow the expansion of the

operational range to higher plasma densities and to perform an initial evaluation of fuelling efficiency of gas versus pellet fuelling and particle transport studies to be performed in this phase, also taking advantage of the almost full baseline diagnostic capabilities. On the basis of the evaluation in Figure 2.5-4, H-mode operation should be possible for both hydrogen and helium plasmas over the density range ($n_e = 0.4 – 1.0 \times n_{GW}$) with NBI and ECRH heating alone. The additional 20 MW of ICRF (assuming coupling issues are not important or have been resolved in PFPO-1) would allow the achievement of helium and hydrogen plasmas at the same level of $P_{input}/P_{L-H} \leq 2$ and to push helium plasmas to levels of $P_{input}/P_{L-H} \leq 3$-4 (if second harmonic hydrogen minority heating is efficient) at 5 MA/1.8 T. It should be noted that for these plasma conditions the fast ion populations from NBI and ICRF will be significant as well as the current driven level [Polevoi, 2012; Maget, 2013]. Therefore the plasmas at the highest power levels may develop instabilities driven by fast particles or by the driven current profile and thus may not be appropriate for the purpose of the characterization of H-mode plasmas for comparison with plasmas at larger plasma currents [Polevoi, 2012]. Details on studies related to the use of the H&CD systems for current drive studies related to long-pulse development and the expected research on fast particles that can be performed at this stage is discussed in sections 2.5.5.9 and 2.5.5.10.

Together with the expansion of the type-I ELMy H-mode operational space, ELM control experiments with the full baseline configuration of the ELM control coil power supplies will be performed. This will include exploration of a range of toroidal mode numbers (most likely from n = 2 to n = 4) and of poloidal spectra over the range of q_{95} = 3.0 - 4.3 at 1.8 T (i.e. I_p = 3.5 – 5.0 MA), as far as possible. In particular the optimization of the spectra to achieve the same level of ELM control/suppression to account for changes in q_{95}, $\langle n_e \rangle$, β, and plasma rotation (that can be varied by adjusting with NBI power level) will be assessed thoroughly. The exploration will also assess the effects of 3-D fields on H-mode access and identify schemes for the time variation of the fields so that their effect on H-mode access is minimized while they provide the required level of ELM control during the stationary H-mode phase. This is an important step that should eventually conclude with the demonstration of ELM suppression for 1.8 T plasmas over q_{95} = 3.0 - 4.3 and that will provide an assessment of what will be required to achieve ELM suppression in ITER. As in the case of PFPO-1, the back-up ELM triggering techniques provided by vertical plasma oscillations and pellet injection (now with 4 available injectors) will be applied to ensure that the minimum level of ELM control is maintained as the 3-D fields by the ELM control coils are retuned for each of the conditions explored, particularly when q_{95} is varied.

The 1.8 T experiments described above are estimated to require 40 operational days and will be shared between hydrogen and helium plasmas. While priority will be given to hydrogen operation, it is not possible to predict the operational sharing between the two species. If the most pessimistic aspects of hydrogen H-mode operation at 1.8 T in ITER materialize (e.g. no viable ICRF coupling because of high ripple issues, etc.) a significant proportion of the experiments would be performed in helium (at least 25-30 of the 40 operational days are estimated). On the other hand, if this is not the case, the operation in helium would be restricted to the minimum required to provide:

- Assessment of the effects of TBMs on H-mode access and confinement and mitigation (if the reference plasmas in PFPO-1 were performed in helium), and
- Reference set of H-mode plasma conditions and requirements to control/suppress type-I ELMs at 5 MA/1.8 T to compare with 7.5 MA/2.65 T helium plasmas in PFPO-2.

In this case, the helium operational period could be reduced to 5-10 days.

Obviously, if this initial assessment of hydrogen H-mode operation at 1.8 T provided, in addition, sufficient confidence that stationary type-I ELMy H-mode are feasible in hydrogen at

7.5 MA/2.65 T (e.g. lower H-mode threshold than expected and/or lower shine-through loads than calculated), then the helium operational period would be shortened or fully eliminated at this stage, depending on whether the PFPO-1 reference H-modes to assess TBM effects were performed in hydrogen or not. If the PFPO-1 reference H-modes are in hydrogen and 7.5 MA/2.65 T stationary H-mode operation is evaluated to be feasible, then there would be no need to have reference H-mode and ELM control experiments in helium plasmas at 5 MA/1.8 T to compare with 7.5 MA/2.65 T and to evaluate the TBM effects, as this would be done in hydrogen.

2.5.5.7.4.2 Expansion of H-mode operation towards 7.5 MA/2.65 T in hydrogen plasmas (10 days)

These experiments will assess first H-mode access at 2.65 T and then explore H-mode operation with increasing power levels and ELM control, in a similar fashion as done for 1.8T during PFPO-2. As discussed in section 2.5.5.7.1, the expected operational range of hydrogen H-modes at 2.65 T is very narrow both due the lack on an ICRF scheme with high SPA as well as to the high NBI shine-through loads expected at low density. Therefore, these initial hydrogen experiments will be focussed towards the determination of the H-mode threshold in hydrogen plasmas at 2.65 T and the assessment of the possible operational range for stationary H-modes. On the basis of the evaluations in Figure 2.5-4 and Figure 2.5-5, it should be possible to access the H-mode in hydrogen plasmas in ITER for densities in the range of $2.4 – 3.6\times10^{19}$ m^{-3}, but the H-mode phase would be limited to ~ 10 s when all available heating power is applied (33 MW of NBI + 20 MW of ECRH). To minimize the probability of accidental melting of the W divertor in this exploration, the experiments will start at 5 MA where melting is not expected to occur, as discussed in Appendix C. At this current level, $\langle n_e \rangle = 2.4\times10^{19}$ m^{-3} corresponds to $0.6\times n_{GW}$ and this density is expected to be achieved with pellet fuelling if required [Militello-Asp, 2016; Garzotti, 2016]. The current level will then be increased in steps of 0.5-1.0 MA towards 7.5 MA, and the temperature of the divertor during ELMs will be monitored at each step. This scan will provide the scaling of the H-mode threshold at 2.65 T for hydrogen plasmas to compare with 1.8 T plasmas in PFPO-1 and an evaluation of possible effects of q_{95} on H-mode access with low ripple plasmas.

It is important to note, as was the case in PFPO-1, that these operational conditions near the L-H threshold are likely to produce long ELM-free periods that may lead to the termination of the H-mode by W accumulation with a sudden H-L transition. Similarly, the limitations to NBI heating associated due to the shine-through loads will restrict the possibilities of providing a soft landing of the H-mode by ramping down the power slowly in this phase. Therefore, significant effort will be required to ensure that these plasmas do not terminate abruptly, for which a key ingredient is to maintain ELM control throughout the H-mode entrance and exit phases, as demonstrated in present experiments [Köchl, 2016]. This will be provided by the back-up ELM triggering schemes available for these plasmas (vertical plasma position oscillations and pellet injection); developing an ELM control scheme with 3-D fields in these marginal H-mode conditions would require a significant amount of time and is expected to have a low probability of success. Based on the evaluations in Appendix C for the low density range of the proposed scans, the divertor power loads for these H-mode plasma conditions are sufficiently high to consider the use of impurity seeding to reduce them or to carefully limit the plasma time in these low density conditions to avoid excessive W recrystallization (to less than few hundred seconds). The total time estimated to perform this initial investigation of hydrogen H-mode access and operational range is 6 days.

On the basis of the findings of these initial experiments, it would possible to assess whether the operational space of stationary H-modes at 2.65 T is zero or very narrow, as predicted by the evaluation in Figure 2.5-4 and Figure 2.5-5, or wider. On the basis of this assessment, the experiments would continue along the steps below (no operational space for pure hydrogen plasmas

at 2.65 T) or move to the program discussed in section 2.5.5.7.4.5 (wide operational space and H-mode characterization and ELM control at 2.65 T to be developed with hydrogen plasmas).

Assuming that the evaluations in Figure 2.5-4 and Figure 2.5-5 are correct, the next step would be to investigate ways to widen sufficiently the H-mode operational space in predominantly hydrogen plasmas so as to provide a good basis for the experiments in section 2.5.5.7.4.5. Two approaches can be considered:

- One would follow the same line as in PFPO-1 by introducing ~10% helium into the hydrogen plasma to decrease the H-mode threshold, and
- The alternative approach explores the possibility of neon seeding the hydrogen plasma to decrease the shine-through loads by increased ionization of the injected neutrals, thus allowing longer pulses at low plasma densities where the margin to the threshold is largest.

For the first approach, it is assumed that injected helium at levels of ~ 10% will decrease the H-mode threshold of hydrogen to the intermediate values between hydrogen and helium. Thus, the threshold for $\langle n_e \rangle = 3.5\times10^{19}$ m^{-3} predominantly hydrogen plasma at 2.65 T (allowing a 30-40 s NBI heating pulse with acceptable shine-through loads) would be in the range of ~ 35.7- 41.5 MW, depending on the helium H-mode threshold value. While some tests on the viability of this approach will have been done in PFPO-1 with 1.8 T plasmas (and possibly earlier in PFPO-2 if the reference pulse for the assessment of effects on TBMs is established with H+10% He), it is possible that its full potential cannot be exploited due to high ripple issues at 1.8 T and, therefore, it is proposed to study it again at 2.65 T. This reduced H-mode threshold in mixed hydrogen-helium plasmas can thus provide some operational range in type-I ELM H-mode with 53 MW of total heating, particularly if the H-mode threshold is near the lower end of the estimates. In addition, the presence of 10% helium in the plasma decreases the shine-through loads approximately in proportion to the helium concentration, so that the duration of 30-40 s full power NBI for H+10%He plasmas with $\langle n_e \rangle = 3.5\times10^{19}$ m^{-3} is conservative.

The other approach relies in increasing the density of impurities in the plasma, as this increases significantly the effective ionization cross section of the plasma for the fast NBI neutrals (charge-exchange capture by highly ionized impurities) and decreases the shine-through loads for a given value of $\langle n_e \rangle$. The drawback of this approach is that core radiative losses increase and may lead to a reduction of the edge power flow (this should be maximized for H-mode access). In addition, the presence of impurities may raise the H-mode threshold itself [Maggi, 2014; Bourdelle, 2014], as discussed in Appendix B. Simulations carried out for ITER 7.5 MA/2.65 T plasmas show that seeding with neon can open a window for operation for hydrogen plasmas with full NBI + ECRH power during long pulses with acceptable shine-through loads, as shown in Figure 2.5-6. For this purpose, medium-Z impurities are optimum as they are fully ionized in the ITER core plasma and thus do not contribute to an increase of the radiative losses.

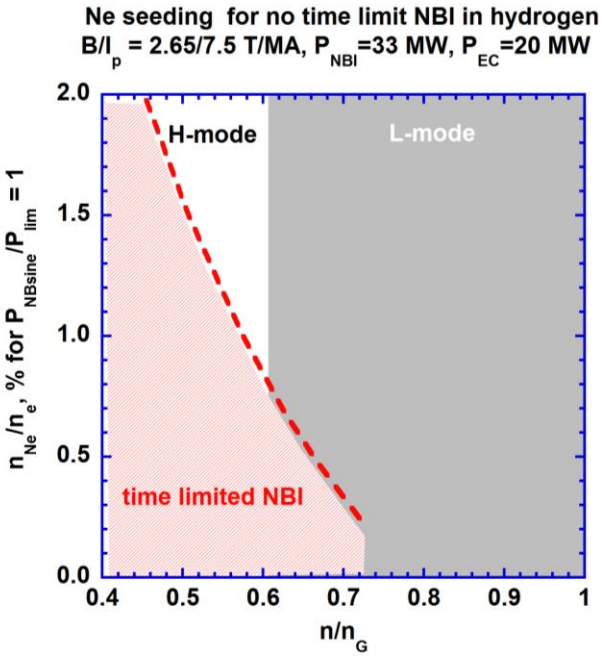

Figure 2.5-6: Required neon concentration for unlimited application of full power NBI heating with acceptable shine-through loads in hydrogen at 7.5 MA/2.65 T versus normalized (to Greenwald density) plasma density, showing the density range in which H-mode access is possible.

The total time estimated for the assessment of H-mode access in hydrogen and hydrogen-dominant plasmas following the approaches outlined above is 10 days. The sharing among the three possible approaches (pure-H, H+10% He and H+1% Ne) will be determined by the results of the experiments themselves and by the degree of complexity of the scenario control issues (sudden H-L transitions, avoidance of long ELM-free periods, plasma radiative collapse etc.). These have to be faced when operating near the H-mode threshold and may be more difficult to resolve in some of the approaches than in others.

At this point of the experimental program a decision will be taken whether to proceed with the 2.65 T H-mode characterization and ELM control demonstration in hydrogen or hydrogen dominant plasmas (i.e. going directly to program of section 2.5.5.7.4.4), or to perform these experiments in helium. Given the reduced operational range predicted for hydrogen plasmas and predominantly hydrogen plasmas, the reference strategy is to switch to helium plasmas at this stage. If this is not required, the allocated 15 operational days in section 2.5.5.7.4.3 to develop helium H-mode access and make an initial characterization of H-mode behaviour could be dedicated to the expansion of the operational range of hydrogen plasmas towards high currents and fields described in section 2.5.5.7.4.5.

2.5.5.7.4.3 Expansion of H-mode operation towards 7.5 MA/2.65 T in helium plasmas (15 days)

If robust H-mode access and long-pulse type-I ELMy H-mode cannot be obtained at 2.65 T in hydrogen or predominantly hydrogen-dominant plasmas, helium plasmas will be studied. The type of scans will be similar to those described in section 2.5.5.7.4.2, starting with 5 MA/2.65 T plasmas to avoid melting of the W divertor, and then increasing the current towards 7.5 MA. Given the much lower H-mode threshold, lower shine-through loads and the wider flexibility in heating mix (NBI, ICRF and ECRH) for helium than is predicted for hydrogen plasmas, the range of plasma densities that can be explored will be much wider than in hydrogen (in principle, from the minimum density determined by mode-locking up to $\langle n_e \rangle \sim 6\times10^{19}$ m^{-3} = $n_{GW\text{-}7.5MA}$). In practice, the achievable $\langle n_e \rangle$ range in H-mode is expected to be limited to relatively low values of $\langle n_e \rangle / n_{GW}$ due to the detachment of the divertor for He plasma, which limits the separatrix density to

$2.0 - 2.5\times10^{19}$ m^{-3} for P_{SOL} = 40 - 60 MW, as shown in Appendix C, due to the lack of pellet fuelling for these plasmas. Integrated simulations of ITER scenarios show that even with this restriction from divertor detachment on the separatrix density, and the possibility of gas fuelling only, stationary H-modes with $\langle n_e \rangle \geq 0.5\times n_{GW}$ should be achievable for 7.5 MA/2.65 T in He plasmas with the standard assumptions regarding particle transport in ITER [Polevoi, 2013; Militello-Asp, 2016].

Operation in He H-modes should thus allow studies of the q_{95} and density dependence of the power threshold in low ripple conditions (2.65 T) which is not possible in hydrogen plasmas. Otherwise the same issues regarding the control of the plasma in these experiments will need to be faced as for hydrogen plasmas (e.g. avoidance of long ELM-free periods, etc.), but may be quantitatively different. For example, W sputtering by helium will be larger than for hydrogen, due both to the higher mass and to the higher divertor plasma temperatures (for the same neutral pressures), as shown in Appendix C. This may restrict the minimum density that can be explored and require a more careful control of ELM-free periods. On the other hand, the ELM power pulses are expected to be longer in helium than in hydrogen due to the longer ion transit time [Loarte, 2003; Eich, 2003], thus reducing the accidental risk of melting of the W divertor in these experiments. Similarly, the wider possibilities for additional heating in helium will ease significantly the control of the plasma in the H-mode access and exit phases, thus decreasing the risk of disruptions in these helium experiments compared to that in hydrogen.

Depending on the range of parameters over which helium H-modes have been characterized in PFPO-2, additional experiments on H-mode access at 1.8 T along the lines of those discussed in section 2.5.5.7.4.1 may be also required at this stage to obtain a matching set of conditions at 1.8 T and 2.65 T (for example, with the same toroidal ripple level).

The foreseen operational time required for these helium access experiments is 15 days. This is longer than for hydrogen in view of the wider range of parameters to be explored at 2.65 T in helium compared to hydrogen and the possible need to perform additional experiments at 1.8 T in order to obtain a matching set of conditions at the two values of the toroidal field.

2.5.5.7.4.4 Characterization of H-mode operation up to 7.5 MA/2.65 T including ELM control and resolution of scenario integration issues (40 days)

The experiments described in section 2.5.5.7.4.2 or section 2.5.5.7.4.3 will provide an assessment of the power requirements for H-mode access and post-transition H-mode plasma evolution at 2.65 T and will determine which main ion species (hydrogen or helium) will be used in the further characterization of stationary H-modes and ELM control. During this follow-up phase, the experiments will follow a similar strategy as that foreseen for 1.8 T in section 2.5.5.7.4.1, but with a much wider scope. The objective of this phase of experiments is to provide a fully integrated H-mode scenario at 7.5 MA/2.65 T which can then be used as the starting point for H-mode experiments in DD plasmas during FPO.

The experiments will start at 5 MA/2.65 T, where melting of the divertor target during uncontrolled ELMs is not expected, and gradually increase firstly the heating power level and duration beyond the initial ~10 s stationary level demonstrated in the experiments of section 2.5.5.7.4.2 or section 2.5.5.7.4.3 towards ~50 s of stationary heating power. For each power level the density will then be increased and this will allow the characterization of the changes to pedestal and SOL plasmas and overall H-mode confinement to be performed. Depending on whether the experiments are performed in hydrogen or helium, a comparison of gas fuelling and pellet fuelling will be performed (only possible for hydrogen) at each level of the heating power. The foreseen level of

heating for each density level will be between ~ 20% above the measured L-H threshold up to the maximum heating power allowed by shine-through loads (< 73 MW at 5 MA).

ELM control with RMP fields will be developed taking advantage of the full baseline set of power supplies and building up on the experience developed at section 2.5.5.7.4.1 for 1.8 T plasmas over a range of $q_{95} = 3.0 - 4.3$. The effects of the RMP fields on ELM control/suppression, H-mode confinement, impurity exhaust and fast particle losses will be determined for a range of heating mixes with a varying level of NBI and optimized (both for ELM control optimization versus confinement degradation and core W accumulation avoidance) while ensuring that fast particle power fluxes on plasma-facing components are acceptable. This will allow the development of RMP optimization schemes with varying levels of toroidal plasma rotation for each density level and/or to identify the level of toroidal plasma rotation/input NBI torque that is required for optimum confinement for a given level of ELM control. In order to ensure that ELMs remain controlled to the required level while ELM control schemes with RMPs are developed, the ELM back-up triggering schemes: vertical plasma oscillations and pellet pacing (if hydrogen plasmas) will be applied. As these experiments will focus on ELM control with RMPs during the stationary heated flat-tops, the ELM back-up triggering schemes will be essential to ensure ELM control in the access and exit phases to stationary H-modes.

Once 5 MA/2.65 T stationary H-modes with ELM control have been developed, the plasma current level will be increased in steps of 0.5 - 1.0 MA towards 7.5 MA. Continuous monitoring of the divertor temperature during ELMs will be performed to ensure that no melting is caused by uncontrolled ELMs; this is expected to occur at the monoblock edges for currents of ~7.5 MA [Gunn, 2017]. At each step, various levels of heating power and power mixes will be applied and the density will also be varied (with gas and pellets if in H plasmas, if He then only gas). The optimization of the RMP fields applied for ELM control will be performed for each level of q_{95}, plasma parameters (chiefly β for the plasma response effects) and heating mix are varied. This optimization is potentially very time-consuming and the sequence of steps will need to be carefully selected on the basis of previous experience in PFPO-1 and PFPO-2 to ensure that it can be performed with a reasonable investment of time. These experiments will provide an excellent characterization of H-mode confinement, pedestal characteristics and SOL plasma parameters with increasing level of plasma current and decreasing recycling neutral source (as the divertor/SOL ionization becomes more effective with increasing levels of plasma density). Similarly, if the increasing plasma β and decreasing q_{95} leads to the triggering of NTMs, schemes to control/suppress them by the use of ECRH/ECCD will be implemented; this together with the need to avoid central W accumulation may restrict the range of heating mixes that can be explored above a given I_p.

For the lower core neutral sources expected at 7.5 MA, low density gradients are expected to appear in the pedestal (similar to DT operation). This should lead to profound changes to W impurity transport as neoclassical screening dominates in the pedestal [Dux, 2104; Dux, 2017; Polevoi, 2016], which can affect the balance of W exhaust between ELMs and at the ELMs. If these effects are identified at this level of plasma current, dedicated studies to determine the optimization of RMP fields to provide control of both power fluxes during ELMs and W exhaust will be performed. In these conditions with dominant pedestal impurity screening, increasing the ELM frequency and reducing ΔW_{ELM} may not provide W exhaust from the core plasma on longer timescales, as shown in Figure 2.5-7 (in this modelled case for DT plasmas) [Polevoi, 2016].

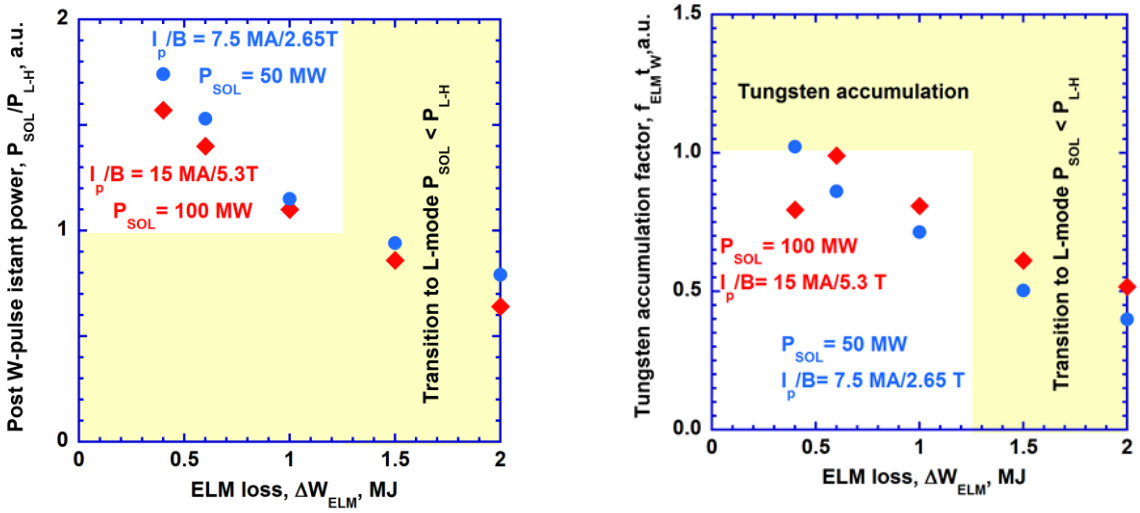

Figure 2.5-7: H-mode operating space for I_p/B_t = 15 MA/5.3 T with separatrix P_{SOL} = 100 MW, and for I_p/B_t = 7.5 MA/2.65 T with P_{SOL} = 50 MW, assuming no W prompt redeposition at the divertor during ELMs and that average transport during ELMs can be described by a diffusive model ($P_{ELM} = f_{ELM} \times \Delta W_{ELM} = 0.2 \times P_{SOL}$): (left) ratio of P_{SOL} to P_{L-H} following post-ELM W influx leading to increased core radiation; (right) long timescale W tungsten accumulation factor; a value larger than 1 implies uncontrolled increase of the W density in the core plasma and termination of the H-mode by an L-H transition.

Together with the expansion of the plasma scenarios towards 7.5 MA not only the transient ELM power fluxes to plasma-facing components but also the stationary power fluxes and W sputtering source will increase, as the SOL power width is predicted to scale as I_p^{-1}. To ensure that stationary power fluxes remain within the ranges required for the W divertor target (see Appendix C) and to prevent core W contamination, additional impurities are expected to be injected to provide increased divertor radiation and decrease both divertor surface temperature (to prevent recrystallization, see Appendix C) and plasma temperature. In addition, time-variation of the RMP perturbation [Loarte, 2014] may need to be applied to avoid the local power fluxes exceeding the limits in Appendix C. If this is required as part of the plasma scenario development above a given current/power level, then as part of the experimental program above, the effects of RMPs of high density radiative divertor conditions and divertor power fluxes will be characterized at this stage. If not, dedicated experiments to assess the effects of RMPs on radiative divertor plasmas and power fluxes in semi-detached divertor conditions and to decrease off-separatrix localized power fluxes by time variation of the applied 3-D fields will be performed at this stage. This is likely to require a retuning of the applied fields (including the use of cyclic variations in time) to integrate an increasing range of requirements (ELM control, W control, radiative divertor operation with low core plasma impurity contamination) which may affect pedestal plasma parameters and core plasma confinement. Therefore, experiments to re-optimize the applied RMP perturbation and heating-mix will be performed to identify the best compromise between core and edge integration in these plasmas which will guide the development of the ELM controlled H-mode plasma scenarios in DT. Similarly, experiments to test specific aspects of the control of stationary and ELM-caused power fluxes, such as those related to operation with reduced wall clearance (especially at the top of the first wall near the secondary X-point), will be performed at this stage for 7.5 MA/2.65 T plasmas.

The experiments above will provide fully integrated and optimized stationary H-mode plasma scenarios in terms of plasma confinement, controlled stationary and ELM-caused power fluxes and impurity exhaust by 3-D fields. The remaining set of experiments will aim at demonstrating the

integration of ELM control, power fluxes and impurity exhaust during the H-mode access and exit phases with 3-D fields, which will be required for DT operation. As mentioned before, in the experiments above ELM control in these phases is assumed to be provided by the back-up ELM triggering schemes: vertical plasma oscillation and pellet triggering (if hydrogen plasmas).

To address the control of H-mode access and exit with 3-D fields, two sets of experiments will be performed:

- At two levels of I_p (5 and 7.5 MA), 3-D fields will be applied before or just after the L-H transition and will be switched-off at the H-L transition or afterwards for a suitable range of plasma densities, levels of input powers and heating mixes determined by the experiments above. The goal of these experiments is to demonstrate robust access from L-mode to a high confinement H-mode and controlled H-mode exit with control of ELMs, impurity exhaust and power fluxes to PFCs provided by 3-D fields. Given the expected effect of 3-D fields optimally aligned for ELM control on the L-H transition [Fenstermacher, 2010; Ryter, 2013], these experiments will most likely concentrate on developing strategies to optimize the time variation of the applied fields in this phase to prevent deleterious effects on the L-H and H-L transition while providing the ELM control required.
- 3-D fields will be applied during the current ramp-phases (at 5 MA for a flat-top current of 7.5 MA) in which the L-H and H-L transition will be triggered by changes in additional heating. The switch-on and off of the fields around the L-H and H-L transitions will follow the strategies developed in the previous experiments and then the 3-D fields will be varied in time to provide ELM control through the current ramp-up/down H-mode phases in which q_{95} will be varying. The experiments will include a range of density and power waveforms and current ramp-up/down rates for which the 3-D fields will be optimized. To optimize the tuning of the 3-D fields during the q_{95} ramps the experience developed for ELM control in stationary conditions with $q_{95} = 3.0 - 4.5$ in 2.65 T H-mode plasmas earlier in this experimental phase will be very useful.

Again, as in all the H-mode experiments performed in PFPO-2, the back-up ELM triggering schemes: vertical plasma oscillation and pellet triggering (if hydrogen plasmas) will be used to provide the required level of ELM control while the applied 3-D fields are being optimized to provide ELM control.

The experiments in this PFPO-2 phase are estimated to require 40 operational days and will provide fully integrated scenarios, including the H-mode access and exit phases, which are optimized in terms of plasma confinement, plasma fuelling and controlled stationary and ELM-driven power fluxes and impurity exhaust provided by 3-D fields. These will be used as template for further development in DD/DT and towards higher plasma currents in FPO.

2.5.5.7.4.5 Demonstration of long-pulse H-mode operation (6 days)

The last series of experiments in PFPO-2 will perform a demonstration of a long-pulse H-mode scenario (potentially up to ~ 1000 s) with the purpose of assessing issues related to processes that may evolve on very long timescales such as those related to changes in the current profile, etc.

These experiments will build on the results of the assessment of the current drive capabilities of the ITER systems described in section 2.5.5.10, for which synergies with the experiments in section 2.5.5.7.4.4 will be exploited. Assuming that, in the experiments in section 2.5.5.10, the current drive capabilities of the ITER NBI and ECRH systems are found in agreement with present estimates and that fast particle-related instabilities do not cause major effects in the plasma, it will be possible to

achieve ~ 1000 s long pulses in 7.5 MA/2.65 T H-modes even without any significant use of the lifetime of the central solenoid. This is due to the fact that the current drive efficiency of the NBI for these plasmas is estimated to be ~ 2.5 – 3 MA [Polevoi, 2012; Maget, 2013]. This, together with the pedestal bootstrap current leads to 60% of the current to be non-inductively driven, as shown in Figure 2.5-8. This allows a stationary H-mode of 1000 s to be feasible even with a premagnetization current of 30 kA (compared to the maximum of ~ 45 kA) in the central solenoid for which lifetime consumption is negligible; Figure 2.5-9 summarizes the achievable flat-top durations for a range of plasma conditions versus premagnetization current. As described above, these demonstration experiments will focus on the determination of effects that may need very long timescales to develop in ITER such as those associated with the relaxation of the current profile which can affect plasma and impurity transport, long timescale evolution of processes related to plasma-wall interactions, etc., and to develop strategies for their control if required. The total operational time estimated to be required for these experiments is 6 days. However, at this point in the experimental program, the H-mode duration is likely to be limited by the pulse duration for which reliable high power operation of the H&CD systems has been established; the development outlined here assumes that it has been possible to commission the high power operation of the H&CD systems required up to the necessary pulse lengths, or that the extension of the pulse length required can readily be achieved within the allocated experimental time.

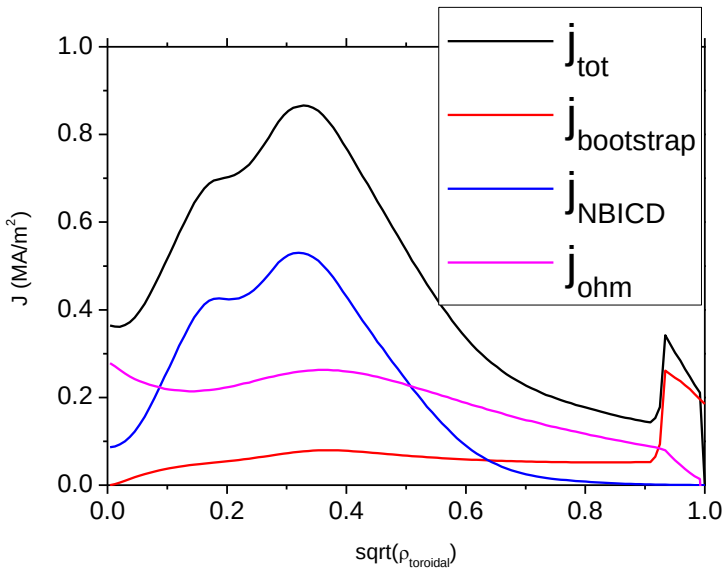

Figure 2.5-8: Current profile for a 7.5 MA/2.65 T He H-mode with 33 MW of NBI and 20 MW of ECRH and 20 MW of ICRF showing the main components to the total current (bootstrap, NBICD and ohmic).

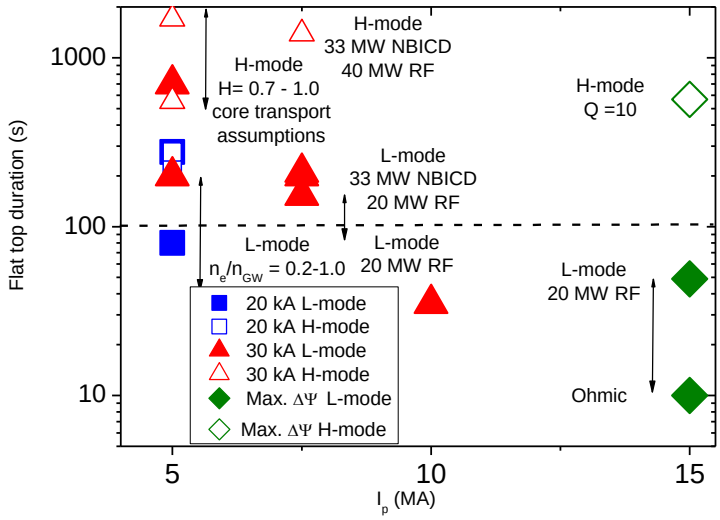

Figure 2.5-9: Flat-top duration versus plasma current level for a range of premagnetization currents and scenarios for each current level.

2.5.5.7.4.6 Option for low ripple hydrogenic H-modes: H-mode in hydrogen at either 3.0 - 3.3 T and up to 8.5 or 9.5 MA respectively

An option exists for obtaining hydrogen H-modes in regimes with low TF ripple by increasing the value of the toroidal field beyond 2.65 T to enable ICRF schemes with SPA based on the three-ion scheme [Kazakov, 2015] with ~10% He^4 and ~1% He^3, following its demonstration in Alcator C-Mod and JET [Kazakov, 2016]. Although the increase of the toroidal field from 2.65 T to 3.0 - 3.3 T increases the H-mode threshold power by 10 - 20%, the possibility of utilizing ICRF heating at up to 20 MW and the possible reduction of the H-mode threshold by the presence of ~10% He, may open a range for predominantly hydrogenic H-mode plasmas at these higher fields. For example, for a hydrogen plasma with $\langle n_e \rangle = 4.5\times10^{19}$ m^{-3} and ~ 10 % He^4 at 3.0 T, for which the application of NBI at full power is not restricted, the corresponding H-mode threshold could be in the range of 47 – 55 MW, significantly less than the total available input power of 73 MW. Several issues need to be assessed before this option can be considered sufficiently viable to be added to those in sections 2.5.5.7.4.2 and 2.5.5.7.4.4, or, indeed, to replace one of the strategies presented in those sections. These include the experimental demonstration of the three-ion heating scheme with the ion species considered for ITER, the confirmation of the effect of quantities in the range of ~ 10% He^4 in decreasing the hydrogen H-mode threshold and an assessment of the fast ion losses associated with this scheme. The heating scheme specified produces very high energy He^3 ions and, for these fields in ITER, has a heating deposition profile which is well off-axis, so that there might be significant fast ion losses to the first wall. Preliminary modelling results show that the off-axis fast He^3 tail accelerated by the ICRF is well-confined, both at 3 T and 3.3 T [Joly, 2017], although the application of 3-D fields for ELM control may modify this. A further reason for concern is the possible W accumulation in the core with predominantly off-axis heating. This is not considered to be very critical because the ICRF heating scheme also provides a significant central heating due to wave damping on electrons (~30 - 40% of the ICRF power). In addition, the ECRH deposition profiles for these fields are moderately centrally peaked at 3.0 T in O-mode (at 170 GHz and 104-110 GHz), although predominantly off-axis for 3.3 T. H-mode experiments combining central and off-axis ICRF heating have been performed in Alcator C-Mod without any significant impact of

high-Z (Molybdenum) accumulation [Rice, 2002], indicating that this may not be a problem in these ITER conditions. However, both the ICRF scheme and the issue of W accumulation in these ITER H-mode conditions needs further assessment by modelling and experiment before this can be adopted as one of the main approaches for H-mode operation to be considered for PFPO-2.

2.5.5.7.5 Deliverables for the H-mode scenarios studies in PFPO-2

Consistent with the objectives of the initial H-mode operation in PFPO-1, the deliverables from H-mode operation in PFPO-2 are:

- *Quantifying power required for H-mode access and sustainment and characterization of H-mode plasmas in FPO-like conditions:* For PFPO-2 the operating scenarios and planned experiments are designed to confirm the assessment of the L-H transition power (P_{LH}) for both hydrogen and helium and the level of margin above this threshold to achieve high H-mode confinement for at least two different toroidal fields. These experiments (particularly those at 7.5 MA/2.65 T) will provide the first H-mode plasmas in FPO-like conditions (e.g. low core recycling neutral source) that will allow the development of optimization strategies for H-mode confinement in ITER (e.g. variations of additional heating mixes). From these results it is also expected that the threshold power needed for H-mode access and sustainment in deuterium and DT plasmas can be predicted with confidence. This will provide the final confirmation in advance of DD/DT operation that the baseline level of 73 MW is appropriate to achieve ITER's Q = 10 goals and, if not, a quantification of the upgrade in power required.
- *ELM control:* The ELM control work in PFPO-2 is designed to verify the techniques to tune the applied RMP spectrum to optimize the control of ELMs for two values of the toroidal field and several edge safety factors using the full complement of power supplies for the internal coils. The range of q_{95} values (3.0 - 4.5) will span the values needed for the scenarios in the FPO campaigns from 7.5MA/2.65T to high-Q operation including Q=10 (15 MA/5.3 T) and long-pulse Q = 5 (11.2-12.5 MA/5.3 T). The ELM control validation with RMPs for multiple q_{95} values and during current ramps is very important for the detailed planning of H-mode operation in the first FPO campaign at higher field and current, for which unmitigated ELMs would cause melting of the PFCs. Similarly, the studies on ELM control with various heating mixes will provide information regarding the role of heating mixes on ELM control and its optimization for minimum confinement deterioration. This can provide information regarding possible upgrades of the ITER systems to improve this optimization (e.g. the 3rd HNB to increase torque input).
- *Document the effect of the TBMs on H-mode performance and develop schemes for their mitigation:* Plasma pulses produced in the presence of the TBMs in PFPO-2 will match those established in PFPO-1 without the TBMs, and will allow documentation of the effects of the TBMs on H-mode performance, albeit at 1.8 T and most likely for the ITER reference plasma shape that has a high level of ripple at this toroidal field value. Mitigation schemes for these effects (if the effects are sizeable) will be developed using the error field correction coils and the ELM control coils at 1.8 T and applied to plasmas at 2.65 T, which have a much lower of TF ripple.
- *Initial validation of predictions of SOL power width in ITER:* The variation of the plasma current for both hydrogen and helium H-mode plasmas planned for PFPO-2 will provide data to validate predictions of the width of the SOL power flux, i.e. that it scales inversely with current (linearly with poloidal field) and that does depend on the toroidal field. This

data is important for the planning of high power H-mode operation at high currents in FPO, in particular the need and schemes for divertor power load control with radiative divertor operation discussed in Appendix C.

- *Assessment of scenario compatibility issues for ELM control with 3-D fields (Pellet Fuelling, Impurity exhaust and radiative divertor).* The experiments in PFPO-2 will demonstrate these three key scenario compatibility issues of ELM control with 3-D fields, although marginally for pellet fuelling if experiments are done in He plasmas. These are required for the application of this scheme in high-Q plasmas in FPO. The PFPO-2 experiments will provide guidance on how to use the large spectral flexibility of the ITER ELM control coils for this demonstration.
- *An initial assessment of long-pulse H-mode operation.* The first demonstration of a long pulse (~ up to 1000 s, if allowed by progress in the H&CD commissioning) 7.5 MA/2.65 T H-mode scenario with ~ 60% driven current would help to identify processes that may develop over long timescales in ITER affecting plasma confinement/impurity transport/MHD stability and the schemes required to control them. This would provide guidance on how to control such phenomena, which will be used for the long H-mode pulses required for the demonstration of the Q =10 and Q =5 goals in FPO.

2.5.5.7.6 Assessment of diagnostic capabilities for performing H-mode research during PFPO-2

By PFPO-2 most of the ITER diagnostics will already be in final configuration; the only diagnostics that will become available for FPO are those for additional neutron measurements (not essential for hydrogen and helium plasmas) and for fast particle measurements. The latter are possibly the only systems which might be needed in PFPO-2 as the level of additional heating increases and, in particular, the use of NBI heating at high power levels starts. The triggering of fast particle driven MHD instabilities (see section 2.5.5.10), together with the application of 3-D fields for ELM control, might lead to increased fast particle losses (especially from the NB-injected ions) for whose characterization the additional capabilities of the lost fast particle diagnostics would be useful. It should be noted, however, that if the fast particle losses in PFPO-2 are significant the local high power fluxes associated with them will be measured with the IR cameras. Therefore, an initial quantitative evaluation of the magnitude of the fast particle losses will be possible and the highest risk of such localized losses to plasma operation will be avoided.

2.5.5.8 Scenarios for long-pulse operation

Long-pulse operation is desirable in PFPO-2 (even in PFPO-1, time permitting) for commissioning all plant operations for FPO requirements. Of principal concern are the magnetic sensors and the heating and current drive systems. In addition, long pulses facilitate verification of the current drive efficiencies of the various H&CD systems as these systems and the required diagnostics become available.

The ITER Research Plan includes two basic scenarios for long-pulse operation in PFPO-2 both at 7.5 MA/2.65 T. The first is a hydrogen L-mode scenario at 7.5 MA/2.65 T with reduced NBI energy/power and ECRH for retention studies (with D spiking, see section 2.5.5.12 and Appendix A) and a flat-top length of ~100 s. The second is an H-mode scenario (in hydrogen or helium) at 7.5 MA/2.65 T, with 33 MW of NBI and 20 – 40 MW of ECRH+ICRF, having a maximum potential flat-top length of ~ 1000 s. Both scenarios can be performed with 30 kA premagnetization and thus without significant consumption of the CS fatigue lifetime. Additional, specific issues related to the development of long-pulse scenarios Q ~ 5 scenarios for FPO are also described in

section 2.5.5.10 within PFPO-2 although many of them do not necessarily require long pulses. Due to the availability of diagnostics (e.g. MSE) and H&CD (e.g. HNB and full ICRF in addition to ECRH), it is more appropriate to perform these studies and long-pulse H-mode operation in PFPO-2 than in PFPO-1.

Although not specifically mentioned in the Research Plan, long-pulse scenarios are also possible in PFPO-1 and could be used for ECRH and ICRF commissioning, diagnostic commissioning, etc. Given the relatively narrow operational space for H-mode operation in PFPO-1 (see section 2.5.4.9) and the reduced set of diagnostics at this stage (see Appendix H), it would be more effective to perform such long discharges in hydrogen L-modes. The achievable flat-top durations for 5 MA plasmas with 20 MW of RF heating are in the range 200 – 700 s, depending on the value of the plasma density ($<n_e> = 0.2 – 1.0 \times n_{GW}$ - see Figure 2.5-9) for 30 kA premagnetization and thus no significant CS lifetime consumption. These L-mode plasmas would be a natural extension of the commissioning activities at 1.8 T discussed in section 2.5.4.5 if the reliability of the ECRH and ICRF systems is sufficient to attempt this long-pulse operation at this stage.

2.5.5.9 Demonstrate critical system performance (including heat loads)

2.5.5.9.1 Key elements of critical system performance

Experimental operation during the FPO phase will rapidly lead to activation of the tokamak structures, implying that maintenance, repair and upgrade activities will require remote handling and are likely to be time consuming. To minimize in-vessel interventions, it is therefore essential for all operational systems to demonstrate that they are capable of operating as close to their performance and pulse length specifications as is feasible during PFPO-2. Due to limitations imposed by flux consumption, achieving long-pulse operation of up to 400 s, or longer, in PFPO-2 is likely to require operating at modest plasma currents of ~7.5 MA (e.g. Figure 2.5-9). The program would likely involve both L- and H-mode plasmas, according to the system test involved, but, as discussed below, certain tests will benefit from H-mode operation. Further optimization of plasma scenarios may therefore be required to allow the exploitation of the maximum baseline power capability under relevant conditions, which provide the most demanding tests of the tokamak, auxiliary and plant systems. The PCS must also demonstrate as much of its advanced control capabilities as possible in H/He plasmas to ensure that any modifications required of the actuators and diagnostic systems can be carried out prior to FPO. Similarly, critical plasma-related interlock and safety functions within CIS and CSS must be fully commissioned during PFPO-2. The pellet and gas fuelling systems must demonstrate adequate fuelling capability up to 15 MA operation, and so some elements of this program can be addressed within the 15 MA/5.3 T development discussed in section 2.5.5.11.

Once all H&CD systems have been commissioned to their rated power levels, operation at currents of at least 7.5 MA has been developed and reliable H-mode operation with acceptable ELM control has been established in PFPO-2, the long-pulse, heat management capabilities of the device will be tested under quasi-stationary long-pulse conditions. The pulse duration of high power plasmas will be progressively extended to the maximum allowed by the available poloidal flux. Flat-top pulse lengths exceeding 100 s are possible (e.g. Figure 2.5-9) according to the experimental time available for commissioning of the H&CD, fuelling, diagnostics, control systems, etc. up to longer pulse lengths. To reach divertor heat flux levels approaching those expected in the DT phase of operation, maximum available power will be required in plasmas at the maximum current and field at which satisfactory H-mode operation can be sustained (see Appendix C). Monitoring of the heat handling capabilities of all critical systems (e.g., H&CD systems, in-vessel components, plasma-

facing surfaces in the divertor) will be essential. Given that power densities are expected to be beyond those previously investigated in an actively cooled tokamak divertor, it is anticipated that this will be a demanding step, requiring, perhaps, several months, and longer if repairs or modifications are necessary. Operation in H-mode is preferred, since this will produce the most challenging combination of quasi-stationary and transient heat fluxes on the divertor, and feedback control of the edge radiation through impurity injection will be essential. These experiments will provide insight into the range of heat loads that may be expected in the future, verify the capability to measure these heat loads in real time and to take appropriate control actions on a routine basis. In addition, the output from this phase will provide valuable data for the assessment of divertor codes. With longer pulses, the heating of all components and structures inside and attached to the vacuum vessel will require careful monitoring.

The Torus Cooling Water System (TCWS) and cryoplant must also demonstrate the capability of maintaining sufficient cooling within prescribed limits at up to 73 MW of auxiliary heating power, both at high (preferably full) plasma current and for pulse lengths potentially up to several hundred seconds at lower current levels. The cooling capability must be demonstrated with sufficient margin to give confidence in the ability of these systems to handle the additional expected heat loads due to fusion power in the subsequent FPO phase. Indeed, a related issue is that the AC heat loads in the Magnet system must be characterized (and be within acceptable limits) to provide a basis for the extrapolation of plasma scenario demands to the $Q = 10$ and $Q = 5$ scenarios foreseen in DT operation. The combined heating and coil power supply systems must keep (pulsed) electrical grid demand within the 500 MW site limit and avoid excessive fluctuations on the grid for the most demanding emergency termination scenarios.

2.5.5.9.2 Critical system performance deliverables in PFPO-2

The deliverables of critical system performance during PFPO-2 include:

- ECRH, ICRF, and NB heating systems must demonstrate full power with pulse lengths limited only by the available experimental time for commissioning;
- Gas and pellet fuelling systems must demonstrate full fuelling capability for 15 MA plasmas;
- Demonstration of satisfactory heat load control on first wall and divertor to full auxiliary heating power capability;
- Radiation and impurity profile control demonstrated up to full auxiliary heating power and available pulse length;
- TCWS and the cryoplant must demonstrate sufficient cooling capability at full auxiliary heating power and available pulse length to extrapolate to full fusion burn conditions;
- All systems must demonstrate that they operate within the 500 MW site power limit without excessive fluctuations on the grid up to the full auxiliary heating power for the most demanding emergency termination scenarios;
- CIS and CSS plasma-related interlock and safety functions must be fully commissioned.

2.5.5.10 Initial studies of current drive efficiency, target q-profile formation and fast particle physics

2.5.5.10.1 Assessment of H&CD and diagnostic capabilities for performing current drive studies during PFPO-2

The primary goal of this research in PFPO-2 is to start the demonstration of the essential components for the development required to achieve the two long-pulse high-Q ITER goals. These are a stable long-pulse (target 1000 s, high non-inductive fraction $f_{NI} \sim 0.6$, $Q \sim 5$) and fully non-inductive steady-state pulse (target 3000 s, $f_{NI} = 1.0$, highest achievable Q, aiming at $Q \sim 5$) [Gormezano, 2007]. During these preliminary exploration stages in H/He the research will concentrate on the assessment of non-inductive current drive efficiencies by various auxiliary (ECRH, ICRF, NBI) and plasma (bootstrap) means, and on the deployment of advanced real-time control techniques for maintaining plasma stability (β) and desired current and kinetic profiles.

The experiments will be focussed on the range of $q_{95} = 3.5$ to 6. Operation at $q_{95} = 4$ will target long-pulse operation in hybrid discharges [Luce, 2003; Staebler. 2005; Joffrin, 2005; Hobirk, 2012], while steady-state operations (fully non-inductive) will be targeted by operation at $q_{95} = 5$ [Kamada, 1994; Söldner, 1999; Wolf 2003]. The capabilities of the baseline H&CD systems (33 MW of HNB, 20 MW of ICRF, and 20 MW of ECRH/ECCD) and of the diagnostics (in particular those related to the determination of the current profile shape, such as polarimetry and MSE) already available by this PFPO-2 stage will be used for this research. The overarching objective of the PFPO-2 experiments is to assess current drive capabilities of the baseline H&CD systems in low-β L- and H-modes (He or H, although H is preferable) at $q_{95} = 4$ and $q_{95} = 5$. In order to allow these studies to be performed in H-mode plasmas, a toroidal field of 2.65 T is selected (see section 2.5.5.7) and, thus, the plasma scenarios to be explored will range over 4.5 - 5.6 MA/2.65 T. From the evaluation of the operational space in hydrogen H-modes with the baseline heating schemes at 2.65 T in section 2.5.5.7.1, it is expected that most of the experiments in stationary H-modes will be performed in He. However, if the approaches discussed in section 2.5.5.7.4.2 are successful in expanding the hydrogen H-mode operational space, it might be possible to perform those carried out at 5.6 MA/2.65 T, $q_{95} = 4$ in hydrogen plasmas.

In order to accomplish the goals of this phase, it is firstly necessary to have the full baseline H&CD systems available. In addition to these systems, MSE, polarimetry and magnetic equilibrium calculations incorporating kinetic profiles are required in order to determine the current profiles produced by these systems. These capabilities should be available by PFPO-2 as well, but it is important that these have reached sufficient maturity for their application to support the execution of the experiments. An additional requirement for this phase of operation includes the availability of real-time control algorithms for plasma formation, maintaining stability and H&CD actuator control for the production of desired target current profiles. The experiments should have stationary plasma conditions in order to produce relaxed j(r) profiles. This will require density and ELM control systems to be fully operational and demonstrated for H-mode plasmas, which is foreseen in the PFPO-2 plan (see section 2.5.5.7), as well as the use of ECRH/ECCD for NTM control in these scenarios, if required.

As discussed in Appendix E, the flexibility of the baseline H&CD systems is not expected to be sufficient for high-Q operation in steady-state DT plasmas. Therefore, it is anticipated that a major activity during this initial scenario development will be to evaluate the capability of these systems to produce steady-state operation and to establish a firm physics basis for decisions on potential upgrades of these systems. It is anticipated that, even if fully non-inductive operation cannot be

achieved with baseline heating and current drive systems at this stage, the required q-profile can be maintained for sufficient duration ($t < t_{RESISTIVE}$) to allow assessments of the associated plasma performance, fuelling requirements, control needs, divertor compatibility and MHD plasma stability in PFPO-2. The results of these studies will provide first experimental evidence for the choice of baseline heating and current drive upgrades to be implemented to ensure that the Q ~ 5 long-pulse and steady-state goals of ITER can be achieved in FPO. From the evaluations in Appendix E, these are likely to be a 3rd HNB (to provide more current drive and input torque) or/and an additional 20 MW of ECRH/ECCD (to provide more heating and j(r) control capability).

To a large degree in parallel with this research, but also with the program of H-mode studies (section 2.5.5.7) and L-mode studies (section 2.5.5.11) in PFPO-2, investigations of fast particle populations and their effects on MHD stability will be launched at this stage. This will require the commissioning of the relevant diagnostics which will be available in PFPO-2 or before. Possibly some additional points along the experimental scans already included in the main program activities will be required to characterize or control specific fast particle physics processes. One of the key physics issues to be assessed in this phase is whether the NBI fast ion confinement can be described by classical processes, or whether it is anomalous due to the presence of Alfvén Eigenmodes or other MHD processes. To this end, it is important that as many fast ion diagnostics as possible are functional for these experiments and, therefore, it would be beneficial if the installation and commissioning of the fast ion loss detector and the vertical and radial gamma ray spectrometers were accelerated so that they are available by PFPO-2; presently these are foreseen for FPO.

The overall distribution of the experimental time among the various issues to be address in this period is given below:

- Scans of the ECRH/ECCD power deposition at constant density in the current flattop of stationary H-modes to evaluate heating and current drive: **4 days**
- Scan of NBI beam sources (on-axis vs. off-axis) in the current flat-top of stationary H-modes and the assessment of NBI fast ion confinement: **2 days**
- Attaining target j(r) at the end of the current ramp-up phase (L-mode) using real-time control algorithm and extension ~10 s: **10 days**

2.5.5.10.2 Risk to the initial studies of current drive efficiency, target q-profile formation and fast particle physics

The major risks to this campaign are associated with technical difficulties related to the available heating and current drive systems and/or their integrated control, insufficient fast particle diagnostics and uncontrolled behaviour of plasmas in ITER, namely:

- *Heating and current drive and/or control schemes cannot provide the required capabilities to produce and/or sustain the target j(r) required for the experiments:* Depending on whether these issues are related to specific features of the H/He plasmas or not the mitigation strategy will vary. To mitigate this risk more experimental time could be allocated to refine the control schemes in PFPO-2. If the inefficiency in current drive or control results from the specific features of these H/He plasmas (e.g. T_e is too low for efficiency current drive, density control in He H-modes does not allow a proper evaluation of CD efficiency, etc.), which are not expected to occur in D/DT plasmas, then this operational period would be shortened as it is not likely to provide useful information. On the other hand, if the inefficiency in current drive is expected to affect D/DT plasmas, it will be necessary to ensure that this is mitigated by the beginning of FPO, for which an upgrade of the baseline heating and current drive systems would be required.

- *Plasma density and temperature cannot be sufficiently well controlled to assess current drive efficiency:* This is a possible risk by this stage, although not likely due to the extensive H/He L-mode and H-mode program in PFPO-2 that will have been performed before these experiments. However, if this becomes an issue, additional dedicated experiments to refine the level of kinetic plasma control will be required.
- *Deficiencies to diagnose specific plasma parameters may affect the execution or interpretation of the experimental results:* Possible issues are related to the measurement of the current profile and of fast particles characteristics. The former are well covered by the available diagnostics in PFPO-2 (which are the same as those in FPO for this) but it may be found that these are not sufficiently accurate. In this case an upgrade of the back-end diagnostics could be required before proceeding to long-pulse experiments in FPO. Regarding fast particles, the capabilities to measure them are more restricted in PFPO-2 than in FPO due to the lack of neutrons. Fast particle measurements are mostly based on the diagnosis of their effects on the plasma (fast magnetics, SXR, ECE, interferometry and polarimetry) and the measurements of their losses on the first wall and divertor (infrared), as described in Appendix H. Otherwise, the only other available diagnostic at this stage is the neutral particle analyzer that would provide a line integrated measurement. Therefore it is essential that the fast ion charge exchange diagnostic upgrade foreseen for PFPO-2 in Appendix H is implemented and brought to its fully functional capabilities at this stage. In addition, it would be highly desirable to advance the fast ion loss detector and gamma ray spectrometers to be functional in PFPO-2; they are presently foreseen for FPO.

2.5.5.10.3 Detailed experimental plan for the initial studies of current drive efficiency, target q-profile formation and fast particle physics (16 days)

Initial research towards producing high non-inductive current fraction and ultimately fully non-inductive discharges with significant fusion power production will start during the non-active PFPO-2 campaign. An efficient progression to the development of non-inductive steady-state plasmas would require a detailed assessment of the capabilities of the heating and current drive systems and the associated operating space during the H and D phases. In particular, the current drive in low-β L-mode and H-mode plasmas (H or He) will be assessed at $q_{95} = 4$ (5.6 MA/2.6 5T) and $q_{95} = 5$ (4.5 MA/2.65 T). Specific experimental activities and objectives of this research include:

- Commissioning of the various H&CD systems for their respective current drive missions and identification of the restriction for their application, if this has not been done up to this stage (shine-through for NBI, incomplete absorption of ECRH, etc.).
- Commissioning of start-up scenarios consistent with these limitations for 5.6 MA/2.65 T and 4.5 MA/2.65 T and of the systems required for q-profile control during the ramp-up phase. It should be noted that if MSE is required for the q-profile control scheme in the ramp-up phase, the HNB energy should be substantially reduced to allow injection in the ramp-up or short beam blips will be required.
- Producing the target current profiles required for hybrid and non-inductive scenarios at end of the ramp-up phase. This includes development for partially non-inductive hybrid discharges ($q_{95} = 4$) as well as for ultimately fully non-inductive, steady state scenarios ($q_{95} = 5$) in H-mode. The stability and confinement properties of the plasmas obtained will be assessed for a range of current/pressure/(and if NBI can be applied) rotation profiles.

- Assessing the ability to sustain the target current profile obtained at the end of the ramp-up during the current flat-top beyond the confinement time scale, e.g. up to 10 s. This will require the tuning of the H&CD capabilities as well as of the plasma density to maintain this current profile control, in particular if H-mode conditions are attempted at the start of the flat-top.
- Determining the EC current drive efficiency through scans of the EC deposition location by measuring the resulting j(r) for q_{95} = 4 and = 5 stationary L-mode and H-mode plasmas and a range of densities and temperatures (controlled by the application of the other heating schemes NBI and ICRF).
- Determining the NB current drive efficiency through a scan of the NB deposition location by measuring the resulting j(r) for q_{95} = 4 and q_{95} = 5 stationary H-mode plasmas and a range of densities and temperatures. The specific scans considered in this period rely on the use of one HNB on-axis and one off-axis. The scans will include assessing the heating and current drive of both beams separately as well as simultaneously in H-mode plasmas. This will include scans with similar total input power (i.e. ICRF or ECRH should be applied to replace the reduced HNB power when one HNB is not used) and others in which the total power is scanned.
- Validating the models that describe current drive. For inductive operation, this will include assessing Spitzer versus neoclassical conductivity models. For non-inductive operation, neoclassical bootstrap models will be assessed as well as whether neutral beam ion confinement is classical or anomalous due to the presence of Alfvén Eigenmodes or other modes. The assessment of ICRF current drive will only be performed for He plasmas for which an effective heating scheme at 2.65 T is available.
- Determining the experimental behaviour of fast ions and validating the models for fast ion behaviour resulting from the fast ion populations arising from all heating systems. In particular, if MHD instabilities are observed, determining the nature of the instabilities observed (e.g. global TAE modes in the outer region of the plasma) [Pinches, 2015].
- If Alfvén Eigenmodes (AE) become unstable, investigating the effects of the various heating and current drive systems on this instability and of the capabilities of these systems to affect AE instability by local modification of plasma parameters (since heating influences the Landau damping experienced by these modes and also changes the spectrum of compressional and Alfvénic modes) [Lauber, 2015]. If suitable actuators are established for AE control then development and refinement of AE control techniques and associated controllers could start at this stage.
- Determining and validating the effects of ELM control coils on fast ion losses for plasmas with q-profiles as required for hybrid and steady-state plasmas. This would be complementary to the experiments in PFPO-2 for the inductive scenario in section 2.5.5.7.

It is important to note that many of the activities above may involve the same experimental conditions and do not require separate experiments. For instance, the experiments to determine the efficiency of ECRH/ECCD in H-modes with NBI (+ ICRF) heating are also likely to provide information regarding the possible use of ECRH/ECCD to affect AE stability if AEs are driven unstable by the NBI. In addition, other experiments carried out in PFPO-2 inductive H-mode scenarios (see section 2.5.5.7) may have addressed some of the issues above already or will provide guidance for experiments in this phase, thus shortening the required experimental time. For example, the measurements of NB current drive efficiency may be already available from similar

experiments where the heating mix will be varied to identify effects on H-mode performance and ELM control. Similarly, the effects of ELM control coils on fast ion losses will have been characterized as part of the ELM control experiments within a range of q_{95} = 3 - 6, etc..

2.5.5.10.4 Deliverables for the initial studies of current drive efficiency, target q-profile formation and fast particle physics

The main deliverables from this phase are:

- Initial demonstration of fully integrated scenarios with q_{95} = 4 and 5 and j(r) profiles required for advanced H-mode scenarios sustained over ~10 s, including the formation of suitable j(r) profiles in the ramp-up phase;
- Definition of control algorithms to achieve the target j(r) profiles for q_{95} = 4 and 5 and to sustain it in L-mode and initial attempt at H-mode plasmas;
- Assessment of NBCD in H-mode plasma conditions for q_{95} = 4 and 5 and j(r) profiles required for advanced H-mode scenarios, which can substantiate the need for a 3rd HNB to achieve the Q ~ 5 long-pulse goal;
- Assessment of ECCD in L-mode and H-mode for q_{95} = 4 and 5 and j(r) profiles required for advanced H-mode scenarios, which can substantiate the need for additional ECRH/ECCD power to achieve the Q ~ 5 long-pulse goal;
- Assessment of j(r) formation by application of ECRH/ECCD in the ramp-up for q_{95} = 4 and 5 scenarios foreseen for advanced H-modes and of its flattop sustainment with ECRH/ECCD and other heating schemes;
- Assessment of the level of ECRH/ECCD required for NTM control for q_{95} = 4 and 5 and j(r) profiles required for advanced H-mode scenarios, which can substantiate the need for additional ECRH/ECCD to achieve the Q ~ 5 long-pulse goal;
- Assessment of the level of ECRH and ICRF needed for W control for q_{95} = 4 and 5 and j(r) profiles required for advanced H-mode scenarios. This is expected to be different in these scenarios as core MHD is likely to change (e.eg less frequent or not sawteeth) and can substantiate the need for additional ECRH/ECCD to achieve the Q ~ 5 long-pulse goal;
- Assessment of the fast particle behaviour and impact on MHD stability for q_{95} = 4 and 5 and j(r) profiles required for advanced H-mode scenarios and identification of possible actuators to control this behaviour;
- Validation of models required to design hybrid and steady-state scenarios to be further developed in FPO.

2.5.5.11 Plasma operation at full technical performance (15 MA/5.3 T)

Once plasma operation, plasma control and, especially, the disruption management/mitigation capabilities are sufficiently reliable, the research program will address the extension of the operational space to full current (I_p = 15 MA). In preparation of the Fusion Power Operation (FPO), this phase (PFPO-2) will provide the first experience of high current operation in ITER. The main aim of this phase is to develop the basis of high current plasma scenarios and to provide the technical demonstration that ITER can operate at its baseline design parameters in terms of plasma current and toroidal field. It will assess the reliability of magnetic control, in particular vertical stability control, the robustness of the plasma current ramp-up and ramp-down, the efficiency of

plasma fuelling with gas and pellets, as well as developing schemes for divertor heat flux control and W production-transport control.

Commissioning of the heating systems and heating schemes will be an integral part of this activity as well as further optimization of the disruption mitigation scheme. Deliberate unmitigated disruptions at high current, in particular at 15 MA, are not required to proceed to the FPO phase: disruption loads will be extrapolated to 15 MA from the disruption tests at lower plasma currents, using appropriate disruption models (as described in section 2.5.5.5). Unmitigated disruptions at plasma currents above I_p = 7.5 MA should be avoided as far as possible to ensure a fast progress towards the FPO. This requires a well-developed disruption mitigation function (mitigation scheme, mitigation trigger) and effective disruption avoidance schemes as well as a targeted operational campaign to demonstrate high current operation within the proposed operational time. This is estimated to amount to 25 operational days and to consist of several I_p/B_t steps along an approximately constant q_{95} path.

The extension to high current in PFPO-2 will be developed via hydrogen L-mode operation, in view of the limitations on H-mode operation at plasma currents and fields above 7.5 MA/2.65 T both for H and He plasmas (see Appendix B and section 2.5.5.7.1). The target flat-top duration at full current and field for hydrogen L-mode operation is ~ 50 s. Operation at 15 MA/5.3 T requires the full capabilities of the central solenoid and optimization of the current ramp-up/down together with the use of additional heating. Scenario simulations of 15 MA/5.3 T plasmas shown in Figure 2.5-9 indicate that, for ohmic plasmas, a flat-top of 10 s can be achieved, while 20 MW of RF heating (ECRH or ICRF) will allow the extension of the flat-top to 50 s. For lower values of the plasma current, similar or longer flat-top lengths can be achieved in heated L-mode plasmas but in this case at lower premagnetization currents for the CS (≤ 30 kA) and, thus, with negligible fatigue lifetime consumption.

2.5.5.11.1 Requirements

Before proceeding to expand the operational space towards 15 MA/5.3 T in hydrogen L-mode plasmas, the following scenarios/technical demonstrations will have been performed:

- Operations in hydrogen L-mode plasmas with 7.5 MA/2.65 T and additional heating power levels of ~ 20 MW will have been demonstrated, in particular with on-axis and off-axis ECRH heating, as well as for 7.5 MA/5.3 T plasmas. The off-axis case is essential to address the risk of the foreseen L-mode scenarios at intermediate fields between 2.65 and 5.3 T, as, for some of them, ECRH heating will be rather off-axis. Plasmas with off-axis heating can be prone to W accumulation (although this phenomenon is more likely in H-modes) and this can significantly increase the risk for disruptions.
- Operations with plasma currents above I_p = 7.5 MA will significantly increase the potential for large electromagnetic disruption forces. Unmitigated disruptions in this research phase should be thus avoided as much as possible. Therefore, as mentioned above, this operational phase can only start when ITER operation has demonstrated a satisfactory capability of disruption avoidance and when the disruption mitigation function (mitigation scheme, mitigation trigger) has reached reliable performance.
- The heating and current drive systems will have been commissioned to both power and durations levels to allow high I_p/B_t operation with flat-top durations of at least 50 s, which can require heating of the plasma during the current ramp-up phase. This is essential to achieve this flat-top duration at 15 MA/5.3 T, as it has been assessed that for ohmic plasmas

only a 10 s flat-top is achievable, following a 65 s ramp-up, as shown in Figure 2.5-9. For lower plasma currents, the use of plasma heating allows the achievement of these flat-top lengths without the need for a fully charged CS at breakdown and, thus, without consuming CS fatigue lifetime for these experiments.

- The execution of this experimental program requires the availability of the full gas injection system (for hydrogen and impurity fuelling) and of the four hydrogen fuelling pellet injectors, full axisymmetric PF control capabilities, vertical stability systems VS1 and VS3, etc.
- By the beginning of PFPO-2, the ITER diagnostic set will be close to its final configuration (except some neutron and fast particle diagnostics) and, therefore, it is found to be appropriate for the foreseen L-mode operation.

2.5.5.11.2 Risks to L-mode plasma operation at full technical performance (15 MA/5.3 T)

The major risks for this operational phase are:

- Issues associated with the development of breakdown scenarios at intermediate fields between 2.65 T and 5.3 T. This may require additional experimental time for this development and if, unsuccessful, the need to adjust the current and toroidal field level for the intermediate I_p/B_t steps. In the worst possible case, all the intermediate steps would be performed at B_t = 5.3 T and thus with q_{95} varying from 6 to 3.
- Recurrent W accumulation for plasmas with intermediate fields between 2.65 T and 5.3 T and thus off-axis ECRH. This will require additional experimental time to develop these scenarios and if, unsuccessful, the need to adjust the current and toroidal field level for the intermediate I_p/B_t steps. In the worst possible case, all the intermediate steps would be done at B_t = 5.3 T and thus with q_{95} varying from 6 to 3.
- Occasional failures in the mitigation of disruptions as I_p/B_t are increased. Unmitigated disruptions above 7.5 MA can potentially produce large electromagnetic forces and have serious consequences for the plasma-facing components. Such events could slow down the experimental program towards 15 MA.

2.5.5.11.3 Detailed experimental plan for the expansion of L-mode plasma operation towards full technical performance (15 MA/5.3 T) (25 days)

This operational phase is estimated to require 25 operational days and in them the plasma current will be increased in gradual steps from I_p=7.5 to 15 MA. The gradual increase of I_p/B_t allows the building of robust scenarios at one current level before proceeding to the next step and thus avoiding unexpected problems at higher currents. This requires that at each step it is verified if: a) there are operational limitations which affect their feasibility, e.g. enough available auxiliary power is available; b) the step is useful; that is, if it provides an appropriate stepping stone for operation at higher currents; and c) it provides relevant, new information and does not duplicate other experiments already done within the Research Plan. Further details of the non-active operations scenarios can be found in [Kim, 2016].

The time allocated to this operational phase is optimized to achieve the deliverables which are required for FPO and special care should be taken in this phase of operations, as unmitigated disruptions at high currents could delay the start of FPO. The choice of the intermediate B_t steps requires the optimization of two constraints related to the location of the ECRH resonance: one is related to the need to ensure that EC-assisted breakdown remains effective and the other that the

ECRH deposition profile does not move to a position so off-axis that is ineffective in preventing W accumulation. This is an issue that can lead to increase disruptivity and thus to be avoided when increasing I_p beyond 7.5 MA. The assessment of this issue for 7.5 MA/2.65 T plasmas with on-axis and off-axis heating is thus included in PFPO-1.

The detailed steps in the proposed increase of I_p/B_t to 15 MA/5.3 T depend, therefore, on the results of this ECRH on- and off-axis assessment and of the commissioning of the VS system. The increase of I_p/B_t is proposed to be carried out at values of constant q_{95} = 3 - 4, as this has advantages related to the avoidance of disruptions, for which forces increase gradually as ~$I_p \times B_t$. Maintaining an approximately constant q_{95} from one I_p/B_t step to the next ensures that the plasma MHD stability for the next higher I_p can be inferred from the previous one. This reduces the risk of disruptions and, in particular, the need to redevelop the ramp-up/down and heating termination scenarios for each step of I_p/B_t, which are usually the more critical phases of the discharges in this respect (although the termination of heating may be less critical for these L-mode discharges than for later ones in H-mode). The operational steps proposed in this phase are shown in Figure 2.5-10. Point 1 in the development path lies underneath point 2 - the difference between the two scenarios is the setting of the poloidal launch angles, such that for point 1 the ECRH deposition is as central as possible, and for point 2 it is tuned off-axis to match the innermost radial range accessible with ECRH at point 3 (the 2nd harmonic resonance moves to the low field side as the field is increased). Points 4-6 correspond to a similar radial range of off-axis heating using the fundamental resonance on the high field side. For points 7 and 8, the ECRH is deposited centrally again. Note that the centre of the ECRH heat deposition profile depends on the temperature profile. The optimum values of the intermediate fields must therefore be confirmed by modelling.

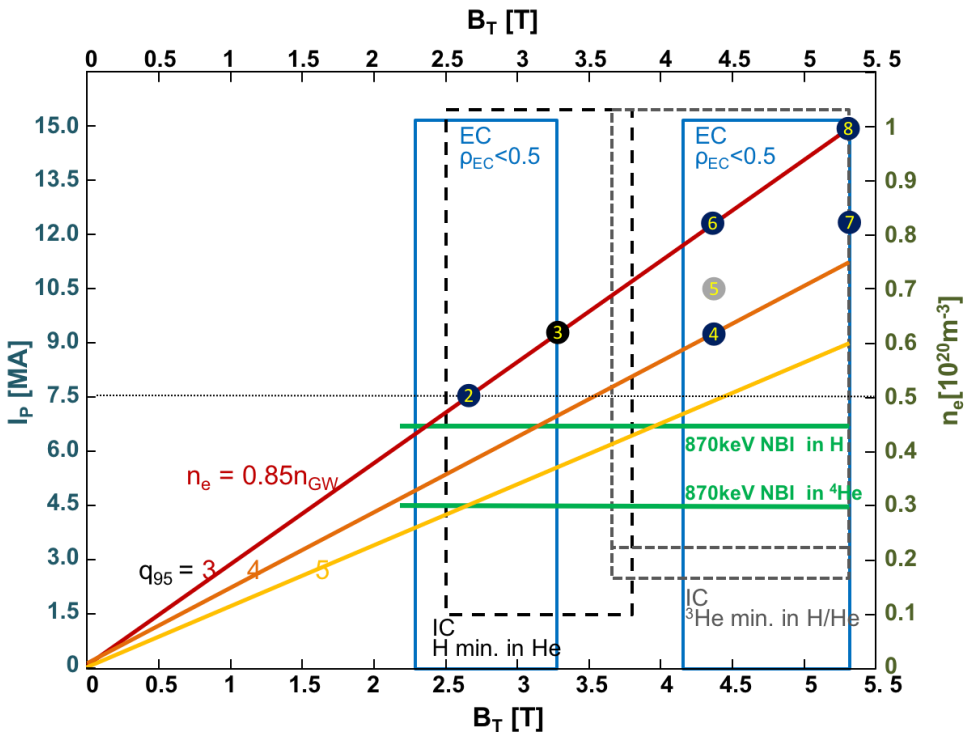

Figure 2.5-10: Operational path (in I_p/n_e versus B_T space) from 7.5 MA/2.65 T hydrogen plasmas towards 15MA/5.3T L-mode operation, indicated by a numbered series of scenarios.

For each I_p/B_t level, optimization of the current ramp-up/down to minimize flux consumption compatible with an acceptable level of W concentration will be performed. This will include the use the various heating systems applicable (mostly of ECRH and ICRF) to heat the plasma in these phases; NBI can possibly be used but with lower energy/power due to the low densities expected during the lower current phases of the ramp-up/down. Similarly, gas fuelling and pellet fuelling scans will be performed. In particular, pellet fuelling in hydrogen L-mode plasmas is likely to be routinely applied for the unrestricted application of NBI in these hydrogen L-mode plasmas for which $\langle n_e \rangle \geq 4.5\times10^{19}$ m^{-3} is required [Militello-Asp, 2016]. These fuelling scans (including gas versus pellet comparisons and gas+pellet optimization) will be performed also for the flat-top phase together with additional power scans (including variations of the heating mix). It is expected that, for high power levels (potentially up to 73 MW of power can be coupled to the plasma for the steps with $B_t > 4.5$ T) or/and low values of $\langle n_e \rangle$, the level of power load to the divertor will be significant and W sputtering may also need to be reduced/controlled. This will require the development of divertor load mitigation and W sputtering reduction schemes by access to radiative divertor conditions with extrinsic impurity seeding in advance of the exploration of these plasma conditions. The final goal of the experiments will be the demonstration of fully integrated L-mode scenarios in terms of W and divertor power load control (including ramp-up/down) by the application of the additional heating and fuelling systems in ITER, which minimize flux consumption and that are MHD stable (including VS) up to 15 MA/5.3 T. These will be the basis for the further development of the DD and DT corresponding L-mode scenarios on which the H-mode scenarios will be built on.

In addition to the scenario development discussed above, these experiments will provide the first experimental assessment of core particle and energy transport and core plasma confinement at high I_p/B_t in ITER. Their dependence on plasma density and fuelling schemes will certainly be assessed, as well as on additional heating power level and mix, within the general scenario development plan discussed above. For specific conditions, or for the assessment of specific physics effects, dedicated experiments will be performed beyond those strictly required for scenario development. Experiments of this type could be, for example, the evaluation of the effect of torque input on L-mode transport and confinement for pure NBI heating versus ECRH or ICRF or ECRH+ICRF heating, the evaluation of the effect of more localized power deposition profile, versus wider ones on plasma confinement and transport, etc.

It may turn out that not all the steps 1-8 in Figure 2.5-10 are feasible, as the efficacy of ECRH to provide both assisted breakdown and W accumulation control may not be sufficient. Depending on the results of the experiments assessing these issues (preferably done in PFPO-1 as planned, or, if not possible, then earlier in PFPO-2), two paths are considered to achieve the final goal of this phase, which is a 15 MA/5.3 T L-mode hydrogen plasma scenario with ~50 s of flat-top. These are described in Table 2-7 for the path assuming that off-axis ECRH heating can meet the required scenario needs and in Table 2-8 for the last steps of the path (after 7.5MA/2.65T) which relies on maintaining on-axis ECRH heating, as far as possible, in most of the steps. For the latter it is assumed that control of W accumulation control will be less efficient with off-axis ECRH heating and thus the number of pulses with use of ECRH off-axis are decreased in order to reduce the number of possible disruptions.

In both cases, scenario #5 (in Figure 2.5-10) is deemed not necessary for the hydrogen L-mode phase. However, this will be developed in deuterium L-mode plasma in preparation for the deuterium H-mode in the FPO phase, which will follow a more careful approach when increasing I_p/B_t (as discussed in section 2.6.3.6 and section 2.6.3.3), as not only the magnetic forces increase, but also the plasma energy is higher, which can lead to localized melting of first wall and divertor target plasma-facing components during transients.

Table 2-7 – Path to 15 MA/5.3 T (in hydrogen) <u>with</u> ECRH off-axis (except #7and #8)

#	I_p/B_t	Available heating		
		P_{ECRH} (MW)	P_{ICRF} (MW)	P_{HNB} (MW)
2	7.5 MA/2.65 T	20	0	10-33*
3	9.5 MA/3.3 T	20	0	> 10**
4	9.5 MA/4.5 T	>13	20	> 10**
6	12.5 MA/4.5 T	>13	20	33
7	12.5 MA/5.3 T	>13	20	33
8	15 MA/5.3 T	>13	20	33

** These NBI power ranges have been calculated for different assumptions of Greenwald density fraction [Kim, 2016]; see also section 2.5.5.7 (H-mode PFPO-2)].*

*** NB heating above 10 MW shall be possible for all scenarios with a proper adjustment of the acceleration voltage and power modulation to limit shine-through losses. These will determine the level of NBI heating applicable in these cases and remains to be evaluated.*

Table 2-8 – Path to 15 MA/5.3 T (in hydrogen) <u>with</u> ECRH on-axis

#	I_p/B_t	Available heating		
		P_{ECRH} (MW)	P_{ICRF} (MW)	PH_{NB} (MW)
4	9.5 MA/4.5 T	>13	20	>10*
6	12.5 MA/4.5 T	>13	20	33
7	12.5 MA/5.3 T	>13	20	33
8	15 MA/5.3 T	>13	20	33

** NB heating above 10 MW shall be possible for all scenarios with a proper adjustment of the acceleration voltage and power modulation to limit shine-through losses. These will determine the level of NBI heating applicable in these cases and remains to be evaluated.*

2.5.5.11.4 Deliverables for the experimental plan for the expansion of L-mode plasma operation towards full technical performance (15 MA/5.3 T)

The main deliverables of this operational phase are:

- Demonstration of first L-mode operation at full current and field (15MA/5.3T) with ~ 50 s flat-top full integrated plasma scenarios including plasma position and vertical stability control, power load control, W accumulation control, etc.
- Demonstration of the intermediate I_p/B_t steps to be followed to achieve 15 MA/5.3 T L-mode plasmas along a $q_{95} = 3 - 4$ path, which will form the basis of the further development of L-mode scenarios in DD and DT (and for the corresponding H-mode scenarios) in FPO.

- Assessment of the effects of gas fuelling and pellet fuelling and additional heating power level and mix on plasma transport and confinement in ITER L-mode scenarios up to 15 MA/5.3 T including ramp-up/down phases.
- Optimization of flux consumption in L-mode ramp-up/down phases by using the ITER systems' flexibly, in particular, regarding the current ramp rate, and for plasma fuelling and heating in these phases.

2.5.5.12 Edge physics and PWI studies in PFPO-2

2.5.5.12.1 Wall conditioning

The efficiency for the removal of medium Z impurities of hydrogen or helium GDC and ICWC, for which scenarios will have been developed in PFPO-1, will be further assessed in PFPO-2. Here it is expected that PFCs will have evolved with operation time and that significant co-deposition of impurities with Be eroded from the first wall will have occurred. Continuous follow-up of wall conditions and routine monitoring of impurity sources in reference pulses (see Appendix D) will therefore be pursued. Since the amount of available ICRF power will be increased in PFPO-2, ECWC is no longer considered (cf. section 2.5.4.10.1.2), though scenarios will have been made available in PFPO-1.

During PFPO-2, the efficiency of ICWC as a method for the control of the T-inventory build-up in the machine during the FPO phase can be studied in detail. However, isotopic exchange between H and D with ICWC can only be quantified if D-trace experiments can be performed or if D-ICWC discharges are allowed. If so, this implies the development of half and full field ICWC scenarios at f/B_t = 7.0 – 10.5 MHz/T, in H as well as in in D, knowing that D-ICWC will *in fine* be operated for the control of the T-inventory in the FPO phase. As in PFPO-1, machine operation time will be required to optimize isotopic exchange efficiency vs. pressure, power, poloidal field patterns and duty cycle. The benefit of using the 2nd ICRF antenna at a higher frequency (55 MHz), as demonstrated in ASDEX-Upgrade and JET-ILW may also be assessed. In addition to torus pressure measurements and RGAs for the gas balance, partial regeneration (to ~100 K) of the cryopumps will allow the quantity of removed and retained isotopes to be measured using gas chromatography.

2.5.5.12.2 Fuel retention and material migration

2.5.5.12.2.1 Deuterium trace experiment

With the availability of the divertor erosion, dust and tritium monitor diagnostics, PFPO-2 offers the possibility for detailed validation of material migration and fuel retention modelling. Such an exercise requires well-defined and diagnosed plasma conditions, detailed information on material erosion and transport, co-deposition rates and fuel content in the co-deposits. The best approach is therefore to perform a dedicated experiment at the end of PFPO-2, during which the same discharge is repeated to accumulate incident particle fluence on the wall and divertor and sufficient thickness of co-deposits. The tritium monitor, a combined laser-induced desorption and lock-in thermography system, is designed to measure the fuel content in and thickness of Be co-deposits forming on the baffle region of the inner divertor. The system requirements indicate a minimum measurable thickness of 1 μm and a measurement range of 1 - 500 μm.

To provide more information on the spatial distribution of Be deposition and fuel retention in the divertor, it is proposed to remove a divertor cassette from the machine during Assembly Phase IV, immediately following PFPO-2, to allow post-mortem analyses in a way similar to what is

performed routinely after a JET-ILW campaign. Preliminary discussions indicate that a new set of plasma-facing units can be fitted on the extracted cassette which could then be re-installed in the machine for the start of the FPO phase. This would avoid the need to use one of the four divertor cassette spares. Once removed, samples could be extracted destructively from the plasma-facing units and various surface analysis techniques deployed to measure the poloidal distribution of the Be co-deposition.

One important output from this exercise is that information on the density and fuel content of the formed Be co-deposits will be available to assist in the validation of the tritium monitor diagnostic. However, an issue with analyzing the H content from surface analysis techniques is that the measurements are complicated by the existence of extrinsic sources (such as atmospheric water when the surface is exposed to air), which is why laboratory experiments use deuterium instead. The use of trace deuterium during this experiment will therefore strongly increase the accuracy of the post-mortem analyses. A suitable L-mode target discharge has been identified (see Appendix A) for such a migration experiment. Simulations indicate that the tritium production rate and in-vessel activation will be low enough to allow a meaningful number of discharges to be executed.

To determine the feasibility of these experiments, DIVIMP and WALLDYN simulations have been performed for the discharge described in Appendix A (I_p = 7.5 MA, B_t = 2.65 T (q_{95} = 3), P_{IN} = 30 MW, f_d = 0.375, $n_{e,sep}$ = 1×10^{19} m^{-3}). Two assumptions have been made to describe the far-SOL and extend the plasma solution right up to all plasma-facing surfaces: either an exponential extrapolation of the SOLPS solution (case 00d) or an increased radial velocity of 100 $m.s^{-1}$ to account for the existence of a high density shoulder (case 00l). The RACLETTE code has also been used to calculate the surface temperature profile in the divertor from the heat fluxes calculated from SOLPS.

Figure 2.5-11 shows the Be deposition rate in the divertor for the low and high far-SOL density, respectively. At the inner divertor baffle (corresponding to the area of interest for the T-monitor), deposit growth rates in the range 0.01-0.5 $nm.s^{-1}$ are predicted, the highest deposition rates being found for the higher far-SOL density case. A measureable peak Be deposition ~1 µm would be obtained for plasma durations of the order of 10^4 s, or about 100 discharges with 100 s flattop.

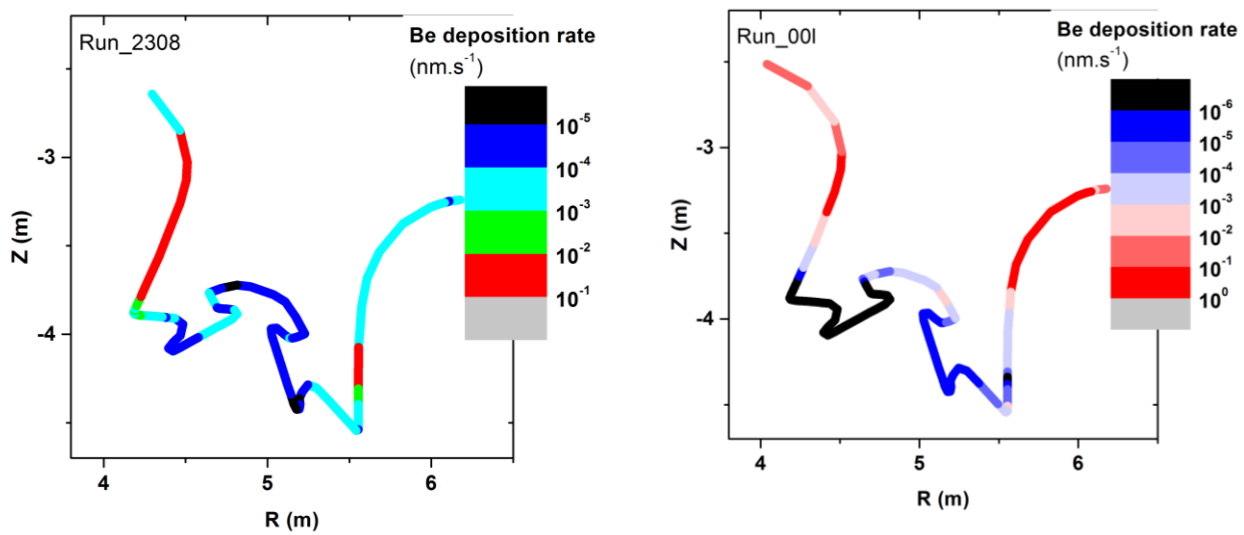

Figure 2.5-11: Beryllium deposition rate in the ITER divertor calculated with DIVIMP/WALLDYN for an L-mode plasma with I_p = 7.5 MA, B_t = 2.65 T (q_{95} = 3), P_{IN} = 30 MW, f_d = 0.375, $n_{e,sep}$=1×10^{19} m^{-3}, and a low density far-SOL (left panel) and a high density far-SOL (right panel).

These estimates have been made for the baseline (burning plasma equilibrium) equilibrium, but a decrease of the outer wall gap could be considered to increase the Be source and deposition rate into the divertor region. The predicted retention rates are 2×10^{-4} gs^{-1} and 10^{-3} gs^{-1} respectively, so that between 2 and 10 g of fuel would be retained in the vessel after 100 discharges much higher than the minimum measurable retention by the T-monitor, which is specified for a minimum in-vessel retention of 1 g. Development time for this discharge would be required. Note that the discharge flattop durations for the scenario explored in Appendix A are indeed on the order of 100 s. The use of trace D also significantly increases the accuracy of the gas balance analysis since background D levels are extremely low. A full gas balance analysis can therefore be executed during this experiment. Cryopump regeneration will be performed before and after the discharge campaign, which would be simply a repeat of identical discharges until the required accumulated discharge time has been attained. The amount of D in the exhaust gas, after regeneration of the cryopumps, can be very accurately measured using gas chromatography.

Importantly, this dedicated migration experiment can be used as a first validation of the fuel removal strategy. After the experiment, ICWC conditioning can be applied to recover D from the walls, and can be followed by a 350°C divertor bake (walls at 240°C). Using gas balance to estimate the in-vessel retention after each step (plasma discharges, ICWC, baking) would permit an estimation of the efficiency of the different techniques, whilst the post-mortem analyses would validate the estimates of remaining D in Be co-deposits formed in the divertor.

In summary, the following methodology is proposed:

- Execute a series of repeated 7.5 MA/2.65 T hydrogen L-mode discharges at the end of PFPO-2 with trace D injection to accumulate divertor fluence and build measurable deposition in the divertor;
- Perform a gas balance analysis over the trace D discharge series to accurately estimate the D retention rate;
- Use the T-monitor to evaluate the thickness and fuel content of co-deposits on the inner divertor baffle;
- Apply ICWC discharges in hydrogen to recover D from the wall. Assess the amount of recovered D from gas balance analyses and local measurements using the T-monitor;
- Perform a bake-out of the PFCs (240ºC for the FW, 350ºC for the divertor) and assess the amount of released D from gas analysis and measurements with the T-monitor;
- Extract a divertor cassette during the following assembly phase for post-mortem analysis.

It is important to mention that the use of trace-D is also desirable for the TBM Program in order to evaluate the permeation rates of fuel species from the plasma to the TBM cooling systems (see section 3.2.2). More detailed calculations and assessment of the experimental detection limits are required to establish if the type of discharge proposed in Appendix A and the total discharge time required for the migration study would also be suitable for the TBM Program.

2.5.5.12.2.2 Ammonia formation during nitrogen-seeded H-modes

The higher available input power during PFPO-2 should allow the investigation of ammonia formation rate during nitrogen seeded H-mode discharges. Since such discharges are likely to be required for testing of divertor power load control, ammonia formation rates can probably be studied without the need for dedicated discharges. Assuming that plasmas executed during this phase will have higher divertor heat loads and higher wall fluxes, it should be possible to assess/confirm the role of these parameters on the ammonia formation rate. The approach used will be identical as that described for the PFPO-1 (section 2.5.4.10.3.1). The main requirement will be to

perform a high temperature regeneration of the divertor cryopumps to recover the ammonia trapped on the active charcoal panels.

2.5.5.12.2.3 Dust generation and characterization

In common with the in-vessel tritium retention, there are inventory limits for the amount of dust inside the vacuum vessel. The maximum permitted amount of mobilizable dust in the vessel is 1000 kg. To prevent the risk of hydrogen explosion following the accidental ingress of air and water into the vessel, the amount of dust on hot surfaces must be kept below 18 kg (9kg Be, 9kg W). It is therefore necessary to be able to diagnose the vacuum vessel dust inventory and to ensure that safety limits are not exceeded.

Several mechanisms may contribute to dust formation. Amongst them, the most significant are expected to be droplet ejection during transient events (especially from melting of the Be wall) and flaking of layers forming as a result of first wall erosion, material migration and subsequent deposition. Uncertainties remain as to how much dust can be generated during a disruption because it is currently unclear how much of the melted material can be ejected in the form of droplets and the proportion of these droplets that can convert into dust. Recent simulations have in fact shown that droplets could be ablated in the disrupting plasma which would potentially strongly reduce the dust formation rate. Given that the wall heat loads during disruptions in ITER will be higher than in any current device, it is unlikely that reliable, experimentally validated extrapolations will be possible before the start of ITER operations. It is therefore important to quantify the dust production rates in ITER, and to determine the characteristics of the produced dust (size distribution, composition) prior to the start of nuclear operations.

An endoscope-based dust monitor system is being designed to view and collect particles below the divertor (both on the cassette body and on the vacuum vessel floor). The system is planned to become available during PFPO-2 and will allow regular inspection during the campaign. In parallel, regular monitoring of the wall erosion/damage will be possible using the In-Vessel Viewing System (IVVS), which has the capability to perform direct viewing and measurements of height changes (with ~85% coverage of the FW) on surfaces, should be foreseen to identify the locations of damage formation and help adapt plasma scenarios to prevent further damage. The IVVS will also allow the monitoring of excessive erosion, either due to direct sputtering/evaporation or due to material redistribution from melt layer motion. A full vessel inspection requires about 8 hours and is therefore most likely to be performed during short-term maintenance periods.

Deployment of the dust monitor and IVVS should probably occur after a disruption or sequence of disruptions in which camera observations show particles being released. No dedicated experimental time is required but the required deployment time must be factored in the planning. After PFPO-2, a complete dust collection through vacuum cleaning of the divertor should be performed to quantify the dust creation during the whole campaign. Dust collection on the vacuum vessel floor is not possible unless divertor cassettes are removed so that if a cassette is removed for post-mortem surface analysis (sections 2.5.5.12.2.1 and 2.5.5.12.2.4), this would provide an opportunity to inspect the vessel floor in this location and possibly aspirate debris before active operations begin.

2.5.5.12.2.4 Post-campaign analysis of Plasma-Facing Components

The divertor plasma-facing material in ITER will be exposed to unprecedented ion fluences and possibly to a very large number of heavy transient heat loads. Damage (melting, cracking) could occur early during operations, and it is important to document its occurrence and evolution. High resolution inspection of the high heat flux regions of the divertor targets will provide information on

the surface morphology and on the occurrence of melting and melt motion. The planned Erosion Monitor (based on Speckle interferometry) can be deployed at the end of each operation day and provides high resolution measurements of the surface morphology at a single toroidal location to characterize surface roughening (caused by melting or thermal shocking). This rather limited coverage, however, calls for additional characterization.

A further concern with the tungsten divertor is to which extent early operations, including those in helium, have modified the W thermo-mechanical properties and how this might impede later higher power operations. To date, no such characterization is foreseen. Removal and full inspection of a divertor cassette after PFPO-2 appears to be the most straightforward option, and, as mentioned in section 2.5.5.12.2.1, would greatly contribute to the characterization of Be migration. Once removed, samples can be extracted (destructively) from the plasma-facing armour and sent out for dedicated analyses. The results of this characterization would indicate whether the W material/components are still compatible with the expected loads during high power operations. In addition, as mentioned in section 2.2.10, removal of a cassette would allow a full characterization of the erosion/deposition pattern in the divertor, in a way similar to what is performed at JET after each campaign. Finally, as in PFPO-1, removal of the First Wall Samples will be performed after PFPO-2 for analysis to determine erosion by charge exchange neutrals and retention by implantation.

The exact strategy with respect to post-mortem analysis of samples (including dust) extracted from the machine is currently undecided. In 2014, a workshop was held at ITER Organisation (IO) to review the suite of diagnostics foreseen for tritium retention/dust/erosion measurements. The panel recommended the study of possible on-site facilities allowing the evaluation of erosion/deposition, surface composition and fuel retention of first wall samples and dust [Philipps, 2014]. As a result, a conceptual design has been developed for a laboratory to be located within the Hot Cell building [Galliez, 2017]. A formal decision on the actual implementation has not yet been taken. In parallel, contacts have been made with several laboratories specialized in analyses of radioactive materials.

2.5.5.12.3 Heat loads during divertor operations

Experiments in the PFPO-2 phase will access for the first time heat loads approaching those possible during FPO when additional heating is supplemented by fusion power. L-modes in hydrogen with close to maximum P_{IN} (73 MW), B_t = 5.3 T and high current (up to 15 MA) could deliver values of P_{SOL} which can drive separatrix parallel heat fluxes to values up to ~50% of those to be expected in baseline burning plasmas, depending on the assumed values of SOL heat flux width (see *Heat and Nuclear Load Specifications* [ITER_D_2LULDH, 2009]) and plasma density. At these levels of $q_{||}$, divertor heat flux control becomes mandatory depending on the achieved divertor neutral pressures, though the lack of ELM activity means that the scenarios will not be equivalent to a high power H-mode in terms of testing power load control in a fully integrated sense for future operation in D and DT plasma.

As discussed in sections 2.5.4.9 and 2.5.5.7, there are various options for H-modes at lower B_t and I_p, but the lack of an ICRF coupling scheme at 2.65 T in hydrogen probably means recourse to 1.8 T and thus lower I_p or more exotic 3-ion absorption schemes at slightly higher B_t (3.0 – 3.3 T) for hydrogen H-modes. High power H-modes in He, which should be possible at 7.5MA/2.65 T, are attractive for first wall and divertor power load characterization, including the contributions of ELMs, but much less attractive for divertor heat load control since the dynamics of divertor detachment differ substantially to those in hydrogenic plasmas due to the very different divertor radiation in He (section 2.2.1). In this sense, high power L-modes in hydrogen may be preferred for the testing of impurity seeding for detachment control in this phase.

In general, PFC heat load experiments in PFPO-2 should follow the methodology of those in PFPO-1 (section 2.5.4.10.5), studying L-mode power widths, divertor spreading factors and general detachment behaviour for a larger range of I_p at higher input power and B_t. Such studies benefit from the addition of the divertor Thomson scattering in PFPO-2. Characterization of inter-ELM and ELM divertor power loads and SOL widths can expand with the further development of hydrogen H-modes at 1.8 T and in He and possibly in hydrogen at 7.5 MA/2.65 T. One of the key aims here is to establish a firmer scaling for the SOL heat flux width over a wider range of I_p, with H-mode a priority, but also recognizing the strong link between the L and inter-ELM H-mode power widths (section 2.2.2). Main chamber power loads should also be studied as in PFPO-1 over the wider parameter range which will be available in PFPO-2, using scans in separatrix separation and plasma density to study profile broadening and possible links to detachment.

Divertor power flux control methods, tested first in PFPO-1 should be further developed at the higher power flux densities achievable in PFPO-2 L-modes at higher I_p and B_t. Seeding of both N_2 and Ne can be tested, with the L-mode a more benign regime for such higher power experiments, but in which SOL opacity will still require the use of core fuelling in conjunction with edge gas injection of fuel and impurity. Such experiments must be conducted in hydrogen plasma to be of relevance owing to the very different radiation distributions in He. Tests of the divertor plasma response to loss of divertor seeding and asymmetric toroidal divertor injection will be required.

Assuming a robust hydrogen target discharge is available at higher power in PFPO-2, more relevant, integrated detachment control of ELMy H-mode N_2-seeded plasmas can be further developed from the initial work in PFPO-2, but will again be limited in the range of density which can be studied if these plasmas have to be operated at low field and current. Having a full set of ELM control coils power supplies in this phase should allow optimization of the 3-D spectrum and tests of rotation of the perturbation so that further measurements of divertor heat load patterns can be performed, even if the density will be limited for low-I_p H-modes.

2.5.6 Summary of experimental activities and operational time in the PFPO Phase

An ambitious experimental program is foreseen for the PFPO phase, advancing the facility operational capabilities from sustainment of the simplest plasma breakdown, with plasma currents of less than 1 MA, to fully integrated L- and H-mode plasma scenarios in the range 5 – 15 MA which exploit essentially all of the tokamak, auxiliary and plant systems. The overall objectives of this phase are to demonstrate essentially the full technical capability of the ITER systems (accepting that the limiting capability in areas such as heat loads, pulse length etc., might not be accessible until significant fusion power is produced), to achieve robust and routine plasma operation over the accessible L- and H-mode parameter range, to perform initial exploration of fusion plasma physics at the ITER scale, and to prepare the scientific, technical and operational basis for the transition to DT operation, leading to significant fusion power production.

The PFPO research program will already allow extensive testing of many elements of the physics basis developed to support the ITER design and performance predictions. The values of key physics parameters such as collisionality and normalized Larmor radius, as well as ‘engineering parameters’ such as plasma current, major/minor radius etc., accessible during this phase will extend the tokamak physics basis very considerably and allow numerous comparative studies of predictions derived from the ITER physics basis in plasma transport and confinement, MHD stability, divertor and plasma wall interactions, heating and current drive efficiency, plasma control and scenario integration, and possibly also energetic particle physics (but still with anisotropic velocity distributions). Perhaps the key caveat in this respect is that, although a substantial program addressing H-mode physics (access conditions, energy and particle confinement, ELM

characterization and control etc.) is planned, the extent to which key aspects of H-mode physics can be addressed adequately will probably depend on achieving satisfactory H-mode performance in hydrogen as well as helium – key physics tests in this area might otherwise await the transition to deuterium operation in the FPO phase. Overall, therefore, and despite the inevitable emphasis 'on commissioning with plasma activities' within the presentation of the PFPO research program, this phase of ITER operation will provide significant opportunities for studies of fusion plasma physics at the ITER scale and will allow access to plasma and operational parameters substantially beyond those of current experiments.

The experimental program implemented during PFPO will also provide wide-ranging tests of much of the ITER technology under challenging conditions. It will, in particular, launch the first phase of the TBM testing program (see section 3.2.2.2), a central element of the ITER mission. Operation of major systems and components such as the superconducting magnets, plasma facing components, heating and current drive systems, Diagnostics, fuelling and vacuum systems, control systems, power supplies, the cryogenic system, tokamak and auxiliary cooling water systems (and even remote handling systems, which are required in this phase simply due to the scale of ITER components) will already yield an invaluable database on system performance and reliability over pulse lengths ranging from several tens to several hundreds of seconds. The upper limit of this range in pulse length will rely on successful commissioning and operation of the tokamak, auxiliary and plant systems, as well as successful implementation of the scientific research program, which will determine the rate of progress through the various performance milestones, potentially releasing time for commissioning of the key tokamak and facility systems, in particular, the H&CD systems, to extended pulse lengths of several hundred seconds.

The routine operation of plasma pulses with long durations during the PFPO phase would be a desirable, and significant, achievement, which would give additional confidence in operational reliability in advance of the FPO phase. This would be a major advantage in the preparation for the transition to DT operation, and could be expected to shorten the experimental time required to achieve long-pulse operation at high fusion power in DT plasmas. Nevertheless, if all other elements were in place to allow a timely transition to D/DT operation in late 2035, as scheduled, reliable L- and H-mode operation over a range of plasma scenarios with flat-top durations of several tens of seconds would be an adequate criterion to support this transition, given the emphasis on ITER's role in demonstrating fusion power production as rapidly as possible.

Table 2-9 and Table 2-10 provide an overview of the experimental activities implemented in each of the PFPO phases and of the operational time estimated as necessary to meet the objectives defined for each phase. There are, of course, significant uncertainties in these estimates, given the complexity of some of the 'commissioning with plasma' activities which it is planned to implement during the PFPO phase and the reliability issues which might be encountered in commissioning plant and auxiliary systems for the first time. For comparison, the estimated experimental time required for PFPO-1 is between 412 and 468 days (including the programmatic options considered) compared to an estimate of 470 operational days available (see Table 2-1), implying that there is little contingency in the estimated time schedule. For PFPO-2, the proposed program is estimated to require 418 – 433 days, as compared to the estimated 545 operational days available. Thus the PFPO-2 program does include contingency against unexpected developments in the program. This potentially offers opportunities to place a greater emphasis on the commissioning of H&CD systems to long-pulse operation and to exploit this capability in the experimental program.

Bringing all ITER systems from the initial phase of Integrated Commissioning to preparedness for DT operation, establishing the required range of plasma scenarios and demonstrating the required

Table 2-9 – Overview of experimental activities and estimates of required operational days for the PFPO-1 research program

Activity	Days
Plasma control/ Plasma scenario development	**155**
PF Null/ Breakdown optimization	7
Commissioning of gas and pellets for density/impurity control	9
Scenario development/ plasma magnetic control to 3.5 MA Limiter	17
Scenario development/ plasma magnetic control at ~5 MA/2.65 T Divertor	32
Scenario development/ plasma magnetic control at ~7.5 MA/2.65 T Divertor	40
Scenario development/ plasma magnetic control at ~7.5 MA/5.3 T Divertor	50
Disruption management	**64**
Disruption load validation	10
Commissioning/ Optimization of disruption prediction/ detection	11
Commissioning/ Optimization of disruption mitigation	43
Commissioning of auxiliary systems	**75**
Diagnostics	10
ECRH commissioning at 170 GHz (plus ~11 days for First Plasma)	25 [75]*
ECRH commissioning at 104/110 GHz	10 [30]*
ICRF commissioning	30 [60]*
Commissioning of advanced control functions	**79**
Advanced control functions (wall/divertor protection, MHD control etc.)	54
Termination scenarios, exception handling, shared actuator management	25
Divertor and PWI studies	**39**
Divertor/wall heat loads in divertor configuration and detachment control	5
Limiter heat loads	15
Disruption heat loads	5
Wall cleaning	10
PWI studies (fuel retention, He effects etc.)	9
Option: 1.8 T H-mode studies	**44**
H/He H-mode access at 5 MA/1.8 T (including ELM control)	31
Studies related to TF ripple effects on H-modes (preparation for TBM effects)	10
Assessment of H-mode power threshold variation with B_t	3
Option: Extension of plasma operation towards 10 MA	**12**
Total	**412 [+56]**

** The total estimated time for initial commissioning is shown in brackets, with an allocation of 1/3 to 1/2 of the time to dedicated experiments.*

Table 2-10 – Overview of experimental activities and estimates of required operational days for the PFPO-2 research program

Activity	Days
Axisymmetric magnetic control	**5**
Plasma scenario commissioning	**10**
Kinetic control commissioning	**50**
MHD and error field control	**30**
Advanced control functions (auxiliary specific, actuator sharing etc.)	**34**
Disruption Management	**27**
Disruption load validation	1
Commissioning/ Optimization of disruption prediction/ detection	6
Commissioning/ Optimization of disruption mitigation	20
Commissioning of auxiliary systems	**70**
Diagnostics	10
ECRH commissioning	10
HNB + DNB commissioning	25 [50]*
ICRF commissioning	25 [50]*
Divertor and PWI studies	**40**
Divertor/wall heat loads in divertor configuration and detachment control	7
Limiter heat loads	15
Disruption heat loads	2.5
Material migration	5
Fuel retention/ management	5.5
PWI studies (wall cleaning, He effects etc.)	5
H-mode studies	**111 - 126**
H-mode studies at 5 MA/1.8 T (TBM effects)	40
Expansion of H-mode operation towards 7.5 MA/2.65 T, incl. ELM control	65 - 80
Development of long-pulse H-modes	6
Development of 15 MA/5.3 T L-mode	**25**
Current drive efficiency, target q-profile formation, fast particle effects	**16**
Total	**418 - 433**

** The total estimated time for initial commissioning is shown in brackets, with an allocation of fraction of the time to dedicated experiments.*

level of operational reliability to support the transition to the FPO phase within the scheduled period of experimental operation of ~40 months is, as noted above, ambitious. There is a range of risks, in terms of hardware reliability/performance and plasma performance (as discussed in preceding sections and consolidated in Appendix J), which, if encountered, will need to be addressed and resolved, or mitigated, rapidly to ensure that the schedule towards DT operation proposed within the Staged Approach is maintained. Many of these risks are being addressed in ongoing physics and technology R&D programs. Nevertheless, given the scale of the extrapolation from current devices

to ITER, the associated uncertainties in the underlying physics basis, and the novelty of elements of ITER's integrated plasma scenarios, it is inevitable that expectations of plasma behaviour and performance, in particular, must be tested in the ITER environment. As indicated in the discussion in previous sections, a significant outcome of these tests and of measures to address the consequences of risks realized in the research program will be the specification of system upgrades required to improve operational reliability and assure the required plasma performance in later phases of the Research Plan (see also the detailed discussion of potential upgrades developed in section 4).

2.6 Fusion Power Operation Phase (FPO)

The Fusion Power Operation Phase, as discussed in this version of the Research Plan, encompasses the first experimental campaign of the FPO phase, which involves both D and DT plasmas and focusses on the development of inductive plasma operation to fusion power production levels of several hundred megawatts, and the second and third campaigns, in which long-pulse operation is developed in inductive, hybrid and non-inductive DT plasma scenarios, with the aim of meeting the project's mission goals of $Q \geq 10$ for periods of $300 - 500$ s, and $Q \geq 5$ in fully non-inductive operation for periods of up to 3000 s.

2.6.1 Objectives for the Fusion Power Operation Phase

During FPO, ITER will operate with all its baseline ancillary systems at full performance, including the T-Plant. In this phase, the three ITER DT high-Q goals should be successfully demonstrated. The initial focus of the research will be towards the achievement of $Q \geq 10$ for ~ 50 s, following which it will shift to extending the $Q = 10$ burn regime towards the $300 - 500$ s goal and subsequently to developing the long-pulse and steady-state scenarios towards $Q = 5$. It is expected that upgrades to the ITER ancillaries will be available for operation, either from the start of FPO (e.g. HNB3) or soon after the initial years, if the upgrades are required to achieve the $Q = 5$ goal, but are not implicated in achieving $Q = 10$ (e.g. additional ECRH power, RWM control power supplies, etc.). Similarly the T-Plant will be commissioned and will start providing significant quantities of T for the experimental program ~ 1 year after the start of FPO, allowing an extended program of DT operation to start.

The FPO phase can be divided into four blocks.

Initial D and trace-T operation:

In this phase all ITER systems will be commissioned (or recommissioned) for nuclear operation and the target scenarios of PFPO-2 will be reproduced in D plasmas. This implies the recommissioning of the ITER H&CD for D operation (mainly the HNBs, for which the injected species will change to D, and ICRF), diagnostics (chiefly the neutron-related diagnostics), fuelling (change to D), etc.

In this phase the plasma conditions achieved in H and/or He plasmas will be reproduced, namely L-mode operation will be expanded to 15 MA/5.3T and H-mode operation will be explored up to 7.5 MA/2.65 T. The operational strategies and control schemes developed during PFPO will be applied and refined/ retuned to the higher plasma energies expected in D plasmas. This phase will provide first experimental confirmation of the plasma parameters expected in DT plasmas in this current range, as the plasma characteristics are expected to be similar in D and DT plasmas except for those related to high fusion power production. Once D operation is reliably established, trace-T experiments will be performed with special focus on the 7.5 MA/2.65 T H-mode scenario, including

also the L-mode phases. Tritium transport and fuelling experiments will be performed and the results will be used to optimize fuelling and mixture control strategies for DT.

In this phase, research to confirm the key ingredients of the long-pulse/ steady-state scenarios will be confirmed. This will include experiments similar to those in PFPO-2 to develop the target-q profiles in the ramp-up, to sustain them for ~ 10 s in the flat-top and to determine the current drive efficiency of each of the H&CD systems (chiefly NBI and ECRH) in H-mode plasmas. The extent to which these experiments will be performed will be determined by progress on the H-mode program and the availability of the T-plant for DT plasma operation.

The main objectives of this operational block are:

- Commission plasma control, interlock and safety systems with plasma to the required level to support the experimental program;
- Commission the additional diagnostic systems (particularly those related to neutrons), validation of data and integration into control/ interlock systems;
- Recommission the installed H&CD systems for D plasmas to their installed power level for at least 50 s;
- Extend the capability for disruption prediction, avoidance and mitigation to parameters characteristic of the highest performance plasma achievable in D plasmas;
- Demonstrate D L-mode operation to 15 MA/5.3 T;
- Demonstrate robust NTM control in high confinement D H-mode plasmas;
- Develop D H-modes to 7.5 MA/2.65 T (~50 s) with reliable ELM control and stationary divertor power load control;
- Physics characterization of ohmic, L-mode and H-mode plasmas in D;
- Perform trace-T experiments in D L- and H-mode plasmas to assess T transport and T fuelling requirements and schemes;
- Characterization of key aspects of plasma-wall interactions in the ITER environment in D plasmas;
- Preparatory studies of hybrid/ non-inductive scenarios in D plasmas;
- Preparatory studies of ‘burning plasma’ issues (e.g. helium exhaust, fuel mixture control in trace T, etc.).

Initial DT operation with non-trace T level:

In this phase, the amount of T provided by the T-plant should allow operation with T concentrations in the range of 10-70% for up to ~ 50 s. Fusion energy production will start to be significant and neutron measurements will start to be important to evaluate it, as well as for the execution of the experimental program. As a consequence of the fusion energy production, the effects of neutron heating on the superconducting coils will start to be measurable and, although this is not expected to raise any issues for operational durations of ~ 50 s, the consequences for longer pulse operation at high Q will need to be evaluated at this stage. This may call for further optimization of the scenarios to be implemented at this stage to reduce AC losses. With the increased level of power in DT H-modes, routine operation of the scenarios with ELM control and radiative divertors will be required; this is expected to necessitate development and/or retuning of the control schemes developed for D at lower currents, with the same applying for the disruption avoidance and mitigation schemes. Similarly, the T throughput will start to be non-negligible, and already in this phase T-retention

measurements and removal schemes are expected to become part of the operation cycle in preparation for their routine use in the next operational DT phase.

The plasma regimes to be explored in this phase start with 7.5 MA/2.65 T plasmas, which will be characterized extensively both in L-mode and H-mode over a range of T concentrations. In these experiments, the first effect of α-heating will be documented, as well as fuelling requirements and possible new edge-core integration requirements that could arise due to the present of T in the plasma. Once a fully integrated 7.5 MA/2.65 T H-mode scenario in DT has been developed, the plasma current/toroidal field will be increased in steps towards 15 MA/5.3 T, and the demonstration of Q = 10 for ~50 s. It is expected that the steps will be similar to those in the L-mode D program, except that additional steps in current/ field will be added between 12 and 15 MA to account for the large change of plasma energy with I_p in H-mode. For each step, the T concentration will be scanned and fully integrated scenarios will be developed, including ELM control, fuelling and divertor power load control. It should be noted that the range of T concentrations that will be explored will decrease as the plasma current increases because the α-heating will become an essential part of the scenario to sustain the high confinement H-mode. It is expected that, in the expansion towards high-I_p/ high-Q, control of MHD stability will become more challenging and significant time will have to be dedicated to the control of NTMs and sawteeth in this phase.

In this phase, research to perform an initial development of Demo-relevant long pulse scenarios will start. This will include current ramp optimization in DT L-modes and H-modes (during the ramp-up), as well as sustainment of the flat-top H-mode phase. It is likely that, in this first operational phase, the sustainment will be limited to a few tens of seconds with relatively low Q, due to the limited operational time available and the available H&CD schemes.

The main objectives of this operational block are:

- Commission plasma control, interlock and safety systems with plasma to the required level to support the DT experimental program towards Q = 10;
- Commission additional diagnostic systems (e.g. for fusion power and fusion products), validation of data and integration into control/ interlock systems, as required;
- Commission ICRF heating scenarios for DT plasmas to installed power level for at least 50 s;
- Extend capability for disruption prediction, avoidance and mitigation to parameters characteristic of the highest performance in DT plasmas;
- Develop DT H-modes at 7.5 MA/2.65 T (~50 s) with reliable ELM control, NTM control and radiative divertor operation;
- Expand DT H-mode operational space from 7.5 MA/2.65 T plasmas culminating in 12- 15 MA/5.3 T DT H-mode operation with full feedback control at fusion powers of 200 – 300 MW for at least 50 s;
- Extend operation to 15 MA (if not done above) and optimize fusion gain to demonstrate $Q \geq 10$ for at least 50 s;
- Optimize fuel mixture control, burn control and plasma-facing component protection in DT plasmas;
- Physics characterization of ohmic, L-mode and H-mode plasmas in DT;
- Explore options for current profile control in DT plasmas to identify most promising approaches for long-pulse/ steady-state operation.

It should be noted that it is not expected that the initial target of Q = 10 for ~50 s will be achieved in the first FPO campaign: the foreseen target for the end of the first FPO campaign is a fusion power target of 200 - 300 MW with a fusion gain of Q ~ 5 sustained for ~ 50 s. Expanding this firstly towards a scenario with Q ≥ 10 for 50 s and then extending the burn duration to 300 - 500 s is expected to occur after the first experimental FPO campaign lasting 16 months.

Second phase of DT operation:

In this phase, the Q = 10 scenario will be extended towards 300-500s and the long-pulse and steady-state scenarios will be developed. The rate of progress of these developments will depend, of course, on the results of the experiments and on the physics itself, as well as on the status of implementation of upgrades which may be required to achieve the Q ~ 5 goals (e.g. additional ECRH/ECCD, power supplies for RWM control, etc.). During this phase the T throughput will reach its maximum value and T retention measurement and removal schemes will be routinely applied as part of the operation cycle. Similarly, neutron heating of the TF coils is also likely to reach its maximum, and this may require re-optimization of the scenarios to decrease AC losses. With the increased burn length, fusion power/ power load to components and inductive current fraction, plasma control in general and event handling, in particular, are expected to become significantly more complex and a substantial fraction of the operational time to extend the burn length is expected to be dedicated to solving such issues.

The main objectives of this operational block are:

- Develop DT plasma scenarios with Q ≥ 10 at P_{fus} ~ 500 MW for 300 – 500 s;
- Characterize key aspects of PWI in the ITER environment in high fusion power/ high gain plasmas;
- Develop program of burning plasma studies around high fusion power/ high gain inductive plasmas;
- Demonstrate satisfactory tritium accounting, retention measurement and removal techniques;
- Provide required support to the TBM testing program;
- Investigate optimization of fusion power with Q > 10 during stationary inductive conditions and characterize plasma behaviour in these conditions;
- Identify needs for upgrades to improve fusion performance, or to improve potential for non-inductive operation (e.g. ELM control coils power supplies for RWM control, if not previously possible to do so);
- Establish robust current profile control techniques for DT plasmas;
- Establish DT plasma scenarios with current profile control, improved H-mode confinement having a burn duration of ~ 1000 s and several hundred megawatts of fusion power based on the hybrid/improved H-mode scenario at q_{95} ~4;
- Establish non-inductive plasmas with the longest sustainable pulse duration (> 1000 s) and moderate fusion performance (Q ~ 2);
- Optimize fusion gain and pulse duration to establish plasmas with durations beyond 1000 s and Q ≥ 5;
- Optimize Q in fully non-inductive DT plasmas towards Q ~ 5;
- Start the characterization of key aspects of PWI in the ITER environment over very long durations (e.g. impact on fuelling, erosion/ redeposition, fuel retention, etc.).

It should be noted that, depending on the suitability of the upgrades implemented by this phase and the need for additional measures to achieve the non-inductive goal, the latter part of the research and development in this phase may be implemented in the next and final phase of FPO.

Long-term DT fusion R&D research:

In this phase, R&D issues related to the long-term goals of ITER towards Demo will be addressed. This is likely to require specific Demo-related upgrades discussed in section 4, which will be identified and implemented in this phase, together with the completion of those required to achieve the Q ~ 5 non-inductive goal.

The main objectives of this operational block are:

- Conduct a program of burning plasma studies to characterize physics of non-inductive DT scenarios;
- Perform systematic characterization of key aspects of PWI in the ITER environment over very long durations (e.g. impact on fuelling, erosion/redeposition, fuel retention etc.);
- Provide required support to the TBM testing program;
- Identify options for further upgrades to prepare longer-term Demo-targeted studies.

2.6.2 Assumptions

The research program in FPO is based on the assumption that all the ITER baseline systems will be fully operational (including H&CD, fuelling, etc.) with all ECRH gyrotrons at a frequency of 170 GHz. Table 2-11 lists the final elements of the baseline diagnostic systems which should be installed to satisfy the essential measurement requirements for the FPO phase. It also shows a range of upgrades which would enhance the studies of burning plasma physics and which could be installed if the necessary funding were available sufficiently in advance of the first FPO campaign. It is furthermore assumed that the T-Plant will start to provide a significant throughput for DT operation (at least 10% concentration for ~50 s) not later than one year after the start of D operation. It would also be of significant benefit to the experimental program if all upgrades identified in PFPO as required for achieving the Q = 10 goal were to be installed before the start of FPO operation.

Regarding plasma scenarios, it is assumed that fully integrated scenarios have been developed for L-mode plasmas up to 15 MA/5.3 T and for H-modes up to 7.5 MA/2.65 T (including ELM control, power load control, etc.), which will require retuning, but not full redevelopment in D/DT. If the latter is not achieved in PFPO due to difficulties in accessing the H-mode regime in H/He plasmas, additional experimental time in D plasmas will be required to determine H-mode access conditions, assess H-mode plasma behaviour at the ITER scale and develop control schemes, as part of the integrated scenarios assumed for D/DT. Similarly, it is assumed that disruption mitigation and avoidance schemes have been developed in PFPO for the same range of scenarios and that retuning, but not full re-development, will be required for D/DT.

As discussed above, it would be desirable that upgrades identified as required to achieve the long-pulse/ steady-state goals were already implemented before the start of FPO (e.g. additional ECRH/ECCD power). Obviously this does not concern the possible upgrade of a 3rd HNB, for which certain measures must already be taken well before the start of FPO, in particular the installation of the captive components, and whose installation, if required, must take place in the last assembly phase (Assembly IV) before the start of FPO (see Appendix G). However, as the first operational period will be focussed towards the achievement of the Q = 10 goal, and this is likely to

take more than the first 2 years, a later implementation of these upgrades (if not delayed by more than ~3 years after the start of FPO) are not likely to severely affect the development of the research program to achieve the Q ~ 5 goal.

Table 2-11 – Overview of <u>additional</u> measurement requirements and <u>additional</u> diagnostic systems installed for the FPO-1 campaign[*]

Measurement Requirement	Installed Diagnostic Systems
14 MeV neutron diagnostics and neutron profile cameras	• Radial Neutron Camera • Vertical Neutron Camera • Neutron Calibration (14 MeV)
Confined- and lost-α diagnostics[**]	• *Collective Thomson Scattering* • *Lost Alpha Monitor*
Additional fusion product diagnostics[**]	• *High Resolution Neutron Spectrometer* • *Tangential Neutron Spectrometer* • *Vertical Gamma Ray Spectrometer* • *Radial Gamma Ray Spectrometer*
PWI/ Heat Load characterization	• Tritium Monitor (fully operational)

[*] *The table illustrates the additional diagnostic systems planned for installation prior to FPO to meet the additional measurement requirements. The installation planned for Assembly Phase IV should essentially complete the Diagnostic baseline specification. However, a variety of upgrade options to extend the baseline measurement capability has been identified for which funding might become available on this timescale – see Appendix H for a discussion of these upgrade options and Section 4 for a summary of the possible benefits to the research program.*

[**] *All diagnostic systems in these categories are currently categorized as unfunded upgrades.*

2.6.3 Operation plan for deuterium plasma experiments

2.6.3.1 Plasma restart in FPO, including H&CD and Diagnostic commissioning

The plasma restart in FPO should establish routine plasma operation in deuterium at 7.5 MA/2.65T after the installation and first commissioning of the tritium plant and completion of the final preparations for DT operation. This is the first time that diagnostics will see significant neutron fluxes; therefore, careful commissioning of the shape and current control, vertical position control, and first wall heat flux management systems must be carried out at the beginning of FPO. The main restart activity for the H&CD systems will be the commissioning of the NB systems for deuterium operation.

Plasma initiation in deuterium will be slightly different from hydrogen and helium operation in the previous phases. Once a robust initiation is found at 2.65 T and 5.3 T, the only further dedicated time to work on plasma initiation that may be required is when the full CS performance is required. The optimized initiation sequence at reduced CS capability may make use of coil current combinations that are not allowed at maximum precharge of the CS due to force or field limits. Optimization of the plasma initiation can be done parasitically during other restart activities.

Recommissioning of the plasma shape, current and vertical position control will follow the procedures developed in the previous phases. The key issue is to look for effects of radiation-induced voltages in the sensors. Precise shape control will be needed for recommissioning of the first wall heat flux protection similar to the protocols developed in the previous phases. The milestone for this element of the restart is robust 7.5MA/2.65 T operation.

Density control will need to be retuned to account for the different transport behaviour of deuterium neutrals and ions from previous experience in hydrogen and helium. Integrated use of the tritium plant for supplying the gas and pellet injectors is necessary. Fuel mix control will have been developed for ICRF and H-mode operation using H/He mixtures in previous phases. This will need to be adapted for DT mix control, plus minority concentration control for ICRF.

The DMS system should be recommissioned using reference pulses from PFPO-2 and any changes to DMS hardware installed during Assembly Phase IV must be commissioned. Operation at 5.3 T will be necessary to demonstrate that runaway mitigation is maintained in deuterium.

The major activity of restart of the H&CD systems will be the commissioning of the HNB systems in deuterium. This will be the first operation at 1 MeV acceleration voltage and in the presence of significant neutron flux. The change in working gas in both the beamline and the plasma will require requalification of the internal protection systems in the beamline and port. The ICRF coupling control will need to be re-optimized for deuterium. There should be no changes required for ECRH operation. All three systems should be recommissioned to at least 50 s operation in order to support the research program. If the systems were commissioned to longer pulse in PFPO-2, it would be good to demonstrate that longer pulse capability again in the restart phase, if time permits.

Once H&CD power in excess of 40 MW is available, the divertor heat flux management system will need to be recommissioned. The controls will need to be re-optimized for the different behaviour of deuterium neutral and ion transport.

New control issues associated with the introduction of significant self-heating such as entry to burn, exit from burn, and robust normal and off-normal termination schemes will be developed within the research phase.

2.6.3.2 Disruption management program in FPO

The disruption program in FPO will focus on monitoring disruption budget consumption and taking corrective actions when needed. This also involves monitoring the performance of the DMS at higher energies and with possibly additional RE seed mechanisms (Tritium decay, Compton scattering). Priorities will be given to reducing disruption rates by appropriate event handling of the PCS (see section 2.5.4.4) and by active MHD control (see section 2.6.3.3). The thermal quench mitigation rate in FPO will be determined by the thermal loads themselves, but also by the need to suppress runaway formation that could potentially follow from strong tungsten influx. The requirements for the current quench mitigation rate will already be identified from the EM load and current quench heat load scaling carried out in PFPO-2 and is expected to be close to 100%. This effective current quench mitigation will be based on the disruption detection that has been established in PFPO-2. Especially because of the thermal energies achieved in FPO, there might be the need to further optimize the mitigation sequence or species composition to achieve higher radiation rates, while keeping radiation peaking and thus heat loads to the first wall (FW) at acceptable values. Note that the impurity quantity is limited by the need to keep eddy current loads on blanket modules in the acceptable range during the current quench and it may not be sufficient for thermal load mitigation at higher thermal energies. This may put further constraints on the required disruption rate. On the other hand, it has been observed in experiments that the energy at the time of the thermal quench is in many cases significantly lower than the maximum energy that was achieved during that pulse. In PFPO-2 high energy thermal quenches are expected mainly for VDEs. In FPO, depending on the plasma scenarios, other disruption types may become relevant that have higher energies at the time of the thermal quench, also demanding higher TQ prediction rates. Improving plasma performance can also introduce new stability limits (e.g. pressure driven

instabilities). This, together with possible changes in diagnostic capabilities will require adapting the disruption prediction schemes to ensure long enough warning times to activate avoidance capabilities or the DMS.

2.6.3.3 Advanced control commissioning in FPO

Advanced control commissioning for the FPO phase will extend the advanced control commissioning from the previous operational phases to high performance operation in D and DT plasmas. It is not yet clear whether there will be new or upgraded actuators in FPO, but there will be new diagnostics for fusion products, and the additional fusion power will enhance plasma performance, requiring significant changes to advanced control schemes, particularly for kinetic control, MHD control, integrated control, and event handling. Neutron and gamma ray emission from fusion reactions may also impact some actuators and measurements so that additional commissioning of advanced control functions that depend on the systems impacted may be required. Note that considerations for disruption-related control in FPO have been already described in section 2.6.3.2. The run-time estimates given here are for commissioning of advanced control schemes, but further development of the physics R&D needed to develop robust control is likely to require significantly more run-time as part of the physics program.

2.6.3.3.1 Plasma kinetic control

The additional load on the first wall due to fusion power in the D and DT phases up to several hundred MW will require significant changes to first wall protection. With longer pulse durations and higher fusion performance, first wall protection will become more challenging, requiring well commissioned robust control schemes. Additional commissioning of first wall protection has been allocated 5 run days in the FPO phase.

Divertor protection with up to 73 MW from all three heating systems and several hundred MW of fusion power will also be significantly more challenging in the FPO phase. At high plasma performance, divertor heat flux control is essential for investment protection requiring well commissioned robust control schemes. Additional commissioning of divertor protection is allocated 5 run days in the FPO phase.

The plasma β and stored energy control will require changes due to the additional fusion power in the FPO phase and it will be coupled to the fusion burn control scheme. Model-based control will require the addition of α-particle heating to the controller model. Additional commissioning of β and stored energy control is allocated 2 run days in the FPO phase.

The temperature and pressure profile control system should be largely commissioned by the start of the FPO period, but the additional fusion power will be concentrated in the plasma core and will dominate the control scheme at high fusion power. It will also be coupled to fusion burn control. Model-based control will require the addition of α-particle heating to the controller model. Additional commissioning of temperature and pressure profile control is allocated 2 run days in the FPO phase.

The rotation profile control system should be nearly fully commissioned by the start of the FPO period. There may be some impact of neutron and gamma ray emission on rotation profile measurements that could require additional commissioning. Alteration of NTV due to possible non-ambipolar loss of α-particles or changes of the uncorrected error field due to the new TBM implementation in the FPO phase may require changes to a model-based control algorithm. Additional commissioning of rotation profile control is allocated 2 run days in the FPO phase.

The current density profile control system should be nearly fully commissioned by the start of the FPO period. There may be some impact of neutron and gamma ray emission on current density profile measurements that could require additional commissioning. Increased plasma performance will affect the central current density and the edge bootstrap current and affect current density profile control. Additional commissioning of current density profile control is allocated 2 run days in the FPO phase.

The FPO phase will finally permit the development of fusion burn control, which will use all H&CD systems and DT fuel mixture control with gas and pellet injection as actuators. Impurity injection may also be used to radiate energy and also control the fusion burn. Indeed, many of the other advanced control schemes will affect the fusion burn, so it will be a strongly coupled system that can only be studied once ITER reaches fusion burn conditions and will require model-based control schemes. The control of the accumulation of helium ash from the fusion burn in the core will also affect burn control, particularly for longer burn durations. Additional commissioning of fusion burn control is allocated 2 run days in the FPO phase, but it will require much more development within the physics program to develop robust long-pulse burn control.

2.6.3.3.2 MHD and error field control

The ELM control schemes commissioned during the previous operational phases should still apply to the FPO phase, though ELM control will be essential at high fusion performance and thus it must be well commissioned and robust before high fusion performance is achieved. No dedicated commissioning time has been allocated to ELM control in the FPO phase, though the development of robust ELM control will be a significant part of the physics program.

NTM control schemes should already be developed to an advanced state by the start of the FPO phase and should remain applicable. The additional plasma performance in this phase will drive large sawteeth and ELMs that provide seed islands for exciting NTMs, particularly at high-β. Before high fusion performance can be achieved, effective, robust NTM control must be commissioned to the extent that it becomes routine. An upgrade of the ITER ECRH system may be needed prior to the FPO phase to ensure effective NTM control. To develop NTM control to full maturity, ITER will have to allow for substantial experimental time within the physics program.

The DEFC and RWM control system should be largely commissioned by the start of the FPO phase. The new TBMs in this phase may change the intrinsic and dynamic error fields of the device that may necessitate further commissioning to ensure that adequate correction is available. Moreover, the use of deuterium and, with the transition to DT operation, the addition of significant α-heating will increase the plasma performance and raise the stored energy closer to plasma β-limits, leading to greater plasma amplification of error fields and potential RWM destabilization. A model-based control system should be upgraded to include the changes to the TBMs.

Sawtooth control should be well developed by the start of the FPO phase. The additional plasma performance and energetic α-particles in this phase will drive large sawteeth and affect their control, which is likely to be essential for maintaining high performance operation. The schemes developed in the PFPO-2 phase should apply to some extent but, because energetic α-particles are likely to affect sawtooth stability, this will require significant changes to the control schemes. The development of high fusion performance will include robust sawtooth control as part of the physics program.

Initial Alfvén Eigenmode control will have been developed during the PFPO-2 phase, but the additional fast α-particles in the FPO phase will change significantly both the drive and damping of

Alfvén Eigenmodes. Significantly more R&D along the lines of [Van Zeeland, 2016] is needed on existing devices to develop Alfvén Eigenmode control for ITER. The large α-particle drive on ITER, however, will probably require significant development of Alfvén Eigenmode control on ITER itself through an extensive physics program.

2.6.3.3.3 Supervisory control

The supervisory control functions of the PCS should be well developed by the start of the FPO phase. The additional plasma performance in this phase will probably lead to more significant plasma events that will require additional commissioning to handle the required control changes and the nuclear heating of some components such as the superconducting magnets will require additional model-based exception handling to avoid exceeding operating limits. At high plasma performance, exception handling becomes particularly critical for investment protection and needs to be well commissioned and robust before high fusion power levels are reached. In particular, the thermohydraulic models for operating the superconducting coils with eddy currents combined with nuclear heating must be optimized to ensure proper event handling with model-based control, particularly to maintain high plasma performance for long pulse operation.

Shared actuator management will be largely developed prior to the FPO phase, but the addition of fusion power and burn control will even more strongly couple all of the advanced control functions that affect plasma performance. Thus the physics program will have to include further development of actuator sharing and model-based control as part of the high fusion performance development program.

2.6.3.3.4 Deliverables for advanced control commissioning in FPO

The deliverables for advanced control commissioning in the FPO phase include:

- Routine operation of first wall and divertor heat flux control with fusion power;
- Implementation of thermohydraulic model-based control of the superconducting coils with eddy current and nuclear heat loads and event handling;
- Establish fusion burn control, β, and stored energy control;
- Commission temperature, pressure, rotation, and current density profile control;
- Reliable ELM control with additional fusion power;
- Sawtooth control with fast α-particles;
- Robust and routine NTM control with additional fusion power;
- Alfvén Eigenmode control with fast α-particles;
- Commission dynamic error field correction and RWM control at high plasma performance.

2.6.3.4 Development of deuterium L-mode operation to 15 MA/5.3 T and first assessment of H-mode access at 2.65 T in D plasmas

2.6.3.4.1 Summary of scenarios and overall objectives

The development of the L-mode scenarios in deuterium mimics the development in hydrogen (section 2.5.5.11) and aims at the same final target of 15 MA/5.3 T L-mode plasmas with ~ 50 s flat-top duration. As in the case of the hydrogen plasmas, the L-mode development will start from 7.5 MA/2.65 T plasmas in deuterium and will progress to 15 MA/5.3 T is steps of I_p/B_t along a q_{95} = 3 - 4 path, with fuelling and power scans being performed at each of the steps. This is expected to require the Plasma Control System (PCS) for density control and heat load control and the disruption management/mitigation and avoidance schemes to be retuned from their specifications

for hydrogen plasmas to adjust to the characteristics of deuterium plasmas. In parallel with this program some elements of the disruption management activities described in section 2.6.3.2 will be implemented. In addition to the program in L-mode within this operational phase, a precise assessment of the power threshold to access the H-mode will be performed in deuterium plasmas at 2.65 T. This will include the determination of the density dependence and possible q_{95} dependences of the H-mode threshold, in particular at q_{95}=3 where some experiments show increased power threshold at high B_t compared to that at q_{95} = 2.7 or 3.3 [Hillesheim, 2016].

The precise determination of the power required to access the H-mode in D plasmas over a range of conditions is planned at this point, in order to perform the final check (in advance of DT operation) that the baseline power level is sufficient to achieve H-mode DT plasmas at 15 MA/5.3T, required for the Q = 10 goal, and if not to proceed with the necessary upgrades. Due to the time required to implement the upgrades, if they are started at this stage, this is likely to lead to a delay of the high I_p/Q DT campaign until the upgrades are functional, as only low I_p/Q DT plasmas will be possible in H-mode. The proposed plan assesses this possible need early in D operations to minimize this delay.

Assuming that significant relevant experience has been gained in the PFPO-2 hydrogen L-mode campaign reaching 15 MA/5.3T, the corresponding activities in D (plus H-mode access) described in this section are estimated to require 32 days of experimental time (plus several additional days for the disruption management program), divided as follows:

- **Development of deuterium L-mode operation to 15 MA/5.3 T (26 days)**
- **L-H transition studies in preparation of H-mode operation in D plasmas (6 days)**

2.6.3.4.2 Requirements

The experimental plan proposed for this phase considers that the following steps have been demonstrated:

- Operation in hydrogen L-mode plasmas up to 15 MA/5.3 T with ~ 50 s successfully demonstrated;
- Disruption avoidance and prediction/mitigation functions have been developed satisfactory and can be applied without major modifications to deuterium plasmas;
- Additional heating systems have been commissioned to full power in D plasmas.

2.6.3.4.3 Risks to the development of deuterium L-mode operation to 15 MA/5.3 T and first assessment of H-mode access at 2.65 T in D plasmas

The main specific risks for this phase are:

- For the L-mode development itself, the main risks are those identified for hydrogen plasmas, which are related to the use of off-axis ECRH heating for breakdown assist and W control in the intermediate fields between 2.65 and 5.3 T.
- For the H-mode access experiments the main risk is that no mitigation scheme is available to avoid long ELM-free periods and large ELMs after the L-H transition in D plasmas. At I_p = 7.5 MA this could lead to melting of the W divertor monoblock edges and should be avoided. These schemes will have been developed already in H plasmas but their application to D plasmas may not be straightforward due to the different pedestal parameters after the L-H transition for D than for H plasmas. The mitigation strategy for this risk would be to first assess L-H access at 5 MA/2.65 T and develop the mitigation schemes in these

conditions, which avoid W divertor melting, and then increase plasma current. The drawback is that q_{95} varies from 4.5 to 3.0 in this approach. A similar strategy at constant q_{95} would be possible by starting at 5 MA/1.8 T but this requires pure ohmic breakdown (without ECRH) to be effective at 1.8 T, as the gyrotron frequency will be 170 GHz by this operational phase. Either mitigation strategy is likely to require additional operational time.

2.6.3.4.4 Detailed experimental plan for the development of deuterium L-mode operation to 15 MA/5.3 T and first assessment of H-mode access at 2.65 T in D plasmas (32 days)

2.6.3.4.4.1 Detailed experimental plan for the development of deuterium L-mode operation to 15 MA/5.3 T (26 days)

This L-mode operational phase follows the same development of the hydrogen plasmas and is expected to require 26 days. The deuterium plasma development follows the same I_p/B_t steps already shown in Figure 2.5-10 and includes scenario #5 to reduce the I_p/B_t step. Table 2-12 describes the scenarios to be explored in this phase; compared to hydrogen plasmas there is significant additional flexibility for heating of deuterium plasmas because the lower density for unrestricted NBI use with tolerable shine-through loads is much smaller (~ 2.5×10^{19} m^{-3} in D versus ~ 4.5×10^{19} m^{-3} in H) and because for low fields (3.3 T) a viable scheme for ICRF heating exists (H-minority). This is expected to make less critical the issue of off-axis ECRH heating for W control in D plasmas, as more heating mix possibilities exist. Otherwise, the experimental plan is similar to that for H plasmas (section 2.5.5.11) consisting of fuelling scans, power and power mix scans, etc., in the flat-top and ramp-up/down with specific experiments to assess core transport and confinement properties of D L-mode plasmas. Similarly, there will be experiments to optimize flux consumption for these scenarios and to control divertor power loads as well as W production and W accumulation control in the main plasma; this may be already necessary at high additional heating levels (see Appendix C).

Table 2-12 – Path to 15 MA/5.3 T (in deuterium)

#	I_p/B_t	Available heating		
		P_{ECRH} (MW)	P_{ICRF} (MW)	P_{HNB} (MW)
2	7.5 MA/2.65 T	20	20	33
3	9.5 MA/3.3 T	20	20	33
4	9.5 MA/4.5 T	20	20	33
5	10.5 MA/4.5 T	20	20	33
6	12.5 MA/4.5 T	20	20	33
7	12.5 MA/5.3 T	20	20	33
8	15 MA/5.3 T	20	20	33

2.6.3.4.4.2 L-H transition studies in preparation of H-mode operation in D plasmas (6 days)

To prepare for H-mode operation an assessment of the L-H threshold in D plasmas will be performed, which is expected to require 6 operational days. This includes the scaling of the H-mode threshold with density and heating mix at 2.65 T and an assessment of the q_{95} dependence at q_{95} ~ 3, as some experiments show increase H-mode power threshold at this precise value, which is the reference value for Q = 10 operation in ITER. An initial assessment of H-mode access at q_{95} ~ 5, which is a typical value for steady-state Q = 5 operation in ITER, will also be performed. The

H-mode access assessment at q_{95} ~ 3 will be carried out around scenario #2 in Table 2-12 by varying the plasma current by up to ±10%. The outline of the foreseen experimental conditions covering the ranges to be explored is summarized in Table 2-13.

As already discussed above the main technical issues of these experiments are:

- to achieve the required level of ELM control to avoid long-ELM free periods that can cause edge melting of the divertor W monoblocks and W accumulation in the main plasma. For this purpose, ELM control by in-vessel coils as well as by the back-up ELM triggering schemes (pellet triggering and vertical position oscillation) will be applied following the operational experience in H/He plasmas in PFPO-1 and PFPO-2.

Table 2-13 – L-H transition scenarios (in deuterium)

I_P FT (MA)	B_t (T)	Density (f_{GW} %)	Heating mix	q_{95}	
7.5	2.65	40	NBI+ICRF+ECRH	3	Density scan
7.5	2.65	80	NBI+ICRF+ECRH	3	
7.5	2.65	40	NBI	3	Heating mix scan
7.5	2.65	40	ECRH+ICRF	3	
7.5-10%	2.65	40	NBI+ICRF+ECRH	3+10%	q_{95} scan
7.5+10%	2.65	40	NBI+ICRF+ECRH	3-10%	
7.5-10%	2.65	80	NBI+ICRF+ECRH	3+10%	
7.5+10%	2.65	80	NBI+ICRF+ECRH	3-10%	
4.5	2.65	40	NBI+ICRF+ECRH	5	H-mode access in q_{95} of steady state scenario density scan
4.5	2.65	80	NBI+ICRF+ECRH	5	

2.6.3.4.5 Diagnostic adequacy for D plasma L-mode scenario studies in FPO

By this stage of the operational program all ITER diagnostics should be available for operation, including those related to neutron and fast particle measurements. Assuming that no issues appear related to the functioning of diagnostics until this phase, it is expected that the available diagnostic set will provide all the measurements required to develop these L-mode scenarios and to characterize the plasmas obtained in this phase.

2.6.3.4.6 Deliverables for the development of deuterium L-mode operation to 15 MA/5.3 T and first assessment of H-mode access at 2.65 T in D

The main deliverables of this operational phase are:

- Demonstration of first L-mode operation in D plasmas at full current and field (15 MA/5.3 T) with ~ 50 s flat-top full integrated plasma scenarios including plasma position and vertical stability control, power load control, W accumulation control, etc.
- Demonstration of the intermediate I_p/B_t steps to be followed to achieve 15 MA/5.3 T L-mode D plasmas along a q_{95} = 3 - 4 path, which will form the basis of the follow-up development of the H-mode scenarios in DD and DT;

- Assessment of the effects of gas fuelling and pellet fuelling and additional heating power level and mix on plasma transport and confinement in ITER L-mode D scenarios up to 15 MA/5.3 T including ramp-up/down phases;
- Optimization of flux consumption in D L-mode ramp-up/down phases by using the ITER systems' flexibly, in particular, regarding the current ramp rate, and for plasma fuelling and heating in these phases;
- Assessment of the power required to access the H-mode in 2.65 T D plasmas for a range of densities and $q_{95} = 3 – 5$, with specific detail on the possible q_{95} dependence at $q_{95} \sim 3$.

2.6.3.5 Development of deuterium H-mode plasmas towards full performance

2.6.3.5.1 Scenarios and overall objectives

The main aim of this first phase of H-mode development in deuterium will be to build a complete H-mode scenario at half current/half field, which is foreseen to require 40 operational days. This will have to be reliable, robust to disruptions, MHD stable with controlled ELMs, and will be used as basis to learn how to use and optimize the additional heating schemes, the tools for ELM control, NTM stabilization, fuelling and divertor heat load control for H-mode plasmas in ITER. Depending on the availability of tritium the operational range of H-mode plasma will be expanded towards higher current and fields in pure deuterium or this expansion will already take place with dominantly deuterium plasmas but with some level of tritium beyond the trace level.

Taking into account the time foreseen to:

a) commission the various systems in deuterium plasmas;

b) develop the associated L-mode and H-mode access program required before stationary D H-modes can be studied, and;

c) commission the Tritium Plant;

the present plan considers that the expansion of the H-mode operational space in FPO beyond 7.5 MA/2.65 T will be performed in D-dominant plasmas (with T content in the several % level) and not in pure D plasmas in order to optimize operational time, as described in sections 2.6.4.2 and 2.6.4.3. If the Tritium Plant were not available, part of this H-mode operational range expansion would be performed in this phase with pure D plasmas and could require a significant increase of the operational time allocated depending on the current/ field reached before the Tritium Plant is available (up to factors of ~3 - 4).

The main part of the H-mode studies in the first campaign of FPO phase will be carried out in D plasmas at 7.5 MA/2.65 T, $q_{95} = 3$ and will explore the requirements for ELM control with in-vessel coils building on the findings of PFPO-2. In order to minimize the risk of melting of the divertor monoblock edges by uncontrolled ELMs in these experiments an option considered is to perform the initial D H-mode characterization and ELM control studies with 5 MA/1.8 T plasmas, where the risk to divertor melting by uncontrolled ELMs is very low (see Appendix C). This option has the advantage to provide an H-mode development path at $q_{95} = 3$ and thus self-similar MHD stability to 7.5 MA/2.65 T plasmas. However, requires the previous demonstration of unassisted breakdown at 1.8 T, as the ECRH gyrotrons will operate only at 170 GHz following the start of FPO. An alternative approach to reach 7.5 MA/2.65 T H-mode plasmas while avoiding the risks of divertor melting due to uncontrolled ELMs is to start at 5.0 MA/2.65 T and increase the plasma current successively; the disadvantages of this approach is that q_{95} varies from 4.5 to 3 as the current is

increased towards 7.5 MA and thus different MHD stability has to be taken into account when developing the scenarios. It should be noted that the restrictions to operation of 5 MA H-modes in DD in terms of the application of NBI heating are much less serious than in PFPO-2 due to the lower shine-through loads; unrestricted application of NBI only requires plasma densities above 2.5×10^{19} m^{-3}, as shown in Figure 2.6-1. This density value corresponds to ~ $0.6\times n_{GW}$ for 5 MA plasmas in ITER, which has been shown to be achievable in L-mode with gas and pellet fuelling [Militello-Asp, 2016]. The lower restrictions regarding the application of NBI, together with the expected H-mode threshold of 14-19 MW (for 1.8 T and 2.65 T respectively) at the shine-through (minimum) density limit of $2.5\times10^{19}m^{-3}$ for D plasmas, is expected to considerably simplify the issues related to the access and sustainment of H-modes at this level of plasma current, which should have been extensively studied in PFPO-2.

Similarly, if L-H threshold studies in D plasmas (see section 2.6.3.4) show that small deviations from q_{95} = 3 are required to optimize H-mode access, this will affect the exact value of the plasma current at which H-mode access is performed for the 2.65 T experiments and whether this plasma current value is kept for the rest of the discharge or later increased to 7.5 MA. Depending on the possible deviation from q_{95} = 3 required to optimize H-mode access and sustainment, possible consequences for achieving ITER project targets at 5.3 T will, then, have to be fully assessed by comprehensive modelling, benchmarked on the ~7.5 MA/2.65 T performance.

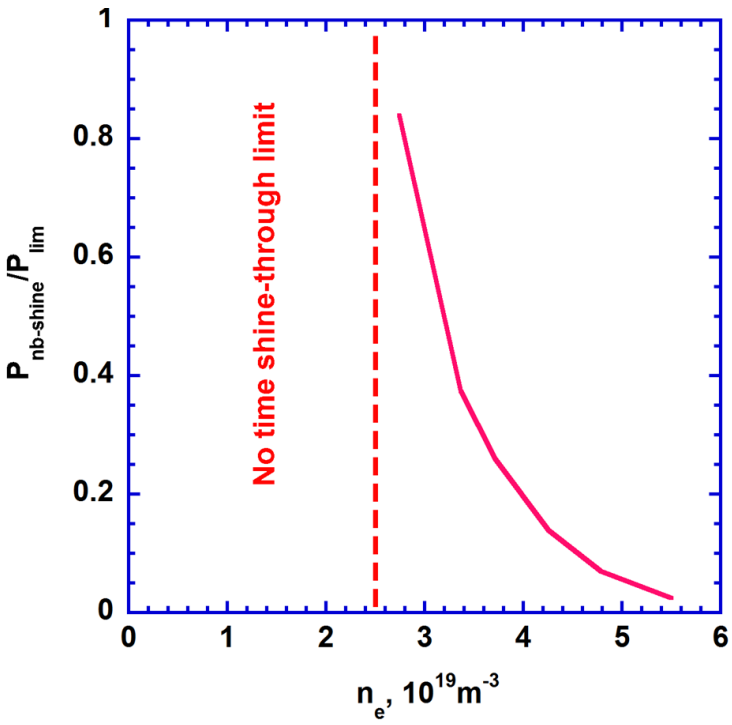

Figure 2.6-1: Normalized NBI shine-through loads (to the value required for unlimited application of 33 MW of NBI power) for 1 MeV D beams in D plasmas versus plasma density.

2.6.3.5.2 Risk to the success of the D H-mode studies in FPO

Most of the risks related to H-mode operation in D plasmas in FPO are linked to the same general H-mode access/sustainment and ELM control issues previously discussed in PFPO-2 in section 2.5.5.7, namely: H-mode access, sustainment and confinement achievable versus P_{inp}/P_{L-H}, conflicting requirements for stationary and ELM power load control, W control and development of

ELM control schemes and the avoidance of melting of plasma-facing components. At this point of the Research Plan it will be known if these risks have materialized or not and whether the mitigation strategies proposed for PFPO-2 are effective or not. In addition to these risks there are a few additional ones that are specifically related to deuterium operation:

- *1.8 T plasma breakdown is not possible without ECRH assist.* In this case 5 MA/1.8 T operation would not be possible and, thus, a q_{95} = 3 H-mode D plasma with low risk of divertor edge monoblock melting would not be available. The mitigation strategy would be based on two approaches whose suitability depends on the findings during PFPO-2. One possible approach would be to consider 5 MA/2.65 T plasmas to characterize the H-mode and then to develop the ELM control strategies with in-vessel coils at q_{95} = 4.5. Increasing the plasma current from 5 MA to 7.5 MA would then involve a decrease in q_{95} towards 3.0 and will require the tuning of the magnetic field perturbation for each step in q_{95} to ensure that ELMs are appropriately controlled to avoid edge monoblock melting, as plasma current is increased. The other possible approach would be to start the H-mode experiments already at 7.5 MA/2.65 T and make use of the back-up ELM triggering schemes (vertical plasma oscillations and pellet pacing) to provide ELM control. The possible risk of edge monoblock melting at 7.5 MA/2.65 T will already have been assessed for H-mode plasmas in PFPO-2, as well as the efficiency of the back-up ELM triggering schemes to provide ELM control. The operational experience gained in PFPO-2 will thus determine which the lower risk approach (for divertor melting avoidance) and fastest approach is to achieve 7.5 MA/2.65 T H-modes in D plasmas in FPO.

- *Power threshold and/or the P_{inp}/P_{L-H} to achieve high confinement are higher than expected for D plasmas.* The D H-mode FPO operational plan is based on the assumption that the experiments in H and He will provide a more precise evaluation of the power requirements to access and sustain H-mode D plasmas in ITER. The extrapolation from the power requirements in H and He to D in ITER will be done on the basis of the understanding developed in experiments in other tokamak experiments but final confirmation will only be available at the beginning of FPO. Given the expected H-mode threshold values for 7.5 MA/2.65 T plasmas, which is in the range of 19-35 MW for $\langle n_e \rangle = 0.4 - 1.0 \times n_{GW}$, and the available heating power of 73 MW, only substantial underestimates of the power required to access and/or sustain high quality D H-modes on the basis of PFPO-2 results are likely to put at risk the Research Plan in this phase up to 7.5 MA/2.65 T. If the power required to access and/or sustain high quality D H-modes is significantly higher than expected, this would imply that 7.5 MA/2.65 T D H-mode plasma operation would necessarily be performed at high levels of input power. This would require a high level of availability of the ITER H&CD systems and the early development and retuning of the control schemes for stationary power load control developed in PFPO-2 already from the start of H-mode operation in FPO. The implications of these issues, however, are more important for later phases of FPO when higher I_p/B_t will be explored and higher P_{inp} will be required. If this risk would materialize at the beginning of FPO an upgrade of the H&CD capabilities would be required to proceed with a significant part of the remaining of the FPO program, as the baseline capability of 73 MW would not be sufficient to achieve the Q = 10 goal in ITER. The results of H-mode operation in D plasmas at 7.5 MA/2.65 T would thus provide guidance regarding the most appropriate upgrades of the baseline H&CD systems to be implemented in order to ensure the achievement of ITER Q = 10 goals. It should be noted that, as discussed in Appendix G, depending on the upgrade path required this may imply an

extension of the D and/or the low-Q DT phase, as the Q = 10 operational phase would not start until these upgrades have been implemented.

- *Core-edge integration schemes (ELM control, stationary power load control, W control) developed in PFPO-2 are not applicable for D plasmas*. The higher pedestal pressure, higher confinement/higher β H-mode plasmas achievable in D are expected to lead to changes of the effects of fields applied by the ELM control coils on the plasma, as well as on W production, transport and exhaust due to changes in plasma response, higher sputtering yields during ELMs, differences in anomalous and neoclassical transport between H/He and D, etc. The FPO operational plan assumes that the core-edge integration schemes developed for H/He plasmas in PFPO-2 will require retuning for D plasmas to account for these changes but not a complete redevelopment. If this proves not to be true, a significant additional operational time would be required in this phase to redevelop viable core-edge integration schemes in 7.5 MA/2.65 T D H-mode plasmas before proceeding to higher plasma current H-modes in D and DT.

2.6.3.5.3 Details of experimental plan for D plasma H-mode scenarios in FPO (40 days)

The development of the initial deuterium H-mode scenario will, in many respects be parallel to that of the non-active H-mode development discussed in section 2.5.5.7. Due to the differences in the recycling and atomic properties of deuterium and hydrogen/helium and the expected consequences for the pedestal plasma, ELM dynamics and overall H-mode confinement, the phenomenology of H-mode plasmas in deuterium is expected to be quantitatively (and, possibly, qualitatively in some aspects) to that of hydrogen/helium plasmas.

The experiments will start with 5 MA plasmas and then progressively increase current towards 7.5 MA in steps of 0.5-1.0 MA preferably following a ~ constant q_{95} approach or, if not possible, a constant B_t = 2.65 T approach, as discussed above. In each step, as far as ELM divertor power loads allow without edge monoblock melting, uncontrolled Type ELMy H-mode characterization will be performed similar to that foreseen in PFPO-2 for heating pulses of similar duration (~ 50 s) and then the ELM control strategies with RMP fields, W impurity exhaust and those for the control of stationary power loads with impurity seeding developed in PFPO-2 will be retuned to D plasmas.

The experimental time required for this program is 40 days. It builds-up on the experience gained in PFPO-2 and will include scans in power levels above the L-H transition, variations in power mixes, gas versus pellet fuelling comparisons, to determine effects on H-mode confinement, pedestal and SOL plasma characteristics, etc., as detailed in PFPO-2. This experimental period will conclude with an integrated demonstration of a 7.5 MA/2.65 T D H-mode plasma scenario which fulfils all requirements necessary to achieve Q = 10 operation regarding core confinement and core-edge integration issues such as W impurity exhaust and controlled stationary and ELM transient power loads to PFCs.

Operation in D H-mode plasmas raises issues that require specific experimental focus or different/additional experiments beyond those detailed for the corresponding phase of PFPO-2. These include:

- *Development of optimized additional heating strategies to maximize plasma confinement while maintaining global MHD plasma stability*. The different behaviour of D plasmas versus H/He plasmas is expected to lead to higher plasma energy/β and thus to different plasma response to error fields. It is, therefore, foreseen that dedicated experiments will be required to retune the correction of error fields with the external error field correction coils

and to optimize the power mix as plasma β increases. At this point it will also be explored whether dynamic error field correction by the in-vessel coils is required to optimize H-mode performance in ITER, given the fact that at these current levels there should be margin in the ELM control coil system to provide both ELM control and error field correction functionality (i.e. the current level expected for ELM control is ≤ 45 kAt for a maximum coil current capability of 90 kAt). Similarly specific tests and optimization of vertical stability control in the presence of ELMs, with abrupt l_i and β_p changes, will be included in this phase as well of the control of NTMs by ECRH/ECCD. In parallel with these developments the DMS will be retuned to provide the required disruption mitigation as the plasma energy increases.

The additional heating optimization will include assessment of specific issues related to the use heating systems in D plasmas such as:

a) control of the H minority concentration to provide reliable ICRF heating at 2.65 T, which will have been demonstrated in He plasmas in PFPO-2 and thus with a very different recycling and pumping behaviour;

b) demonstration and optimization of ICRF coupling in the varying edge plasma conditions expected in D H-mode plasma scenarios;

c) re-assessment of the NBI shine-through loads with deuterium NBI in deuterium H-mode plasmas;

d) optimization of the sharing of ECRH/ECCD power between equatorial launcher and upper launcher to provide both W core transport control (W accumulation avoidance) and NTM control, etc.

In particular, if 5 MA/1.8 T plasmas are chosen as the first step of the D H-mode program, specific studies will be required given the expected difficulties to heat these plasmas with ICRF (second harmonic minority hydrogen would be required) and also with ECRH (third harmonic heating of ohmic plasmas may not be effective). Specific strategies to increase the plasma temperature with NBI alone in L-mode plasmas and to access the H-mode will have to be employed that could be similar to those already applied in the PFPO-2 phase (i.e. a reduction of the NBI energy and input power) or more advanced (i.e. reduction in the time-averaged NBI power by cyclic changes of the injected power). The former would allow the injection of NBI with tolerable shine-through loads at the levels of plasma density which are expected to be achievable at this current level in ohmic/low power L-mode plasmas ($1.0 - 1.6\times10^{19}$ m^{-3}) [Romanelli, 2015; Militello-Asp, 2016]. However, the corresponding reduction of the NBI power is significant (a factor of ~ 2) and thus reduces the NBI power to values close to the expected H-mode power threshold at 5 MA/1.8T (10 MW at $\langle n_e \rangle = 1.6\times10^{19}$ $m^{-3} = 0.4\times n_{GW}$). In this case, robust H-mode operation will require ECRH heating together with the NBI, which should be effective with third harmonic heating in these NBI preheated L-mode/marginal H-mode plasmas. The second NBI power-reduction strategy for H-mode access would allow (through the time variation of the NBI power) to build up the plasma density in L-mode to the level in which unrestricted NBI operation is possible [Militello-Asp, 2016], thus enabling studies of NBI-alone and NBI + ECRH heating of 5 MA/1.8 T D H-modes to be performed.

- *Studies of plasma fuelling in the stationary H-mode phase and of H-mode access and exit phases with pellets and gas fuelling and of the density evolution during confinement and pellet transients.* These studies are key to validating predictions of the fuelling efficiency of

gas fuelling and recycled neutrals in ITER D and DT plasmas, which is expected to be very low, to optimize H-mode access and exit through the control of the plasma density in these phases as well as to optimize pellet fuelling. Some initial experimental evidence on these issues is expected from PFPO-2 in hydrogen (gas and pellet fuelling) and helium (gas fuelling alone) H-mode plasmas. However, dedicated experiments in deuterium are essential to provide a quantitative assessment of the above issues with a view to DT operation, due to differences in edge and pedestal plasmas that affect edge ionization and transport, as well as in core transport, between H/He and D plasmas. In addition, the restricted operational space for H-mode plasmas in hydrogen is likely to restrict the H-mode experiments in PFPO-2 and it is possible that no significant experimental assessment of these issues can be made in hydrogen H-mode plasmas during PFPO-2. The experiments will explore the range of stationary H-mode operational conditions and the degree of control of the plasma density in the H-mode access and exit phases that can be obtained with gas fuelling, pellet fuelling and the combination of both for a range of currents 5.0 - 7.5 MA, P_{inp}/P_{L-H}, pellet specifications (size, frequency and injection velocity) and pumping throughput (controlled through shot-to-shot variations of the cryopumps' opening valves). These experiments will perform a full exploration of the effects of various fuelling and pumping choices on ITER H-mode plasma scenarios, thus providing essential data to assess the accuracy of the particle transport physics models and to develop the best H-mode fuelling strategies for access and exit from burn required for the development of the DT research program.

- *Exploration of the different scenario options for entrance and exit to high confinement H-modes, including H-mode entrance in the ramp-up phase and exit in the ramp-down phase, and phasing of the pellet fuelling ramp-up/down versus the heating ramp-up/down.* These experiments will build up on the initial experience in PFPO-2 and will expand these results to relevant conditions with a view to their application to DT plasmas. The experiments will be carried out in plasmas with a flat-top current of 7.5MA and their main aim is to determine:

  a) the evolution of plasma parameters (including l_i and core W concentration) in these H-mode access/exit transient phases, and;

  b) to which level these can be controlled by the heating and fuelling waveforms.

  This is essential to start the development of the higher I_p scenarios in DT where the margin to the H-mode threshold is lower and optimization of α-heating is required to have robust access and exit schemes to burning plasma conditions that avoid fast back transitions to L-mode and W accumulation [Loarte 2016-2] because, in the higher I_p scenarios in DT, the fine details of access to and exit from burning H-mode plasmas depend on the evolution of plasma parameters in the core and pedestal in these transient phases (e.g. pedestal plasma formation for low edge grad-n conditions expected with gas fuelling). The knowledge of ELM control during these transient phases acquired during PFPO-2 will be applied and retuned to D plasmas. The final goal of these experiments will be the demonstration of the optimum scheme to provide ELM control with RMP fields throughout the H-mode access and exit phases up to stationary conditions, both when these access/exit phases take place at the flat-top current of 7.5 MA as well as during the current ramp-up/down from 5.0 - 7.5 MA in which q_{95} varies within 3.0 - 4.5. The ELM triggering back-up schemes (vertical plasma oscillations and pellet triggering) will be applied during the transient phases to ensure that ELM control is maintained following the guidance of the PFPO-2 results.

- Specific experiments to demonstrate full edge-core integrated scenario at 7.5 MA/2.65 T with the required performance for the achievement of Q = 10 in 15 MA/5.3 T plasmas. These experiments will put together the knowledge acquired in this phase regarding the control of ELM transient loads with 3-D fields, W impurity exhaust and stationary divertor exhaust by impurity seeding in stationary H-mode conditions and H-mode access/exit phases and will integrate them to demonstrate a robust H-mode scenario that meets the requirements for Q = 10 operation scaled to 7.5 MA/2.65 T. While this will have been preliminarily explored in PFPO-2, it is likely that this exploration will have been done only for He H-mode plasmas (given the low margin for hydrogen H-mode operation) and, even if in hydrogen, at relatively low β. Due to the significant changes expected in the SOL, pedestal and core plasma when operating in deuterium, and the consequences for edge-core integration issues (ELM control by 3-D fields depends strongly on plasma response, pedestal W transport and λ_q are expected to depend on neoclassical-related effects, etc.), it is expected that significant differences will result in the optimization of the various schemes and strategies for D compared to those applied in PFPO-2. In particular, operation in D allows an appropriate assessment of the effect that the margin above the L-H transition and β have on the overall optimization of the scenarios and the achievable H-mode confinement providing core-edge integration in ITER as, for D plasmas in these conditions, the ratio of the input power to the L-H transition threshold power can be varied over a wide range $P_{inp}/P_{LH} = 1.0 – 4.0$ for $\langle n_e \rangle = 0.4 - 1.0 \times n_{GW}$.

2.6.3.5.4 Diagnostic adequacy for D plasma H-mode scenario studies in FPO

By this stage of the operational program all ITER diagnostics should be available for operation, including those related to neutron and fast particle measurements. Assuming that no issues appear related to the functioning of diagnostics until this phase, it is expected that the available diagnostic set will provide all the measurements required to develop these H-mode scenarios and to characterize the plasmas obtained in this phase.

2.6.3.5.5 Deliverables for D plasma H-mode scenario studies in FPO

The main deliverables for this phase are:

- Robust 7.5 MA/2.65 T, $H_{98} = 1$ deuterium H-mode scenario with integrated fuelling, NTM and W accumulation control, error field correction, ELM control with 3-D fields from in-vessel coils to provide acceptable transient power loads and impurity exhaust, stationary power load control through radiative divertor and with low disruptivity and efficient DMS when disruptions occur. This provides the basis for predictive modelling and for the operational development of the 15 MA/5.3 T DT H-mode scenario to be demonstrated in FPO.
- Evaluation of the power level and power mix required to access and sustain high confinement H-modes in deuterium plasmas. This will provide a high confidence estimate of what would be required for DT plasmas. If the baseline additional heating level is found to be insufficient for successful Q = 10 operation at this late stage, upgrades of the ECRH and/or ICRF systems could be implemented to ensure the achievement of the Q = 10 goal, although the high-Q DT research would need to be delayed until such upgrades are fully functional.
- First evaluation of key plasma behaviour in deuterium H-modes required for the optimization of plasma scenarios in D and DT plasmas including the degree of control of

pedestal and core plasma density, temperature and l_i by tuning of the heating and fuelling schemes and waveforms in the transient H-mode access/exit phases and in the stationary ELM-controlled H-modes.

- Confirmation of the ELM control capability that can be expected from ELM control coils in relevant deuterium plasmas during transient H-mode access/exit and stationary phases over a current range of 5.0 MA – 7.5 MA allowing a high confidence evaluation of these capabilities for later high I_p operation in D and DT. If these are found to be insufficient or marginal, an upgrade of the back-up ELM triggering scheme based on pellet pacing will be implemented at this stage (e.g. addition of two pellet injectors specially designed for pellet pacing).

In parallel with the deuterium H-mode scenario development, hydrogenic retention studies, diagnostic validation and investigations of intrinsic and extrinsic impurity behaviour, etc., will be performed.

2.6.3.5.6 Progress towards full machine parameters in D H-modes

The main goal of this phase would be to demonstrate a reliable ELMy H-mode scenario at parameters as close as possible to 15 MA/5.3 T with the required performance extrapolable to DT operation. Based on the considerations above, it is planned to perform this study with plasmas containing some level of tritium, as discussed in detail in section 2.6.4.1 and these are not included in the pure deuterium experimental plan in this section. Here we give a short description of the proposed Research Plan if delays in the commissioning of the Tritium Plant would lead to these studies to be done in pure D plasmas.

From the full integrated demonstration at 7.5 MA/2.65 T, the range of plasma currents and fields would be expanded towards 15MA/5.3T along an approximately constant $q_{95} \sim 3$ line, similar to the L-mode development plan (I_p = 9.5, 12.5 and 15 MA) in Figure 2.5-10. The precise value of current and fields to be used in the intermediate steps will be the subject of studies during the development, as they are expected to be determined by the need of central heating by ECRH and ICRF to avoid W accumulation and the need of off-axis ECRH/ECCD to control NTMs, etc. Given the expected H-mode threshold in deuterium plasmas and the available maximum additional heating of 73 MW, it is likely that the maximum plasma current/field where stationary H-mode operation can be sustained in D is ~ 12.5 MA/4.5 T, as shown in Figure 2.6-2 Operation at higher plasma currents and in marginal H-modes is considered to be risky due to possible difficulties in controlling plasma behaviour in marginal H-mode conditions and the high risk of high I_p disruptions that this entails.

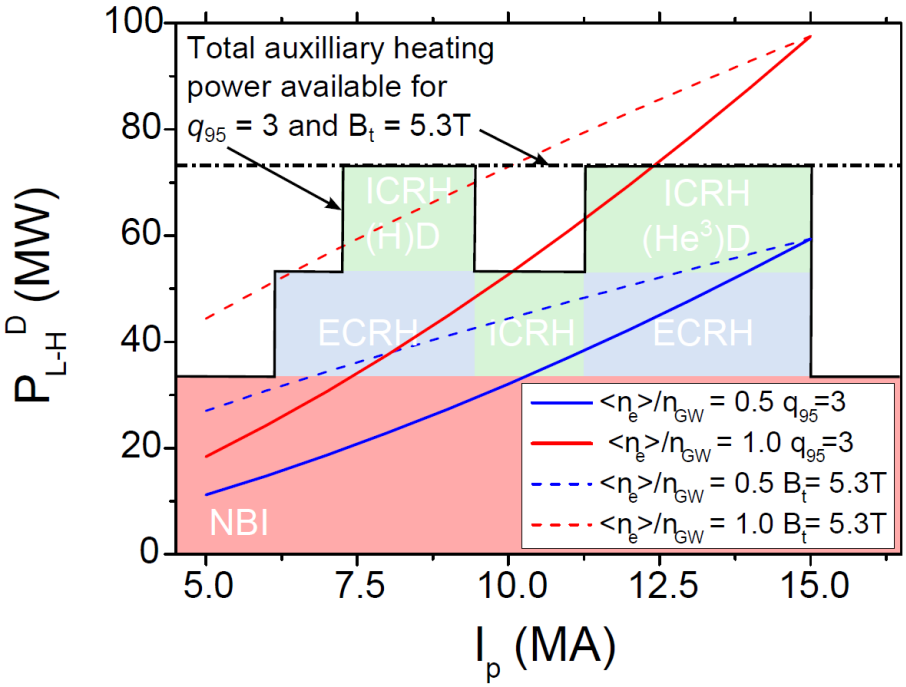

Figure 2.6-2: Dependence of the L-to-H power threshold, P_{L-H}, in deuterium plasmas versus current, I_p. The available heating power with central deposition profiles (ρ < 0.5) for operation at q_{95} = 3 and B_t = 5.3 T is also shown.

For each current level a similar set of experiments to those at 7.5 MA/2.65 T is foreseen. This phase would conclude with a demonstration of an integrated H-mode scenario at each current level. The total number of days foreseen for these studies would be 120 days but this is not included in the plans for pure deuterium operation described earlier (the experiments are planned to be done already containing tritium). This time takes into account the more complex development of scenarios as the plasma current increases. This is due to the increasing deleterious effects of disruptions and the need to tune the ECRH and ICRF systems to provide both central W accumulation control and NTM control as the toroidal field varies with increasing plasma current, because the deposition profiles for ECRH and ICRF are dependent on this.

2.6.3.6 Edge physics (including heat loads) and PWI studies in D plasmas

2.6.3.6.1 Wall conditioning

During the FPO phase, only D-ICWC is of relevance, either at half or full field with f/B_t = 7.0 – 10.5 MHz/T, depending on the IC frequency. As in the PFPO phases, the efficiency of D-ICWC for the removal of medium Z impurities can be further evaluated in FPO whenever cleaning discharges are required for programmatic or operational needs. Dedicated trace-T removal experiments using isotopic exchange with D-ICWC can be also executed in the D phase of FPO (analogous to possible H, D trials in PFPO-2 – section 2.5.5.12.1). Gas balance will be performed, as before using torus pressure measurements, RGAs and analysis by gas chromatography of the gas released from the partial cryopump regeneration (to ~100 K). Once experience gained on the operational parameters to be used (pressure, power, duty cycle and poloidal fields), D-ICWC can be applied to effectively control the T-inventory build-up in the vacuum vessel, expected to be due principally to Be co-deposition in the divertor.

Extrapolations from current devices, in particular the JET-ILW, show that isotopic exchange in D-ICWC discharges could remove an amount of T comparable to that of the estimated retention per nominal DT pulse [Brezinsek, 2013-1; Shimada, 2011] (section 2.2.8). However, this may only hold if these discharges are regularly operated before too thick T-rich co-deposits accumulate. Only in this case will ICWC be able to contribute to mitigation of the T inventory build-up (the so-called 'good housekeeping approach' [Counsell, 2006]).

2.6.3.6.2 Fuel retention and material migration

By the time pure deuterium operations begin, fuel retention measurements by gas balance will be well established and operations with pure D will increase the measurement accuracy, allowing estimates obtained during PFPO phases to be further refined. In particular, characterization of D retention during H-mode operations at high power with ELM control and a radiative divertor will expand the existing database. The higher mass of deuterium will lead to an increase of the Be sputtering from the first wall both in-between and during ELMs. It is therefore important to monitor material migration regularly. This can be done parasitically during operations through visible spectroscopy and regular operations of the tritium and erosion monitors. In addition, regular execution of the reference pulse (Appendix D) will allow for routine monitoring of impurity sources.

Most of the fuel retention characterization will not require dedicated machine time and will be performed in parallel with the main scientific program. It will be beneficial, however, to perform a dedicated fuel removal experiment before the start of trace-T experiments. This will consist in D-removal by hydrogen ICWC followed by a full bake of the PFCs. Since co-deposits will have accumulated during this phase, benchmarking of the fuel removal simulations can be performed with thicker deposits, allowing validation of the knowledge gained during the PFPO phases.

A similar strategy will be pursued during trace-T experiments where T removal using isotopic exchange with D can now be developed and validated. An important additional aim of this campaign will be to develop/validate the T accounting strategy which relies on measurements performed in the Tritium Plant for global accounting (including decay), with gas balance measurements to determine in-vessel retention and neutron measurements for determination of the burn-up fraction. Performing another fuel removal exercise before the start of DT operations is also important to validate earlier measurements. It is particularly important in serving to determine the frequency at which these techniques will need to be employed during DT operations to ensure that the in-vessel T-inventory remains below regulatory limits.

2.6.3.6.3 Heat loads and detachment control

With the exception of lower power operation at very low density/divertor neutral pressure, (likely to be associated with issues of W control), or improper control of plasma position/shape etc., it is only in the FPO phases that stationary first wall and divertor target heat loads can attain engineering limits. By the time FPO begins, power load monitoring and control should have reached a level of maturity allowing the progressive increase of input power and current in H-mode which will be made possible by the switch to deuterium. Progression beyond H-modes at half current and high input power will in fact not be possible until feedback schemes and robust divertor heat load control have been fully optimized and shown to be robust and reliable.

High input power ($P_{SOL} \gtrsim 40$ MW) deuterium H-mode operation without extrinsic seeding at 7.5 MA/2.65 T ($q_{95} = 3$) is expected to produce power flux densities in the strike point regions close to steady state power handling limits, and considerably above them at low neutral pressure

(Appendix C). Such operation will thus require active detachment control and can be performed at densities high enough for meaningful application of extrinsic seeding. It is also the point at which unmitigated ELM energy densities are expected to produce clear W divertor monoblock toroidal gap edge melting and potential problems with ELM driven W impurity influxes, requiring that ELM mitigation or suppression be fully developed.

With the progressive increase of plasma current in H-mode which will be possible in FPO, the database of inter-ELM power $\lambda_{q,near}$ can be expanded beyond the lower power H-modes accessible in the PFPO phases, permitting the evaluation of the extent to which the predicted $\lambda_{q,near} \propto 1/I_p$ scaling is preserved with increasing performance. If the scaling is found to apply on ITER up to the highest currents, the operational window is likely to constrict and detachment control will become even more stringent as the plasma current is increased.

Heat load characterization should proceed as in the PFPO phases, using first L-modes in deuterium to expand the PFPO database and applying the detachment control techniques developed in PFPO-2. The application of 3-D fields at higher current and thus density in L-mode will allow the study of the effect of divertor dissipation on the perturbed divertor target heat load distribution. Even 7.5 MA/2.65 T deuterium H-modes are likely to require integrated scenarios coupling ELM control with impurity seeding, thus requiring the detailed investigation of divertor heat load patterns in the presence of dissipation and magnetic perturbations, including possible rotation of the perturbation.

Divertor heat load characterization will thus occur along with the scenario development and may not require much, if any, dedicated experimental time. Some specific experiments will be necessary to study main chamber power loads, along the lines performed in PFPO-1 and PFPO-2 (e.g. effect of separatrix separation on steady state loading at the top of chamber), though if performed in H-mode there will again be limits to what is possible imposed by the divertor (e.g. the study of unmitigated ELM impact on the first wall will not be possible if such ELMs are incompatible with divertor power loads or W influx).

For the first time heat flux control by impurity seeding in H-mode can be rigorously tested under relevant conditions, including tests of response to loss of impurity injection, the effect of impurity injection through the main chamber and divertor gas inlets, the detailed dynamics of the combination of divertor/main chamber fuelling with impurity seeding. A key aspect to examine will be the relative merits of N_2 versus Ne seeding (see section 2.2.5), which, until the advent of higher power H-mode operation in deuterium, may be difficult to study with respect to extrapolation to fusion conditions as a result of lower pedestal temperatures and plasma densities in lower power hydrogen H-modes (He H-modes are not useful for the investigation of extrinsic seeding dynamics/detachment control in view of extrapolation to D or DT). These early H-mode experiments in D, before the introduction of T, should allow a much clearer assessment of whether or not, as indicated by plasma boundary simulation for ITER, Ne will be as efficient as N_2 as a divertor radiator (section 2.2.5). The use of nitrogen seeding alone will also be important to further quantify the rate of ammonia formation (section 2.2.4) in more relevant, higher power H-mode conditions (higher surface temperatures), for which studies will have begun in PFPO-2 and possibly in PFPO-1. At this stage, first tests of main chamber radiation (Ar) may also be started in preparation for later higher power fusion plasmas, along with associated feedback control methods.

2.6.3.7 Trace Tritium H-mode experiments

2.6.3.7.1 Summary of scenarios and objectives

At this stage of the Research Plan, the tritium plant is expected to be able to provide sufficient quantities of tritium to perform trace tritium H-mode experiments in D plasma, i.e. with a much smaller throughput (typically more than 100 times lower) than that required for Q = 10 operation in 300 - 500 s burn pulses. This trace tritium campaign is expected to require 12 days of operation and its main aims are to carry out fuelling and particle transport studies of T into D H-mode plasmas, perform an initial evaluation of tritium retention in H-mode plasmas and to start commissioning the diagnostics required for the DT experimental phase, especially of the 14 MeV neutron diagnostics, which are key to perform the investigation of core physics processes involving nuclear fuel (tritium transport, DT fuel mixture, etc.) in this phase and later in the full DT phase.

The basic scenario to be used for these experiments is the integrated D H-mode scenario at 7.5 MA/2.65 T q_{95} = 3 developed in section 2.6.3.5 and the main research to be performed will concentrate on tritium fuelling, particle transport and tritium retention studies with a total operational time of 12 days.

2.6.3.7.2 Risk to the success of the trace tritium H-mode experiments in FPO

The main risks to the success of these experiments are linked to issues related to the provision of tritium fuel, to its diagnosis and to the associated modelling. The risks associated with H-mode operation in D plasmas at 7.5 MA/2.65 T are assumed to have been satisfactorily resolved by this stage:

- *Late availability of the Tritium Plant.* This is not a scientific/technical risk but a scheduling risk. If this materializes it can be mitigated by pursuing the H-mode research program from 7.5 MA/2.65 T towards 15 MA/5.3 T in D plasmas rather than in DT. In this case the experiments described in section 2.6.3.5.6 would start at this stage and the program would revert to the trace tritium experiments as soon as the required tritium throughput is available.
- *Key diagnostics to determine the concentration of tritium in the confined plasma (e.g. neutron spectrometer, neutral particle analyzer), in the recycling fluxes (e.g. H_α and visible spectrometers/cameras) or retained in the plasma-facing components (e.g. tritium monitor) are found not to have the sensitivity required to determine trace amounts of tritium (~ 1%) in 7.5 MA/2.65 T H-mode plasmas after commissioning.* Depending on the sensitivity problems and the diagnostics affected, this could be solved by performing the experiments at a higher tritium level at this stage (~10% T), if this can be provided by the Tritium Plant or by delaying the experiments until sufficient tritium throughput is available.
- *Modelling of tritium transport is not yet mature enough at this stage.* Modelling of multi-species particle transport in ITER-like plasmas is expected to be very mature at this stage of the experimental program. This allows its validation and fine tuning with the trace tritium experiments and to apply it to the detailed planning of DT experiments. If this turns out not to be the case there is no risk for the trace T experiments as such but for the follow-up DT campaign. The DT campaigns will thus have to be fundamentally based on experimental findings, which will slow down the progress towards maximum fusion performance until adequate and reliable numerical predictive tools are available.
- *Trace tritium experiments reveal that tritium retention in ITER PFCs is larger than expected or tritium removal is less efficient than foreseen.* This again is not likely to put at risk the

trace T experiments as such, due to the small amounts of tritium fuelled into the plasma but is a risk for the follow-up DT campaign. Identifying if this risk materializes as an issue as early as possible in FPO is essential to develop improvements to the foreseen tritium removal techniques in ITER before routine long-pulse DT operation takes place.

It should be noted that delaying the trace tritium experiments is not a desirable option, as the results from these experiments are important to understand the behaviour of tritium in ITER H-mode plasmas and to validate the models on which the detailed planning of the follow-up DT operation will be based.

2.6.3.7.3 Details of experimental plan for the trace tritium H-mode experiments in FPO (12 days)

As describe above, the basic scenario to be used for these experiments is the integrated D H-mode scenario at 7.5 MA/2.65 T q_{95} = 3 developed in section 2.6.3.5. This scenario will be used to perform specific experiments to address tritium fuelling transport and retention with tritium concentrations at the trace level of ~ few %. The diagnostics for tritium measurements in the confined plasma are designed to measure T concentrations to the 1% level with a time resolution of 100 ms and 20% accuracy [ITER_D_28B39L, 2017]. However, the final capabilities of the diagnostics is dependent on plasma parameters and it may be the case that, for very low values of the T concentrations, the achievable time resolution is longer than 100 ms if 20% accuracy is required. Optimization of the trace tritium level for accurate diagnostic measurements is, therefore, included as the first item in the experimental plan, which consists of the following steps:

- Optimization of the trace tritium concentration level (by T-doped deuterium pellet fuelling) into 7.5 MA/2.65 T plasmas in order to ensure the highest quality measurements and to allow the commissioning of other diagnostics that will be required for the DT phase beyond those required to determine the T concentration (e.g. 14 MeV neutron measurements);
- For at least two trace tritium levels, fuelling experiments will be performed by injecting the trace T by gas puffing and T-doped deuterium pellets. DT mix control experiments will be performed both for stationary H-mode conditions and during the H-mode access and exit phases. The main goals of these experiments are:
  - Validate the predictions for T fuelling efficiency by gas fuelling and pellet fuelling performed on the basis of experiments in D H-mode stationary plasmas and the optimization of pellet fuelling for efficient core fuelling;
  - Validate the predictions for core T transport performed on the basis of experiments on stationary D H-mode plasmas and identify possible effects associated with the different mass of T versus D on both anomalous transport and neoclassical transport [Loarte, 2016-2] and ELM control, and to re-optimize the trace T gas/pellet fuelling schemes accordingly;
  - Study T fuelling (most likely by pellets) in the transient H-mode access/exit phases with a view to optimize T throughput and to provide robust H-mode access/exit phases in DT plasmas. These experiments will specifically address the requirements and effectiveness of tritium fuelling to change the DT mix (at the trace level) in the H-mode access/exit phases by varying the time to start/stop of tritium injection with respect to the start/end of the H-mode for a range of D L-mode densities (pre and post H-mode);

- In parallel with the above, experiments to diagnose tritium retention by in-situ diagnostics as well as by gas balance will be performed. This will be accompanied by studies to demonstrate in-situ removal techniques between shots such as ICWC.

2.6.3.7.4 Diagnostic adequacy for trace tritium H-mode scenario studies in FPO

By this stage of the operational program all ITER diagnostics should be available for operation, including those related to neutron and fast particle measurements. The main open issue, as discussed above, is whether the sensitivity/time resolution/accuracy for the trace T experiments will be sufficient to draw quantitative conclusions and to validate the T transport models required to plan DT operation. This is most likely to affect the experiments that concern transients rather than those related to determination of the time-averaged T fuelling efficiency in stationary H-mode conditions. It is possible that the time resolution of the T concentration may have to be increased beyond 100 ms to maintain measurement accuracy for trace T levels and, depending on the increase, this may affect the T concentration measurements during H-mode access/exit phases and during particle transport experiments targeted to characterize the post-pellet inwards diffusion of T in the H-mode stationary phases.

2.6.3.7.5 Deliverables for the trace tritium H-mode experiments in FPO

The main deliverables for this phase are:

- First assessment of the T fuelling efficiency in ITER integrated H-mode scenarios (at 7.5 MA/2.65 T) and of the capabilities for DT mix control by gas and pellet fuelling both for stationary and transient phases;
- Essential data on T transport for the benchmarking the numerical models to be used to predict the schemes which will be required to achieve DT mix control for optimum burn access/exit and stationary burn optimization;
- Initial assessment of T retention in relevant conditions for DT operation to confirm the evaluation performed on the basis of D experiments and of the effectiveness of between-shot T removal techniques such as ICWC.

2.6.3.8 Initial development of hybrid/ advanced scenarios

2.6.3.8.1 Summary of scenarios and overall objectives

The overarching objective for this campaign is to optimize non-inductive current drive fraction in high-β, low collisionality integrated q_{95} = 4 (hybrid) and q_{95} = 5 (steady-state) scenarios. The results from this campaign will establish the basis for those in the DT campaign, ultimately achieving the 1000 to 3000 s highly or fully non-inductive discharges with significant levels of fusion power production. Plasma scenarios with q_{95} = 4 and 5 at both 2.65 T (5.6 MA and 4.5 MA respectively) and 4.5 T (9.5 and 7.5 MA respectively) will be the basis for these studies. Consistent with the strategy followed for deuterium H-modes in section 2.6.3.5, the experiments performed at 2.65 T will most likely be performed in D pure plasmas while those at 4.5 T will most likely be performed with some level of T (a concentration of at least 10%), taking advantage of the availability of the T-Plant at this stage. Should the available T throughput not be sufficient at this stage, the 4.5 T experiments will be carried out in D plasmas.

In order to accomplish these goals, it is first of all necessary to have full heating and current drive systems operation for ~ 50 s, fast ion diagnostics and current profile measurements, real-time β and

current/pressure profile control developed. The DMS should be fully available and functional and stationary H-modes with robust ELM, density control and divertor detachment real-time control developed for 2.65 and 4.5 T plasmas with $\langle n_e \rangle / n_{GW} \geq 0.5$. This implies that these experiments can only be performed after the corresponding H-mode program in section 2.6.3.5 for 2.65 T and the possible follow up in DT for 4.5 T in section 2.6.4.3 have successfully demonstrated these scenarios.

The estimated operational time required for achieving the overall objectives of this phase is described below. Obviously, these estimates depend on the development performed and research results from other areas in the program such as H-mode scenario development (section 2.6.3.5) and the commissioning of advanced control schemes (section 2.6.3.3):

- Application of β/current/pressure profile control algorithms using target current profiles for q_{95} = 4 and 5 at 2.65 T in stationary H-mode conditions: **10 days dedicated plus experience from other experimental areas;**
- Optimization of performance and non-inductive current drive in 2.65 T discharges at q_{95} ~ 4 to 5 (I_p ~ 4.5 to 5.6 MA): **10 days;**
- Optimization of performance and non-inductive current drive in 4.5 T discharges at q_{95} ~ 4 to 5 (I_p ~ 7.5 to 9.5 MA): **0 to 20 days** (the amount of time in D plasmas depends on whether the corresponding H-mode experiments are performed in D or in D + 10% T).

2.6.3.8.2 Risk to the initial development for hybrid/ advanced scenarios

The main risks in this phase are related to the capability of the ITER actuators and control loops to achieve the required plasma control and the lack of ability to extrapolate the results in PFPO-2 to D plasmas. In addition, the general risks affecting the development of the Q ~5 scenarios in Appendix J also apply:

- *Uncontrolled impurity accumulation (from W and seeding impurity) degrading plasma performance and current drive:* This can be more problematic in this phase than in PFPO-2 due to the higher plasma currents and associated power loads and may require a higher level of central heating than in PFPO-2, which may conflict with other j(r) and MHD control requirements. It is important to note that this issue may not necessarily be problematic in the corresponding DT plasmas with significant α-heating, which provides a central power source, and probably not likely to be found at this stage for the 2.65 T scenarios for which similar plasmas will have been extensively studied in the H-mode program (see section 2.6.3.5).
- *Higher β operation leads to additional MHD-related phenomena affecting the scenarios:* The β of the D plasmas in this phase will be higher than that in the H/He plasmas in PFPO-2. This may lead to new MHD phenomenology affecting NB current drive and fast particle losses (e.g. AEs, enhanced losses with 3-D fields for ELM control due to larger plasma response [Kurki-Suonio, 2017], etc.). If this is the case, experimental time will be required at this stage to characterize and control these phenomena and to mitigate their effects on the plasma.
- *Heating and current drive flexibility not sufficient to develop the scenarios:* Due to the increasing requirements on the H&CD it may be the case that the sharing of missions among the various H&CD systems cannot be satisfactorily met (e.g. ECRH/ECCD may be required for core W control, AE control and NTM control, etc.). If this is the case, an assessment of

whether this will be an issue for DT or not will be made and, if so, the upgrade required for successful Q ~5 long-pulse operation in DT identified.

- *Experience developed in PFPO-2 not relevant:* i.e. D plasmas in these scenarios might be significantly different from those in H/He plasmas so that the operational recipes developed in H/He do not apply. As an example, the current ramp-up scenarios developed in H/He L-mode may not be applicable to D plasmas due to the lower H-mode threshold if the H&CD power level applied in this phase is higher than this level, as was the case for D and DT plasmas at JET [Söldner, 1999]. In this case the scenarios would need to be redeveloped at this stage by adjusting heating level, current ramp-up rate, density, etc.

2.6.3.8.3 Detailed experimental plan for the initial development of hybrid/ advanced scenarios (20-40 days)

Given the large number of issues that need to be assessed and demonstrated in the Research Plan before these experiments are performed, as well as the remaining physics uncertainties of the extrapolation of the hybrid and advanced regimes to ITER and of their integration with operational requirements, it is not possible to give a detailed plan for the precise conditions for the q_{95} = 3.5-6.0 (with focus in q_{95} = 4 and 5) plasmas at 2.65 and 4.5 T that will be explored. Despite this, it is possible to identify the specific experimental objectives that will be addressed in these operational days:

- Assessment of the diagnostic and control capabilities in longer-pulse plasmas towards developing control techniques for accessing current profiles consistent with steady-state operation in ITER;
- Establishment of a basis for fully non-inductive plasma performance in ITER including initial tests of closed-loop feedback capabilities;
- Development and sustainment of q_{95} = 4 hybrid discharges with $H_{98} \geq 1$ integrated with all ITER operational scenario requirements including edge-core integration (fuelling, power loads, impurity exhaust, etc.), MHD control, etc., and evaluation of expected fusion performance in DT;
- Establishment of (~ 50 s) plasmas with optimized non-inductive current drive fraction integrated with all ITER operational scenario requirements including edge-core integration (fuelling, power loads, impurity exhaust, etc.), MHD control, etc., and evaluation of expected fusion performance in DT;
- Assessment of MHD stability (NTM, AEs, etc.) and confinement properties of long-pulse q_{95} = 4 hybrid and steady-state plasmas to determine the control requirements for stable operation;
- Development of disruption avoidance and detection schemes for highly non-inductive plasmas and demonstration of disruption mitigation, which are likely to be deviate from those for q_{95} = 3 - 4 plasmas. This will include the assessment of the need for RWM control, which will be explored within the installed capabilities of the ELM control coils (90 kAt, 5 Hz rotation) and the current level margin available beyond that required for ELM control. For the I_p/B_t levels in these plasmas, this spare current capability for RWM demonstration is expected to be > 45 kAt for 2.65 T and > 15 kAt for 4.5 T plasmas;
- Assessment of the pedestal characteristic of hybrid and steady-state scenario plasmas and of the coupled core and pedestal optimization at the expected operating points for hybrid and

steady-state operation in DT. This is expected to require optimization of the heating power level and mix, torque input, fast particle content and, possibly, plasma density to determine the dominant physics process that leads to enhanced plasma confinement above H_{98} in these plasma scenarios;

- Complete the validation of models for ECRH, ICRF and NBI heating and current drive in D plasmas to enable extrapolation to the corresponding hybrid and steady-state plasmas in DT. This interaction between simulation and experiment is also key to providing input regarding the decision to go ahead with an ECRH/ECCD upgrade at this stage, if this is essential for long-pulse Q ~ 5 DT operation, although this would delay that research until this system is available (see details in Appendix G). It is essential that the validation of the individual models used for these simulations receive high priority during all phases of the steady-state scenario development, starting with PFPO-2 and most importantly in this initial stage of FPO. Success in validating these models will provide a powerful tool for planning experiments during the later DT campaigns in FPO, and ultimately will provide increased confidence in the ability to project steady-state scenarios achieved on ITER towards Demo. In this respect, it should be noted that the 3rd HNB upgrade decision should be taken before FPO (see in Appendix G). Therefore this capability could be available for this operational period providing more flexibility than the previous experiments in PFPO-2;
- Determining the experimental behaviour of fast ions and validating the models for energetic ion behaviour resulting from the fast ion populations arising from all heating systems in D plasmas will be performed in these experiments. These are different from PFPO-2 because among other things the HNBs are changed from H to D and the ICRF minority at 4.5 T will be He^3, rather than the H minority used at 2.65 T (see details in section 2.5.3). In particular, if MHD instabilities are observed, determining the nature of the instabilities observed (e.g. global TAE modes in the outer region of the plasma) [Pinches, 2015] will be a focus of the experiments;
- If Alfvén Eigenmodes (AE) become unstable, investigating the effects of the various heating and current drive systems on these instabilities and of the capabilities of these systems to affect AE instability by local modification of plasma parameters (since this influences the Landau damping experienced by these modes and changes the spectrum of compressional and Alfvénic modes) [Lauber, 2015] will be a focus of the experiments. If suitable actuators are established for AE control then establishment and refinement of AE control techniques and associated controllers could continue at this stage [Van Zeeland, 2016];
- Determining and validating the effects of ELM control coils on fast ion losses for plasmas with q-profiles as required for hybrid and steady-state D H-mode plasmas [Garcia-Munoz, 2013] will be performed. This would be complementary to the experiments in FPO for the inductive scenario in section 2.6.3.5.

2.6.3.8.4 Deliverables for the initial development of hybrid/ advanced scenarios

The main deliverables from this operational phase are:

- Assessment of the effect of the different isotopes/species (H/He/D) on hybrid and non-inductive scenarios development in H-mode;
- Establishment of a validated model basis for extrapolation of the D plasma scenarios to long-pulse and steady-state DT operation;

- First assessment of β/j(r)/p(r) control in D H-modes and its consequences for plasma performance;
- First assessment of the current drive capabilities of the H&CD systems in D H-mode plasma at q_{95} ~ 4 and 5 for two B_t-field values in long-pulse H-mode plasma. This assessment will lead: to refinement in the application of the available H&CD, to the establishment of the upgrade requirements for the control system sensors and actuators, including an ECRH/ECCD upgrade for long-pulse development and/or NTM control and the need to upgrade power supply for RWM active control;
- Development of closed-loop feedback control algorithms for core performance and edge-core integration (fuelling, power loads, impurity exhaust, etc.) control;
- Demonstration of $q_{95} = 4$ hybrid discharges with $H_{98} \geq 1$ integrated with all ITER operational scenario requirements including edge-core integration (fuelling, power loads, impurity exhaust, etc.), MHD control, etc.;
- Demonstration of long-pulse (~ 50 s) plasmas with optimized non-inductive current drive fraction integrated with all ITER operational scenario requirements including edge-core integration (fuelling, power loads, impurity exhaust, etc.), MHD control, etc.

2.6.4 Operations Plan for Deuterium-Tritium (DT) Plasma experiments towards Q = 10

2.6.4.1 Plasma scenarios for the experimental program towards Q = 10 operation

The experiments in DT will start from the 7.5 MA/5.3T D and D+trace-T integrated scenarios described in sections 2.6.3.5 and 2.6.3.7 and proceed by increasing I_p and B_t in steps along a q_{95} ~ 3 line (with I_p = 9.5, 12.5 and 15 MA plus a possible intermediate step at 13.5 MA at constant B_t) aiming at a stationary H-mode duration of ~ 50 s. For each of the current levels explored, the T concentration will be varied from trace levels to ≥ 60 % to determine the effects on the plasma of the increasing α-heating and the optimum T concentration for maximum fusion power production. As discussed in section 2.6.3.5, it is expected that stationary H-modes with trace T levels will not be achievable beyond 12.5 MA/4.5 T due to the baseline heating power installed 73 MW and the D H-mode threshold level. Above this current level, plasmas with significant T concentrations will be required to achieve stationary H-modes both because the presence of T decreases the H-mode threshold and because of the increased heating power provided by the additional α-heating. In this respect, performing this development with significant fractions of T instead in pure D plasmas can mitigate the risks related to changes in the ECRH and ICRF power deposition profiles, which can become less central for some values of the intermediate fields between 2.65 T and 5.3 T. In these cases, α-heating will remain centrally peaked and even for the low Q values (~ 1-2) expected at low I_p levels, the resulting α-heating power will be in the range of 10's MW and thus sufficient to have an important effect on the W concentration according to ITER modelling in [Loarte, 2016-2], shown in Figure 2.6-3.

The research program is divided into three main phases:

- The first main phase concentrates on the characterization of H-mode access in DT and the thorough exploration of DT H-modes and on the solution of operational issues in 7.5 MA/2.65T H-mode plasmas requiring 66 operational days;

- The next phase expands the H-mode operational range in DT plasmas up to 15 MA/5.3 T concluding with the demonstration of Q = 10 operation for burn lengths of ~ 50 s, which is expected to require 180 operational days;
- The final phase performs the developments to increase the Q = 10 burn length to 300 - 500 s and thus concludes with the demonstration of the ITER inductive goal; this is expected to require ~100 additional operational days.

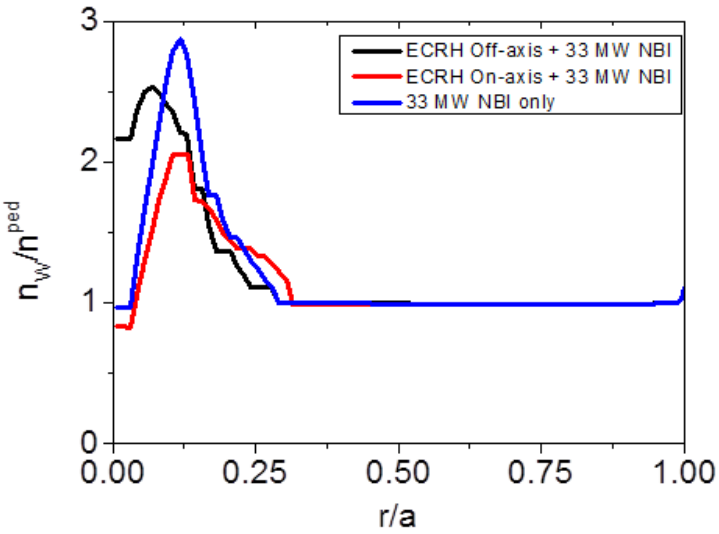

Figure 2.6-3: W density profiles, normalized to the pedestal value, for ITER DT 7.5 MA/2.65 T plasmas with 33 MW of NBI and 0/20 MW of RF for a range of heating schemes modelled with ASTRA. Core particle and energy transport assumptions where anomalous transport is negligible are those of neoclassical transport for DT ions and electrons.

It is important to note that it is not expected to reach the Q = 10 short pulse goal during the first operational period in FPO of 16 months, which amounts to 415 operational days, due to the significant commissioning and operational development activities that will have to be undertaken with the start of D and DT operations. On the basis of the present Research Plan, it is expected that by the end of the first operational period in FPO fusion power production at the level of ~ 250 MW for ~ 50 s and Q ~ 5 will have been demonstrated. The plasma scenario in which this will be achieved depends on the result of the research performed within this initial phase of FPO. It is currently expected that this will be either with I_p ~ 12.5 MA and $\langle n_e \rangle \sim 10^{20}$ m^{-3} (i.e. $\langle n_e \rangle \sim n_{GW}$) or with I_p = 15 MA and $\langle n_e \rangle \sim 0.7\times10^{20}$ m^{-3} (i.e. $\langle n_e \rangle \sim 0.6\times n_{GW}$) [Polevoi, 2015] for the τ_E predicted by the ITER-H98(y,2) scaling, as shown in Figure 2.6-4.

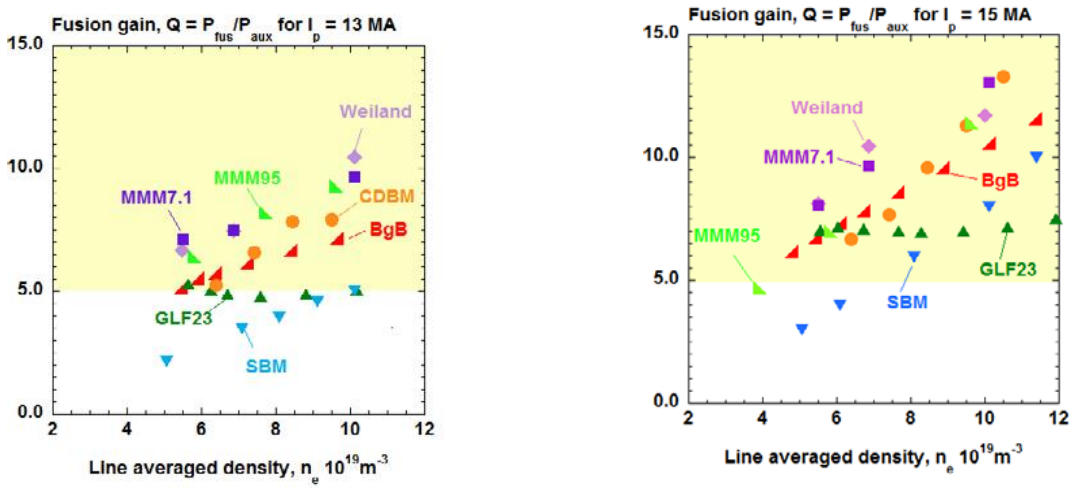

Figure 2.6-4: Fusion gain factor, Q, predicted by different core transport models for 13 MA (left) and 15 MA (right) DT plasmas in ITER plasmas with P_{inp} = 50 - 53 MW. The predictions with the SBM model (Scaling Based Model) correspond to $H_{98}(y,2) = 1$.

It should be noted that by this phase of operation, ITER will be equipped with the full contingent of diagnostics required for DT operation. Therefore, no diagnostic limitation specific issues are discussed further in the sections below. These could arise if key diagnostics do not provide the required measurements with the foreseen accuracy or if the measurement requirements prove to be inappropriate in view of the achieved plasma parameters in ITER; i.e. if the achieved plasma parameters differ substantially from those predicted on the basis of existing knowledge that has been used for diagnostic design. This will only be known when this stage in the operational plan is reached and at that point appropriate mitigation actions will have to be implemented.

In addition, by this point in the operational campaigns, all the tools needed to characterize fuel retention and material migration will have been validated and a good understanding of erosion/redeposition will have been reached. Measurements would then become part of routine monitoring to check the power handling capabilities and thermal response of PFCs, ensure that FW erosion remains within allowable limits and that fuel retention rates are as expected and do not change with time. One important aspect, as wall fluence and integrated material erosion accumulates, will be to monitor the occurrence of co-deposit flaking, which is known to occur when co-deposits become too thick. As mentioned earlier, this would represent a potential source of dust creation in the machine, and would be the dominant dust production mechanism when the disruption mitigation/avoidance system has reached its target for mitigation rates.

2.6.4.2 Optimization of DT plasma scenarios at 7.5 MA/2.65 T (66 days)

2.6.4.2.1 Experimental plans for the characterization of H-mode access (6 days)

To prepare for the following DT H-mode operation an assessment of the L-H threshold of DT plasmas will be performed, which is expected to require 6 operational days. This includes the scaling of the H-mode threshold with T concentration, plasma density and heating mix at 2.65 T at q_{95} ~ 3 and an initial study of H-mode access at q_{95} = 5 in the current ramp-up, will also be performed.

An assessment of the mass dependence of the H-mode threshold will be completed by exploring H-mode access in DT plasmas up to 50% T concentrations, as soon as the T plant allows, by comparing with the previous D results. Similar to H/He plasmas, H-mode access in the current ramp

will be explored by accessing the H-mode at ~2/3 of the flat-top level (i.e. 5 MA). These points are essential for the next development of the H-mode scenarios in DT where the optimization of the DT mix and the heating mix to achieve a robust H-mode transition is required both for the flat-top and the current ramp-up phase. The outlines of the foreseen experimental conditions covering the ranges to be explored are summarized in Table 2-14 for the stationary DT plasmas and in Table 2-15 for the current ramp-up experiments in DT.

As already discussed above, the main technical issues for these experiments are:

- to achieve the required level of ELM control to avoid long-ELM free periods that can cause edge melting of the divertor W monoblocks and W accumulation in the main plasma. For this purpose, ELM control by in-vessel coils as well as by the back-up ELM triggering schemes (pellet triggering and vertical position oscillation) will be applied following the previous operational experience in H/He plasmas in PFPO-1 and PFPO-2 and in D in FPO;
- to ensure robust DT mix control for the experiments where the T concentration is scanned by gas fuelling and/or pellets.

Table 2-14 – L-H transition scenarios in DT

I_P FT (MA)	B_t (T)	Density (f_{GW} %)	Heating mix	q_{95}	
7.5	2.65	40	NBI+ICRF+ECRH	3	Density scan with 10%T
7.5	2.65	80	NBI+ICRF+ECRH	3	
7.5	2.65	40	NBI+ICRF+ECRH	3	Density scan with 50%T
7.5	2.65	80	NBI+ICRF+ECRH	3	
7.5	2.65	40	NBI	3	Heating mix scan with 50% T
7.5	2.65	40	ECRH+ICRF	3	

Table 2-15 – L-H transition scenarios in DT during I_p ramp-up

I_P ramp (MA)	B_t (T)	Density (f_{GW} %)	Heating mix	q_{95}	
5	2.65	40	NBI+ICRF+ECRH	4.5	Density scan with 50%T
5	2.65	80	NBI+ICRF+ECRH	4.5	

2.6.4.2.2 Experimental plans for the exploration of DT H-mode at 7.5 MA/2.65 T (60 days)

Beginning with the 7.5 MA/2.65 T D and D+trace-T plasmas, which will have been extensively explored and understood by this stage, the tritium content of the H-mode phase of the discharge will be gradually increased, producing higher and higher levels of α heating until the optimum T concentration is exceeded and α heating decreases. In principle, the modification of plasma characteristics as the T concentration increases in DT 7.5MA/2.65T plasmas is expected to be gradual, as the maximum level of α-heating will be moderate compared to the external heating sources (< 20%) and the reduction in the H-mode power threshold from pure D plasmas to ~50/50 DT plasmas is expected to be 25%. On the other hand, new physics phenomena may appear with the introduction of two isotopes that change the behaviour of the plasma qualitatively. For example, neoclassical DT transport effects due to the different masses of D and T are expected to cause

density gradients in the central plasma region to appear, which are not existent in D plasmas, that can affect W transport [Loarte, 2016-2], as shown in **Figure 2.6-5**.

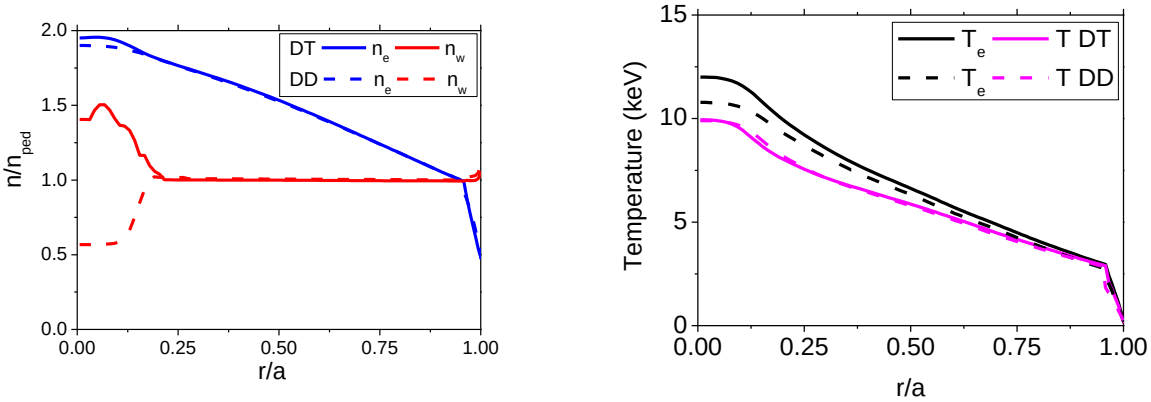

Figure 2.6-5: Plasma density and W profiles (left) and electron and ion temperatures (right) for two 7.5 MA/2.65 T ITER plasmas with P_{inp} = 50 - 53 MW, one in D and the other in DT. Due to neoclassical transport effects associated with the different masses of D and T the density profiles are more peaked for DT in the central plasma region than for D plasmas and this leads to an increased W peaking in DT compared to D plasmas.

The specific plan for this phase relies on a variation in the tritium concentration from levels of ~10% (well above the trace-T level) to levels in excess of 60-70% and, thus, well beyond the optimum concentration for fusion power production. Various levels of additional heating and additional heating mixes will be explored and the impact of the increasing T concentration core/edge/boundary plasma characteristics will be characterized. An important ingredient for this characterization to be possible is the demonstration of the capabilities to control the DT mix, which will have been developed on the basis of the D+trace-T experimental results. For the highest fusion powers some helium production will take place, although probably at a level one order of magnitude lower than for Q =10, that allow fusion-produced He exhaust experiments to start. Most likely this will require decreasing the pumping throughput to ensure that the core He concentration exceeds the minimum measurable of 1%.

During this phase, moderate length pulses, few tens of seconds, are likely to be required to assess long time-scale stability of established feedback algorithms, such as those required for the control of the DT mix. Therefore, it is foreseen that the stationary phase of these plasmas is at least ~ 50 s long (i.e. ~ 25 τ_E). The final part of the experiments will concentrate on the optimization of fusion performance and its control with fuelling and additional heating schemes to develop strategies that will be used in later experiments at higher plasma currents and higher fusion power where development of such schemes is more difficult due to the need to control, simultaneously with the development, the higher power loads to plasma-facing components. This initial DT H-mode phase with 7.5MA/2.65T plasmas is expected to require ~ 60 days of operation.

The main experimental activities in this phase are:

- Scans of the core plasma T concentration, starting ~10% and going beyond optimum DT mix, most likely by pellet fuelling, for various levels of additional heating power/additional heating mix and stationary H-mode plasma density to assess the effects of increasing T concentration on:

  - The L-H power threshold, which is expected to decrease with increasing T concentration;
  - Edge pedestal plasma characteristics and ELM power loads (uncontrolled if allowed); the pedestal pressure and the associated uncontrolled ELM energy losses are expected to increase with increasing T-fraction;
  - MHD stability of the core plasma including fast particle effects in DT plasmas (from NBI, ICRF and fusion-produced α-particles);
  - He concentration in the plasma and its exhaust through uncontrolled ELMs (if allowed) and controlled ELMs and other collateral effects (e.g. ICRF parasitic resonances, divertor PWI effects, etc.).

- The assessment and retuning of control schemes which depend on increasing tritium concentration and plasma energy (energy confinement is expected to follow T concentration) and specific scenario issues for DT plasma (preliminarily developed for D and D+trace-T plasmas):
  - T fuelling optimization for stationary H-modes (pellet, size, injection velocity, etc.) H-modes and studies of burn control by fuelling;
  - Development of robust schemes for robust H-mode access/exit phases including the optimization of the density waveform before and after the H-mode and the build-up and ramp-down of the T concentration towards/downwards the target DT mix in stationary conditions (e.g. reaching the target DT mix in L-mode and maintaining it through the H-mode, increasing the T-fraction once the plasmas is in H-mode, etc.);
  - Re-optimization/redevelopment of the schemes to obtain stationary power control by operating in the radiative divertor regime and evaluation of the consequences for core plasma confinement, as both W impurity production and transport are expected to be affected by increasing T concentration;
  - Re-optimization/redevelopment of the 3-D fields applied by the in-vessel coils to provide ELM control, which is expected to be required given the effects of increasing T concentration on the pedestal plasma (increasing pedestal pressure and ELM energy losses). This re-optimization should integrate other scenario requirements such as radiative divertor operation, impurity and helium exhaust and low losses of fast particles in the applied 3-D fields;
  - Re-optimization of NTM control schemes, sawtooth control schemes, error field correction, disruption and runaway mitigation, etc., which may be required due to the increase in plasma β and changes to the current profile caused by the increased T-fraction (e.g. lower l_i driven by a higher pedestal bootstrap, etc.);
  - Re-optimization of the H&CD schemes to avoid W accumulation with varying D and T concentrations.

In parallel with these studies, further studies on T retention and removal (e.g. ICWC) will be performed to quantify T retention and the effectiveness of T removal techniques now in plasma conditions very similar to those expected in Q = 10 plasmas.

2.6.4.2.3 Risks for exploration of DT H-mode at 7.5 MA/2.65 T

The major risks for the success of this phase are:

- Predictive and interpretative modelling of fuelling, transport and α-particle effects not mature enough for detailed planning of DT operations at this stage. This will require that the experimental plan progresses on a more empirical basis, which will require more experimental time and possibly smaller T concentration steps and wider parameter scans for each condition.
- Sudden non-linear changes of plasma behaviour above a given T concentration. The experimental plan above is based on the effects of the T concentration being gradual, as observed in existing experiments. This allows continuous retuning of the application of the actuators and control schemes from one T concentration to the next. If this is not the case, alternative experimental paths would need to be followed. For instance, ELM behaviour could already be significantly different at ~10 % T concentration compared to trace-T (or from one T concentration level to the next). This could render the ELM control strategies followed in D and D+trace-T plasmas invalid and risk melting the divertor monoblock edges. In this case, the alternative strategy would be to perform the T-fraction explorations in 5 MA plasmas (at 1.8 T or 2.65 T depending on the D and D+trace-T experience) and then gradually increase the plasma current up to 7.5 MA. This would avoid the risk of divertor melting but would require more experimental time.
- General risks to ITER DT operation could materialize already at this stage, even if a priori not expected, such as large α-particle losses caused by fast particle driven modes, high T retention etc. These are issues that need to be resolved to achieve the Q = 10 goal and if they appear at this stage, additional experimental time would be required to resolve them before continuing with DT program at higher plasma currents.

2.6.4.2.4 Deliverables from the exploration of DT H-mode at 7.5 MA/2.65 T

The main deliverables of this experimental phase are:

- Determination of the H-mode threshold with varying concentrations of T in DT plasmas at 2.65 T for stationary H-modes with q_{95} = 3 and during the current ramp-up at q_{95} = 5;
- Robust 7.5 MA/2.65 T H_{98} = 1 DT H-mode scenario over a range of densities and additional heating power with integrated fuelling and DT mix control, NTM and W accumulation control, error field correction, ELM control with 3-D fields from in-vessel coils to provide acceptable transient power loads and impurity exhaust (including He exhaust), stationary power load control through radiative divertor and with low disruptivity and efficient DMS, when disruptions occur. This scenario will be used to benchmark the predictive modelling to be used to guide the operational development of the rest of the DT program up to 15 MA/5.3 T Q = 10;
- Validated and optimized schemes to control the DT mix in H-mode plasmas in ITER including H-mode access and exit transient phases with minimum T throughput;
- Documented experimental behaviour of DT H-mode plasmas including their reaction to heating and fuelling actuators, which is essential to design the burn control strategies and schemes that will be required in the next step of the experimental program;
- Operational experience and experimental data for model benchmark of the re-optimization of the schemes to control ELM transient loads (ELM control coils) and stationary power loads (fuelling and impurity seeding) with increasing β and Tritium fraction, which will

allow a faster progress in the next phase of the DT program at higher plasma currents where both schemes will be routinely required for operation;

- First evaluation of the magnitude of T retention and of the efficiency of removal techniques (e.g. ICWC) in H-mode plasma conditions very similar to those expected in Q = 10;
- First assessment of nuclear heating of the toroidal field coils in DT H-mode plasmas. This together with the AC losses during H-mode operation will indicate if the combination of both is likely to be problematic for high current/Q operation. If this is the case, the minimization of AC losses will be an important ingredient of the next operational phase.

2.6.4.3 Optimization of fusion power in DT plasma scenarios towards 15 MA/5.3 T Q = 10 (~ 50 s) demonstration (180 days)

Starting from the experience gained in the experiments in section 2.6.4.2 with 7.5 MA/2.65 T H-mode, the operational space of DT H-mode will be expanded towards the final demonstration of the ITER Q = 10 goal for burn lengths of ~ 50 s. This is expected to require 180 operational days and will follow a similar route to that in the development of L-mode plasmas towards 15 MA/5.3 T discussed in section 2.6.3.4. The approach foreseen for the H-mode development follows the same route of gradually increasing current and field while keeping q_{95} ~ 3, namely the steps of 7.5 MA/2.65 T, 9.5 MA/3.3 T, 12.5 MA/4.5 T, 12.5 MA/5.3 T and 15 MA/5.3 T. The values of the step ladder to be followed in DT H-modes will be chosen on the basis of those finally found to be optimum for L-mode, which may be different from those above. Operation along this path makes use of the flexibility of the ITER H&CD systems to maintain power deposition in the central part of the plasma $r/a < 0.5$, which is required both for plasma performance and to prevent W accumulation, which should have been demonstrated in L-mode by this stage. In this respect, as already mentioned before, the increasing production of α-heating in these experiments is at a level that it is predicted to have a significant effect on W transport and may reduce the demands regarding the central localization of the deposition profiles of ECRH and ICRF for intermediate fields between 2.65 and 5.3 T. If this is not sufficient and W accumulation would occur for some of the I_p/B_t steps above, an alternative route for optimum central ECRH/ICRF deposition would be followed when increasing I_p, e.g. increase of I_p and constant B_t = 5.3 T, for which q_{95} would vary.

Plasma operation in this phase will make routine use of the strategies and schemes developed in the experiments in section 2.6.4.2 for DT mix control, divertor power load control, ELM control, etc., because at these current levels the uncontrolled stationary and transient loads are already not compatible with the ITER PFC lifetime or power handling capabilities, as discussed in Appendix C. The experiments will consist of steps in I_p/B_t, additional heating power and T concentration until the Q = 10 goal is achieved and 500 MW are produced in a controlled way.

As mentioned in section 2.6.4.2, in this phase a wide range of T concentrations will be explored at the lower current levels where DT H-mode can be sustained by additional heating alone (no need for α-heating) while for higher plasma currents only high T concentrations will be explored. As mentioned in the D H-mode (section 2.6.3.5.6), the expected H-mode threshold for 12.5 MA/4.5 T plasmas at $\langle n_e \rangle = 0.85 \times n_{GW}$ (the same adopted for Q = 10 operation) in pure D plasmas is 67 MW compared to an additional heating power of 73 MW so that stationary H-mode operation and low T- fractions will be limited to low densities near the minimum H-mode threshold of $\langle n_e \rangle = 0.4 \times n_{GW}$ where $P_{inp}/P_{LH} \sim 1.6$.

The experimental strategy adopted streamlines the development of high current H-modes towards DT by merging the development that was separated in D and DT plasmas in previous versions of

the ITER Research Plan. It should be noted, however, that this relies on the tritium plant being able to deliver an increasing T throughput during this phase to match the increasing T needs associated with high T-fraction/high I_p operation.

Within this experimental strategy, the experimental results obtained for 12.5 MA/4.5 T plasmas at $\langle n_e \rangle \sim 0.5 \times n_{GW}$ will be crucial to determine the optimum way to proceed towards higher I_p/B_t in the next step. These plasmas will be gas-fuelling dominated and are, thus, expected to have relatively low density gradients in the pedestal. Present estimates with integrated modelling, assuming that the reduction of transport in the edge transport barrier is not affected by density gradients, indicate that the fusion performance that can be achieved in these conditions can be significant (Q > 3) [Polevoi, 2015; Romanelli, 2015] as shown in Figure 2.6-6 , which is due to the high pedestal temperatures that can be sustained in these conditions within the calculated edge MHD stability limits. If this is confirmed by experiments, it would open a route to access high-Q operation in ITER of much easier

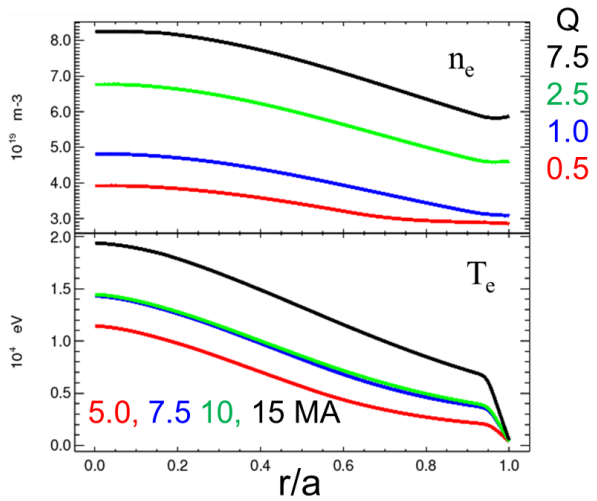

Figure 2.6-6: JINTRAC modelled gas fuelled DT plasmas for a range of plasma currents and with P_{NBI} = 33 MW and P_{ECRH} = 20 MW with the GLF23 core transport model. Note the low density gradients in the pedestal and the high pedestal and overall plasma temperatures and achieved Q for these DT H-mode plasmas.

development (i.e. with a more gradual increase of α-heating with increasing current), by operating at $\langle n_e \rangle \sim 0.5 \times n_{GW}$ as the current increases, than the conventional one based on pellet fuelling and $\langle n_e \rangle \sim 0.85 \times n_{GW}$. In this $\langle n_e \rangle \sim 0.5 \times n_{GW}$ approach $P_{additional\text{-}heating}/P_{LH} \geq 1.7$ all the way to 15 MA/5.3 T and, thus, the H-mode plasmas are more controllable with the additional heating and more weakly dependent on the optimization of the α-heating to ensure robust H-mode operation.

In this approach, access to $\langle n_e \rangle \sim 0.85 \times n_{GW}$ Q=10 operation at 15 MA would be undertaken starting from $\langle n_e \rangle \sim 0.5 \times n_{GW}$, Q ~5, 15 MA plasmas by increasing gradually the density by pellet fuelling at this stage. Indeed, an initial phase of $\langle n_e \rangle \sim 0.5 \times n_{GW}$, Q ~5 to build up α-heating before increasing the plasma density to the nominal $\langle n_e \rangle \sim 0.85 \times n_{GW}$ of the Q = 10 scenario at 15 MA/5.3T has been modelled to provide a more robust access and exit phases to/from burning plasma conditions both in terms of H-mode control as well as for W accumulation avoidance [Köchl, 2014; Motojima, 2015; Köchl, 2016; Militello-Asp, 2016; Loarte, 2016-2], as shown in **Figure 2.6-7**(a) and **Figure 2.6-7**(b). Otherwise, direct access from L-mode to $\langle n_e \rangle \sim 0.85 \times n_{GW}$, Q = 10 conditions relies on the use of the full additional heating power of 73 MW in all discharges [Kessel, 2015] because $P^{max}_{additional\text{-}heating}/P_{LH} \sim 1.0$ for $\langle n_e \rangle \sim 0.85 \times n_{GW}$ at 15 MA/5.3 T.

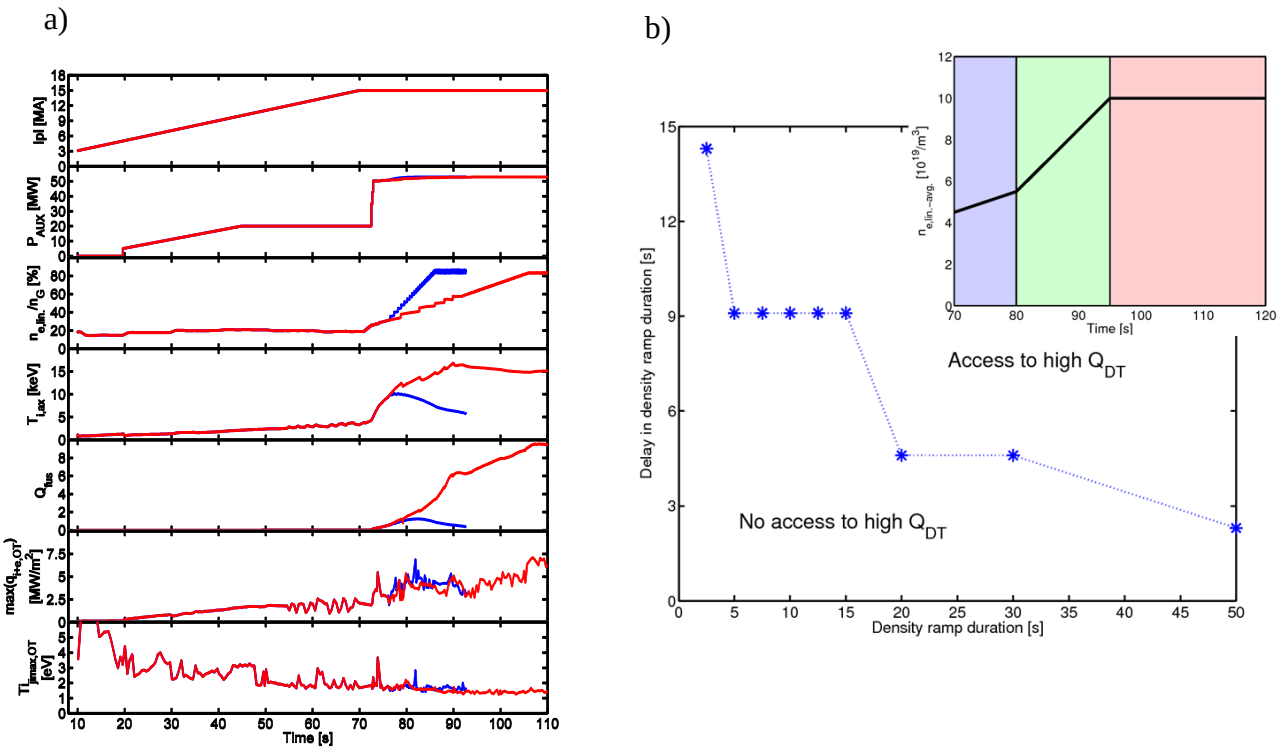

Figure 2.6-7: (a) Modelled current ramp-up for ITER DT baseline scenario with L-H transition at 15MA. Slow (red) and fast (blue) pellet density ramp after the transition. From top to bottom: plasma current, additional heating level, line average density, Q and maximum divertor power flux and temperature. The level of 10 MWm^{-2} is not exceeded in the H-mode access phase. (b) Operational space for the achievement of a transition to high-Q_{DT} ~ 10, 15 MA/5.3 T H-mode in ITER for P_{AUX} = 53 MW in terms of the duration of the pellet fuelled ramp to the nominal density (green phase in inset) and of the delay of the pellet fuelling with respect to the start of the high heating power (blue phase in inset).

The experimental plan foresees performing experiments for each level of I_p/B_t and T-fraction at various levels of plasma density (at least three $\langle n_e \rangle$ ~ 0.5, 0.7, $0.9 \times n_{GW}$) and two levels of additional heating one to match β_N ~ 1.8 and the other to match the expected P_{inp}/P_{L-H} for Q = 10 plasmas. At each of these steps, the schemes previously developed to avoid/control limiting instabilities such as NTMs, sawteeth, etc., may need additional optimization time. Similarly, it is likely that at each step the schemes to provide control divertor power loads and ELM control will have to be retuned. This will become increasingly more complex as the plasma current and fusion power increases, as the schemes to control divertor power loads and ELMs are likely to affect fusion power production (e.g. through the dilution of the plasma by seeded impurities and the effects of ELM control on plasma energy) requiring the control loops and the use of actuators to become increasingly more sophisticated.

Depending on the processes that limit edge MHD stability on ITER plasmas (more ballooning or more peeling) the pedestal pressure is expected to scale as $P^{peeling}_{ped} \sim I_p \times B_t$ or $P^{ballooning}_{ped} \sim I_p^2$ [Snyder, 2011; Polevoi, 2015] and thus, if ballooning dominated, an intermediate current point between at 5.3 T between 12.5 MA and 15 MA may be required to avoid large steps in the edge plasma parameters. These large steps would make very difficult to ensure that ELM control is maintained from one I_p step to the next one (i.e. both q_{95} and edge pedestal pressure would change significantly when going from 12.5 to 15 MA).

Other specific tests and studies of the effects linked to disruptions and runaway mitigation with increasing I_p and/or B_t and plasma energy are addressed separately in section 2.6.3.2 and are not part of the experiments described here.

In view of the above plan, the main experimental activities foreseen in this phase are:

- Increasing the plasma current and field following as much as possible the first two I_p/B_t points in the step ladder for the L-mode scenarios namely 9.5 MA/3.3 T, 12.5 MA/4.5 T. For these two current levels the same type of experiments foreseen for 7.5 MA/2.65 T DT H-mode operations in the previous section will be performed for at least two levels of additional heating. This will lead to an increase of the α-heating in small steps thus allowing the tuning of the operational schemes to ensure that the plasmas obtained remain within the compatibility requirements for ITER operation in terms of power loads, NTM and sawtooth control, etc.; these will become more complex as the I_p and B_t and plasma heating power increase. As mentioned in the description of the overall plan in this phase, with increasing levels of α-particle specific issues related to their effect on plasma MHD stability, α-particle losses due to these effects and to the 3-D fields applied for ELM control as well as He exhaust may arise at this stage. If this occurs, specific experiments will be required at this stage to eliminate such possible deleterious effects or to mitigate them before proceeding to higher current levels. In particular the experimental results obtained for 12.5 MA/4.5 T plasmas at $\langle n_e \rangle \sim 0.5 \times n_{GW}$ will be crucial to determine the optimum way to proceed towards higher I_p/B_t in the next step as discussed in detail above.
- From 12.5 MA/4.5 T plasmas at $\langle n_e \rangle \sim 0.5 \times n_{GW}$, the range of low T concentrations that will be explored will be reduced because significant T-fractions (> 10%) may be required to both have an effect on the H-mode threshold and to provide α-heating for H-mode sustainment and W accumulation avoidance Within this reduced T concentration range two routes are considered feasible to proceed towards 15 MA/5.3 T, Q = 10 plasmas: one based on increasing I_p/B_t with $\langle n_e \rangle \sim 0.5 \times n_{GW}$ and the other with $\langle n_e \rangle \sim 0.7 - 0.9 \times n_{GW}$ that are described below. It is important to note that in both approaches it is required that scenario control is maintained in the q_{95} step (3.0 to 3.6) from 12.5 MA/4.5 T to 12.5 MA/5.3 T. Given that this is a variation of only 0.6 in q_{95} and the experience accumulated on H-mode control with varying q_{95} (i.e. ELM control by RMP fields, NTM control) at this stage, this is foreseen to be a feasible target but it is likely to require the use of the back-up ELM triggering scheme of pellet pacing to minimize the risks of this development.
- For option 1 ($\langle n_e \rangle \sim 0.5 \times n_{GW}$) better control of the H-mode scenario can be achieved with the additional heating, thus making the development less dependent on the optimization of α-heating in the next two higher I_p/B_t steps in the ladder (12.5 MA/5.3 T and 15 MA/5.3 T). This will allow a wider range of T concentrations to be explored and a more gradual increase of the α-heating, which is expected to ease the progress of experiments. Scenario control issues are expected to become more complex with increasing current and additional power levels as well as α-power production. At this phase (if already not materialized at 12.5 MA/4.5 T) it is expected that burning plasma physics processes will start to be dominant allowing both to tackle the issues related to scenario control for Q =10 plasmas as well as the burning plasma physics issues described in section 2.6.6. Similarly many ITER systems will start to operate near the maximum of their operational range (i.e. ELM control coils reaching maximum current capability, ECRH power sharing for NTM and W control maybe routinely required, etc.) and the need to control the DT mix will increase, as the range of T-fractions over which stationary H-modes can be sustained decreases with

increasing current. Every step upwards in additional heating power, T concentration and plasma current from 12.5 MA to 15 MA at ($<n_e> \sim 0.5 \times n_{GW}$) will require the development of a fully integrated H-mode scenario before proceeding to the next step, which is expected to require significant experimental time. In principle, this can be optimized by matching, as far as possible, the edge power flow level of the 12.5 MA plasmas with high T-fraction with that of the 15 MA plasmas with lower T-fractions. Once the 15 MA at ($<n_e> \sim 0.5 \times n_{GW}$) $Q \sim 5$ scenario has been achieved, the plasma density would be raised in small steps at a T-fraction of ~50% towards the final goal of $<n_e> \sim 0.85 \times n_{GW}$, $Q = 10$. This strategy is not foreseen to entail special difficulties regarding the sustainment of stationary H-mode conditions because the H-mode threshold in these DT conditions is expected to increase with $<n_e>^{0.72}$ while the α-heating power increases with $\sim <n_e>^{1.5}$ so that P_{tot}/P_{LH} increases with $<n_e>$. By choosing the number of steps to be ~ 5 one can ensure that the increase of α-heating from one plasma condition to the next one will be of not more than 20% (e.g. fusion power is expected to increase from 50 to 100 MW and thus 10 MW per step). Advancing from each step to the next one will require the development of a fully integrated H-mode scenario to account for the increase of edge power flow due to the α-heating, higher He exhaust required, changes to pedestal parameters and edge stability (increasing n_{ped} and decreasing T_{ped} etc.), increasing plasma β and possibly more strict requirements for NTM control etc. However, by choosing the density steps judiciously this development could be simplified, as the changes to plasma parameters, α-particle properties, etc., can potentially be made as gradual as required. Obviously, phenomena which only occur once a given physics threshold is exceeded (e.g. fast particle driven instabilities) in this process of increasing density and doubling α-heating from 15 MA, $Q = 5$ to $Q = 10$ will require dedicated fine-scan experiments for its study and avoidance or for the mitigation of its effects if required.

- For option 2 ($<n_e> \sim 0.7 - 0.9 \times n_{GW}$) careful build-up of the α-heating is required to ensure that appropriate margin of the edge power flow is maintained in each step to provide stationary H-mode operation; in this case the baseline additional heating is not expected to be sufficient to sustain stationary H-modes without α-heating. This implies the need for additional dedicated experiments to optimize DT mix control compared to option 1. For this type of scenario, the key issue for the access and exit from burning plasma conditions is the build-up/ramp-down of the α-heating with respect to that of the plasma density. A too fast density increase after the L-H transition can prevent the plasma from reaching stationary H-mode conditions as shown in Figure 2.6-7(a). Dedicated experimental time would be required in this option compared to option 1 to investigate and optimize the scenarios in this respect, as this option will most likely rely on H-mode access/exit in the current ramp-up/down. This will include optimization of the fuelling waveform and of the DT mix and the power waveform both for access/exit to H-mode in stationary conditions as well as during the current ramp-up/down (typically at $I_p = 2/3 \times I_p^{\text{flat-top}}$). Every step upwards from 12.5 MA to 15 MA in I_p, $<n_e>$, additional heating power, and T concentration (within the narrow range that will be explored) will require the development of a fully integrated H-mode scenario. Given the potential large increase of α-heating from 12.5 MA to 15 MA in DT plasmas at these high densities (a factor of ~ 2) it is likely that at least one intermediate current point at 13.8 MA will be required in this approach. The development of this option concludes with the achievement of 15 MA, $Q = 10$ plasma conditions with $<n_e> \sim 0.85 \times n_{GW}$ for ~50 s, as in the case for option 2.

Both options have advantages and disadvantages and which one will be chosen will depend both on the results of physics processes in ITER (pedestal characteristics and achievable H-mode performance in gas-fuelling dominated plasmas, robustness of stationary H-mode operation with ELM control for $P_{tot} \sim P_{LH}$, etc.), as well as on the efficiency of some control schemes versus others (e.g. efficiency and time response of DT mix control, efficiency of ELM control in varying plasma conditions, etc.). At present it is not possible to judge which one will be finally implemented.

On the other hand, there are many operational and physics issues which are common to both options. These have to do with the access to burning plasma conditions and the new physics research that this will allow, as well as the additional scenario integration issues that will have to be addressed. In both approaches experiments on burning plasmas will be performed at various levels of α-heating to refine schemes for burn control, transient high-Q phases (through additional heating step-down experiments) will be explored, if a robust scenario can be developed, to determine the behaviour of burning plasmas fully dominated by α-particles, etc.

Regarding scenario integration issues, it is important to note that by this stage of operation many of the ITER systems may have to operate near the maximum of their operational capabilities (i.e. ELM control coils reaching maximum current capability, ECRH power sharing for NTM and W control maybe routinely required, etc.). This is likely to require additional operational time to ensure that the scenario requirements can be matched by the hardware capabilities. Examples of this would be:

a) optimization of the rotation profiles by varying the power mix for minimum current requirements for ELM control, if the 12.5 MA experiments show that this would be marginal for 15 MA operation;

b) optimization of the power mix for W control, if the requirements for off-axis NTM control would not allow sufficient central ECRH power to be available for this mission;

c) re-optimization of the current ramp-up/down rate and the stationary H-mode phases, if it is found that flux consumption and/or AC losses in the PF coils are excessive, etc.

The precise scenario optimization experiments that will be implemented obviously depend on the physics results obtained and the limitations in the hardware which will be identified at this stage. The operational plan includes time to perform this type of experiments in order to ensure that the Q = 10, ~50 s goal is obtained within the allocated operational period of 180 days.

With the increasing α-heating production and plasma energy, the verification of key systems for Q = 10 operation will have to be carried out, including: the disruption mitigation system, the effects of neutrons on diagnostics, possible further calibration and cross-check of neutron diagnostics at higher neutron production rates as well as the measurements of the neutron heating of the superconducting coils with ~ 50 s pulses. This together with the determination of the AC losses is a key step before proceeding to longer high-Q pulses.

As mentioned above, it is likely that not all of the research under this item will be finished within the first operational campaign in FPO (i.e. the first 18 months of nuclear operation). The actual target for the first operational campaign is, therefore, the achievement of several hundred (200-300) megawatts of fusion power for ~ 50 s with Q ~ 5. The plasma scenario in which this will be achieved will depend on which of the two options discussed above is selected in the final implementation of the Research Plan.

2.6.4.3.1 Risk to the optimization of fusion power in DT plasma scenarios towards 15 MA/5.3 T Q = 10 (~ 50 s) demonstration

By this stage of the operational plan many of the general risks to the achievement of the ITER Q = 10 goal may materialize. These are general to the project goals and are discussed in Appendix J. Below we discuss the specific risks that can affect the operational plan in this phase:

- *H-mode confinement insufficient when integrated with ELM control by 3-D fields with in-vessel coils (plus pellet pacing) to achieve Q = 10 or ELM control capability is insufficient for 15 MA due to hardware limitations.* This would require a reformulation of the research program above the plasma current level on which either of these two issues is identified. Possible mitigation strategies would consist of: a) switching to the hybrid/advanced scenario development at this stage and proceed to its optimization for Q > 5 and/or b) to proceed to develop other high confinement regimes ELM-less regimes such as QH-mode or I-mode at this stage. This can make use of the existing systems (e.g. ELM control coils in non-resonant mode to control edge rotation for the QH-mode) but may also require hardware upgrades to be implemented. In the latter case, this would be a major strategic decision for the project to take at this stage which will need appropriate justification by dedicated experiments to be performed in this phase.
- *Predictive and interpretative modelling of particle and thermal transport through the core to the edge, and of α-particle behaviour required to develop the scenarios and burn control within them are not mature enough.* This will require the progress of the experimental program to be based mostly on an empirical basis and, thus, slower progress of the research as the steps in I_p/B_t, additional heating level, T-fraction, etc., may have to be smaller than strictly required in order to ensure that the plasma in the scenarios remain integrated with the operational/hardware constraints and MHD stable to ensure low disruptivity.
- *Tritium throughput provided by the T-Plant not sufficient at the beginning of the experimental phase.* Although it is expected that the T plant will be able to provide the required throughput to sustain Q = 10, ~50 s operation by the end of this operational phase, it may not be able to provide the required throughput at the beginning when 9.5 MA and 12.5 MA DT plasmas with high T-fraction are foreseen to be explored. Depending on the actual limitations, various mitigation strategies could be used. One is to develop these plasma scenarios only at low T-fractions first and then at higher T-fractions (the present plan is sequential in I_p and for each I_p step the T-fraction is scanned). The other would be to proceed with the present plan as it is but shorten the burn length by a factor of ~ 2 (25 s would still provide pulses ~ $10\times\tau_E$ long). The drawback of the latter option is that particle transport timescales maybe longer than the duration of the stationary H-mode phase and some experiments would need to be repeated later with longer burn lengths to ensure that the findings reached with shorter burn lengths remain valid.
- *Nuclear heating and/or AC losses of the superconducting coils are found to be much larger than expectations.* It is only during this phase that the final levels of several hundreds of megawatts of nuclear heating expected in high-Q experiments will be reached, together with high current operation in the relevant conditions for high-Q long-pulse scenarios, to allow these issues to be quantitatively evaluated. It is not expected that such findings would limit operation at this phase due to the short burn length of ~50 s. However, as already mentioned above, such findings would require additional scenario development before attempting long-pulse Q ~ 5 plasmas. Given that nuclear heating of the superconducting coils can only be reduced by decreasing neutron production, the additional development of the scenarios

should focus on reducing AC losses either by optimization of the scenario itself or of the control schemes.

- *Flux swing provided by the CS/PF system marginal for H-mode operation at 15 MA.* Although the L-mode operation at 15 MA would have already provided some indications if flux swing would be an issue, it is only in this phase when a realistic evaluation of the flux consumption of the complete H-mode scenario, including the burn access and burn exit phases, will be available. If it would be found out that the flux swing is marginal for 15 MA Q = 10, 300 – 500 s operation, further optimization studies of the scenario will be required at this stage. Part of these studies are already included in the research plan for this phase (e.g. access/exit from H-mode at $2/3 \times I_p^{flat\text{-}top}$) but they should probably be expanded with the specific target to further decrease flux consumption in the burn access/exit phases.

2.6.4.3.2 Deliverables for the optimization of fusion power in DT plasma scenarios towards 15 MA/5.3 T, Q = 10 (~ 50 s) demonstration

The main deliverables from this operational phase are:

- H-mode plasma scenarios over a range of I_p = 12.5 – 15 MA and q_{95} = 3.0 – 3.6 delivering hundreds of megawatts of fusion power integrated with all ITER operational requirements and with demonstrated burn control for periods of ~ 50 s. These are important not only with a view to develop the next phase of the Q = 10 scenario towards 300 - 500s burn length, but also for the development of the Q = 5, t_{burn} > 1000 s scenarios;
- The Q =10 H-mode plasma scenario at I_p = 15 MA and q_{95} = 3.0 delivering 500 MW fusion power integrated with all ITER operational requirements and with demonstrated burn control for periods of ~ 50 s, essential for the development of the next phase of the Q = 10 scenario towards 300 – 500 s;
- First results of plasma behaviour in burning conditions allowing the identification of the physics processes that control this behaviour and the validation/development of models to be used in the further development of burning plasmas scenarios in ITER and for the interpretation of the required diagnostics measurements;
- First results of the TBMs operating at relevant neutron fluxes for high-Q operation (although at reduced fluences);
- First assessment of the nuclear heating of the superconducting coils at the levels of several hundreds of megawatts and of the AC losses for a range of plasma scenarios expanding a current range of I_p = 12.5 – 15 MA, which provide key information for the further development of the Q = 10 scenario towards 300 – 500 s burn length and of the Q = 5, t_{burn} > 1000 s scenarios.

2.6.4.4 Extension of the Q = 10 scenario towards long-pulse inductive operation (300 – 500 s) (100 days)

After the capability to achieve Q = 10 burning plasma conditions at 15 MA has been demonstrated for ~50s, the plasma discharges will be developed towards longer durations of 300 - 500s, which is expected to require 100 operational days. This experimental campaign will not only include the development of the Q = 10 scenario to long pulse length, but also assessments of long-pulse operation at a range of Q-values and specific experiments to achieve Q > 10. Obviously, as the pulses become longer additional technical issues will arise such as those related to handling of

exceptions by the control system and the control of the plasma termination will become more complex, as the central solenoid will be operating near its flux swing limit in this phase. While the Q = 10, t_{burn} ~ 50 s will have provided demonstration of scenario integration with many processes related to power deposition control, α-particle physics, thermal and particle transport, DT mix control, etc., there are processes in ITER which are expected to develop on longer timescales such as:

- MHD-related processes determined by the shape of the current profile, which could lead to the triggering of tearing modes, Alfvén Eigenmodes, etc., as the current profile changes shape during the burn phase. This is expected to take from 100 s to 1000 s to reach its final shape depending on whether the central part of the plasma or the whole plasma is considered as shown in Figure 2.6-8;
- Anomalous transport processes which are influenced by the evolving current profile shape. The evolving magnetic shear can lead to the onset or change of intensity of turbulent transport, as shown in Figure 2.6-9 for ITER integrated plasma simulations [Parail, 2013];
- Processes controlled by neoclassical particle transport, particularly in the central plasma region where anomalous transport is low. The values of the neoclassical transport coefficients both for D, T as well as for W are very low for 15 MA/5.3 T plasmas, as shown in Figure 2.6-10 [Loarte, 2015; Loarte, 2016]. This implies that the typical time evolution for the DT and W profiles in the central plasma region is of the order of several tens of seconds and that they may not have reached the fully relaxed conditions in the ~ 50 s burn foreseen for the previous experimental phase;
- Other physics processes whose development time could be of the order of tens of seconds. This could be, for example, sawteeth which are expected to have repetition periods of ~ 50 s [Hender, 2007], as shown in Figure 2.6-11 and can be stabilized by fast particles in ITER.

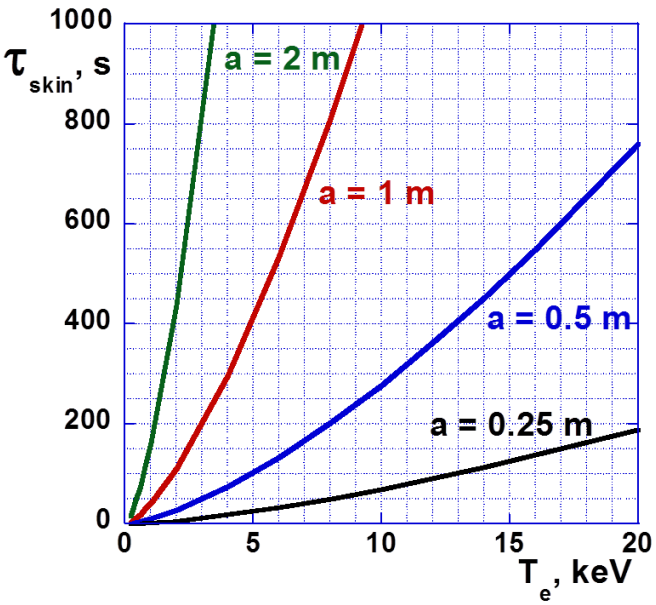

Figure 2.6-8: Current relaxation time, as characterized by the skin time ($\boldsymbol{\tau_{skin}} = \boldsymbol{\mu_0 \frac{a^2}{\rho_{\parallel}}}$, $\boldsymbol{Z_{eff} = 1.2}$, with Spitzer resistivity) versus plasma radius for a range of electron temperatures in ITER.

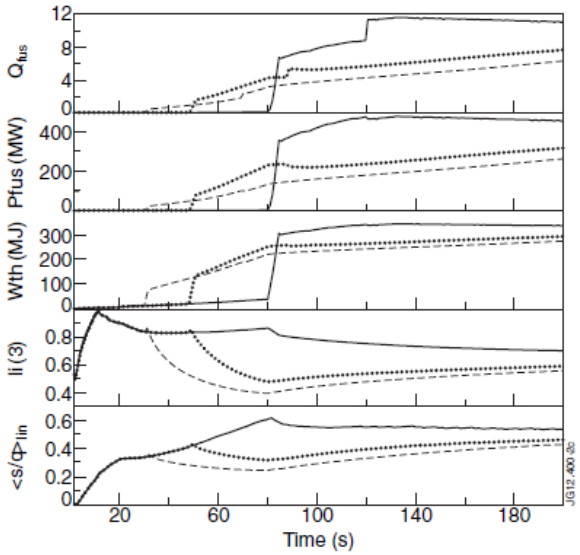

Figure 2.6-9: From top to bottom: fusion Q, P_{fus}, W_{th}, $l_i(3)$ and line-averaged s/q ratio for ITER JINTRAC simulations of the entrance to burn including: a reference case with the L–H transition at 15 MA (solid), and two simulation cases with early L–H transition at 10MA (dotted) and 7MA (dashed), showing the long-term evolution of the fusion power over time scales exceeding 50s as the current profile shape relaxes. In the latter case a Greenwald density fraction of 60% was applied to avoid the NB shine-through limit after the transition.

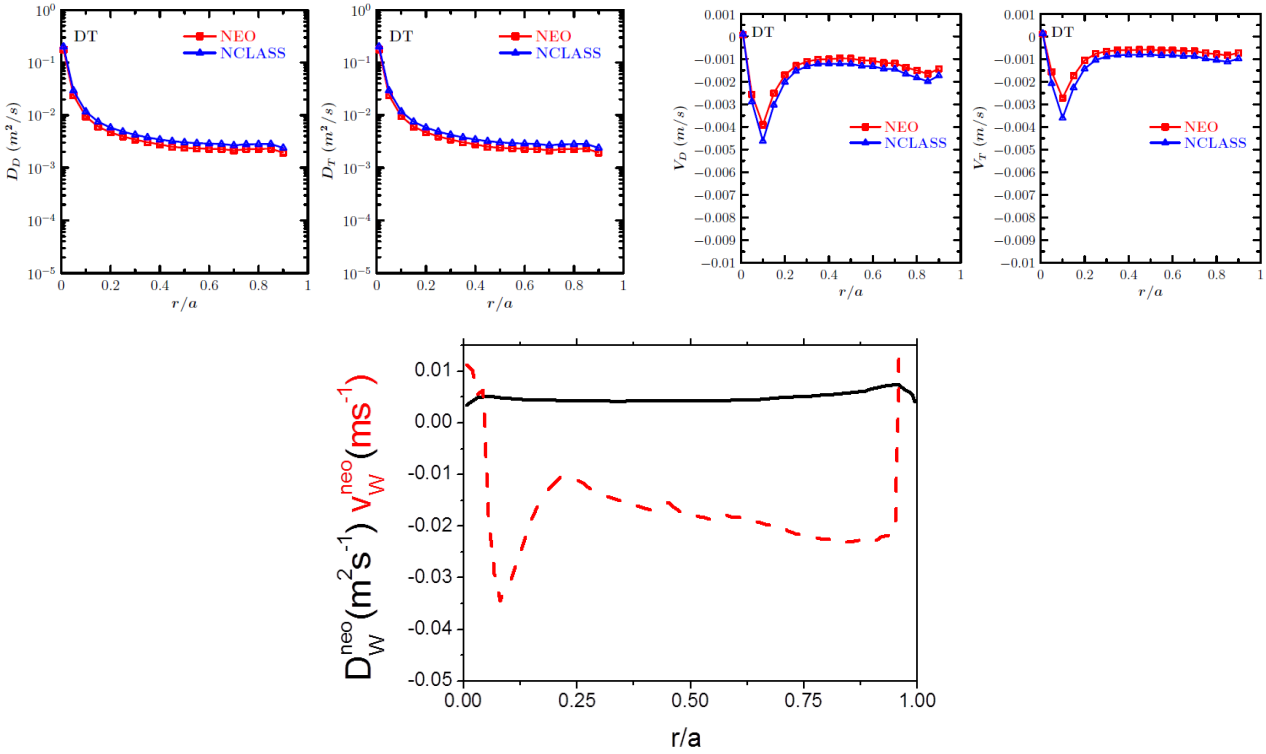

Figure 2.6-10: top: Neoclassical diffusion coefficients and pinch velocities for D and T in calculated by NCLASS and NEO; bottom: Neoclassical diffusion coefficient and pinch velocity for W calculated by NCLASS. Both D-T and W coefficients are for 15 MA/5.3 T Q = 10 plasmas.

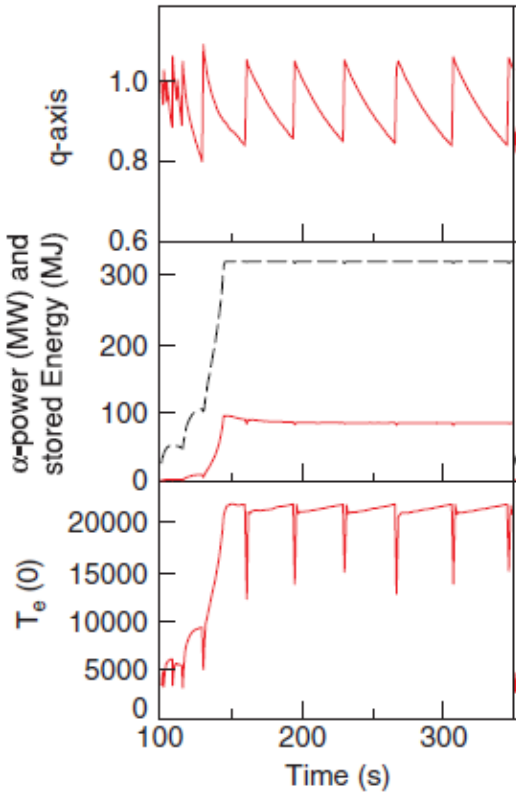

Figure 2.6-11: ITER simulations using the GLF23 transport model and the complete reconnection model for the sawteeth. The top frames show the axial q value, in the middle frames the α-power is the solid line and stored energy the broken line, and the bottom frames show the axial temperature [Hender, 2007].

Processes related to long time scale evolution of plasma-wall interactions seen in present experiments are unlikely in ITER due to the fact that particle/power fluxes are much larger than in present experiments and to the fact that the vessel and all in-vessel components are water cooled; the typical timescales for in-vessel components to reach thermal equilibrium is few seconds. However, there could be additional issues such as building up of thick co-deposited beryllium layers for longer pulses that could lead to their overheating and/or detachment for Q = 10, t_{burn} = 300 – 500 s pulses, which are less likely to occur for the ~50 s pulses, and may pose specific operational issues when the burn length is extended.

To ensure that these processes and other operational limitations do not increase the likelihood of disruptions, the extension of the burn length will be done gradually (e.g. in steps of ~ 50 s) and most likely starting with a lower value of Q. For instance, Q = 5 could be obtained by operation with $\langle n_e \rangle = 0.5 \times n_{GW}$ for 15 MA/5.3 T or for higher $\langle n_e \rangle$ if T-fractions higher than 50% are used (lower T-fractions would not allow H-mode operation for 15 MA/5.3 T due to the higher H-mode threshold). Given the lower Q, plasma behaviour can be more effectively controlled with the H&CD actuators than for Q = 10. Once the Q = 5 scenario is demonstrated for a given burn length, the Q = 10 scenario with the same burn length will be developed and the process will be repeated until the Q = 10 burn length reaches 300 – 500 s. In parallel with these experiments, assessment of the burning plasma physics processes described in section 2.6.6 and dedicated experiments to characterize them will be performed.

This operational period will conclude with a series of experiments to attempt increasing fusion performance above Q = 10 during transients and during stationary phases taking advantage of the

ITER H&CD flexibility and the favourable interaction of fast particle pressure with edge stability through the increased Shafranov shift (and possibly through a direct influence on anomalous transport) [Garcia, 2015; Urano, 2016]. By this time of the operational plan the tritium throughput from the tritium plan will have reach its peak and tritium retention and removal will have become a routine part of ITER operation. Therefore, it is foreseen that in parallel with the experimental program, diagnosis of T retention will be done routinely and that T removal schemes between discharges, overnight and/or over routine maintenance or operational breaks, and/or specific phases of the discharge designed to remove the trapped tritium will be routinely implemented as part of the ITER operation cycle.

Consistent with the above global description the main experimental activities during this phase of the experimental plan will be:

- Starting at 15 MA/5.3 T, Q = 5 with ~50 s burn, the burn duration will be increased by ~50-100 s and a full integrated scenario demonstrated. This includes control of stationary and ELM-related power fluxes, pumping, DT mix, burn control, He exhaust, MHD stability, etc., over the longer timescales.
- Once this is achieved, the same scenario will be repeated for Q = 10 and the necessary retuning of the actuators will be implemented. This sequence will be repeated until Q = 10 for 300 – 500 s is achieved. With increasing burn length flux consumption will be monitored to ensure that there is enough current margin in the solenoid to provide a robust (i.e. disruption-free) termination of the burn phase and of the discharge as a whole. This is likely to require re-optimization of the entry-to and exit-from burn phases of the discharge and possibly of the L-mode ramp-up/down phases that will have to be performed before the longest burn Q = 10 pulses are attempted.
- In parallel, or within the above research activity, specific experiments will be performed. These will deal with specific control aspects of burning plasmas over long time scales as well as with the characterization of burning plasma physics phenomena. If deleterious physics effects, as those described above, appear when the pulses extend over long time scales, specific experiments will be required to mitigate their effects. These could consist of experiments to control the evolution of the current profile by local heating and/or current drive to avoid MHD instabilities, use of H&CD to affect core particle transport and avoid W accumulation, use of the H&CD systems to modify the fast particle distributions and/or the current profile shape/local plasma parameters to prevent the growth of Alfvén Eigenmode instabilities, implementation of specially designed D phases within the high-Q discharges (or special D discharges between high-Q discharges) to remove the retained T, etc.
- This experimental period will conclude with attempts to achieve $Q > 10$ plasmas at 15 MA/5.3 T. This could be done during transient phases which are expected to last several τ_E (i.e. tens of seconds at most) by gradually decreasing the additional heating power or by using the flexibility of the ITER H&CD systems to improve fusion performance in stationary conditions. One such experiment would consist of the use of He^3 minority for ICRF heating during the burn (this is presently foreseen only for H-mode access/exit in view of the high He^3 consumption expected in ITER). This is expected to increase the level of central ion heating thus increasing core reactivity and Q (up to $\Delta Q = 1.5$ is expected from this effect [Wagner, 2010]). Other experiments are foreseen to focus on the optimization of the favourable interlink between Shafranov shift and edge stability leading to improved plasmas confinement, which is seen in present experiments. The flexibility of the ITER H&CD systems can be applied to maximize the central fast particle pressure (e.g. by

injecting the beams as close to the plasma centre as possible) and thus Shafranov shift, which can then lead to improved confinement and Q > 10 plasmas in ITER. To which level this is possible without triggering fast particle-driven MHD instabilities in ITER will have to be demonstrated. It is also likely that by this stage of the experimental program other ideas regarding the optimization of H-mode confinement and fusion performance in ITER will have emerged and these will be exploited as well, before concluding this experimental phase.

After this operational phase is completed, the experimental program will more strongly focus on the Q = 5, t_{burn} > 1000 s ITER objective. In this subsequent operational phases, additional inductive Q = 10 experiments will certainly be performed to assess specific burning plasma issues and, possibly, to provide high neutron fluence for TBM-dedicated experiments. However, in terms of scenario development, the emphasis will shift towards ITER's Q = 5 goals and the need to achieve H_{98} > 1 confinement with a significant fraction of driven current, as described in section 2.6.5.

2.6.4.4.1 Risks and deliverable from the experimental phase to extend the Q = 10 scenario towards long-pulse inductive operation (300 – 500 s)

The risks for this experimental phase have either been described in section 2.6.4.3.1 or form part of the overall risks of ITER to achieve its goals, which are described in Appendix J.

The main deliverables for this phase are:

- Demonstration of robust and integrated H-mode scenarios to achieve Q = 5 and Q = 10 operation for 300 – 500 s, thus achieving the ITER inductive goal;
- Determination and control of physics processes taking place in burning plasmas in time scales of hundreds of seconds. This is important both for the achievement of the Q = 10 inductive goal as well as for the further development of t_{burn} > 1000 s, Q = 5 scenarios;
- First thorough exploration of burning plasma physics processes in ITER and its control aspects over long timescales;
- Demonstration of Q > 10 operation over short and (if experiments are successful) long time scales;
- Demonstration of routine operation with acceptable T retention over long pulses and operational periods at high T throughput;
- Testing of the TBMs at high neutron fluxes and fluences.

2.6.5 Operational plan for hybrid/non-inductive DT plasma experiments

2.6.5.1 Summary of scenarios and overall objectives

The data obtained during the first FPO campaign will allow an initial assessment of the most favourable path towards long-pulse and steady-state operation. Based on this assessment, the next step will be to extend the chosen scenarios towards long-pulse operation (q_{95} = 4 hybrid) up to 1000 s and steady-state operation (q_{95} = 5) up to 3000 s. While fusion performance will be a consideration at this point, the overriding consideration will be given to demonstrating long-pulse operation. Once long-pulse, high-β_N operation has been demonstrated (target 1000 s, high non-inductive fraction $f_{NI} \geq 0.6$, Q ~ 5). The research program will focus on demonstrating steady-state fully non-inductive operation (target 3000 s, f_{NI} = 1.0, optimized Q with Q $\geq$ 2 target).

The achievement of the final high-Q long-pulse and steady-state goals will require the optimization of plasma energy confinement together with driven current (by bootstrap current and external current drive) while ensuring MHD plasma stability and plasma edge compatibility. The requirements for high energy confinement are less demanding for long-pulse operation (i.e. with non-inductive current fraction $f_{NI} < 1$) at high plasma currents. The long-pulse Q = 5, 1000 s goal is expected to be achievable (and possibly exceeded in terms of burn length) for $H_{98} \sim 1.0$-1.1 in ITER with I_p in the range 13 to 15 MA ($q_{95} \sim 3.5$-3) [Polevoi, 2015] and low average densities ($\langle n_e \rangle \sim 0.5 \times n_G$), as shown in Figure 2.6-12 [Luce, 2014]. Long-pulse operation at lower currents ~ 11 MA ($q_{95} \sim 4$) requires higher plasma density operation and is more demanding with regards to energy confinement ($H_{98} \sim 1.3$), requiring confinement values which are typical for 'hybrid scenarios' at $q_{95} \sim 4$ in present tokamaks [Luce, 2014]. Thus the development path of the long-pulse Q = 5 scenario will have to explore the trade-off between the level of plasma current and energy confinement that can be achieved in ITER. This will finally determine whether the 'hybrid' approach or the low density 'conventional' H-mode approach will be more suitable in achieving this goal. In this section we consider the development path of the hybrid approach towards the Q = 5 long-pulse goal as this has more synergies with the development path for the Q = 5 steady-state goal, which requires lower plasma current operation with high energy confinement in order to ensure $f_{NI} = 1.0$.

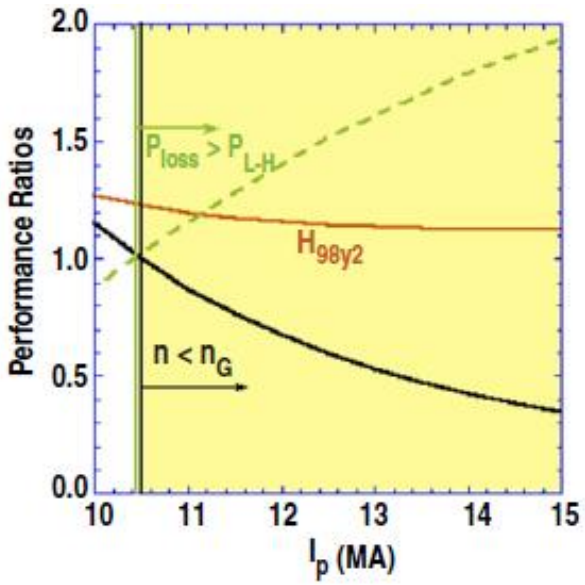

Figure 2.6-12: ITER operational space diagram for advanced inductive operation at the nominal ITER toroidal field of B = 5.3 T with P_{aux} = 50 MW and burn duration of 3000 s. The black curve is the ratio of the density to the Greenwald value, the green curve is the ratio of the loss power to the predicted L–H threshold power, and the red curve is the confinement quality measured by the H-mode scaling [Luce, 2014].

The development path for the Q = 5 steady-state goal ($f_{NI} = 1.0$) is subject to larger uncertainties associated with the achievable energy confinement, core density peaking (key to generating core bootstrap current), edge MHD stability (key to providing high energy confinement and pedestal bootstrap current) and achievable current drive. Figure 2.6-13 shows, as an example, the steady-state scenarios that can potentially be explored in ITER for 50 MW of additional heating and current drive power (33 MW NBI plus 17 MW of ECRH) and a core density peaking factor of 1.3, assuming that the required energy confinement can be achieved. As shown in this figure the achievement of Q = 5 requires $H_{98} \geq 1.7$ and I_p = 8.2-9.1 MA at this power level, while Q = 2.5 can be achieved for I_p = 9 MA in steady-state for H_{98} = 1.4 under these conditions. A more detailed review of the sensitivity of the Q = 5 steady-state scenario to transport, density peaking factor, and heating and current drive power levels and schemes is provided in Appendix E.

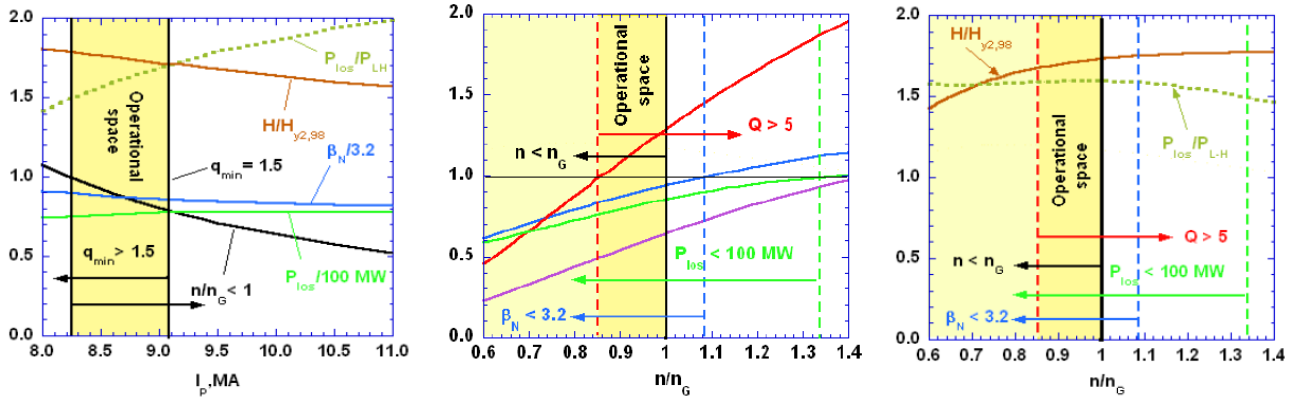

Figure 2.6-13: ITER steady-state operational space with 33 MW of NBI and 17 MW of ECRH and density peaking of 1.3: a) at prescribed Q=5; b) and c) at prescibed plasma current, I_p =9 MA [Polevoi, 2010].

Therefore, the experimental program in this phase will explore systematic variations of main plasma parameters (e.g., density, plasma current, applied heating, current profile) and the edge conditions required for core-edge integration (e.g. divertor radiation for stationary power load control, ELM control, etc.) will be utilized to optimize performance (core and edge integration) towards the goal of fully non-inductive operation. During these scans, the control techniques developed previously in PFPO-2 and earlier in FPO will need to be adjusted in each case to optimize the control algorithms for the specific plasma conditions. Significant time will be required during this phase to optimize confinement and real-time MHD stability control in order to sustain operation near MHD stability boundaries.

At this point in the Research Plan, the main Q = 10 performance objective will have been obtained, and it is envisioned that an extended operational period of several years will be available for long-pulse/ steady-state research. In addition, the required upgrades for the heating and current drive systems and plasma control systems (e.g. RWM) that have been identified in earlier phases of the Research Plan will have been implemented and available for use in the development of the scenarios. The estimated operational time and overall research activities that will be performed in this period are:

- Application of β/current/pressure profile control algorithms using target current profiles in stationary DT discharges: **25 days dedicated, synergies with work in other DT experiments.** This research can, in principle, be carried out at any time within the Q = 10 DT development program in FPO, if difficulties in developing that scenario are encountered;
- Optimization of non-inductive current drive in 2.65 T discharges at $q_{95} \sim 4$ (hybrids) and assessment of the influence of isotope (D versus DT): **25 days.** This research can, in principle, be carried out at any time within the Q = 10 DT development program in FPO, if difficulties in developing that scenario are encountered;
- Optimization of non-inductive current drive in 5.3 T discharges at $q_{95} \sim 4$ (hybrids): **125 days.** This research can, in principle, be carried out at any time within the Q = 10 DT development program in FPO, if difficulties in developing that scenario are encountered;
- Optimization of performance (with target Q ~ 5) and discharge length (up to 1000 s) in long-pulse full-field hybrids (q_{95} = 4): **100 days;**
- Demonstration of 3000 s, $q_{95} \geq 5$ steady-state (fully non-inductive) plasma with Q ~ 2: **100 days;**

- Optimization of 3000 s, $q_{95} \geq 5$ steady-state (fully non-inductive) plasma with target Q ~ 5): **200 days.**

The major research focus within this phase will be given to the optimization of the core-pedestal coupling following on the initial results of FPO on this issue and its integration with the ITER metallic wall. This will include the assessment of the role of fast particles and plasma rotation on the virtuous feedback loop between core and pedestal for high-β_N ITER plasmas with a large fraction of fusion-born fast α-particles [Garcia, 2015]. In synchrony with this, significant efforts to understand and optimize/control MHD instabilities triggered by fast particles and to reduce fast particle losses (by MHD instabilities or non-axisymmetric magnetic field effects) are likely to be required at this stage.

It is important to note that, should the long-pulse, high-β_N operation (target 1000 s, high non-inductive fraction, $f_{NI} \geq 0.6$, Q ~ 5) development encounter insurmountable difficulties, there exist alternatives to achieve the 1000 s, Q = 5 goal that do not require a very high inductive current drive fraction or enhanced confinement ($H_{98} > 1$), assuming that the remaining pedestal physics issues are resolved satisfactorily. These are based on the $\langle n_e \rangle = 0.5 \times n_{GW}$ approach discussed in section 2.6.4.3 and are a natural extension of the Q = 10 scenario to lower densities and, therefore, to higher plasma temperatures, implying lower resistive flux consumption. Although this is a less attractive option from the perspective of fusion energy development towards Demo, it remains a viable approach to the achievement of the 1000 s, Q = 5 goal in ITER.

2.6.5.2 Risks to operational plan for hybrid/non-inductive DT plasma experiments

These long-pulse and steady-state scenarios require fully integrated capabilities, and the lack of any of these would affect the accomplishment of this aspect of the project's mission goals. In addition to the general risks to the Q = 5 long-pulse and steady-state goals registered in Appendix J, the major specific risk for this operation phase is that the scenarios developed for D (particularly in the ramp-up phase) may not be viable for DT due to the different H-mode power threshold, as observed in JET [Söldner, 1999]. An important issue could arise if the heating and current drive requirements to establish the required target current profiles at the end of the ramp-up are incompatible with the required plasma confinement regime in the plasma ramp-up, e.g. if the ramp-up scenarios should require L-mode confinement to achieve a given j(r), but the required H&CD level during the ramp were to cause the plasma to enter the H-mode. If this risk materialized, then specific additional studies, e.g. to prevent access to the H-mode regime to ensure a successful j(r) target at the end of the current ramp-up, would be required at this stage.

2.6.5.3 Experimental plan to develop DT scenarios for long-pulse hybrid and steady-state operation with high fusion power production

The ultimate objectives during the DT campaign are: 1) to develop hybrid, $q_{95} = 4$ scenarios with pulse lengths of up to 1000 s having high fusion performance (target Q-values of up to 5) and non-inductive current drive fractions above 60%; 2) to develop fully non-inductive steady-state discharges, probably with $q_{95} \geq 5$, having pulse lengths of up to 3000 s (of the order of the magnetic flux diffusion time) with target Q-values of up to 5.

To provide a detailed experimental program for the achievement of these goals to the same level of that for Q = 10 (section 2.6.4) is not possible at this stage of the project because such details will depend critically on the research results of previous operational phases (PFPO-2 and the initial phase of FPO) and on the upgrades of the H&CD and other control systems (e.g. power supplies for

RWM control) that should have been implemented in preparation for addressing these elements of the Research Plan.

On the basis of the present analysis of long-pulse operation for ITER (see Appendix E for details), the experimental program needs to develop self-consistent scenarios, in terms of core and edge plasma confinement (e.g. pedestal MHD stability), and which also satisfy the constraints on core and global MHD stability, in order to achieve the project's mission goals. This will need to be achieved by the adjustment and control of the plasma current and pressure profiles using the available H&CD actuators and by exploitation of RWM stabilization. These scenarios will have to be established while satisfying the common requirements for ITER scenarios regarding core-edge integration (radiative divertor operation, ELM control, impurity exhaust) – these requirements are expected to give rise to specific issues associated with these novel scenarios due to the high edge power flows and the lower plasma currents and plasma densities that are expected. Similarly, fast particle physics and the control of the associated MHD instabilities may require substantial experimental time, as the proportion of fast particles in these plasma and their contribution to the total plasma pressure are expected to be larger than in the intermediate steps towards the Q = 10 goal described in section 2.6.4. This is due to the larger values of the ratio $P_{heat}/\langle n_e \rangle$ for the long-pulse high-Q scenarios compared to conventional H-modes at similar I_p: an increase in $P_{heat}/\langle n_e \rangle$ should increase β_N and enhance plasma confinement (by the favourable core/pedestal feedback loop generating improved confinement) and provide the current drive needed for long-pulse operation.

Although the experimental program to achieve the ITER high-Q long-pulse goals cannot be defined in detail at this stage, it is anticipated that it will consist of the development of a series of DT plasma scenarios at various levels of plasma current and field towards the final ITER goals. In many of these plasma scenarios (particularly at low values of plasma current), the value of Q will be low, so that the influence of α-particles on the scenarios themselves is not expected to be significant. This allows better control of the plasma behaviour by external actuators in the development of these scenarios but, on the other hand, implies that the effects of significant α-particle heating/fast α-particle densities may only be identified rather abruptly in the final steps of scenario development when the highest Q (~5) will be achieved. This can potentially increase the risk of disruptions at high levels of plasma energy, if core modes are destabilized by the increased α-pressure, and so may require significant scenario redevelopment/retuning in the last steps to achieve the high Q; the outline experimental program discussed below is intended to mitigate such deleterious effects.

At this stage of the operational program, it is assumed that the target current profiles for these scenarios, which require tuning of the current ramp-up phase (additional heating power, plasma density, ramp-up rate, etc.), have already been developed in the previous phases of FPO. If this is not the case or additional issues appear when the T concentration is increased, additional time will be required to address these issues; this is not included in the experimental plan below.

The outline experimental plan for the achievement of the ITER long-pulse scenario, Q = 5 goals is expected to be developed according to the following steps and research objectives:

- *Development and demonstration of β/current/pressure profile control algorithms using target current profiles in stationary DT discharges (25 days):*

The aim of the experiments will be to develop and demonstrate control algorithms with the available actuators (H&CD, fuelling, etc.) to control total plasma pressure and current/pressure profiles in DT plasmas for the range of plasma currents and magnetic fields foreseen in the development path of the ITER high-Q, long-pulse scenarios. These experiments will be performed

in plasmas with optimized target current profiles at the end of the ramp-up and will focus on the control aspects themselves, rather than on the optimization of plasma confinement and pulse duration. This research has synergies with other experiments in the DT program and could, in principle, be carried out at any time in the FPO program together with the Q = 10 development. However, as the actuators for these experiments at this stage of the experimental plan are likely to have improved capabilities and/or versatility as result of H&CD upgrades, it is considered more appropriate to carry out these experiments once a substantial research activity towards the achievement of the long-pulse, high-Q ITER goals is launched.

- *Optimization of non-inductive current drive in 2.65 T discharges at $q_{95} \sim 4$ (hybrids) and assessment of the influence of isotope (D versus DT) in hybrid plasmas (25 days):*

The 5.6 MA/2.65 T hybrid plasmas will have been developed during the D phase in FPO, and they will serve as a basis for assessing the influence of the isotopic mix on discharge development during the DT phase, which will be very important for the follow-up development at higher toroidal fields. The experiments will explore a range of D/T ratios (while demonstrating mix control), plasma densities and H&CD mixes, and will aim to optimize current drive and overall plasma confinement for 2.65 T hybrid plasmas. The low value for the minimum density for acceptable shine-through loads in DT ($\sim 2.5\times10^{19}$ m^{-3}) allows unrestricted application of NBI H&CD for $\langle n_e \rangle / n_{GW} > 0.6$ in these plasmas, facilitating the achievement of very large current drive fractions even with moderate H-mode like energy confinement, although generating current profiles which may pose issues for MHD stability (including fast particle effects). This, together with the use of ECRH for heating and current drive and, possibly, ICRF for plasma heating, will allow systematic studies of current drive and an initial assessment of the influence of fast particles and plasma rotation on the enhancement over H-mode confinement that may be achievable in ITER in hybrid plasmas. Due to the relatively low level of plasma current in these plasmas, it is expected that the edge integration aspects (divertor power loads, W source and transport control, ELM control, etc.) will pose moderate demands on the development of these scenarios, although especially dedicated experiments may be required for the highest levels of additional heating and the lowest densities explored. Similarly, the effects of α-particle heating/fast α-particles in these plasmas are expected to be small due to the low values of Q expected; on the other hand, the influence of fast particles generated by the heating systems (NBI and ICRF) may be significant.

- *Optimization of non-inductive current drive in 5.3 T discharges at $q_{95} \sim 4$ (hybrids) (125 days):*

These experiments will extend the experience gained in 5.6 MA/2.65 T plasmas to ~ 11.2 MA/5.3 T plasmas. Although the emphasis in this program will be on optimizing current drive at the levels of plasma current and toroidal fields required for the high-Q, 1000s pulse goal in ITER, the experiments in this phase will also perform an initial assessment to determine whether the findings regarding H-mode confinement optimization for hybrid plasmas at 2.65 T also apply at 5.3 T. It is important to note that the hybrid experiments for 5.3 T plasmas are expected to be significantly more complex than those at 2.65 T and thus will require more experimental time due to the following issues:

a) Operational experience of hybrid plasmas 11.2 MA/5.3 T in D is unlikely to be available, as hybrid operation is only foreseen up to 9.5 MA/4.5 T plasmas in D, due to H-mode access issues. Therefore an intermediate step at 4.5 T with DT plasmas will be required before exploring these plasma conditions in DT at 5.3 T;

b) Due to the higher plasma currents, toroidal fields and additional heating levels, the edge integration issues (divertor power loads, W source and transport control, ELM control, etc.)

will have to be addressed as an integral part of the scenario development; in addition to requiring additional experimental time, this may limit exploration of current drive at the highest plasma temperatures, emulating conditions expected for Q ~ 5 conditions in this scenario, which require low density operation;

c) The α-heating expected in these experiments, although much smaller than the additional heating, may already be significant ($Q \geq 2$) and influence the development of the experiments themselves (e.g. triggering fast particle MHD instabilities that decrease current drive efficiency). This may impose restrictions on the range of DT isotopic mixes in which current drive efficiency can be explored and/or may have implications for the strategy followed in varying the isotope mix.

- Optimization of performance (with target Q ~ 5) and discharge length (up to 1000 s) in long-pulse full-field hybrids (q_{95} ~ 4) (100 days):

This experimental phase will concentrate on the achievement of the ITER 1000 s, Q = 5 goal. To a large degree, the development of scenarios to achieve this goal will be based on the results of the previous step at 11.2 MA. The experimental results in the 11.2 MA step will indicate the plasma current level at which the Q = 5 goal is most likely to be achieved; this will depend on the level of energy confinement and current drive efficiency achieved, as well as on possible (deleterious) MHD-related effects. An important aspect of the scenario development and performance optimization is to avoid large changes in Q from one experimental step to the next to ensure a gradual tuning of the edge integration and MHD control schemes as plasma fusion performance is increased. In this respect, it is important to note that the hybrid scenario plasmas can be subject to positive feedback loops between core and pedestal confinement driven by α-particle heating/ fast-α β that can potentially lead to significant increments in Q when the scenario is being developed towards higher values of Q. Maintaining overall plasma control while sustaining fusion power production under such conditions will have to be developed and demonstrated. Depending on the findings of the previous experimental step, two strategies can be considered to reach the Q = 5, 1000 s goal:

a) To develop a high confinement, MHD-stable (most likely by active control), fully integrated and controlled scenario with DT plasmas and long burn (>1000 s) at 9.5 MA/4.5 T with the highest achievable Q, and subsequently to proceed to the development of the equivalent scenario at 11.2 MA/5.3 T to demonstrate the final Q = 5, 1000 s goal; or

b) To develop an optimized scenario by initiating the development at 11.2 MA/5.3 T, or even higher current (depending on the previous findings), with the necessary adjustment of MHD control, edge integration schemes, etc., as the burn length and fusion performance increase.

Whether the final experimental path to the Q = 5 goal will follow one or other path, or a combination of the two, cannot be foreseen at present. As described above, an important operational issue that may be encountered in such development paths is that of significant changes in Q from one step to the next due to the occurrence of a positive feedback loop between core confinement and edge pedestal stability as fusion performance increases. One approach to avoiding these potentially large increments in Q is to optimize the scenarios first in T-rich plasmas, taking advantage of the lower α-heating production and lower H-mode threshold in T-rich plasmas than in 50-50 DT plasmas, followed by a progressive change in the DT mix towards 50-50, thus increasing Q gradually. Note that using D-rich plasmas in such a development path is not a suitable option due to the higher H-mode power threshold in D plasmas (e.g. for an 11.2 MA/5.3 T D plasma at $n_e = 0.8 \times n_{GW}$, the H-mode power threshold is ~ 70 MW), which this strongly reduces the flexibility

in the choice of heating and current drive that can be explored to develop the experimental path to the desired scenario.

- Demonstration of 3000 s $q_{95} \geq 5$ steady-state (fully non-inductive) plasma with Q ~ 2 (100 days):

The achievement of this fully non-inductive objective requires H_{98}-factors of ~1.2 with Greenwald factors of ~0.85 (see Appendix E). Achievement of this goal, however, is likely to require significant H&CD upgrades, including the addition of the 3rd HNB as well as an additional 20 MW of ECRH (case 12 in Appendix E, Table E.2 with q_{95} = 5.7). The additional NBI injector is currently considered to be the most important component of the H&CD upgrade to achieve this goal: with the baseline H&CD, the Q value for fully non-inductive operation may fall to 1.3 for H_{98} ~ 1.2 (case 2 in Appendix E, Table E.2 with q_{95} = 7.6).

While the operational experience in FPO and, in particular, the two preceding series of experiments for hybrid plasmas will have provided important input for this phase, significant issues will remain open and will have to be addressed as part of this development program. Establishing full non-inductive operation under essentially stationary conditions imposes significant requirements on the external current drive sources, which also inject substantial heating power and create significant fast particle densities in the plasma (in particular, NBI). These affect both the current and pressure profiles, which determine global MHD plasma stability (see Appendix E; internal modes rather than external ones are more likely in this case given the moderate total plasma β). Fast particle driven instabilities can also have an important influence on global plasma behaviour in these plasma scenarios. Significant experimental time will therefore have to be dedicated to the optimization of the current and pressure profiles via appropriate application of the H&CD and other actuators to achieve and maintain the required plasma conditions over the target duration of 3000 s.

In principle, the level of energy confinement enhancement required for this plasma scenario is in line with expectations for hybrid plasmas in present experiments as well as in ITER, and it is therefore assumed that it will have been demonstrated in the set of experiments that precede this development program. The main focus of this phase is to produce an integrated scenario that demonstrates the steady-state goal at a moderate value of Q (~2). The demonstration of this goal will require an increase in the fraction of self-driven bootstrap current and, thus, it is expected that these experiments will also provide the first empirical insight under ITER conditions into possible approaches to the optimization of plasma confinement and to the control of MHD stability in steady-state plasmas. Such experience will be essential for the development of the next phase of the experimental program discussed below. It can be anticipated that the strategy followed for the development of moderate Q plasmas will be based on the DT hybrid scenario development, and will proceed either by starting from the 9.5 MA/4.5 T scenario, by increasing the field to 5.3 T and decreasing the current to 9 MA, or from the 11.2 MA/5.3 T scenario, by decreasing the current to 9 MA. If the change in q-profile in following these approaches is found to cause difficulties for the development of this scenario in DT plasmas (e.g. control difficulties leading to disruptions), an alternative would be to start the development from the initial scenario at q_{95} = 5 in D at 4.5 T (7.5 MA/4.5 T) already characterized (see section 2.6.3.8), redeveloping the scenario in DT and then increasing current and field to 9 MA/5.3 T.

In this phase, edge integration issues are not likely to be significantly more challenging than those for the Q = 5 hybrid plasmas that will have been developed previously. These fully-inductive plasmas will require a high level of additional heating (to increase plasma β and to provide the level of current drive required to sustain fully non-inductive operation) and will have a lower plasma density than the hybrid plasmas (due to the lower plasma current), which are in principle more

challenging for edge integration. This is, however, compensated to a certain degree by the lower α-heating levels targeted in this phase compared to those in the preceding hybrid plasmas.

- Optimization of 3000 s $q_{95} \geq 5$ steady-state (fully non-inductive) plasma with a target of Q ~ 5 (200 days)

As discussed in detail in Appendix E, the achievement of this goal requires optimization of the use of the upgraded H&CD systems and other control schemes available in ITER to ensure full current drive and global MHD stability (including core MHD modes and the control of RWMs) while maintaining very high energy confinement levels ($H_{98} \geq 1.6$ for $q_{95} = 4.5$ - case 9 in Appendix E, Table E-2). Establishing such plasma conditions is expected to require a significant experimental program, particularly for the achievement of the very high energy confinement levels required. The details of such a program will depend critically on the experience gained in the development of hybrid and the fully non-inductive Q ~ 2 scenarios discussed – results from these explorations will provide essential guidance on potential strategies for combining high-Q (~5) and fully non-inductive operation under burning plasma conditions.

It is important to note that if the achievable purely non-inductive and fully integrated plasma scenario (including all considerations regarding plasma fusion performance, MHD stability and edge integration) cannot finally reach the required fusion performance of Q = 5, other options to achieve the Q = 5 goal during 3000 s can be explored. These correspond to plasmas with a high proportion of current drive (but not 100%) for which the burn duration can extend to 3000 s (very long hybrid-like plasmas). In these scenarios the plasma current level is larger than for purely non-inductive operation but lower than for hybrid plasmas. This reduces the required energy confinement enhancement (i.e. beyond the reference H-mode level) to achieve the Q = 5 goal; more details on such scenarios can be found in Appendix E.

Regardless of whether the 3000 s, Q = 5 plasmas finally developed are purely non-inductive or not, the edge integration issues in these plasmas will have to be addressed simultaneously with the development of the scenario itself. This will be complex due to the lower plasma densities (lower edge currents) and high edge power flow (similar to those for the Q = 5 hybrid plasmas) expected in these scenarios. This integration aspect therefore represents a significant experimental challenge within this program.

2.6.5.4 Deliverables from the operational plan for hybrid/non-inductive DT plasma experiments

This operational period, if successful, will demonstrate the achievement of the ITER Q = 5 goals in long-pulse (~1000 s) and fully non-inductive ('steady-state' of ~3000 s) with fully integrated scenarios. If not fully successful, it should elucidate what the highest achievable values of Q in ITER are likely to be for both scenarios; this is a very important result for the further development of fusion energy. Specific deliverables for this campaign are:

- Understanding of the effect of the isotope mix on non-inductive scenario development in H-modes and on the development of plasmas scenarios incorporating this insight;
- Determination of the threshold for, and the consequences of, AE instabilities in long-pulse/steady-state plasmas with large α-particle populations and the control/mitigation of their effects as necessary;
- Assessment of the impact of the α-particle population on the scenarios obtained (stability and confinement);

- Development of fuelling techniques, DT mix control and burn control for long-pulse operation;
- Development of edge-core integration schemes to provide stationary and ELM power load control compatible with the high level of fusion performance (high confinement) required for these scenarios;
- Provision of input to the physics basis for the Demo design and guidance on candidate operating scenarios.

As described earlier, upgrades of the heating and current drive systems will enable a broader range of potential steady-state operation scenarios in ITER, in particular those of relevance to Demo design/operation. Due to the limited physics basis currently available for these scenarios, it is not straightforward to anticipate the specific research that will be carried out during this phase. However, it is expected that the experience gained from present-day devices before ITER operation and from the early phases of ITER operation will provide sufficient information for a detailed experimental plan, albeit incorporating a range of experimental options, to be developed prior to this phase. An important output of this program will be an assessment of the viability of, and requirements for, steady-state operation in Demo; the experiments will be able to address some specific Demo physics issues such as:

- Compatibility among high plasma radiative losses (up to the maximum possible radiated power fraction), high density (above the Greenwald value) and high fusion performance, together with integrated stationary power exhaust;
- Development of real-time control of integrated high-Q scenarios with a minimum set of actuators and diagnostics with the power exhaust constraints;
- Development of high fusion performance regimes without off-normal transient events, chiefly edge localized modes and disruptions.

Specific issues that should be addressed within the research activity targeted towards Demo include the attainable fusion gain in the fully non-inductive steady-state regime, the degree of control required to maintain steady-state operation, and the associated diagnostic/control requirements. The additional H&CD upgrades should also allow long-pulse, high gain operation, enabling material and blanket tests at moderate neutron fluence levels. The latter set of tests would be enhanced significantly by running a series of highly reproducible steady-state pulses during the latter phase of ITER operation (see, in particular, section 3.2.2.5.5).

2.6.6 Burning Plasma Physics

2.6.6.1 Opportunities for burning plasma studies in DT plasmas

The range of plasma parameters achievable in ITER provides an opportunity to study the physics of toroidal burning plasmas in a new, currently inaccessible regime, where a significant population of fusion α-particles and self-heating are achieved simultaneously. This is particularly true for operations with $Q > 5$ when the plasma will be dominantly heated by the population of α-particles created as a result of the DT fusion process. It should be noted that in this regard ITER has scientific value in providing the validated models that will serve as a basis for Demo design and operation, even if ITER itself may not provide the explicit experimental demonstration of Demo scenarios.

The research program in the ITER burning plasma campaigns is likely to evolve as an improved understanding of key issues is developed within the fusion community during the Construction and earlier Operation Phases of ITER. However, there are certain research issues for which ITER may be expected to provide the primary contributions to the scientific understanding of the underlying physics. Some of these issues are shown in Table 2-16 and outlined in sections 2.6.6.1.1– 2.6.6.1.5 below. It should be noted that this list is not meant to be exhaustive, but rather illustrative of the research opportunities available on ITER for burning plasma studies in DT plasmas.

Table 2-16 – New phenomena in DT plasmas and expected effects

New phenomena expected in DT	Expected effects and potential issues	Experience from ITER H/He and D phases and present devices	Required additional dedicated experimental study during DT phase
Significant increase of plasma heating power: ~150 MW in DT vs 73 MW in D	Higher heat loads in divertor, ELM control, divertor performance, effect on plasma core confinement, H-mode.	Power density similar or higher have been achieved in present experiments for short pulses.	Explore high-Q>10 regimes consistent with low divertor load, low tritium retention.
He ash accumulation	Plasma dilution, reduction of fusion power.	Externally introduced He.	Investigate He profiles in the core plasma; study of He exhaust.
Self-heating by fusion α-particles	Burn control issues such as transients in fusion power, profile control, etc.	Model experiments with $P \sim W^2$ possible.	Plasma control with minimized auxiliary power.
Fast α-particle population in the plasma core	Additional drive for Alfvén Eigenmode instabilities can cause loss of α-particles, reduction of heating, localized heat loads on the FW; AE phenomena expected to be enhanced in long-pulse plasmas with higher q; effect of α-particles on MHD phenomena; additional wall erosion by α's.	AEs driven by NBI and ICRF minority fast ions in other machines as well as ITER H/He and D phases.	Exploration of stability limits; investigation of loss/redistribution vs plasma parameters.

Isotope effect on plasma confinement and edge plasma performance	Positive effect on plasma confinement and L-H transition is expected; scenario adjustment and optimization could be required.	Experience with H, He, D, DT and T plasmas in other devices and the previous phases of ITER.	Extend ρ* scaling experiments to DT operation.

The initial phases of DT operation, as detailed in sections 2.6.4.1–2.6.4.3, will begin to address these issues associated with α-heating and increased power throughput, culminating in Q ≥ 10 operation for a short pulse, of order (10-20) $\times\tau_E$ (several tens of seconds). At this level, many of the essential burning plasma physics issues can be addressed. The subsequent extension of the burn to the maximum inductive pulse length accessible within the Vs capability of the device in these 15 MA plasma conditions (300 – 500s) will begin to encounter longer time scale phenomena. Broadly speaking, these include issues of particle transport and exhaust, resistive current diffusion, plasma material interactions (e.g. tritium retention and impurity generation), and infrequent off-normal events. While some of the long-pulse development before this phase, may have provided some relevant experience in most of these areas, the interaction with dominant self-heating and fast (and slowing down) α-particles will present new control challenges.

Specific issues to be addressed include:

- Helium ash build-up and exhaust, and control of the optimum fuel mix;
- Burn control in the context of time-varying energy, particle (fuel and impurity), and momentum transport as the q-profile evolves on the resistive timescale;
- Modification of MHD stability properties due to evolution of the q-profile driven by changes in the heating profile, including bootstrap current effects, affecting modes which then interact with the α's, including 'monster' sawteeth, fishbones, various types of Alfvén Eigenmodes and NTMs;
- Interactions of escaping fast α's with first wall structures, potentially resulting in sputtering of impurities;
- Intermittent or aperiodic relaxation phenomena driven by α-heating or instability drive, potentially leading to off-normal events (e.g. disruptions).

2.6.6.1.1 Fast particle physics and effects of non-axisymmetry

Good confinement of α-particles generated in DT reactions is crucial for a fusion power plant. Single classical orbit α-particle confinement is well understood, and α-particle loss is predicted to be relatively low in ITER with corrected toroidal magnetic field ripple. However, a high gradient of fast particle pressure in high-Q plasmas can drive collective instabilities that may cause α-particle loss. Collective modes of concern include different types of Alfvén Eigenmodes (AEs), kinetic ballooning modes, and internal kink modes. In addition to these driven magneto-hydrodynamic modes, there are also fast particle modes (EPMs) characterized by strong dependence on the fast α-particle distribution function [Gorelenkov, 2014].

ITER plasma performance also relies on confinement of fast particles generated by auxiliary heating systems such as NBI and ICRF minority heating. The achievement of H-mode in H/He and

D plasmas as well as the transition to high-Q regimes in DT plasmas is critically dependent on the efficiency of heating systems and their ability to deliver full power to the plasmas. Particle energy, pressure, and density of NBI and ICRF generated fast ions are expected to be comparable with those of α-particles in high-Q operation. It is expected that, by the beginning of DT operations, ITER experiments in the H/He and D phases will already have produced some information on the confinement of fast particles and other effects of fast particles on the performance of ITER scale plasmas. High-Q operation in the DT phase will provide a unique opportunity to study fast particle physics in reactor relevant regimes.

Fast particle effects have been studied in many tokamak experiments using fast ion tails produced by NBI and ICRF plasma heating, as well as fast α-particles in JET [Sharapov, 1999] and TFTR [Nazikian, 1997] DT experiments. However, direct extrapolation from these experiments to a burning plasma is limited, since the values of characteristic dimensionless parameters and the isotropy of the distribution functions are different. Fast particles in ITER will have much smaller normalized gyro-radius and have to be confined for a much greater number of bounce periods than fast particles in present day experiments. Also, the distribution function of fast α-particles in a burning plasma will be nearly isotropic, whereas in present experiments, with fast particle distributions driven by auxiliary heating, distribution functions of fast particles are anisotropic.

Present models predict that the drive due to the α-particle pressure, $\beta_\alpha < 1\%$ in ITER inductive scenarios, is comparable to that from NBI and leads to marginally unstable toroidal Alfvén Eigenmodes (TAEs) with n = 15 – 30 in the outer region of the plasma, r/a > 0.4, as shown in Figure 2.6-14 [Pinches, 2015]. Scenarios with high q_{95} and, in particular, with reversed magnetic shear are expected to be more prone to fast particle instabilities. Initial analysis of non-linear dynamics of EPMs in configurations with reversed shear predicts rapid fast particle redistribution, albeit with a relatively small global particle loss.

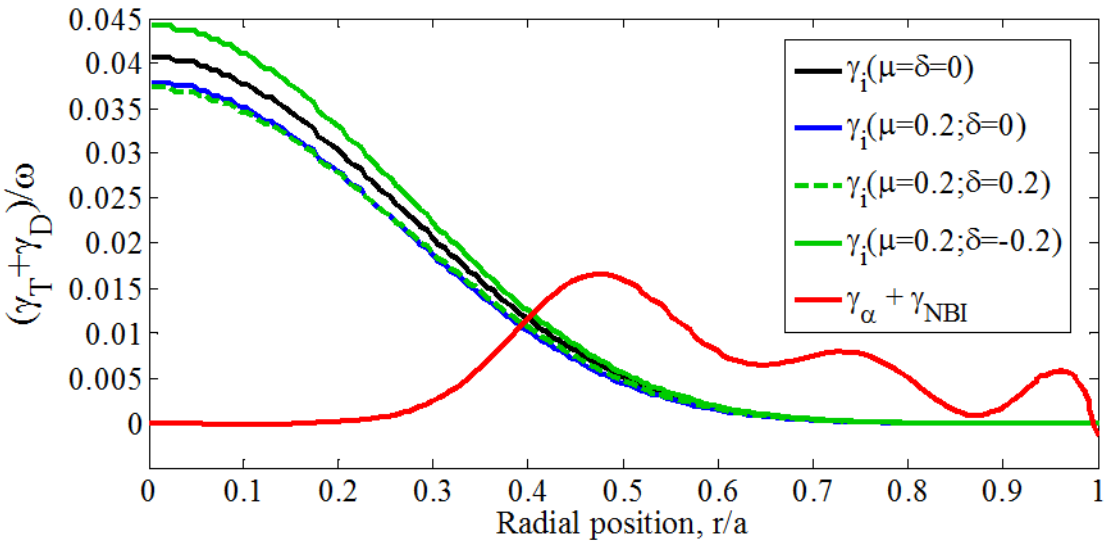

Figure 2.6-144: The sum of α-particle and beam drives (red) compared with the primary AE damping mechanism (ion Landau damping), as a function of normalized radius. The effects of the DT fuel mix ($\delta = 1 - n_T / n_D$) and depletion ($\mu = 1 - \left(n_D + n_T\right) / n_e$) on the damping are also depicted.

Fast particles can transiently suppress the internal m/n=1/1 MHD mode resulting in a large amplitude 'monster' sawtooth crash that redistributes fast particles and plasma parameters inside the affected zone – somewhat larger than the radius of the q(r) = 1 magnetic surface [Campbell, 1988; Chapman, 2007]. The sawtooth crash can induce seed magnetic islands to initiate the growth of neoclassical tearing modes (NTMs). On the other hand, fast particles can destabilize the internal m/n=1/1 MHD mode through a resonant wave-particle interaction at the magnetic precession frequency of the trapped fast ions, and result in fishbone oscillations that can also redistribute the fast particles within the central zone.

Given the large number of instabilities and the complexity of the problem, computational codes predicting α-particle driven instabilities in burning plasma are unavoidably approximate and sensitive to the detailed profiles of the scenarios. This makes the development of predictive capabilities particularly challenging despite ongoing validation exercises against present day experiments.

Physics research in the area of fast particles in burning plasma will require additional measurements such as the profile of fusion power (e.g. neutron tomography), fuel composition including D/T and He/D ratios and impurity concentrations, and MHD fluctuation in the range of Alfvén modes (30-300 kHz). If anomalous loss of fast α-particles is encountered, then measurements of the energy spectrum of confined α-particles and the first wall flux of escaping α's will be required in order to understand the loss mechanism and to try to eliminate the cause. To avoid localized power loads on the FW – which is typical for fast particle loss – a monitoring of localized heat loads on the plasma-facing wall will be necessary, especially for the high-Q operation. Whilst visible/IR cameras are sufficient for machine protection purposes, understanding the physics behind such loss channels will require dedicated fast ion loss detectors that can resolve more information about the specific details of the lost fast ions, e.g. their pitch angle and energy. Such diagnostics are currently under investigation for implementation in the baseline, namely the fast ion loss charge-exchange diagnostic and a fast ion loss detector (see Appendix H).

In addition to non-axisymmetric effects arising from the presence of MHD phenomena, the application of 3-D magnetic fields to influence ELM behaviour will also have an impact on fast particle confinement. Detailed modelling, in which the important effect of the plasma response is retained, has shown that, for the maximum current in the ELM control coils in the baseline scenario (15 MA), an additional fast ion power loading in the divertor region is primarily observed, as illustrated in Figure 2.6-15 [Akers, 2016]. This should be monitored as the populations of fast ions are built up during the experimental program and also as various levels of current and relative phasing are explored in the ELM control coils. Whilst the distribution of fast ion power loading in the divertor is largely determined by the geometry of the divertor structure, the loads onto the first wall are determined by the applied spectrum. If these loads reach levels where they are not tolerable in stationary conditions then it may be necessary to use the flexibility within the ELM control coils to change the applied field during a discharge in order to move the heat loads around whilst simultaneously meeting the requirements for ELM control (e.g. by statically rotating the applied field or changing the harmonic mix to otherwise modify the heat load footprint and protect the first wall during the discharge evolution).

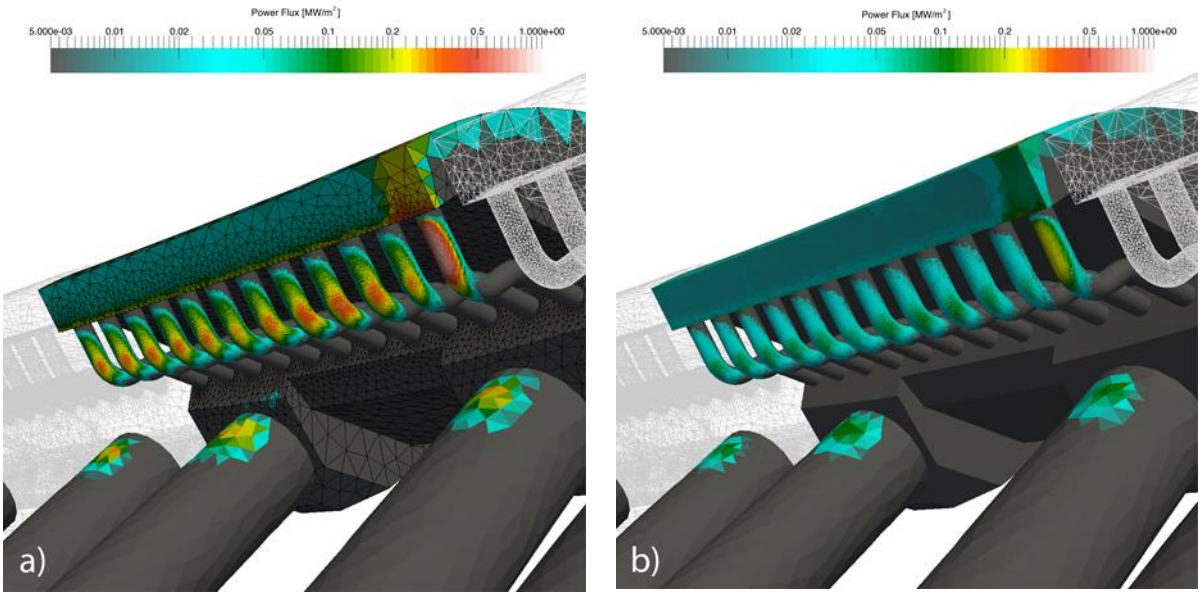

Figure 2.6-15: Fast ion power loading to the ITER under-dome components for 33 MW of 1 MeV NBI into 15 MA flat-top H-mode with 90 kAt of n = 3 ELM control coil field applied (including the n = 6 side-band). The power loads in a) assume that a vacuum approximation holds whilst b) includes the plasma response [Akers, 2016].

2.6.6.1.2 Self-heating and thermal stability

Significant plasma self-heating by α-particles raises the issue of thermal stability of the operating point for burn. While one can conceive burn control simulation experiments in present devices or the earlier phases of ITER operation, in which a fraction of heating power is proportional to W_{th}^2 ($\propto P_{fus}$ in a power plant plasma), thermally stable operating modes for a power plant must be demonstrated in a plasma heated by fusion reactions. The plasma burn in ITER and Demo are expected to be globally stable, with operation located near the stable (right) branch of the ignition curve where the power loss increases faster with temperature than the fusion power [Rebhan, 1997]. An expected increase in fuel dilution by helium ash with rising fusion power is an additional stabilizing factor. However, the consistency between the plasma pressure profile, the current density profile (including bootstrap current), and the plasma stability requirements may raise multi-faceted feedback and profile control issues that could be important, especially for hybrid and steady-state scenarios in which the power degradation of energy confinement is expected to be weaker than in conventional H-modes [Challis, 2015]. In such a case, a simple global control scheme may not be adequate and more sophisticated control of plasma current and pressure profiles may be required.

Possible actuators for fusion power control in ITER include auxiliary power, fuelling, and impurity injection. Even at $Q \approx 10$, substantial external heating power is still required at the burn point, and a control strategy for regulating the fusion power by modulation of P_{aux} seems feasible. Actuators for particle control include gas puffing and cryogenic pellet injectors. Reduction of the fuel ion density reduces the reactivity as $\langle n_{DT} \rangle^2$, but the response to the fuelling source (primarily pellet injection) is on the slower particle confinement time scale. More importantly, reduction in the core density tends to reduce the radiated power fraction unless additional impurity seeding is provided simultaneously, thus aggravating the power exhaust challenge to the divertor.

Conversely, positive excursions in the density to counter a decrease in reactivity are bounded by the proximity to the density limit. The concept based on controlling the fuel mixture (ratio n_D/n_T) could be tested on ITER using independently timed pellet injectors for D and T fuelling.

Measurements for the various quantities of interest for control will be available in ITER. The fusion power (proportional to P_α) itself is observable with essentially zero lag by monitoring the flux of 14.1 MeV neutrons. This is an important consideration, since the plasma response to variations in reactivity experiences a lag associated with the α–particle slowing down time and the energy confinement time, typically amounting to a delay of several seconds. Real-time spatial profiles of the kinetic quantities n_e, T_e, T_i, and to some extent of radiating impurities, are expected to be available on ITER using the foreseen diagnostic set. Real-time measurements of global quantities such as the plasma current and plasma pressure (β), and of the plasma shape, will be available from magnetic sensors. Measurements of the fuel mix at the plasma edge, or in the divertor region using neutral emission (e.g. D_α/T_α) seems feasible, as does monitoring of the exhaust gas. Alternatively, there is the possibility of inferring the relevant core ratios from simultaneous observation of the 2.45 and 14.1 MeV neutrons arising from the D(T,He^4)n and D(D,He^3)n reactions respectively.

Although ITER's objective is the achievement of $Q \geq 10$, much higher Q values, and even ignition in ITER, are not precluded within the range of present uncertainties in projections of ITER plasma parameters. Optimization of operational scenarios with the aim to increase the Q value will be an important part of ITER research program during the DT active phase. As one can expect, an increase in Q to very high values will make plasma control more difficult, but it would provide a unique environment in which to develop plasma control necessary for Demo.

2.6.6.1.3 Macroscopic stability physics and control

Issues of macro-stability research to be addressed during the ITER DT phase operation are centred on four main topics:

- MHD activity driven by the α-particles, discussed in section 2.6.6.1.1;
- Confinement limiting instabilities, exemplified by NTM modes in the core and pedestal stability and relaxation mechanisms in the edge;
- Ultimate pressure (β) limiting instabilities, exemplified by RWM;
- Off-normal events, in particular disruptions.

These effects must be understood and dealt with in ITER in order for the facility to achieve its performance objectives. Moreover, research into these instabilities on ITER is essential in order to provide data in support of Demo and reactor facilities, either by directly demonstrating relevant conditions or to validate theoretical extrapolation to parameters not actually achievable in ITER itself.

DT operation in ITER will provide a unique combination of β_α, a/ρ_α, and $v_\alpha/v_{Alfvén}$ for the study of α-driven instabilities, especially Alfvén Eigenmodes. While the projected value of β_α (<1%) in ITER is smaller than might be expected in a reactor, for example, the comparable value of the ρ_α, isotropic source distribution, and self-heated burn dynamics make the ITER data an invaluable extension to the database in this area by providing a vital testbed for validation of linear and non-linear theoretical models of these phenomena. The ITER research program in the area of α-driven instabilities would therefore incorporate:

- Validation of linear stability boundaries in the relevant range of parameter space;

- Validation of non-linear predictions of α-transport and redistribution in unstable regimes, including potential of coupling to thermal plasma modes either through direct excitation, e.g. generation of seed islands for NTM, or modification of pressure or current profiles;
- Tests of active control or mitigation of α-driven instabilities.

Studies of NTM physics and application of ECRH/ECCD-based NTM control should have already begun during the non-active and deuterium phases of ITER operation. Control of these modes is expected to be required to allow achievement of the plasma pressure necessary for the target $Q \geq 10$ inductive operation, and thus a relevant demonstration of NTM suppression is required [La Haye, 2006]. However, due to the limitations on available auxiliary power in the D phase it may be necessary for this demonstration to be conducted at less than full (dimensional and non-dimensional) parameters. While NTM physics has been extensively studied in smaller devices, validation of theoretical projections to reactor-scale ρ* is a unique capability of ITER, as is the possible interaction of NTMs with α-driven modes and profile modifications associated with self-heating. The ITER research program into NTM physics during inductive operation in the DT phase would emphasize physics validation and control optimization in non-dimensional parameter regimes (β, ν*, ν/ω*, ρ*) not accessible during the D phase, and identify and investigate aspects associated with α-particle effects and self-heating. During hybrid mode operation, ITER research will investigate the beneficial role of saturated NTMs in maintaining $q_0>1$ at reactor-relevant ρ* and in the presence of α-heating.

Non-inductive, high-β plasmas produced in support of the steady-state $Q \geq 5$ goal at high q_{95} are likely to present more stringent requirements on the NTM control algorithms, as a number of potentially unstable modes must be tracked and suppressed as the q-profile evolves. As the kink β-limit is approached, Δ' is increased, destabilizing the classical tearing mode which can then grow as an NTM. To the extent possible, control algorithms will have been tested at similar β and q-profiles, but at reduced absolute parameters, during the non-active and D phases. The extension to the burning plasma conditions during the active phase of operations will introduce a unique combination of parameters, as well as confronting coupling of the self-heating to the pressure and current profiles. Optimization of the feedback/feedforward tearing mode control strategy is essential to realization of the steady-state $Q \geq 5$ target. While neither the bootstrap fraction nor the β achievable in ITER will reach the values anticipated for a steady-state Demo based on advanced scenarios, the interaction of self-heating and α-driven instabilities with the NTM control represents an irreplaceable testbed for validation of models and control algorithms for extrapolation to Demo and reactor conditions.

In the steady-state regime, ITER is expected to operate close to or above the no-wall β-limit and will therefore require active control of the resistive wall mode (RWM). Much of the underlying physics associated with control of these modes is known (in principle), and has been, or will be, validated on medium-sized non-burning tokamaks. There will remain some issues, however, which can only be fully elucidated by experiments at the reactor scale. The first research problem to be confronted by high-β experiments on ITER is likely to be exploration and validation of models of the passive (rotational) stability boundary, below which active feedback is not required. Kinetic effects, including thermal and fast particles, are important elements of the MHD physics of wall stabilization, and of course the rotation in the absence of strong external torque will depend on transport phenomena. Therefore, experiments at the ITER ρ* and including fast ions (initially from MeV NBI in the D phase, then by the more isotropic α-particle distribution in the DT phase) will provide essential checks on the theory. A powerful tool supporting such experiments is the capability to diagnose the proximity to RWM instability by means of active MHD spectroscopy

[Chapman, 2009-2]. This could be achieved on ITER by using the in-vessel ELM control coils to apply a rotating $n = 1$ perturbation while measuring the amplitude and relative phase of the plasma response and comparing (or fitting) to theoretical models.

The results of these experiments will need to be incorporated into the design of model-based controller algorithms for feedback stabilization above the wall-stabilized limit [Liu, 2009]. To the extent possible, specific control algorithms and actuators to be used for steady-state operation will be tested in ITER prior to DT operation by accessing the relevant β at half-field, provided the auxiliary power is adequate in the absence of α-heating. Since the extrapolation in ρ^* to full field DT operation will be less than a factor of two, these experiments would provide confidence in the approach and methodology. The additional RWM physics associated with DT operation will arise primarily from the addition of an isotropic fast ion (α) distribution, and from the couplings associated with self-heating, which imposes additional constraints on pressure and current profiles, impacting the stability and requiring even more of a MIMO (Multiple-Input Multiple-Output) control strategy. At a projected target of $Q = 5$ ($P_\alpha = P_{loss}/2$) and $f_{bs} \sim 0.5$, the ITER experiments should retain sufficient control authority in the external actuators (possibly including upgrades in H&CD systems) to sustain the steady-state scenario. Significant experimental time will be required to validate and optimize the controllers using the installed capabilities, and to explore the boundaries of controllability.

A major focus of the research on ITER should then be to address the more strongly coupled system anticipated in an 'advanced scenario Demo', with higher Q (perhaps approaching 40) and f_{bs} approaching 0.9, with only weak actuator availability, and operation close to the ideal wall limit. Aspects of such a research program would include model validation, and could encompass simulation of strong coupling by feedback on the additional heating and current drive. Upgrades to power supplies of the ELM control coils so that they can provide RWM control to access higher β would need to be considered to extend the ITER advanced scenario operational regime closer to physics limits.

A particularly important stability issue for ITER is that of disruptions, due to the potential impact of disruptions on the research program [Lehnen, 2015-1] (see also section 2.3). In addition to the electromagnetic and thermal loads imposed on the tokamak internal structures, which can be estimated to some degree from experience on smaller devices, disruptions at the ITER scale are predicted to be associated with substantial avalanche runaway electron generation at levels not previously encountered. This prediction should be tested already during the PFPO phase on ITER, together with qualification of mitigation techniques. The technical demands on the mitigation system during the DT phase are expected to be only quantitatively, not qualitatively, different, primarily owing to the increased stored thermal energy, except in conditions in which the additional sources of seed electrons in DT plasmas are sizeable [Martín-Solís, 2017]. Of course, the reliability of the mitigation algorithm must be assured before DT operation, and reconfirmed as full parameters are approached.

While disruption mitigation will be relied upon to prevent melting of the ITER plasma-facing components and large electromagnetic forces to vessel and in-vessel component, the recovery time associated with even mitigated disruptions represents a significant cost to the ITER research program, especially during the high-Q inductive DT phase. Moreover, while the consequences of such off-normal events in terms of lost research time are serious for ITER, the tolerance for such occurrences in a Demo or a reactor will be orders of magnitude less. To this end, research on ITER should aim to develop real-time control algorithms that avoid (as much as possible) instabilities that may lead to disruptions and to control methods for stabilizing instabilities that may occur. The

development of these control techniques and information on the scaling of disruption effects with machine size will be extremely valuable in the design of the next-generation of fusion devices.

2.6.6.1.4 Multi-scale transport physics

The physics governing magnetic fusion plasmas covers an enormous range of spatial and temporal scales. ITER will represent the first opportunity for the fusion community to assess plasma transport in a system with a reactor-relevant ratio of the ion gyroradius to the system size (i.e. at very low ρ^*). Because ρ^* is the only dimensionless parameter governing plasma transport that cannot be matched in present-day devices, the research conducted on ITER in this area will provide significant leverage in the scaling of present databases to future devices. Another important issue that ITER will help resolve is the impact of electron transport on overall confinement in reactor-like conditions in which the α-particle energy will primarily be coupled to the plasma electrons.

Detailed turbulence characterization studies on ITER will be more challenging than on present-day devices. However, some diagnostics seem to be feasible for diagnosing turbulence in ITER (e.g. Beam Emission Spectroscopy fluctuation measurements) and are being considered for incorporation into the baseline (see Appendix H). These diagnostics will allow comparisons of plasma turbulence in ITER and those in smaller devices.

Plasma rotation will also be a critical issue for ITER. It is well established that increased plasma rotation can have beneficial effects on both the transport and stability properties of tokamak plasmas. Yet, the extent to which ITER plasmas will rotate is still uncertain. Due to the limited capability to apply external torque with NBI (1MeV energy), self-generated torques may be equally (or more) important than the external torque in generating rotation. Measuring the rotation and, more importantly, identifying the mechanisms responsible for the observed rotation should be a high priority research topic on ITER. Such research may point the way to optimization of a future device to take advantage to the extent possible of the self-generated plasma rotation.

A closely related topic is that of transport barrier formation, sustainment and avoidance. Present knowledge suggests that these barriers can be formed by a combination of plasma rotation and compression of the magnetic field on the outboard side of the plasma. While ITER's tools are limited in the ability to control rotation, the significant current drive capability of ITER should allow manipulation of the current drive profile over a wide range to assess the capability to produce transport barriers in the presence of significant α-particle heating. Such knowledge may be necessary to achieve the mission objectives of the long-pulse $Q \sim 5$ scenarios.

2.6.6.1.5 Physics of the plasma-boundary interface

ITER will represent a major step towards reactor-like edge conditions, simultaneously requiring a high pedestal temperature, dissipation of high heat fluxes, low tritium retention, and adequate exhaust of the helium ash produced by the fusion process. While many aspects of the plasma boundary interface issue that are required for successful operation of ITER have been demonstrated individually in current devices, ITER experiments will play a crucial role in obtaining physics data for developing specifications for power and particle exhaust and plasma-wall interactions in Demo.

Simulations of ITER performance suggest that the strength of the H-mode edge transport barrier will play a major role in the ability to achieve high-Q operation. At the moment, a first-principles understanding of the structure of this edge region (i.e. pedestal) is still being developed. The operating conditions of ITER (low ρ^*, low collisionality, high pedestal density relative to the Greenwald density, moderate β, low neutral source) will be distinct from those accessible in current devices, providing an opportunity to develop more fully the physics understanding of the processes

that determine the edge plasma structure. Integrally linked to this issue is the control of ELMs to reduce large transient heat fluxes to the divertor targets. Research on ITER to control the edge evolution and/or structure through the use of non-axisymmetric magnetic fields (resonant magnetic perturbations), or other means (for example pellet pacing, vertical kicks, etc.) will take on added importance as ITER performance increases towards its design goals [Loarte, 2014].

A large part of the Research Plan will be devoted to the study of the performance of plasma-facing components [Pitts, 2011]. The ITER research program has to demonstrate, to the extent possible, that most of the energy arriving in the divertor region can be radiated, that tritium retention can be kept within acceptable levels (i.e. below 1%), that adequate helium exhaust can be provided, that acceptable core impurity concentrations can be maintained, and that plasma-facing materials have a tolerable lifetime. In brief, having established an adequate mode of divertor operation that satisfies the requirements of ITER's fusion performance mission goals, the ultimate goal of the ITER Research Plan in this area will be to explore the extent to which this mode of operation can be developed further to provide a divertor physics and technological solution basis adequate for a reactor.

Regarding tritium retention, by the time of DT exploitation, a sufficient knowledge base will have been acquired from non-active phase operations so that a robust scheme for fuel retention management can be developed. Moreover, DT operations will see the deployment and validation of the global tritium accounting scheme using tritium accounting through the T-plant, determination of burned fuel through neutron rate measurements, gas balance measurements and local retention measurements using the planned tritium monitor, which first becomes available in PFPO-2 (Appendix H). With the development of long-pulse DT discharges, not only T retention but also permeation through components to the cooling water can be characterized. While permeation through beryllium is expected to be negligible, this is not the case for stainless steel components visible to the plasma (Diagnostic First Wall, TBM front surfaces, blanket module surfaces not completely covered by first wall panels, etc.) in which permeation will probably occur during baking of the in-vessel components and needs to be accounted for to close the tritium cycle. Although the dpa (displacement per atom) levels in ITER will be relatively modest compared to those expected in Demo, ITER will provide valuable information on the evolution of the retention and permeation rate of neutron damaged materials (especially for W and steel) in the tokamak environment for the next step.

As operations progress towards DT and longer discharges, and as the requirements on disruptivity get tighter, it is anticipated that during FPO dust production mechanisms evolve from melt generated droplets to solid particles resulting from the delamination of thick co-deposits. Assuming a peak Be deposition rate of ~0.2 $nm \cdot s^{-1}$ in the divertor (an average of values obtained from WALLDYN simulations [Schmid, 2015]), a film thickness of ~50 microns will be reached by the end of FPO-1. This is a value for which Be layer delamination has been observed in laboratory experiments. Monitoring the formation of thick co-deposits and their delamination will be important to avoid the creation of loose material on surfaces, which could, for example, be detrimental during plasma initiation.

Regular monitoring of first wall erosion will be important to validate earlier estimates of the first wall lifetime and inform the need for slight adjustment of the magnetic equilibrium in case of pronounced localized wall erosion. In essence, it is expected that the wall erosion rate is sufficiently understood at this stage that the FPO phases will serve only for the validation of existing models, providing important data for the design of the Demo first wall in terms of erosion lifetime. If, as expected, long-term wall erosion in Demo devices will be dominated by charge-exchange neutral

impact, then ITER is likely to be the only device in which this can be (at least partially) verified, largely through the application of models together with the experimentally determined overall migration balance; the latter requires routine long-pulse operation. Although the experienced gained through the PFPO phases will be helpful, it is also likely to be only as a result of long-pulse fusion power operation that proper assessments can be made as to the need and timing of an upgrade to the in-vessel components (see Section 4.4). However, the long timescales for supply of upgraded PFCs implies that decisions may need to be taken rather early in the nuclear phase.

It is important to note that during FPO-1, the divertor material in the high heat flux region will be regularly operated close to the tungsten recrystallization temperature. Such conditions are unlikely to be obtained, even with full power in PFPO-2. Regular execution of a reference pulse (see Appendix D) will allow the evolution of the divertor power handling capabilities to be carefully characterized during operations. As the discharge duration is increased, the ion fluence onto the divertor and the number of mitigated ELMs will also reach very high values. Since the end of FPO-1 is also likely to correspond to the time where the divertor is replaced, careful analysis of the exposed material will provide important information on modifications of the material thermal and mechanical properties, supplying guidelines for the possible development of advanced tungsten-based materials for Demo. In general, it is expected that ITER will provide key information on the use of a divertor with solid targets (as opposed to liquid plasma-facing surfaces) at the reactor scale.

During the FPO-1 phase mixed He-D-T plasma interactions with tungsten at elevated temperatures will take place for the first time in ITER; under these conditions the formation of 'fuzz' is more likely than during pure He operation in PFPO [De Temmerman, 2018]. The formation of fuzz, or other He-induced morphology changes, might strongly affect the surface emissivity and thus will require regular calibration of the infrared and visible diagnostics to account for this and to derive reliable measurements. At the same time, observations of emissivity changes will provide information on the formation/evolution of any He-induced morphology changes.

2.6.7 Summary of experimental activities and operational time in the FPO Phase

The overall duration of the FPO Phase will be determined by the ITER Members at an appropriate time in the light of the Project's success in achieving significant fusion power production, but considering also the mission goals defined in the ITER *Project Specification*, the terms of the ITER Agreement and the Members' (evolving) strategies towards the exploitation of fusion energy for electricity production. The research program for the FPO phase developed within the current version of the ITER Research Plan encompasses only the first 3 DT campaigns with the aim of presenting a plausible experimental plan to achieve the principal scientific goals and some elements of the fusion technology mission, to illustrate the issues and risks that will need to be addressed in establishing the necessary high fusion gain plasma scenarios and to consider the key aspects of burning plasma physics to which the ITER program will give access. Clearly, many details of this plan will evolve in response to the experimental results obtained during ITER operation and in the light of the experience gained in the study of burning plasmas following the introduction of DT fuel.

The plan presented in section 2.6 initially emphasizes the development of (predominantly) inductive scenarios, in particular, the 'conventional' ELMy H-mode regime in D and DT plasmas, since this, at present, has the most developed quantitative physics basis for extrapolation to fusion power production in ITER. The initial D phase of operation is primarily foreseen to allow the development of DT-relevant scenarios in parallel with the continuing commissioning of the Tritium Plant and the gradual rise in T throughput, leading to the establishment of plasmas with a sufficient T concentration to initiate significant fusion power production (say ~ 50 MW). As discussed in the

previous sections, much can be learned from these experiments in D plasmas, not least in terms of scenario optimization, since they should allow easier access (i.e. lower threshold power) to H-mode operation than the H and He plasmas available during the PFPO phase. Nevertheless, a rapid transition to DT operation, if allowed by progress in the T-Plant commissioning, would be favourable for the achievement of high fusion power/ high fusion gain and the associated studies of burning plasma physics, due to the additional heating power provided by the α-particle population and the further reduction in the H-mode power threshold expected. It should be emphasized that this emphasis on the conventional ELMy H-mode as the principal path towards the demonstration of Q = 10 plasmas in ITER will be kept under review in the light of results from the ongoing R&D programs in current devices and, indeed, in response to the results of initial operation of ITER; it is clear that ITER should exploit the most favourable plasma regime for the achievement of high fusion gain according to the understanding developed at the time of the implementation of the FPO phase, some 20 years hence.

Progress towards higher fusion power and fusion gain will necessitate the integration of scenario elements such as fuel mix control, burn control, heat load control, helium exhaust and MHD stability control, providing capabilities which can be exploited as other burning plasma scenarios are developed. Several parallel programmatic threads are therefore likely to emerge within the DT experiments, as approaches to longer pulse operation are developed and specific aspects of burning plasma physics are explored. In the present version of the ITER Research Plan, it is assumed that the important milestone of achieving fusion power levels of ~300 – 500 MW with Q ~ 10, even for 'short' burn durations of several tens of seconds, will take priority due to its wider implications for fusion energy development. Demonstration of this level of fusion performance would, in all probability, generate significant support for the longer-term exploitation of ITER and provide motivation for wide-ranging exploration of ITER's potential for fusion power production. This logic forms the basis of the detailed discussion of the early FPO campaigns developed in section 2.6, in which achievement of this initial milestone is followed by lines of research exploring several modes of long-pulse operation, from conventional ELMy H-mode, through hybrid/improved H-mode scenarios to fully non-inductive operation. The precise evolution of these lines of research will, of course, depend very strongly on results emerging from initial investigation of such modes of operation in the burning plasma regime. The discussion presented here has, therefore, proposed a strategy based on current expectations, but these expectations will evolve very significantly in the coming decades. Nevertheless, the achievement of significant fusion power production in ITER will open the path to an extensive exploration of viable plasma scenarios and to wide-ranging studies of the physics of burning plasmas.

In parallel with the scientific program towards high fusion power, high fusion gain, long-pulse operation and burning plasma studies, the technology R&D program will assume greater significance in the FPO phase, since this provides a first opportunity to investigate the performance of numerous Demo-relevant technologies in the burning plasma environment with significant fluxes of 14.1 MeV neutrons (even if the ultimate neutron fluences in ITER will be significantly lower than in a Demo device or fusion power plant). The progress towards long-pulse operation will provide insight into the reliability of many components and systems when operating at their performance limits over long durations of up to 3000 s. In addition, as presented later in section 3.2.2, the TBM program will make use of these early DT campaigns to test various aspects of TBM and ancillary system performance, leading to an integrated test of modules capable of breeding tritium and generating high grade heat, scheduled for FPO-3. This will also be a significant milestone for the project, being the first practical demonstration of a novel technology, which is critical for the realization of electricity production from DT fusion.

Table 2-17 summarizes the activities within research program developed around D and DT plasmas during the first 3 campaigns of the FPO phase, and provides an estimate of the operational days required to achieve the objectives of this phase of the Research Plan, in particular to achieve the project's mission goal of demonstrating long-pulse (300 – 500 s) operation at $Q \geq 10$ and to make significant progress towards the mission goal of fully non-inductive operation for durations of up to 3000 s with $Q = 5$. The estimates made for the duration of specific activities, particularly those related to the development of burning plasma scenarios, are necessarily uncertain, since ITER will furnish the first opportunity for the magnetic confinement program to establish and study this entirely new regime of fusion plasmas. The challenges which are likely to emerge in the development of fully non-inductive DT scenarios are particularly uncertain, given the present state

Table 2-17 – Overview of experimental activities and estimates of required operational days for the FPO research program

Activity	Days
Axisymmetric magnetic control	**5**
Plasma scenario commissioning	**5**
Kinetic control commissioning	**28**
MHD and error field control	**20**
Advanced control functions (auxiliary specific, actuator sharing etc.)	**24**
Disruption Management	**11**
Commissioning of auxiliary systems	**25**
Diagnostics	10
H&CD system commissioning	15
Divertor and PWI studies	**12.5**
Deuterium plasma studies	**104 - 124**
Development of D L-mode plasmas to 15 MA/5.3 T	32
Development of D H-mode plasmas to high power at 7.5 MA/2.65 T	40
Trace-T H-mode experiments	12
Initial development of hybrid/ advanced scenarios in D	20-40
Optimization of DT H-mode plasmas at 7.5 MA/2.65 T	**66**
Optimization of DT fusion performance towards Q = 10 at 15 MA/5.3 T	**180**
Extension of DT Q = 10 scenario towards pulse lengths of 300 – 500 s	**100**
Development of hybrid/ non-inductive DT plasma scenarios	**575**
Control of β/ current/ pressure profiles in stationary DT plasmas	25
Optimization of non-inductive current drive at $q_{95} \sim 4$ (2.65 T)	25
Optimization of non-inductive current drive at $q_{95} \sim 4$ (5.3 T) - hybrids	125
Optimization of Q (target Q ~ 5) in long-pulse (~1000 s) hybrids at 5.3 T	100
Demonstration of 3000 s fully non-inductive ($q_{95} \geq 5$) plasma with Q ~ 2	100
Optimization of 3000 s fully non-inductive ($q_{95} \geq 5$) plasma towards Q ~ 5	200
Total	**1155 - 1175**

of understanding of non-inductive operation in existing devices. As the discussions in section 5.4.5 and Appendix E illustrate, there is much that can be learned during ITER construction and the initial years of ITER operation, through collaboration with the international fusion community, to establish a stronger basis for the development of such scenarios. Nevertheless, it is clear from the time estimates derived for the DT research program that the achievement of these key scientific mission goals is likely to stretch over several FPO campaigns: the estimated duration of the proposed research program, 1155 – 1175 days, essentially corresponds to the duration of the first 3 FPO campaigns (415 operational days per campaign – Table 2-1). Achieving the mission goal of fully non-inductive operation at $Q = 5$ may also require upgrades to one or more of the ITER H&CD systems and, possibly, to the power supplies of the ELM control coils for RWM control, in order to provide both the current drive capability and the flexibility required for the more complex control environment of fully non-inductive plasmas. Assuming that ITER were successful in meeting the principal mission goals during the first few DT campaigns (even if there were some deviation from the precise numerical targets established in the *Project Specification*) the later FPO experimental campaigns, beyond the initial campaigns discussed here, will provide opportunities to develop substantial physics and technology bases for the design and operation of Demo devices (the more successful ITER is, the more likely it will be that a range of Demos will be constructed by individual ITER Members). Further upgrading of the ITER tokamak and auxiliary systems could, for example, lead to a focussed program aiming to simulate burning plasma operation under Demo-relevant constraints and with Demo-relevant plasma-facing components, H&CD systems, Diagnostics etc.

3 Technology Research Program

3.1 Introduction

As outlined in section 1, the ITER project will carry out an extensive research program in fusion technology in fulfilment of its mission goals and in pursuit of its overall programmatic objective, defined by the *Project Specification*:

- The device should demonstrate the availability and integration of technologies essential for a fusion reactor (such as superconducting magnets and remote maintenance);
- The device should test components for a future reactor (such as systems to exhaust power and particles from the plasma);
- The device should test tritium breeding module concepts that would lead in a future reactor to tritium self-sufficiency, the extraction of high grade heat and electricity production.

Wide-ranging R&D activities have already been undertaken across the entire scope of key fusion technologies for ITER to provide the technical basis for the design and manufacturing of ITER's tokamak, auxiliary and plant systems, e.g. in superconducting materials and magnets, plasma-facing materials and components, heating and current drive systems, diagnostics, fuelling and vacuum technology, tritium handling, remote handling, control systems, power supplies, cryogenic and cooling systems, and an ambitious Test Blanket Module Program has been launched to develop and construct a series of tritium breeding blanket modules, together with the required ancillary systems, with key features relevant to a fusion reactor.

These technologies will be tested intensively during ITER operations, providing a technical basis for most of the fusion technology required for construction of a Demo device. The research program which will be undertaken in each of these technology areas will be developed in the coming years to ensure that a comprehensive definition is in place in advance of the ITER Operations Phase. As these plans become available, they will be integrated into the overall Research Plan in the course of its regular updating. At present, the analysis of the TBM testing program is considerably more advanced than that of other technology areas, as it is necessary to specify how the staged testing of various aspects of TBM technology will be integrated into the operations program (and on what timescale) to provide guidance to the TBM development program; this must deliver a sequence of TBMs through the operations program, leading to the integrated testing of tritium breeding and high grade heat extraction during the FPO phase.
The following discussion of the Technology Research Program is therefore limited in the present version of the Research Plan to the detailing of the TBM testing program, with an initial scope of about 10 years, extending from PFPO-2 to the end of the 3rd DT campaign. The longer-term TBM Program might be expected to undergo significant evolution, as further developments of blanket concepts emerge in response to the Members' design studies of potential Demo devices in support of the exploitation of fusion energy for electricity generation. In addition, it can be expected that the discussion in this section will be significantly expanded in future versions of the Research Plan to encompass the full scope of technology testing activities which will be implemented during ITER operations.

3.2 Test Blanket Module (TBM) Testing Program in ITER

3.2.1 Test Blanket Module Program

3.2.1.1 Background and context for the TBM Program

In order to prepare for Demo, ITER has the mission to test mock-ups of design concepts of tritium breeding blankets relevant to a reactor, called Test Blanket Modules (TBMs), in three equatorial ports called 'ITER Test Ports'. TBMs and associated systems (called Test Blanket Systems, TBSs) inserted in ITER from the H/He phase are the principal means by which ITER will provide the first experimental data on the still open issue on the path to fusion power, the performance of breeding blankets.

The three equatorial ports allocated to TBM testing are the ports # 2, # 16 and # 18. In each of these ports it is expected to insert a TBM Port Plug (PP) that is formed by a water-cooled steel frame (see Figure 3.2-1) and 2 TBM-Sets. Each TBM-Set is formed by the TBM and the associated required shield.

Each TBM must be relevant for the corresponding Demo breeding blanket (in design, materials and operating parameters). Each TBS includes several associated systems (e.g., primary and secondary cooling, tritium management and control, and measurement systems). The integration of each TBS in ITER implies the presence of several interfaces with the ITER machine and buildings that have to be taken into account in the ITER machine and buildings design [Giancarli 2012].

A large R&D and validation program has to be performed during the ITER construction phase to ensure the installation in ITER of six reliable and safe TBSs in order not to jeopardize ITER performance while producing Demo-relevant testing results.

More than 10 TBS designs have been initially proposed by the ITER Members for testing in ITER. Among them, six TBSs have been selected for installation in ITER. They will be designed and fabricated by the ITER Members and delivered to the ITER Organization for installation. Each TBS is developed by a Member Leader (TL) or by a Partnership of Members. The formal way of creating a Partnership is discussed in TBM Arrangement (TBMA) Article 12.

The six selected TBSs (including concepts with both solid (SB) and liquid (LB) breeders), their port allocations, and the corresponding Member Leaders are the following [Giancarli 2016]:

1) Helium-Cooled Lithium-Lead (HCLL) TBS (Port #16/TL: EU). The Helium is operated at 8 MPa and at inlet-outlet temperature of 300-500 °C. The structural material is a Reduced-Activation Ferritic/Martensitic (RAF/M) steel, the EUROFER. The Lithium-Lead is a liquid metal with melting temperature of 235 °C acting as both tritium breeder and neutron multiplier;
2) Helium-Cooled Pebble Beds (HCPB) TBS (Port #16/TL: EU). It makes use of ternary lithium oxide ceramic pebbles as tritium breeder and Beryllium pebbles as neutron multiplier. The Helium is operated at 8 MPa and at inlet-outlet temperature of 300-500 °C;
3) Water-Cooled Ceramic Breeder (WCCB) TBS (Port #18/TL: Japan). It makes use of ternary lithium oxide ceramic pebbles as tritium breeder and Beryllium pebbles as neutron multiplier. The Water is operated at 15.5 MPa and at inlet-outlet temperature of 280-325 °C;
4) Helium-Cooled Ceramic Breeder Graphite Reflector (HCCR) TBS (Port #18/TL: Korea). It makes use of ternary lithium oxide ceramic pebbles as tritium breeder and Beryllium pebbles as neutron multiplier. The Helium is operated at 8 MPa and at inlet-outlet

temperature of 300-500 °C. A graphite reflector region is added in the back-side of the TBM;

5) Helium-Cooled Ceramic Breeder (HCCB) TBS (Port #02/TL: China). It makes use of ternary lithium oxide ceramic pebbles as tritium breeder and Beryllium pebbles as neutron multiplier. The Helium is operated at 8 MPa and at inlet-outlet temperature of 300-500 °C;

6) Lithium-Lead Ceramic Breeder (LLCB) TBS (Port #02/TL: India). It makes use of 2 coolants: Lithium-Lead (p = 1.2 MPa, inlet/outlet temperature = 300-460 °C) and Helium (p = 8 MPa, inlet/outlet temperature = 300-500 °C). It makes use of 2 breeders: Pb16Li and lithium titanate ceramic pebbles. Pb16Li acts also as neutron multiplier.

The structural material for all the above Test Blanket Modules are Reduced-Activation Ferritic/Martensitic (RAFM) steels, as these are considered mandatory for a Demo, and for Fusion Power Plant designs. Note that RAFM steels are ferromagnetic.

The following two additional 'strategic' requests were made by the ITER Members and agreed by the TBM-Programme Committee:

1) The USA requested to reserve the option of leading a TBM concept at a later phase of ITER operations. Specifically, the USA request noted that nothing in the TBM technical plans preclude testing of the Dual-Coolant Lithium-Lead (DCLL) concept. To meet this request, an additional set of inlet and outlet He-coolant connection pipes are designed and installed in Port #18. The associated characteristics would be the following:

   - Dual-Coolant Lithium-Lead (DCLL) TBS (provisional TL: US). It makes use of 2 coolants: Lithium-Lead and Helium (p = 8 MPa, inlet/outlet temperature = 300-500 °C). Pb16Li acts also as tritium breeder and neutron multiplier. The structural material is an RAFM steel;

2) The EU requested to not preclude the testing of a Water-Cooled Lithium Lead TBS or of a DCLL TBS in Port #16. To meet this request, an additional set of inlet and outlet coolant connection pipes (able to use either pressurized water or Helium) are designed and will be installed in Port #16. The characteristics of the DCLL-TBS would be very similar to those described above for the USA; the characteristics of the WCLL-TBS would be the following:

   - Water-Cooled Lithium-Lead (WCLL) TBS. It makes use of lithium-lead as tritium breeder and as neutron multiplier. The Water is operated at 15.5 MPa and at inlet-outlet temperature of 270-325 °C. The structural material is a Reduced-Activation Ferritic/Martensitic (RAFM) steel, the EUROFER.

ITER may be the only opportunity for testing breeding blankets mock-ups in a real fusion environment before the construction of a Demo reactor ensuring:

i) in the Pre-Fusion-Power Operation: relevant magnetic fields, relevant plasma regimes (e.g., H-mode), surface heat fluxes, H (and, possibly, trace D) permeation in the First wall coolant and disruption-induced loads; this phase will also be essential to learn how to operate a TBS in a reliable and controlled way from the control room and to confirm several operation data that will be part of the ITER nuclear licensing file;

ii) in the Fusion Power Operation phase: additional relevant neutron flux, volumetric heat, and tritium production with corresponding tritium-management capabilities.

The most serious limitation for blanket testing in ITER is that the magnitudes of neutron flux and volumetric power density are lower than that expected in a Demo reactor and that ITER operation

features relatively short pulse length (compared to the quasi-continuous operation expected in a Demo). The countermeasure is that, for each selected blanket concept, several TBMs have to be developed making use of 'engineering scaling' for testing specific 'act-alike' TBMs during different ITER-phases in order to address different aspects of the TBM performances (neutronics, thermo-mechanics, thermo-hydraulics, etc.).

In addition, neutron fluence in ITER is too low (up to 3 dpa after 20 years of operation compared with about 70 dpa expected in Demo for 2 years of operation) to test long-term irradiation effects on materials, and, therefore, they must be determined by other means and in dedicated facilities (e.g. IFMIF/DONES).

Taking into account these limitations, the major overall testing objectives of the TBM programme in ITER are the following:

i) validation of structural integrity theoretical predictions under combined and relevant thermal, mechanical and electromagnetic loads;

ii) validation of tritium breeding rate predictions;

iii) validation of tritium recovery process efficiency and T-inventories in blanket materials;

iv) validation of thermal predictions for strongly heterogeneous breeding blanket concepts with volumetric heat sources;

v) demonstration of the integral performance of the blanket systems.

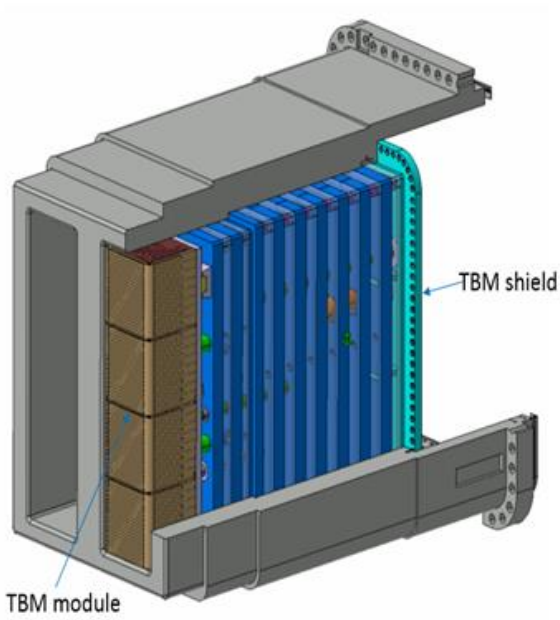

Figure 3.2-1: Schematic view of a TBM Port Plug.

TBSs have to be installed early in ITER operation because very important data have to be obtained during the non-active operational phase (H/He PFPO phase). Within current Integrated Project Schedule (IPS-2017) most TBMs are expected to be installed during Assembly Phase III in 2031 (see section 3.2.2.1 and Figure 2.2-1: Operations Plan within the Staged Approach.) before PFPO-2. However for some of them, and for most of the TBSs ancillary systems, the installation may occur during the Pre-Fusion Power Operation 1 in 2028-2031. The main results expected in the non-active phase are the following:

i) demonstration of the structural integrity of the TBM structures and attachment during disruptions and Vertical Displacement Events (VDEs);

ii) assessment of the impact of RAFM steel, used as the structural material for the most part of TBMs, on the 3-D tokamak magnetic field structure and evaluation/mitigation of its effects on plasma confinement, fast ion losses, plasma rotation, etc.;

iii) demonstration of all the functionalities of the TBM systems;

iv) essential data relevant for safety in order to obtain authorization to proceed with the nuclear phase of ITER operation.

3.2.1.2 TBM research program accompanying construction

Each installed TBM must be relevant for the corresponding Demo breeding blanket in term of design, materials, manufacturing techniques and operating parameters. In order to ensure the installation of reliable TBSs, several specific steps have to be completed in advance. They include essential R&D activities, relevant for material and manufacturing qualification, safety and licensing documentation. Moreover, because of the ferromagnetic behaviour of the TBM structures, several experiments have been and should be further performed in present-day tokamaks to ensure the compatibility of the TBMs with the foreseen plasma operations and fusion performance objectives in ITER.

3.2.1.2.1 R&D to be performed on TBMs and associated systems

For each TBS, the main required R&D activities prior to testing in ITER and the corresponding required time schedule (assuming that the TBSs are installed in Assembly Phase III, around 2031) are the following:

- Out-Of-Pile characterization of Demo-relevant structural material and TBM fabrication process validation (at industrial level); for each TBM, these activities require the selection of a reference material to be used in all experiments in order to obtain a coherent and complete set of data. Such a reference material will be used for the manufacturing of all mock-ups and for the TBMs. To be achieved before the TBM final design reviews planned in the range 2022-25;
- TBS preliminary design; it has to be based on the reference structural material database and it has to be used for deriving the design and manufacturing of the medium/large scale mock-ups necessary to validate the TBM design. To be achieved in the range 2019-22;
- Fabrication and testing of medium/large size mock-ups of TBMs and TBS components addressing critical aspects (industrial manufacture or, at least, industrially compatible manufacture). These tests should be able to guarantee a sufficient reliability of the TBMs prior installation in ITER. To be achieved by the end of the final design phase;
- Construction of databases for structural material and joints for use in design codes and codes and standards; these activities correspond to several experimental campaigns able to validate material properties on a sufficient number of samples for reduction of uncertainties. To be achieved in support of the final design;
- Construction of databases under irradiation (at least, 1 dpa) for structural material and joints and for functional materials (e.g., ceramic breeder pebble beds, beryllium pebble beds), obtained in experimental campaigns performed in fission reactors; these data have to be used to perform the detailed design of the TBMs. To be achieved in support of the final design;

- Design, fabrication, acceptance tests (expected to be done by the manufacturer) and delivery of the first TBMs (TBM-EM) to the ITER Organization on the ITER Site expected in 2029 for assembly of the TBM Port Plugs (2 TBM-Sets in each frame), Port Plugs acceptance tests and installation in ITER.

3.2.1.2.2 Effect of TBM ferromagnetic structural material on plasma H-mode performance and fast ion losses

Because of the use of ferromagnetic RAFM steel as TBM structural material, the presence of TBMs produces localized magnetic field perturbations in the TBM Port area (about 0.6% of the local field per TBM). Experiments in JET had shown that periodic ripple of the toroidal magnetic field could have a negative impact on the quality of the plasma confinement in H-mode. Significant perturbations start at a ripple level of about 0.3%. Since the physics phenomena behind such an effect have not yet been fully understood, it is uncertain to what extent localized TBM-induced perturbations have the same impact on the H-mode as toroidally periodic ripple.

In 2010, a Workshop on 'TBM Impact on ITER Plasma Physics and Potential Countermeasures' was organized by the ITER organization to assess the impact of Test Blanket Modules (TBMs) on ITER physics operations and to consider possible countermeasures and strategy to be adopted to allow the execution of the TBM Program within the constraints dictated by the achievement of ITER's fusion performance goals. Almost 50 scientists participated to the two-and-a-half day Workshop, including representatives from the ITER Organization, from the TBM teams of all 7 ITER Members, from the international plasma physics community, from the ITER TBM Program Committee (TBM-PC) and from the ITER Science and Technology Advisory Committee (STAC).

The main conclusions from the physics side were:

1) impact of the expected magnitude of magnetic fields produced by the TBMs is small in low performance (L-mode) and low-β plasmas; however, the plasma performance may be degraded in high performance plasmas and, therefore, there is a significant risk of affecting the first-priority ITER mission of achieving Q = 10;

2) in particular, the experimental results show that ripple causes density pump out and significantly reduces plasma rotation, increasing the risk of plasma disruptions;

3) theory and modelling of how these magnetic perturbations lead to degradation of plasma confinement are not yet sufficiently mature and, therefore, the predictive capability is lacking to quantify the impact of these issues on ITER high-β plasma performance.

The main conclusions from the TBM design side were the following:

1) both the reduction of the TBM ferromagnetic mass and the increase of the TBM recess distance from the plasma would lead to a significant reduction of the tritium production in the TBMs that is already at the minimum acceptable level for being able to extrapolate results to Demo; therefore, the main testing objectives would be jeopardized;

2) use of correction coils in the TBM Port Plugs themselves will add significant further constraints to the TBM tests (e.g., increase of the replacement frequency due to the limited coils lifetime under neutron irradiation (less than 2 years)).

The consequences from the TBM-design side have been to fix a recess of 12 cm from the plasma and a maximum weight of 1.3 tons for the ferromagnetic material present in each TBM. Recommendation of further decreasing such weight has also been taken as a guideline for the TBM design development.

From the plasma-side several experiments were performed in DIII-D, the last occurring in 2014. The experiments on DIII-D have demonstrated that low-torque ITER baseline scenarios with uncorrected fields introduced by a Test Blanket Module (TBM) mock-up coil are highly susceptible to rotation collapse and disruption. However, this loss of stability can be recovered (Figure 3.2-2 and Figure 3.2-3) using only n =1 compensation fields generated by ex-vessel control coils similar to those planned for ITER, enabling sustained operation at ITER performance metrics (T_{NBI} ~ 0.7 Nm, I_p/aB = 1.41, β_N = 1.8) [Lanctot, 2017]. Companion experiments in high-β plasmas have also demonstrated that n = 1 error field correction leads to recovery of β and rotation degradation, and a significant reduction of localized heat loads on plasma facing components associated with the TBM local magnetic field disturbance. These results validate concepts of a single dominant mode to the plasma response and show that correction of the n = 1 component recovers most of the performance impact of the TBM, while optimization of n = 2 fields showed little further recovery of the plasma rotation. Correction of TBM error fields has enabled full restoration of low torque access to ITER baseline-like scenarios on DIII-D.

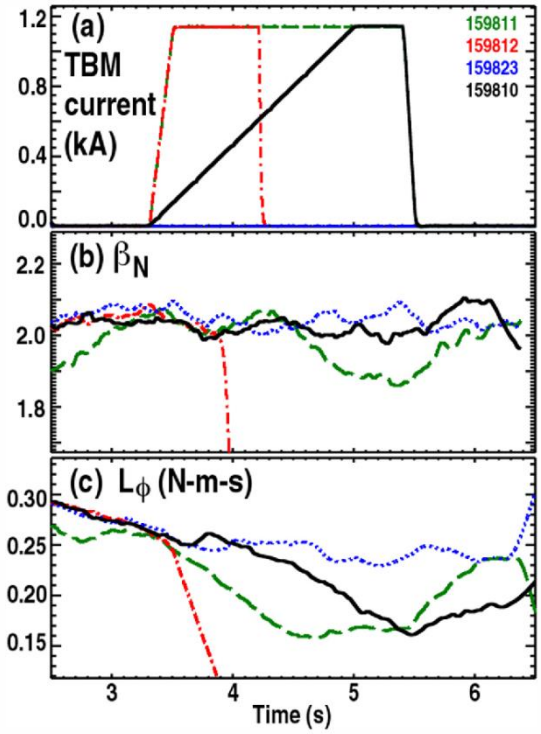

Figure 3.2-2: Evolution of : (a) the TBM coil current, (b) β_N, and (c) L_ϕ in low-torque discharges for three TBM field settings: no TBM field (dotted blue), uncorrected TBM field (dash–dot red), and compensated TBM field (dashed green and solid black traces). In every discharge, a 5/4 NTM is present when the TBM coils are energized. Onset of a 4/3 NTM instability in 159811 (green) at 4390 ms reduces energy and particle confinement, and modifies the torque balance [Lanctot, 2017].

The DIII-D results provided great encouragement for the viability of the TBM Program on ITER, and the important knowledge development that it will enable for fusion energy. They show that TBM error field compensation is essential in ITER, but this can be readily achieved with the external n=1 correction coils, recovering performance losses and eliminating associated localized heat loads. This increases our confidence that ITER will be able to achieve its scientific mission while developing the TBM technology, which is critical for Demo.

The experimental setting in DIII-D allowed simulating a pair of TBMs in only one location with an equivalent mass to that of the three pairs of TBMs that will be present in ITER. Additional experiments to take into account the distribution of three pairs of TBMs (in Port #2, Port #18 and Port #16) with TBM mock-up coils in three equatorial ports would be more representative of the actual situation in ITER.

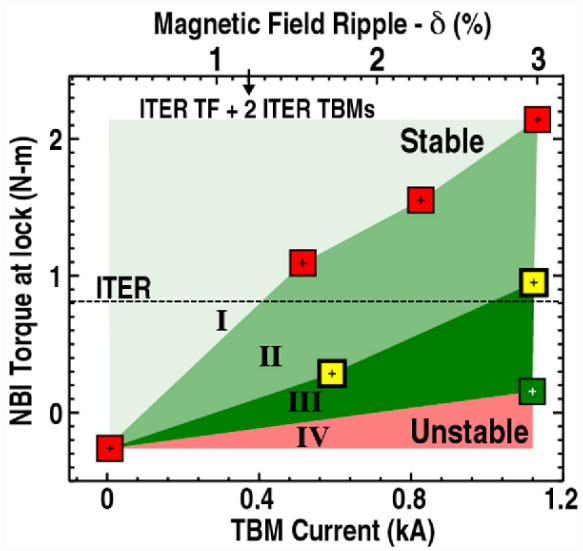

Figure 3.2-3: Torque access as a function of TBM field strength expressed in terms of TBM coil current and total magnetic field ripple for combinations of TBM and TBM-compensated fields: no n = 1 EFC (red), with optimal n = 1 EFC (green) and with partial n = 1 EFC (yellow). Region I can be accessed without encountering an n = 1 locked mode. Regions II and III are stable only with EFC and inaccessible otherwise. Region IV cannot be accessed even with optimized EFC of the TBM field. The dashed line marks the expected ITER-equivalent torque level in DIII-D. The total field ripple expected from a pair of 1.3 ton TBMs in ITER together with the TF ripple is 1.2% [Lanctot, 2017].

In any case, it is not likely that experimental tests in present tokamaks and physics/model-based extrapolation to ITER will provide a fully conclusive evaluation of the effects of ferromagnetic TBMs on ITER plasma performance, particularly for the high Q scenarios. The operation of the TBMs during the non-nuclear phase, particularly the comparison of ITER operation without TBMs in PFPO-1 to that with TBMs in PFPO-2, will probably give the necessary knowledge to understand if the effects of ferromagnetic TBMs on ITER operation and plasma performance can be mitigated to the level required to achieve the Q = 10 inductive and/or Q = 5 long pulse and steady-state goals or if more drastic measures need to be adopted for some critical operational phases (e.g. replacement of the TBMs by non-ferromagnetic dummy TBMs during some operational periods).

Finally, it is important to recall that error fields associated with the use of ferromagnetic RAFM steels are not an issue in a tokamak where all blanket modules are made of this material, e.g. in a Demo tokamak, unlike in ITER where RAFM steels are only used for the TBMs.

3.2.2 Experimental program during operation of the TBM Testing Program in ITER

Within the revised ITER schedule based on the Staged Approach, the TBM testing program is expected to start during PFPO-2, and continue throughout the FPO phase. As discussed in section 2.6.6, the first experimental campaign of the FPO phase will include both D plasmas and the first DT plasmas, while subsequent FPO campaigns will be developed around a variety of DT plasma scenarios.

In the operation of the TBSs, the successful operation of the tokamak and accompanying physics experiments is essential, so that the TBM program needs to be flexible enough to adjust, if necessary, to the needs of the rest of the ITER program. This includes start-up and shutdown periods and the adjustment to unscheduled down-times.

The adopted approach for the TBM testing program is to consider it as a ‘piggy back’ experiment where the TBMs will be exposed to ITER plasma discharges in a range of operational scenarios, as long as the presence of the TBMs would not impede the goals of the specific physics experiments/scenario development. This approach implies the need for the TBM teams to work with the ITER physics/scenario development program closely; this is essential to the success of the TBM testing program. An example of this kind of requirement is the estimated need of having, in the last part of an FPO campaign, at least six days of back-to-back pulses in order to reach a

sufficient pseudo-equilibrium of the tritium-related parameters in the TBM, thereby being able to measure relevant tritium-related data.

3.2.2.1 Overall TBM testing strategy and objectives

The 6 TBSs have to be installed early in ITER operation because very important data have to be obtained during PFPO-2. The majority will be installed with their ancillary systems during the Assembly Phase III, and they are all expected to be completely installed before the end of the Assembly Phase IV shutdown in 2034-35, before the start of the FPO phase (see Figure 2.2-1).

For each of the 6 TBSs types, it is planned to have up to four TBM versions (to be confirmed) to be tested in two main phases, a first phase that can be called the 'learning/qualification' phase and a second phase that can be called the 'Demo-relevant data acquisition' phase.

The 'learning/qualification' phase includes the PFPO-2 and first FPO campaign. It lasts about 5 calendar years and it is mainly devoted to:

- Verify/qualify the TBSs operation in ITER operational environment. It includes:
  - checking on how to integrally operate the various ancillary systems such as: i) cooling systems (CSs) including pressure drops in TBMs and connection pipes, effects on CSs pipes thermal expansion; ii) liquid metal systems including impact of MHD effects and filling and draining procedures; iii) detritiation systems (using trace D and/or T); iv) CODAC systems and connection with the Central Safety System and the Central Interlock System (for investment protection);
  - verifying port plug mounting/dismounting operations, Remote Handling systems and related operations including in the Hot Cell;
  - studying effects of magnetic field in all dynamic equipment associated with TBSs (e.g. pumps, valves, diagnostics, etc.);
- Verify the TBS response and the margins for control under abnormal conditions, such as plasma disruptions, Vertical Displacement Events and power excursions. Identify the operational margins covering all possible operating conditions and confirm/justify them; validation of TBS integrity;
- Solve all ITER/TBS interface issues such as: a) impact of ferromagnetic structures on plasma confinement and ion losses; b) demonstration of the capability of TBMs to withstand plasma disruptions; c) check tolerances with other components; d) check interferences with other ITER systems;
- Collect all relevant data and procedures needed for the licensing process, including demonstration of the capability to withstand disruption-induced loads. This information is needed significantly before the beginning of the start of the D-phase in FPO;
- To start preliminary measurements on TBM neutronic responses in order to verify and validate neutronic calculations;
- Demonstrate the coolant capability of the TBMs First Walls;
- Confirm the essential data and validate the assumptions made for the TBMs to be tested in the nuclear phase (compliance with the ITER license).

This phase is essentially covered by the operation of the first two TBM versions, the Electro Magnetic module (EM-TBM), in the PFPO-2 H/He phase and of the second TBM, the Thermal-Neutronic module (TN-TBM), in the D-phase and initial DT-phase, i.e. the 1st campaign of FPO.

The 'Demo-relevant TBS data acquisition' phase encompasses the later experimental campaigns in FPO, i.e. after FPO-1 for the purpose of this discussion. It lasts about 5 calendar years and it is mainly devoted to obtaining from the TBSs all data and information needed for the design and manufacturing of the corresponding Demo breeding blanket. The main expected results in this phase are the following:

- Validation of the capability of the neutronic codes and existing nuclear data to predict TBM nuclear response, including neutron fluxes and spectra, the tritium production rate, nuclear heat deposition, neutron multiplication and shielding efficiency;
- Investigation of the TBMs thermo-mechanical behaviour at relevant temperatures taking into account, for the first time, appropriate volume heat sources; assessment of adopted fabrication technologies, in particular for joints, and the validation of the adopted manufacturing processes under low-level irradiation; additional information for SB TBMs on the thermo-mechanics of pebble beds and for LB TBMs on tritium permeation barriers (either coatings or natural oxide layers);
- Demonstration of the operational behaviour of the blanket components for heat extraction and for tritium management, including, for instance, the assessment of tritium permeation and of methods for its reduction, of tritium extraction and coolant purification;
- Performance of an integrated test campaign in order to extend the reliability and operational performance database for the tested breeding blankets in a DT fusion device under Demo-relevant operating conditions (except for neutron fluence) for an extended period of time.

This phase is covered by the operation of the third TBM version, the Neutronic-Tritium/Thermo-Mechanical module (NT/TM-TBM), in the FPO-2 campaign and of the fourth TBM version, the INTegral module (INT-TBM) in the FPO-3 campaign.

It is assumed here to have the same approach for all six selected TBSs. This approach has therefore to be considered as 'generic'. In reality, minor differences can be expected from one TBS to another to account for their specific characteristics; such variation will be taken into account in a future version of the TBM testing plan. The four TBM versions considered for each breeding blanket concept, to be used throughout the various plasma operational phases, correspond to the four experimental campaigns shown in Figure 2.2-1 (PFPO-2 through to FPO-3). The detailed objectives for each campaign are given in the following sections.

In fact, the TBM testing program presented below reflects the adaptation of the initial TBM testing program, which was defined by the Test Blanket Working Group as an answer to the ITER-STAC-3 issues and presented at the STAC meeting in April 2008. In the test plan presented below, the initial testing strategy of the four TBM versions has been kept unchanged, although the scope and objectives of each test campaign have been revised to take into account the loading conditions in each campaign. Therefore, the TBM Leaders are in the process of further analyzing the impact of the newly defined ITER operational phases in the Staged Approach and the associated loading conditions to confirm the number of TBM versions to be tested as well as the associated scope of the tests in each phase. The possibility to extend the scope of tests associated with a given version of TBM or to combine 2 TBM versions into a single one is not precluded at this stage of the assessment.

Similarly, the tests in the successive campaigns of FPO, after FPO-3, have not yet been clearly defined. It is, however, expected that they will include the continuation of the operation of the INT-TBM systems to address reliability/availability issues and performance of advanced functional materials (e.g. coatings, beryllides). In this phase it is also envisaged to test other types of TBM systems, in particular more advanced ones whose technology is not sufficiently mature for being tested at the beginning of ITER operation.

It is assumed that all four TBM versions will share the same basic architecture, in particular their structural part (including the attachment system) whose design will be qualified during the testing program in laboratory facilities before TBM commissioning and checked/monitored step-by-step during the different phases of ITER operation. This strategy ensures a relatively stable interface between the TBMs and the other ITER tokamak and ancillary systems during the whole operational time with benefits for the availability and safety of the machine.

An important difference in the design of each TBM version will concern the integration of the specific instrumentation and the design of internal components; in particular of the breeding zone, which could be modified to test optimized design variants or to achieve the required testing conditions. For instance, the thickness of the breeder material could be increased to achieve Demo-relevant temperatures, and the ^{6}Li enrichment could be modified to obtain the desired test conditions.

Each TBM will include a monitoring system of all the features relevant for the control and safe operation of the TBM systems. This includes coolant and liquid metal circuit inlet and outlet temperatures (including by-pass in case of He), pressure measurements in coolant and liquid metal circuits, mass flow rates and neutronics responses inside the fluids (for the D- and DT operational phases). The TBM ancillary equipment will also have to be adapted to the different loading conditions that the various TBMs tested in the different ITER operational phases will be subject to.

3.2.2.2 Testing objectives for the Electro Magnetic Module (EM-TBM)

3.2.2.2.1 Role of the Electro Magnetic Module

Electromagnetic transients in tokamak reactors (e.g. disruptions, vertical displacements) constitute a severe issue as far as the capacity of the mechanical structure to withstand the induced mechanical forces and torques is concerned. These electromagnetic loads also play an important role for the general design of the TBMs, almost determining the design and the dimensions of the mechanical supports. In past years, several computational procedures and models have been developed and validated for the analysis of electro-mechanical transients in tokamak reactors. Some work has been dedicated to analyze the influence of magnetic materials such as the RAFM steels that are envisaged for Demo applications. Such steels show a non-linear ferromagnetic behaviour so that the distribution and magnitude of the loads on the reactor components during electromagnetic transients are significantly modified in comparison to non-magnetic structures.

Furthermore, ferromagnetic materials also cause distortions of the magnetic field; in ITER the TBMs magnetized structures produce an increase of the local ripple in the toroidal magnetic field which can lead to loss of confinement of high energy particles and localized power fluxes on the first wall as well as to a possible impact on the quality of the plasma confinement achievable in the H-mode regime.

Hence, the validation of computational tools suitable for the design of reactor components based on these materials is an issue. This validation can be carried out to some degree on the basis of suitable experiments in dedicated laboratory facilities or in existing tokamaks such as ASDEX Upgrade,

JET, EAST or KSTAR, etc. However, ITER will offer the possibility of performing tests in which geometry, materials, intensity of magnetic fields and plasma disruptions are relevant for reactor conditions, which cannot be reproduced together in any facility/present tokamak experiments. The EM-TBM is a mock-up of the Demo blanket having geometry and material composition that are relevant for EM testing. It will be instrumented so that specific electromagnetic parameters (such as magnetic fluxes, eddy currents and magnetic forces) will be evaluated from real measurements, allowing a comparison with calculated values and validation of the models.

For TBMs using liquid metals, an additional field to be studied is the MHD aspects. The liquid metal flows are affected by MHD effects that can be subdivided into: i) pipe flow in fringing B-field, ii) flow in manifolds (toroidal and poloidal), and iii) flow between structural components and cooling plates. These flows are sources of several specific issues with respect to pressure drop and velocity distribution. Electrical coupling between structural components and cooling plates may cause multi-channel effects leading to additional pressure drops, and also influencing the flow distribution. For HCLL TBMs, as the liquid metal throughput is quite small, the temperature gradient in the structural components may generate mixed convection and thus might alter the flow distribution.

The EM-TBM, seen as the first module of a series of similar modules, will provide a demonstration of the capability of the structural construction of the TBMs to withstand the mechanical loads associated with plasma disruptions. As far as heat loading is concerned, relevant tests for the FW are possible, anticipating the conditions of later phases of ITER operation. Finally, the EM-TBM will give the possibility to test the overall system and its remote handling (RH) procedures in a tritium uncontaminated environment and without activated materials, offering ideal conditions to detect early defects and allow corrections and/or, eventually, repairs.

Therefore, the Electro Magnetic module (EM-TBM) is used in the H/He phase to investigate the response of the structure to electromagnetic transients, to test operational functions (start-up and shutdown, cooling systems, remote handling, safety, MHD and trace D-permeation issues for the liquid breeder TBMs (if possible in this phase), etc.) and to collect essential data for the licensing process to be completed in advance of the transition to nuclear operations. It will also provide operational experience that would give confidence in being able to operate the TBS with reasonable reliability during the nuclear phase.

The use of ferromagnetic structural materials will have some effects on the ITER magnetic field configuration. At present, the most important issue is considered to be the creation of localized magnetic field perturbations, which may have a negative influence on plasma confinement in H-mode and lead to loss of fast particles and localized power fluxes to the first wall. Since the phenomena associated with these effects are not yet well understood, it has not yet been possible to theoretically assess the potential impact of the EM-TBM in ITER operation and plasma performance, although experiments in DIII-D are very encouraging regarding the possibility of mitigating such effects. The present designs for EM-TBMs do not include local active schemes to correct such effects (by coils creating a field that nulls the magnetic field perturbation introduced by the ferromagnetic mass) because it has not been demonstrated that this scheme would be very effective and because this complicates considerably the design of the TBM Port Plugs. If further analysis or new experiments would show that it is not possible to mitigate the effects of the TBMs on the ITER plasma performance to the required level, other possible countermeasures will be assessed (e.g. reducing ferromagnetic material masses in TBMs, further recession of TBMs from the plasma separatrix, optimization of the ferromagnetic inserts around the TBM ports).

3.2.2.2.2 General objectives

- Assess the overall functionality of TBM systems, both in the TBM (e.g., heaters if needed, measurement devices such as thermocouples, sensors, etc.) and in the ancillary equipment for coolant-circuits (pumps, heat exchangers, flow-meters, thermocouples, etc.) and Liquid Metal circuit (pumps, valves, tritium extractors, etc.). For the latter, confirm the start-up and shutdown procedures including heat losses, kinetics for heating and cooling of the circuits and liquid metal draining;
- Validate the performance and predictability of heat extraction from the first wall, taking into account the deposited surface heat, thermocouple measurements in structures and the FW cooling circuit;
- Validate the structural integrity of the box and of the attachment system (especially during disruptions and Vertical Displacement Events). This validation is of extreme importance for the safety dossier and licensing for the acceptability of similar TBMs in the DT phase;
- Record TBS performance data to be used for confirmation/justification of operational margins;
- Assess the effect of reduced activation ferromagnetic (RAFM) steel on the deformation of magnetic fields and determination of the induced ions losses with consequent additional heat loads on neighbouring components such as shield blanket modules (expected to be acceptable from theoretical estimates) and the schemes for their mitigation;
- Assess the impact of reduced activation ferromagnetic (RAFM) steel on plasma confinement and stability during plasma H-mode operation and the schemes for their mitigation;
- Check and validation of TBM exchange procedures including the RH system both in the port cell and the hot cell, TBM installation/dismantling procedures including TBM inspection techniques; and possible feedback to relevant procedures and manuals;
- Collect all relevant data and procedures needed for the licensing process.

3.2.2.2.3 Specific objectives/ measurements for the Lithium-Lead TBM Systems

- Measurement of Liquid Metal (LM) pressure drops, velocity profiles and temperature profiles as a function of LM flow-rate (capacitive pressure transducers, electrical potential probes, thermocouples, gyrostatic and electromagnetic flow meters) at different flow channels;
- Measurement of the steady state magnetic field as input for MHD simulations;
- Measurement of transient magnetic fields and currents in the breeder units to validate assumptions in EM calculations;
- Measurement of corrosion products concentration in LM as a function of the LM flow rate and cooling plate average temperature.

3.2.2.2.4 Specific objectives/ measurements for the Ceramic-Breeder TBM Systems

- Measurement of magnetic fields and currents in the Beryllium and ceramic beds to confirm the design assumptions used in EM calculations.

3.2.2.2.5 Special requirements for plasma operation scenarios in the PFPO-2 campaign

The EM-TBMs and associated systems are expected to be able to operate in all types of plasma scenarios achieved in the H/He phase. Few specific requirements from the TBM Program on plasma operations may be expected for this experimental campaign, ensuring that the data obtained allow accurate estimates for the worst operating conditions that the TBSs have to withstand in that operational phase and the following ones. The specific requirements from the TBM Program on plasma operations cannot yet be fully substantiated for the PFPO-2 experimental campaign. For example, there should be a consideration whether 25 days of high plasma current L-mode operation up to 15 MA/5.3 T is a long enough operational time for TLs to confirm essential data and validate the assumptions made for the design of the TBSs to be tested in the nuclear phase in compliance with the license requirements, such as safety measures functions expected during a particular incident/accident scenario.

In order to check the heat extraction capability of the FW, it would be necessary to have, for a couple of weeks, plasma pulses with predictable and constant heat flux on the FW. Even if this heat loads are low (<0.1 MWm^{-2}), if they are at fixed value and known in advance, it will be possible to set the appropriate coolant parameters in such a way to have gradients that could be close to the value achievable in the nuclear phase. It may well be that specific tests with varying FW surface temperature would be required for the overall ITER first wall heat load diagnosis.

To have trace-D injected in the later part of PFPO-2 plasma operations would be desirable in order to measure the D-permeation from the FW (TBMs but also frames, if feasible), and support assessments of tritium permeation rates during FPO. This would require typically a week or more of continuous operation of the TBMs at defined preheating conditions, and repeated well-defined plasma parameters. There are significant synergies between this type of experiments and those required to check the heat extraction of the TBM FW with those being considered for the characterization of fuel retention (see section 2.5.5.12.2.1), so that a common set of experiments could most likely address both the retention characterization aspects and the EM-TBM specific needs towards the end of PFPO-2.

3.2.2.3 Testing objectives for the Thermal-Neutronic Module (TN-TBM)

3.2.2.3.1 Role of the Thermal-Neutronic Module

The Thermal-Neutronic module (TN-TBM) is used mainly for investigation of neutronic responses during the FPO-1 campaign with D-D and initial DT-operation, and to confirm the thermal behaviour of the TBM FWs. In particular, the TN-TBM main objective is the validation of the capability of the neutronic codes and existing nuclear data to predict TBM nuclear responses, including neutron fluxes and spectra, nuclear heat deposition, and shielding efficiency. In relation to these nuclear responses, this module will permit accurate measurement of tritium production in order to verify the tritium breeding predictions. It will also give preliminary information on the capability of the TBSs to extract surface and low-level volumetric heat loads, the latter being applied for the very first time on the breeding blanket component.

Instrumentation for the TN-TBM will include thermocouples, and activation foil stacks, fission micro-chambers, and/or scan wires to monitor and assess neutron fluence and energy spectrum.

3.2.2.3.2 General objectives

- Measurement of neutronic fluxes and spectra in selected positions of the TBM. The data will be used (together with the information derived from other ITER diagnostics) to validate

neutronic calculations (activation foils, fission chambers and scan wires) and to define tritium sources;

- Neutron and gamma load measurements on the FW (bi-chromatic infrared camera + thermocouples, activation foils);
- Assessment of the shielding efficiency of the TBM: neutron flux at the back plate (BP) rear face (e.g. by three neutron detector counters), activation foils in the back-shield layers;
- Calibrate most of the nuclear and thermal measurements equipment (to save testing time during later DT campaigns);
- Preliminary demonstration of the TBS capability to extract heat loads coming from both surface heat loads on the first wall and low-level volumetric heat loads in the various blanket materials;
- Confirm the effects of reduced activation ferromagnetic (RAFM) steel on plasma confinement and stability during plasma H-mode operation and on induced fast ion losses and the schemes for their mitigation (as assessed during PFPO-2).

3.2.2.3.3 Specific objectives/ measurements for the Lithium-Lead TBM Systems

- For Pb16Li TBMs, preliminary Pb16Li activation measurements for measurement systems' calibration, including trace tritium measurements;
- Confirmation of tritium-control and management performance (e.g., permeation) using trace D and/or trace T.

3.2.2.3.4 Specific objectives/ measurements for the Ceramic-Breeder TBM Systems

- Preliminary activation measurements for Be and ceramics;
- Confirmation of tritium control and management performance (e.g. permeation) using D and trace T.

3.2.2.3.5 Special requirements for plasma operation scenarios in the FPO-1 campaign

The TN-TBMs and associated systems are expected to be able to operate in all types of plasma scenarios achieved in the FPO-1 campaign. No specific requirements from the TBM Program on plasma operations are expected for this experimental campaign. The only requirement is to know in advance the most extreme operating conditions that the TBSs will experience during this phase, in particular concerning wall loads and allow tuning of neutron flux/fluence measurements in the TBM, and initial production of Tritium in the breeder zone.

3.2.2.4 Testing objectives for the Neutronic-Tritium/Thermo-Mechanic Module (NT/TM-TBM)

3.2.2.4.1 Role of the Neutronic-Tritium/Thermo-Mechanic Module

The Thermo-Mechanic module (NT/TM-TBM) is mainly used for investigation of the TBM structural behaviour at relevant temperatures and to determine the nuclear responses at Demo-relevant 14.1 MeV neutron flux, in particular the tritium production. Typical TBM thermal time constants are 100 – 200 s for the front part of the TBM and longer for the rear part. Therefore, with ~ 400 s pulses thermal equilibrium can be reached, at least in the front part of the TBMs. Typical

time constants for tritium control and management are of several days and therefore only measurements of T-sources are expected to be achieved during this DT operational phase.

Additional objectives are: for the ceramic Breeder TBMs, the thermo-mechanics of pebble beds and tritium extraction by purge gas; for the Lithium-Lead TBMs, investigation on tritium control. These objectives will be assessed during the FPO-1 campaign, which will have both low and high duty cycle operation with DT pulses.

Instrumentation for this NT/TM-TBS will include thermocouples, flow-meters, pressure transducers, stress and strain gauges and T-concentration sensors, and other instrumentation in various parts of the ancillary circuits and components. In relation to the nuclear responses, the instrumentation will include activation foil stacks to monitor neutron fluence and energy, fission micro-chambers, and/or scan wires and measurement systems allowing the determination of Tritium inventories.

For the Lithium-Lead NT/TM-TBMs the main objectives are twofold: First is the measurement of the thermo-mechanical characteristics of the TBM (temperature and stress/strain distribution) under neutron flux to validate calculation assumptions and results. Second is the measurement of the inlet and outlet tritium concentration (both in the coolant and LM circuits) that will be carried out in order to validate a local model simulating the tritium transfer in the TBM and allowing the determination of a global tritium mass transfer coefficient. This global mass transfer coefficient will characterize the global permeation from the LM to the He circuits through the RAFM steel structure in a system model. Furthermore, thermal measurements could be used to estimate the actual heat flux on the first wall and the nuclear heat deposition. Then, an equivalent Neutron Wall Loading (NWL) could be estimated and the tritium production could be calculated. This procedure would allow checking if tritium production could be assessed using temperature measurements. However, for all measurements related to tritium the interpretation of the obtained values is quite complex due to the pulsed operation with a quite long exhaust time.

For the Ceramic Breeder TBMs, the NT/TM-TBM will be mainly dedicated to the testing of the Pebble bed thermo-mechanics, a critical issue for the temperature control of this kind of concept and to ensure correct performance of the T purging flow. The thermo-mechanical behaviour of pebble beds is determined by numerous effects, e.g. the differential thermal expansion between the beds and the structure, elastic and plastic deformation of the pebble bed and structure, thermal creep, ‘bed ratcheting’, gap formation, and irradiation swelling. These effects play an important role for the design-relevant properties of the beds, in particular the thermal conductivity, the bed-to-wall heat transfer coefficients, and the modulus of elasticity. The design of a blanket using a breeder and multiplier in form of a pebble bed requires the development of efficient computer codes. The validation of these codes and of the implemented models is an important part of the development work which has to be carried out on the basis of suitable experiments, up to now either out-of-pile or in fission reactors. However, these experiments suffer from severe physical and technical restrictions, especially the lack of the non-uniform volumetric heating. Hence, tests under conditions closer to fusion power reactor blankets are necessary and the test in ITER will inherently provide such conditions. Of particular importance for thermo-mechanical pebble bed testing are the neutron flux and spectrum in large volumes, and the related volumetric heat sources in the DT phase, which allows the installation of test modules with pebble beds of representative size. A limitation of the experimental validation can be the length of the burn pulses; preliminary calculations have shown that a full steady state condition in the overall TBM is reached only for pulses of about 1000 s; however, some TBM regions have a shorter time constant (~10 s in the FW vs. the surface heating flux) so that the use of shorter pulses can be used for this kind of validation.

In any case, the main restriction of this kind of experiments in ITER is the relatively low neutron fluence which implies that end-of-life conditions (in comparison to Demo) in the pebble beds cannot be reached.

Other appropriate test conditions must be established by selecting appropriate design parameters. One important parameter is the maximum temperature in the pebble beds. The relatively low neutron flux and resulting power density can be compensated by increasing the thickness of the pebble beds or increasing ^{6}Li enrichment (in comparison to a Demo design). First estimates have shown that the thickness of the breeder pebble bed in ITER must be about 25 mm at 90% ^{6}Li enrichment to achieve the same maximum breeder temperature (~920°C) as in a power reactor blanket. Another design parameter is the orientation of the pebble beds with respect to gravity; in current Demo blanket concepts, the beds are horizontal at the tokamak mid-plane with the inclination increasing in the poloidal direction. In single-null divertor reactors, vertical beds exist at the top of the poloidal cross section of the torus (opposite the divertor x-point). In vertical beds, gravitational forces additionally affect the thermo-mechanical behaviour of the pebble beds, and ratcheting effects may lead to bed compaction and void formation. The experimental investigation of this phenomenon should be included in the thermo-mechanics test program.

3.2.2.4.2 General objectives

- Measurement of temperature and stress/strain distributions in selected parts of the TBM structure in order to validate computational codes and modelling;
- Assessment of the thermal stresses on joints and corresponding joints' behaviour to validate computational codes and modelling;
- Further validation of the performance and predictability of heat extraction from the first wall, taking into account the deposited surface heat and thermocouple measurements in structures and in the FW cooling circuit;
- Validation of the performance and predictability of heat extraction from the structures and breeding zone, taking into account the deposited volume heat (for the first time);
- Measurement of tritium and gamma production (activation foils, fission chambers) for comparison with the neutronic calculations in order to assess the tritium breeding capability of each blanket design;
- Assessment of the tritium permeation towards the coolant and initial validation of tritium-extraction techniques;
- Irradiation of samples of structural and functional material for determination of material nuclear responses. Measurements of Neutron Fluxes (> 1 MeV), α and proton production rates near the FW and welds (activation foils, fission chambers) for material damage estimations.

3.2.2.4.3 Specific objectives/ measurements for the Lithium-Lead TBM Systems

- Influence of the Pb16Li flow rate and chemistry control on Pb16Li and He average tritium concentrations;
- For Pb16Li TBMs, Pb16Li activation measurements (T with gamma spectrometer in line and integral, Po and other reaction products with counters and spectrometers);
- Influence of the ^{6}Li enrichment and, therefore, of the volume ratio of ^{6}Li/RAFM steel.

3.2.2.4.4 Specific objectives/ measurements for the Ceramic-Breeder TBM Systems

- Test of the thermo-mechanical behaviour of the pebble beds under different configurations. Measurement of the temperature field and (if possible) stresses. Comparison with computational code predictions;
- Tests of fluid-dynamic performance of the purge flow, including measurement of pressure drops and investigation of possible causes of performance degradation during operation due to pebble fragmentation and deposition of dust;
- Test of the effect of the purge gas flow rate and purge gas chemistry (hydrogen addition, impurities) on tritium extraction from the breeder material.

3.2.2.4.5 Special requirements for plasma operation scenarios in the FPO-2 campaign

The NT/TM-TBMs and associated systems are expected to be able to operate in all types of plasma scenarios achieved in the FPO-2 campaign. The first requirement for the TBMs is to know in advance the most extreme operating conditions that the TBSs will experience during this operational phase. A further important requirement in the FPO-2 campaign is to have several series of pulses with a good in advance knowledge of their characteristics in order to adapt the TBM operating parameters to the expected loads and durations.

3.2.2.5 Testing objectives for the INTegral TBM (INT-TBM)

3.2.2.5.1 Role of the INTegral Module

The INTegral TBM (INT-TBM) is used to demonstrate the operational behaviour of the blanket components for heat extraction and tritium management during the FPO-3 experimental campaign (DT operation at high duty cycle). The overall objective of the integrated test campaign is to extend the reliability and operational performance data base for the tested breeding blankets in a DT fusion device under Demo-relevant operating conditions (except for neutron fluence) for an extended period of time.

Instrumentation will include thermocouples and flow-meters, pressure transducers, stress and strain gauges, tritium concentration sensors. In this case, the installed instrumentation will be reduced, in a compatible way with the required measurements, in order to reduce the impact of the detectors on the TBM functionality.

The INT-TBM should perform its designated mission without failure, enabling parametric studies related to thermal response, prove thermal and mechanical predictions, demonstrate the on-line tritium handling capability and provide general experience for system improvements.

The INT-TBM ‘looks-like’ the corresponding Demo blanket module, suitably scaled in order to fit in the Test Blanket port. It represents, to the largest extent possible, all synergetic effects acting in a blanket module of a power reactor, such as e.g., cooling the FW and other structures, local heat generation and transport and tritium generation and release. The low Neutron Wall Load (NWL) in ITER compared to Demo necessitates compromises, where necessary, between the look-alike Demo design in favour of an act-alike Demo design (e.g. multi-pass helium coolant channels in the FW) in order to achieve reactor-relevant operating conditions. These are achieved mainly in terms of temperature level and distribution (both in the box and in the breeder zone), coolant conditions such as inlet/outlet temperature and pressure or coolant parameters such as Reynolds and Nusselt numbers and, for the Pb16Li-based TBM, Pb16Li relevant parameters, such as Hartmann, Stuart and Sherwood numbers.

This campaign will cover testing of the tritium systems (on-line extraction and removal) in a long period of long pulse operation and back-to-back series of pulses (about six days of continuous back-to-back pulses are required). Pulses of several thousand seconds would be required to approach steady state conditions for the thermal performance of the TBM. The objective is to validate a dynamic model of the tritium transfer in the TBM system and obtain relevant data allowing an extrapolation to a Demo blanket concept and its technological components.

3.2.2.5.2 General objectives

- Validation of the on-line tritium processing systems designed for the different TBM concepts. This will require a relatively long period of back-to-back series of reference pulses (about six days of continuous back-to-back pulses) as well as the development of on-line tritium measurement techniques/sensors with suitable accuracy;
- Validation of a dynamic model of the tritium transfer in the TBM system through relevant experimental data allowing an extrapolation to Demo (blanket concept and technological components);
- Parametric analysis on the impact of the main circuits' functional parameters (purge gas flow-rate, He chemistry, efficiency of tritium permeation barriers) on the global tritium system performance in order to obtain relevant information for extrapolation to Demo.

3.2.2.5.3 Specific objectives/ measurements for the Lithium-Lead TBM Systems

- As a first step, the model of the global mass transfer coefficient of the TBM will be finalized and validated. Tritium concentration inlets (in He and Pb16Li circuits) will be considered as inputs. Tritium concentration outputs will be measured and compared with calculations;
- As a second step, the predictive capacity of the tritium system model and component recovery models will be assessed. Only system functional parameters and tritium recovery parameters will be the considered as inputs, the overall inlet and outlet concentrations of both He and Pb16Li concentrations will be compared with calculations.

3.2.2.5.4 Specific objectives/ measurements for the Ceramic-Breeder TBM Systems

- Monitoring of temperatures and stresses in the solid breeder zone and of the pressure drop in the purge systems;
- Test of the effect of the purge gas flow rate and purge gas chemistry (hydrogen addition) on tritium extraction from the breeder.

3.2.2.5.5 Special requirements for plasma operation scenarios in the FPO-3 campaign

As noted above, in this experimental campaign the TBM testing program will require about six days of continuous back-to-back pulses. In this period, particularly towards the end of FPO-3, ITER long pulse plasma operation should be well developed so that disruptions will be infrequent. Ideally, long pulses at high fusion power and with a period of 6 days (to be confirmed) of back-to-back pulses, e.g. with high FW heat loads, should be dedicated to TBM testing. Pulses of several thousand seconds would be required to approach steady state condition for the thermal performance of the TBM.

3.2.2.6 Overall achievements in the TBM Testing Program from PFPO-2 to the FPO-3 campaign – implications for later operations

As illustrated in Figure 2.2-1, the revised schedule within the Staged Approach foresees (where start and end dates are inclusive):

- First Plasma: December 2025 – June 2026;
- PFPO-1: December 2028 – May 2030;
- PFPO-2: June 2032 – February 2034;
- FPO campaign 1 (DD + first DT): starts December 2035 (16 months campaign);
- FPO campaign 2: starts December 2037 (16 months campaign);
- FPO campaign 3: starts December 2039 (16 months campaign).

The schedule outlined above assumes that the long-standing pattern of ITER operational campaigns developed in the original RAMI analysis will be maintained.

The transition to 'partial' nuclear operation at ITER begins with the introduction of tritium into the Tritium Plant, which is foreseen in present planning to coincide with the start of Assembly Phase IV, and an initial regulatory authorization is required for this step. Authorization for full nuclear operation of the ITER facility is expected later, towards the end of Assembly Phase IV.

The majority of TBSs are expected to be installed during the Assembly Phase III in 2030 - 2031 and the planned operations for the four TBM-versions are expected to last until March 2041. From the point of view of the TBM Program, these 10 calendar years can be divided in two large phases, a first phase that can be called the 'learning' phase and a second phase that can be called the 'Demo-relevant data acquisition' phase.

The 'learning' phase includes the PFPO-2 and the FPO-1 campaign 1. It lasts about 6 calendar years and it is mainly devoted to:

- Verify/qualify the TBSs operation in the ITER operational environment. It includes:
  - checking how to operate the various ancillary systems such as: i) cooling systems including pressure drops in TBMs and connection pipes, effects on CS pipe thermal expansion; ii) liquid metal systems including impact of MHD effects and filling and draining procedures; iii) tritium-detritiation systems (using D); iv) CODAC systems and connection with the Central Safety System and the Central Interlock System;
  - verify port plugs mounting/dismounting operations, RH handling systems and related operations including in the Hot Cell;
  - effects of magnetic field in all dynamic equipment associated with TBSs (e.g. pumps, valves, diagnostics, etc.);
- Identify the operational margins covering all possible operating conditions and confirm/justify them; validation of TBMs integrity;
- Solve all ITER/TBS interface issues such as: a) impact of ferromagnetic structures on plasma confinement and fast ion losses; b) demonstration of the capability of TBMs to withstand plasma disruptions; c) check tolerances with other components; d) check interferences with other ITER systems;

- Collect all relevant data and procedures needed for the licensing process, including demonstration of the capability to withstand disruption-induced loads. This information is needed significantly before the end of the PFPO phase;
- To start preliminary measurements on TBM neutronic responses in order to verify and validate neutronic calculations;
- Demonstrate the coolant capability of the TBMs First Walls.

This phase is essentially covered by the operation of first TBMs, the Electro Magnetic module (EM-TBM), in the PFPO-2 campaign and of the second TBM, the Thermal-Neutronic module (TN-TBM), in the FPO-1 campaign.

The 'Demo-relevant data acquisition' phase concerns the FPO-2 and FPO-3 campaigns involving experiments in DT plasmas. This phase lasts about 4 calendar years and is mainly devoted to obtaining all data and information from the TBSs relevant for the design and manufacturing of the corresponding Demo breeding blanket. The main objectives of this phase are the following:

- Validation of the capability of the neutronic codes and existing nuclear data to predict TBM nuclear response, including neutron fluxes and spectra, the tritium production rate, nuclear heat deposition, neutron multiplication and shielding efficiencies;
- Investigation of the TBMs' thermo-mechanical behaviour at relevant temperatures taking into account, for the first time, appropriate volume heat sources; assessment of adopted fabrication technologies, in particular for joints, and the validation of the adopted manufacturing processes under low-level irradiation; additional information for SB TBMs on the thermo-mechanics of pebble beds and for LB TBMs on tritium permeation barriers (either coatings or natural oxide layers);
- Demonstration of the operational behaviour of the blanket component for heat extraction and for tritium management including, for instance, the assessment of tritium permeation and of methods for its reduction, of tritium extraction and of coolant purification;
- Performing an integrated test campaign in order to extend the reliability and operational performance database for the tested breeding blankets in a DT fusion device under Demo-relevant operating conditions (except for neutron fluence) for an extended period of time.

This phase is covered by the operation of the third set of TBMs, the Neutronic-Tritium/Thermo-Mechanical module (NT/TM-TBM), in the FPO-2 campaign and of the fourth set of TBMs, the INTegral module (INT-TBM) in the FPO-3 campaign.

These data and information will allow the design and manufacture of a Demo breeding blanket, provided that high neutron fluence material data are obtained in parallel in another facility; since the expected total neutron fluence in ITER is much smaller than the one expected in Demo, the neutron fluence-induced effects on materials cannot be assessed in ITER.

As a consequence, the objectives for later FPO campaigns (i.e. FPO campaigns after FPO-3) can be twofold depending on the fusion program strategy assumed by each Member:

- Those Members supporting a 'fast track' approach to fusion energy development will likely proceed immediately to the detailed design and construction of Demo using the information on TBSs described above. In this case, the later FPO campaigns can be used to continue the tests on the same TBSs as in the earlier DT campaigns in order to collect further data useful to determine the reliability of the corresponding breeding blanket system;

- Those Members having a longer-term approach to fusion energy development may wish to test more advanced breeding blanket concepts in ITER in order develop high-performance breeding blankets. In this case, the FPO campaigns after FPO-3 will be partially used to repeat the operations performed in the previous phases for the initial TBSs but now for the new advanced concepts. The constraints are that the new advanced TBSs should use the already existing pipes, connections, and equipment.

3.2.3 Summary and Conclusions

In this preliminary adaptation of the TBM Program to the revised ITER schedule within the Staged Approach, the previous TBM testing strategy of testing in sequence four TBM versions for each type of TBM designs has been maintained.

It must be stressed that this proposal may be modified in the future when the following uncertainties have been resolved:

1) Impact of the TBM ferromagnetic structural material on plasma performance - if no definitive experimental evidence is available before testing of the TBMs in ITER and/or if the effects of TBMs are identified by comparison of PFPO-1 and PFPO-2 plasmas but cannot be satisfactorily mitigated, it may be necessary to add a partial use of dummy TBMs made of non-ferromagnetic materials during the PFPO-2 phase until mitigation schemes for the effects of ferromagnetic TBMs have been developed and implemented;
2) Eventual duration of the different ITER TBM phases - the possibility of extending the scope of tests associated with a given version of TBM, or to combine 2 TBM versions into a single version with a single testing campaign, cannot be precluded at this stage of analyses;
3) Delivery date of each Test Blanket System – It may happen that some TBSs are delivered later than the others.

Nevertheless, it can be concluded that the integration of the TBM Program into the Staged Approach schedule is possible, confirming its robustness for adaptation to modified ITER operational plans without jeopardizing the TBM testing objectives.

4 Upgrade Options and Required R&D

The aim of the proposed upgrade plan within the context of the ITER Research Plan is twofold: (i) to minimize the risks to the achievement of ITER's goals by implementing timely upgrades of systems in view of the results obtained from the scientific exploitation of ITER itself and by the R&D carried out by the ITER Members during construction and the initial phase of ITER operation; and (ii) to expand the capabilities of the ITER device by suitable upgrades of ancillary systems emphasizing the demonstration of physics and technologies that will be required in Demo.

The specific upgrades which could be envisaged at present and their rationale are provided in the following sub-sections. The corresponding time-windows within which upgrade decisions for key systems contributing to the achievement of ITER's goals could be taken, based on preceding operational experience, are described within the deliverables for sections 2.5.4, 2.5.5, 2.6.3, 2.6.4 and 2.6.5; these are summarized below. It should be noted that the implementation of some upgrades requires significant timescales (~5 years), as described in Appendix G for the H&CD systems. Early decisions may be required, therefore, to avoid delays in the progress of the experimental program during DT operation, when such upgrades may well be essential to the satisfactory completion of the ITER mission. Table 4-1, at the end of this section, provides an overview of the main options for upgrades in each of the major categories of tokamak and auxiliary systems which can be foreseen at present as potentially required (or simply 'desirable' for improved physics studies) at each stage of the IRP.

Possible required upgrades following the results of the PFPO-1 operational campaign:

PFPO-1 will provide first operational experience for: L-mode plasmas up to 7.5 MA and for H-mode plasmas up to 5 MA with ELM control by the application of 3-D magnetic field perturbations. On this basis the following upgrades could be identified at this stage:

- *Need to increase the additional heating level:* if the power required for H-mode operation exceeds expectations – there might be a preference for ECRH or ICRF (if the corresponding antenna is available), depending on operational experience;
- *Need to upgrade the pellet injection system*: to provide ELM control capabilities, if ELM control by 3-D fields is found inefficient (for stationary H-modes or for transient H-mode phases, i.e. access/exit and with varying q_{95});
- *Possible need to upgrade the NBI system with the 3rd HNB:* if ELM control with no-torque input (only RF heated plasma discharge with ECRH and, possibly, ICRF will be performed in this phase) proves difficult or leads to excessive confinement degradation.

Possible required upgrades following the results of the PFPO-2 operational campaign:

PFPO-2 will provide first operational experience for: L-mode plasmas in the range 8 - 15 MA, H-mode plasmas around 7.5 MA with ELM control by the application of 3-D magnetic field perturbations, and current drive capabilities for long-pulse operation in ITER. On this basis the following upgrades could be identified at this stage (if the assessment of PFPO-1 is not conclusive):

- *Need to increase the additional heating level:* if the power required for H-mode operation exceeds expectations, with the preference among ECRH, ICRF or NBI options being developed based on operational experience;

- *Need to upgrade the pellet injection system:* to provide fuelling and ELM control capabilities, if either fuelling is found insufficient at higher plasma currents or ELM control by 3-D fields is found inefficient (for stationary H-modes or for transient H-mode phases, i.e. access to/exit from the H-mode and with varying q_{95});
- *Need to upgrade the NBI system with the 3rd HNB*: either for ELM control (if ELM control in H-modes with 2 HNBs proves difficult, or excessive confinement degradation is observed due to the low input torque), or to achieve the required current drive for steady-state operation (if, for any reason, the current drive provided by the HNBs is lower than expected);
- *Need to upgrade the ECRH system:* if the level of current profile control in the current ramp-up and flat-top is insufficient for long-pulse/steady-state scenarios in DT, or the requirements for NTM control by ECCD make power sharing demands on ECRH difficult to manage at the baseline power level (i.e. the baseline ECRH power level provides insufficient scenario flexibility when using ECRH both for core heating and NTM control).

As detailed in Appendix G, a decision on the installation of the 3rd HNB upgrade taken at this stage would lead to a significant delay of the FPO phase, whereas a decision at the end of PFPO-1 is not expected to have any impact on the start of FPO.

Possible required upgrades following the results of the first FPO operational campaign:

FPO will provide first operational experience for D and DT plasmas, in particular for high-Q operation at 15 MA, and the first experience on the issues which must be resolved for the development of the Q ~ 5 long-pulse and steady-state scenarios. By this time most of the upgrades required to achieve these goals should have been implemented. However, a need for further upgrades might be identified at this late stage from the exploration of high-β DT plasma conditions, which can lead to requirements that cannot be met by the installed systems at that time and that would not have been identified by previous operation in PFPO-1/PFPO2:

- *Need to upgrade the pellet injection system:* to provide DT fuelling mix control and ELM control capabilities, if either DT fuelling or mix control with the (baseline) 4 pellet injectors is found insufficient in DT plasmas, or ELM control by 3-D fields is found inefficient (for stationary H-modes or for transient H-mode phases, i.e. access/exit and with varying q_{95});
- *Need to upgrade the ECRH system*: if the level of current profile control is insufficient for the development of long-pulse/steady-state scenarios in DT, or if the required power level to provide W accumulation control and NTM control in high-Q plasmas exceeds the baseline power level of 20 MW;
- *Need to upgrade the ICRF system*: if studies on the effect of heating mixes reveals that a higher level of ICRF power optimizes Q in integrated H-mode scenarios;
- *Need to upgrade power supplies for Resistive Wall Mode control:* if the capability provided by the baseline power supplies for the ELM control coils is not sufficient to ensure the required level of RWM for high-Q/high-β scenarios.

In addition to these upgrades, others may be required to ensure robust ITER operation, i.e. essentially disruption-free, but with routinely successful mitigation when disruptions do occur. The need for these upgrades (vertical stability control, disruption mitigation upgrades, etc.) is likely to be identified as the expansion of the ITER operational space proceeds towards: higher plasma currents (PFPO-2) and plasma energies (PFPO-2 and FPO), and with the start of DT operation

(FPO). However, without ITER's operational experience, it is not possible to provide a specific point in the experimental program where the need for such upgrades will be identified.

4.1 Heating and current drive systems

As specified in the *Project Requirements* [ITER_D_27ZRW8, 2014], The maximum installed power foreseen for H&CD in ITER is 130 MW, of which a maximum of 110 MW can be injected simultaneously into the tokamak due to limits in the total site power for steady operation. A review of analyses of the exploitation of H&CD systems in candidate non-inductive plasma scenarios in ITER is given in Appendix E, while options for upgrading of the H&CD systems are discussed in Appendix G. The *Project Requirements* identifies options for 4 H&CD upgrade scenarios, leading to a total installed power of ~130 MW:

1. The addition of 20 MW each of ECRH, ICRF and LHCD to the baseline capability;
2. An upgrade of NBI to 50 MW with the addition of a 3rd HNB line, plus the addition of 20 MW of ECRH and LHCD; the removal of one ICRF antenna while upgrading of the performance of the other to maintain 20 MW of IC;
3. An upgrade of NBI to 50 MW with the addition of a 3rd HNB line, plus the addition of 20 MW of ECRH and ICRF;
4. An upgrade of NBI to 50 MW with the addition of a 3rd HNB line, plus the addition of 40 MW of LHCD; the removal of one ICRF antenna while upgrading of the performance of the other to maintain 20 MW of ICRF.

As discussed in Appendix G, allocation of ports to meet H&CD and Diagnostics requirements within the Staged Approach has resulted in the deprioritization of LHCD as an H&CD upgrade option. Priority in the development of H&CD upgrades is now given to:

- A 3rd HNB line to increase the NBI power from 33 MW to 50 MW;
- An increase of the ECRH power from 20 to 40 MW (maintaining the same number of ports);
- An increase of the ICRF power by bringing the two antennas from 20 to 40 MW.

For the baseline heating systems, the estimated time required to perform the upgrades of existing H&CD systems (from procurement to installation) is in the range of 5-6 years. Therefore, a decision immediately after PFPO-1 is required in order to have upgraded systems ready by the beginning of the FPO phase. The choice of upgrade options would then depend on experimental observations and operational experience during PFPO-1, as well as on R&D results from ITER Members' facilities. These experimental observations are expected to provide the first quantitative information regarding the required level of additional heating to achieve ITER's $Q \geq 10$ goal. In addition, uncertainties regarding the required conditions for H-mode access and stationary type-I ELMy H-mode operation in ITER, in particular its dependence on isotope and plasma species, are expected to be reduced by R&D studies. Proposals are already under development to ensure that H&CD upgrades could be implemented at a sufficiently early stage to allow their exploitation early in FPO, as discussed in Appendix G.

4.1.1 Baseline H-mode access capabilities

Although the technical feasibility of delivering 10 MW of ICRF during PFPO-1 has not yet been demonstrated, in the context of the IRP it is assumed that the 10 MW of ICRF power will be available for PFPO-1, and therefore that 30 MW and 73 MW of auxiliary heating power should be

routinely available for the PFPO-1 and PFPO-2 campaigns respectively. Access to H-mode in helium (and possibly hydrogen) is expected during PFPO-1 within the program based on the 5 MA/1.8 T option once the installed H&CD systems are commissioned for short pulse (a few tens of seconds) operation. However, stationary type-I ELMy H-mode operation in helium and hydrogen plasmas at higher currents and fields may require the full baseline auxiliary heating power foreseen in PFPO-2.

In the case of hydrogen plasmas, the lack of a reliable heating scheme for ICRF at 7.5 MA/2.65 T is an issue and, thus, under these conditions the maximum level of coupled power from this system may be significantly lower than that specified (10 MW in PFPO-1, 20 MW in PFPO-2). Therefore, during PFPO-2, operation in helium at half field is expected to provide the best experimental evaluation of the auxiliary H&CD power required for Q = 10 operation in ITER. This information would complement observations from 5 MA/1.8T hydrogen and helium plasmas during PFPO-1 and PFPO-2.

4.1.2 Strategy towards H&CD upgrades

A decision on upgrades to the existing heating systems to ensure the success of the $Q \geq 10$ mission could be based on experimental results from the PFPO-1 phase. The objective of such as decision would be to have the upgraded systems ready for DT operation to achieve the $Q \geq 10$ goal as early as possible. If the results from experiments conducted in PFPO-1 were unclear, any decision on H&CD upgrades would be postponed until PFPO-2, in which case the upgraded heating systems would only be available later in the FPO campaigns, possibly influencing the timescale for the achievement of the $Q \geq 10$ goal. However, delaying a decision on the preferred H&CD upgrades until PFPO-2 could also cause a delay in the transition to the FPO phase, if further optimization of plasma scenarios were required in advance of DT operation or if installation of upgraded (for some) H&CD systems were to be undertaken prior to activation of the tokamak structures – the strategy for upgrading of the HNB system discussed in Appendix G is designed to avoid this latter issue.

Even if early operational experience confirms that the baseline H&CD power will provide an adequate basis for meeting the $Q \geq 10$ mission, it would still be sensible to plan for an H&CD upgrade, with priority given to improving the current drive capabilities of the device to achieve the $Q \geq 5$ steady-state goal, once the initial inductive DT experiments reach the $Q \geq 10$ milestones. The choice of preferred current drive upgrade (NBCD, ECCD) will depend on: (i) the results of research in ITER on the real capabilities of each H&CD system, in particular the level of the current drive obtained with the existing systems (HNB and ECRH); (ii) the experimental evaluation of the role played by plasma effects on the localization of the driven current in ITER compared with standard resistive current diffusion; and (iii) R&D carried out at the ITER Members' facilities on the development of plasma scenarios for steady-state operation in ITER, as described below.

4.1.3 R&D needs to support decisions on H&CD upgrades

In parallel with the analysis of H&CD upgrade proposals, several R&D activities would need to be pursued to provide an adequate basis for meeting the $Q \geq 10$ baseline and $Q \sim 5$ steady-state operation goals.

1. Identification of the EC current drive efficiency and requirement for an ECRH system upgrade (to 40 MW) to provide more power and greater flexibility for other applications, for example, active control of NTMs, which will become a potential issue during the high performance H-mode operation in PFPO-2; depending on the progress of commissioning and operation of the ECRH plant in advance of First Plasma, a staged upgrade of the ECRH

system could start earlier (after First Plasma), which would allow additional power for PFPO-2 and FPO. In particular, increased power for off-axis current drive for NTM control, while maintaining 20 MW for central heating, would significantly enhance the flexibility for scenario development and control;

2. Identification of the ICRF power coupling to the plasma during PFPO experiments, and the requirement for an ICRF system upgrade (to 40 MW) for handling issues related to fast ion driven modes, such as Alfvén Eigenmodes;
3. Identification of the NB current drive efficiency and influence on fast ion driven modes, and the requirement for a NBI system upgrade (3rd HNB) to provide more power and current drive for long-pulse and non-inductive steady-state operation;
4. Optimization of H&CD mixes for high performance, non-inductive, steady-state operation within plasma stability boundaries.

4.2 Fuelling and pumping upgrades

SOLPS modelling for the reference 15 MA ITER scenario indicates that the required pumping speed for acceptable helium concentration (an edge concentration of 3%) and power load at the divertor is typically <60 m^3s^{-1}. This pumping speed is about 40% lower than that foreseen for 300 - 500 s $Q \geq 10$ pulses, for the neutral pressures in the range of several Pa expected in these conditions. Thus, an upgrade of the foreseen pumping capability is not expected to be required for He removal, at least for Q = 10 operation. Despite this, and because our understanding of neutral H, D, T and He behaviour under ITER divertor conditions is not very accurate, it will be important to perform helium pumping investigations early in the non-active and deuterium campaigns (in H-mode for helium and deuterium) so that the currently predicted performance can be confirmed.

A further issue which could lead to a reconsideration of the pumping requirements in ITER is that of density control. For the long pulses which ITER targets, wall saturation is expected, so that the only effective particle removal will be provided by active pumping. The baseline requirement for a maximum throughput of 200 Pam^3s^{-1} (~10^{23} atom·s^{-1}) is significantly larger than the expected core plasma outflux on the basis of global scalings for Q = 10 plasma conditions ($N_{plasma}/\tau_E < 3\times10^{22}$ s^{-1}), and is, in fact, similar to that in present devices. For example, ITER-like discharges on JET with $<n_e>/n_{GW} \sim 0.85$ and I_p = 2.5 MA have $N_{plasma} = 7\times10^{21}$ particles with τ_E = 0.4 s and a steady fuelling/ pumping rate of ~ 2×10^{22} s^{-1}. The main difference between present devices and ITER is that the recycling particle flux is typically a factor of ~10 larger than the core particle outflux (equal to the pumped flux for stationary conditions) in current tokamaks, while it is a factor of 100 for ITER Q = 10 plasma conditions. Thus, particle control in ITER is subject to larger uncertainties with respect to recycling flux behaviour, such as outfluxes from saturated walls, than present devices. Early operation in the non-active phase of ITER, particularly in helium (and in H-mode), for which pumping is lower than in hydrogen, will show whether or not there is a need to increase the initial pumping speed in order to achieve satisfactory plasma density control in the expected conditions for Q = 10.

An increase of a factor of 1.5 in pumping speed can be easily achieved by modifying the reference operation scheme of the cryopumps. The ITER pumping system operates with 6 isolatable cryopumps connected to pumping ports at the divertor level. For Q = 10 operation, the system is operated with 4 pumps active during the discharge while the other 2 are being regenerated and brought back to operation for the next plasma. For high neutral pressure operation, in which the system is not conductance limited, the pumping speed can therefore be increased by operating all

pumps simultaneously. An additional increase of a factor of 2 (i.e. a factor of 3 in total with respect to the baseline, if all pumps are used simultaneously) is possible, if the pulse duration is reduced - this would be compatible with the theoretical maximum value of the peak fuelling rate, though the overall consistency with the operation of the fuel reprocessing cycle would need to be confirmed. The drawbacks of this high pumping speed operation mode are that: (i) the discharge duration would need to be shortened to meet safety requirements (in this respect, the deflagration limit in the pumps is likely to be more important than the total in-vessel tritium inventory limit) and to maintain the total throughput per discharge within the capability of the Tritium Plant; (ii) the discharge repetition rate would be affected, since all pumps would have to be regenerated between pulses.

If the pumping speed needed upgrading beyond this factor of 3 higher than baseline level, this would have considerable implications for ITER operations (possibly including further shortening of the pulses to remain within the limit on the time-averaged throughput of the Tritium Plant). The practical implementation of such an upgrade would need to be investigated in detail, but currently the most viable route would rely on improvements in cryopump design and/or technology and the replacement of the initial cryopumps by others with higher pumping speeds. Otherwise, additional ports would need to be allocated to pumping, which requires a major redistribution of the equipment and applications foreseen for the lower ports in ITER – the feasibility of such a reconfiguration of the port allocation, together with the required access through the cryostat, would need to be assessed in detail, in particular for the period following the initiation of DT operation.

Implementation of the pellet fuelling system at ITER will be carried out in a phased approach, so that upgrading of the system is foreseen and requires a relatively simple implementation procedure. The initial pellet injection system for PFPO-1 will have two injectors that can individually inject hydrogenic (H in PFPO and later H/D/DT in FPO) pellets at a frequency of 4 - 16 Hz with a pellet volume in the range 17 - 92 (±20%) mm^3, covering the needs from pellet pacing (of ELMs) to pellet fuelling with two injection geometries (low and high field sides). Within the Staged Approach, the number of pellet injectors is planned to increase by 2 before PFPO-2, to ensure reliable fuelling of ITER hydrogenic plasmas. The pellet injection capability is further upgradeable to a system of up to 6 injectors, which can be used simultaneously for both pellet pacing and fuelling. Initial experimental results of the capabilities of the system will be obtained by hydrogen pellet fuelling of hydrogen plasmas and helium plasmas (in L-mode and, as far as possible, in H-mode) during the PFPO phase of ITER operation, although for helium H-modes, the hydrogenic content needs to be kept low. Tests of pellet pacing of ELMs at high injection frequencies of up to 32 Hz (in PFPO-1) and 64 Hz (in PFPO-2) will be performed for helium and, if possible, hydrogen type-I ELMy H-mode plasmas. The expected frequency of uncontrolled ELMs in 7.5 MA/2.65 T DT plasmas is 3 Hz [Loarte, 2014]. He H-mode plasmas with similar densities and ratios of P_{in}/P_{LH} to those in D plasmas have a similar ELM frequency [McDonald, 2004; McDonald, 2010]. Therefore, it is expected that for He plasmas at this level of plasma current the uncontrolled ELM frequency will remain at around several Hz. These tests will most likely be performed in PFPO-2, where a pellet injection frequency of up to 64 Hz can be achieved.

Depending on the outcome regarding pellet requirements for pellet pacing during the PFPO phases and the associated effective fuelling with hydrogen of helium plasmas, experiments on pellet pacing in helium plasmas may be possible in stationary conditions or only for timescales of several seconds, the timescale on which the concentration of H in the He plasmas is expected to evolve. In either case, the results obtained in helium and, where possible, hydrogen plasmas, together with the results of ELM control using 3-D fields in stationary H-modes and in transient access/exit phases, will provide a basis for decision-making on the choices for the upgrade path to be followed that will be confirmed by further experiments in deuterium.

Upgrade of the pellet fuelling and ELM pacing system to its full performance (6 injectors) can be implemented on the timescale of a few years, so that a timely decision during PFPO-2 would allow the system to be operational for DT operation, or possibly even for the D phase. This upgrade will allow simultaneous use of pellets for pacing at frequencies in the range of ~40 Hz (as predicted to be required for producing controlled ELMs of an acceptable amplitude) together with fuelling (frequencies of 4 - 8 Hz [Loarte, 2014]). As part of this upgrade, the maximum injected pellet size could be increased, if required, for more effective fuelling; this could allow ITER to explore regimes at 15 MA with densities at or beyond the Greenwald density.

A more substantial upgrade of the pellet system would be required if the baseline LFS pellet injection geometry/ size/ velocity prove inadequate for ELM control by pellet pacing, either because ELMs are not triggered by these pellets, or because the pellets required to trigger ELMs in this geometry lead to excessive plasma fuelling. In this case, a more extensive use of the HFS injection geometry for pellet-pacing, or the installation of a LFS high speed injector of small pellets could probably need to be considered for ELM control.

The fuelling upgrades described above can lead to operation of ITER beyond the maximum average design throughput of 200 $Pam^{-3}s^{-1}$ for some experimental conditions. It is foreseen that the duration of flat-top phases of the pulses in such experiments would be shortened (from the reference 300 - 500 s) as required to ensure that the in-vessel inventory of all hydrogenic species condensed on the cryopumps during a plasma pulse, as well as the in-vessel tritium inventory, remains within safe limits. The average total gas throughput per pulse must also be kept within the limits foreseen for the operation of the Tritium Plant.

4.3 Diagnostic upgrades beyond the 2016 Baseline

The possible diagnostic upgrades beyond the 2016 baseline for ITER can be grouped into several categories.

Firstly, one can consider upgrades of the specifications of present systems, for example to increase their time/space resolution, or their radiation hardness, or the completeness of the system in a more or less straightforward fashion, in particular for these cases:

- High Temperature Core Thomson Measurements;
- Edge Thomson Scattering coverage;
- Fast pellet tracking through fast Visible/IR cameras;
- Development of rad hard soft X-ray detectors, neutron detectors, preamps, optical transmission, ADC;
- Equipment for laboratories in the Hot Cell facilities;
- Contingency for systems which do not meet performance requirements.

Secondly, ‘new’ diagnostics whose usefulness for ITER is acknowledged, but for which complete funding is not yet available or for which satisfactory design solutions are still under development, can be considered. As discussed in Appendix H, some of these systems, particularly those related to fusion products, will already be ‘enabled’, for example via the installation of in-vessel components:

- Fibre Optic Current Sensor (FOCS);
- Collective Thomson Scattering;
- Radial and Vertical Gamma Ray Spectrometer;
- High Resolution Neutron Spectrometer and Tangential Neutron Spectrometer;
- Measurements of lost α-particles;

- Measurements of dust and retained tritium;
- In-Vessel Transporter (IVT) or Multi-Purpose Deployer (MPD) related tools, e.g. for neutron calibration and MPD tools for PWI investigations;
- IR bolometer system to increase the diversity of that system;
- Water leak detection spectroscopic wide angle viewing system.

In the third category are upgrades of diagnostic capability that are perhaps less straightforward, but would enhance the device performance, for example, by progressing from a simple measurement to a measurement that can be used to improve tokamak control capability, or from inputs into the plasma control system (PCS) to inputs for investment protection systems in a more direct way such as:

- Vis/IR and bolometers, planned to feed into PCS, could be upgraded to feed more directly into investment protection systems.

The fourth category includes those new diagnostics installed for demonstration in fusion-relevant conditions and intended for eventual implementation in Demo, or to demonstrate operation of ITER in a Demo-like mode such as:

- Radiation hard imaging solutions in Visible and IR range;
- Bolometers which are substantially 'harder' against radiation;
- New diagnostics for helium concentration and T_i measurements which are not based on CXRS;
- Diagnostics for steady-state operation (new magnetic sensors, etc.).

The upgrades to installed diagnostics are likely to be stimulated as a consequence of plasma operation as the ITER program develops and plasma measurements become available. These are expected to consist of hardware improvements (improved signal-to-noise ratio, detection limits, etc.) and/or improvements in space/time resolution. Most ITER diagnostics are already foreseen to be upgradeable in this way and forward planning in this respect can be carried out on a relatively short timescale (~1-2 years) if no port plug modification is needed for the upgrade. This would increase to 5 years if a new port plug were required.

An additional driver for upgrades will be the continued development of the control aspects of various measurements from the operational experience on ITER. Related to this are the expected incremental improvements to the CODAC interface. This development of control aspects is important as it will help to determine the ultimate utility of the various diagnostics for tokamak operation. As just one example, the primary diagnostics for q-profile control (at present) in ITER are MSE, polarimetry, and the underlying equilibrium reconstructions based on the magnetics ensemble. How well these measurements work in concert will determine their utility for control, as opposed to a simple determination of the q-profile *post hoc*. A corollary to this is the value of early experience –the deployment of much of the diagnostic ensemble should be undertaken as early as is feasible from the schedule and budget perspectives. Similarly, delays in the commissioning of the full NBI capability will delay the ability to make MSE measurements. While not critical in the early operational phases of ITER, such measurements will play a role in determining the q-profile control capability for the later phases.

On a longer timescale, development of new diagnostics towards Demo should be considered. This involves tests of diagnostics for helium concentration and T_i measurements which are not based on CXRS, diagnostics for steady-state operation (new magnetic sensors, etc.), as well as possible modifications to present diagnostics for their use in control schemes aimed at Demo control demonstration, such as increased resolution of soft X-ray cameras, polarimetry, etc. For the higher

P_{aux} regimes (~110 MW) that one could foresee for Demo-like operation simulations, the fast α-particle pressure is expected to increase by a factor of at least 1.4 with respect to that foreseen in the reference scenarios. It is possible that such pressure increase may have a noticeable influence on the MHD stability of the discharges, as the reference scenarios are expected to be close to stability thresholds in this respect. With this outlook, upgrades to diagnostics of α-particles and, in particular, the fast α-particle population, are an obvious option. This could imply two types of actions: (i) increasing the lines of sight and/or power launched into the plasma for collective Thomson scattering measurements of the perpendicular α-particle energy distribution, and/or (ii) installing a new viewing geometry that allows direct diagnosis of the parallel α-particle energy distribution. This second option would most likely require the installation of the necessary waveguides before the active phase of ITER exploitation.

4.4 Upgrades of plasma-facing components and materials

Regarding PFCs, upgrades naturally separate into modifications to the divertor and first wall. The modular divertor design and the possibility for in-situ replacement of the First Wall Panels (FWPs) protecting each blanket module mean that upgrades can proceed independently and in all cases fully by remote handling [Merola, 2014].

4.4.1 Divertor

Before the decision to eliminate the first CFC/tungsten divertor in 2013 [Pitts, 2013], the original upgrade path for the ITER divertor foresaw two further full divertor exchanges, with the first, a full-W variant installed in the pre-nuclear shutdown and a third unit (reusing some components of the non-activated first divertor set) planned for deployment after the first ~10 years of nuclear operation. Two divertor replacements are still retained in the revised schedule in the case of ITER extended operations (see [ITER_D_3T6DZ9, 2015]), but no decision has been taken as to the details of future upgrades. What is clear is that design-to-manufacturing and assembly completion requires a minimum of ~7 years, and so this time interval must be respected for any new divertor upgrade. In the current baseline planning, design activities for the second divertor would begin at the start of the PFPO-1 campaign.

The present full-W divertor, to be installed from the start of PFPO-1 operations, will be qualified according to defined numbers of load cycles to 10 MWm^{-2} (~5000) and 20 MWm^{-2} (~300, qualified as ‘slow transients’), themselves derived from earlier versions of the Research Plan in which operation phases were broken down into H-He I, H-He II, DD and DT [Carpentier, 2014]. The revised plasma operation in the present version of the ITER Research Plan, consistent with the Staged Approach, anticipates that these cycle numbers could be attained within the first ~2 years of the FPO campaigns (section 2.6.4) and, thus, according to the present definition of divertor engineering-lifetime, this would be the logical point to replace the first units. It may also be coincident with the time at which other upgrades (e.g. H&CD systems) are being installed.

Given the long development and manufacturing lead times, it is clear that a divertor upgrade in a matter of years following the start of FPO could not benefit from much operational experience regarding exposure in the tokamak environment. Moreover, early non-active operation cannot attain high heat fluxes, significant transient energy densities or the largest electromagnetic forces. Nevertheless, it is expected that the lessons learned from the manufacture, assembly and installation of the first divertor will contribute enormously to the development of the second, even before the component is exposed to plasma. If a decision is taken to replace the divertor after only a relatively

short period of nuclear operation, it is therefore inevitable that the second divertor will resemble the first preserving, in particular, the vertical target geometry.

A significant research effort is currently devoted to the development of new tungsten-based materials, aiming, for example, at improving the material ductility, reducing the possibility for macro-crack formation and propagation [Coenen, 2016; Pintsuk, 2016], and mitigating the formation of plasma-induced morphology changes [El-Atwani, 2014]. This research is linked primarily to expected Demo requirements, with the tacit assumption that ITER will continue using pure tungsten as a plasma-facing material. Given the wealth of research in this area, and the fact that the recent development of high flux/high fluence plasma generators allows the testing of materials/components to extremely high fluences, it is important to keep the option open for the use of an advanced tungsten-based material for any future divertor upgrade in ITER.

Based on current materials R&D and issues already experienced with regard to the design and prototyping of the first divertor, the following options could be considered:

- Splitting the inner and outer targets into separately cooled high heat flux and baffle regions; such an option was already proposed qualitatively in the 2011 Deferral Workshop at the time that the option to eliminate the CFC/W variant was being considered (see *Physics basis for the first ITER divertor* [ITER_D_6JCJ5T, 2011]);
- Use of more advanced W materials for the monoblocks in the high heat flux areas;
- Modifications to monoblock surface shaping based on early experience in the PFPO campaigns;
- Upgrades/refinements/replacement of the first set of in-vessel diagnostics installed on divertor cassettes.

Regarding a third divertor, in addition to the further refinement of materials which will doubtless be possible as R&D proceeds through the ITER construction and first operational years, the major modifications are most likely to be in the area of divertor geometry; one potentially important issue, however, is radiation damage at the CuCrZr cooling pipes for a divertor exposed to higher neutron fluences – to some extent this may already be problematic for the second divertor.

Two main geometrical changes can be foreseen within the interface constraints of the present cassette structure. The first concerns modification of the vertical target and/or dome geometry to optimize operation at high fusion power and acceptable helium exhaust. The second would be a complete change to a horizontal plate geometry, maximizing plasma volume and plasma current capability within the design limits of the PF system. Such a modification would also likely require changes to the blanket module geometry in the lower outer regions of the poloidal cross-section. An upgrade of this type is only likely to be performed if experiments in the first years of FPO show that radiative power dissipation in burning plasma conditions is effective and is only weakly dependent on divertor target geometry and/or that the SOL power e-folding length in ITER (and therefore that foreseen for Demo devices beyond ITER) is substantially larger than presently foreseen. If this does turn out to be true, ITER operation will have demonstrated that the problem of power handling is less severe than currently foreseen for thermonuclear plasmas. In such a case solutions which optimize the volume available inside the vacuum vessel for use by the plasma should be examined in ITER.

4.4.2 First wall

The FWP design is such that replacement of the entire first wall material is possible once in the device lifetime. From an engineering qualification point of view, the Be wall panel lifetime is

designed on the basis of 50% of the full 30,000 cycle budget for the central solenoid full flux swing. An obvious long-term upgrade, in view of support to a conventional Demo, would be the switch to a full high-Z wall (either tungsten or steel), allowing ITER to perform Demo-like plasma-wall interaction studies (albeit at low wall temperature), and to examine the compatibility of a high-Z wall at the reactor scale in terms, for example, of edge power load control studies in the absence of low-Z intrinsic impurities and core high-Z impurity control. Such studies are naturally linked to heating system upgrades allowing ITER to approach Demo plasma conditions more closely.

An upgrade to a full-W wall may also profit from the advances in materials described above and from the ongoing assessments of the most suitable Demo first wall material. Developments in power handling technology may also be such that specific panels could be deployed in high heat flux areas, notably in the upper main chamber, opening up the possibility of quasi-double null operation and possible access to small ELM regimes, should ELM control prove to be insufficient on ITER in baseline configurations. The first upgrades to power handling technology and materials may, in fact, occur in a gradual approach, whereby the transition to full-W begins, for example, in the midplane (start-up) and upper main chamber regions. Such upgrades may even be envisaged at the end of the PFPO phases, for installation during the pre-nuclear shutdown. This might be necessary if damage occurs on certain Be panels (for example due to melting in the current quench phases of disruptions), or if early operation demonstrates that higher heat handling capacity is required. This will only be possible, however, if a decision is taken early enough to allow production of the required hardware. It should be mentioned that the Enhanced Heat Flux first wall panels use a hypervapotron cooling technology which is also used for the divertor reflector plates and dome, while the Normal Heat Flux Panel use a steel pipe liner embedded into a CuCrZr heat sink. Although the divertor reflector plates and the dome umbrella use hypervapotron technology with flat tungsten tiles, dedicated R&D will be needed to develop a tungsten FWP, depending on the required thickness and size of the individual tungsten tiles.

Depending on the observed rates of T permeation through steel during ITER operations, modification of steel surfaces visible to the plasma might be required. Several options could be considered, such as coating of the existing steel surface with a permeation barrier material, complete replacement of the 316L(N), etc. All will require a dedicated development/qualification program to ensure they are compatible with operation conditions. Such an upgrade could be performed during the replacement of the FWP.

4.5 Upgrades of disruption mitigation systems

The present ITER strategy for disruption mitigation is based on the injection of large quantities of high-Z atoms to dissipate the thermal and magnetic energy through radiation. Whereas a high level of confidence exists that this scheme can mitigate the electromagnetic and the thermal loads, there is a significant uncertainty as to whether it will prevent runaway electron formation or will be able to mitigate the consequences of a runaway beam once it forms. The main technique chosen for the ITER disruption mitigation system (DMS) to inject the impurities, and possibly also large quantities of hydrogen or deuterium for runaway avoidance, is the Shattered Pellet Injection (SPI). The ITER DMS design has the maximum flexibility in terms of quantities, species and injection location that is possible within the technical constraints. However, there is the risk that the mitigation performance is insufficient at some point during the execution of the research program when approaching high current or high energy operation. In that case, an alternative scheme or a possible upgrade option must be available to minimize the impact on the execution of the experimental program. Therefore, it is essential that in parallel to the implementation of the DMS baseline design, R&D studies are performed that aim at exploring alternative injection or mitigation

concepts and which prepare the efficient use of the ITER DMS. Besides alternatives to the present baseline DMS, an upgrade could also involve the use of different injection locations or an increase in the injection capabilities.

Alternative injection concepts would aim at improving the deposition of the injected material inside the plasma, on increasing the assimilation efficiency and on allowing flexibility in the injected species. Possible candidates, such as compound pellets, shell pellets or rail gun systems, would require further exploration to allow their performance to be characterized and to come to a more mature design stage. Alternative mitigation schemes would aim at techniques other than material injection. These could include, for example, the use of wave-particle interactions or passive protection schemes.

Any of the above mentioned upgrades of the DMS will result in major impact on the operational schedule and on other systems which are integrated in the relevant port plugs. Minor upgrades, such as changing the pellet sizes of the existing injectors, are possible without significant impact on the operational schedule.

4.6 Upgrades to plasma magnetic control (verstical stabilization, shape, error fields, resistive wall modes)

4.6.1 Plasma vertical stabilization

Reliable plasma vertical stabilization (VS) is essential to limit the frequency of VDEs and, as a consequence, to reduce the impact of thermal and electromagnetic VDE loads on the machine lifetime. The capability of the VS system also determines the operational space for plasma axisymmetric magnetic control, in the terms of maximum plasma elongation and maximum value of the plasma-wall gap on the plasma outboard side for given plasma current and plasma conditions. A capability to increase this gap may be important for first wall protection, taking into account possible static and dynamic errors in axisymmetric magnetic control and 3-D distortion of the plasma boundary caused by various sources of non-axisymmetric magnetic fields (e.g. currents in the ELM control coils). For example, according to the study reported in [Chapman, 2014], the RMP-induced 3-D distortion of the plasma boundary foreseen in the ITER 9 MA steady state scenario can be up to ±5 cm.

The level of low frequency noise in the measurement signal of the vertical velocity of the plasma current centre, *dz*/*dt*, used in the feedback loop for stabilization of plasma vertical displacements, is an important parameter affecting plasma vertical stabilization [Gribov, 2015]. In ITER, the relevant frequency band lies below ~300 Hz. A high level of the noise in the *dz*/*dt* signal: (i) increases the probability of VDEs during operation with low values of the stability margin, m_s, (e.g. operation with high plasma elongation and/or with a high value of the plasma-wall gap on the plasma outboard side); (ii) increases heating of the VS in-vessel coils and their busbars; (iii) causes disturbances in plasma-wall gap control (due to coupling of the ‘fast’ plasma vertical stabilization and the ‘slow’ gap control), increasing the amplitude of oscillations in the plasma-wall gap control (the dynamic error in gap control); (iv) increases AC losses in the superconducting magnets, due to the increase in amplitude of current and magnetic field oscillations in the superconductors, and increases joule heating in the structures surrounding the superconductors. If necessary, measures for reduction of the low frequency noise in the *dz*/*dt* diagnostic signal should be taken based on ITER operational experience.

In nominal operation, plasma vertical stabilization is provided by the VS in-vessel coils (the vertical stabilization system VS3) in combination with the system VS1 (which controls the differential

current in the external coils PF2, PF3 and PF4, PF5). In this mode of operation, VS1 is used for reduction of the time-averaged component of the current in VS3 [Gribov, 2015]. If necessary (e.g. for deliberate plasma vertical oscillations generated with the aim of ELM triggering in low current H-mode plasmas, [Gribov, 2015]), an upgrade of the vertical stabilization system VS3 could be performed, increasing the velocity of the cooling water in the VS coils and the on-load voltage of the VS3 power supply (a modification of the VS3 power supply is required).

Algorithms for in-service assessment of the fatigue lifetime of the VS in-vessel coils, based on the waveforms of currents flowing in the coils, should be developed. The residual fatigue lifetime of the in-vessel VS coils should be periodically reassessed based on the data obtained in the course of ITER operation. It will also be important to gain experience of plasma vertical stabilization without the in-vessel coils, but using only a stabilizing feedback loop based on VS1, should the residual fatigue lifetime of the VS3 coils assessed on the basis of operating experience be predicted at some point to be insufficient for the entire ITER operational life, or in the case of failure of the VS3 coils. Experimental optimization of the plasma magnetic configuration (in particular, the maximum value of the separatrix elongation and location of the strike points), allowing operation without the VS3 coils while retaining a low probability of VDEs, as well as optimization of the VS1 stabilization algorithms and of the *dz*/*dt* diagnostic, should be performed, preferably at low plasma currents, where the impact of VDEs on the machine is significantly lower.

If necessary (e.g. when the residual fatigue lifetime of the VS3 coils becomes low, or when the coils fail), the plasma stabilizing system VS1 can be upgraded. This upgrade consists of an increase in the VS1 power supply on-load voltage from 6 kV to 9 kV, which allows an increase of the plasma vertical stabilization operational boundary when using only the VS1 ex-vessel coils by about 25% [Gribov, 2015]. Another upgrade for VS control involves an additional system utilizing ex-vessel coils to further improve plasma vertical stabilization. This system, referred to as VS2, varies the differential current in the coils CS2U and CS2L. The VS2, with an on-load power supply voltage of 6 kV, allows an additional increase of the operational boundary (relative to that for VS1 with a voltage limit of 6 kV) by about 25% [Gribov, 2015].

Depending on the need, these upgrades of the vertical stabilization capability could be implemented as early as in the shutdown period between PFPO-1 and PFPO-2.

4.6.2 Control of plasma current position and shape

Should it turn out that the voltage requested from certain coil power supplies for the control of plasma current and plasma-wall gaps in key ITER plasma scenarios can potentially exceed the installed voltage capability, the number of converters in the corresponding circuits can be increased (within the voltage limits for the coil insulation tests). Depending on need, this could be considered as early as in the shutdown period between PFPO-1 and PFPO-2.

4.6.3 Control of error fields

18 ‘saddle’ superconducting correction coils with 9 independent power supplies will be used for minimization of error fields with toroidal mode number $n = 1$. In addition to these correction coils, 27 ELM control coils with 27 independent power supplies will be used for identification of the error field structure and, in scenarios when these coils are not used for ELM control or in scenarios when the coil currents required for the ELM control leave sufficient margin, the ELM control coils could be used for correction of error fields with $n = 1, 2, 3$.

Dynamic (feedback) error field correction (DEFC) would make use of the ELM control coils, assuming that sufficient 'headroom' exists above the current required for ELM control. The following upgrades of the error field correction system can be envisaged:

- increase of voltage on the ELM control coils, if this is deemed necessary;
- if required, increase the speed of the cooling water in the ELM control coils.

Depending on the need, these upgrades could be considered as early as in the shutdown period between PFPO-1 and PFPO-2.

4.6.4 Control of Resistive Wall Modes

Resistive wall mode (RWM) control and dynamic error field correction via the ELM control coils utilize the same control system and associated upgrades. Therefore, any upgrades of DEFC utilizing the ELM control coils can be applied also to the upgrade of the RWM control capability. The only potential difference between these two control capabilities is the speed of control (with RWM requiring more rapid alteration of the perturbed field than DEFC).

If the current requirements for ELM control determined by operating experience in ITER plasma scenarios allow the application of a significant fraction of the current capability of the ELM control coils to RWM control, the following upgrades of the RWM control system can be envisaged:

- upgrade the power supplies of the ELM control coils (increase of on-load voltage and reduction of the voltage response time) in combination with measures for reduction of the low frequency noise (for frequencies less than ~600 Hz) in the diagnostic signal, $dB_{poloidal}/dt$, used for RWM control;
- if required, increase the speed of the cooling water in the ELM control coils.

Depending on the need, these upgrades could be considered prior to the development of DT hybrid and non-inductive operational scenarios.

Algorithms for the assessment of the fatigue lifetime of the ELM control coils, based on the waveforms of currents flowing in the coils, should be developed. The residual fatigue lifetime of the ELM control coils should be periodically reassessed based on operational experience gained in ITER scenarios using ELM and/or RWM control.

4.7 Upgrades required for maintaining long-pulse operation

According to the *Project Requirements* [ITER_D_27ZRW8, 2014], "The extended burn duration under the hybrid and non-inductive operations may be accomplished with additional investment for auxiliary systems". A critical element in providing access to long-pulse operation is the H&CD capability, and the upgrade options have been summarized in section 4.1. A detailed review of the analyses of candidate non-inductive plasma scenarios in ITER, including the influence of the H&CD capability on pulse duration and fusion performance, is given in Appendix E, while options for upgrading of the H&CD systems are discussed in detail in Appendix G.

An initial assessment of the implications for system performance associated with the requirement to support very long pulses has highlighted that a more detailed analysis of system performance should be performed in advance of $Q \geq 5$, 3000 s operation, based on experience from early ITER operation. Systems that should be analyzed in this respect are: (i) the diagnostic neutral beam; (ii) magnetic measurements and possible back-up measurements should magnetics become unreliable on such long timescales; (iii) fuelling and pumping systems; and (iv) cooling water system (pulse

length and pulse repetition rate needs to be assessed for long-pulse scenarios taking into account the seasonal temperature variation and the heat transfer from the basin due to water evaporation and other heat loss by radiation and convection).

4.8 Upgrades for exploration of Demo plasma regimes and for Demo technology demonstration in ITER

During the FPO phase, ITER can be expected to deploy improved plasma heating and current drive schemes, as well as components to test first wall and heat extraction technologies, which would be suitable for initial deployment on Demo. These would comprise evolutionary updates to existing or planned heating and current drive systems to provide greater flexibility, reliability and survivability and/or higher power density. ICRF launchers, for example, would employ advances in materials and cooling concepts that are suitable for Demo (e.g. gas cooling) and adapt these approaches to additional requirements (such as electrical conductivity) to produce rugged designs. Alternative ICRF launcher approaches such as the folded waveguide design could be tested in ITER as Demo prototypes. Launchers for high-frequency microwaves used in ECRH and EBW heating and ECCD have different requirements and opportunities. The survivability of copper mirrors used in the present ITER design is a significant concern. An alternative is to implement remote steering utilizing angled injection into an oversized-corrugated waveguide. The ohmic loss on this waveguide is very low so that it can be made of any metal, including a high resistivity metal, such as tungsten-molybdenum. A remote steering upgrade would serve as a prototype for Demo, or it may be required if operational experience shows that the present front steering mirror concept is not reliable.

Such H&CD upgrades should bring the level of coupled power to the plasma to the maximum of ~110 MW and, together with the upgrades for fuelling and first wall components described above, would make ITER an ideal test bed for integrating the technology and plasma regimes foreseen in Demo. Such upgrades would allow ITER to explore plasma operation with Demo-like heating and current drive schemes and first wall divertor materials under Demo-relevant plasma conditions: high P_{loss}/P_{L-H}, high β_N, high P_{rad}/P_{tot}, high $\langle n_e \rangle / n_{GW}$, high Q ($\geq$10) and steady-state Q ($\geq$5) with Demo-like H&CD, etc., albeit not simultaneously and/or not at the highest currents. Given the uncertainty in the foreseen H-mode threshold in ITER, an increase of the heating power level may also be required to access very high $Q \geq 10$ regimes in 17 MA inductive operation, which would allow the study of quasi-self-sustained thermonuclear plasmas in ITER.

ITER can also make significant contributions to the testing of advanced Demo-relevant first wall (not yet included in the first 4 modules of the TBM testing program – see section 3.2) and divertor materials and structures together with associated heat extraction technologies in an integrated fusion environment. Such tests would focus on studying the synergetic effects of neutron irradiation and high plasma fluxes on the sputtering of advanced materials and in the tritium uptake, retention and diffusion through high performance helium-gas cooled first wall and divertor panels operating at elevated temperatures (higher than 600 °C). Attractive advanced plasma-facing/structural material combinations, such as tungsten joined to oxide dispersion strengthened low activation steel, could be tested in a mid-plane port or in a dedicated divertor sector that would expose test samples to various degrees of plasma impingement (and heat flux) under controlled conditions.

Table 4-1(a) – Overview of potential system upgrades at each phase of the IRP

Upgrade after phase	H&CD	Fuelling and Pumping	Diagnostics, PFCs & Materials	Plasma and MHD Control
PFPO-1	**ECRH:** Upgrade if power required to operate in H-mode higher than expected or if ICRF coupling lower than expected. **ICRF:** Upgrade if power required to operate in H-mode higher than expected and good ICRF coupling experienced. **HNB:** Launch upgrade if power required to operate in H-mode higher than expected and/or if low-torque operation with controlled ELMs is not robust.	**Fuelling:** Upgrade to 4 pellet injectors is included in the Staged Approach baseline. **Pumping:** If density control proves insufficient, plan for upgrade after PFPO-2, as mitigation measure *pro tem* in PFPO-1 and PFPO-2, use more pumps simultaneously (up to 6 with no upgrade) if density control insufficient.	**Diagnostics:** - Increase Edge Thomson Scattering coverage. - Fast pellet tracking through fast VS/IR cameras.	**DMS:** Improve shattered pellet injector (pellet sizes, etc.), if required for disruption mitigation. **VS:** Implement measures to reduce noise in dz/dt to minimize use of VS3 coils. **Shape:** Increase main converter voltage of CS and PF within coil voltage limits for fast ramp-up/down and improved plasma-wall gap control if problems envisaged for 15 MA L-mode operation. **Error Field:** Upgrade ELM control power supplies for dynamic error field correction if 'no-torque' operation is not robust for $I_p < 7.5$ MA.
PFPO-2	**ECRH:** Upgrade if power required to operate in H-mode at 2.65 T is higher than expected. **ICRF:** Upgrade if power required to operate in H-mode at 2.65 T is higher than expected. **HNB:** Upgrade if power required to operate in H-mode higher than expected and/or if low-torque operation at 2.65 T with controlled ELMs is not robust. **(FPO would be delayed until 3rd NBI ready)**	**Fuelling:** Upgrade with 2 additional pellet injectors if pellet fuelling less efficient than expected, or if pellet pacing is required for robust H-mode operation at 2.65 T. **Pumping:** Upgrade pumping (new cryopump technology or allocation of more divertor pumps to pumping) if density control is insufficient.	**Diagnostics:** - High Temperature Core Thomson Scattering. - Radiation-hard soft X-ray and neutron detector, and associated equipment. - Fibre Optic Current Sensor for steady-state magnetic measurements. - Implement lost-α detector. - Implement measurements of dust and in-situ T-retention. - In-vessel tools (for RH systems) for neutron calibration and PWI studies. **PFCs&Materials:** - Upgrade parts of the first wall to W if damage to Be is excessive in some areas.	**DMS:** Improve shattered pellet injector (pellet sizes, etc.) if required for disruption mitigation at high I_p. - Implement new disruption mitigation systems if improved SPI is not sufficient at high I_p. **(FPO may have to be delayed until new DMS is implemented)** **VS:** Implement measures to reduce noise in dz/dt with increasing I_p to minimize use of VS3 coils. - Increase water cooling and/or on-load voltage of VS3 PS if required for high I_p operation. **Shape:** Increase main converter voltage of CS and PF within coil voltage limits for fast ramp-up/down and improved plasma-wall gap control if problems envisaged for 15 MA H-mode operation. **Error Field:** Upgrade ELM control power supplies for dynamic error field correction if low-torque operation is not robust for $I_p = 15$ MA. - Increase cooling capabilities of ELM control coils if required for dynamic error field control up to 15 MA.

Table 4-1(b) – Overview of potential system upgrades at each phase of the IRP

Upgrade after phase	H&CD	Fuelling and Pumping	Diagnostics, PFCs & Materials	Plasma and MHD Control
FPO-1	**ECRH:** Upgrade if power required to operate in H-mode at 5.3 T in DT is higher than expected, or if ECCD is lower than expected. **ICRF:** Upgrade if power required to operate in H-mode at 5.3 T in DT is higher than expected.	**Fuelling:** Upgrade to 6 pellet injectors if pellet fuelling less efficient than expected in high I_p H-modes, if DT mix control more complex than expected, or if pellet pacing is required for robust H-mode operation at high I_p. - Upgrade to a new LFS injector (port based) if pellet pacing is required but is not effective with baseline geometry. **Fuelling:** Upgrade pumping (new cryopump technology or allocation of more divertor pumps to pumping) if density control or He exhaust for Q = 10 scenario is insufficient.	**Diagnostics:** - Collective Thomson Scattering. - Radial/Vertical Gamma Ray Spectrometer. - High Resolution Neutron Spectrometer. - Tangential Neutron Spectrometer. - Water leak detection by spectroscopic wide angle view. - Improve q-control by MSE, polarimetry and high precision equilibrium reconstruction. - Improve divertor diagnostics if second divertor is installed at this stage. **PFCs&Materials:** - Install a second divertor with improved geometry, cooling arrangement and/or W materials towards Demo. - Upgrade parts of the first wall to W, or increase coverage (if already initiated at the end of PFPO-2) if damage to Be is excessive in some areas as plasma currents/energies increase.	**DMS:** Improve shattered pellet injector (pellet sizes, etc.) if required for disruption mitigation up to 15 MA/350 MJ in DT plasmas. - Implement new disruption mitigation systems if improved SPI is not sufficient for 15 MA/350 MJ. **(FPO-2 may have to be delayed or program constrained until new DMS is implemented)** **VS:** Implement measures to reduce noise in dz/dt with increasing I_p and nuclear heating to minimize use of VS3 coils. - Increase water cooling and/or on-load voltage of VS3 PS if required for high I_p operation with high nuclear heat loads. - Upgrade VS1 to 9 kV and/or VS2 to 6 kV, if required by the possible deterioration of the VS3 system. **Shape:** Increase main converter voltage of CS and PF within coil voltage limits for fast ramp-up/down and improved plasma-wall gap control, if problems found in the Q =10 scenarios and/or in the initial development of Q = 5 scenarios. **Error Field:** Upgrade ELM control power supplies for dynamic error field correction if low torque operation is not robust for 15 MA/Q = 10 scenario. - Increase cooling capabilities of ELM control coils if required for dynamic error field control for 15 MA/Q = 10 scenario (increased nuclear heating). **RWM:** Upgrade ELM control coil PS for RWM in preparation of FPO-2.

Table 4-1(c) – Overview of potential system upgrades at each phase of the IRP

Upgrade after phase	H&CD	Fuelling and Pumping	Diagnostics, PFCs & Materials	Plasma and MHD Control
FPO-2	**ECRH:** Upgrade if more ECCD or more ECRH power is required to optimize $Q \geq 10$ scenario, or to achieve $Q = 5$ hybrid or steady-state goals. **ICRF:** Upgrade if more ICRF power is required to optimize $Q \geq 10$ scenario, or to achieve $Q = 5$ hybrid or steady-state goals.	**Fuelling:** Upgrade to 6 pellet injectors if DT mix control more complex than expected or if pellet pacing is required for robust H-mode operation at high l_i. - Upgrade to a new LFS injector (port based) if pellet pacing is required for long-pulse $Q = 5$ scenario and not effective with baseline injection geometry. **Pumping:** Upgrade pumping (new cryopump technology or allocation of more divertor pumps to pumping) if density control or He exhaust for $Q = 10$ scenario is insufficient.	**Diagnostics:** - IR bolometer system. - Link VIS/IR and bolometers to investment protection system. - Improve divertor diagnostics if second divertor is installed at this stage. **PFCs&Materials:** - Install a new divertor with improved geometry, cooling arrangement and/or W materials towards Demo (if not installed after FPO-1). - Upgrade parts of the first wall to W, or increase coverage, if damage to Be is excessive in some areas as plasma currents, energies and pulse lengths increase.	**DMS:** Improve shattered pellet injector (pellet sizes, etc.) if required for disruption mitigation of long-pulse $Q = 5$ plasmas. - Implement new disruption mitigation systems if improved SPI is not appropriate for disruption mitigation of long-pulse $Q = 5$ plasmas. **(FPO-3 may have to be delayed until new DMS is implemented)** **Shape:** Increase main converter voltage of CS and PF within coil voltage limits for fast ramp-up/down and improved plasma-wall gap control if problems encountered in $Q = 5$ scenarios. **Error Field:** Upgrade ELM control power supplies for dynamic error field correction if low torque $Q = 5$ long-pulse operation is not robust. **RWM:** Upgrade ELM control coil PS for RWM if not implemented earlier. - Upgrade water cooling capability of ELM control coils to facilitate application for RWM control under long-pulse/high nuclear heating conditions.

Table 4-1(d) – Overview of potential system upgrades at each phase of the IRP

Upgrade after phase	H&CD	Fuelling and Pumping	Diagnostics, PFCs & Materials	Plasma and MHD Control
FPO-3	**ECRH:** Implement new ECRH/ECCD and EBW with Demo-like features. **ICRF:** Implement ICRF antennas with Demo-like cooling and configuration.		**Diagnostics:** - Improve divertor diagnostics as divertor upgrades permit. - Higher radiation hardness bolometers, visible and IR systems for use in Demo. - New diagnostics (non-CXRS based) for He concentration and T_i in Demo. - New magnetic sensors for steady-state operation for Demo. - Improved α-particle distribution diagnostics. **PFCs&Materials:** - Install a new divertor with improved geometry, cooling arrangement and/or W materials towards Demo (if not installed after FPO-2). - Upgrade first wall to W with Demo-like materials. - Install a Demo test station for plasma facing components in equatorial port (e.g. low activation steel with W element with helium-gas cooling at 600 °C).	**VS:** Upgrade VS1 to 9 kV and/or VS2 to 6 kV to demonstrate Demo-like vertical stability operation. **Shape:** Increase main converter voltage of CS and PF within coil voltage limits for Demo-like operation with Demo-like magnetic sensors/on-line equilibrium reconstruction. **Error Field:** Increase voltage of power supplies of side correction coils for Demo-like dynamic error field correction for long-pulse operation at high Q. **RWM: Earlier analysis indicates that RWM control with external correction coils impractical in ITER, and so it is not clear at this stage what upgrades relevant to Demo operation can be implemented.**

5 Research Program Accompanying Construction

5.1 H-mode issues

The research in present and near future tokamak experiments (ASDEX-Upgrade, DIII-D, EAST, JET, JT-60SA, KSTAR, WEST, etc.) should be focussed towards H-mode research in plasmas with the specific features of the ITER H-mode plasmas, in order to understand and develop validated models that can be used to predict plasma behaviour in H-mode scenarios in ITER. This involves not only the study of stationary conditions but also of the access/exit phases to/from H-modes, where plasma behaviour is already more difficult to control in present experiments, particularly with W PFCs. In ITER this is further complicated by the relatively low margin of P_{sep}/P_{L-H} and the need to maintain ELM control in these transient phases.

The main H-mode issues that should be the focus of H-mode research to improve ITER H-mode performance and to refine the ITER Research Plan are:

- Characterization of H-mode plasmas (core, pedestal and overall confinement) in ITER-like conditions, chiefly with electron dominant heating, low torque input, low core particle source and peripheral pellet fuelling;
- Characterization of the evolution of the pedestal and core plasma parameters (density, temperature, impurity concentrations, etc.) in the L-H and H-L transition and development of schemes to control them based on ITER-like actuators (particularly heating and current drive, fuelling, impurity seeding, etc.);
- Determination of the plasma parameters that determine the L-H transition in ITER-like conditions (e.g. low neutral core particle source) and development of schemes to decrease the required additional heating power to access and sustain high confinement H-modes;
- Characterization of the effects of impurities and gas fuelling, required for radiative divertor conditions in ITER, on the plasma edge of H-modes with metallic PFCs and on divertor power loads and development of schemes to improve H-mode performance in radiative divertor conditions that are extrapolable to ITER;
- Development of ELM controlled/suppressed H-mode scenarios by application of 3-D fields with ITER-like plasma features (electron dominant heating, low torque input, low core particle source and peripheral pellet fuelling) including current ramp-up/down phases (i.e. control of ELMs by 3-D fields with varying pedestal parameters and q_{95});
- Determination of the impacts of ELM control with 3-D fields on H-mode thermal, particle and fast ion confinement, impurity exhaust and divertor radiative conditions and development of schemes to optimize them for integrated H-mode operation with ITER-like actuators;
- Characterization of the (core-pedestal) physics processes that determine the changes of H-mode plasma confinement with increasing β for $q_{95} = 3 – 6$, and development of optimization schemes with ITER-like actuators. While this is of importance for the $Q = 10$ inductive goal, it is essential for the $Q = 5$ long-pulse and steady-state goals which rely on H-mode plasmas at $q_{95} > 3.5$ and $H_{98} > 1$ confinement.

The experimental research in the areas described above must be accompanied by equally intense modelling and theoretical development programs to provide:

- physics basis on which to extrapolate the findings in present tokamaks to ITER; and,
- validated models on which to design ITER plasma scenarios for the ITER Research Plan.

In addition to these overall research issues, specific topics have been identified for each of the research plan phases where H-mode experiments are performed; these are described below.

5.1.1 H-mode research related to PFPO-1

Additional research issues of importance for this phase are:

- Characterization of the effect of TF ripple on the L-H power threshold, pedestal and core H-mode parameters and ELM characteristics in ITER-like H-modes. Most of the experimental H-mode plasmas on which ITER H-mode performance projections are based are NBI heated and, on this basis, significant pedestal degradation (20 - 30%) is expected for 1.8 T plasmas with 1.3% ripple, as discussed in Appendix B. However, it is not yet known if the same behaviour is expected for RF dominated plasmas with electron heating as the ITER plasmas will be;
- Further studies of ICRF plasma coupling at large antenna-separatrix distances and with second harmonic H majority and minority (in He plasmas) schemes. The former is important to determine the way to maintain coupling in ITER hydrogen H-modes at this stage if the ICRF antenna is available and ripple needs to be reduced to ~0.5%, as this requires a plasma separatrix-antenna distance of ~ 55 cm in ITER. The latter determines whether ICRF heated H-modes will only be viable in H or also in He plasmas;
- Studies of L-H transition and H-mode performance in mixed H+10% He plasmas. This can open a wider operational window for H plasmas in ITER in PFPO-1 and, more importantly, in PFPO-2. Potentially, it may allow performing all H-mode programs in PFPO-1 and PFPO-2 with plasmas of this type rather than pure He H-modes.

5.1.2 H-mode research related to PFPO-2

Besides the specific research for PFPO-1 also relevant for PFPO-2, other research issues of importance for this phase are:

- Validation of shine-through loads in hydrogen and helium plasmas with NBI at high ion energy $E_{NBI} \geq 500$ keV. This can be performed in JT-60SA in advance of ITER PFPO-2 operation and it is essential to determine whether hydrogen plasmas at 2.65 T have a sizeable operational space in H-mode in ITER;
- Validation of modelling for fast particle losses with 3-D fields for ELM control in ITER with present experiments for a range of 3-D field spectra and NBI ion injection energy. This is required to determine the way to optimize the spectra applied to obtain ELM control while minimizing fast particle losses from NBI;
- Validation of the single pass absorption, power deposition profiles and possible orbit losses of accelerated minorities for ICRF heating with the three-ion scheme ($H\text{-}He^4\text{-}He^3$) proposed to heat ITER hydrogen plasmas at either 3.0 or 3.3 T.

5.1.3 H-mode research related to deuterium and trace T plasmas in FPO

In addition to the general H-mode physics R&D above and the specific issues in PFPO-1 and PFPO-2 which are of relevance for the D phase, the following issues would benefit from dedicated R&D in present experiments to refine the operational plan:

- Evaluation of the need for ECRH to assist plasma breakdown in ITER at 1.8 T. Ideally, this should be performed in devices operating with high-Z divertor/PFCs and with a highly conducting vacuum vessel (plus ITER-like 1.3% TF ripple at the outer midplane) and scaled current/voltages in the PF systems to mimic the expected conditions in ITER. This is required to determine whether the D H-mode development path from a current level of 5 MA to 7.5 MA in this phase should follow a constant q_{95} approach or a constant B_t = 2.65 T approach;
- Assessment of effectiveness of W accumulation control versus location of the power deposition profiles and electron/ion heating in devices operating with high-Z divertor/PFCs. This is important to determine the operational strategy to proceed upwards in current and field from 7.5 MA/2.65T in D and DT H-mode plasmas in FPO.

5.1.4 H-mode research related to hybrid and steady-state D plasmas in FPO

The specific issues to assess by R&D for the refinement of the research plan for hybrid and steady-state D plasmas in FPO are:

- Evaluation of the ITER q_{95} = 4 hybrid and q_{95} = 5 steady-state target scenarios including the optimization of current drive to achieve these target scenarios with real-time control schemes;
- Development of validated models (on the experimental assessment above) able to perform accurate simulations for ITER to define the required real time control schemes, as well as to predict the expected performance of these plasmas in ITER. This can provide important information on the heating and current drive upgrades necessary to achieve the high non-inductive current fraction, high-Q plasma scenarios required for the long-pulse and steady-state goals in ITER.

5.1.5 H-mode research related to inductive DT plasmas in FPO

In addition to the general H-mode physics R&D above and the specific issues in PFPO-1, PFPO-2 and D H-modes which are of relevance for the DT phase, the following issues would benefit from dedicated R&D in present experiments to refine the operational plan:

- Improvement of the physics basis for T transport in mixed DT H-mode plasmas through dedicated experiments and modelling. Both isotopic effects on anomalous and neoclassical transport need to be understood. In particular the role of core neoclassical transport in determining the central T concentration for plasmas with low DT central source needs to be determined;
- Improvement of the physics basis for DT effects on W transport and core W accumulation. This is in part linked with the above issue and to the level that the central levels of DT density peaking are set by neoclassical transport in mixed DT plasmas. This would make the experience on W control gained for D plasmas in ITER not to be applicable to DT;
- Development of robust H-mode access and exit schemes compatible with ITER requirements that take into account the effect of plasma parameter evolution on edge power

flow to simulate the changes to α-heating in ITER (e.g. by real-time variation of a fraction of the additional heating power with plasma energy in the H-mode access and exit phases);

- Determination of the physics processes that determine edge stability limits and overall H-mode confinement in conditions with low grad-n in the pedestal and evaluation of their relevance to ITER and of the expected H-mode confinement in these conditions.

5.1.6 H-mode research related to hybrid and steady-state DT plasmas in FPO

The specific issues to assess by R&D for the refinement of the research plan for hybrid and steady-state DT plasmas in FPO are:

- Development of control schemes required for hybrid and steady-state scenarios (such as β, current/pressure profile, edge-core integration, etc.) and demonstration of their application to optimize performance in H-mode plasmas with a large non-inductive current fraction including: the development of access route to these high confinement/large non-inductive current fraction H-modes and demonstration of their compatibility with metallic PFCs (including divertor power load control);
- Identification of the conditions required to obtain H-modes with high q_{95}, high H_{98} (~1.6), and characterization of the properties of these plasmas in these conditions in a wide range of experimental devices. The objective here would be to obtain a relevant experimental database of these H-mode plasmas to improve the physics basis for the $H_{98} \sim 1.6$, $Q \sim 5$ steady-state scenario in ITER.

5.2 Plasma-wall interaction issues

Section 2.2 has treated at length the most important plasma boundary physics and plasma-wall interaction issues in the context of the challenge that ITER will face and the areas which will require particular attention on ITER. R&D required in the coming years was implicitly (often explicitly) covered in that section and is summarized here briefly in the form of a list of issues which should be addressed in the years up to the beginning of ITER exploitation. It is worth mentioning that unlike many of the other key physics/operational areas, plasma boundary issues cover both physics and materials and, as such, require R&D on tokamaks, linear plasma devices and transient heat pulse devices (e.g. electron beams, plasma guns), as well as advances in theory and simulation.

Plasma boundary physics:

- The inter-ELM near-SOL heat flux channel width (section 2.2.2 and Appendix C): is the experimental scaling $\lambda_{q,near} \propto 1/I_p$ preserved at high current in ITER? The question is far from resolved, and there are opposing theoretical positions, but if the values of $\lambda_{q,near} \sim 1$ mm at 15 MA implied by the experimental scaling and neoclassical drift theory were to be confirmed on ITER, the operational window for burning plasma operation may be substantially reduced, particularly given that divertor target component shaping significantly reduces tolerable parallel heat fluxes. The important question appears to be whether electron filamentary (blobby) turbulence 'washes out' the ion drift scale at high current in ITER. Further theoretical development/simulations and new experimental data (e.g. additional measurements in JET at high power/high current) are required to resolve this key issue.

- Equally, the study of what physics determines the far-SOL power and particle widths and the possible link to detachment (divertor/SOL collisionality) should continue experimentally and theoretically. What is the driving mechanism for filament formation, where and at what frequency will filaments form on ITER and how will their impact on Be first wall surfaces determine the net erosion source? It currently remains unclear whether the broad far SOL profiles seen universally in L-mode at higher density in current experiments will persist in H-mode at ITER. Recent H-mode experiments on JET, for example, find that broad SOL density shoulders are not typically seen for vertical target configurations, but are seen for outer strike points on the bulk, quasi-horizontal tungsten target [Wynn, 2018]. This calls into question the leading explanation for the formation of broad shoulders, i.e. the strong correlation seen with divertor plasma collisionality [Carralero, 2015]. It may instead be linked rather to plasma-neutral interactions in the divertor target regions.
- The recent experimental scaling for the peak outer target ELM parallel energy density, $\varepsilon_{\parallel}$ for uncontrolled ELMs (section 2.2.3 and Appendix C) is a favourable development for ITER in the sense that H-mode experiments with unmitigated ELMs may be possible at higher currents than previously thought (subject to satisfactory control of tungsten influxes). To date, the same scaling dependence has also been found for mitigated ELMs. More experimental work is required here in the coming years to expand the databases for both controlled and uncontrolled ELMs, for larger numbers of devices and for a wider range of operating scenarios. An improved understanding of the scatter in the scaling database, and in particular in the dependence $\varepsilon_{\parallel} \propto (\Delta W_{ELM})^{\alpha}$ (with α in the range 0-1) is required. More data are also required for the inner target on additional devices since, as a result of the ITER target design and magnetic geometry, this may be the location which sets the limit on allowable transient energy density. The dependence of $\varepsilon_{\parallel}$ on pressure at the pedestal top means that mitigating ELMs will still not be sufficient at the highest performance in ITER, so that either full suppression, or H-mode regimes with naturally smaller ELMs and good confinement (including the ability of highly dissipative divertors for ELM energy dissipation, provided the incoming energy pulse is low enough), is required. Exploration of these approaches should therefore continue in current devices, as should theoretical development and simulation to consolidate the experimental scaling findings.
- An outstanding issue is the degree to which Ne seeding will be possible for detachment control on ITER (section 2.2.5). From the simulation point of view, ITER is large and powerful enough for N_2 and Ne to be roughly equivalent, yet thus far on most of today's devices, Ne enrichment is too low for it to be a useful divertor radiator. Here, higher power experiments on JET with the relevant ITER wall material mix will be key. Developments in theory and simulation must continue along the lines already being successfully pursued to fully include drifts and a proper description of impurity transport in the non-trace limit into plasma boundary simulations (see e.g. [Sytova, 2018]). This will also provide more realistic predictions for the likely target power loading asymmetries in ITER at high power and a better description of the SOL flows, so important for the determination of migration patterns. In parallel, the 3-D simulation capability must be developed, such that the physics model (drifts, recombination, etc.) attains similar maturity to that of the 2-D codes, in order to properly simulate the likely power loading in the presence of magnetic perturbations for ELM control, particularly in the dissipative limit, with strong impurity seeding. The very general issue of proper detachment modelling is a central theme here (together with the problem of narrow heat flux channels – see above), since the inclusion of divertor target shaping means that stronger detachment will be required for given incoming parallel heat

flux, particularly at the outer target, compared to an unshaped divertor target. All these elements ultimately combine during the development of reliable and routine detachment control strategies (section 2.2.9). This is an area which must be assigned higher priority in current devices in the approach to ITER operation, paying specific attention to the pursuit of methods deploying the same sensors and actuators as will be present on ITER. In particular, the very extensive IR coverage of first wall and divertor surfaces in ITER requires that operating tokamaks devote more effort to the use of IR for heat flux control.

- The castellated ITER divertor target design has stimulated a great deal of recent R&D focussed on the power loading of component edges (section 2.2.7). Calculations, validated in part on present machines, show that this gap edge loading (Appendix C) may set a lower limit on allowable energy loss per ELM, and it seems difficult to avoid this by shaping design. Experiments should thus continue to study edge power loading and the effect of finite ion orbits to build more confidence that the extrapolations to ITER may be trusted.

Plasma-materials interaction:

- Loss of material strength during tungsten recrystallization has been shown to favour the appearance of macro-cracks which can propagate down to the cooling tube. To avoid these deleterious effects, an operational budget will need to be defined which takes into account the fact that recrystallization is a time- and temperature-dependent effect. To date, the recrystallization kinetics of the tungsten material to be used in ITER is not well characterized and detailed studies are needed to allow a reliable operational budget to be defined for ITER operations.

- Even if deep recrystallization is avoided by proper control of the steady-state divertor heat fluxes, surface roughening/cracking/melting can occur, depending on the ELM energy density. The evolution of the surface damage and its dependence on the base material temperature have been studied in detail, and it is clear that the damage threshold is very low for ITER. One big unknown for ITER, however, is whether and how such surface damage might affect the material compatibility with high performance plasmas. In particular, it is at present impossible to define a tolerable level of damage before the degraded material properties would start to have an impact on plasma performance because of enhanced tungsten release or reduced power handling capabilities. This is clearly an area where further research is needed before the start of ITER operations.

- The effect of long-term stationary and transient plasma exposure (be it H, D, DT or He) on the thermo-mechanical properties of W clearly remains an important topic where little information is available. Although indications exist of material property modifications following plasma exposure, extrapolations to the very high fluence expected in ITER are currently hazardous. Results from high fluence ($>10^{28}$ m^{-2}) experiments are currently very scarce, especially for the case of mixed species (including extrinsic seeded impurities), although the recent development of high flux steady-state plasma devices should expand the existing database. These experiments will need to be accompanied by detailed mechanical measurements allowing the quantification of changes in material properties such as ultimate strength, ductility, etc., which will require a systematic use of micro-mechanical measurements. Understanding long-term plasma exposure effects will also require the development of multi-scale material modelling capable of describing the evolution of the material properties at different temporal and spatial scales, therefore bridging the gap from the plasma-surface interaction processes (occurring close to the surface) to the long range diffusion of D/T/He atoms and their effect on the material bulk.

- Related to the above, the existence and importance of synergetic effects should be investigated in more detail in the coming years. This includes, for example, the possible role of plasma-induced defects (voids, bubbles) on the recrystallization kinetics of the tungsten material. Recent investigations have indeed revealed a possible retarding effect of plasma exposure on recrystallization. An additional issue is the effect of stresses created by the high local concentration of plasma species in the near-surface region on the material thermal shock behaviour.
- Systematic analysis of the JET bulk tungsten divertor lamella would provide important information for ITER. Even if the conditions in JET (inertial cooling, different stress distribution) are quite different from those in ITER, the tungsten material in JET has been exposed to significant plasma fluence in the presence of a large number of ITER-relevant ELMs, providing unique information about the effect of long-term exposure to the tokamak environment on tungsten.
- Formation of tritiated ammonia might represent an issue for the duty cycle of ITER operations, since high temperature regeneration of the cryopumps would be needed to recover ammonia (and the tritium within) from the active charcoal used in ITER for H/D/T and He pumping. Ongoing studies of ammonia formation rates during nitrogen injection should be continued and complemented by edge plasma simulations where the nitrogen/hydrogen chemistry is accounted for. The recent development of a reaction database for the SOLPS-ITER code is a first step in this direction, but would benefit from additional data on surface reaction rates, which are crucial since ammonia formation mainly proceeds through surface reactions. In parallel, the possibility of preventing ammonia formation during nitrogen seeding should be explored in a fashion similar to the so-called scavenger effect, which was promoted to mitigate the formation of tritium-rich carbon co-deposits.

5.3 MHD stability issues

A number of MHD stability control issues continue to be the subject of active research during the ITER construction phase. The Plasma Control State-of-the-art and R&D Plan [Snipes, 2016-2] from the PBS-47 Plasma Control System Preliminary Design Review gives a good overview of recent R&D and suggestions for future R&D for all of the plasma control functions, including MHD stability control. A brief summary of the recommended MHD stability control R&D is given below.

5.3.1 Disruption characterization, prediction and mitigation

Specifying mitigation success rates for ITER disruption management requires more input on the characterization of electromagnetic loads as well as on the energy deposition distribution during runaway electron impact. The ITPA disruption database shows that some tokamaks encounter frequently halo current amplitudes at levels of ITER load category III [Eidietis, 2015]. However, it is also seen that machine specific ‘hidden’ parameters appear to determine the halo current fraction and the toroidal peaking. This has to be further understood to improve predictions for ITER. During the ‘progressive start-up’ approach, EM loads will be monitored and models will be validated as plasma parameters are increased in the course of the implementation of the Research Plan. A better understanding of the physics of asymmetric VDEs is required to ensure that these can be assessed appropriately in applying this approach. Models describing these events have to be assessed and validated through experiments. Initial modelling has been performed to address the impact of runaway energy deposition on the first wall or divertor components to specify critical plasma

currents for which runaway formation would represent a significant risk for water leaks [Lehnen, 2016]. A full assessment requires more information on RE energy, the deposition process and the resulting energy load distribution.

The disruption predictor inside the PCS aims to trigger the DMS within its reaction times [Pautasso, 2016]. High levels of prediction success will have to be achieved for high energy plasmas [Lehnen, 2016]. Predictors currently under development are either physics-based threshold approaches or statistical methods using training data sets. R&D in this area is required to extend threshold approaches, such as that described in [de Vries, 2015], to reach the required success rates. Disruptions in which the prediction algorithm has failed in current devices have to be assessed with respect to their severity. In this respect, it is important to identify the expected disruption types in ITER and to assess those critical for disruption mitigation. Training and testing data sets have to be selected such that they reflect the expected types of disruptions in ITER. The threshold-based predictor will be used from the beginning of operation and may be complemented at a later stage of the project with a data-driven predictor. All of these approaches have to ensure portability and scalability between devices to avoid excessive commissioning/training in ITER and also to reduce the risk of insufficient prediction success rates when progressing in the operational space and when transiting to new operational scenarios (e.g. from L-mode to H-mode).

The ITER strategy for establishing reliable and effective disruption mitigation is based on a step-wise approach to account for the gaps in the present physics and engineering basis. Most urgent R&D has to focus on physics and technology issues related to the baseline DMS that will use shattered pellet injection (SPI) systems distributed across several ITER port plugs to effect thermal, electromagnetic and runaway electron load mitigation at disruptions. Given the current understanding of the challenges in implementing a DMS with the required level of reliability in ITER, extensive R&D is required to provide the basis for a timely upgrade of the baseline system should results from the ongoing R&D, or, subsequently, from ITER operation, reveal that the baseline specification does not adequately meet the mitigation requirements. A final element of the R&D program for ensuring that ITER will have a satisfactory disruption mitigation capability at the highest plasma performance is the exploration of alternative approaches to disruption mitigation. These could be related to more efficient material delivery to the plasma or to modifications of the present mitigation scheme, which is primarily based on energy dissipation through radiation. This provides an element of risk mitigation for the baseline implementation of the DMS concept (i.e. SPI) given the critical role played by the DMS in the successful implementation of the IRP.

The two main outstanding issues in understanding the physics of disruption mitigation are the suppression or avoidance of runaway formation during the disruption mitigation process (i.e. during the initial intervention aimed at mitigation of thermal and electromagnetic loads) and – as a second layer of defence – the dissipation of runaway energy should a runaway beam have formed in spite of the initial intervention. Therefore, physics R&D needs to focus on improving the understanding of all processes that drive RE seed formation, including the role of the thermal quench MHD and the impact of the impurity source distribution (determined by, e.g., pellet fragment ablation). Similarly, physics R&D needs to address all mechanisms that impact on the efficiency of the energy dissipation scheme, such as the runaway interaction with impurities, the impurity penetration process and the evolution of the runaway beam, including possible instabilities.

The R&D needs around the implementation of the DMS baseline concept can be divided into three groups: a) integration of the system in the port plugs, b) the pellet generation and injection process, and c) the effectiveness and robustness of the system during ITER operation. Addressing these areas will require experimental work in laboratories as well as at tokamaks together with modelling

and theory development. The work related to groups a) and b) is very much technology oriented and includes, for example, adapting the SPI technology to the specific restrictions in ITER on space and port plug availability, but also to addressing questions specific to SPI, such as optimizing pellet release and the shattering process to ensure high reliability and effectiveness of the system.

Work related to group c) focusses on matching the SPI parameters to the needs for most efficient mitigation. This includes addressing the optimum size distribution of the pellet fragments, the optimum pellet velocities and injection directions, as well as the effectiveness of multiple pellet injection. Finally, extensive tests at present devices with mitigation systems representative of the final design choice for the ITER baseline system will be required to minimize the risk that the mitigation performance is insufficient at some point during ITER operation when approaching high current or high energy operation. Currently, SPI experiments are performed at DIII-D and are in preparation for JET. These experiments focus on narrowing down requirements for the DMS, such as injection angles, effectiveness of multiple injections, etc. Priority should be given specifically to R&D on the validation of the concept of material injection to avoid runaway formation and on confirming the required injection quantities, sequences, and species. The effectiveness in dissipating the runaway energy as a second layer of defence has to be further addressed as some experimental results [Reux, 2015; Commaux, 2016] and recent modelling work [Konovalov, 2016] have raised questions on the viability of this strategy. Radiation heat loads can be an issue for mitigated disruptions with high thermal energy. To date, radiation asymmetries have been assessed only for MGI mitigated disruptions [Izzo, 2013; Shiraki, 2016; Lehnen, 2015-2] and must be assessed for SPI. Theory and modelling work is needed to conclude on the required injection quantities and shard sizes, and on the allowable fraction of gas and liquid during SPI. Here, it is important to account for the various plasma scenarios for which mitigation is required - this can have a significant impact on ablation rates and thus assimilation efficiency.

5.3.2 Sawtooth control

It is important to extend the methods that have been demonstrated to be effective for controlling sawteeth in present experiments by further exploiting localized current drive or fast ion generation supported by model validation that would allow application in ITER. Requirements for heating and current drive actuators for sawtooth control have been described in detail in an ITPA report [Chapman, 2011]. While ECCD has been shown to control sawteeth effectively for decades, only recently have such demonstrations been replicated in the presence of core energetic particles. Sawtooth destabilization of long period sawteeth induced by ICRF generated core fast ions with energies $\geq$0.5MeV was achieved in Tore Supra, even with modest levels of ECCD power [Lennholm, 2009a; Lennholm, 2009b]. More recently, sawtooth control using ECCD has been demonstrated in ITER-like plasmas with a large fast ion fraction, wide q=1 radius and long uncontrolled sawtooth periods in DIII-D [Chapman, 2012]. As expected from simulations, the sawtooth period is minimized when the ECCD resonance is inside the q=1 surface. Sawtooth control using driven current inside q=1 allows the avoidance of sawtooth-triggered NTMs, even at much higher pressure than required in the ITER baseline scenario [Chapman, 2010; Chapman, 2013-2]. Operation at β_N=3 has been achieved in ITER demonstration plasmas – which otherwise often experience sawtooth-triggered 2/1 or 3/2 NTMs – when sawtooth control is applied using only modest ECCD power [Chapman, 2012]. Such avoidance of NTMs permitting operation at higher pressure than otherwise achievable by application of steerable core ECCD sawtooth control has also recently been demonstrated in ASDEX Upgrade [Chapman, 2013-1].

TCV has demonstrated feedback control of the sawtooth period by actuating on the EC launcher injection angle in order to obtain the sawtooth period at a predetermined value [Paley, 2009]. Fine

control over the sawtooth period has been demonstrated on Tokamak à configuration variable (TCV) using either `sawtooth pacing' via modulated ECCD with real-time crash detection [Goodman, 2011], or `sawtooth locking', where the sawtooth period is controlled even in the absence of crash detection in a reduced region of duty-cycle vs. pulse-period parameter space [Lauret, 2012; Witvoet, 2011]. The applicability of these control methods to ITER has been tested [Kim, 2014] and sawtooth locking experiments have been performed on KSTAR [Kim, 2015; Jeong, 2015] and AUG [Kim, 2015] in the presence of energetic particles.

Control of sawteeth by ICRF in the presence of core energetic particles has been widely exploited on JET, e.g. [Eriksson, 2004; Eriksson, 2006; Sauter, 2002]. The fundamental difference between ECCD and ICRF for sawtooth control is that ECCD modifies the local magnetic shear at the q=1 surface, while the ICRF kinetically destabilizes the kink mode. Furthermore, ICRF control has also been demonstrated in plasmas with significant heating power on-axis from neutral beam injection and high β_p well above the critical threshold for triggering of 3/2 NTMs in the absence of sawtooth control [Coda, 2007]. Subsequently, it was noted that the sensitivity of sawtooth destabilization by ICRF was very high and effective sawtooth control required an accuracy of the resonance position with respect to the q=1 surface of less than 0.5% (i.e. within 1 cm of the q=1 surface in JET), far more sensitive than expected from a control mechanism involving a modification of the magnetic shear. Recent JET experiments using ^{3}He minority heating (so that the driven current was negligible) on the high field side just outside the q=1 surface lead to a strong destabilization for counter-propagating waves (-90°) and a strong stabilization for co-propagating waves (+90°) [Graves, 2010]. This sawtooth control scheme via affecting the kink mode potential energy has subsequently been demonstrated in H-mode plasmas with significant core heating too [Graves, 2012], adding credibility towards its applicability in ITER. Finally, real-time control through variation of the ICRF frequency has been attempted with some success on JET [Lennholm, 2011], though the frequency variation is much slower than anticipated in ITER.

A detailed experimental program on sawtooth control in ITER should be developed around dedicated R&D on existing devices, performed with the goal of optimization of the commissioning of sawtooth control for ITER. Experimental activities should include minimization of the number of the dedicated shots, assessment of required duration of the plasma current flattop, q_{95}, etc., optimization of the control methods and algorithms, and development of requirements for diagnostics at each phase of the IRP. The corresponding R&D should be carried out using diagnostics and actuators similar (to the extent possible) to those in ITER.

5.3.3 ELM control

For plasma currents exceeding 6 – 9 MA, depending on the assumed wetted area of the heat flux [Loarte, 2010], type-I ELMs must be controlled or mitigated in ITER to avoid excessive intermittent heat load and subsequent material erosion from the first wall blanket modules and divertor target plates; at high plasma performance, ELM control is critical for machine protection. This edge instability is believed to be an interplay of low to intermediate mode number peeling-ballooning modes and high mode number kinetic ballooning modes whose onset is well predicted in existing devices by the EPED model [Snyder, 2011].

It has been found experimentally that the ELM amplitude decreases with increasing ELM frequency [Lang, 2003]. ELM pacing has been demonstrated on several machines with deuterium pellets [Lang, 2004; Lang, 2011; Lang, 2013] and with lithium granules [Mansfield, 2012]. Deuterium pellet injection at up to 64 Hz can potentially be used in ITER to induce ELMs frequently enough so that the ELM amplitude remains relatively small. This frequency is expected to be sufficient to

reduce ELM perturbations to acceptable levels with $\Delta W_{ELM} < 0.7$ MJ for the Q=10, 15 MA inductive scenario [Loarte, 2010]. However, the pellet size must be chosen to have sufficient penetration to trigger the ELM and yet have little impact on fuelling. Resonant magnetic perturbations have also been shown to stabilize or mitigate ELMs under some conditions in existing devices [Evans, 2008; Suttrop, 2011]. The in-vessel ELM control coils will be used to actively drive an n = 3 or n = 4 edge magnetic perturbation to stabilize or mitigate ELMs. An ELM control coil current of up to 90 kAt will provide a magnetic perturbation in the edge pedestal region of up to $6.6\times10^{-4} \times 5.3$ T, which is expected to be sufficient to stabilize ELMs based on extrapolation from existing devices [Loarte, 2010]. To better distribute the heat load, the ELM control coil perturbation will be capable of rotating at up to few Hz at full coil current.

5.3.4 Neoclassical tearing mode control

Neoclassical tearing modes represent a significant challenge for present tokamaks and are expected to be even more important in ITER. Sawtooth and ELM control will help to avoid creating seed islands for NTMs [Sauter, 2002]. The most effective means of NTM control has been demonstrated with localized ECCD inside the magnetic island, as demonstrated in DIII-D [La Haye, 2002; Humphreys, 2006] and ASDEX Upgrade [Günter, 2003; Zohm, 2007]. The precise specifications for an effective NTM stabilization system with ECCD on ITER are still an active area of research within the fusion community [La Haye, 2009; Sauter, 2010]. The response time to initially turn on EC to full power is 10 ms and to turn EC power on from standby state is 1 – 10 ms. The time required to begin sweeping the UL mirrors following a request by PCS is ~200 ms and the sweep can cover one third of the plasma cross-section in ~3 s (~6º/s). This sweep rate should be adequate for NTM control to move between the q = 1.5 and q = 2 surfaces [La Haye, 2009]. The EC full power modulation will be available with a frequency up to 5 kHz, with a variable duty cycle. Modulated ECCD with absorption and current drive in the O-point of the islands only (ECCD power off for X-points) can be yet more effective than CW ECCD, if island widths are substantially narrower than that of the ECCD as demonstrated in ASDEX-Upgrade [Maraschek, 2007]. However, the change in the ITER ECRH launcher mirrors to front steering, which was implemented during the design review, allows narrow ECCD deposition, which may obviate the need for modulation so that CW ECCD may be effective enough, if well-aligned on the rational surface, for the stabilization of NTMs in ITER.

Techniques to allow a ‘saturated’ island to occur and then turn on and align ECCD for stabilization are inadequate in ITER where 2/1 islands must be kept small to avoid locking. However, some experiments have been successful in avoiding or quickly stabilizing NTMs when they first start to grow [Nagasaki, 2003; La Haye, 2005]; this is the approach modelled for ITER [La Haye, 2009]. After stabilization of an NTM and/or before it ever occurs, it was shown that ‘active tracking’ of the real-time MSE EFIT location of the q=2 surface and of the location of the ECCD by TORAY, TORBEAM or a refraction analogue based on interferometers, in order to keep alignment good enough between the ECCD driven current and the q=2 location, is a feasible strategy to prevent the NTM modes from reappearing and/or to never occur [Prater, 2007]. However, this strategy for NTM mode control requires gyrotron power to be applied throughout the high-β phase and the alignment relies on the real-time estimation of the mode location which can have uncertainties. Recent TCV experiments have introduced a new way to implement this strategy by sweeping ECCD around the estimated mode location to compensate these possible uncertainties from real-time estimations [Kim, 2015].

Dedicated R&D on existing devices should also be undertaken with the goal of optimization of the commissioning strategy for NTM control in ITER. This program should include minimization of

number of the dedicated shots, assessment of the required duration of the plasma current flattop, q_{95}, β_N, etc., optimization of control methods and algorithms, and development of requirements for diagnostics at each phase of the IRP. The corresponding R&D should preferably be performed using diagnostics and actuators as similar as possible to those available in ITER.

5.3.5 Error field control

Error field control in ITER is necessary to correct for small misalignments in the CS, PF, and TF coils and asymmetries in the coil feeders, and to minimize the influence of ferromagnetic inserts, TBMs, NB Magnetic Field Reduction system, holes and port plugs in the vacuum vessel and other non-axisymmetric features of the magnetic field topology in ITER, in order to avoid locked modes and to enable the generation of a local field null for plasma initiation. Such error fields can induce a torque slowing down the plasma toroidal rotation, which can then lead to a higher incidence of locked modes and disruptions. Ramps in the n=1 error field produced by external coils can be used to determine the low density locked mode threshold [Buttery, 1999; Luxon, 2003; Wolfe, 2005; Buttery, 2012]. Error fields also enhance resistive wall modes (RWMs) at high β and thus their control will help avoid RWMs. The control of error fields and their effects on locked modes have been studied for many years on a number of devices [Scoville, 2003; Buttery, 2000; Morris, 1992; La Haye, 1992; Park, 2007]. Recent dedicated experiments on DIII-D have studied the effects of error fields due to TBMs particularly on H-mode confinement and plasma rotation [Snipes, 2010]. Three sets of 6 top, bottom, and side external correction coils (CC) will be used in ITER to minimize error fields within the 320 kAt top and bottom and 200 kAt side correction coil current limits. In the addition to the correction coils, ELM control coils will be used for identification of the error field structure and, in scenarios when these coils are not used for ELM control, or in scenarios when the coil currents required for ELM control leave sufficient margin, the ELM control coils could be used for error field correction.

Historically, analysis of n = 1 mode error fields leading to mode locking (LM) in ITER has been performed using two LM criteria. The first is the '*3-mode*' criterion [Hender, 2007], which was used for the ITER design since the Engineering Design Activities (EDA) [ITER Technical Basis] and it was also used in the *Project Requirements* up to version 5.3 [ITER_D_27ZRW8, 2014]. The second is the '*overlap*' error field criterion, which is the criterion on the resonant error field for the n = 1 toroidal mode. This was developed around the analysis performed with the IPEC code for three fiducial ITER plasmas [Park, 2008]. The review of progress made in the last decade in the area of error fields, summarized in the report of MHD Topical Group of the International Tokamak Physics Activity (ITPA) [Park, 2017], concludes that: i) the *3-mode* criterion must be retired and ii) as far as the LM avoidance is concerned, only the *overlap* (resonant) criterion should be used. It should be noted, that the criteria for error field correction are not final and they are studied in the ITPA framework. In particular the database of the *overlap* n = 1 criterion will be increased, and criteria for correction of n = 1 non-resonant error fields (e.g. effecting plasma rotation and L to H mode transition), as well as criteria for n = 2 modes remain to be developed.

Optimization of error field control commissioning should be investigated within the R&D programs of existing devices in order to develop a suitable methodology allowing minimization of the time allocated to this activity in ITER. The program should include minimization of the number of the dedicated shots, assessment of required duration of the plasma current flattop, q_{95}, β_N, etc., optimization of control methods and algorithms, and development of requirements for diagnostics at each phase of the IRP. The corresponding R&D should be undertaken using diagnostics and actuators similar to those available in ITER.

5.3.6 Resistive Wall Mode control

To achieve high values of Q in steady-state regimes, high values of the normalized pressure, β_N, are required. Plasmas with low l_i and high β_N may be unstable to Resistive Wall Modes (RWM). Unstable RWMs can be generated from a plasma initially below the ideal low-n kink/ballooning no-wall limit, such as the ITER baseline scenario, by local increases of pressure gradients via transport barrier formation [Maingi, 2010], or other events that significantly increase the plasma pressure profile peakedness (e.g. H-L mode back-transition) and thus substantially lower the ideal no-wall limit [Sabbagh, 2004].

RWM stabilization is best accomplished by a combination of passive kinetic stabilization [Betti, 2004] and an active feedback control system capable of sensing low-n RWM activity [Okabayashi, 2001; Sabbagh, 2006]. Calculations using kinetic RWM theory for ITER by two independent groups (using the MARS-K and MISK codes) show that passive kinetic stabilization is possible in ITER through the combination of thermal and energetic particle effects (including α-particles), but that the operational space of interest is largely unstable, and thus that passive stabilization must be supplemented by active control [Liu, 2009; Berkery, 2010]. The studies conducted for ITER using the MISK code utilize a theoretical model that has been quantitatively benchmarked against the NSTX and DIII-D experiments.

In ITER, the ELM control coils may be used for feedback stabilization of RWMs with an upgrade to their power supplies, if necessary. These coils provide a flexible set of actuators capable of handling feedback control of multiple toroidal mode numbers up to $n = 3$, and different poloidal field perturbation spectra at a given n (multi-mode control at constant toroidal mode number) [Sabbagh, 2010; Sabbagh, 2011]. The power supplies driving the ITER ELM control coils will need to create an AC toroidally rotating field to track RWM rotation during feedback control.

A study of RWM active stabilization in ITER by the ELM control coils was performed with the CarMa code for two 9 MA plasmas with weak reverse shear having $\beta_N = 2.94$ ($\gamma \approx 15\ s^{-1}$) and $\beta_N = 3.14$ ($\gamma \approx 40\ s^{-1}$). The best achievable performance of the ELM control coils has been computed in terms of the maximum allowable initial perturbations of the vertical (poloidal) magnetic field, measured by the outboard in-vessel sensors, which is recoverable by any feedback controller with currents and voltages inside the design limits of the power supplies. If all three sets of ELM control coils (Upper, Equatorial and Lower) are used for RWM stabilization, the maximum recoverable magnetic field perturbation is about 40 mT for both reference 9 MA plasmas. The maximum recoverable initial perturbation reduces to about 20 mT, if only the Equatorial ELM control coils are used for the RWM stabilization.

5.4 Scenario development issues

Operational scenarios need to cover all phases of the discharge consistently – the breakdown, ramp-up, flat-top, burn and ramp-down – with the time evolution providing proper linkage between and during these phases. Most of the attention in describing ITER operation has focussed so far on the burn phase. But, as known from the experience of operation in present devices, it is necessary to identify controlled sequences that arrive at the optimum conditions to achieve high performance stationary plasmas even when these plasmas are not dominated by the physics of burning plasmas. In addition to the constraints imposed by, for example, MHD stability control or plasma-surface interactions, operational scenarios must link the plasma breakdown, ramp-up, flat-top and ramp-down stages in a manner that is consistent with the control systems. Additional constraints may apply when operating at lower field and current or with a species other than DT fuel (e.g. low current operation in hydrogen or helium H-mode operation) in ITER that do not make these

scenarios any easier to operate due to these additional constraints (marginal H-mode operation, shine-through limits, etc.), as studied in [Kim, 2016] and also discussed in detail in section 2.5.3.

Research and development activities in the area of plasma control will be a central aspect of the research program in the scenario development area. Burning plasma scenarios in ITER will make extensive demands on the ITER control capability. Limitations on actuator capabilities or capacities require an integrated control approach, with the possibility of actuator sharing. Demonstrating not only that the many plasma control techniques that are being developed in the present experimental programs (e.g. MHD stability control, radiative power control, Internal Transport Barrier (ITB) control, current profile control) can be turned into reliable and robust control technologies that can be applied to ITER in an integrated plasma scenario, is a major research activity which will accompany ITER construction.

It is, furthermore, very important that these experimental studies are accompanied by a substantial effort in the simulation of ITER operational scenarios. Present day devices will never be capable to fully emulate ITER operational scenarios, but they can validate individual models that can be used for the predictive simulation of such scenarios. ITER operation is expensive and any component damage resulting from operational errors can potentially lead to high repair costs and significant downtime of the facility. Hence predictive simulations, using the ITER integrated modelling platform (IMAS), to assess plasma control, develop operation scenarios and prepare experiments, will be essential for reliable and efficient ITER operation [Parail, 2009; Imbeaux, 2015; Pinches, 2016]. IMAS must meet the challenge of simulating complete discharges including all phases from plasma initiation to termination, prior the experiment, to anticipate their behaviour and performance, and to tune controls and scenarios accordingly. The ITER integrated modelling platform shall equally be capable of reconstructing experimental discharges based on the actual measurements in order to ensure the understanding of all physics aspects related to the experiment.

5.4.1 Breakdown and burn-through

The large size of ITER brings an immediate challenge, namely achieving effective and reliable plasma initiation. Although calculations based on the existing tokamak experience suggest that breakdown using only the inductive electric field should be achievable, the margin appears to be low and breakdown assisted by several MW of ECRH, is foreseen. To obtain a greater confidence that the breakdown has an adequate margin to establish reliable initial plasmas for the ramp-up phase, detailed modelling of the breakdown using the ITER geometry, PF system, ECRH sources as well as passive components, such as for example the vacuum vessel, is needed. This modelling should also include an accurate treatment of the impurity behaviour. Variations, in the first wall (e.g. a steel limiter for First Plasma, and a Beryllium main chamber wall from PFPO-1 onwards), applied poloidal flux (e.g. the CS precharge) and, most importantly, breakdown at third and half of the full ITER toroidal field of 5.3 T, should be also included in these studies.

Progress has been made in this area over the recent years, e.g. by: rehearsing ITER breakdown in present devices [Sips, 2009; Jackson, 2010], assessing the effect of a beryllium wall [Kim, 2012-1; Kim, 2013; de Vries, 2013] as well as use ECRH to assist plasma formation [Jackson, 2011], culminating in fully simulated ITER plasma initiations [Kavin, 2017]. However, better models of ECRH assisted pre-ionization and breakdown need to be developed, as well as a better understanding of the impact of the ITER vessel size with respect to the breakdown area, in order to predict accurately and to optimize plasma initiation in ITER.

5.4.2 Current ramp-up

The current ramp-up phase raises several operational issues that need to be addressed self-consistently. The constraints imposed by the PF system during the current ramp-up are considerable: forming an X-point and controlling its position through the remainder of the current rise, maintaining the internal inductance, l_i, in an acceptable range, minimizing resistive losses to increase the duration of the burn phase, avoiding current, field force, and voltage limits on the coils, etc. [Sips, 2009; Jackson, 2010]. X-point formation may also have to be done early in the current ramp-up in ITER using a reliable shape control to avoid the excessive power loads on the beryllium first wall panels due to narrow power e-folding lengths in the near-separatrix limiter SOL.

A large theoretical and experimental effort has been devoted to improving the understanding of plasma confinement in present tokamak plasmas and to evaluate the implications for ITER. However, most of this effort has addressed flat-top conditions in H-mode plasmas while ohmic and L-mode plasmas always precede the H-mode in the current ramp-up in ITER and dictate the initial conditions for the flat-top, or burn conditions. One of the most critical issues is the evolution of the current profile during current ramp-up, where the radial profile of the thermal conductivity and the resulting resistivity profile determine whether the current profile will be peaked and lead to sawtooth activity (higher l_i) or broad (lower l_i) and will more easily connect with high performance conditions for the advanced scenarios, such as hybrid and steady-state operation. Predictive modelling of the current profile behaviour during the ramp-up is still not satisfactory [Voitsekhovitch, 2010]. Moreover, the influence of high-Z impurities on this phase should be better understood [Hogeweij, 2015]. The transition to H-mode conditions, if performed in the current ramp-up, introduces another dimension to the evolution of the internal inductance through the appearance of the bootstrap current in the pedestal when the plasma enters the H-mode. A low l_i from a large edge current increases the demands on the PF system (i.e. PF6) for control of the X-point.

A second aspect is the increase of plasma density simultaneously with the current during the ramp-up phase. This will not be as straightforward in ITER as in present devices, due to the limited efficiency of edge neutral fuelling [Kukushkin, 2013-2]. This, and the slow response of the ITER gas fuelling injection system with the valves located far from the vessel, may complicate density control. Pellet injection may be necessary to assist in fuelling and controlling plasma density in the ramp-up phase. However, this will be limited for helium operation scenarios, scheduled during PFPO-1 and PFPO-2, due to the dilution of the helium plasma by the hydrogen pellets. Detailed modelling of the fuelling of ITER ramp-up scenarios, for all species, as well as assessing the achievable density control, will provide a better insight in the expected density behaviour during this critical scenario phase [Garzotti, 2012; Ravensbergen 2015; Militello-Asp, 2016].

5.4.3 Current flat-top

As the main phase of a tokamak discharge, the current flat-top usually attracts most attention in scenario development. In the scope of the analysis of R&D for ITER there are a number of issues that should be considered: the achievable flat-top duration, the reliable entry to high performance operation (i.e. access to H-mode operation and eventually entry to burn) and the integration of various control schemes.

A proper assessment of the maximum current flat-top duration, will depend on a number of factors, the magnetic flux consumed during plasma initiation and ramp-up, the consumption during the flat-top, which depend on the plasma resistivity (i.e. related to the plasma temperature and plasma heating) and on the non-inductively driven current and also on other factors such as the cooling

capacity of the superconducting coils, and the achievable control of the plasma current density profile. All these factors will eventually determine the burn duration of the ITER baseline Q = 10 DT as well as of advanced scenarios, but also the available flat-top length for lower current, lower temperature (i.e. higher resistivity) non-active scenarios to be explored during PFPO-1 and PFPO-2.

The entry to H-mode will need to be controlled with the accompanying change in β, which will require integrated control of the auxiliary heating sources and plasma radial position. The transition to high performance, especially concerning the transition to burn, requires the gradual application of control of the steady-state heat flux to the divertor and also the transient loads due to ELMs. Although heat flux and ELM control techniques have been applied in present devices in stationary conditions, controlled transitions to high power H-modes are rarely explored.

Controlling the plasma performance, and more specifically kinetic profiles, in present tokamaks has advanced significantly, which helps to support the case for operation of ITER close to its theoretical and empirical performance limits [Kim, 2012-2; Felici, 2012]. Under these conditions, plasma control becomes more sensitive to the desired flat-top plasma regime. During the flat-top the discharge performance, fuelling, stability and exhaust need to be controlled. Present devices have developed numerous schemes to control sawteeth, NTMs or ELMs and the applicability to ITER has been assessed. However, there is still a need to develop a reliable methodology to integrate these control schemes into one operation scenario, with high performance together with MHD stability, kinetic plasma and current profile, fuelling and exhaust control. Larger emphasis should be given to such integration and verification, identifying how these control schemes may interact with each other or to identify how they are linked. The latter may impose additional requirements to the individual control schemes; for example the use of auxiliary heating systems to control MHD instabilities will impact on the control of the exhaust. The sharing of auxiliary heating sources to either control MHD instabilities or the kinetic profiles need to be assessed, while the MHD stability itself may in turn depend on the kinetic and current density profiles. Burn control will also require, besides density control, the control of the fuel ratio. This will require better models for to the fuelling of high performance plasmas, in particular using pellets [Garzotti, 2012].

5.4.4 Plasma termination

The controlled termination of high performance plasmas is an important, but often overlooked, phase of the tokamak discharge. For ITER, considerable effort will have to be devoted to the development of appropriate plasma terminations, with special attention to the transition from a largely self-driven burning state to one that is controlled by the auxiliary systems [Sips, 2009]. In some sense, this mirrors the entry into burn phase, but there are significant differences in the dynamics, such as the density decay and current profile development, that are opposite. These differences complicate the control with respect to the entry phase that makes it difficult to avoid operational limits in many circumstances; this, in the worst cases, may lead to a disruption. This control problem is exacerbated by the fact that at the end of the discharge, the device is usually operating close to its technical limits (e.g. CS current limit). For unplanned terminations, triggered by off-normal events, the situation is further complicated. The ability to carry out a well-controlled termination contributes significantly to the avoidance of disruptions.

The termination phase should achieve a simultaneous ramp-down of the plasma current, kinetic energy and particle density while maintaining control over the radiation levels, plasma position and shape (i.e. to avoid overheating the first wall) and VS, staying within the capabilities of the poloidal field coils and power supplies and heating systems. Stability boundaries and general operational limits must also be avoided. ITER will operate at high densities and a controlled density decay is

important to avoid the density limit in the termination phase, while also managing the H-L transition timing and exit from fusion burn. ITER power supply limitations and the thick low resistivity vacuum vessel slow the control response for vertical stability (VS) and the radial position that can be achieved. Increasing the current ramp-down rate leads to higher l_i, which affects the plasma vertical stability and its control, while the associated β drop for fast H-to-L back transitions may compromise the radial position control. A further concern is the control of impurities and radiation during this phase [Loarte, 2016-2].

As mentioned above, significant effort in the scenario development R&D has focused on the high performance flat-top phase of the plasma scenarios. The dynamic behaviour of e.g., the H-mode pedestal decay, H-to-L transition or the density behaviour during current ramp-down is, on the other hand, much less well understood. A greater experimental effort combined with dedicated simulations is needed to address these scenario development issues for transient phases (particularly in high performance terminations), such that reliable and robust termination scenarios can be developed [de Vries, 2016] for ITER.

5.4.5 Impact of scenario development issues on operation

Scenario development traces the progression of the ITER Research Plan. It is important that at each stage, the new scenarios that need to be explored can make use of the development and understanding gained in previous ITER operational phases. PFPO-1 will dedicate a significant fraction of experimental time to the assessment and optimization of control schemes that will be the basis of operation in PFPO-2 and later phases. For example, plasma initiation and start-up in the hydrogen phase will address several fundamental issues for all future operating scenarios and control schemes. Plasma breakdown, possibly assisted with ECRH, and early divertor formation will be tested. Model validation to enhance the confidence in predictive simulation of the next operational phase scenarios will accompany the execution of the ITER Research Plan.

The development of the ITER Research Plan will also benefit from validation of plasma scenario modelling tools on present tokamaks, including models for plasma initiation, control schemes, and models to describe the evolution of the temperature, density and current profiles. In particular, radial transport models for electron and ion energy and particles in Ohmic and L-mode plasmas that were developed many years ago should be re-examined using the more extensive diagnostic capabilities of present devices so that they can be used to plan more optimal ITER ramp-up scenarios that maintain the internal inductance, l_i, within an acceptable range for control.

The basis for establishing ITER baseline Q = 10 DT operation, the initial major goal of the ITER Research Plan, is reasonably well established. But the experimental development of advanced (i.e. hybrid and steady-state) scenarios is more challenging, as they require operation at the limits of the hardware capabilities of any given tokamak where they are explored (i.e. operation at high power for a maximum time duration, close to plasma stability limits, etc.). With regards to operation of ITER in regimes with enhanced core confinement, such as hybrid scenarios, but especially those that feature ITBs, none of the predictive models for such regimes are as yet in a position to make reliable projections. For the global scaling approach, the limitation may be intrinsic, in that the development and sustainment of ITBs depends on local plasma parameters (i.e. on detailed plasma profiles), which are not captured in scalar databases. For the transport models, while progress has been made in replicating ITB formation and sustainment, further work is required before projections can be made with confidence of such regimes to ITER. Advanced operation in ITER with enhanced core confinement is becoming an increasingly realistic and attractive prospect, but a major experimental emphasis is required to demonstrate that such an advanced operation is compatible

with reactor operating conditions. Substantial advances have been made in improving the physics content and reliability of transport modelling and simulation codes, but a fully consistent and integrated (core and edge) predictive capability that can accurately describe all transport channels remains to be developed. These also need to be coupled with control schemes that can be implemented on ITER, consistent with the diagnostics, PF, auxiliary heating, and current drive capabilities.

References

This ITER Technical Report may contain references to internal technical documents. These are accessible to ITER staff and External Collaborators included in the corresponding ITER Document Management (IDM) lists. If you are not included in these lists and need to access a specific technical document referenced in this report, please contact us at ITR.support@iter.org and your request will be considered, on a case by case basis, and in light of applicable ITER regulations.

[Aiba, 2011] N. Aiba et al., Nucl. Fusion **51** (2011) 073012.

[Akers, 2016] R.J. Akers et al., Proc. 26th IAEA Fusion Energy Conf. (Kyoto, Japan, 2016) TH/4-1.

[Alberti, 2005] S. Alberti et al., Nucl. Fusion **45** (2005) 1224.

[Amoskov, 2016] V. Amoskov et al., "TF ripple with Ferromagnetic Inserts "Baseline 2016" (regular sectors of the vacuum vessel)": https://user.iter.org/?uid=TEEWB5.

[Andrew, 2004] Y. Andrew et al., Plasma Phys. Control. Fusion **46** (2004) A87.

[Andrew, 2008] Y. Andrew et al., Plasma Phys. Control. Fusion **50** (2008) 124053.

[Arnoux, 2013] G. Arnoux et al., Nucl. Fusion **53** (2013) 073016.

[Artaud, 2008] J-F. Artaud et al., Proc. 35th European Physical Society Conf. on Plasma Physics (EPS) (Hersonissos, Greece, 2008) vol. 32D ECA P-5.068.

[Artaud, 2010] J-F. Artaud et al., Nucl. Fusion **50** (2010) 043001.

[Asakura, 2007] N. Asakura et al., J. Nucl. Mater. **363-365** (2007) 41.

[Asakura, 2009] N. Asakura et al., Nucl. Fusion **49** (2009) 115010.

[Austin, 2011] M.E. Austin, Fusion Sci. Technol. **59** (2011) 647.

[Baelmans, 2011] M. Baelmans et al., Nucl. Fusion **51** (2011) 083023.

[Baylor, 2013] L.R. Baylor et al., Phys. Rev. Lett. **110** (2013) 245001.

[Baylor, 2015] L.R. Baylor et al., IEEE 26th Symposium on Fusion Engineering (SOFE) (Austin, USA, 2015), DOI: 10.1109/SOFE.2015.7482362.

[Behn, 2015] R. Behn et al., Plasma Phys. Control. Fusion **57** (2015) 025007.

[Berkery, 2010] J.W. Berkery et al., Phys. Plasmas **17** (2010) 082504.

[Belyakov, 2003] V.A. Belyakov et al., Plasma Devices and Operations **11** (2003) 193.

[Bernard, 2015] E. Bernard et al., J. Nucl. Mater. **463** (2015) 316.

[Bernert, 2017] M. Bernert et al., Nucl. Mater. Energy **12** (2017) 111.

[Betti, 2004] B. Betti et al., Phys. Rev. Lett. **93** (2004) 105002.

[Beunas, 2009] A. Beunas et al., IEEE Transactions on Electron Devices **56** (2009) 864.

[Bialek, 2001] J. Bialek et al., Phys. Plasmas **8** (2001) 2170.

[Boozer, 1995] A.H. Boozer, Phys. Plasmas **2** (1995) 4521.

[Borodin, 2011] D. Borodin et al., Phys. Scr. **T145** (2011) 014008.

[Bourdelle, 2014] C. Bourdelle et al., Nucl. Fusion **54** (2014) 022001.

[Brezinsek, 2013-1] S. Brezinsek et al., Nucl. Fusion **53** (2013) 083023.

[Brezinsek, 2013-2] S. Brezinsek et al., J. Nucl. Mater. **438** (2013) S303.

[Brooks, 2014] J.N. Brooks et al., Contrib. Plasma Phys. **54** (2014) 329.

[Burrell, 1990] K.H. Burrell, et al., Phys. Fluids B-Plasma Phys. **1** (1990) 1405.

[Buttery, 1999] R.J. Buttery et al., Nucl. Fusion **39** (1999) 1827.

[Buttery, 2000] R.J. Buttery et al., Nucl. Fusion **40** (2000) 807.

[Buttery, 2012] R.J. Buttery et al., Phys. Plasmas **19** (2012) 056111.

[Campbell, 1988] D.J. Campbell et al., Phys. Rev. Lett. **60** (1988) 2148.

[Carpentier, 2014] C. Carpentier-Chouchana et al., Phys. Scr. **T159** (2014) 014002.

[Carralero, 2015] D. Carralero et al., Phys. Rev. Lett. **115** (2015) 215002.
[Carralero, 2017] D. Carralero et al., Nucl. Mater. Energy **12** (2017) 1189.
[Challis, 2015] C.D. Challis et al., Nucl. Fusion **55** (2015) 053031.
[Chang, 2017] C.S. Chang et al., Nucl. Fusion **57** (2017) 116023.
[Chankin, 2007] A.V. Chankin et al., Nucl. Fusion **47** (2007) 479.
[Chankin, 2017] A.V. Chankin et al., Plasma Phys. Control. Fusion **59** (2017) 045012.
[Chapman, 2007] I.T. Chapman et al., Plasma Phys. Control. Fusion **49** (2007) B385.
[Chapman, 2009-1] I.T. Chapman et al., Nucl. Fusion **49** (2009) 035006.
[Chapman, 2009-2] I.T. Chapman et al., Nucl. Fusion **51** (2009) 055015.
[Chapman, 2010] I.T. Chapman et al., Nucl. Fusion **50** (2010) 102001.
[Chapman, 2011] I.T. Chapman et al., "Power requirements for ICRH and ECCD for sawtooth control in ITER - Final Report": https://user.iter.org/?uid=7JFHVR.
[Chapman, 2012] I.T. Chapman et al., Nucl. Fusion **52** (2012) 063006.
[Chapman, 2013-1] I.T. Chapman et al., Plasma Phys. Control. Fusion **55** (2013) 065009.
[Chapman, 2013-2] I.T. Chapman et al., Nucl. Fusion **53** (2013) 066001.
[Chapman, 2014] I.T. Chapman, et al., Nucl. Fusion **54** (2014) 083006.
[Chatelier, 2007] M. Chatelier, Nucl. Fusion **47** (2007) S579.
[Citrin, 2015] J. Citrin et al., Nucl. Fusion **55** (2015) 092001.
[Coenen, 2016] J.W. Coenen et al., Phys. Scr. **T167** (2016) 014002.
[Commaux, 2016] N. Commaux et al., Proc. 26th Fusion Energy Conf. (Kyoto, Japan, 2016) EX/9-2.
[Corre, 2011] Y. Corre et al., Fusion Eng. Des. **86** (2011) 429.
[Counsell, 2006] G. Counsell et al., Plasma Phys. Control. Fusion **48** (2006) B189.
[Cui, 2017] S. Cui et al., J. Nucl. Mater. **486** (2017) 267.
[Degtyarev, 1997] L. Degtyarev et al., Comput. Phys. Commun. **103** (1997) 10.
[Delabie, 2015] E. Delabie et al., Proc. 42nd European Physical Society Conf. on Plasma Physics (EPS) (Lisbon, Portugal, 2015) vol. 39E ECA O13.113.
[Delabie, 2016] E. Delabie et al., Proc. 26th IAEA Fusion Energy Conf. (Kyoto, Japan, 2016) EX/P5-24.
[De Temmerman, 2008] G. De Temmerman et al., Nucl. Fusion **48** (2008) 075008.
[De Temmerman, 2011] G. De Temmerman et al., J. Vac. Sci. Technol. A **30** (2012) 041306.
[De Temmerman, 2017] G. De Temmerman et al., Nucl. Mater. Energy **12** (2017) 267.
[De Temmerman, 2018] G. De Temmerman et al., Plasma Phys. Control. Fusion in press (2018).
[de Vries, 2013] P.C. de Vries et al., Nucl. Fusion **53** (2013) 053003.
[de Vries, 2016-1] P.C. de Vries et al., Proc. 26th IAEA Fusion Energy Conf. (Kyoto, Japan, 2016) EX/P6-41.
[de Vries, 2016-2] P.C. de Vries et al., Fusion Sci. Technol. **69** (2016) 471.
[de Vries, 2016-3] P.C. de Vries et al., Nucl. Fusion **56** (2016) 026007.
[Do, 2011] H. Do et al., Fusion Eng. Des. **86** (6-8) (2011) 992.
[Douai, 2011] D. Douai et al., J. Nucl. Mater. **415** (2011) S1021.
[Douai, 2016] D. Douai et al., Proc, 26th IAEA Fusion Energy Conf. (Kyoto, Japan, 2016) EX/P8-31.
[Dumont, 2014] R.J. Dumont et al., Plasma Phys. Control. Fusion **56** (2014) 75020.
[Dux, 2014] R. Dux et al., Plasma Phys. Control. Fusion **56** (2014) 124003.
[Dux, 2017] R. Dux et al., Nucl. Mater. Energy **12** (2017) 28.
[Eich, 2003] T. Eich et al., J. Nucl. Mater. **313–316** (2003) 919.
[Eich, 2013] T. Eich et al., Nucl. Fusion **53** (2013) 093031.

[Eich, 2017] T. Eich et al., Nucl. Mater. Energy **12** (2017) 84.
[Eidietis, 2015] N.W. Eidietis et al., Nucl. Fusion **55** (2015) 063030.
[Ekedahl, 2010] A. Ekedahl et al., Nucl. Fusion **50** (2010) 112002.
[El-Atwani, 2014] O. El-Atwani et al., Nucl. Fusion **54** (2014) 083013.
[Eriksson, 2004] L-G. Eriksson et al., Phys. Rev. Lett. **92** (2004) 235004-1.
[Eriksson, 2006] L-G. Eriksson et al., Nucl. Fusion **46** (2006) S951.
[Escourbiac, 2017] F. Escourbiac et al., "Assessment of critical heat flux on tungsten monoblocks of the ITER divertor vertical targets", to be submitted to Fusion Eng. Des..
[Evans, 2004] T.E. Evans et al., Phys. Rev. Lett. **92** (2004) 235003.
[Evans, 2008] T.E. Evans et al., Nucl. Fusion **48** (2008) 024002.
[Falchetto, 2014] G. Falchetto et al., Nucl. Fusion **54** (2014) 043018.
[Felici, 2012] F. Felici et al., Plasma Phys. Control. Fusion **54** (2012) 025002.
[Feng, 2017] Y. Feng et al., Plasma Phys. Control. Fusion **59** (2017) 034006.
[Fenstermacher, 2010] M.E. Fenstermacher et al., Proc. 23rd IAEA Fusion Energy Conf. (Daejeon, Korea, 2010) ITR/P1-30.
[Fitzpatrick, 2002] R. Fitzpatrick, Phys. Plasmas **9** (2002) 3459.
[Fukuda, 2000] T. Fukuda et al., Plasma Phys. Control. Fusion **42** (2000) A289.
[Futatani, 2014] S. Futatani et al., Nucl. Fusion **54** (2014) 073008.
[Galliez, 2017] K. Galliez et al., '' Conceptual Design of Hot Cell Building Laboratory'': https://user.iter.org/?uid=TN254B.
[Garbet, 2010] X. Garbet et al., Phys. Plasmas **17** (2010) 072505.
[Garcia, 2008] J. Garcia et al., Plasma Phys. Control. Fusion **50** (2008) 124032.
[Garcia, 2015] J. Garcia et al., Nucl. Fusion **55** (2015) 053007.
[Garcia, 2016] O.E. Garcia et al., Phys. Plasmas **23** (2016) 052308.
[Garcia-Munoz, 2013] M. Garcia-Munoz et al., Nucl. Fusion **53** (2013) 123008.
[Garcia-Munoz, 2015] M. Garcia-Munoz et al., Proc. 14th IAEA Technical Meeting on Energetic Particles in Magnetic Confinement Systems (Vienna, Austria, 2015): 14th IAEA TM on Energetic Particles/Website/Papers/Garcia.pdf.
[Garofalo, 1999] A.M. Garofalo et al., Phys. Plasmas **6** (1999) 1893.
[Garofalo, 2002] A.M. Garofalo et al., Nucl. Fusion **42** (2002) 1335.
[Garofalo, 2008] A.M. Garofalo et al., Phys. Rev. Lett. **101** (2008) 195005.
[Garzotti, 2012] L. Garzotti et al., Nucl. Fusion **52** (2012) 013002.
[Garzotti, 2016] L. Garzotti et al., Proc. 43rd European Physical Society Conf. on Plasma Physics (EPS) (Leuven, Belgium, 2016) vol. 40A ECA O4.113.
[Giancarli 2012] L.M. Giancarli et al., Fusion Eng. Des. **87** (2012) 395.
[Giancarli 2016] L.M. Giancarli et al., Fusion Eng. Des. **109-111** (2016) 1491.
[Giroud, 2017] C. Giroud et al., Proc. 25th IAEA Fusion Energy Conf. (St. Petersburg, Russia, 2014) EX/P5-25.
[Goetz, 1999] J.A. Goetz et al., Phys. Plasmas **6** (1999) 1899.
[Gohil, 2010] P. Gohil et al., Nucl. Fusion **50** (2010) 064011.
[Gohil, 2011] P. Gohil et al., Nucl. Fusion **51** (2011) 103020.
[Gohil, 2012] P. Gohil et al., Proc. 24th IAEA Fusion Energy Conf. (San Diego, USA, 2012) ITR/P1-36.
[Goldston 2011] R.J. Goldston, Nucl. Fusion **52** (2011) 013009.
[Goldston, 2012] R.J. Goldston et al., Nucl. Fusion **52** (2012) 013009.
[Goldston, 2015] R.J. Goldston, J. Nucl. Mater. **463** (2015) 397.
[Goniche, 2014] M. Goniche et al., Phys. Plasmas **21** (2014) 61515.

[Goodman, 2011] T.P. Goodman et al., Phys. Rev. Lett. **106** (2011) 245002.
[Gorelenkov, 2014] N.N. Gorelenkov et al., Nucl. Fusion **54** (2014) 125001.
[Gormezano, 2007] C. Gormezano et al., Nucl. Fusion **47** (2007) S285.
[Goumiri, 2017] I.R. Goumiri et al., Phys. Plasmas **24** (2017) 056101.
[Graves, 2009] J.P. Graves et al., Phys. Rev. Lett. **102** (2009) 065005.
[Graves, 2010] J.P. Graves et al., Nucl. Fusion **50** (2010) 052002.
[Graves, 2012] J.P. Graves et al., Nat. Comms. **3** (2012) 624.
[Gribov, 2007] Y. Gribov et al., Nucl. Fusion **47** (2007) S385.
[Gribov, 2015] Y. Gribov et al., Nucl. Fusion **55** (2015) 073021.
[Gribov, 2016] Y. Gribov, "Overview-of-operation-scenarios": https://user.iter.org/?uid=U2D9MR.
[Gribov, 2017-1] Y. Gribov, "15MA hydrogen ohmic scenario with Be and W impurities": https://user.iter.org/?uid=UHBUWT.
[Gribov, 2017-2] Y. Gribov, "DINA simulation of 15MA H ohmic scenario: 15MA H-DINA2017-01": https://user.iter.org/?uid=UG69U4
[Guillemaut, 2017] C. Guillemaut et al., Plasma Phys. Control. Fusion **59** (2017) 045001.
[Gunn, 2017] J.P. Gunn et al., Nucl. Fusion **57** (2017) 046025.
[Gunn, 2017] J.P. Gunn et al., Nucl. Mater. Energy **12** (2017) 75.
[Günter, 2003] S. Günter et al., Nucl. Fusion **43** (2003) 161.
[Hakola, 2017] A. Hakola et al., Nucl. Fusion **57** (2017) 066105.
[Harris, 1990] G.R. Harris, "Comparisons of the current decay during carbon-bounded and beryllium-bounded disruptions in JET", Rep. JET-R(90)07, JET, Abingdon (1990).
[Hawryluk, 2014] R.J. Hawryluk et al., Proc. 25th IAEA Fusion Energy Conf. (St. Petersburg, Russia, 2014) PPC/P2-33.
[Hender, 2007] T.C. Hender et al., Nucl. Fusion **47** (2007) S128.
[Hillairet, 2012] J. Hillairet et al., Fusion Eng. Des. **87** (2012) 275.
[Hillairet, 2015] J. Hillairet et al., Fusion Eng. Des. **94** (2015) 22.
[Hillesheim, 2016] J. Hillesheim et al., Proc. 26th IAEA Fusion Energy Conf. (Kyoto, Japan, 2016) EX/5-2.
[Hirai, 2018] T. Hirai et al., Fusion Eng. Des. **127** (2018) 66.
[Hobirk, 2012] J. Hobirk et al., Plasma Phys. Control. Fusion **54** (2012) 095001.
[Hogeweij, 2015] D. Hogeweij, Nucl. Fusion **55** (2015) 063031.
[Hohnle, 2011] H. Hohnle et al., Nucl. Fusion **51** (2011) 083013.
[Hollmann, 2015] E.M. Hollmann et al., Phys. Plasmas **22** (2015) 021802.
[Horacek, 2015] J. Horacek et al., J. Nucl. Mater. **463** (2015) 385.
[Horacek, 2016] J. Horacek et al., Plasma Phys. Control. Fusion **58** (2016) 074005.
[Horton, 1999] L.D. Horton et al., Nucl. Fusion **39** (1999) 17.
[Humphreys, 2006] D.A. Humphreys et al., Phys. Plasmas **13** (2006) 056113.
[Humphreys, 2015] D.A. Humphreys et al., Phys. Plasmas **22** (2015) 021806.
[Imbeaux, 2015] F. Imbeaux et al., Nucl. Fusion **55** (2015) 123006.
[Itami, 2009] K. Itami et al., J. Nucl. Mater. **390–391** (2009) 983.
[ITER Technical Basis] "ITER Technical Basis", ITER EDA Documentation Series No. 24, IAEA, Vienna 2002.
[ITER_D_2FB8AC_v1.0, 2008] ITER Research Plan (IRP-v1.0): https://user.iter.org/?uid=2FB8AC&version=v1.0.
[ITER_D_28B384, 2009] SRD-54 (LHH&CD) from DOORS: https://user.iter.org/?uid=28B384.

[ITER_D_2FB8AC_v2.2, 2009] ITER Research Plan (IRP-v2.2): https://user.iter.org/?uid=2FB8AC&version=v2.2.
[ITER_D_2LULDH, 2009] Heat and Nuclear Load Specifications v2.3: https://user.iter.org/?uid=2LULDH.
[ITER_D_2DY7NG, 2010] Project Specification v2.0: https://user.iter.org/?uid=2DY7NG.
[ITER_D_346RPL, 2010] Proposal for the Revision of the ITER Research Plan (v2.3): https://user.iter.org/?uid=346RPL&version=v1.1.
[ITER_D_6JCJ5T, 2011] Day 1-05 Physics basis for the first ITER divertor: https://user.iter.org/?uid=6JCJ5T.
[ITER_D_28WBXD, 2012] ITER RAMI ANALYSIS PROGRAM v4.3: https://user.iter.org/?uid=28WBXD.
[ITER_D_ETLLQC, 2013] Project Change Request: PCR-496 - Space reservation for EC & IC systems upgrades: https://user.iter.org/?uid=ETLLQC.
[ITER_D_KTP2H5, 2013] ITER-Research-Plan-v2-3_Appendix-F_Updated_Sep-Oct13: https://user.iter.org/?uid=KTP2H5.
[ITER_D_27ZRW8, 2014] Project Requirements v.5.3: https://user.iter.org/?uid=27ZRW8.
[ITER_D_ETJB4Q, 2014] Project Change Request: PCR-439 - Equatorial and Upper Port Plug Handling and Dogleg Configuration: https://user.iter.org/?uid=ETJB4Q.
[ITER_D_L9ABVC, 2014] PBS54 – Loads Table for EP's substantiation –Tokamak bldg. 11-L1 Walls/Ceiling: https://user.iter.org/?uid=L9ABVC.
[ITER_D_NSHUQ7, 2014] IC/STAC-16/2.3 Report on the development of the ITER Research Plan: https://user.iter.org/?uid=NSHUQ7.
[ITER_D_28B39L, 2017] SRD-55 (Diagnostics) from DOORS (approved version): https://user.iter.org/?uid=28B39L.
[ITER_D_3T6DZ9, 2015] Divertor Maintenance Scenarios v2.1: https://user.iter.org/?uid=3T6DZ9.
[ITER_D_QFF9XY, 2015] Mechanisms of ammonia formation in low-T plasmas and fusion-relevant conditions: https://user.iter.org/?uid=QFF9XY.
[ITER_D_QNDHTV, 2015] Summary of the Second Workshop on First Mirror Surface Recovery, 9 – 10 February 2015: https://user.iter.org/?uid=QNDH7V.
[ITER_D_RD59AJ, 2016] PCS Document Production Plan (RD59AJ): https://user.iter.org/?uid=RD59AJ.
[ITER_D_SN28YH, 2016] WP09-HCD-03-01 "LH4IT": https://user.iter.org/?uid=SN28YH.
[ITER_D_SNE6G8, 2016] Staged Approach Configuration PBS Level 3, v3.1 (2016): https://user.iter.org/?uid=SNE6G8.
[ITER_D_SSKMMC, 2016] Final report from the Magnetic Axis Working Group: https://user.iter.org/?uid=SSKMMC.
[ITER_D_ TFJJNH, 2016] ITER Divertor Monoblock Shaping Workshop, 13 – 15 September 2016 Presentations: https://user.iter.org/?uid=TFJJNH.
[ITER_D_T7KUNB, 2016] BIPT67 FPPC update by R. Hunt (First Plasma Protection Components): https://user.iter.org/?uid=T7KUNB.
[ITER_D_TF3RCZ, 2016] Local heat loads to be expected on plasma-facing components during the Second Plasma Phase ("Pre-Fusion Power Operation 1"): https://user.iter.org/?uid=TF3RCZ.
[ITER_D_TL5ACR, 2016] ITER Research Plan Workshop, 26 - 28 July 2016 - Presentations and Material: https://user.iter.org/?uid=TL5ACR.
[ITER_D_TL5BR3, 2016] Project Change Request: PCR-738 - Establishment of the 2016 ITER Baseline: https://user.iter.org/?uid=TL5BR3.

[ITER_D_TMT985, 2016] 5 MA H-mode helium scenario in toroidal magnetic field 1.8T (20MW of ECH during 245s of current flattop): https://user.iter.org/?uid=TMT985.

[ITER_D_TP3QQA, 2016] 5 MA/1.8T H-mode He scenario (20MW of ECH, 20kA limit on CS current, 245s of flattop): https://user.iter.org/?uid=TP3QQA.

[ITER_D_TVUZP2, 2016] PCS Physics Requirements Document for the Preliminary Design: https://user.iter.org/?uid=TVUZP2.

[ITER_D_TXQ5E8, 2016] ITER ECE operation at 1.8T: an assessment: https://user.iter.org/?uid=TXQ5E8.

[ITER_D_TVG7YK, 2017] Staged Approach Configuration - Preliminary Functional Description v1.5 (2017): https://user.iter.org/?uid=TVG7YK.

[ITER_D_TTPHKZ, 2017] MPP-M030 Presentation 3 - Capability of WAVS for detection of faulty IVT monoblocks: https://user.iter.org/?uid=TTPHKZ.

[ITER_D_UFAXKQ, 2017] Lost Alpha Monitor Workshop Summary: https://user.iter.org/?uid=UFAXKQ.

[Izzo, 2013] V.A. Izzo, Phys. Plasmas **20** (2013) 056107.

[Jackson, 2010] G.L. Jackson et al., Phys. Plasmas **51** (2010) 056116.

[Jackson, 2011] G.L. Jackson et al., Nucl. Fusion **51** (2011) 083015.

[Jeong, 2015] J.H. Jeong et al., EPJ Web of Conferences **87** (2015) 02016.

[JET Team, 1993] JET Team, Plasma Physics and Controlled Nuclear Fusion Research 1992 (Proc. 14th Int. Conf., Würzburg, 1992) Vol 1, IAEA, Vienna (1993) 429.

[Joffrin, 2005] E. Joffrin et al., Nucl. Fusion **45** (2005) 626.

[Joly, 2017] J. Joly et al., Proc. 22nd Topical Conf. on Radiofrequency Power in Plasmas (Aix-en-Provence, France, 2017) to be published.

[Jones, 2001] T.T.C. Jones et al., Proc. 28th European Physical Society Conf. on Plasma Physics (EPS) (Funchal, Portugal, 2001) ECA vol. 25A 1197.

[Kallenbach, 2010] A. Kallenbach et al., Plasma Phys. Control. Fusion **52** (2010) 055002.

[Kamada, 1994] Y. Kamada et al., Nucl. Fusion **34** (1994) 1605.

[Kavin, 2013] A.A. Kavin et al., "15MA hydrogen L-mode scenario with maximum auxiliary heating": https://user.iter.org/?uid=GNREJL.

[Kavin, 2015] A.A. Kavin et al., "3.2MA ohmic scenario with plasma current flattop 10s and minimum currents in Central Solenoid": https://user.iter.org/?uid=RSFZPQ.

[Kavin, 2016-1] A.A. Kavin et al., "7.5MA (2.65T) scenarios with different assumptions on W content (5MW of ECRF heating)": https://user.iter.org/?uid=SMV7QL.

[Kavin, 2016-2] A.A. Kavin et al., "First plasma scenario with 20 kA limit on currents in CS coils": https://user.iter.org/?uid=SNTCNG.

[Kavin, 2016-3] A.A. Kavin et al., "Duration of plasma current flattop in 7.5MA (2.65T) hydrogen scenarios with different assumptions on tungsten content (20MW of ECRF heating)": https://user.iter.org/?uid=SNTBP8.

[Kavin, 2016-4] A.A. Kavin et al., "Study of ohmic plasma initiation in toroidal magnetic field 1.8T with the transport code SCENPLINT": https://user.iter.org/?uid=T8J6UV.

[Kavin, 2016-5] A.A. Kavin et al., "Low current ohmic hydrogen scenarios (3MA & 5MA) in toroidal magnetic field 1.8T": https://user.iter.org/?uid=T8FFS9.

[Kavin, 2016-6] A.A. Kavin et al., "Study of He plasma initiation in toroidal magnetic field 1.8T with transport code SCENPLINT": https://user.iter.org/?uid=TFJCRA.

[Kavin, 2016-7] A.A. Kavin et al., "5MA/1.8T H-mode He scenario (20MW of ECH, 20kA limit on CS current, 245s of flattop)": https://user.iter.org/?uid=TP3QQA.

[Kavin, 2016-8] A.A. Kavin et al., "First plasma: study of ohmic plasma initiation in hydrogen at half toroidal magnetic field (2.65 T) with Fe limiter by the transport code SCENPLINT": https://user.iter.org/?uid=TTNNX5.

[Kavin, 2017-1] A.A. Kavin et al., "5MA/1.8T helium H-mode scenario with increased outboard plasma-wall gap (20MW of ECH, 20kA limit on CS currents)": https://user.iter.org/?uid=UD7XPF.

[Kavin, 2017-2] A.A. Kavin et al., "Study of 1st plasma initiation using SCENPLINT code with revised model of runaway electrons": https://user.iter.org/?uid=UCVKY4.

[Kazakov, 2015] Y.O. Kazakov et al., Nucl. Fusion **55** (2015) 032001.

[Kazakov, 2015] Y.O. Kazakov et al., Phys. Plasmas **22** (2015) 082511.

[Kazakov, 2016] Y.O. Kazakov et al., Bull. Am. Phys. Soc. **61** (2016) NI3.00005.

[Kessel, 2007] C.E. Kessel et al., Nucl. Fusion **47** (2007) 1274.

[Kessel, 2015] C.E. Kessel et al., Nucl. Fusion **55** (2015) 063038.

[Khayrutdinov, 1993] R.R. Khayrutdinov and V.E. Lukash, Jour. Comp. Physics **107** (1993) 106.

[Kim, 2012-1] H-T. Kim et al., Nucl. Fusion **52** (2012) 103016.

[Kim, 2012-2] S-H. Kim, Nucl. Fusion **52** (2012) 074002.

[Kim, 2013-1] H-T. Kim et al., Plasma Phys. Control. Fusion **55** (2013) 124032.

[Kim, 2013-2] S-H Kim et al., Proc. 7th IAEA-TM on Steady-State Operation (Aix-en-Provence, France, 2013) O8.

[Kim, 2014] D. Kim et al., Phys. Plasmas **21** (2014) 061503.

[Kim, 2015] D. Kim, "Real-Time Control of Sawteeth and NTMs in TCV and ITER", EPFL Thesis No.6539. (2015).

[Kim, 2016] S.H. Kim et al., Proc. 26th IAEA Fusion Energy Conf. (Kyoto, Japan, 2016) TH/P2-22.

[Kim, 2017] S.H. Kim et al., Nucl. Fusion **57** (2017) 086021.

[Klimov, 2009] N. Klimov et al., J. Nucl. Mater. **390-391** (2009) 721.

[Kocan, 2015] M. Kocan et al., J. Nucl. Mater. **463** (2015) 709.

[Kocan, 2015] M. Kocan et al., Nucl. Fusion **55** (2015) 033019.

[Köchl, 2014] F. Köchl et al., Proc. 25th IAEA Fusion Energy Conf. (St. Petersburg, Russia, 2014) TH/P3-24.

[Köchl, 2016] F. Köchl et al., Proc. 26th IAEA Fusion Energy Conf. (Kyoto, Japan, 2016) EX/P6-15.

[Kogut, 2015] D. Kogut et al., Plasma Phys. Control. Fusion **57** (2015) 025009.

[Kogut, 2016] D. Kogut et al., Phys. Scr. **T167** (2016) 014062.

[Kolesnikov, 2013] R.A. Kolesnikov et al., Nucl. Fusion **53** (2013) 083021.

[Kovari, 2018] M. Kovari et al., Nucl. Fusion **58** (2018) 026010.

[Krieger, 2013] K. Krieger et al., J. Nucl. Mater. **438** (2013) S262.

[Kukushkin, 2003] A.S. Kukushkin et al., Nucl. Fusion **43** (2003) 716.

[Kukushkin, 2011] A.S. Kukushkin et al., Fusion Eng. Des. **86** (2011) 2865.

[Kukushkin, 2013-1] A.S. Kukushkin et al., J. Nucl. Mater. **438** (2013) S203.

[Kukushkin, 2013-2] A.S. Kukushkin et al., Nucl. Fusion **53** (2013) 123024.
[Kurki-Suonio, 2017] T. Kurki-Suonio et al., Plasma Phys. Control. Fusion **59** (2017) 014013.
[Kwon, 2011] M. Kwon et al., Nucl. Fusion **51** (2011) 094006.
[La Haye, 1992] R.J. La Haye et al., Nucl. Fusion **32** (1992) 2119.
[La Haye, 2002] R.J. La Haye et al., Phys. Plasmas **9** (2002) 2051.
[La Haye, 2005] R.J. La Haye et al., Nucl. Fusion **45** (2005) L37.
[La Haye, 2006] R.J. La Haye et al., Nucl. Fusion **46** (2006) 451.
[La Haye, 2009] R.J. La Haye et al., Nucl. Fusion **49** (2009) 045005.
[Lanctot, 2017] M J. Lanctot et al., Nucl. Fusion **57** (2017) 036004.
[Lang, 2003] P.T. Lang et al., Nucl. Fusion **43** (2003) 1110.
[Lang, 2004] P.T. Lang et al., Nucl. Fusion **44** (2004) 665.
[Lang, 2011] P.T. Lang et al., Nucl. Fusion **51** (2011) 033010.
[Lang, 2013] P.T. Lang et al., Nucl. Fusion **53** (2013) 073010.
[Lauber, 2015] P. Lauber, Plasma Phys. Control. Fusion **57** (2015) 054011.
[Lauret, 2012] M. Lauret et al., Nucl. Fusion **52** (2012) 062002.
[Lehnen, 2015-1] M. Lehnen et al., J. Nucl. Mater. **463** (2015) 39.
[Lehnen, 2015-2] M. Lehnen et al., Nucl. Fusion **55** (2015) 123027.
[Lehnen, 2016] M. Lehnen et al., Proc. 26th IAEA Fusion Energy Conf. (Kyoto, Japan, 2016) EX/P6-39.
[Lennholm, 2009-1] M. Lennholm et al., Phys. Rev. Lett. **102** (2009) 115004.
[Lennholm, 2009-2] M. Lennholm et al., Fusion Sci. Technol. **55** (2009) 45.
[Lennholm, 2011] M. Lennholm et al., Nucl. Fusion **51** (2011) 073032.
[Lerche, 2015-1] E. Lerche et al., AIP Conference proceedings, **1689** (2015) 040003.
[Lerche, 2015-2] E. Lerche et al., J. Nucl. Mater. **463** (2015) 634.
[Lisgo, 2014] S. Lisgo et al., "Material migration, tritium retention and dust formation in ITER", ITER Workshop on Erosion/Deposition/Dust/Tritium Diagnostics, February 2014: https://user.iter.org/?uid=MBRTGQ.
[Litaudon, 2006] X. Litaudon, Plasma Phys. Control. Fusion **48** (2006) A1.
[Litaudon, 2017] X. Litaudon et al., Nucl. Fusion **57** (2017) 102001.
[Liu, 2009] Y.Q. Liu et al., Nucl. Fusion **49** (2009) 035004.
[Loarte, 2000] A. Loarte et al., Contrib. Plasma Phys. **40** (2000) 508.
[Loarte, 2003] A. Loarte et al., Plasma Phys. Control. Fusion **45** (2003) 1549.
[Loarte, 2008] A. Loarte et al., 22nd IAEA Fusion Energy Conf. (Geneva, Switzerland, 2008) IT/P6-13.
[Loarte, 2010] A. Loarte et al., 24th IAEA Fusion Energy Conf. (San Diego, USA, 2012) ITR/1-4.
[Loarte, 2011] A. Loarte et al., Phys. Plasmas **18** (2011) 056105.
[Loarte, 2014] A. Loarte et al., Nucl. Fusion **54** (2014) 033007.
[Loarte, 2015] A. Loarte et al., Phys. Plasmas **22** (2015) 056117.
[Loarte, 2016-1] A. Loarte et al., "Evaluation of neutron power production in ITER from initial DD operation to DT2", March 2016: https://user.iter.org/?uid=PAT5T8.
[Loarte, 2016-2] A. Loarte et al., Proc. 26th IAEA Fusion Energy Conf. (Kyoto, Japan, 2016) PPC/2-1.
[Loewenhoff, 2011] T. Loewenhoff et al., Phys. Scr. **T145** (2011) 014057.
[Lu, 2014] G.H. Lu et al., Nucl. Fusion **54** (2014) 086001.
[Luce, 2003] T.C. Luce et al., Nucl. Fusion **43** (2003) 321.
[Luce, 2014] T.C. Luce et al., Nucl. Fusion **54** (2014) 013015.

[Luxon, 2003] J.L. Luxon et al., Nucl. Fusion **43** (2003) 1813.
[Lyssoivan, 2012] A. Lyssoivan et al., Plasma Phys. Control. Fusion **54** (2012) 074014.
[Ma, 2012] Y. Ma et al., Nucl. Fusion **52** (2012) 23010.
[Maddison, 2011] G.P. Maddison et al., Nucl. Fusion **51** (2011) 082001.
[Maget, 2013] P. Maget et al., Nucl. Fusion **53** (2013) 093011.
[Maggi, 2012] C.F. Maggi et al., Proc. 39th European Physical Society Conf. on Plasma Physics (EPS) (Stockholm, Sweden, 2012) vol. 36F ECA O3-108.
[Maggi, 2014] C.F. Maggi et al., Nucl. Fusion **54** (2014) 023007.
[Maingi, 2010] R. Maingi et al., Phys. Rev. Lett. **105** (2010) 135004.
[Mansfield, 2012] D. Mansfield et al., Proc. 24th IAEA Fusion Energy Conf. (San Diego, USA, 2012) PD/8-15.
[Maraschek, 2007] M. Maraschek et al., Phys. Rev. Lett. **98** (2007) 025005.
[Martin, 2008] Y.R. Martin et al., J. of Phys. Conf. Series **123** (2008) 012033.
[Martín-Solís, 2017] J.R. Martín-Solís et al., Nucl. Fusion **57** (2017) 066025.
[Maruyama, 2015] S. Maruyama et al., IEEE 26th Symposium on Fusion Engineering (SOFE) (Austin, USA, 2015), DOI: 10.1109/SOFE.2015.7482363.
[Matthews, 2016] G.F. Matthews et al., Phys. Scr. **T167** (2016) 014070.
[Mayoral, 2004] M-L. Mayoral et al., Phys. Plasmas **11** (2004) 2607.
[McDonald, 2004] D.C. McDonald et al., Plasma Phys. Control. Fusion **46** (2004) 519.
[McDonald, 2010] D.C. McDonald et al., Proc. 23rd IAEA Fusion Energy Conf. (Daejeon, Korea, 2010) EXC/2-4Rb.
[McKee, 2009] G.R. McKee et al., Nucl. Fusion **49** (2009) 115016.
[Merola, 2014] M. Merola et al., Fusion Eng. Des. **89** (2014) 890.
[Mertens, 2009] Ph. Mertens et al., Fusion Eng. Des. **84** (2009) 1289.
[Mikhailovskii, 1997] A.B. Mikhailovskii et al., Plasma Physics Reports **23** (1997) 844.
[Militello-Asp, 2016] E. Militello-Asp et al., Proc. 26th IAEA Fusion Energy Conf. (Kyoto, Japan, 2016) TH/P2-23.
[Mitchell, 2016] N. Mitchell et al., "1.8T Operation of the TF Coils with 5MA and 3MA plasma scenarios": https://user.iter.org/?uid=TRUJUN.
[Mitteau, 2011] R. Mitteau et al., J. Nucl. Mater. **415** (2011) S969.
[Mitteau, 2015] R. Mitteau et al., J. Nucl. Mater. **463** (2015) 411.
[Miyamoto, 2011] M. Miyamoto et al., J. Nucl. Mater. **415** (2011) S657.
[Morris, 1992] A.W. Morris, Plasma Phys. Control. Fusion **34** (1992) 1871.
[Motojima, 2015] O. Motojima, Nucl. Fusion **55** (2015) 104023.
[Mück, 2005] A. Mück et al., Plasma Phys. Control. Fusion **47** (2005) 1633.
[Murakami, 2011] M. Murakami et al., Nucl. Fusion **51** (2011) 103006.
[Nagasaki, 2003] K. Nagasaki et al., Nucl. Fusion **43** (2003) L7.
[Nazikian, 1997] R. Nazikian et al., Phys. Rev. Lett. **78** (1997) 2976.
[Neu, 2013] R. Neu et al., J. Nucl. Mater. **438** (2013) S34.
[Neuwirth, 2012] D. Neuwirth et al., Plasma Phys. Control. Fusion **54** (2012) 085008.
[Noterdaeme, 2003] J-M. Noterdaeme et al., Nucl. Fusion **43** (2003) 202.
[Nunes, 2012] I. Nunes et al., Proc. 24th IAEA Fusion Energy Conf. (San Diego, USA, 2012) FT/P2-1Rb.
[Okabayashi, 2001] M. Okabayashi et al., Phys. Plasmas **8** (2001) 2071.
[Okabayashi, 2005] M. Okabayashi et al., Nucl. Fusion **45** (2005) 1715.
[Pacher, 2015] H.D. Pacher et al., J. Nucl. Mater. **463** (2015) 591.
[Paley, 2009] J.I. Paley et al., Plasma Phys. Control. Fusion **51** (2009) 055010.
[Panayotis, 2017] S. Panayotis et al., Fusion Eng. Des. **125** (2017) 256.

[Parail, 2009] V. Parail et al., Nucl. Fusion **49** (2009) 075030.

[Parail, 2013] V. Parail et al., Nucl. Fusion **53** (2013) 113002.

[Park, 2007] J-K. Park et al., Phys. Rev. Lett. **99** (2007) 195003.

[Park, 2008] J-K. Park et al., Nucl. Fusion **48** (2008) 045006.

[Park, 2017] J-K. Park et al., "Assessment of Error Field Correction Criteria for ITER": https://user.iter.org/?uid=UMLSUW.

[Park, 2013] S. Park et al., Fusion Sci. Technol. **63** (2013) 49.

[Paul, 2016] E. Paul et al., Proc. 58th Meet. American Physical Society Division of Plasma Physics (APS) (San Jose, USA, 2016) BP10.063.

[Pautasso, 2016] G. Pautasso et al., Proc. 26th IAEA Fusion Energy Conf. (Kyoto, Japan, 2016) EX/P6-38.

[Paz-Soldan, 2014] C. Paz-Soldan et al., Nucl. Fusion **54** (2014) 073013.

[Pereverzev, 2002] G.V. Pereverzev et al., "ASTRA automated system for transport analysis", IPP-Report IPP 5/98 (2002).

[Philipps, 2014] V. Philipps et al., "Summary of ITER Workshop on Erosion/Deposition/Dust/Tritium Diagnostics", February 2014: https://user.iter.org/?uid=NEE8HV.

[Pinches, 2015] S.D. Pinches et al., Phys. Plasmas **22** (2015) 021807.

[Pinches, 2016] S.D. Pinches et al., Proc. 26th IAEA Fusion Energy Conf. (Kyoto, Japan, 2016) TH/P2-14.

[Pintsuk, 2016] G. Pintsuk et al., Phys. Scr. **T167** (2016) 014056.

[Pitts, 1997] R.A. Pitts et al., J. Nucl. Mater. **241-243** (1997) 867.

[Pitts, 2003] R.A. Pitts et al., J. Nucl. Mater. **313-316** (2003) 777.

[Pitts, 2011] R.A. Pitts et al., J. Nucl. Mater. **415** (2011) S957.

[Pitts, 2013] R.A. Pitts et al., J. Nucl. Mater. **438** (2013) S48.

[Pitts, 2015] R.A. Pitts et al., "The ITER divertor concept: physics and engineering design": https://user.iter.org/?uid=RF2HCM).

[Pitts, 2016] R.A. Pitts, "Introduction to ITER first plasma": https://user.iter.org/uid=U39LSW.

[Pitts, 2017] R.A. Pitts et al., Nucl. Mater. Energy **12** (2017) 60.

[Polevoi, 2010] A.R. Polevoi et al., Proc. 37th European Physical Society Conf. on Plasma Physics (EPS) (Dublin, Ireland, 2010) vol. 34A ECA P2.187.

[Polevoi, 2012] A.R. Polevoi et al., Proc. 39th European Physical Society Conf. on Plasma Physics (EPS) (Stockholm, Sweden, 2012) vol. 36F ECA P4.032.

[Polevoi, 2013] A.R. Polevoi et al., Nucl. Fusion **53** (2013) 123026.

[Polevoi, 2015] A.R. Polevoi et al., Nucl. Fusion **55** (2015) 063019.

[Polevoi, 2016] A.R. Polevoi et al., Proc. 26th IAEA Fusion Energy Conf. (Kyoto, Japan, 2016) EX/P6-44.

[Polevoi, 2017] A.R. Polevoi et al., Nucl. Fusion **57** (2017) 022014.

[Poli, 2012] F.M. Poli et al., Nucl. Fusion **52** (2012) 063027.

[Prater, 2007] R. Prater et al., Nucl. Fusion **47** (2007) 371.

[Rapson, 2014] C. Rapson et al., Fusion Eng. Des. **89** (2014) 568.

[Raupp, 2017] G. Raupp et al., Fusion Eng. Des. **123** (2017) 541.

[Ravensbergen, 2015] T. Ravensbergen et al., Proc. 43rd European Physical Society Conf. on Plasma Physics (EPS) (Leuven, Belgium, 2015) vol. 40A ECA P4.068.

[Rebhan, 1997] E. Rebhan and U. Vieth, Nucl. Fusion **37** (1997) 251.

[Reich, 2012] M. Reich et al., Fusion Sci. Technol. **61** (2012) 309.

[Reimerdes, 2007] H. Reimerdes et al., Plasma Phys. Control. Fusion **49** (2007) B349.

[Reux, 2015] C. Reux et al., Nucl. Fusion **55** (2015) 093013.
[Rice, 2002] J.E. Rice et al., Nucl. Fusion **42** (2002) 510.
[Righi, 1999] E. Righi et al., Nucl. Fusion **39** (1999) 309.
[Rognlien, 2004] T.D. Rognlien et al., Contrib. Plasma Phys. **44** (2004) 188.
[Romanelli, 2015] M. Romanelli et al., Nucl. Fusion **55** (2015) 093008.
[Ryter, 2002] F. Ryter et al., Plasma Phys. Control. Fusion **44** (2002) A407.
[Ryter, 2009] F. Ryter et al., Nucl. Fusion **49** (2009) 062003.
[Ryter, 2013] F. Ryter et al., Nucl. Fusion **53** (2013) 113003.
[Ryter, 2014] F. Ryter et al., Nucl. Fusion **54** (2014) 083003.
[Sabbagh, 2004] S.A. Sabbagh et al., Nucl. Fusion **44** (2004) 560.
[Sabbagh, 2006] S.A. Sabbagh et al., Phys. Rev. Lett. **97** (2006) 045004.
[Sabbagh, 2010-1] S.A. Sabbagh et al., Nucl. Fusion **50** (2010) 025020.
[Sabbagh, 2010-2] S.A. Sabbagh et al., Proc. 23rd IAEA Fusion Energy Conf. (Daejeon, Korea, 2010) EXS/5-5.
[Sabbagh, 2011] S.A. Sabbagh et al., Proc. 38th European Physical Society Conf. on Plasma Physics (EPS) (Strasbourg, France, 2011) vol. 35G ECA P5.104.
[Sabbagh, 2013] S.A. Sabbagh et al., Nucl. Fusion **53** (2013) 104007.
[Sabbagh, 2016] S.A. Sabbagh et al., Proc. 26th IAEA Fusion Energy Conf. (Kyoto, Japan, 2016) EX/P4-33.
[Saibene, 2007] G. Saibene et al., Nucl. Fusion **47** (2007) 969.
[Saibene, 2008] G. Saibene et al., Proc. 22nd IAEA Fusion Energy Conf. (Geneva, Switzerland, 2008) EX/2-1.
[Sauter, 2002-1] O. Sauter et al., Plasma Phys. Control. Fusion **44** (2002) 1999.
[Sauter, 2002-2] O. Sauter et al., Phys. Rev. Lett. **88** (2002) 105001.
[Sauter, 2010] O. Sauter et al., Plasma Phys. Control. Fusion **52** (2010) 025002.
[Schmid, 2015] K. Schmid et al., Nucl. Fusion **55** (2015) 053015.
[Schmitz, 2016] O. Schmitz et al., Nucl. Fusion **56** (2016) 066008.
[Schneider, 2016] M. Schneider et al., "Integrated scenario modelling with METIS in IMAS, with a slight glance to available ICRH schemes": https://user.iter.org/?uid=TH5SDS.
[Schneider, 2017-1] M. Schneider et al., "H&CD scenarios for each operational phase of the IRP within the 4-stage approach" (scenario table): https://user.iter.org/?uid=UG4UCX.
[Schneider, 2017-2] M. Schneider et al., "The case for outer midplane gas injection in the vicinity of the ITER ICRF antennas": https://user.iter.org/?uid=V2QFQ3
[Scoville, 2003] J.T. Scoville et al., Nucl. Fusion **43** (2003) 250.
[Shaing, 2015] K.C. Shaing et al., Nucl. Fusion **55** (2015) 125001.
[Sharapov, 1999] S.E. Sharapov et al., Nucl. Fusion **39** (1999) 373.
[Shimada, 2011] M. Shimada and R.A. Pitts, J. Nucl. Mater. **415** (2011) S1013.
[Shimomura, 2007] K. Shimomura et al., Fusion Eng. Des. **82** (2007) 953.
[Shinohara, 2006] K. Shinohara et al., Proc. 21st IAEA Fusion Energy Conf. (Chengdu, China, 2006) FT/P5-32.
[Shiraki, 2015] D. Shiraki et al., Nucl. Fusion **55** (2015) 073029.
[Sieglin, 2015] B. Sieglin et al., Rev. Sci. Instr. **86** (2015) 113502.
[Sieglin, 2016] B. Sieglin et al., Plasma Phys. Control. Fusion **58** (2016) 055015.
[Singh, 2017] M. Singh et al., New J. Phys. **19** (2017) 055004.
[Sips, 2009] A.C.C. Sips et al., Nucl. Fusion **49** (2009) 085015.

[Sips, 2017] A.C.C. Sips, "Plasma breakdown at low loop voltage", ITPA Integrated Operation Scenarios TG Meeting, (Frascati, Italy, October 2017).

[Snipes, 2010] J.A. Snipes et al., Proc. 37th European Physical Society Conf. on Plasma Physics (EPS) (Dublin, Ireland, 2010) vol. 34A ECA P1.1093.

[Snipes, 2016-1] J.A. Snipes, "Plasma scenarios and Plasma Control Program": https://user.iter.org/?uid=T6XTTN

[Snipes, 2016-2] J.A. Snipes et al., "Plasma Control State-of-the-art and R&D Plan for the Preliminary Design": https://user.iter.org/?uid=TX2FY8.

[Snyder, 2011] P.B. Snyder et al., Nucl. Fusion **51** (2011) 103016.

[Söldner, 1999] F.X. Söldner et al., Nucl. Fusion **39** (1999) 407.

[Sommer, 2015] F. Sommer et al., Nucl. Fusion **55** (2015) 033006.

[Stacey, 2016] W.M. Stacey et al., Phys. Plasmas **23** (2016) 012508.

[Staebler, 2005] A. Staebler et al., Nucl. Fusion **45** (2005) 617.

[Stober, 2011] J. Stober et al., Nucl. Fusion **51** (2011) 083031.

[Suttrop, 2011-1] W. Suttrop et al., Phys. Rev. Lett. **106** (2011) 225004.

[Suttrop, 2011-2] W. Suttrop et al., Plasma Phys. Control. Fusion **53** (2011) 124014.

[Sytova, 2018] E. Sytova et al., Contrib. Plasma Physics in press (2018): https://doi.org/10.1002/ctpp.201700135.

[Takizuka, 2004] T. Takizuka et al., Plasma Phys. Control. Fusion **46** (2004) 227.

[Takizuka, 2017] T. Takizuka, Plasma Phys. Control. Fusion **59** (2017) 034008.

[Tobita, 1995] K. Tobita et al., Nucl. Fusion **35** (1995) 12.

[Treutterer, 2017] W. Treutterer et al., Fusion Eng. Des. **115** (2017) 33.

[Urano, 2006] H. Urano et al., Plasma Phys. Control. Fusion **48** (2016) A193.

[Urano, 2011] H. Urano et al., Nucl. Fusion **51** (2011) 113004.

[Urano, 2016] H. Urano et al., Proc. 26th IAEA Fusion Energy Conf. (Kyoto, Japan, 2016) EX/3-4.

[van den Brand, 2012] H. van den Brand et al., Plasma Phys. Control. Fusion **54** (2012) 094003.

[van den Brand, 2013] H. van den Brand et al., Nucl. Fusion **53** (2013) 013005.

[Van Zeeland, 2009] M.A. Van Zeeland et al., Nucl. Fusion **49** (2009) 065003.

[Van Zeeland, 2016] M.A. Van Zeeland et al., Nucl. Fusion **56** (2016) 112007.

[Voitsekhovitch, 2010] I. Voitsekhovitch et al., Plasma Phys. Control. Fusion **52** (2010) 105011.

[von Hellerman, 2017] M. von Hellerman, "Loose Ends in Fast Ion CXRS Modelling Issues", ITPA Energetic Particles TG Meeting (Seville, Spain, April 2017).

[Wagner, 2010] F. Wagner et al., Plasma Phys. Control. Fusion **52** (2010) 124044.

[West, 2009] W.P. West et al., J. Nucl. Mater. **390-391** (2009) 461.

[Wiesen, 2017] S. Wiesen et al., Nucl. Mater. Energy **12** (2017) 3.

[Wirtz, 2017] M. Wirtz et al., Nucl. Mater. Energy **12** (2017) 148.

[Wischmeier, 2003] M. Wischmeier et al., J. Nucl. Mater. **313-316** (2003) 980.

[Witvoet, 2011] G. Witvoet et al., Nucl. Fusion **51** (2011) 103043.

[Wolfe, 2005] S.M. Wolfe et al., Phys. Plasmas **12** (2005) 056110.

[Wolf, 2003] R.C. Wolf et al., Plasma Phys. Control. Fusion **45** (2003) R1.

[Wynn, 2018] A. Wynn et al., Nucl. Fusion in press (2018).

[Yoshida, 2005] N. Yoshida et al., J. Nucl. Mater. **337-339** (2005) 946.

[Zhu, 2006] W. Zhu et al., Phys. Rev. Lett. **96** (2006) 225002.

[Zohm, 2007] H. Zohm et al., Nucl. Fusion **47** (2007) 228.

Appendix A: Use of Deuterium Seeding to Characterize Fuel Retention during PFPO-2 Phase

The possibility of limited operation in deuterium during the non-active phases, or of 'deuterium spiking' in hydrogen discharges, has been discussed in earlier versions of the ITER Research Plan (in **Appendix D** of the IRP-v1 [ITER_D_2FB8AC_v1.0, 2008], **Appendix C** of the IRP-v2.2 [ITER_D_2FB8AC_v2.2, 2009] and **Appendix C** of the IRP-v2.3 [ITER_D_346RPL, 2010]). With the development of the new baseline schedule, the decision in 2011 to eliminate the CFC-tungsten first divertor and the improved understanding and modelling of retention processes in a beryllium-tungsten environment afforded by the ILW experiments on JET, the justification for an early look at retention before deuterium operations begin has not diminished. This Appendix therefore takes a new and more quantitative look at a possible deuterium spiking scenario which would allow early assessment of fuel retention levels and efficiency of fuel recovery, testing of dedicated retention diagnostics in advance of nuclear operation and calibration of migration/retention models. Such an experiment may also provide sufficient D outflux for testing of hydrogenic permeation into TBMs in support of the assessment of tritium permeation rates during FPO. Detailed calculations of the feasibility of this latter measurement have yet to be made. The example plasma scenario considered here can be used as a basis and modified at a later stage depending on the outcome of such calculations.

The case chosen is a hydrogen L-mode which would be executed in PFPO-2 at 7.5 MA/2.65 T using hydrogen neutral beams and ECRH power. The rationale for choosing L-mode is the following:

1. Lower required heating power provides increased guarantee that the discharge can be executed reliably and repeatedly (a prerequisite if the scenario is to be used for retention studies);
2. Higher quantities of deuterium gas injection permit to maximize D/H ratio for retention/permeation studies (SOL less opaque);
3. Lower confinement, reducing fusion reactions and hence lower neutronic activation (DD neutrons) and low triton production;
4. More stable conditions, avoiding difficulties of ELMy H-modes and staying away from operational boundaries (disruptions).

The experiment, should it go ahead, would be programmed at the end of PFPO-2, benefitting from the fact that stable, long-pulse L-mode discharges should be well established at this point. Moreover, the proposed discharges are intended to provide sufficient material migration for meaningful beryllium deposits to grow in the divertor under well controlled conditions. If, as proposed, one or more divertor cassettes can be removed following the experiment for post-mortem analysis of long-term retention (to complement global gas balance), this will only be possible if the experiment occurs at the beginning of the pre-nuclear shutdown.

To assess the target discharge, and provide input to further modelling specific to plasma-wall interactions, analysis has been performed using a crude iterative process deploying 1.5-D transport modelling with the ASTRA code for the plasma core and the SOLPS-ITER plasma boundary code whose output is used to provide a complete plasma background solution for subsequent migration calculations in support of fuel retention predictions.

The ASTRA simulations use the framework described in [Polevoi, 2017], based on the analysis in [Pacher, 2015], in which scalings for key SOL and divertor parameters derived from a database of

SOLPS-4.3 simulations targeting the baseline burning plasma scenario are used to provide boundary conditions for the core transport model: separatrix values of T_e, T_i, n_e, n_{He}, n_{DT}, the ionization source from edge neutrals into the core plasma consistent with the power and particle fluxes into the SOL and the SOL gas puff strength required to maintain the divertor peak power flux density at tolerable levels). ASTRA simulates heat and particle transport in the core according to scaling-based models with prescribed profiles for heat diffusivities (assuming $\chi_{\perp e} = \chi_{\perp i}$) and the empirical relationship $D_\perp = C\chi_\perp$ with C = 0.2 (see section 2 of [Polevoi, 2017]). It contains models for pellet ablation and, using the SOLPS boundary scalings, is able to account for SOL opacity and thus select an appropriate balance of core (pellet) and edge (gas) fuelling to satisfy a given prescription on divertor neutral pressure for given P_{SOL}.

A problem with the approach is that the boundary parameterization derived from the SOLPS-4.3 database applies to a specific (burning plasma) operating space: H-mode like SOL transport ($D_{\perp,0}$ = 0.3 m^2s^{-1}, $\chi_{\perp,0}$ = 1.0 m^2s^{-1}) with 60 < P_{SOL} < 140 MW (the implicit assumption is that this will be at I_p = 15 MA). These transport coefficients lead to near SOL power channel widths of $\lambda_{q,0}$ ~ 3-4 mm in the SOLPS simulations (see Appendix C).

Applying these boundary conditions to a core transport calculation for a lower power L-mode at lower I_p will not capture the wider SOL resulting from higher L-mode transport and thus will not correctly describe the SOL opacity (neutral penetration and thus the core ionization source). To compensate approximately for this, an adjustment has been made (see below) to the coefficient multiplying P_{SOL} in the scalings, representing an effective increase in the upstream power width by a factor $f_q = (\chi_\perp/\chi_{\perp 0})^{1/2}(15/I_p)$, where $\chi_\perp$ is the value fitted in the scaling-based model used in ASTRA for the core transport simulation to reproduce the L-mode scaling for the energy confinement time. The degree to which the low power ASTRA simulation output is consistent can then be checked by running a single SOLPS-ITER case with the same fuel throughput, pumping speed, P_{SOL}, split between edge and core fuelling, and using the separatrix values of $D_\perp$ and $\chi_\perp$ computed by ASTRA.

The case chosen for the ASTRA study has the following key parameters:

I_p = 7.5 MA, B_t = 2.65 T (q_{95} = 3), P_{IN} = 30 MW, f_d = 0.375

P_{IN} the total auxiliary power, chosen to remain below the L-H transition threshold for a hydrogen plasma at 2.65 T. It is comprised of P_{ECRH} = 20 MW, P_{HNB} = 10 MW, provided by reducing the (hydrogen) beam energy to 500 keV. Factor $f_d \propto (G_{tot}/S_{pump})^{0.83}(P_{SOL}/f_q)^{-0.52}$ is the desired 'detachment parameter', equivalent to the normalized divertor neutral pressure μ in (see eqn. (1) in [Pacher, 2017]) and is a measure of the degree of detachment (f_d = 1 corresponds to the point at which the total ion flux at the divertor target falls to 80% of its maximum value as divertor neutral pressure, p_n increases). Here, G_{tot} is the total fuel throughput (including H and D) and S_{pump} is the pumping speed. An existing SOLPS-4.3 simulation at P_{SOL}= 40 MW, G_{tot} = 96 Pam^3s^{-1}, $D_{\perp,0}$ = 0.3 m^2s^{-1}, $\chi_{\perp,0}$ = 1.0 m^2s^{-1}, p_n = 3.1 Pa, S_{pump} = 31 m^3s^{-1} (about 50% of the maximum available on ITER) is used to fix f_d at the chosen value, representing a divertor plasma far from strong detachment.

Deuterium is assumed to be provided only as gas from the edge, whilst hydrogen can be puffed from the edge and/or introduced into the core using high field side pellet injection. For the chosen f_d, the SOLPS parameterization (modified for L-mode transport) provides ASTRA with the edge gas puff strength required to maintain the desired degree of detachment, $n_{e,sep}$, $T_{e,sep}$, $T_{i,sep}$ and G_{sep}, the core ionization source due to the neutral influx at the separatrix. The remainder of G_{tot} is provided by HFS pellets at the level required to maintain the core density above the beam shine-

through limit (~3×10^{19} m^{-3} for 500 keV H^0). Two ASTRA code runs have been made with these input parameters assuming that D constitutes 10% and 100% of the input gas puff.

The most important output parameters from these first stage simulations are summarized below:

$n_{sep} = 1.15\times10^{19}$ m^{-3}, $T_{e,sep} = 66$ eV, $T_{i,sep} = 101$ eV

$P_{SOL} = P_{IN} + P_{\Omega} - P_{RAD} = 30 + 3.13 - 1.76 = 31.4$ MW

$n_{e,avge} = 3.2\times10^{19}$ m^{-3}, $n_{e,0} = 3.5\times10^{19}$ m^{-3} (Greenwald fraction = 0.52)

$T_{e,0} = 4.6$ keV, $T_{i,0} = 4.1$ keV

Total core ionization source (coming from SOL gas puff) = 14 Pam^3s^{-1}

Core fuelling (HFS pellets) = 53 Pam^3s^{-1}, edge gas puffing = 30 Pam^3s^{-1} (G_{tot} = 83 Pam^3s^{-1})

$D_{\perp,sep} = 1.0$ m^2s^{-1}, $\chi_{\perp,sep} = 6.0$ m^2s^{-1} (thus $f_q = 4.9$)

Triton production rate = 3.6×10^{11} s^{-1} (10% D in gas puff), 3.9×10^{13} s^{-1} (100% D in gas puff)

Triton burn-up fraction < 2%

$n_D/n_H = 0.014$ (10% D in gas puff), $n_D/n_H = 0.134$ (100% D in gas puff)

Maximum possible flat-top duration ~100 s

$q_{pk} = 0.39$ MWm^{-2} (peak divertor power flux density obtained from the boundary parameterization).

The calculated L-H transition threshold power for these conditions is $P_{LH} = 44.4$ MW, well above P_{SOL}. Recent results from a pure hydrogen campaign in the ILW environment [Litaudon, 2017] indicate that the maximum core D concentrations found in this ITER D-spiking study (~13%) may be marginal with respect to reducing P_{LH} and pushing this L-mode discharge closer to the H-mode threshold. If this were problematic, operation at higher B_t could be considered to move away again from the threshold.

At these DD fusion rates, the total tritium production is ~1.8×10^{-4} μg /100 s pulse for 10% D in the edge gas puff. For 100% D gas puffing, the production rate increases by ~100 due simply to the order of magnitude increase in the core D concentration ($\propto n_D^2$). A proposed migration/retention experiment aiming for, say, 20,000 s of reproducible L-mode plasma with maximum D concentration would thus require 200 such pulses, requiring ~2 weeks of machine time (13 pulses/day) and producing at most ~ 3.6×10^{-2} μg and a total DD neutron production (2.45 MeV) of ~ 7.2×10^{15} (assuming 50% probability for the two DD fusion reaction branches: D+D → T+p and D+D → ^{3}He + n).

This tritium production for the proposed 10% D-spiked retention/migration experiment is about twice the 2×10^{-2} μg estimated as the maximum quantity which could be produced throughout the non-active phases using hydrogen plasmas due to the natural concentration (~0.015%) of D in H. It is orders of magnitude lower than the maximum quantity of tritium which can be discharged annually without a functioning tritium plant in ITER. The resulting vessel activation needs to be assessed and this has not been performed here. The arguments demonstrating acceptable activation in *Tritium production and activation for the hydrogen phase* will not apply, since the spiking experiment would be performed in a short, concentrated period, though the levels will still be extremely low given the very low neutron production from these low performance L-modes.

To provide a boundary plasma suitable for material migration studies and to check consistency with the ASTRA run based on boundary parameterization, a SOLPS-ITER simulation has been performed using some of the ASTRA output to determine the key input parameters:

P_{SOL} = 31.4 MW, $D_\perp$ = 1.0 m^2s^{-1}, $\chi_{\perp,}$ = 6.0 m^2s^{-1}, edge gas puff = 30 Pam^3s^{-1}, outflux to the inner core boundary = 53 Pam^3s^{-1}.

The simulation has been run in the first instance with pure H and all-metal walls (but no W sputtering switched on), though SOLPS-ITER can deal with mixed hydrogenic species. The standard reference magnetic equilibrium at q_{95} = 3 (~9 cm outboard midplane separation between first and second separatrix) has been used to generate a numerical grid, even though for a dedicated future material migration/gas balance experiment a more optimized plasma shape would likely be chosen. An existing converged solution at higher density was used to start the simulation, but with density scaled down such that $n_{e,sep} \sim 1.0\times10^{19}$ m^{-3}, close to the ASTRA output value (see above). Fluid drifts are deactivated.

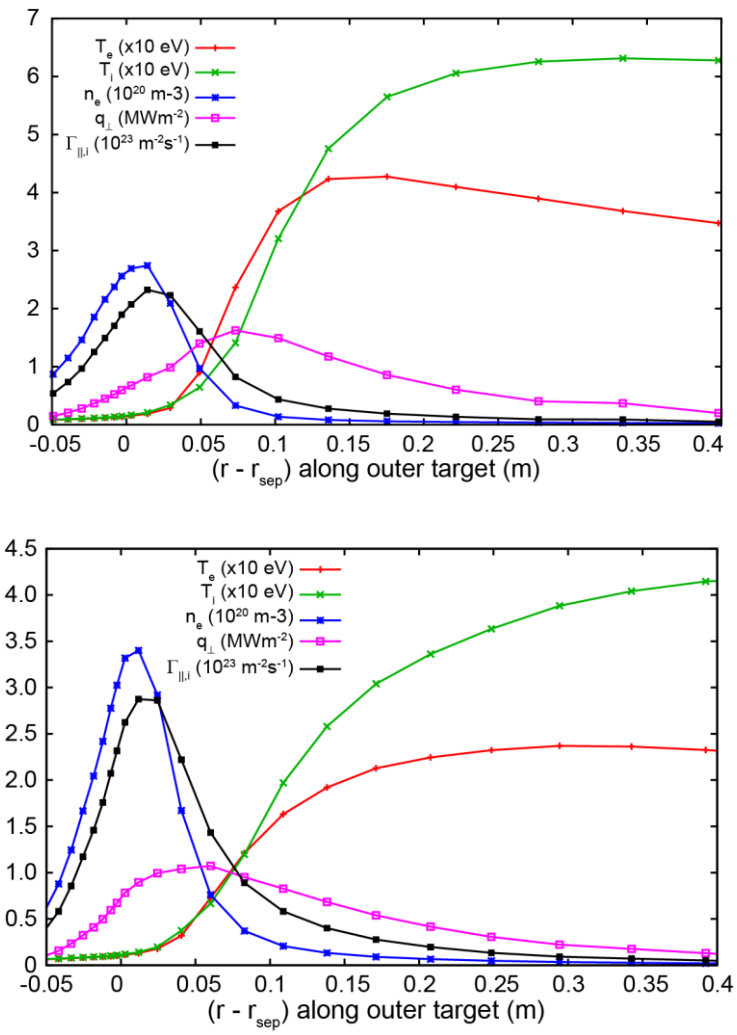

Figure A-1: Outer (top) and inner (lower) divertor profiles of T_e, T_i, target power flux density ($q_\perp$) and parallel ion flux density for the SOLPS-ITER simulation consistent with the ASTRA code run at $n_{e,sep} \sim 1.0\times10^{19}$ m^{-3}, P_{SOL} = 31 MW.

An example of the code output is shown in Figure A-1, which compiles profiles of T_e, T_i, n_e, $q_\perp$ and parallel ion flux density, $\Gamma_{\|,i}$ at the inner and outer divertor targets ($q_\perp$ is the perpendicular heat flux density assuming an axisymmetric (unshaped) divertor).

This simulation has the following upstream separatrix parameters:

$n_{e,sep} = 1.0\times10^{19}$ m^{-3}, $T_{e,sep}$ = 100 eV, $T_{i,sep}$ = 150 eV,

and it is comforting to note that the upstream power flux width correction to the SOLPS parameterization in ASTRA, $f_q \sim 5$, corresponds to $\lambda_{q,near} = f_q\lambda_{q,0} \sim 17$ mm, to be compared with $\lambda_{q,near} \sim 18$ mm obtained from this dedicated SOLPS-ITER code simulation.

Likewise, the calculated SOLPS-ITER core ionization source is 14.9 Pam^3s^{-1}, extremely close to the ASTRA value of 14 Pam^3s^{-1} for the same gas puff and core fuelling. This means that the modified boundary parameterization for the L-mode case produces a core source consistent with the full boundary plasma simulation and that the core D concentrations can be trusted.

A total of 3.3 MW is radiated in the divertor, all from neutral hydrogen. The neutral pressure is 2.1 Pa. As shown in Figure A-1, $q_{pk} \sim 1.6$ MWm^{-2} at the outer target, about a factor 4 higher than predicted by the boundary parameterization. There is a moderate plasma pressure loss in a narrow region around the strike point (~factor 2) and thus the plasma is not as deeply detached as would be expected for the low $n_{,sep}$. Despite the low P_{SOL}, this divertor plasma solution has reasonable q_{pk} and would likely be suitable for migration studies.

The study described here should in no way be taken as definitive. There is evidently much scope for tuning. Future true integrated modelling would allow scoping and refining, without relying on the application of boundary scalings taken out of the range of parameters from which they were derived. However, the degree of agreement obtained between the key outputs from the dedicated SOLPS-ITER and ASTRA simulations increases confidence that this case study can act as a reasonable basis for concluding that a series of low power D-spiked discharges in the non-active phase suitable for material migration and gas balance/fuel recovery studies can be realistically executed without exceeding regulatory limits or requiring a functioning tritium plant.

Appendix B: L-H Threshold and Toroidal Field Ripple effects on H-modes

B.1 L- to H-mode power threshold uncertainties when extrapolating towards ITER

B.1.1 Summary

Due to the large scatter in the ITPA database used for the L-H power threshold prediction for ITER, its 95% confidence interval gives a wide range of possible values for the L-H transition in ITER: from 0.54 to 1.86 times the scaling value given by $P_{th,D} = 0.049.\overline{n_e}^{0.72}.B_T{}^{0.8}.S^{0.94}$. This introduces significant uncertainties on the range of plasma conditions over which the H-mode will be achievable in ITER with the baseline heating schemes. The uncertainties in the scaling reflect the impact of divertor geometry, input torque, Z_{eff}, etc., on the power required to access the H-mode. Some of them are expected to lead to lower power threshold in ITER than predicted by the scaling (lower Z_{eff} than C wall machines, lower torque input than NBI-heated present machines, etc.) while others could lead to a significantly increased power threshold (divertor geometry impact of the temperature profile at the target and the associated edge electric field E_r, etc.).

The minimum power threshold with respect to the plasma density is expected to range between 20 to 40% of the Greenwald density on the basis of the existing database. A more physics based scaling has been recently proposed but it is not yet universally accepted.

The impact of the H isotopes and species on the H-mode threshold is based on a range of experimental results and has uncertainties, particularly for He plasmas. For H isotopes the power threshold decreases inversely with the isotopic mass. The impact of He versus D on the power threshold either leads to higher or unchanged thresholds depending on the experimental devices; so far these results are unexplained. Thus, for the isotope effect ITER predictions are based on $P_{th} \propto M^{-1}$ and for He the power threshold is expected to be between 1 to 1.4 times the D power threshold.

Until scalings accounting for the numerous specific impacts are available or, conversely, until a better theoretically based understanding is able to unify the various observations, it is a reasonable approach to use the 'n, B, S' scaling [Martin, 2008]. However, it should always be considered that the 95% confidence interval of this scaling is rather large and this can have significant impact on the Research Plan for ITER.

B.1.2 ITER L-H power threshold estimates

The ITPA 2008 scaling [Martin 2008] is used to extrapolate towards ITER the L to H mode power threshold such that:

$$P_{th,D} = 0.049 \times \overline{n_e}^{0.72} \times B_t{}^{0.8} \times S^{0.94} \quad \text{(B.1-1)}$$

S is the plasma surface, taken to be 683 m^2 for ITER plasmas.

The volume line averaged density $\overline{n_e}$ (usually quoted as a percentage of the Greenwald density: $n_{GW} = \frac{I_p}{\pi a^2}$).

B_t is the toroidal magnetic field on the magnetic axis.

In H, the power threshold is taken to be such that $P_{th,H} = 2 \times P_{th,D}$.

In He, the power threshold is taken to be such that $P_{th,He} = [1\ to\ 1.4] \times P_{th,D}$.

In DT, the power threshold is taken to be such that $P_{th,DT} = 0.8 \times P_{th,D}$.

This leads to the H-mode threshold values displayed in Figure B-1.

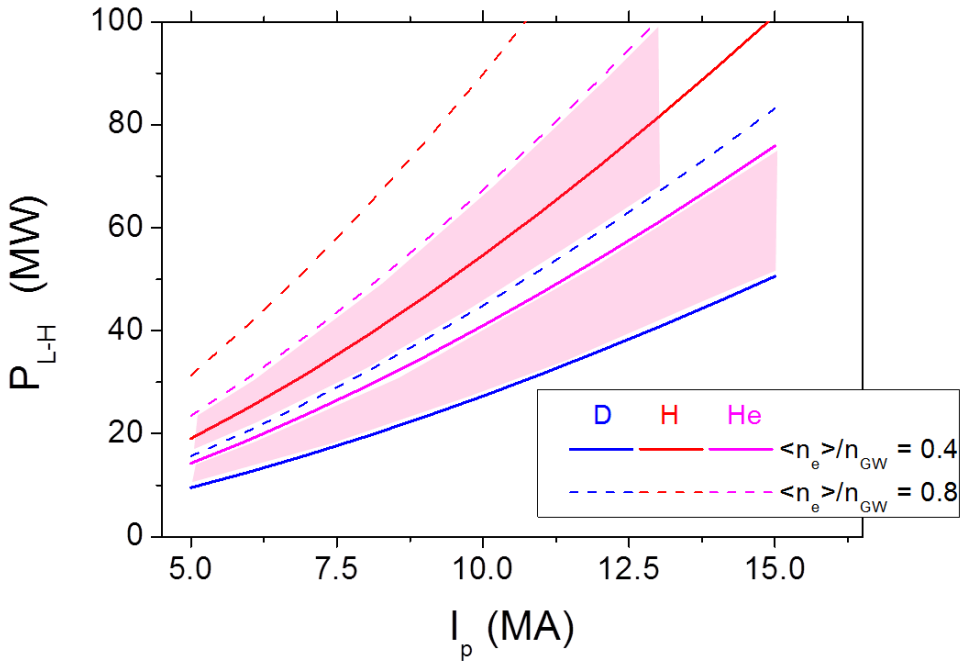

Figure B-1: Expected L-H threshold power on the basis for the B.1-1 scaling for H, He and D plasmas in ITER over a range of plasma currents for q_{95} = 3 and two values of the plasma density. For He plasmas the range $P_{th,He} = [1\ to\ 1.4] \times P_{th,D}$ is shown.

B.1.3. Existing ITPA scalings

In [Martin, 2008] the power scaling was derived with 1024 data points. The root mean square (RMS) value of the fit is 30.8%. This means that the 95% confidence interval of the power threshold is between 54 and 186% of the extrapolated power value. This reflects the very large deviations in the data used. Even when selecting only JET data, one finds a factor 5 variation of the measured power threshold with respect to the scaling value, as illustrated on Figure 1 of [Martin, 2008].

The previous ITPA scaling was produced in 2004 [Takizuka, 2004] and it accounted for the impacts of the aspect ratio and effective charge, as well as density, magnetic field and plasma surface. When reduced to density, B and S this scaling is very similar to that of [Martin, 2008] within a standard deviation of 0.36:

$$P_{th,D} = 0.06 \times \overline{n_e}^{0.7} \times {B_T}^{0.7} \times S^{0.9} \quad \text{(B.1-2)}$$

B.1.4 Impact of ion species

Based on T, DT, D and H experiments at JET, the dependence of the threshold power on the ion mass number M is given by $P_{th} \propto M^{-1}$ [Righi, 1999]. Experiments in H versus D have also been carried out in other tokamaks to explore further the isotope impact on the power threshold and found that $P_{th} \propto M^{-1}$ provides a good guideline for the isotopic effect, although the precise value of the multiplier from H to D depends of plasma parameters.

He versus D has also been explored on DIII-D, ASDEX-Upgrade, Alcator C-Mod and JET, most of the experiments in a C wall environment [Gohil, 2012; McDonald, 2010]. When comparing He with D plasmas, either the power threshold is unchanged (ASDEX-Upgrade), unchanged or somewhat increased depending on density (JET) or largely increased by up to factors of 3 at some densities (DIII-D and Alcator C-Mod).

Recent experiments from JET show that small amounts of H in D plasmas and He in H plasmas can have significant effects on H-mode access [Hillesheim, 2016]. Although this was identified already in ASDEX-Upgrade for He plasmas [Ryter, 2013], the new JET results indicate that the issue is more complex and can be beneficially exploited to expand the range of ITER H-mode operation in H plasmas.

B.1.5 Impact of density

The [Martin, 2008] scaling exhibits a threshold power increasing with increasing density. In many experiments, the power threshold is minimized at a given density and then rises up at low density again. The position of this minimum density is reported to range between 20 to 40% of the Greenwald fraction [Martin, 2008], as shown in Figure B-2.

Recent work on ASDEX-Upgrade [Ryter, 2014] showed that this minimum density is determined by the role of the edge ion heating in triggering the L-H transition. Based on these results, an expression for the density providing the minimum threshold L-H power has been derived, which also describes well the values found in tokamaks of various sizes.

$$n_{e,min}^{scal}(10^{20}m^{-3}) \approx 0.07\, I_p^{0.34} B_t^{0.62} a^{-0.95} (R/a)^{0.4} \quad \text{(B.1-3)}$$

For ITER, this leads to,

$$\frac{n_{e,min}^{scal}}{n_{GW}} \approx 0.71 \frac{I_p^{0.34} B_t^{0.62}}{I_p} \quad \text{(B.1-4)}$$

For $q_{95} = 3$ conditions in ITER, for which $B_t\,(T) = 0.35 \times I_p\,(MA)$, this corresponds to $n_{e,min}^{scal} \sim 0.4 \times n_{GW}$. Accessing the H-mode at these densities reduces the additional heating power required and this is particularly important for the access to H-mode at 1.8T in PFPO-1 when the installed additional heating power will be in the range of 20-30 MW.

It should be mentioned however, that in JET with the ITER like wall access to H-mode at low densities exhibits a significant increase, as in the ASDEX-Upgrade experiments, although $T_e = T_i$, thus questioning the findings in [Ryter, 2014] that the increase of H-mode threshold at low power is due to the decreased ion power flux due electron-ion thermal decoupling at low densities [Maggi, 2014].

B.1.6 Impact of toroidal field ripple

TF ripple up to 1.1% has been found not to affect the H-mode threshold in JET experiments [Andrew, 2008]. In earlier JET experiments, when switching from 32 to 16 coils, hence with a ripple factor reaching 10%, the H-mode was obtained at a slightly higher power [JET Team, 1993]. Conversely, on JT-60U, the power threshold was reduced when increasing the ripple (before

ferromagnetic inserts) [Tobita, 1995]. In DIII-D, a TBM mock-up insert coil induced a local 3% ripple [Gohil, 2011], which did not modify the L-H threshold value nor its dependence on input torque.

The impact of resonant and off-resonant fields applied for ELM control has been studied on ASDEX-Upgrade, MAST and DIII-D [Gohil, 2012; Fenstermacher, 2010; Ryter, 2013]. Strong resonant components in the Resonant Magnetic Perturbation (RMP) spectrum lead to significant increase in P_{th} for RMP fields above a critical threshold field (i.e. for dB/B_t above $\sim 3\times10^{-4}$), whereas no clear increase in P_{th} is observed below this field. For off-resonant fields, there is a much smaller increase in P_{th} with the applied fields.

Therefore, a priori no significant impact of the magnetic field ripple on H-mode access is expected in ITER, even at the 1.3% expected at 1.8T. On the other hand RMP fields applied for ELM control are expected to have a large effect on the L-H threshold when optimized for ELM control. Therefore the application of these fields when accessing the H-mode should be carefully designed to minimize their effect on H-mode access. Nonetheless, it should be noted that the normalized magnitude of the field perturbation either by ripple of RMPs is not an appropriate dimensionless parameter that should be used to extrapolate towards ITER. More modelling on existing experiments should take place, and the collisionality regimes in which effects are found should be characterized and compared to the ones expected in ITER, in order to draw physics-based conclusions on the effects of TF ripple and 3-D fields applied for ELM control on the H-mode power threshold in ITER.

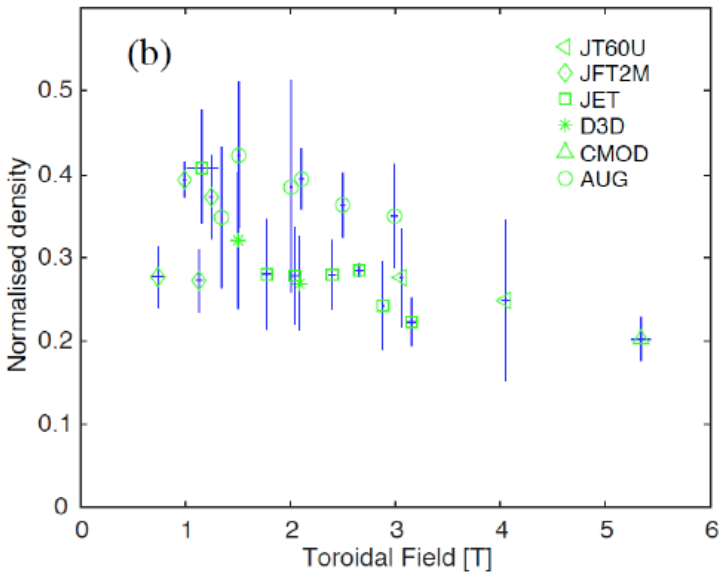

Figure B-2: Plasma density at which the minimum H-mode threshold power is achieved versus toroidal field as a fraction of the Greenwald density (from [Martin, 2008]).

B.1.7 Impact of divertor geometry (Vertical Target versus Horizontal Target and X- point height)

The L-H power threshold has been found to be lower by 20 to 35% with increased divertor closure in JET with Carbon PFCs [Horton, 1999; Andrew, 2004] and in JT-60U [Fukuda, 2000]. In more recent Alcator C-Mod experiments, the slot divertor configuration is associated with a lower power threshold (up to a factor 3) than the vertical target configuration [Ma, 2012].

In DIII-D a lower X-point height leads to a lower threshold (a factor 2 for a 15 cm variation) [Gohil, 2011]. A similar X-point height impact is also reported for JET with Carbon PFCs (a factor 5 for 25 cm variation) [Andrew, 2008]. More recently in JET with the ITER-like Wall, experiments to determine the impact of the vertical versus horizontal target divertor geometry on H mode access, have shown that up to a factor 3 reduction of the threshold is obtained with the horizontal target configuration [Delabie, 2015]. In this later case a qualitative explanation has been proposed by using EDGE-2D/Eirene modelling that shows that lower temperature gradients on the target plate are expected and measured in the vertical target case, leading to lower positive E_r at the separatrix and, hence, potentially reduced E×B shear [Chankin, 2017]. A reduced E×B shear is qualitatively consistent with an observed higher power threshold [Burrell, 1990].

B.1.8 Metallic wall impact on H-mode access

The power threshold is found to be reduced with metallic walls as observed in JET and ASDEX-Upgrade [Maggi, 2012; Neu, 2013]. Several authors have, thus, suggested that the effective charge could be an important parameter [Takizuka, 2004; Bourdelle, 2014]. JET-ILW and C wall data have been shown to be better fitted by the [Takizuka, 2004] scaling, including a Z_{eff} dependence than by the [Martin, 2008] scaling [Maggi, 2014]. This trend is confirmed by N_2 seeding impact on the power threshold demonstrated in JET [Delabie, 2016].

B.1.9 Torque impact

In DIII-D using balanced NBI, a lower P_{th} was found for lower torque input [McKee, 2009]. In ITER, which has a low normalized torque due to the high energy NBI, a lower power threshold might be observed compared to the value extrapolated from the existing scalings, such as [Martin, 2008], where a large number of data are provided from NBI heated plasmas with a significant normalized torque.

B.1.10 Needs for further understanding/characterization

Further studies are required to refine the evaluation of the ITER H-mode power threshold:

- From the existing ITPA ‘n, B, S’ scalings, the confidence interval at 95% is very wide and leads to large uncertainties of 54% and 186% around the predicted power threshold. This is due to hidden parameters that have to be investigated further and understood, including: divertor geometry, X-point height, torque, etc. SOL modelling relating the target temperature to the separatrix radial electric field, as done recently on JET [Chankin, 2017], has to be applied to other tokamaks. The nature of the turbulence stabilization when entering the H-mode has to be characterized and its parametric dependences determined as well. Indeed the competition between turbulent drive and E×B shear is the most commonly shared basis for L-H transition understanding.
- The isotopic effect needs to be further understood in detail. As DT experiments are rare, it is important to perform further H versus D experiments, particularly with metallic walls, to develop the physics understanding that can be used for ITER predictions.
- Depending on the device, either both He and D have the same H-mode power threshold or the power threshold is up to 3 times higher in He. Further experiments, in metallic environments should be performed. Models should address the issue of He versus D impact on the power threshold as well as the impact of small amounts of He into H plasmas, as this has large implications on the ITER Research Plan H-mode studies in the PFPO phases.

- The density impact on the L-H power threshold also has to be investigated. In particular the increase at low density due to a decoupling between ions and electrons might explain all experimental observations. Further consolidation should be provided to these ASDEX-Upgrade experimental observations.
- The impact of the TF ripple and non-axisymmetric fields on the power threshold observed in existing tokamaks should be modelled and extrapolated to ITER to determine its potential effect for the collisionalities pedestal conditions expected in ITER plasmas. This could be carried out by applying stellarator neoclassical transport codes (SFINCS, PERFECT) to ITER [Paul, 2016] and theoretical work, such as [Garbet, 2010], should be applied to ITER to predict the E_r modification due to these effects.

B.2 Effects of the Toroidal Field ripple on H-modes

B.2.1 The effect of Toroidal Field (TF) ripple on pedestal and confinement

In JET, the TF system was configured to feed different currents to the odd and even set of coils out of 32 TF coils [Saibene, 2008]. In this operation mode, the peak TF ripple δ_R can be actively varied by selecting an appropriate differential current between each set of coils. In these experiments, four levels of δ_R = 0.08%, 0.5%, 0.75% and 1% were used. The TF ripple in the JET tokamak, where all TF coils are fed with an equal current, is normally very small at the nominal separatrix radius at the outer midplane (0.08%). A series of H-mode experiments were conducted at 2.6 MA/2.2 T (q_{95}~3) varying δ_R within the range above. Figure B-3.a shows the normalized confinement H_{98} as a function of δ_R. The upper envelope in this plot, which corresponds to the case of unfuelled plasmas (ν^*_{ped} ~ 0.04), indicates a gradual decrease of H_{98} with TF ripple, with up to ~ 20% confinement loss for δ_R = 1%. Figure B-3.b shows the pedestal pressure as a function of TF ripple in this series of experiments, where the high density data are excluded because of the lack of T_e measurements. This shows that the confinement degradation with TF ripple at low density clearly originates from a reduction in the pedestal pressure. On the other hand, the variation of H_{98} for high density discharges (see the lower envelope of the plot in Figure B-3.a) is very small and H_{98} appears to be independent of TF ripple at higher density and/or higher pedestal collisionality (ν^*_{ped} > 0.1). These results are consistent with the observation of a much-reduced density pump-out as the density is increased, independent of TF ripple, as shown in Figure B-3.c. The most striking effect of TF ripple is the strong density pump out, particularly for the case when no gas puffing is applied. As gas fuelling is increased, the steady state density achieved in the discharges becomes more and more similar despite of the increased TF ripple. At the highest fuelling rates (corresponding to n_{ped} ~ 60 – 70% n_{GR}), the difference between an H-mode with 0.08% and 1% TF ripple becomes very small in terms of achievable density and temperature as well as the energy confinement.

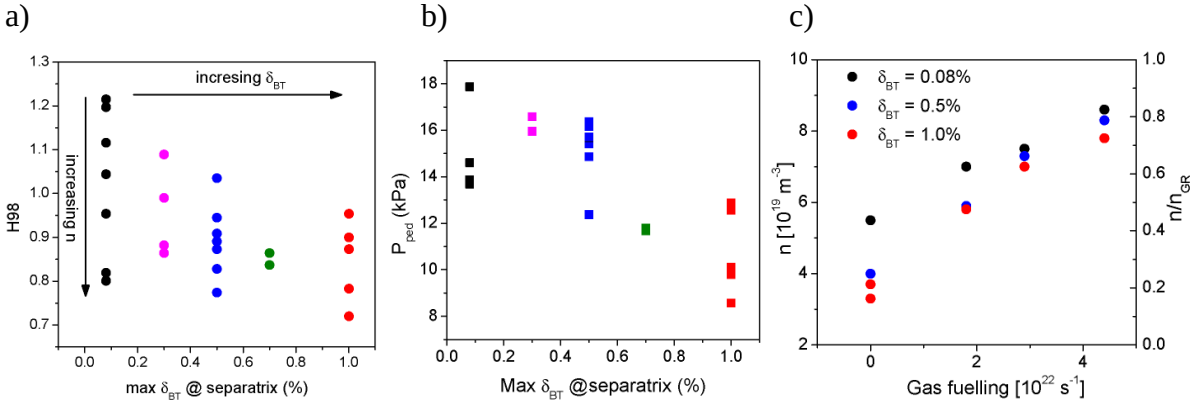

Figure B-3: Dependence of a) H_{98}, b) pedestal pressure and c) line averaged electron density on TF ripple amplitude in the JET ripple scan experiments at 2.6 MA/ 2.2T.

In JT-60U, ferritic inserts (FIs) were installed in the vacuum vessel to reduce the TF ripple in 2005 [Shinohara, 2006]. Similarity experiments between JET and JT-60U with variable TF ripple were carried out for 1.1 MA/ 2.0T plasmas [Urano, 2011] because the FI correction in JT-60U was optimized for TF ripple reduction at B_t < 2 T [Shinohara, 2006]. While the increased TF ripple significantly changed the ELM behaviour as described later, the reduction in the pedestal pressure with TF ripple was small at 1.1MA for both devices as shown in Figure B-4.a. This may indicate that the effect of TF ripple could be more significant at lower collisionality (ν^*_{ped} ~ 0.04), which is consistent with the very small confinement degradation with TF ripple in JET 2.6 MA plasmas at high density (see Figure B-3.a). This characteristic is also seen in the impact of TF ripple on density pump-out in JT-60U and JET. Figure B-4.b and Figure **B-4**.c show n_e/n_{GR} as a function of TF ripple for discharges without gas puffing at low (~1 MA) and high I_p (2.6 MA), respectively.

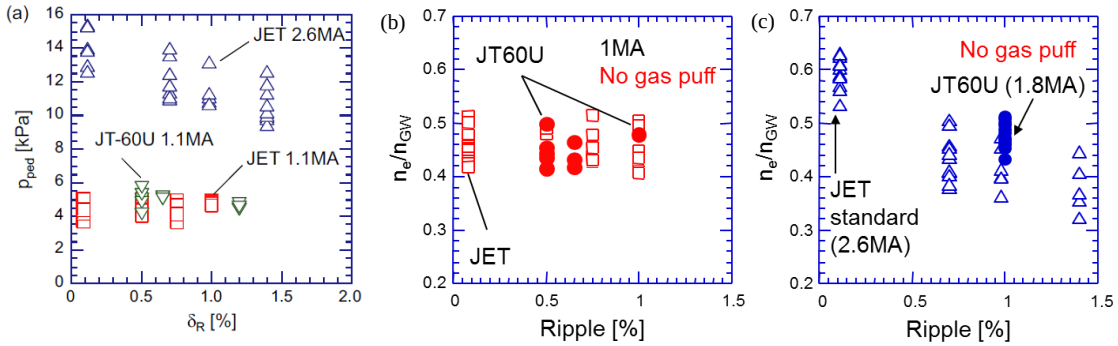

Figure B-4: a) Dependence of pedestal pressure on TF ripple amplitude in JET 1.1 MA, 2.6 MA and JT-60U 1.1 MA ripple scan experiments. Greenwald density fraction as a function of TF ripple for unfuelled plasmas with b) low (~ 1MA) and c) high I_p (2.6 MA).

A strong density pump out of 20-30% at δ_R of 1% is observed at 2.6 MA in JET whereas the reduction in density is negligible at ~ 1 MA with high collisionality (ν^*_{ped} > 0.1). In JET, the effect of TF ripple on H-mode characteristics was also examined at the reduced I_p/B_t of 1 MA/ 1T (q_{95} ~ 3.6) [Saibene, 2008]. In contrast to the results obtained at higher I_p and B_t, the global and pedestal parameters of the 1 MA/ 1T series of H-modes do not change significantly for increasing TF ripple values at high collisionality (ν^*_{ped} ~ 0.1), as shown in Figure B-5. In particular, the plasma stored energy is only slightly reduced at high ripple with constant input power. Despite this, a significant effect of TF ripple on edge toroidal rotation is observed; the plasma rotation is reduced as the ripple is increased, with V_{TOR} approaching 0 at the plasma periphery for δ_R = 1.0%.

B.2.2 Effect of Toroidal Field ripple on type-I ELMs

JT-60U ripple scan experiments showed that ELMs are more sensitively affected by TF ripple than confinement [Aiba, 2011]. Figure B-6 shows the dependence of ELM frequency, ELM energy loss and edge toroidal rotation frequency on the TF ripple in JT-60U 1.1 MA H-mode plasmas at fixed P_{sep} ~ 6 MW. By the installation of FIs, the ELM frequency decreased by ~ 30% and the ELM energy loss increased by a factor of two. The power carried by ELMs increased by ~30% with increasing ripple for a given loss power through the separatrix P_{sep}, at ~ constant plasma energy indicating that the inter-ELM transport is reduced with the increased TF ripple. The edge toroidal rotation, which was in the counter I_p direction because of large TF ripple of ~ 1% before the installation of FIs, was increased towards the co-I_p direction when the FIs were introduced.

Therefore, the significant changes to ELMs in JT-60U when FIs were introduced could be related to the change in the edge toroidal rotation.

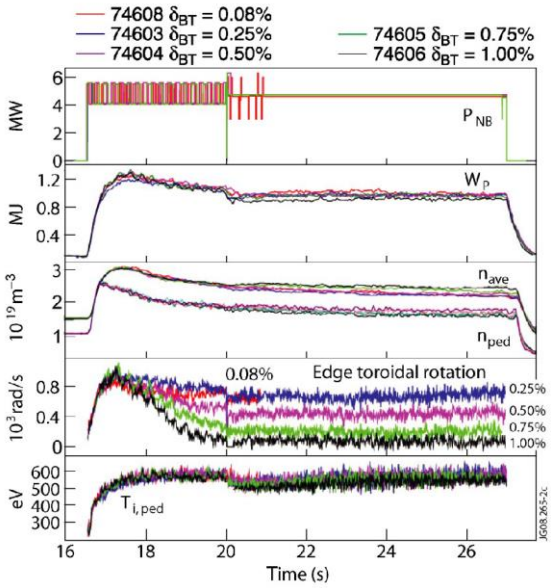

Figure B-5: TF ripple scan H-mode discharges at 1MA/1T in JET.

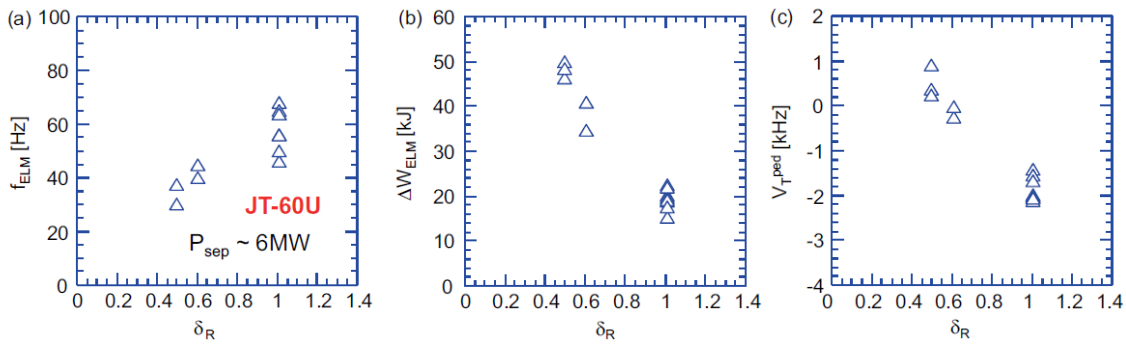

Figure B-6: Dependence of a) ELM frequency, b) ELM energy loss and c) edge toroidal rotation frequency on the TF ripple amplitude in JT-60U 1.1MA H-mode plasmas at P_{sep} ~ 6MW.

In the JET ripple scan experiments at 1 MA/1 T, the effect of TF ripple on edge toroidal rotation was also clearly observed, whereas the change in the pedestal performance was very small [Saibene, 2008]. Figure B-7 shows the dependence of normalized ELM energy loss on edge collisionality in the JET ripple scan experiments at 2.6MA/2.2T. This plot indicates that, for similar edge collisionality, the size of the ELM energy loss is reduced as the TF ripple increases. This is consistent with the JT-60U findings where increased edge toroidal rotation in the counter direction leads to smaller ELMs, while the pedestal parameters are not largely changed [Aiba, 2011].

B.2.3. Implications for ITER 5 MA/ 1.8T operation

From the experimental evidence, the effect of TF ripple on H-mode confinement is not uniform but seems to depend on the plasma parameters, such as the edge collisionality. The JET ripple scan

experiments at 2.6 MA/ 2.2T, which show 20-30% loss of pedestal pressure at δ_R ~1%, were performed at ν_{ped}* ~ 0.04 for the unfuelled plasmas, which is a similar collisionality to that expected for Q =10 15MA/5.3T operation in ITER. On the other hand, the JET ripple scan experiments at 1 MA/1 T and JET/JT-60U similarity experiments at 1 MA, which show very small loss of the pedestal pressure and confinement at δ_R ~1%, were performed at relatively high ν_{ped}* > 0.1.

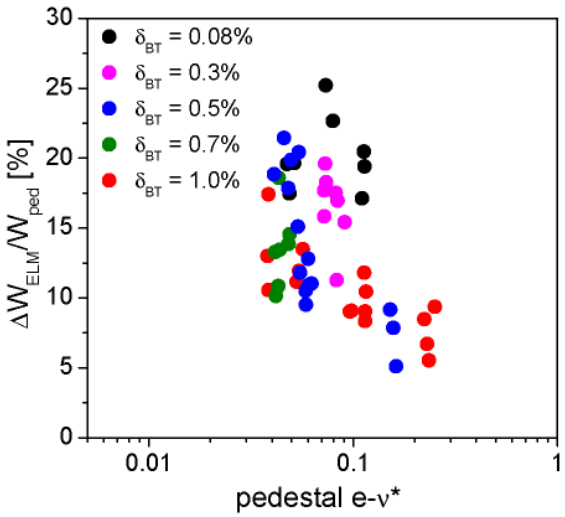

Figure B-7: Dependence of normalized ELM energy loss on edge collisionality in JET ripple scan experiments at 2.6MA/2.2T.

If we assume that collisionality is the key parameter, we can then use the ITER predictions for the pedestal pressure derived from EPED1 [Polevoi 2015] to evaluate the possible effects of ~ 1% ripple on the pedestal plasmas for 5MA/1.8T plasmas in ITER, by first evaluating their characteristics without ripple effects. For q_{95} ~3 the pedestal pressure is found to scale with $p_{ped} \sim I_p^2$. For plasmas with constant $\langle n_e \rangle / n_{GW}$, $n_{ped} \sim I_p$ and this leads to $\nu^*_{ped} \sim I_p^{-1}$. (i.e. the collisionality of 5 MA plasmas with the same $\langle n_e \rangle / n_{GW}$ that Q = 10 plasmas be three times larger than that of 15 MA Q=10 plasmas). However, for the expected plasma conditions in ITER 5 MA/1.8T plasmas (see appendix G), we expect $n_{ped}/n_{GW}|_{5MA} = 0.5\ n_{ped}/n_{GW}|_{15MA\text{-}Q=10}$ and this reduces further the plasma collisionality of these plasmas so that finally for the foreseen ITER 5 MA/1.8T H-mode plasmas $\nu^*_{ped}|_{5MA} \sim \nu^*_{ped}|_{15MA\text{-}Q=10}$. Therefore, ripple effects are expected to be similar at 5 MA/1.8T to those for collisionless experimental plasmas with ITER-like pedestal collisionality implying a reduction of the pedestal pressure by 20-30%. The level of ripple in ITER at 1.8T may be decreased by reducing the minor radius of the plasma and displacing it towards the HFS to reduce the TF ripple amplitude.

From the viewpoint of ELM energy losses and heat loads, this high level of ripple is expected to decrease the ELM energy losses by at least a factor of 2 at δ_R ~ 1%, on the basis of the JET and JT-60U ripple scan experiments. However, these experimental results could be due to the change in the edge toroidal rotation enhanced towards the counter direction by the fast ion losses induced by increasing TF ripple. If this is the case the ELM energy loss reduction with high ripple may not materialize in the electron-heated 5MA/1.8T ITER H-mode plasmas.

Appendix C: Heat Load Management

In the progressive approach to scenario development and preparation for nuclear phase operation, an important issue is the point in operational space at which the divertor target heat load begins to require mitigation. This Appendix attempts to provide some approximate guidelines.

When discussing heat load management, it is in general understood that this refers to steady state power loads. In the case of ELMy H-mode plasmas, this steady load is an average of the inter-ELM and ELM phases. The approach adopted at the ITER Organization during the divertor and first wall design phase has been to estimate the expected power loading using static (i.e. time independent) runs with the SOLPS suite (version 4.3, coupling the B2 fluid code to the Eirene kinetic Monte Carlo neutral code, no fluid drifts). The usual strategy over the years (documented in a number of publications, see e.g. [Kukushkin, 2003]) has been to provide a large number of independent SOLPS code runs, in which key engineering parameters are varied (e.g. power into the SOL (P_{SOL}), fuelling throughput, pumping speed), and from which scaling relationships can be constructed for use as boundary conditions for core plasma models (e.g. separatrix averaged values of electron and ion temperatures, electron densities, etc.).

The original SOLPS-4.3 database constituted mostly burning plasma simulations with CFC divertor targets, but this has now been replaced by a new dataset in which carbon is eliminated in favour of all-metal walls, with the caveat that tungsten impurities (W) themselves are not simulated. To do so would be extremely costly in a computational sense and would bring little additional information to the question of power loading assessment since, if W is present in any quantity sufficient to modify the divertor power balance, then the quantities are too high to be considered trace and the simulation would not correspond to a realistic operational scenario.

Part of the database for $60 < P_{SOL} < 120$ MW was published in [Pacher, 2015] with emphasis on burning plasma operation. Several new data points now exist for $P_{SOL} < 60$ MW. Each point in the database corresponds to a fully converged SOLPS run (usually requiring several weeks or months of clock time), with careful attention paid to particle balance and using the full Eirene capability. Simulations have been performed with both nitrogen (N) and neon (Ne) seeding which, at the highest input powers, is required if peak divertor power flux densities are to remain within technological limits ($q_{pk} \leq 10$ MWm^{-2}).

Given the lack of a realistic method for modelling ELMs in SOLPS and the fact that time dependent code runs are extremely costly (and moreover cannot deploy a physically correct model of the ELM), the simulations assume that the chosen P_{SOL} comprises the power conducted/convected into the SOL both during and in-between ELMs. This is thought to be a reasonable approach for smaller (e.g. mitigated) ELMs for which the inter-ELM and ELM footprints on the targets are expected to be similar.

A fundamental issue when extrapolating to ITER is the choice of cross-field transport which, in the case of heat transport, sets the near-SOL heat flux width, $\lambda_{q,near}$ and thus the peak target power flux density. In recent years, the deployment of high quality infra-red monitoring of divertor targets has allowed an improved determination of the H-mode inter-ELM $\lambda_{q,near}$, which is now being found in current devices to depend essentially only on $1/I_p$ (or $1/B_{pol}$) [Eich, 2013]. This is preserved at least up to the largest device (JET) currently in operation and such a scaling is well matched by a theory in which cross field motion in the separatrix vicinity is assumed dominated by (neo)classical magnetic drifts, giving $\lambda_{q,near} \sim 2a\rho_{pol}/R$ [Goldston, 2012]. For the 15 MA ITER H-mode reference burning plasma scenario, this theory predicts an extremely narrow heat flux channel, $\lambda_{q,near} \sim 1$ mm.

Such narrow widths would in practice be difficult to handle in terms of target power loads. Simulations with SOLPS-4.3, in which heat and particle transport is reduced to very low values to reproduce ~1 mm near SOL widths, find that the additional divertor dissipation required to bring q_{pk} to manageable levels results in extremely high, and perhaps unsustainable, upstream separatrix densities [Kukushkin, 2013]. Very recent calculations using the XGC1 edge gyrokinetic code are finding, however, that at high current at the ITER scale, it is filamentary ('blobby') electron turbulence which dominates over ion magnetic drift, resulting in a much wider $\lambda_{q,near}$ ~ 5-6 mm [Chang, 2017]. It is not currently known if, and at which point in operating space (namely I_p), there would be a transition from one type of transport to the next, so that a prescription for cross-field heat transport in boundary simulations for ITER is uncertain. Moreover, the validity of the XGC1 simulations needs to be further explored.

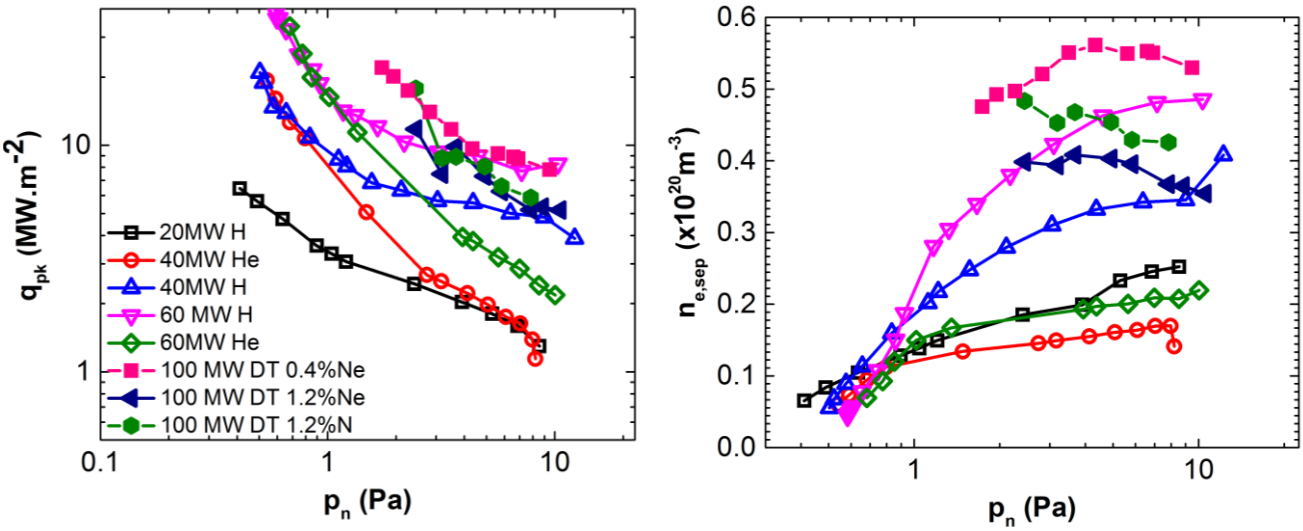

Figure C-1: Left: dependence on sub-divertor neutral pressure of the peak target power flux density for a variety of operating scenarios from non-active operation at low P_{SOL} in H and He to the highest performance at Q_{DT} = 10. Right: the corresponding upstream separatrix densities.

All SOLPS-4.3 simulations performed thus far and which have been used to build scaling relationships for core modelling have concentrated on the baseline equilibrium at q_{95} =3 (I_p = 15 MA/B_t = 5.3 T) for fixed values of cross-field transport coefficients for particles ($D_\perp$ = 0.3 m^2s^{-1}) and heat ($\chi_\perp$ = 1.0 m^2s^{-1}). This yields $\lambda_{q,near}$ ~ 3-4 mm in the simulations, thus a factor ~3 larger than the values predicted by the ion orbit drift model at 15 MA, but lower than the more optimistic XGC1 simulation results. The code runs performed at lower P_{SOL}, for H and He plasma, designed to provide some guidance for non-active phase operation, use the same baseline equilibrium at q_{95} = 3 (thus appropriate to I_p[MA]/B_t[T] = 15/5.3, 7.5/2.65, 5/1.8) and assume the same cross-field transport as for the burning plasma. No attempt has been made to vary the radial transport inside the separatrix so that these simulations do not include any form of H-mode transport barrier.

A subset of the ITER SOLPS database, is shown in Figure C-1 (left), where q_{pk} is given as a function of sub-divertor neutral pressure, p_n, a key control parameter for particle exhaust and a strong indicator of the level of divertor detachment. Here, q_{pk} may be either on the inner or outer targets, but is usually found on the outer. Results are included for H, He and DT operation with P_{SOL} = 20 – 100 MW. The right-hand plot in the figure gives the values of upstream separatrix

density, n_{sep} in the simulations, demonstrating that the points at lowest p_n correspond to $n_{sep} \sim 5\times10^{18}$ m^{-3}.

To put the fixed transport assumption into context, the ion drift based theory in [Goldston, 2012] referred to earlier gives $\lambda_{q,near}$ ~ 2-3 mm for a helium H-mode plasma at 7.5 MA/2.65 T and $\lambda_{q,near}$ ~ 2 mm for a hydrogen H-mode at 5.0 MA/1.8 T, so in both cases not too far from the heat flux channel width produced by SOLPS for the specified fixed cross-field transport strength. Since SOLPS is a 2-D code producing only purely axisymmetric heat fluxes, the values of q_{pk} in Figure C-1 have been scaled up by a factor 1.4 to account for the global divertor target tilting and front surface monoblock shaping used at ITER to ensure avoidance of power overload on leading edges [Pitts, 2017], which reduces the divertor effective area for power handling.

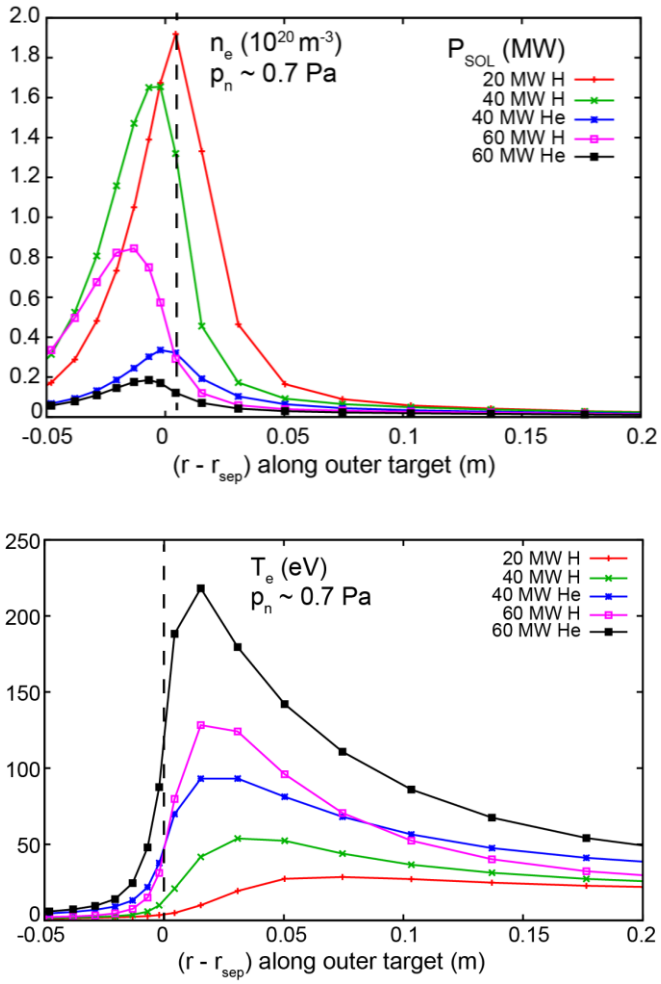

Figure C-2: Outer target profiles of n_e (upper) and T_e (lower) for the H and He scenarios in Figure C-2 at lowest p_n.

This data demonstrates that for all but the lowest P_{SOL} (20 MW), it is possible to find boundary solutions in which q_{pk} can exceed the nominal limit of 10 MWm^{-2}, sometimes significantly. This occurs in general for sub-divertor neutral pressures, $p_n \leq 1$ Pa. At the highest P_{SOL}, corresponding to DT operation, higher p_n will be required as well as extrinsic seeding (Ne and N have been used for the high power scans in Figure C-1) to remain at tolerable q_{pk}. Note, however, that it is generally found that $p_n \geq 10$ Pa corresponds in the simulations to a state of rather deep detachment, which may be considered too close to operational boundaries (e.g. H-L back transitions, disruptions). The

inclusion of shaping, which increases the field line attack angles, reduces the operating space with respect to acceptable target heat loads.

With regard to the operating points at low p_n when target power handling becomes an issue, they are associated in the simulations with a much lower degree of detachment in the strike point region, corresponding to high strike point plasma temperatures. This is illustrated in the steady state target profiles compiled in Figure C-2 for the PFPO operating conditions (namely only H and He plasma) in Figure C-1, at fixed p_n ~0.7 Pa. At these low neutral pressures, for any P_{SOL} > 20 MW, strike point values of T_e are in the many tens of eV range, corresponding to incoming ion energies close to or exceeding the tungsten sputtering yield of fuel ions (H, D, He, T), even without accounting for the higher yields in the case of impurity sputtering (e.g. Be or seeded species). Higher T_e would also, however, increase the prompt redeposition fraction and ELMs, if present, would likely dominate the W net source [Dux, 2017]. Additional simulations are required to address these points to estimate the net source in each case and then to assess the efficiency with which the released W may transport to the core plasma.

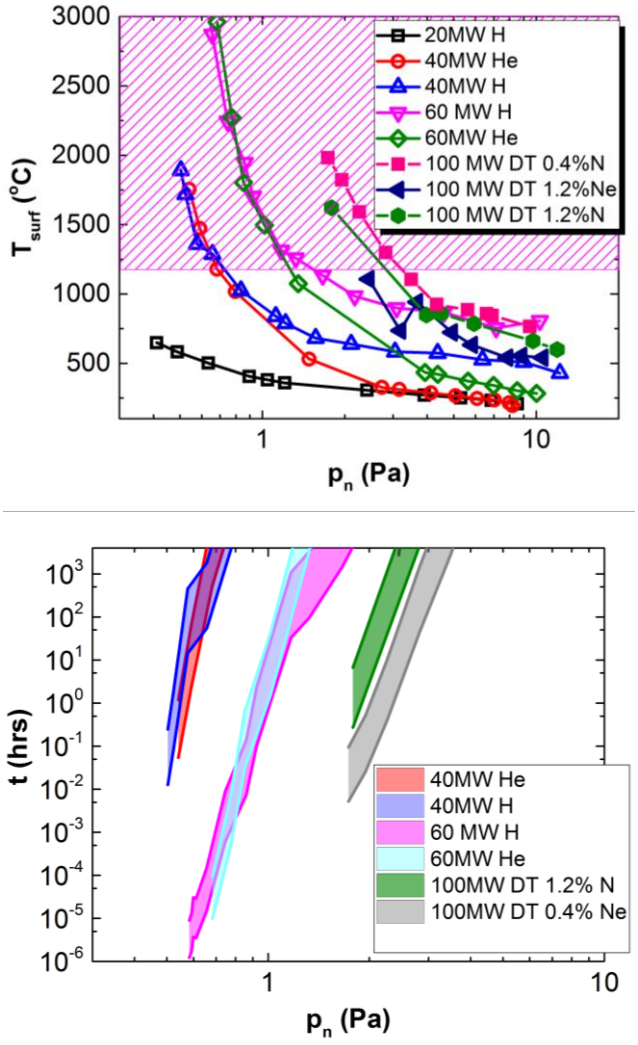

Figure C-3: Upper: the data of Figure C-1 transformed in terms of monoblock top surface temperature values. The purple hashed region corresponds to operating points above the W recrystallization temperature. Lower: estimate of the allowed operating time to recrystallize to a depth of 1 mm from the top surface.

The q_{pk} data in Figure C-1 can be straightforwardly associated with a divertor monoblock front surface temperature value using finite element thermal analysis taking into account the toroidal bevelling of the front surface and the appropriate water cooling parameters. This yields the data in Figure C-3 (upper), where the computed temperature is taken at the toroidal centre of the monoblock and does not, therefore, account for toroidal gap edge heating, a phenomenon which is expected to occur as a result of the castellated nature of the divertor target (namely the use of discrete monoblocks) and the particularities of the magnetic geometry, together with the presence finite ion orbits [Gunn, 2017].

Surface temperature is the key parameter determining the proximity to W recrystallization, long known to be associated with changes in mechanical properties such as a decrease in hardness and strength. Such modifications strongly affect the thermal shock resistance of W and may favour the appearance of deep macrocracks in the centre of the monoblocks (due to the inherent thermal gradients provoked by the geometry of the monoblock) and/or the development of surface crack networks during ELMs [De Temmerman, 2017]. The hashed region in Figure C-3 (upper) represents the approximate operating domain over which the surface recrystallization temperature (T_{recrys}) would be exceeded for the ITER divertor W grade.

In fact, recrystallization is a function of both material temperature and time. Operation above T_{recrys} may thus be permitted, but for strongly decreasing shorter times as the surface temperature increases (the recrystallization fraction depends exponentially on time). The allowable operating space may be characterized through the use of recrystallization kinetics [De Temmerman, 2017]. This has been applied to the temperature data in Figure C-3 (upper) to produce the curves in Figure C-3 (lower), which provide the operating time allowed before recrystallization to a depth of 1 mm into the monoblock surface occurs as a function of divertor neutral pressure.

As mentioned earlier in connection with q_{pk}, what can be seen immediately in the plots of Figure C-3 is that steady state operation at the lowest neutral pressures is to be avoided once heating powers in the PFPO phases permit $P_{SOL} \geq 40$ MW. Such low pressures correspond to low upstream separatrix densities (Figure C-1: lower), but these are not inconsistent with values that may be expected for operation at lower I_p. Although simulations have not yet been performed to quantify this, it is also to be expected that extrinsic seeding will be much less efficient for low p_n operation (high temperatures, lower densities) and thus this may not be an option to reduce q_{pk} in these conditions. The only approach will be to seek operating points at higher p_n (provided this is compatible with the required n_{sep}), in which case Figures Figure **C-1** and Figure **C-3** demonstrate that steady H-mode operation for essentially any accumulated plasma time will be possible for any P_{SOL} before nuclear operation. Note that once the 'threshold' value (to stay below T_{recrys}) of p_n is achieved for He plasmas, q_{pk} reduces rapidly with p_n due to the beneficial additional divertor radiation obtained in helium compared to operation in hydrogen.

The analysis described above has been confined to steady state operation, using time independent SOLPS simulations which do not separate the ELM and inter-ELM components in the power transported into the SOL plasma. Separate operational limits will be imposed when the ELM transient is accounted for and these are discussed below.

A clear limit on the allowed ELM energy density is given by the requirement to avoid W melting. This has recently been assessed in a detailed study [Gunn, 2017], which combines 3-D ion orbit calculations with monoblock thermal analysis to estimate the parallel ELM energy flux densities which would lead to both monoblock top surface melting and toroidal gap edge melting at the outer target for the 3 combinations of I_p, B_t at fixed $q_{95} = 3$. The analysis properly accounts for: the ion species and charge, the nominal ELM rise times for H-mode pedestal parameters characteristic of

the various scenarios, the baseline monoblock geometry (including the assumption of worst case misalignments and manufacturing tolerances) and the variation of stationary (inter-ELM) monoblock surface temperature. The results of this analysis are shown in Figure C-4, where the thresholds for toroidal gap and full surface melting are shown for the three I_p/B_t operating points 15/5.3, 7.5/ 2.65, 5/1.8. Figure C-4 also includes the recent multi-machine ELM parallel energy density scaling [Eich, 2017] applied to ITER, for comparison (the shaded region encompasses the uncertainty boundaries in the scaling). If this scaling is correct, H-mode operation on ITER at 5 MA is outside the boundaries for any monoblock melting. At 7.5 MA, toroidal gap edge melting is already an issue and full surface melting is still to be expected in 15 MA burning plasmas.

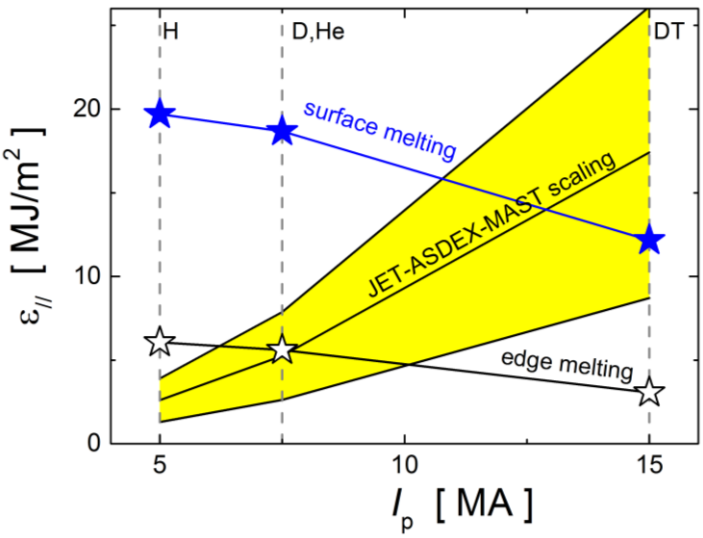

Figure C-4: Threshold on outer divertor target parallel ELM energy density as a function of I_p for full surface and toroidal gap edge melting. The yellow shaded area corresponds to the recent ELM energy density scaling for uncontrolled type-I ELMs (figure modified from [Gunn, 2017]).

These ion-orbit calculations have not yet been performed for intermediate combinations of I_p and B_t. The analysis in [Polevoi, 2017], whilst not including finite ion orbit effects, does attempt to combine the SOLPS boundary scalings mentioned at the beginning of this Appendix with the ELM parallel energy density scaling of Figure C-4 and scalings of pedestal pressure limits based on predictions from stability codes to estimate the point at which ELM-induced monoblock top surface melting becomes an issue on toroidally bevelled monoblocks for the full range of I_p and B_t, P_{SOL} and n_{sep}. The conclusions are slightly more pessimistic than those reached from Figure C-4 for the 7.5 MA/2.65 T case, showing that for the most pessimistic boundary of the ELM parallel energy density scaling, full surface melting could be achieved for $I_p \geq 5.5$ MA. At full toroidal field of 5.3 T this reduces to $I_p \geq 3$ MA, though it is unlikely that the large ELMs obtained in this case (ΔW_{ELM} ~10 MJ) would be compatible with sustained H-mode operation (high ELM energy densities on the first wall and large W influxes due to low ELM frequencies).

Ion orbit calculations are being performed to assess if further monoblock shaping can be applied to prevent ELM heat fluxes from reaching toroidal gaps (see presentations at the *ITER divertor monoblock shaping workshop* [ITER_D_ TFJJNH, 2016]), since toroidal gap edge melting will always occur before full surface melting (Figure C-4). Electron beam loading experiments are also planned to study the consequences of the very localized toroidal gap melting on the monoblocks performance.

Even if melting is completely avoided, ELMs will also contribute to W recrystallization since, although the ELM-averaged monoblock temperature may not exceed T_{recrys}, the ELMs will drive the surface over T_{recrys} for a very short time (< 1 ms). Assessing the cumulative effect of many ELMs in terms of recrystallization kinetics as performed for the steady state (Figure C-3 (lower)) is underway and is a function both of ELM amplitude, ELM frequency and the baseline inter-ELM monoblock temperature.

Finally, it should be stated that the transient energy density threshold for the onset of surface damage (roughening, development of small crack networks) can be extremely low when a large numbers of events are involved (as for example in the case of high frequency mitigated ELMs). Electron beam studies of repetitive fast transients (duration ~0.5 ms) with simultaneous steady state loading have found that for event numbers exceeding ~10^5, ELM energy densities should not exceed ~0.13 MJm^{-2} on the W surface [Loewenhoff, 2011]. This corresponds to ~2 MJm^{-2} parallel to the magnetic field on ITER and is comparable to, but still lower, than the parallel energy density required to avoid toroidal gap edge melting in Figure C-4.

Appendix D: Reference Pulse

A reference or standard discharge is run regularly, and in some cases at the start of every operational day, in many tokamaks, often motivated primarily to assess wall conditions and their evolution over a campaign [Ryter, 2002; Pitts, 2007; West, 2009]. Such a pulse can also be used to track variations in the L-H power threshold, the discharge impurity content and to provide a useful target for diagnostic calibrations, for example by providing information on the degradation of first mirror reflectivity. The plasma behaviour during this reference pulse can help optimize the machine performance by providing indications on the potential need for conditioning. In Tore Supra or JET, reference discharges have also been used to monitor the thermal response of the plasma-facing components and provide information on the presence and evolution of co-deposits [Corre, 2004; Chatelier, 2007] and variations in component surface emissivity (this is of interest depending on whether two-colour capability is eventually provided for the ITER IR camera systems or not). More recently, a dedicated monitoring discharge has been developed at JET to document wall conditions, but also the long-term evolution of erosion fluxes, material migration, material mixing and deposition in remote areas [Brezinsek, 2013-2; Krieger, 2013].

In a fully actively cooled device such as ITER, particularly one in which stationary power flux densities are expected to routinely attain PFC heat handling limits, the regular execution of a reference discharge is particularly appropriate. Signs of thermal fatigue, for example due to degradation of bond interfaces, can be identified by the relative overheating of components subject to the same input power flux density. The thermographic systems on ITER have been designed to cover ~90% of the first wall and divertor surfaces and will be capable, depending on the location in the field of view, of detecting temperature excursions with sufficient accuracy to determine anomalous behaviour (see, e.g., [ITER_D_TTPHKZ, 2017]) of sub-units of plasma facing components. In very critical areas, such as divertor strike point regions, this may allow pre-emptive action to be taken to ensure that degrading parts of plasma facing components do not continue to be overloaded leading to early failure.

As mentioned above, the gradual degradation of mirror reflectivity is a major concern for ITER diagnostics. A substantial R&D program has been underway for several years throughput the ITER Members' institutions to develop mirror cleaning techniques and shutter systems are foreseen for several diagnostics (see [ITER_D_QNDHTV, 2015]), but a periodically executed reference discharge will be required to track the performance of diagnostics relying on first mirrors.

To maximize the usefulness of the reference pulse, it should include several phases with different levels of heating power and different confinement modes. This approach has the advantage that the reference pulse can evolve as the machine capabilities evolve while data from the early phases of the discharge can be compared throughout the entire machine operations. The discharge could comprise an L-mode phase (including limiter operation) and two H-mode phases with different levels of heating power (to vary the wall ion flux and power to the divertor). Some variation of the divertor strike-point position could be included. The details of the scenario would need to be developed, but since the discharge needs to be run already during PFPO-1, it is likely that it should be run at half current/field (7.5 MA/2.65 T) at least for the non-active phases and partly into FPO. Once high current operation is routinely established, the pulse would likely be executed uniquely at the nominal B_t = 5.3 T. The frequency of execution will be decided once operations begin.

Appendix E: Non-inductive Scenarios with/without LHCD

The achievement of $Q = 5$ in very long pulse, fully non-inductive plasmas is an ultimate goal of the ITER project, and it may take a considerable period of experimentation and a variety of upgrades to achieve that goal. Among the potential upgrades of various systems, a lower hybrid (LH) heating and current drive system has been recently considered as a less favourable option due to the technical challenges anticipated in its installation and the lack of research and design activity in the fusion community compared to that being conducted in support of the electron and ion cyclotron wave heating and neutral beam injection systems. In this Appendix, candidate ITER steady-state operation scenarios previously reported in several key publications are reviewed and an assessment that also includes scenarios more recently developed is presented addressing a specific question: does the inclusion of an LHCD upgrade in the ITER H&CD capability confer particular advantages in achieving fully non-inductive operation with $Q = 5$ in ITER?

E.1 ITER steady-state operation scenarios reported in previous publications

Litaudon has performed a scan of the fusion power multiplication factor [Litaudon, 2006] using the 0.5-D METIS code [Artaud, 2008] at a wide range of the plasma confinement enhancement factor (H_{98}) and density profile peaking factor ($n_{e0}/\langle n_e \rangle$). In his work, 73 MW of total auxiliary heating power was assumed including 20 MW LHCD. The flat-top plasma current was allowed to vary with zero loop voltage applied after the start of the flat-top (SOF), and the flat-top phase was extended to achieve stationary non-inductive operation.

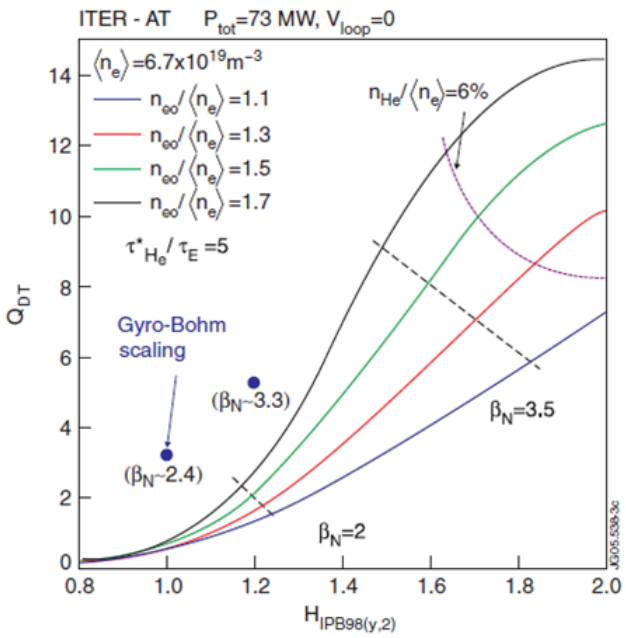

Figure E-1: ITER zero loop voltage operation ($V_{loop} = 0$): fusion gain, Q_{DT}, versus the confinement enhancement $H_{IPB98}(y,2)$ factor assuming ITER geometric parameters and with 73 MW applied power (33 MW NBI, 20 MW ICRF and 20 MW LHCD). Reprinted from [Litaudon, 2006].

The results from this scan are shown in Figure E-1 (reprinted from [Litaudon, 2006]). The fusion power multiplication factor rapidly increased along with H_{98} and density profile peaking factor. The target fusion gain ($Q = 5$) was achieved at $H_{98} = 1.6$ with a density peaking factor of about 1.3, whereas it was only accessible with a high density peaking factor (>1.5) at $H_{98} = 1.4$. Note that the non-inductive scenarios obtained at low H_{98} and Q would have a high Greenwald density fraction (above 1.0) as the flat-top plasma current was reduced while the average density was set to 6.7×10^{19} m^{-3}. This scan does not provide information on the operation space achievable with various ITER H&CD upgrade options. However, the applied modelling approach is useful for the assessment of various non-inductive scenarios with different confinement enhancement and H&CD upgrade options. Therefore, an additional modelling analysis performed using the METIS code is described later in this Appendix to address the specific question on the achievement of $Q = 5$ fully non-inductive ITER operation and H&CD upgrade options.

Various assessments of ITER steady-state operation scenarios developed using different tools and operation assumptions have been previously reported in the literature. In Kessel's study [Kessel, 2007], several ITER steady-state scenarios developed using TOPICS, TSC/TRANSP, CRONOS and ONETWO were compared. In these scenarios with a large variation of the H&CD mix, the flat-top plasma currents were assumed to be 8-9 MA. The non-inductively driven current fraction of about 72% was achieved in the CRONOS scenario by minimizing the use of NBI power, whereas fully non-inductive operation was achieved in the other scenarios. In the TSC/TRANSP and CRONOS scenarios, the fusion gain of $Q = 5$ was achieved with LHCD and high plasma confinement enhancement ($H_{98} > 1.6$). In the ONETWO scenario, $Q = 5.7$ was achieved at relatively lower confinement enhancement ($H_{98} = 1.42$), assuming, however, a high pedestal temperature of about 8 keV and a high density of 1.2 times the Greenwald density. In another CRONOS scenario reported by Garcia [Garcia, 2008], $Q = 6.5$ was achieved at $H_{98} = 1.7$ with only wave heating schemes including 13 MW LHCD. Wagner studied the various H&CD mixes and current drive efficiencies which are necessary for fully non-inductive steady-state operation [Wagner, 2010]. As an optimized case, 27 MW ECRH, 33MW NBI and 20MW ICRF power were selected and the confinement enhancement factor was varied from 1.37 to 1.78. In this scan, $Q = 4.4$-5.2 was achieved with $f_{NI} = 0.82$ - 0.90.

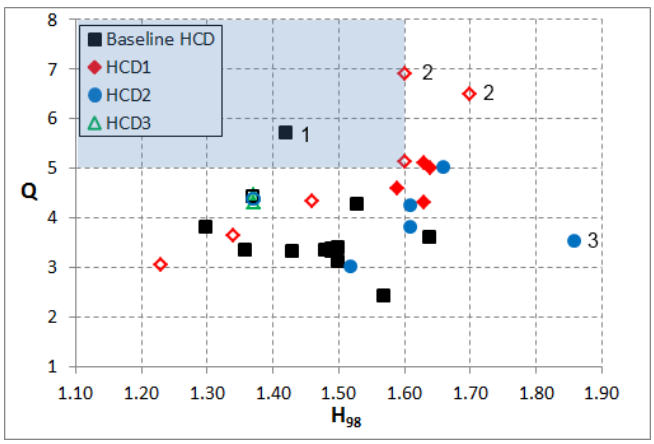

Figure E-2: Fusion gain (Q) versus the confinement enhancement factor (H_{98}) collected from the steady-state scenarios reported in various publications. Filled markers represent non-inductive ($f_{NI} > 0.95$) scenarios and open markers represent scenarios with $f_{NI} < 0.95$. The point indicated by '1' represents the ONETWO scenario. The two points indicated by '2' represent CRONOS scenarios ($f_{NI} < 1.0$). The point indicated by '3' represents the TOPICS scenario. Various HCD mixes are categorized as follows: Baseline HCD (or HCD0): within (33 MW NBI + 20 MW ECRH + 20 MW ICRF), HCD1: Baseline HCD + 13-25 MW LHCD, HCD2: Baseline HCD + 2-20 MW ECRH, HCD3: 53-73 MW ECRH.

Murakami has firstly benchmarked six different scenario modelling tools, TOPICS, TRANSP, CRONOS, ASTRAi, ASTRAk and FASTRAN, by applying the ITER baseline H&CD mix (33 MW NBI, 20 MW ECRH and 20 MW ICRF) to an ITER steady-state scenario ($I_p = 8$ MA) [Murakami, 2011]. The fusion gains obtained from various non-inductive operation scenarios ($f_{NI} \sim 1.0$) were 3-4, but with a relatively wide range of the plasma confinement enhancement ($H_{98} = 1.3$-1.5). An optimization of the fusion gain was attempted by reducing the ICRF power to 5 MW, and a fully non-inductive scenario with $Q \sim 4.3$ was achieved at $H_{98} = 1.53$. Another scan on the achievable fusion gain at different flat-top plasma current was also performed by allowing $f_{NI} < 1.0$. A scenario with $Q = 5$ was achieved at $I_p \sim 9.5$ MA ($f_{NI} \sim 0.8$), however fully non-inductive scenario was only accessible at $I_p \sim 8$ MA and with reduced fusion gain ($Q = 3.5$).

Poli has investigated fully non-inductive steady-state ITER operation with various H&CD mixes using TRANSP [Poli, 2012]. In her work, the desired fusion gain ($Q = 5$) was achieved at $H_{98} = 1.58$ - 1.65 with several H&CD mixes including 20-40 MW of LHCD power. Kim has studied various ITER steady-state operation scenarios using CORSICA [Kim, 2013]. A scan of the fusion gain at constant plasma current ($I_p = 9$ MA) was performed by varying the assumed plasmas confinement enhancement. In this scan with 16.5 MW NBI, 20 MW ECRH and

20 MW LHCD, Q = 3.1 - 5.1 were achieved at H_{98} = 1.23 - 1.60 and f_{NI} = 0.67 - 0.87. A fully non-inductive scenario developed assuming H_{98} ~ 1.6, Q = 4.2 was achieved without including LHCD in the H&CD mix (33 MW NBI and 40 MW ECRH). Polevoi has developed a new approach to explore the operation space for ITER steady-state operation [Polevoi, 2010]. In his study, the fusion gain was constrained (Q = 5) and the required confinement enhancement was calculated. A fully non-inductive operation scenario with 22 MW ECRH and 33 MW NBI required a value of H_{98} of 1.66.

Table E-1 – ITER steady-state scenarios reported in various publications (Power is in MW and the plasma current is in MA)

Author	Code	P_{NB}	P_{EC}	P_{IC}	P_{LH}	H_{98}	I_p	Q	f_{GW}	f_{NI}	HCD
Kessel	TOPICS[3]	33	40	17	0	1.86	9	3.5	<1.0	0.98	2
Kessel	TSC/TRANSP	16.5	0	20	**25**	1.63	8	5.1	<1.0	0.98	1
Kessel	CRONOS[2]	5.9	0	16.3	**20**	1.60	8.4	6.9	<1.0	0.72	1
Kessel	ONEWTWO[1]	33	20	20	0	1.42	9	5.7	**1.18**	1.01	0
Garcia	CRONOS[2]	0	20	20	**13**	1.70	8	6.5	0.90	0.90	1
Wagner	case A	33	20	20	0	1.37	9	4.4	0.97	0.82	0
Wagner	case B	0	53	0	0	1.37	9	4.45	0.97	0.72	3
Wagner	case C	0	73	0	0	1.37	9	4.3	0.97	0.71	3
Wagner	case D	33	40	0	0	1.37	9	4.38	0.97	0.83	2
Murakami	FASTRAN	33	20	20	0	1.49	8	3.31	0.85	1.06	0
Murakami	TOPICS	33	20	20	0	1.48	8	3.32	0.85	1.03	0
Murakami	TRANSP	33	20	20	0	1.43	8	3.31	0.85	0.99	0
Murakami	CRONOS	33	20	20	0	1.30	8	3.8	0.85	1.06	0
Murakami	ASTRAi	33	20	20	0	1.36	8	3.34	0.85	1.04	0
Murakami	ASTRAk	33	20	20	0	1.50	8	3.11	0.85	1.05	0
Murakami	FASTRAN	33	20	20	0	1.49	8	3.36	0.85	1.02	0
Murakami	FASTRAN	33	20	10	0	1.50	8	3.38	0.85	1.01	0
Murakami	FASTRAN	33	20	5	0	1.53	8	4.25	0.85	1.01	0
Poli	TRANSP	33	20	20	0	1.57	7	2.4	1.00	1.00	0
Poli	TRANSP	33	20	20	0	1.64	7.4	3.6	0.99	1.00	0
Poli	TRANSP	33	40	20	0	1.52	9	3	0.84	0.98	2
Poli	TRANSP	33	40	20	0	1.61	9	3.8	0.96	0.95	2
Poli	TRANSP	33	20	0	**20**	1.63	8.85	4.3	0.95	1.00	1
Poli	TRANSP	33	20	0	**20**	1.64	8.85	5	1.05	1.00	1
Kim	CORSICA	16.5	20	0	**20**	1.23	9	3.06	0.80	0.67	1
Kim	CORSICA	16.5	20	0	**20**	1.34	9	3.64	0.80	0.72	1
Kim	CORSICA	16.5	20	0	**20**	1.46	9	4.32	0.80	0.79	1
Kim	CORSICA	16.5	20	0	**20**	1.60	9	5.14	0.80	0.87	1
Kim	CORSICA	24.75	20	0	**20**	1.59	9	4.59	0.80	1.00	1
Kim	CORSICA	33	40	0	0	1.61	9	4.24	0.80	0.99	2
Polevoi	ASTRA	33	22	0	0	1.66	9	5	0.90	1.00	2

The ITER steady-state scenarios reviewed in this Appendix are summarized in Table E-1 and also shown in Figure E-2. The point indicated by '1' represents the ONETWO scenario in which the plasma density was assumed to be quite high (f_{GW} ~ 1.2). The two points indicated by '2' represent the CRONOS scenarios in which NB power was significantly reduced (<6 MW) and inductive current was provided to increase the fusion gain (therefore allowing f_{NI} < 1.0). The point indicated by '3' represents the TOPICS scenario in which H_{98} is increased to a very high value of 1.86. The

other steady-state scenarios were inside the region ($H_{98} < 1.66$ and $Q < 5.1$). By comparing the scenarios reported in these publications, several relevant observations can be drawn. Firstly, a plasma confinement enhancement (H_{98}) of above 1.6 is required to achieve $Q = 5$ operation ($f_{NI} \leq 1$) with the ITER baseline H&CD systems (33 MW NBI, 20 MW ECRH and 20 MW ICRF), if the flat-top density is lower than the Greenwald density and density peaking is limited to 1.5. Secondly, if $H_{98} = 1.6$ is achievable, fully non-inductive $Q \sim 5$ operation may be accessible with several H&CD upgrade options including additional ECRH and/or LHCD power. Lastly, one of the H&CD upgrade options, adding the 3rd HNB, was not explored in the previous studies.

E.2 METIS analysis of fully non-inductive ITER operation scenarios ($f_{NI} = 1.0$)

Based on the review of the previously developed ITER steady-state scenarios, an additional analysis has been performed to study the issues related to fully non-inductive ITER steady-state operation and the H&CD system upgrades. Firstly, potential H&CD upgrade options for achieving $Q = 5$ fully non-inductive steady-state operations were investigated. The confinement enhancement factor of 1.6 was assumed to allow the plasma to access to $Q = 5$ at fully non-inductive operation. Secondly, the confinement enhancement factor has been reduced to 1.2 to examine how plasma fusion performance varies across the various H&CD upgrade options at lower values of the plasma confinement enhancement factor. Lastly, a scan of Q versus H_{98} in fully non-inductive ITER operation was compared with the previous scan performed at a constant I_p ($f_{NI} < 1.0$ is allowed) using CORSICA. These scenarios are summarized in Table E-2 and also shown in Figure E-3.

E.2.1 Assuming a plasma confinement enhancement factor of $H_{98} = 1.6$

To study the achievement of $Q = 5$ fully non-inductive ITER steady-state operation, a confinement enhancement factor of 1.6 has been assumed based on the literature review previously undertaken. Such high confinement enhancement is identified as a necessary condition for accessing fully non-inductive steady-state operation with $Q = 5$. Several METIS scenarios with different H&CD upgrade options have been developed adopting the approach introduced by Litaudon [Litaudon, 2006]. The plasma density was constrained below the Greenwald density along with the achieved flat-top plasma current at a stationary state with zero loop voltage. Various H&CD mixes including several upgrade options are categorized as follows:

- Baseline H&CD (or HCD0) : Within 33 MW NBI + 20 MW ECRH + 20 MW ICRF
- HCD1 : Baseline H&CD + 20 MW LHCD
- HCD2 : Baseline H&CD + 20 MW ECRH
- HCD4 : Baseline H&CD + 16.5 MW NBI
- HCD5 : Baseline H&CD + 16.5 MW NBI + 20 MW ECRH

Note that 20 MW ICRF option was not included in the H&CD upgrade options (HCD1-HCD5) to optimize the fusion gain. In the non-inductive scenario with only the Baseline H&CD mix (Case1), $Q \sim 3.7$ was achieved with a non-inductively driven plasma current of about 7.5 MA. The fusion gain was increased to 4.9 (HCD1), 4.1(HCD2), 4.7(HCD4) and 5.3(HCD5) when the H&CD upgrade options were applied assuming a density profile peaking factor of 1.3. This comparison shows that a similar increment in fusion gain to that achieved by adding 20 MW LHCD power (HCD1) can be also achieved by adding either (16.5 MW NBI – HCD4) or (16.5MW NBI + 20 MW ECRH – HCD5). Replacing 20 MW LHCD (HCD1) by 20MW ECRH (HCD2) seems to be less efficient in optimizing Q as the ECCD efficiency off-axis ($\rho = 0.4$ - 0.5) achieved in this analysis was about half of the LHCD efficiency (2.2×10^{19} $m^{-2}AW^{-1}$). Adding a 3rd HNB (HCD4 and

HCD5) appears to be more efficient than adding 20 MW ECRH (HCD2). The maximum variation of the fusion gain (ΔQ) was about 1.6. The fusion gain can be further increased if higher density profile peaking (> 1.3) or flat-top density ($f_{GW} \sim 1.0$) can be maintained for non-inductive steady-state operation. Note that the dependence on the density profile peaking has been already studied [Litaudon, 2006; Poli, 2012; Polevoi 2010] and is also shown in the Figure E-1.

E.2.2 Assuming a reduced plasma confinement enhancement factor of $H_{98} = 1.2$

The H&CD upgrade options for fully non-inductive ITER steady-state operation were also compared at a reduced confinement enhancement condition ($H_{98} = 1.2$). Operating the plasma at such relatively modest confinement enhancement has been demonstrated in many tokamak devices and may also be more easily achievable in ITER. In the non-inductive scenario only with the Baseline H&CD mix (Case2) as shown in Table E-2 , $Q \sim 1.3$ was achieved with a non-inductively driven plasma current of about 5.9 MA. With the H&CD upgrade options, the fusion gain was slightly increased to 1.7 (HCD1), 1.6 (HCD4) and 1.8 (HCD5, Case12), whereas it remained similar with the ECRH system upgrade option (HCD2). The maximum variation of the fusion gain was about 0.5, indicating that the fusion gain achievable at reduced confinement enhancement would be less sensitive to the H&CD upgrade options. This comparison also shows that the fusion gain may approach $Q \sim 2$ with several H&CD upgrade options if the density profile peaking and flat-top density can be further optimized.

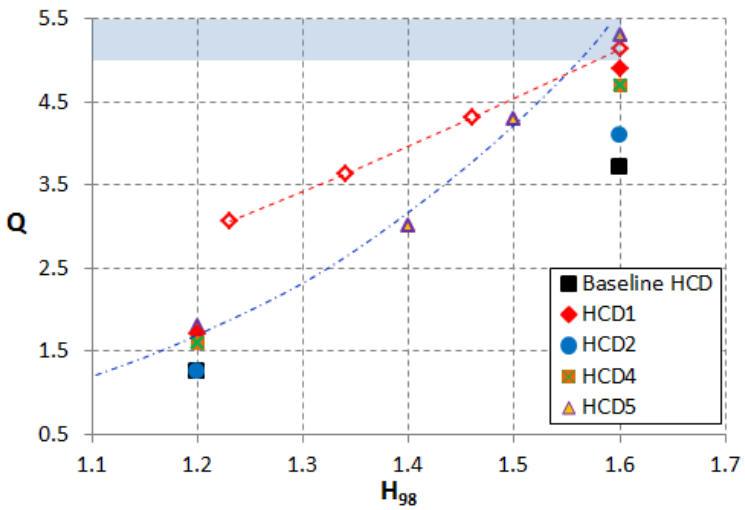

Figure E-3: Fusion gain (Q) versus the confinement enhancement factor (H_{98}) obtained from the scenarios developed using METIS and CORSICA. Open markers (of HCD1) represent CORSICA scenarios at a constant flat-top plasma current of 9 MA (f_{NI} = 0.67~0.87) and the other markers represent fully non-inductive METIS simulations (f_{NI} = 1.0). The blue dash-dot line is replotted from the red solid line (density profile peaking of 1.3) shown in the Figure E-1. Various H&CD mixes are categorized as follows: Baseline H&CD (or HCD0): Within 33 MW NBI + 20 MW ECRH + 20 MW ICRF, HCD1: Baseline H&CD + 20 MW LHCD, HCD2: Baseline H&CD + 20&MW ECRH, HCD4: Baseline H&CD + 16.5 MW NBI, HCD5: Baseline H&CD + 16.5 MW NBI + 20 MW ECRH.

E.2.3 Steady-state operation at a constant I_p ($f_{NI} < 1.0$)

A scan of the Q versus H_{98} in fully non-inductive operation has been additionally performed using METIS (listed in Table E-2), and has been compared with the previous scan at a constant plasma current (I_p = 9 MA) performed using CORSICA (listed in Table E-1). These two scans are compared in Figure E-3. The red dashed line shows the scan at constant plasma current (f_{NI} = 0.67 - 0.87) and the blue dash-dot line shows the scan in fully non-inductive operation (I_p = 7.9 - 10.1 MA). The fusion gain in fully non-inductive operation was rapidly increased as the confinement enhancement factor was increased from 1.2 to 1.6. This was due to the strong dependence of the energy confinement time (τ_E) on the plasma current. This comparison shows that

the dependence of the fusion gain on the confinement enhancement factor is stronger for the fully non-inductive operation (f_{NI} = 1.0), implying that achieving high confinement enhancement (H_{98} ~ 1.6) would be critical for Q ~ 5 fully non-inductive ITER operation. This comparison also shows that modest fusion gains (Q = 2-5) may be achievable in long-pulse operation (~3000 s) with H_{98} = 1.2 - 1.6, if the flat-top plasma current is constrained for better confinement. Note that 20 MW LHCD (HCD1) was included in the CORSICA simulations, whereas the 3rd HNB and an additional 20 MW ECRH (HCD5) were included in the METIS simulations.

Table E-2 – ITER steady-state scenarios developed using METIS: a density profile peaking factor of 1.3 was assumed (power in MW, plasma current in MA)

Case	P_{NB}	P_{EC}	P_{IC}	P_{LH}	P_{Aux}	H_{98}	I_p	Q	f_{GW}	f_{NI}	β_N	HCD
1	33	20	20	0	73	1.6	7.5	3.7	0.90	1	2.8	0
2	33	20	20	0	73	1.2	5.9	1.3	0.85	1	1.9	0
3	33	20	0	20	73	1.6	9.1	4.9	0.93	1	2.8	1
4	33	20	0	20	73	1.2	7.4	1.7	0.91	1	1.8	1
5	33	40	0	0	73	1.6	8.2	4.1	0.95	1	2.8	2
6	33	40	0	0	73	1.2	6.6	1.2	0.89	1	1.8	2
7	49.5	20	0	0	69.5	1.6	8.5	4.7	0.91	1	2.9	4
8	49.5	20	0	0	69.5	1.2	7.0	1.6	0.84	1	1.9	4
9	49.5	40	0	0	89.5	1.6	10.1	5.3	0.84	1	3.4	5
10	49.5	40	0	0	89.5	1.5	9.2	4.3	0.92	1	3.0	5
11	49.5	40	0	0	89.5	1.4	8.6	3.0	0.90	1	2.6	5
12	49.5	40	0	0	89.5	1.2	7.9	1.8	0.85	1	2.0	5

E.3 Plasma stability analysis

A stability analysis has been performed to compare the resulting plasmas from the various H&CD upgrade options with or without LHCD. Two METIS simulations shown in Table E-2 , Case3 (33 MW NBI + 20 MW EC + 20 MW LH) and Case9 (49.5 MW NB + 40 MW EC), have been selected for this comparison. These two simulations were reproduced using the 1.5-D CORSICA code to improve the quality of the scenario simulation taking the ITER H&CD configuration into account as well as to verify the feasibility of steady-state operation in terms of various PF coil and power supply limits. The modelling of the plasma edge pedestal has been also improved with increased radial profile resolution as well as using the EPED1 estimates [Snyder, 2011]. As the plasma temperature was more peaked in the CORSICA simulations (Case3C and Case9C in Table E-3), the Q values were slightly higher than those in the METIS simulations (Case3 and Case9 in Table E-2). These two CORSICA simulations were then repeated using ASTRA [Pereverzev, 2002] to further improve them by including the fast ion pressures in the evaluation of the equilibrium and plasma β. Finally, two plasma stability analysis codes, KINX [Degtyarev, 1997] and MISHKA [Mikhailovskii, 1997], have been applied and the plasma MHD stability of the two scenarios has been studied. As MHD stability issues were identified for Case9C, a variant of Case9C with reduced EC power (30 MW) and plasma density, Case9Ca, has been also additionally developed to reduce the β_N to a value close to that in Case3C. This scenario has been also analyzed to compare MHD stability of plasmas with similar β_N values, but different H&CD mix (Case3C vs Case9Ca). All three cases are summarized in Table E-3 and the KINX plasmas stability analysis is summarized in Table E-4.

To study the MHD stability analysis of a given scenario, β_N has been varied with fixed $j_{||}$ and scaled pressure gradient ($dp/d\psi$) profiles, and marginally stable values were identified for various MHD instabilities. In both Case3C and Case9C, all the critical MHD modes considered were unstable ($\beta_{N,limit} < \beta_N$), although the $\beta_{N,limit}$ values for the n = 1 external mode were slightly increased when the presence of the ITER wall shown in Figure E-4 was considered (compared to the no-wall evaluation). The limit for internal modes was set by the n = 3 mode, and this was particularity unstable in Case9C, with a relatively low $\beta_{N,limit}$ of 2.54. It appears that the higher core plasma pressure gradient, resulting from the high NBI and EC power levels, is responsible for such a low $\beta_{N,limit}$ for the n = 3 internal mode. On the other hand, for Case9Ca, which has a plasma beta comparable with that of Case3C and less peaked core plasma pressure profiles, the $\beta_{N,limit}$ for the n = 3 internal mode was comparable (2.98) to that of Case3C. The n = 1 external mode stability is also improved for both the no-wall and ITER wall studies for Case9Ca compared to Case9C, and the n = 1 external mode with the ITER wall becomes marginally stable ($\beta_{N,limit} \sim \beta_N$). The higher l_i of Case9Ca compared to that of Case3C was identified as beneficial for the improved n = 1 external mode stability of this plasma. MISHKA stability analysis performed in parallel for the same plasmas has confirmed the KINX results.

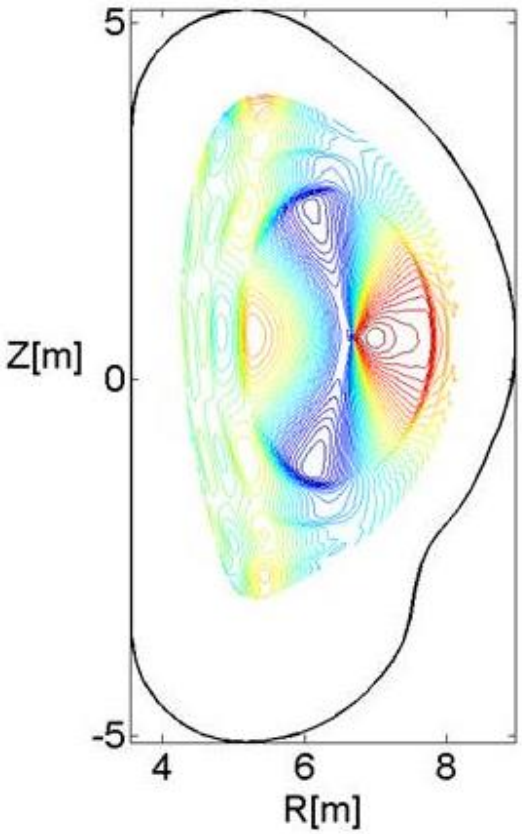

Figure E-4: The model of the ITER conformal wall (black line) used in KINX stability analysis.

Based on these plasma stability analyses and their comparison, the H&CD upgrade option which includes LHCD appears to be less favourable in terms of plasma MHD stability for the achievement of high-β_N non-inductive plasmas. As LHCD provides driven current at a far off-axis location in ITER plasmas, the plasma inductance (l_i) will be reduced compared to values likely to be produced with H&CD upgrade options which do not include LHCD. For the suppression of the n = 3 internal mode, which may require either an optimization of local pressure gradient at the low magnetic shear region or an active control of magnetic shear at the high pressure gradient region, upgrading the ECCD power is shown to be beneficial. As ECCD current drive is less efficient than that of LHCD for a given power level, this needs to be compensated by additionally adding a 3rd NBI beamline when LHCD is removed from the H&CD mix. Therefore, considering the stability of target plasmas for non-inductive operation having similar β_N with and without LHCD, the H&CD upgrade option including both the 3rd NBI beamline and a total of 40 MW EC appears to be equivalent to, and perhaps even more flexible than, the H&CD upgrade option including 20 MW LHCD. It is also worth mentioning that the values of $\beta_{N,limit}$ estimated for the n = 3 internal mode in our studies are likely to be conservative values, because the presence of the fast particles is expected to have beneficial effects in improving the plasma stability against internal modes; this is an effect which is well known and characterized for the n = 1 mode (associated with sawteeth) and that needs to be assessed in detail for the n = 3 mode in these plasmas.

Table E-3 – ITER steady-state scenarios developed using CORSICA: A density profile peaking of 1.3 was assumed (power is in MW and the plasma current is in MA)

Case	P_{NB}	P_{EC}	P_{IC}	P_{LH}	P_{Aux}	H_{98}	I_p	Q	f_{GW}	f_{NI}	β_N	H&CD option
3C	33	20	0	20	73	1.59	9.0	5.7	0.94	0.99	2.91	1
9C	49.5	40	0	0	89.5	1.61	10.0	6.3	0.91	0.98	3.30	5
9Ca	49.5	30	0	0	79.5	1.61	10.0	5.4	0.80	0.98	2.94	5

Table E-4 – $\beta_{N,limit}$ from KINX stability analysis: β_N has been varied with fixed $j_{\|}$ and scaled pressure gradient (dp/dψ) profiles, and marginally stable values were identified for various MHD instabilities; β_N is recomputed using ASTRA including the pressure from fast α-particles and beam-injected ionx; the β_N and l_i computed from CORSICA are indicated by (*).

MHD modes	Case3C $P_{NB}/P_{EC}/P_{LH}$=33/20/20 MW β_N=3.27(2.91*), l_i=0.61*	Case9C P_{NB}/P_{EC}=49.5/40 MW β_N=3.78(3.30*), l_i=0.75*	Case9Ca P_{NB}/P_{EC}=49.5/30 MW β_N=3.34(2.94*), l_i=0.79*
n=1 no-wall	2.26	3.26	2.78
n=1 ITER wall	2.70	3.62	3.37
n=3 internal	2.96	2.54	2.98

E.4 Summary and Conclusions

From the literature review on modelling of ITER non-inductive steady-state operation, several conclusions can be drawn:

- High plasma confinement enhancement (H_{98} >1.6) was required to achieve Q = 5 operation ($f_{NI} \leq 1$) with the ITER baseline H&CD mix and a reasonable density profile peaking assumption (~ 1.3).
- Fully non-inductive steady-state operation at Q ~ 5 was achieved when additional LHCD (20-25 MW) was added.
- If other H&CD upgrade options equivalent to 20 MW LHCD are considered, it is also possible to achieve a fully non-inductive Q ~ 5 operation at H_{98} ~ 1.6.

In the additional analysis performed using METIS, some noteworthy findings are obtained from several comparative studies:

- With a high plasma confinement enhancement of H_{98} = 1.6, fully non-inductive Q ~ 5 operation may accessible with the following H&CD upgrade options and at optimized operation conditions (f_{GW} ~ 1.0, $n_{e0}/\langle n_e \rangle$ ~ 1.3 - 1.5):
    - Q ~ 4.9 with NBI/ECRH/LHCD/ICRF = 33/20/20/0 (i.e. Baseline +20 MW LHCD)
    - Q ~ 4.7 with NBI/ECRH/LHCD/ICRF = 49.5/20/0/0 (i.e. Baseline +3rd HNB)
    - Q ~ 5.3 with NBI/ECRH/LHCD/ICRF = 49.5/40/0/0: (i.e. Baseline +3rd HNB + 20 MW ECRH)

- At a modest plasma confinement enhancement of $H_{98} = 1.2$, fully non-inductive $Q \sim 2$ operation would be accessible with the H&CD upgrade options at optimized operation conditions ($f_{GW} \sim 1.0$, $n_{e0}/\langle n_e \rangle \sim 1.3 - 1.5$):
    - $Q \sim 1.7$ with NBI/ECRH/LHCD/ICRF = 33/20/20/0 (i.e. Baseline +20MW LHCD)
    - $Q \sim 1.6$ with NBI/ECRH/LHCD/ICRF = 49.5/20/0/0 (i.e. Baseline +3rd HNB)
    - $Q \sim 1.8$ with NBI/ECRH/LHCD/ICRF = 49.5/40/0/0: (i.e. Baseline +3rd HNB + 20 MW ECRH)
- Partially inductive ($f_{NI} > 0.6$) long-pulse operation (~3000 s) with $Q = 3$-5 may be possible with several H&CD upgrade options and at $H_{98} = 1.2 - 1.6$, if the flat-top plasma current is optimized for better confinement (i.e. higher I_p than in fully non-inductive operation).

From the plasma stability analysis performed using the KINX and MISHKA stability codes, it can be concluded that:

- Reduction of the internal inductance due to the inherently off-axis LHCD current drive noticeably reduces the MHD stability limit for n = 1 external modes.
- For fully non-inductive plasmas having similar β_N and $Q \geq 5$, from the plasma stability point of view, the H&CD upgrade option including both 3rd NBI and a total of 40 MW EC appears to be equivalent to, and possibly more flexible than, the H&CD upgrade option including 20 MW LHCD.

There are several research areas which require further study and analysis:

- Improvement of the physics basis on stable non-inductive operation at high plasma confinement:
    - Physics mechanism of the non-linearly coupled core-edge confinement improvement [Garcia, 2015].
    - Dynamic evolution of internal transport barriers for their control and/or avoidance.
- Stability of non-inductive scenarios against, in particular, NTMs, internal modes and RWMs together with control requirements for the sustainment of long-pulse operation at high-β_N.
- Optimization of multiple plasma profiles for achieving high plasma confinement ($H_{98} = 1.2 - 1.6$) and improved stability ($\beta_N \geq 4l_i$), using the baseline H&CD mix and its possible upgrades.

As a final summary and recommendation for ITER H&CD upgrade:

- Both 3rd HNB and 20 MW ECRH power upgrade can provide a non-inductive steady-state operation capability comparable to the H&CD upgrade option which includes 20 MW of LHCD.
- Further R&D effort will be necessary to establish routine plasma operation at higher confinement enhancement ($H_{98} = 1.4 - 1.6$).

Appendix F: Physics Analysis and Risks of 5 MA/1.8 T Scenarios

A detailed analysis of the loads on the ITER TF coils has shown that operation of the TF set at a toroidal magnetic field of 1.8 T will be possible with plasma currents of up to 5 MA. The main results and conclusions are summarized in [Mitchell, 2016]. The exploitation of this option becomes attractive if it is possible to operate the heating and current drive systems at these current and field values, since it offers the possibility of access to H-mode operation at lower injected powers, implying that H-modes (and ELM control) might be studied at an early stage of the research program.

The main results of physics studies of plasma scenarios performed at 5 MA/1.8 T are summarized in this Appendix. The basic assumptions considered in these analyses are that ECRH heating at 104 or 110 GHz ($\leq$ 6.7 MW) and at 170 GHz ($\geq$ 13.3 MW) will be available and fully absorbed in the plasma, 10 MW of ICRF will also be available and that the magnetic equilibrium during the current flat-top of these plasmas is essentially identical to that of the 15 MA/5.3 T H-mode scenarios. This allows, in principle the achievement of both He and H H-modes at 5 MA/1.8 T in PFPO-1 and PFPO-2. Specific studies on heating of these plasmas are being performed including detailed simulations of ECRH absorption in these modelled plasma scenarios. The initial simulations performed assumed that 20 MW ECRH heating can be maintained for arbitrarily long periods, whereas there may be limitations for the low-frequency portion of the ECRH power limiting it to pulses lengths of several tens of seconds (see Appendix G).

F.1 Plasma initiation with magnetic field of 1.8 T

Results of the study of plasma initiation with a magnetic field of 1.8 T are described in [Kavin, 2016-1] for hydrogen plasmas and in [Kavin, 2016-2] for helium plasmas. The studies have been performed with the 0-D plasma transport code SCENPLINT [Gribov, 2007], using the electromagnetic input data obtained with the TRANSMAK code [Belyakov, 2003], assuming Be as a single impurity. In the simulations the Be influx to the plasma was described by physical sputtering of the Be first wall due to the wall bombardment by hydrogen (or helium) ions and by Be ions. After breakdown, an additional gas puffing is required (less than about 10^{21} s^{-1}, assuming a total gas volume of 1000 m^3) for ramping-up the plasma density after the plasma initiation and for prevention of runaway electron generation.

The studies performed reached the following conclusions:

- The narrow range of gas pressure required for ohmic plasma initiation at B_t = 1.8 T indicates that its experimental achievement is possible, but very difficult in ITER. The experimental achievement of ohmic plasma initiation in helium appears to be more difficult than in hydrogen;
- ECRH-assisted plasma initiation (at 104 or 110 GHz) broadens the range of helium prefill pressure to $0.2 < p < 0.75$ mPa, assuming that 1 MW of ECRH power is absorbed in the plasma. At these high prefill pressures no generation of the runaway electrons is expected;
- The value of plasma current at the end of plasma initiation (t = 3.5 s) is approximately independent of the ECRH pulse duration, Δt_{ECRH}, if $\Delta t_{ECRH} > 1$ s. If $\Delta t_{ECRH} < 1$ s, the plasma current at t = 3.5 s decreases with a reduction of Δt_{ECRH} (by about a factor of 2 at Δt_{ECRH} = 0.1 s).

F.2 5 MA scenarios in a magnetic field of 1.8 T

Design and simulations of 5 MA full bore plasma scenarios at B_t = 1.8 T were performed using the DINA code [Khayrutdinov, 1993] with feedback and feedforward control of the plasma current, position and shape, assuming a W divertor and Be first wall, and assuming the separatrix position and shape during the current flat-top to be similar to those in 15 MA/5.3 T scenarios. It was also assumed that the maximum value of the current in the central solenoid CS1 coil at the initial magnetization and at the end of current flat-top is 20 kA (the design limit is 45 kA). The value of the initial magnetic flux provided by the PF system with this assumption is ~59 Wb.

F.2.1 5 MA hydrogen ohmic scenarios

The study of the maximum duration of the 5 MA current flat-top in hydrogen ohmic scenarios limited by 20 kA in the CS1 coil is described in [Kavin, 2016-2]. The blue line in Figure F-1 shows the duration of the 5 MA current flat-top versus assumptions on the tungsten content, $\gamma_W = n_W/n_e$, during the flat-top. With increasing γ_W, the duration decreases from 17 s, at $\gamma_W = 3\times10^{-5}$, to 7 s, at $\gamma_W = 25\times10^{-5}$. For comparison the duration of the 3 MA current flat-top is shown by the red line. Modelled electron and ion temperatures and density profiles in ohmic 5 MA/1.8 T hydrogen plasmas modelled with ASTRA are shown in Figure F-2.

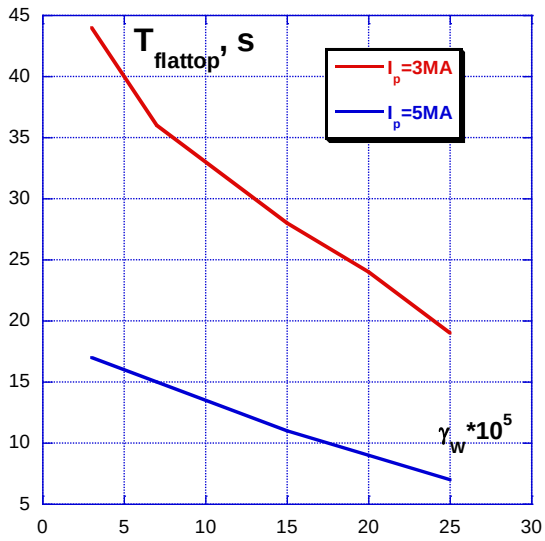

Figure F-1: Duration of the plasma current flat-top in 3 MA and 5 MA hydrogen ohmic scenarios for different assumptions on the W content, $\gamma_W = n_W/n_e$.

F.2.2 5 MA/1.8T helium H-mode scenario with 20 MW of ECRH

The simulation of a 5 MA helium H-mode scenario is described in [Kavin, 2016-4]. It is assumed that the plasma is in H-mode, when the power loss to the SOL, P_{SOL}, is higher than the power threshold value deduced from [Martin, 2008] for deuterium multiplied by C = 1.4 (for helium):

$$P_{SOL} > P_{H\ to\ L} = 0.0488 C n_e^{0.72} B_t^{0.8} S^{0.94}\ [MW,\ 10^{20} m^{-3}, T, m^2]\ ,$$

where $P_{SOL} = P_{heat} - P_{rad} - dW_{th}/dt$. The waveforms of Be, $\gamma_{Be} = n_{Be}/n_e$, and W, $\gamma_W = n_W/n_e$, concentrations assumed in the simulations are shown in Figure F-3.

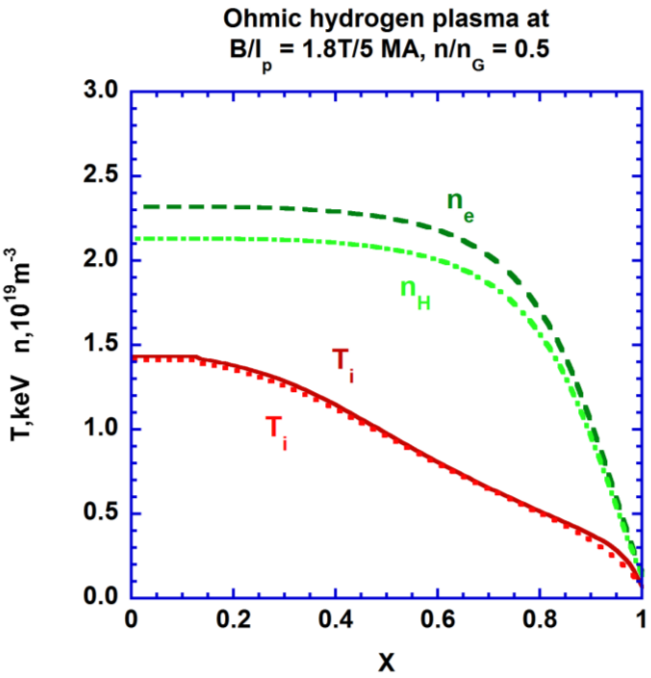

Figure F-2: The electron and ion temperatures and density profiles in ohmic 5 MA/1.8 T hydrogen plasmas simulated by ASTRA [Pereverzev, 2002], here at $<n_e> \sim 0.5 \times n_{GW}$. The simulation displays a very strong electron-ion coupling due to pure ohmic heating, as opposed to the case when 20 MW of EC power is applied described in section F.2.2 .

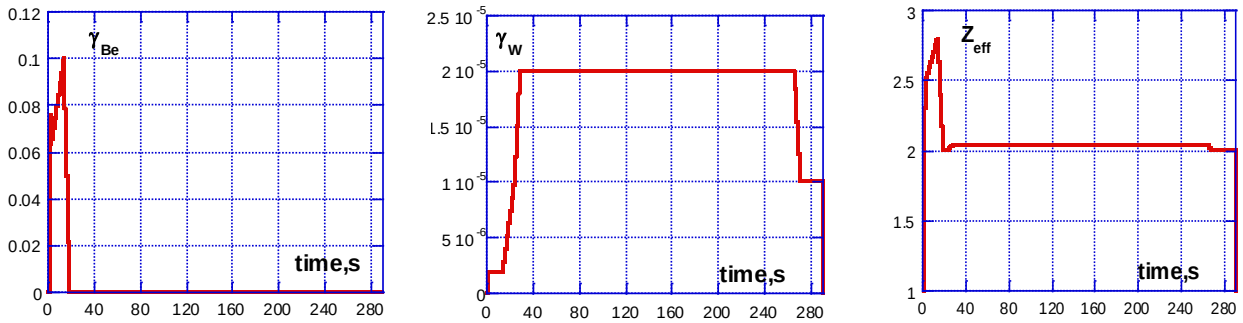

Figure F-3: Assumptions for the contents of Be and W, and the waveform of Z_{eff} obtained in 5 MA helium H-mode scenario.

An example of the scenario simulation with integrated control of plasma current, shape, plasma density with 20 MW of additional heating is shown in Figure F-4. During the plasma start-up, the ECRH (assuming 1 MW absorbed in the plasma) was used only during 2 s for assistance of plasma initiation, from the gas breakdown (t_{BD} = 1.1 s) until t = 3.1 s. The ECRH power is then switched off. The X-point is formed at t_{XPF} = 11.8 s ($I_p \approx$ 3.1 MA). At this time the volume averaged density of He ions is 0.15×10^{19} m^{-3}, and increases to $\sim 0.4 \times 10^{19}$ m^{-3} at the start of current flat-top (t_{SOF} = 20 s). During 4 s the density of He ions increases to from 0.8 to 1.6×10^{19} m^{-3} (t = 24 s), i.e. the ratio $<n_e>/n_{GW}$ increases from 0.2 to about 0.4. At t = 24 s 20 MW of ECRH is applied, leading to the L- to H-mode transition (at t = 25 s) with a subsequent increase in the density of He ions during 5 s to $\sim 2.0 \times 10^{19}$ m^{-3} (t = 29 s). This corresponds to $<n_e>/n_{GW}$ = 0.5 at the subsequent phase of the plasma current flat-top. The energy confinement time in H-mode is about 1.7 s. The plasma

density value is kept constant until the end of the plasma current flat-top (t_{EOF} = 265 s) – which assumes no limitation on the pulse length of the gyrotrons operating at 104 GHz[5].

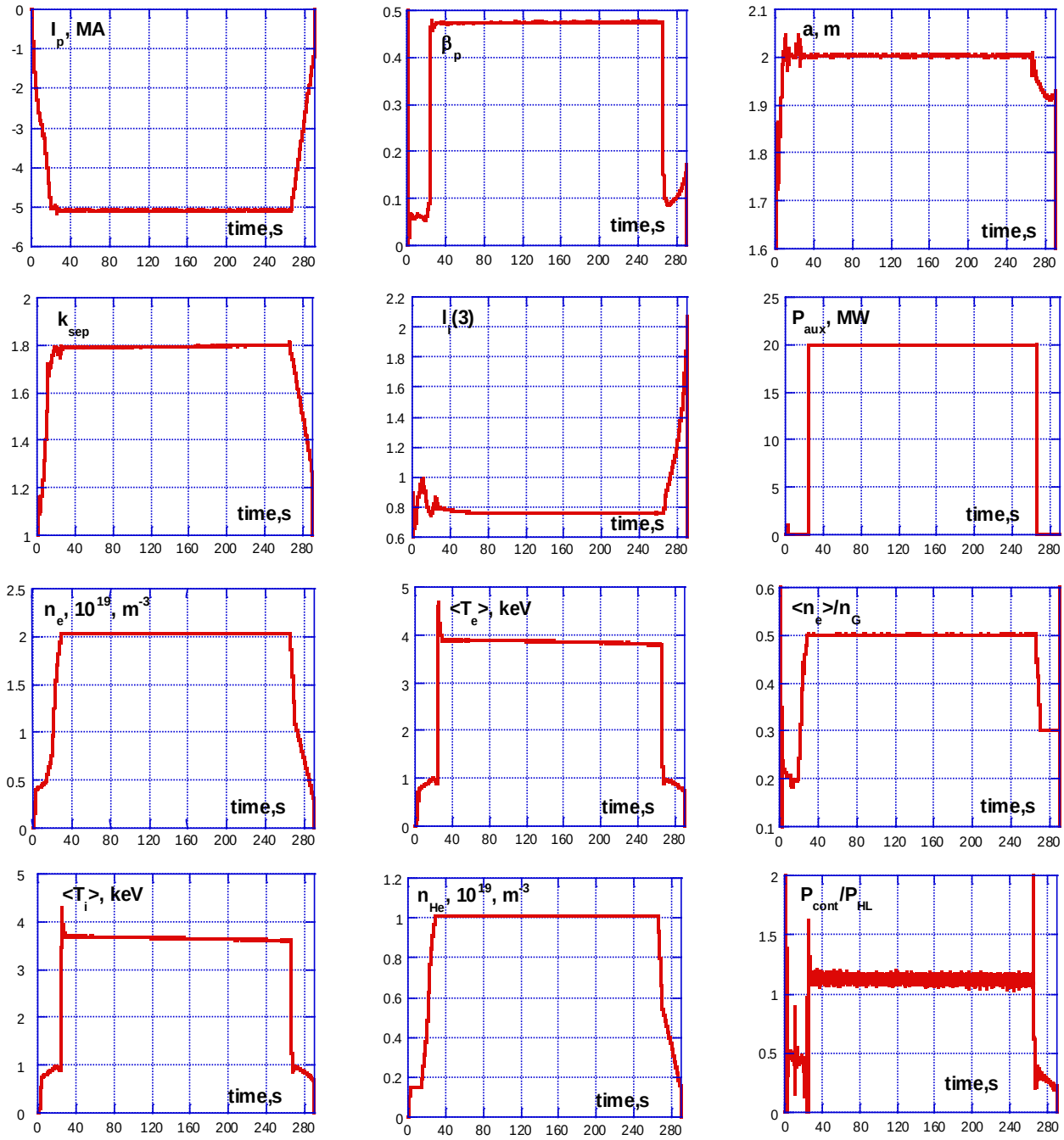

Figure F-4: Time evolution of I_p, β_p, minor radius, elongation, $l_i(3)$, ECRH power absorbed in the plasma in the 5 MA helium H-mode scenario, volume averaged electron density and temperature, volume averaged electron density normalized by the Greenwald density, volume averaged ion temperature, volume averaged helium density, and the ratio of the thermal conductive power loss to the L- to H-transition power threshold in the 5 MA helium H-mode scenario (assuming $P_{LH}^{He} = P_{LH}^{D}$).

[5] It is possible that the ECRH power pulse at 104 GHz may be limited to few tens of seconds; this remains subject of R&D and technical evaluation (see Appendix G).

The density which provides the minimum power for H-mode access, $n_{LH,min}$, has been evaluated on the basis of 1.5-D transport modelling as the density at which the edge ion power flux starts to saturate with increasing density (i.e. $P_i(n)/P_{tot} \approx P_i(n_{LH,min})/P_{tot}$ for $n > n_{LH\text{-}min}$). This follows the findings of ASDEX-Upgrade experiments [Ryter, 2014] that identified the key role that the edge power loss through the ion channel plays in accessing the H-mode, as described in Appendix B. It is found that, for 5 MA/1.8 T plasmas, this minimum density is $\langle n_e \rangle \sim n_{LH,min} \sim 0.4 \times n_{GW}$, as shown in Figure F-5, in agreement with the global multi-machine scaling evaluations described in Appendix B, and corresponds to the maximum of the ratio, $P_i(n)/P_{L\text{-}H}$. The actual ratio at which the edge power flow saturates depends on assumptions regarding the electron and ion transport (ratio χ_i/χ_e), but the value of the density at which saturation takes place depends weakly on this assumption, provided that the overall confinement is assumed to follow the L-mode scaling (this is the normalizing parameter for the actual values of χ_i and χ_e). Therefore, $\langle n_e \rangle \sim 0.4 \times n_{GW}$ can be taken as a good estimate of the density for the minimum H-mode threshold for ITER over a range of main ion species and fields/currents when $q_{95} = 3$, as originally identified for D plasmas in [Ryter, 2014], and discussed in more detail in Appendix B.

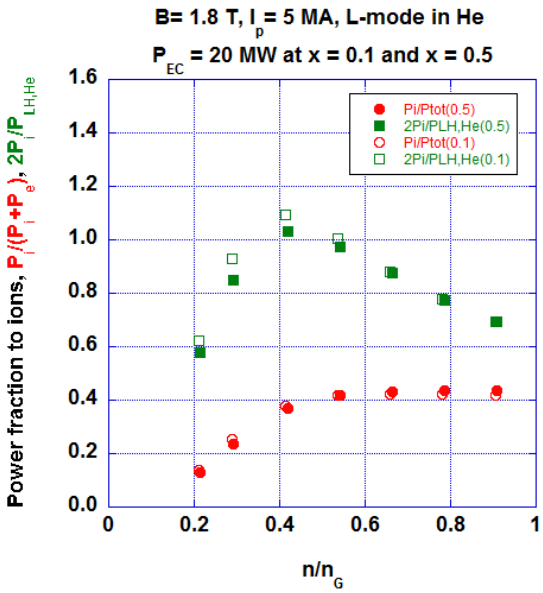

Figure F-5: Fraction of the edge power flow in the ion channel and expected margin to the H-mode threshold assuming that 50% of the value provided by the Martin scaling has to be conducted by the ion channel for 5 MA/1.8T He plasmas and 20 MW of ECRH heating.

Figure F-6 shows the electron and ion temperature and density profiles calculated by the METIS transport solver [Artaud, 2010] and by the 5-D kinetic Qualikiz neural network (NN) for turbulent transport [Citrin, 2015]. The green region represents the validity region of the Qualikiz NN. METIS predicts an electron-ion decoupling $T_e/T_i \sim 2$ while the Qualikiz NN predicts $T_e/T_i \sim 3$. This strong electron-ion decoupling in the plasma central region is due to the fact that these plasmas are heated by ECRH and have a very low plasma density and thus low electron-ion equipartition.

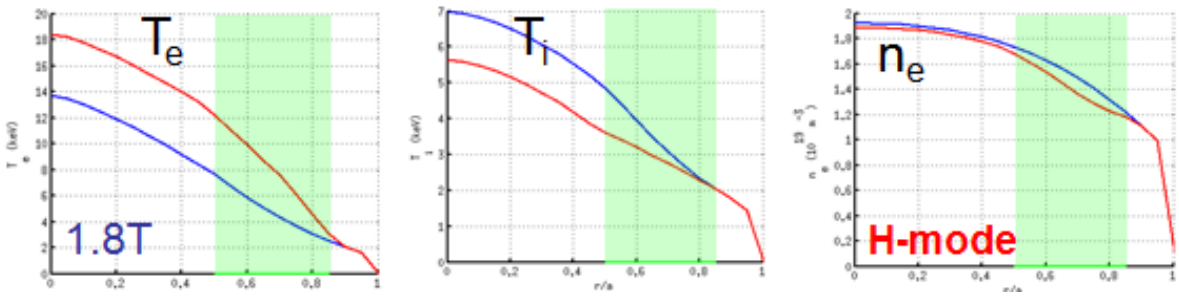

Figure F-6: Electron and ion temperature profiles as simulated by METIS (blue) and the Qualikiz Neural Network (red) for an H-mode helium plasma at 5 MA/1.8 T with 20 MW of ECRH.

Additional studies have been carried out to perform first principle turbulent transport simulations for these plasmas in order to evaluate energy and particle transport in the core plasma and the possible consequences for core confinement of these high T_e/T_i ratios. This modelling has been carried out with ASTRA for D plasmas – to overcome the isotopic effect which is not modelled correctly by first principle models – using the GLF23 and TGLF transport models, for ECRH-heated plasmas with 20 MW of ECRH and $<n_e>/n_{GW}$ ~ 0.5. Resulting kinetic profiles are displayed in Figure F-7. These simulations confirm the strong electron-ion decoupling T_e/T_i ~2.5-3.0 near the plasma centre (central ECRH is assumed in these simulations). Comparison of these ITER simulations with results from ASDEX-Upgrade experiments with ECRH-dominant heating shows comparable scale lengths for density and electron temperature for both GLF23 and TGLF, i.e. R/L_{ne} (~2) and R/L_{Te} (~5), as shown in Figure F-8. For the ion temperature, the scale length evaluated by GLF23 is much lower than in experiment (R/L_{Ti} ~ 2 compared to the experimental value ~ 4-8), while the TGLF values predicted for ITER are closer to those measured in ASDEX-Upgrade. It is important to note that in spite of the strong central decoupling between ions and electrons in the plasma centre, density values of $<n_e>/n_{GW}$ ~ 0.4-0.5 are sufficient to provide the strong coupling of the electrons and ions at the plasma edge, and therefore ensure sufficient ion power flow to sustain the H-mode.

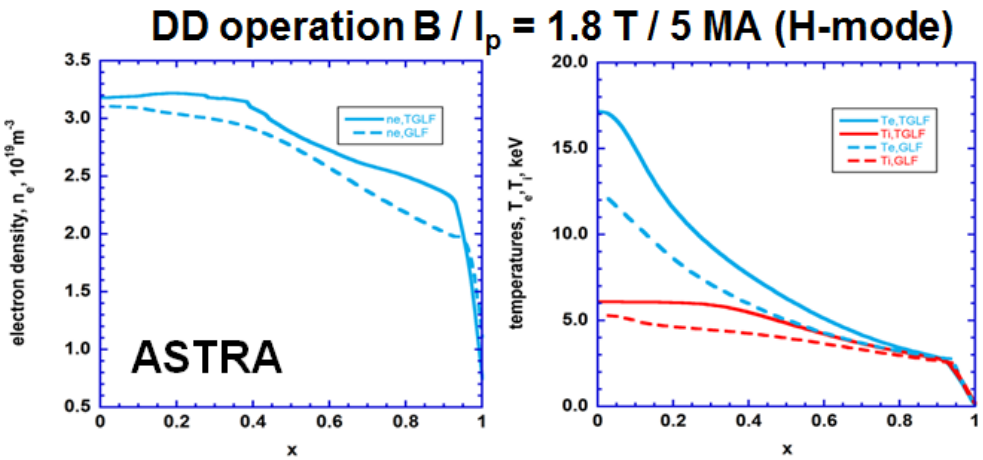

Figure F-7: Density (left) and temperature (right) profiles simulated by ASTRA with GLF23 (dashed lines) and TGLF (solid lines) for D plasmas with 20 MW of ECRH at $<n_e>/n_{GW}$ ~ 0.5.

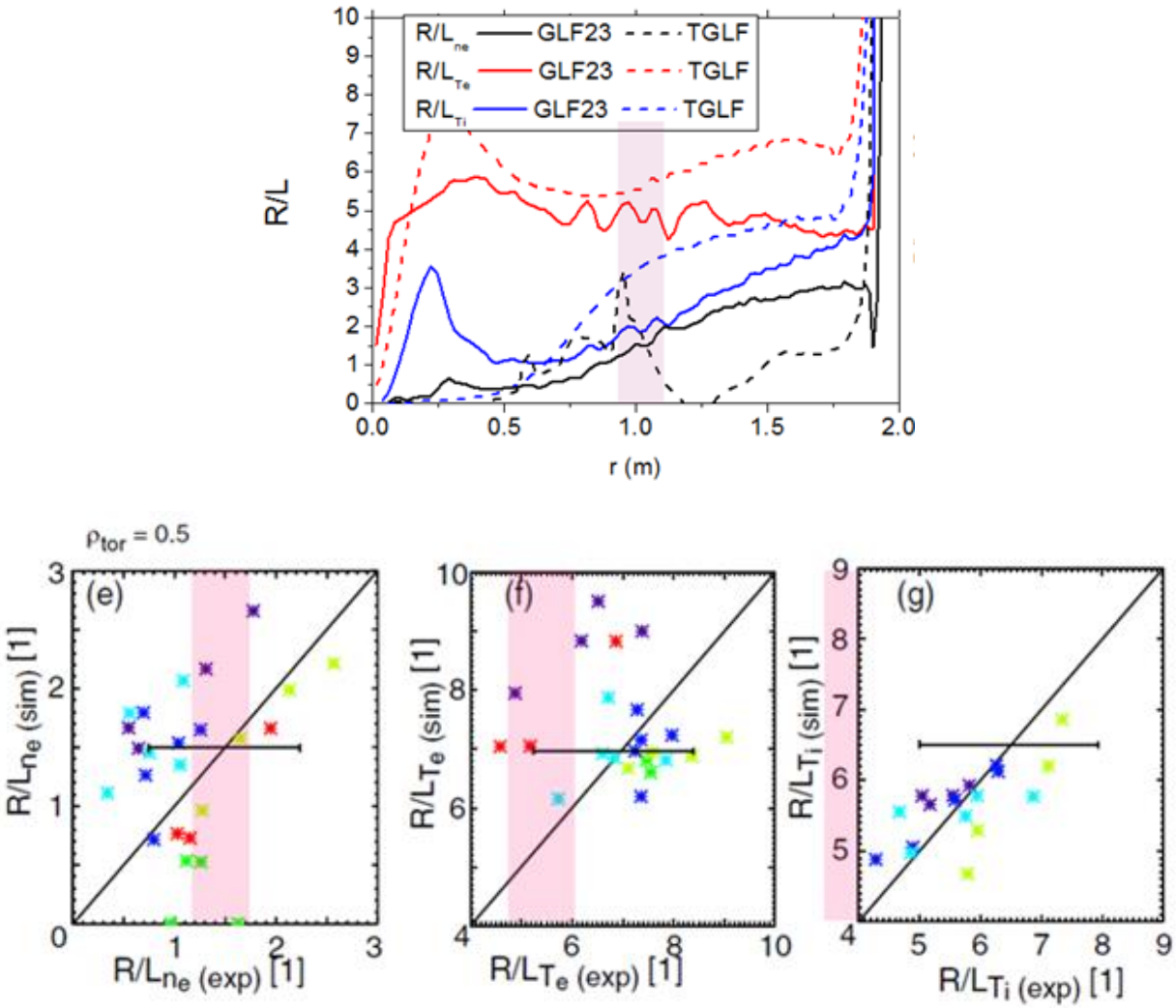

Figure F-8: Top: scale lengths R/L_{ne}, R/L_{Te} and R/L_{Ti} for ITER simulations of ASTRA 5 MA/1.8 T D plasmas with 20 MW of central ECRH and with anomalous transport modelled with GLF23 and TGLF. The pink region around r = 1m corresponds to ρ_{tor} ~ 0.5. Bottom: ASDEX-Upgrade experimental scale lengths for plasmas with dominant ECRH heating [Sommer, 2015]. The equivalent scale lengths for 5 MA/1.8 T D plasmas modelled with TGLF are illustrated by pink region on these figures, demonstrating reasonable agreement.

F.3 Toroidal field ripple for a toroidal magnetic field of 1.8 T

The toroidal field (TF) ripple has been evaluated for the vacuum vessel regular sectors at three levels of toroidal magnetic field (B_t = 5.3 T, 2.65 T and 1.8 T at 6.2 m) taking into account the reduced mass (by ~10%) of the ferromagnetic shielding blocks (ferromagnetic inserts) #30-35 (without change in their geometrical models). Moreover the measured value of the saturation magnetization of the steel SS 430 was used in the calculations ($\mu_0 M_s$ = 1.645 T).

The results obtained are reported in [Amoskov, 2016]. Figure F-9 shows the lines of constant values of the TF ripple in the vacuum vessel regular sectors at three different values of toroidal magnetic field. At 5.3 T, the peak value of the TF ripple is **+0.338**%, at 2.65 T it is **–0.538**% (the TF ripple is overcompensated by the ferromagnetic inserts) and at 1.8 T it is **–1.283**% (the ferromagnetic inserts further overcompensate the TF ripple).

The effect of TF ripple on the L-H power threshold, the pedestal performance and the ELM character and frequency has been described in Appendix B, and is expected to amount to a 20-30% pedestal pressure decrease for 1.8 T plasmas with 1.3% ripple compared to those at lower ripple. A reduction of the TF ripple can be obtained down to ~ 0.5% by decreasing the plasma radius and shifting the outer plasma separatrix inward by 40 cm while keeping q_{95} = 3 by increasing the plasma elongation. This poses no particular problem for He plasmas, which can be sustained by ECRH alone. However, if such ripple reduction strategy is required to obtain high quality H-modes in 5 MA/1.8 T plasmas, this may have deeper implications for hydrogen plasmas: these require ICRF heating to access and sustain the H-mode confinement regime, and coupling with such long distances between the plasma and the antenna (~ 55 cm), which may make ICRF coupling very challenging and thus H-modes difficult to sustain. Finally, the effects of this level of TF ripple on RF-accelerated ions and NBI ions need to be quantified by further modelling to determine whether the associated localized power fluxes on the first wall exceed the power handling limits or not.

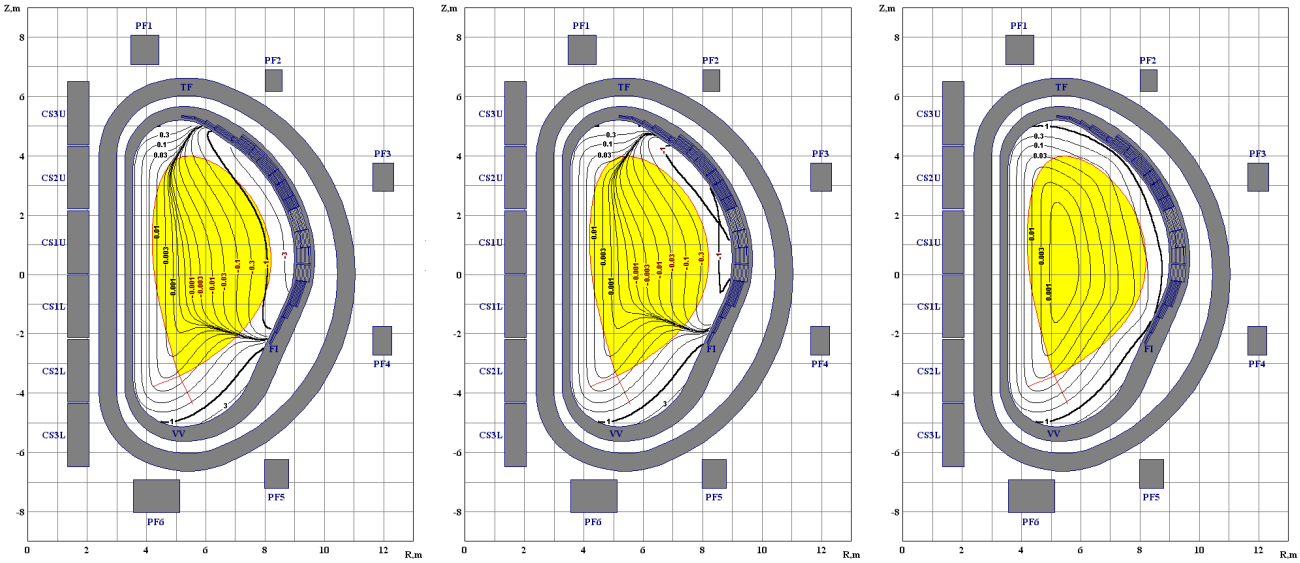

Figure F-9: Lines of constant values of the TF ripple in the vacuum vessel regular sectors at various values of the toroidal magnetic field at R = 6.2 m: 1.8 T (left), 2.65 T (centre), 5.3 T (right).

F.4 Specific issues on H-mode access and operation at 1.8 T

F.4.1 H-mode physics issues

The issues associated with access to H-mode operation at 1.8 T, and in particular during PFPO-1, deserve special discussion. The advantage of operation at 1.8 T to access the H-mode in PFPO-1 is illustrated in Table F-1 , which lists a series of possible scenarios with standard assumptions for the H-mode threshold for H/He/D/DT described in Appendix B. The selected operational density, $n_e \sim 0.4 \times n_{GW}$, corresponds to the expected density for the minimum H-mode power threshold for ITER. This density corresponds to the multi-machine scaling predictions [Ryter, 2014], and is found by ASTRA modelling to ensure good sharing of the edge power flow between the electron and ion channels. Below this density the edge ion power flow decreases with decreasing density. As described in section F.2.2 and Appendix B, this provides a good guideline for the evaluation of this minimum density for H-mode access and it is adopted for ITER evaluations.

Table F-1 – Predictions of H-mode threshold power for several scenarios according to the Martin 2008 scaling and standard ITER assumptions (Density values at $\langle n_e \rangle \sim 0.4 \times n_{GW}$).

$n_{e,min}$ (10^{20} m^{-3})	B_T (T)	S (m^2)	P_{th} - H_2 (MW)	P_{th} - He (MW)	P_{th} - D_2 (MW)	P_{th} - DT (MW)
0.16	1.8	683	20	10 - 15	10	8
0.25	2.65	683	37	19 - 28	19	15
0.5	5.3	683	106	53 - 80	53	43

Finally, as mentioned in section 2.5.4.9 and Appendix B, the effect of ~10 % helium on hydrogen plasmas H-mode access and performance should be further assessed in order to determine if the recent from recent JET [Hillesheim, 2016] can open a sizeable operational space for predominantly hydrogen H-mode plasmas in PFPO-1.

F.4.2 ECRH and ICRF heating of He and H plasmas

Exploiting the option for low field operation in ITER requires not only the ability to operate the TF set at 1.8 T, but also the ability to heat the plasma efficiently. This requires efficient ECRH heating at 1.8 T. The design frequency of 170 GHz corresponds to 3rd harmonic heating at 1.8 T that, *a priori*, may not have the highest efficiency; in addition, it does not allow the ECRH to be exploited for plasma start-up (no successful use of 3rd harmonic breakdown/ burn-through has been achieved on existing devices). A parallel activity to evaluate the possibility of operation of some fraction of the ECRH system at both 170 and 104 GHz or only at 110 GHz has, therefore, been launched, as described in Appendix G. In addition, analysis and design modifications will be required for specific transmission line (TL) and equatorial launcher (EL) components, as described in Appendix G. The aim would be to achieve ECRH pulse lengths of several tens of seconds either at 104 GHz or 110 GHz, which would be suitable for the experimental program foreseen to explore H-mode access at 1.8 T. It should be noted, however, that a recent study suggests that ohmic breakdown may be possible at 1.8 T in ITER [Sips, 2017]. Indeed, JET has demonstrated successful breakdown for B_t = 2.3 T and an electric field of 0.23 Vm^{-1}, confirmed by modelling performed with the DYON code. This indicates that ohmic breakdown in ITER at 1.8 T may be feasible.

Further ECRH commissioning time will be required if plasma scenarios at 1.8 T are to be explored in the PFPO-1 campaign. For the 1.8 T scenarios, commissioning of integrated operation of the ECRH system at 104 or 110 GHz would be undertaken, followed by the use and commissioning of the two frequencies of the ECRH system by combining 104 or 110 and 170 GHz gyrotrons. Using ECRH with 104 or 110 GHz frequency (representing a total EC power of up to 6.7 MW, injecting from the equatorial launcher) would be essential for 2nd harmonic breakdown, if ECRH start-up assist were required, as well as for plasma preheating at 1.8 T, if required to ensure adequate absorption of the main heating ECRH power at 170 GHz. This would provide a maximum absorbed ECRH power of ~20 MW for the development of the plasma scenario. This scenario will be further assessed with appropriate dedicated modelling of ECRH power absorption at these two frequencies integrated into the simulations.

As described in section 2.5.3, the foreseen ICRF scenarios at 1.8 T are 2nd harmonic H heating both in H and He plasmas. While this heating scheme is known to be efficient in H plasmas being a majority heating scheme, the efficiency of 2nd harmonic H minority heating in He plasmas remains to be confirmed and further quantified.

Since increasing the gap between the plasma and the wall is envisaged in order to reduce the magnetic field ripple, comprehensive data on the effect of increased outer separatrix to antenna gap on coupling of RF power to the core plasma is needed to predict the available absorbed ICRF power available for two basic plasma shapes proposed for PFPO-1 (standard and displaced inwards by 40 cm). The efficiency of ICRF coupling in H plasmas in the 5 MA/1.8 T conditions with reduced ripple can potentially have significant impact in the split of the operational time between hydrogen and helium H-modes at 1.8T in PFPO-1 and PFPO-2. Experiments during ITER construction need to develop a detailed database of the effect of ELMy and suppressed-ELM H-mode edge plasmas on coupling of ICRF power. The RF coupling is usually better in L-mode than in H-mode plasmas, due to the smaller edge density gradients. Optimizing the matching algorithm settings for the L- to H-mode transition, during which the coupling varies rapidly, will require due attention, since the H-mode access is only possible with coupled ICRF power for hydrogen plasmas. The acquisition of sufficient experimental data will allow optimization of the algorithm by better anticipation of the transition.

A few initial conclusions can be put forward regarding the ICRF coupling efficiency for these ITER 5 MA/1.8 T plasmas from the observations in JET experiments: 1.8 T H-mode scenarios have a very low density and a low collisionality, as discussed in Appendix B and section 2.5.4.9. Hence, the high energy tail of RF-heated ions may create high local power loads on the first wall, even without considering magnetic field ripple. This behaviour has been observed in JET for low density plasmas, as illustrated in Figure F-10 [Lerche, 2015-1].

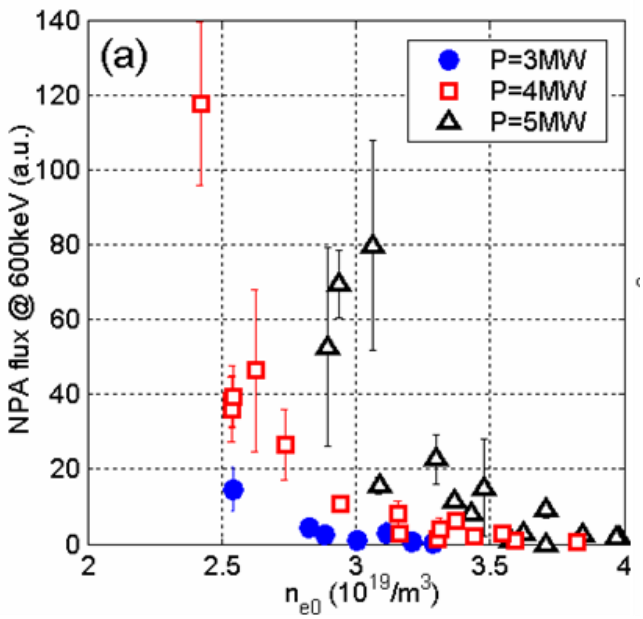

Figure F-10: Increase in the neutral particle analyzer signal for a range of ICRF powers versus plasma density. This increase is due to poor confinement of RF-heated ions at low fields, currents and densities.

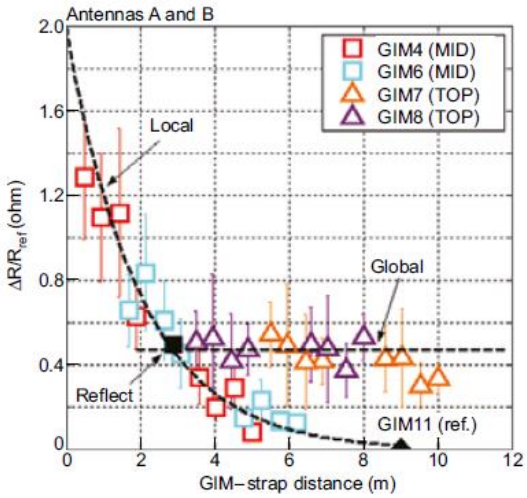

Figure F-11: ICRF coupling resistance as a function of the Gas Injection Module (GIM) - strap distance for mid-plane and top gas injection in JET.

ICRF coupling properties are very dependent on the value of the plasma density and on the location of the gas injection modules. In ITER, gas injection at the top is foreseen to fuel the plasma and to improve ICRF coupling performance. As described in section F.3, increasing the plasma-wall distance is the option to reduce the separatrix value of the magnetic field ripple at 1.8 T, and this may degrade the ICRF coupling efficiency. JET experiments have shown that the coupling does not significantly depend on the GIM-strap distance when using top injection[6] [Lerche, 2015-2], as illustrated in Figure F-11, which displays the coupling resistance versus the GIM-strap distance for top and mid-plane gas injection at JET. These observations suggest that the use of top gas fuelling in ITER should be explored in order to maintain good ICRF coupling if the plasma-antenna distance has to be increased to reduce TF ripple in 5 MA/1.8 T H-mode plasmas. Using a local midplane gas injection system instead of top injection is more likely to increase the coupling efficiency significantly in these conditions, as illustrated in Figure F-11. This modification of the gas fuelling capabilities is under assessment within the project [Schneider, 2017-2].

From the ICRF commissioning point of view, 1.8 T scenarios would be advantageous to test RF capabilities earlier in the research plan, particularly in H H-mode plasmas.

F.5 Physics risks

There are a number of physics risks to the success of these H-mode scenarios, associated with operation at 1.8 T, that need to be carefully considered and evaluated:

- *Plasma heating by ECRH:* for the 170 GHz ITER gyrotrons at 1.8 T, 3rd harmonic, or X3, central heating is available and has been demonstrated to work well in present-day devices, both in TCV plasmas preheated by X2 heating [Alberti, 2005] and in ASDEX Upgrade plasmas without X2 preheating [Hohnle, 2011]. Evaluating the necessity (or otherwise) of X2 preheating in ITER will require further simulation studies, but dual-frequency gyrotron operation if implemented for assisted ECRH breakdown/burn-through would, nevertheless, allow such a scenario in ITER.

[6] The worst case for ICRF coupling performance is divertor injection, the medium case is top injection and the best case is local injection from, e.g., the equatorial plane.

- *EC start-up assist:* reliable plasma start-up in ITER may require an assist from up to ~ 5 MW of ECRH, particularly at 1.8 T, where the connection lengths in the proximity of the toroidal null are shorter, unless ohmic breakdown can be achieved. Since the use of ECRH at 170 GHz in the X3 mode is not feasible due to low absorption at low temperature and density, start-up assist would require X2 ECRH heating at 104 or 110 GHz.
- *Toroidal field ripple:* the peak toroidal field ripple on the separatrix at 1.8 T for regular sectors (i.e. not NBI vacuum vessel sectors) is estimated to be -1.28%, as compared to -0.54% and 0.34% for 2.65 and 5.3 T respectively, as described in section F.3. At this level of ripple, reduced H-mode performance has been observed in present days tokamaks for low pedestal collisionality [Saibene, 2007; Saibene, 2008], although a much smaller effect is found on P_{LH} [Urano, 2006; Andrew, 2008]; further discussions on this topic can be found in Appendix B. If the level of 1.3% ripple at 1.8 T were found to degrade H-mode performance to an unacceptable level in ITER, one option for decreasing the level of ripple is to decrease the minor radius and displace the plasma radially inwards. To achieve a ripple at the separatrix of ~0.55% requires an inward displacement of the outboard mid-plane separatrix location from 8.2 to 7.8 m [Kavin, 2017] and adjustment of the plasma shape to keep q_{95} ~ 3. Although this plasma scenario has been shown to be controllable from the plasma position and vertical stability points of view [Kavin, 2017] the larger distance of the plasma to the ICRF antenna and to the ELM control coils poses specific challenges. Increasing the distance of the plasma separatrix to the wall by ~0.4 m (i.e. from ~ 0.16 m to 0.56 m) may strongly decrease the coupling resistance and this is likely to reduce the coupled ICRF power to very low values for such plasmas. The increase of distance from the plasma to the wall also significantly increases the distance from the ELM control coils to the plasma, which is typically 0.5-0.9 m for the un-shifted plasma position, and this reduces the magnitude of the field from the coils at the separatrix by a factor of ~ 1.5-2.0 depending on the coil location (Upper, Lower or Equatorial). Thus, the current to be applied to obtain a similar value of radial magnetic perturbation at the plasma surface to that in the reference separatrix position needs to be increased substantially.
- *Low density operation:* ITER's reference operating point for $Q = 10$ is at a plasma current of 15 MA and a line averaged density of ~ 10^{20} m^{-3}. However, the empirical H-mode density limit provided by the Greenwald density depends linearly on plasma current, and thus the equivalent operating point at 5 MA corresponds to ~ 0.35×10^{20} m^{-3} (i.e. at 85% of the Greenwald density). As discussed in Appendix B, experimental results indicate that there is a density minimum in the power threshold scaling for a wide range (but not all) of plasma conditions. A possible explanation for this density minimum is the thermal decoupling of ions and electrons at the plasma edge [Ryter, 2014], leading to a density for minimum power to access H-mode in ITER of n_e ~ $0.4\times n_{GW}$, corresponding to a density of ~1.6×10^{19} m^{-3} at 5 MA/1.8 T, in these ITER conditions. In addition, 5 MA/1.8 T operation at plasma densities of n_e ~ 2.0×10^{19} m^{-3} in PFPO-1 and PFPO-2 creates two issues for H-mode operation:
  - The poor collisional coupling between ions and electrons and the dominant electron heating in ITER leads to very large high radial T_e gradients in the plasma core and significant decoupling of the electron and ion channel, which may affect the energy confinement of the H-mode plasmas in this phase;
  - The low density operation in hydrogen plasmas leads to very low absorption of the heating neutral beam (HNB) and thus to large shine-through loads on the first wall and shield block panels. This restricts the power that can be injected in this type of plasmas with NBI in PFPO-2 or the length of the NBI heating pulse, particularly for hydrogen plasmas. On the

basis of recent assessments [Singh, 2017; Kim, 2017] the maximum power for long-pulse HNB operation in hydrogen plasmas with $n_e \sim 2.0\times10^{19}$ m^{-3} is 8 MW while for helium plasmas this is 16.5 MW, where the energy of the NBI ions is reduced to 500 and 650 keV respectively in order to decrease the shine-through loads.

- *Coupling of ICRF power with high ripple levels and through the L-H transition for hydrogen plasmas:* Using ICRF with a minority heating scheme leads to the formation of high energy ion tails and ions that can be trapped in the relatively high ripple (~1.28%) wells. Although the scheme foreseen for ICRF heating of hydrogen plasmas is not one which leads to very high energy tails (second-harmonic majority heating) the expected loads due to ICRF heating in these high ripple conditions need to be evaluated. Another important issue is that ICRF heating is essential to access the H-mode regime for hydrogen plasmas and, thus, good ICRF coupling needs to be maintained throughout the L-mode, L-H transition and H-mode phases. While resolving the issues of ICRF coupling to plasmas in H-modes with controlled and suppressed ELMs is required for the application of ICRF to ITER high-Q scenarios, the specific issue of maintaining good coupling through the L-H transition is critical for hydrogen H-mode operation in PFPO-1. In PFPO-2, the situation is somewhat less critical due to the possibility of using NBI heating at reduced power during this phase. Previous studies have shown that it is possible to maintain sufficient plasma coupling through the L-H transition to provide ~20 MW of ICRF heating in the access phase to $Q = 10$ plasmas; a similar assessment will be repeated for the H-mode access phase of hydrogen H-modes at 5MA/1.8T in the near future.
- *ELM control and MHD control:* Some of the baseline systems for MHD control will not be fully available in PFPO-1. For instance the set of power supplies for the ELM control coils will only allow a restricted set of 3-D field configurations to be produced and at a current level in the coils which will be much lower than in the baseline configuration, where every coil will be connected to its own power supply (e.g. fixed helicity n = 3 with maximum current level of ~30 kAt is foreseen for PFPO-1). This will require adjustment of the alignment between the applied magnetic perturbation and the plasma edge magnetic field through the adjustment of q_{95} in a similar way to current tokamak experiments. This substantially differs from the operational mode planned for PFPO-2 and FPO, where all power supplies will be available and the applied edge magnetic field perturbation will be adjusted to the value of q_{95}. The β_N of the H-mode scenarios is expected to be low (~1.2) and therefore it is not clear if the performance in these plasmas will be strongly affected by neoclassical tearing modes. If this is the case, it should be noted that the flexibility for NTM control in PFPO-1 will be reduced compared to that during PFPO-2 and FPO because of the reduced set of heating schemes in this phase. If a significant amount of off-axis ECRH/ECCD is required to control NTMs in these plasmas, this will reduce the available central heating and will most likely affect the performance of these H-mode plasmas, possibly leading to problems of W accumulation, if the remaining level of central heating is not large enough.

Appendix G: Heating and Current Drive Staging

The Heating and Current Drive systems in ITER are comprised of the Neutral Beam system for heating & current drive (HNB) and diagnostics (DNB), Ion Cyclotron for heating & current drive (ICH&CD) and the Electron Cyclotron for heating & current drive (ECH&CD). The combination of these 3 systems is designed to provide 73 MW of power for the PFPO (H/He) phase of operation, and up to 110 MW of injected power in the fusion power operation phase when including available upgrade options, which potentially range from a choice of a combination of an extra 20 MW of ECRH, 20 MW of ICRF, 16 MW of NBI or up to 40 MW of Lower Hybrid power (LHCD). The total installed power after upgrades can be up to 130 MW.

The current ITER Research Plan is based on PCR-738 that establishes the ITER Baseline [ITER_D_TL5BR3, 2016] and foresees the availability of 6.7 MW of ECRH for the First Plasma (FP) followed by the completion of the installation and operation of the ECRH system up to 20 MW for PFPO-1. In the current Baseline both the NBI and ICRF systems will be functional for the PFPO-2 experimental campaigns. The ITER Research Plan is elaborated on the basis that a further 10 MW of ICRF heating may be available within PFPO-1. Feasibility studies into accelerating the ICRF system to provide 10 MW for PFPO-1 are underway and are reported upon below.

This Appendix covers the following issues for the heating and current drive systems, which are key for the ITER Research Plan within the staged operation approach:

1. The proposal to operate at 1.8 T and the impact, primarily on the ECRH system;
2. The acceleration of 10 MW of ICRF power, to be made available for the PFPO-1 campaign;
3. The status of the investigation into acceleration of the NBI systems;
4. The upgrade possibilities of the heating systems, including the status of the LHCD system.

G.1 Implications of 1.8 T plasma operation for H&CD systems

Within the elaboration of the ITER Research Plan, the participant experts recommended to investigate the possibility of considering 1.8 T operation as this may enable access to H-mode operation within PFPO-1 and offer an H-mode scenario (5 MA/1.8 T) for which uncontrolled ELMs are not predicted to cause divertor monoblock melting in this and later phases of the research program (see Appendix C and sections 2.5.4.9 and 2.5.5.7). At its 21st meeting in October 2016, the STAC recommended further study of the implications of 1.8 T plasmas, both in terms of plasma operation and in relation to the performance of ITER auxiliary systems (especially for heating and current drive and diagnostic systems).

Operation at 1.8 T has primarily an impact on the ECRH system. The ECRH system is available for both PFPO-1 and PFPO-2 plasmas, and 1.8 T operation can have impacts on hardware, design, and requires additional physics analysis in order to maximize the efficiency of operation at this field. Regarding the possibility of combined heating for PFPO-1, taking advantage of the accelerated program for the ICRF system discussed below, it is not envisaged that any hardware changes will be needed. Therefore, there is no impact on the ICRF system hardware and the studies are centred on the optimization of the use of the baseline ICRF hardware for heating of 1.8 T plasmas, as discussed in Appendix F. Similarly the possible operation of 1.8 T with NBI in PFPO-2 does not have hardware implications for the NBI system; the main issue is here is to develop plasma scenarios with acceptable shine-through loads on the blanket shield block modules. This may impose limitations to the length of the NBI heating pulse and/or to the maximum ion beam energy

that can be used during this and, possibly, later phases (see 2.5.5.7 and 2.6.3.6), none of which impact the NBI hardware. The hardware of the ICRF and NBI systems is, therefore, not affected by 1.8 T operation and these systems are not discussed further in this section.

The ECRH system is designed for optimized operation at the nominal field of 5.3 T, and to provide a similar functionality at half field (2.65 T), in addition to reduced functionality at intermediate fields. The present design is compliant with the requirement for depositing the 20 MW across nearly the entire plasma cross section. It includes the potential for a power increase of up to 40 MW, with the addition of 24 1 MW gyrotrons, associated power supplies and transmission lines, located either in an extension to the RF Building or in the Assembly Hall. Note that no changes are required within the Tokamak Building for an ECRH upgrade option, as the additional gyrotrons and transmission lines (TL) will be connected to 56 entries available between the four upper launcher and one equatorial launcher.

This section describes the additional requirements imposed on the ECRH system for operation at 1.8 T, and the subsequent impact on the ECRH system design.

G.1.1 Impact of 1.8 T plasma operations on the ECRH system

Including 1.8 T plasma operation in the IRP (one-third nominal field) would require the ECRH system to provide the following functions:

- Up to 6.7 MW for Plasma start up using either O1 or X2, if required for plasma breakdown and burn-through;
- 20 MW of central heating in a combination of either O1, X2 and/or X3;
- consistency of the inclusion of the above requirements without sacrificing the functional requirements in the range of 2.65 T operation during the PFPO-1, PFPO-2 and FPO operating phases.

The primary impact on the ECRH system is driven by the need to provide breakdown and burn-through at one-third nominal field should this be required, as preliminarily evaluated by modelling in Appendix F. In order to meet this requirement, an additional lower frequency gyrotron operation mode is needed to provide these functions via either the O1 (~60 GHz) or X2 (~110 GHz) using the existing transmission lines (TL) and equatorial launcher (EL). Note that the upper launcher (UL) has a narrower frequency bandwidth not compatible with the above frequencies. The TL and EL offer broadband operation, but the range of 60 GHz is far outside the bandwidth, therefore only the X2 path is being investigated.

In order to maintain functionality at the 2.65 T operation (O1) a dual-frequency gyrotron is assumed, so that a set of up to 8 gyrotrons could either provide the X2 heating (~110 GHz) or the O1 heating (170 GHz). The Toshiba 170 GHz gyrotrons have already demonstrated operation at four frequencies (104, 137, 170 and 203 GHz), and the Japan-Domestic Agency (JA-DA) gyrotrons are configured for the EL steering mirrors that provide the breakdown and burn-through functions. Therefore, a design proposal utilizing the Toshiba tubes at either 104 GHz or 137 GHz, with a back-up option of using the 110 GHz tubes used for JT60-SA, which are compliant with the superconducting magnets and matching optics units of the 170 GHz gyrotrons, is being developed.

Preliminary ECCD analysis was performed by L. Figini and D. Farina (IFP-CNR) assessing the deposition ranges at the two frequencies as a function of the toroidal field and comparing these with the 170 GHz functionality, as shown in Figure G-1.

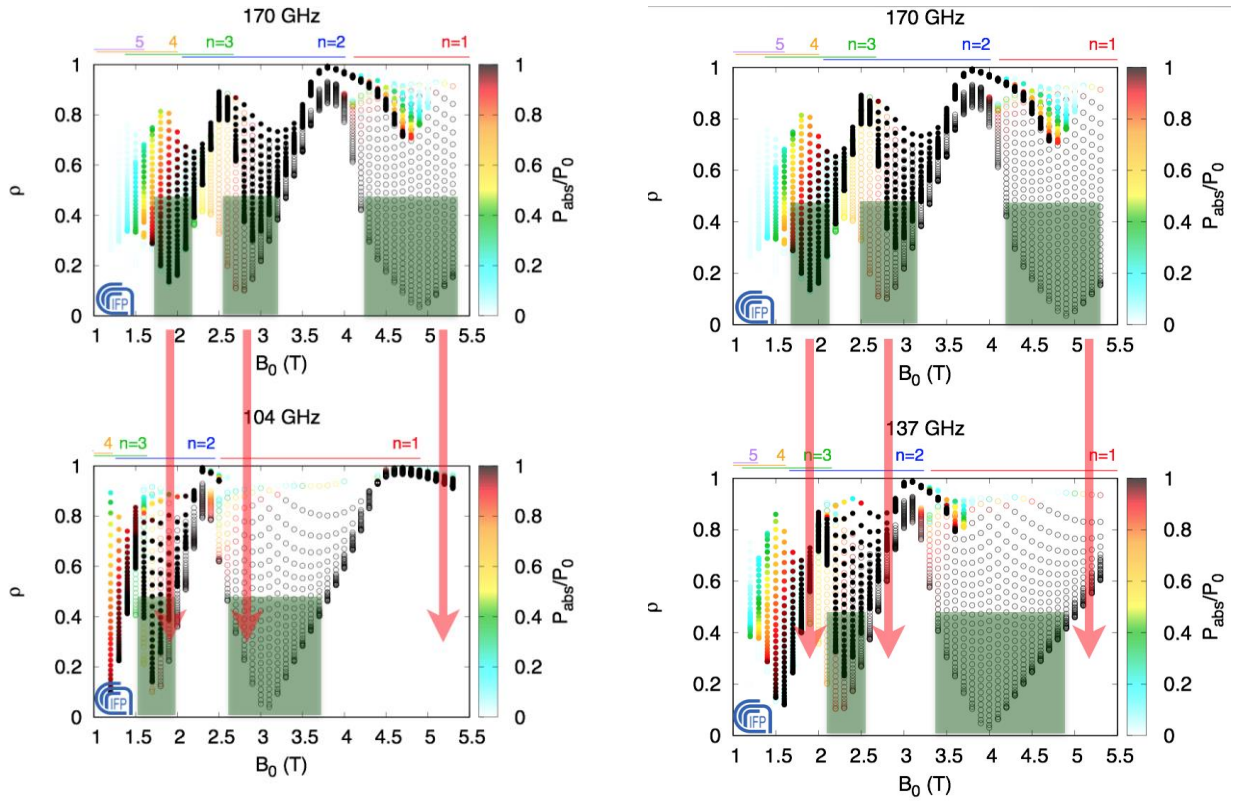

Figure G-1: (left) Comparison of the radial deposition location of the EC beam as a function of the toroidal magnetic field for the 170 GHz and 104 GHz frequencies and (right) the 170 GHz and 137 GHz frequencies. The deposition range is calculated for the end of flat-top, and the density and temperature profiles scaled proportionally with the magnetic field relative to the H-mode 15 MA / 5.3 T scenario.

The 104 GHz option has similar deposition ranges for the 1.8 T and 2.65 T operating ranges, while the 137 GHz option corresponds to poor central deposition for both the 1.8 T and 2.65 T ranges. Therefore, a path pursuing a dual-frequency 104/170 GHz operation is proposed, with the back-up of dedicated 110 GHz gyrotrons that would be replaced in the active phase once the 1.8 T operation has been concluded.

Note that the EC system has been designed for a single-frequency system, as the 170 GHz frequency achieved the required functionality at 2.65 T and 5.3 T considered in previous versions of the ITER Research Plan. Introducing the dual-frequency operation has a significant impact on the gyrotrons, TL and EL, which will be outlined in the following sections. Note that the upper launcher (UL) has a four mirror quasi-optical system that limits the operating bandwidth to a narrow region around 170 GHz, with the 104 GHz far outside this operating window.

G.1.1.1 Impact on Gyrotrons

The primary impact on the gyrotrons is the development of a 104 GHz/170 GHz dual-frequency gyrotron (DFG) with output power ≥0.8 MW and pulse lengths in the range of several tens of seconds. The present 170 GHz gyrotron procurement remains unchanged with the delivery of the eight tubes maintaining the present schedule. In parallel, the DFG would be developed using the present 170 GHz design, but with a three phase optimization, as illustrated in Figure G-2. There is a hold point at each phase that assesses the output power, mode purity and generated stray power. If

the results indicate that the DFG parameters mentioned above cannot be achieved, then the mitigation path of procuring 110 GHz tubes (JT60-SA) will be implemented.

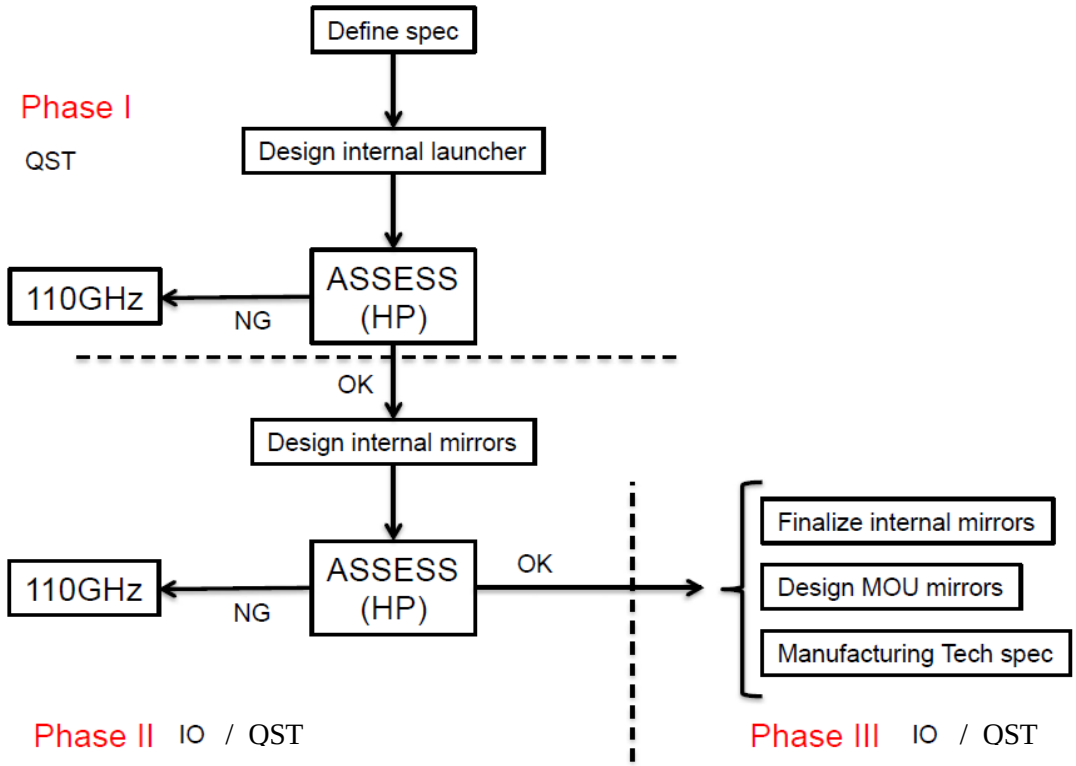

Figure G-2: Description of the different phases for the dual-frequency gyrotron study.

The first two phases will cover the new design of internal critical components: internal launcher and quasi-optical mirrors (see Figure G-3), and the last phase is focussed on the external matching optics unit and design finalization.

The most critical technical issue for developing a dual-frequency tube is to obtain a high efficient conversion from the excited mode in the cavity (either $TE_{19,7}$ for 104 GHz or $TE_{31,11}$ for 170 GHz) to the free space Gaussian mode (TEM_{00} for both frequencies) via the internal launcher. Then the 4 internal mirrors reshape and direct the beam out the diamond window with both frequencies having a common co-linear path; such that the two additional external mirrors can couple to the HE_{11} waveguide (not shown on the picture).

This study aims at finalizing the design of a dual-frequency tube with the following characteristics:

1. Transmission efficiency at diamond window: > 98% (both 104/170 GHz);
2. Gaussian mode at the diamond window: > 95% (both 104/170 GHz);
3. Coupling efficiency of more than 95 % from the TEM_{00} into an HE_{11} mode at the entrance of the waveguide (both 104/170 GHz);
4. Power transmission efficiency at the matching optics unit (MOU) of more than 96 % (both 104/170 GHz).

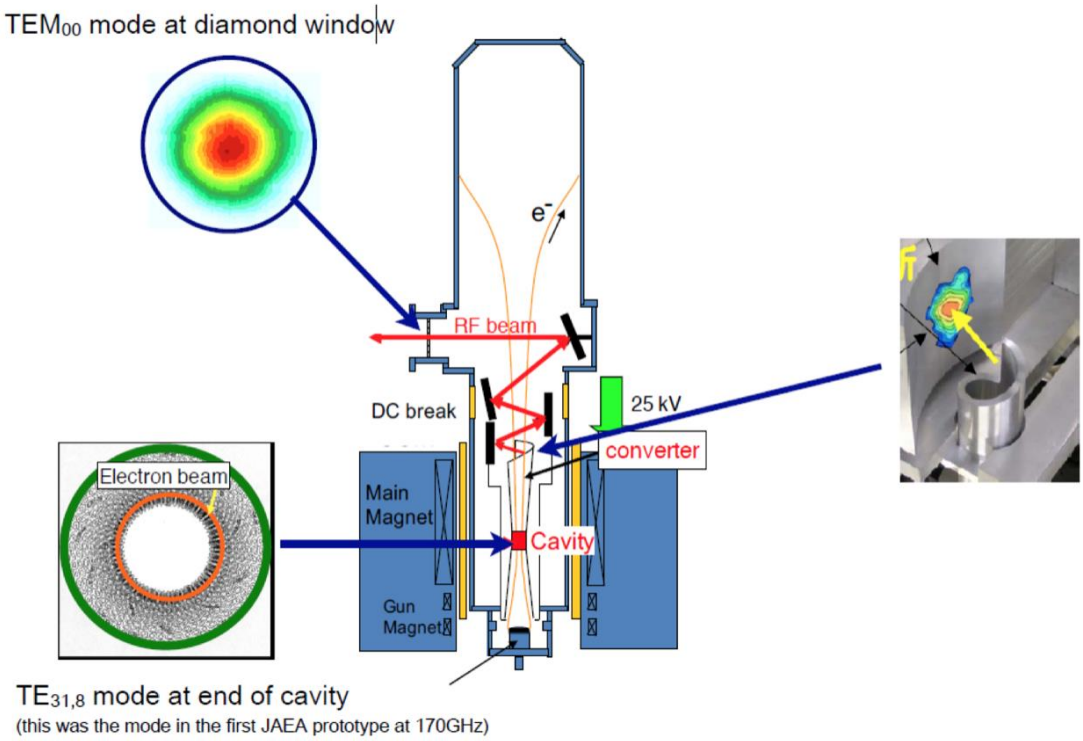

Figure G-3: Sketch of main parts inside the gyrotron showing the critical components to be modified for a dual-frequency tube.

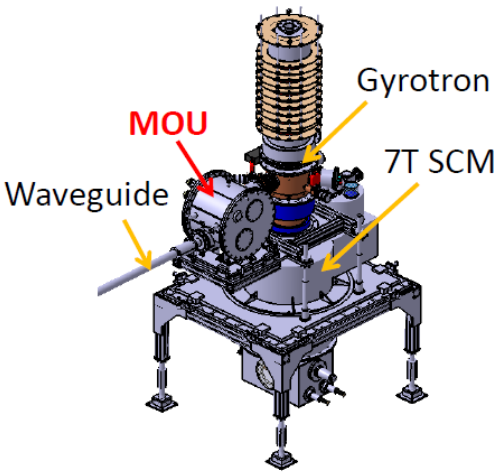

Figure G-4: Model of a gyrotron installed in its superconducting magnet (SCM) and connected to the waveguide through the MOU.

The expected performances will be given at the end of the study, but should not be less than 800 kW at the output of the MOU:

- for a pulse length of 100 s at the frequency of 170 GHz;
- for a pulse length of 30 s at the frequency of 104 GHz.

The development program is scheduled to last 18 months, starting from the signature of a task agreement between ITER Organisation and JA-DA (QST). For reference, a schematic of a gyrotron installed in its superconducting magnet (SCM) and connected to the waveguide through the MOU is shown in Figure G-4.

G.1.1.2 Impact on Transmission Lines

The transmission line (TL) diameter and its corrugations have been optimized for the frequency of 170 GHz. The operation at a lower frequency (be it 104 or 110 GHz) would result in increased power densities primarily near the mitre bends. The lower frequency will generate higher losses at the mitre bends than those for 170 GHz and these losses will be absorbed in the shorter length of the neighbouring waveguide. The resulting power density is typically a factor of 4 higher compared to the 170 GHz case. The design of these components will not be modified at this stage, but an assessment will be performed based on their finite element models to determine the limiting transmitted power and/or pulse length to determine the maximum power handing and pulse length capabilities.

This assessment will require additional resources to re-analyze the finite element models of each component and to assess the limiting power/pulse length possible for the TL. Note that no increase of total loads is envisioned to the Component Cooling Water System that serves the ECRH system (CCWS-2A or CCWS-1).

G.1.1.3 Impact on Equatorial Launcher

The operation of the 104 GHz (or 110 GHz) system will be limited to the equatorial launcher as mentioned above, as the upper launcher quasi-optical design has a much narrower frequency bandwidth that is only a few tenths of GHz in width. The impact on the equatorial launcher includes the following:

1) *Diamond window:* The window has a thickness of 1.11 mm, consistent with the 170 GHz operation, sufficiently thick to withstand all over-pressure load conditions and kept to a minimum to avoid cost increases (proportional to the volume of the disk) and minimize the window absorption coefficient. In order to transmit at both 104 GHz and 170 GHz, the disk thickness has to increase to ~1.5 mm (corresponding to integer half wavelengths for both frequencies). A development program for the qualification of the thicker disk and subsequent procurement of eight windows would be required;
2) *Equatorial Launcher:* The compatibility of the existing optical configuration has to be assessed for 104 GHz transmission. The concern is that the beams expand more rapidly, potentially being too large at each of the two free space mirrors. In this case, the optical design would have to be redesigned for the two frequencies.

Note that the above changes would be implemented for the PFPO-1 operation and be removed after PFPO-2. The upper launchers cannot be used at all at the frequency of 104 (or even 110) GHz as the stray field would be too high and would damage components.

G.1.1.4 Impact on Resources

The additional complexity to the EC system and corresponding management of the design modifications and implementation requires additional engineering resources in the corresponding section of the IO within the Heating systems Division during the period of 2018 to 2037. This

covers the period in which the design, installation, operation and removal of the components for the DFG operation takes place.

G.2 Acceleration program of 10 MW of ICRF power to be made available for the PFPO-1 campaign

The Record of Decisions of the 19th meeting of the ITER Council's (IC-19) states:

> *7.2 The ITER Council:*
> *i. […]*
> *ii. Requested that the IO, Members and their Domestic Agencies (DAs) accelerate the Neutral Beam Injection (NBI) and Ion Cyclotron Resonance Heating (ICRH) systems, making use of existing expertise in the Members and their DAs and of progress that will be achieved in the coming 2-3 years, with a view to enabling the use of the ICRH system for the Pre-Fusion Power Operation-1 in the interests of shortening the period from First Plasma to DT Operation;*

The IO and respective DAs are investigating the feasibility of accelerating the ICRF system with a view to providing 10 MW of ICRF power in the PFPO-1 experimental campaign, as has been assumed for the development of the ITER Research Plan. The report here outlines the current Baseline and plan of work to determine the possibility of accelerating, in particular, the ICRF antenna, which is on the critical path for the ICRF system.

The ICRF system is divided into the following procurements:

1. RF Sources and HV PS;
2. HV PS;
3. Transmission lines and matching units;
4. Antenna;
5. Control system.

The current high-level planning of the ICRF system based on the 4-stage approach in PCR-738 [ITER_D_TL5BR3, 2016] is shown below in Figure G-5.

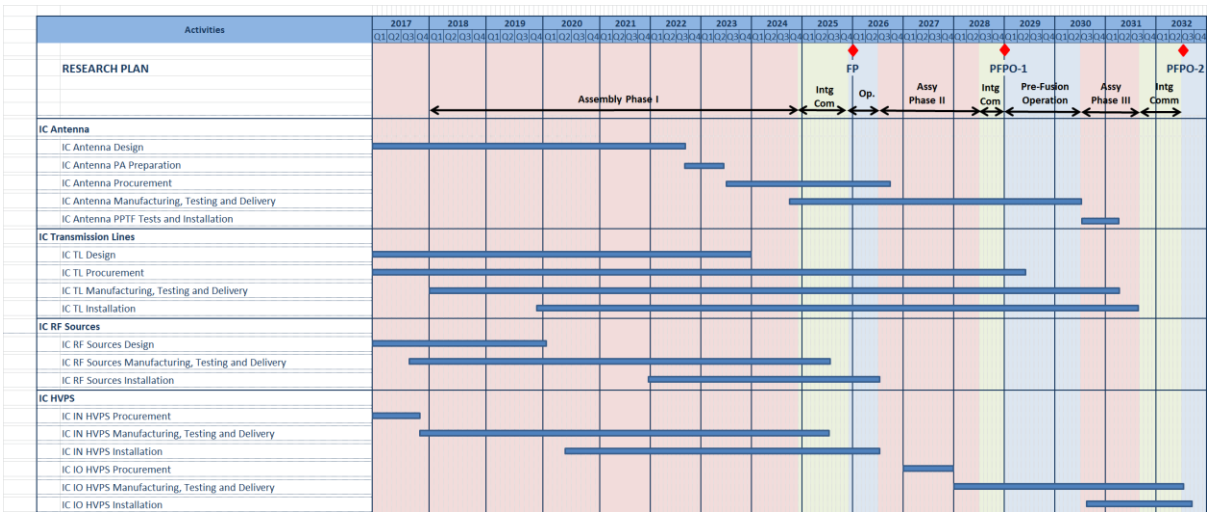

Figure G-5: ICRF system Baseline schedule based on PCR-738.

The staged operation approach has been developed with the inputs of the Configuration Workshop and the cost constraints of the DAs for the relevant procurements. Issues have been identified with the delivery of some of the transmission line components, as current cost constraints and schedule

baselined under PCR-738 are not compliant with the accelerated program. However, the main critical path to ensure 10 MW for PFPO-1 is the antenna, which is currently scheduled to be ready in 2030. This section deals with the antenna acceleration only, as detailed discussions have only started on the TL deliveries. The main assumptions used as a basis of this evaluation are listed here:

- The present procurement strategy is adhered to: need to have technical knowledge of design, knowledge of industry and market for the manufacture and procurement aspects of the antenna project (Note: risk reduction). Therefore, most of the work on design and prototypes is planned to be carried out by the responsible DA (via task agreements);
- Corresponding procurement rules have to be followed;
- No new budget or resource is assumed before second quarter of 2018;
- Assume suitable resource and expertise is available as and when needed;
- No Faraday Screen (FS) mock-ups will need to be manufactured before the prototype. As explained in the next paragraph, part of the proposed acceleration is based on accelerating the critical path work (RF windows). The FS work then becomes the critical path.

The progress made in order to evaluate the feasibility of antenna acceleration is under evaluation with the intention of providing a final report to the IC-22 meeting in June 2018.

In order to accelerate 10 MW of ICRF power (one antenna), so that it is available for Assembly Phase II, would imply that the ICRF antenna would need to be delivered to the IO site by October 2027, thus allowing for six months of testing in the Port Plug Test Facility (PPTF) and three months for the installation, i.e. this would mean that the antenna would need to be installed and ready for the Integrated Commissioning II activity in July 2028. Therefore a three-year acceleration relative to the current antenna schedule (current delivery foreseen in September 2030) would be required.

The current planning of the antenna is shown in Figure G-5 above. There are two main phases, the design phase and the procurement/manufacturing phase.

G.2.1 Design Phase

In evaluating the acceleration of the ICRF antenna in the design phase, the critical path activity for the design and development of a suitable window was considered. The window development could potentially be part of an accelerated program, by combining the contracts that are currently foreseen for demonstration of manufacturability and for production of a prototype to demonstrate functionality. If combined, this would incur a significantly higher cost since the risk to the supplier would be considered higher than the current two-step strategy.

Removing the window from the critical path of the design phase would then result in the Faraday screen being the new critical path. The Faraday Screen mock-ups reported at STAC in May 2014 were planned to be repeated, based on the change of material from copper to stainless steel. From the plan it is clear that if the previous mock-up tests for the rectangular cooling could be used to validate the new cooling channel proposal, bearing in mind that a prototype will in any case be made, then the removal of this activity combined with the window acceleration will save significant time.

The above saving combined with a final acceleration step in the design phase to partially parallel the Final Design Review (FDR) with the Procurement Arrangement preparation (PA) could save ~ 1 year.

G.2.2 Manufacturing and Procurement Phase

Acceleration for the manufacture and procurement phase is currently difficult to evaluate as the detailed procurement strategy has not yet been defined. However, it is assumed that there may be margin for limited acceleration by optimizing the contract strategy. Currently, without further detailed investigation, a six-month acceleration is assumed possible, although an increase in resources will be necessary in such a strategy.

While the above acceleration possibilities may be feasible, it should be remembered that there are currently a number of open issues in the antenna design which need to be addressed, some of which are highlighted here:

- *There is a suitable process, which can be qualified, for the joining of titanium to Stainless Steel (TI/SS):* The current ICRF antenna design has a requirement for the joining of titanium to stainless steel but a straight joint between these two materials is not possible due to the creation of brittle intermetallics. There is some literature available, which suggests that the use of a metallic interlayer for this type of joint is possible with non-trivial mechanical properties. Metallic interlayers to join the titanium to stainless steel are, therefore, being investigated in two processes namely: Ti/SS friction welding and uniaxial diffusion bonding. Initial results for the friction welding look promising and, therefore, if the feasibility of these welding trials proves to be successful, a welding procedure will be produced. If, instead, a technique for joining titanium to stainless steel is not found, then the RF antenna design will have to be altered;
- *The copper plating process is suitable and can be qualified:* The ICRF antenna has some areas within its design which have to be copper coated. However, there is currently no suitable process which can be qualified. The R&D work on the baseline technique, which used copper electroplating for the copper coating of Titanium Grade 2, provided questionable results in both quality and repeatability. There was severe degradation of coatings including Copper lift-off in the presence of braze material (Ticusil/Incusil). An alternative technique, proposed after consultation with appropriate experts, suggested cold spraying techniques as a possible alternative. An R&D contract is underway for cold spraying, the current results look promising;
- *The titanium embrittlement is demonstrated not to be an issue:* The antenna design includes Titanium which is not a commonly accepted material for ITER vacuum applications. It is particularly susceptible to H-embrittlement phenomena, brought about by the ITER water chemistry in the nuclear phase. An evaluation of H-embrittlement effects on the Removable Vacuum Transmission Line (RVTL) materials, in particular the Ti and the Ti-SS joints, is needed to gain the required vacuum compliance (VQC1A) approval and a contract has been placed to start this work;
- *The manufacture of the entire window assembly is possible:* The window design, incorporated in the RVTL of the ICRF antenna, is very complex. The design needs to be validated by building and testing a suitable prototype window. If issues are found, there is a risk that an alternative window solution will have to be found;
- *There is an RF test facility available for the tests when required;*
- *The current design activity will be successful in producing a fully compliant design.*

G.2.3 Additional Risks of an Accelerated Programme

Additionally, other risks need to be considered for an accelerated program and these include:

- As indicated above, there is still a question on the viability of the window design which presents a risk to the overall project timescale. The consequences of this risk are larger for any proposed accelerated program;
- An accelerated window program is likely to imply higher risk and, therefore, higher cost;
- Risk of insufficient resources being available to perform parallel work on the Procurement Arrangement preparation and Final Design Review;
- Risk of insufficient resources being available to prepare and follow up all procurement contracts. The exact amount of additional resources needed is still to be evaluated.

The possibilities examined to date would result in an eventual acceleration of approximately 1.5 years. If possible to implement, the delivery of the antenna would be then occur at the end of 2029, i.e. during the PFPO-1 experimental campaign, and its installation would require a special shutdown to allow some commissioning and operation during PFPO-1. Such acceleration also comes with associated risk and increased human resources. No cost assessment has yet been carried out in relation to risks and resources, and the possibility of achieving the required acceleration to allow 10 MW ICRF to be installed before the start of PFPO-1 remains the subject of analysis. In this respect, it should be noted that further discussions with DAs having the relevant expertise in this area are ongoing to support the analysis of the proposed acceleration activity.

As mentioned previously, a final report will then be made available at the IC-22 meeting in June 2018 and will include the full risk assessment and required additional budget and resources for this acceleration.

G.3 Status of the investigations into the acceleration of the NBI systems

As for the ICRF system, IC-19 has requested a study of the feasibility of accelerating the NBI systems. The current schedule for the HNB systems is shown below in Figure G-6. Note that the schedule for the DNB is the same.

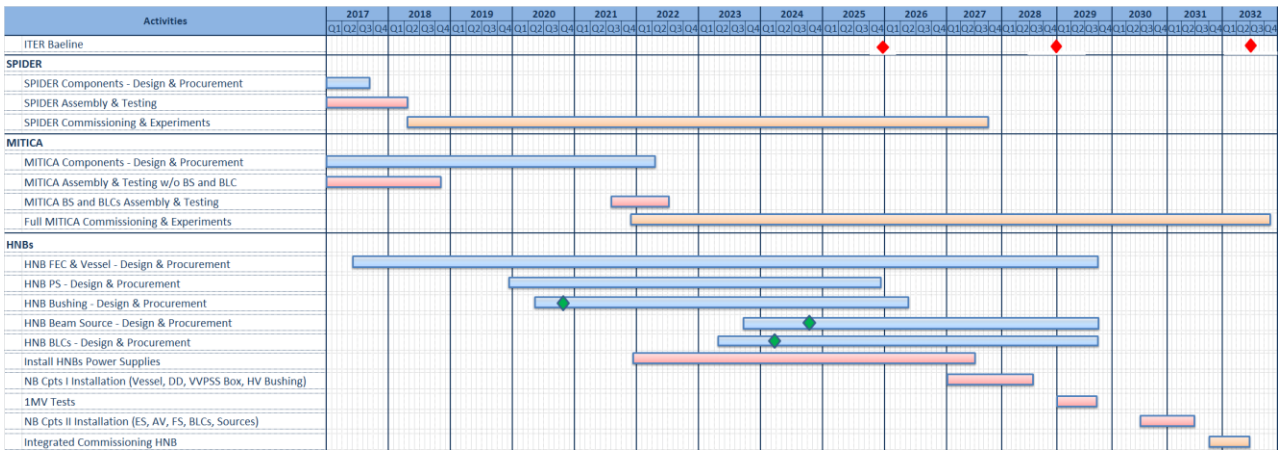

Figure G-6: Baseline schedule for the Neutral Beam Test Facility (NBTF) and NBI system with respect to the ITER Baseline.

The success of the NBI systems for ITER relies heavily on the development program that is underway at the Neutral Beam Test Facility (NBTF), which was considered necessary in order to

mitigate the design, manufacturing and operational risks of the injectors. With the current planning, the timelines in shown Table G-1 are envisaged.

Table G-1 – Experience to be gained in the NBTF facilities prior to ITER NBI operation

Time Line	Experience
SPIDER start of experiments 2018	Four years' experience on the ion source prior to 1 MV beam experiments
MITICA start of experiments 2021	
HNB/DNB to inject into PFPO-2	Ten years' experience on a prototype injector prior to ITER operation of the injectors

In order to have confidence in the above schedule it has been decided to investigate the technically shortest achievable schedule of the NBTF. With the involvement of all of the stakeholders, the NBTF schedule is being developed, and this is based on a deliverable, resource loaded schedule, to provide the input parameters for the beam program at ITER in time for manufacture and procurement of the critical elements of the HNBs.

A roadmap has been developed, which incorporates the risks that could be encountered and the possible modifications from one facility to the next, to result in the final design of the HNBs and DNB. This roadmap forms the basis of the technically fastest achievable schedule from the test facilities of the NBTF through to operation of the beams on ITER. The development of this roadmap has taken into account the expertise both of the DAs who contribute to the NB for ITER and also that of experts in other DAs. It has been concluded that, while some collaborations in the operation and data analysis are possible and welcomed, no significant acceleration can be achieved in the technically shortest schedule which meets the Staged Approach. The work will be continuously reviewed in order to determine if there are any areas which could potentially assist with an accelerated schedule.

G.4 Upgrade possibilities of the ITER H&CD systems (including the status of the LH system)

The *Project Requirements* [ITER_D_27ZRW8, 2014] outline the possible heating and current drive upgrades in section 5.4.3. These upgrades ensure the flexibility of the machine for the different operating scenarios and cover the possible upgrade of all three (construction) baseline H&CD systems, i.e. ICRF, ECRH and NBI, but also define the possible upgrade to incorporate a Lower Hybrid system as a potential upgrade path to increase the capabilities for off-axis current drive. These possible upgrades are considered in the following sections.

G.4.1 Upgrade of the ECRH system

The present ECRH system shall provide a total of 20 MW of RF power at the frequency of 170 GHz in the plasma. The EC system is composed of High Voltage Power Supplies (HVPS), RF power sources (or gyrotrons), the transmission lines (TL), the equatorial (EL) and upper (UL) launcher port plugs plus auxiliary sub-systems and services, control systems and test facilities. The layout is illustrated in Figure G-7, which shows the three buildings that house the ECRH system: RF Building (PS, gyrotrons and TL), Assembly Hall (TL) and Tokamak Building (TL and launchers).

The ECRH system has been designed to be compatible with increased power, which can be achieved in two options. First, the power supplies have been dimensioned to be compatible with a future upgrade of the gyrotron tubes in the range of 1.2 to 1.4 MW (depending on the gyrotrons' required current/voltage requirements and overall efficiency). This can provide an additional 4 - 8 MW with very little changes in the existing infrastructure, as all ECRH components are compatible with this rating and the cooling pipes are dimensioned for the corresponding increased flow.

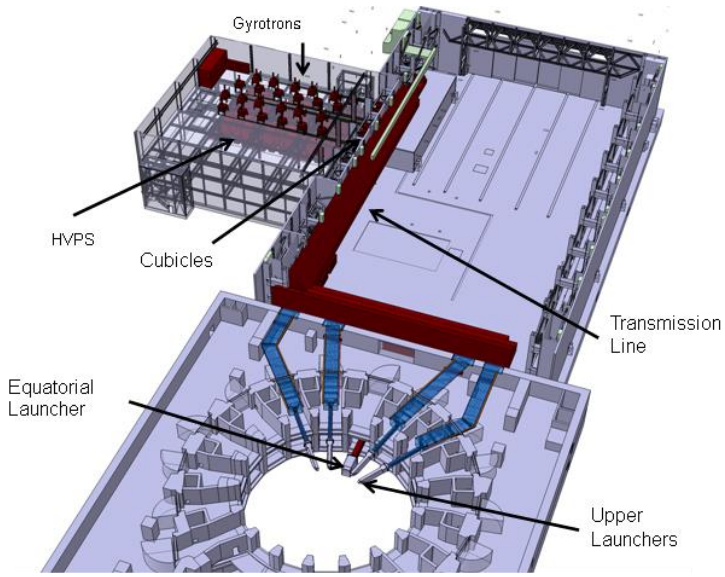

Figure G-7: Layout of the ECH&CD system.

The second option assumes duplicating the ECRH system outside the Tokamak Building thus increasing the total available power for plasma heating by ECRH to 40 MW. This requires the additional space, 12 power supply sets, 24 gyrotrons, 24 TLs leading up to the Tokamak Building and the associated ancillaries. The TL and launchers within the Tokamak Building do not change, as there are 56 entries (24 in the EL and 32 in the UL). The routing and switching mechanisms in the Assembly Hall will be modified to best distribute the total 48 output beams from the gyrotrons to the 56 entries based on the HCD physics requirements.

Note that a combination of both options could be implemented to bring up the injected power between 48 to 56 MW. Obviously, this is strongly dependent on the continued improvements in gyrotron technology, which should not be taken for granted.

G.4.1.1 Location of the 20 MW upgrade of the ECRH system

A 20 MW upgrade would require equivalent space to the one for the existing plant in the RF Building (B15). PCR-496 [ITER_D_ETLLQC, 2013] identified two options for providing this space, as illustrated in Figure G-8:

1) An extension to the RF Building (B15), as represented in the blue shaded area;
2) To install it in the Assembly Hall with an area equivalent to the RF Building, but placed sufficiently far from the tokamak to avoid the stray magnetic field to impact the gyrotrons.

The most cost effective solution is to utilize the space in the Assembly Hall to avoid the additional cost in construction of a building extension. The following assumes that the Assembly Hall option is adopted for the 20 MW upgrade.

A metallic structure is required that mimics the three levels of B15 and would fit between the south side of the building, the metrology lab (to the east) and the Collective Thomson Scattering (CTS) gyrotrons to the north-west as illustrated in Figure G-8. The transmission lines would drop down to the ground level and run along the west wall and feed directly into the EL. Note that eight TLs would have a switch to redirect the power from the EL counter-ECCD entries to the eight UL co-ECCD entries of the upper steering mirrors of UL12 and UL13. The TL routing avoids supports to the building structures to prevent additional distortions of the waveguide and the corresponding mode conversion, as shown in Figure G-9.

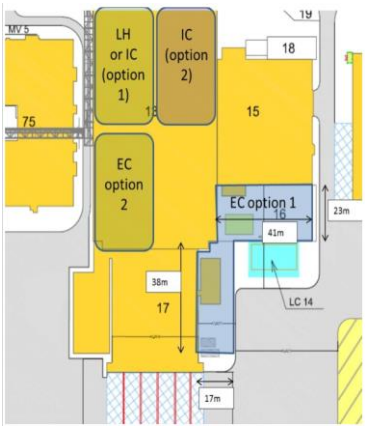

Figure G-8: Space reservations for the EC upgrade with 2 possible options based on PCR-496: 1) An extension to the RF Building (B15), as represented in the blue shaded area; or 2) In the Assembly Hall with an area equivalent to the RF Building, but placed sufficiently far from the tokamak to avoid any influence of stray magnetic field on the gyrotrons.

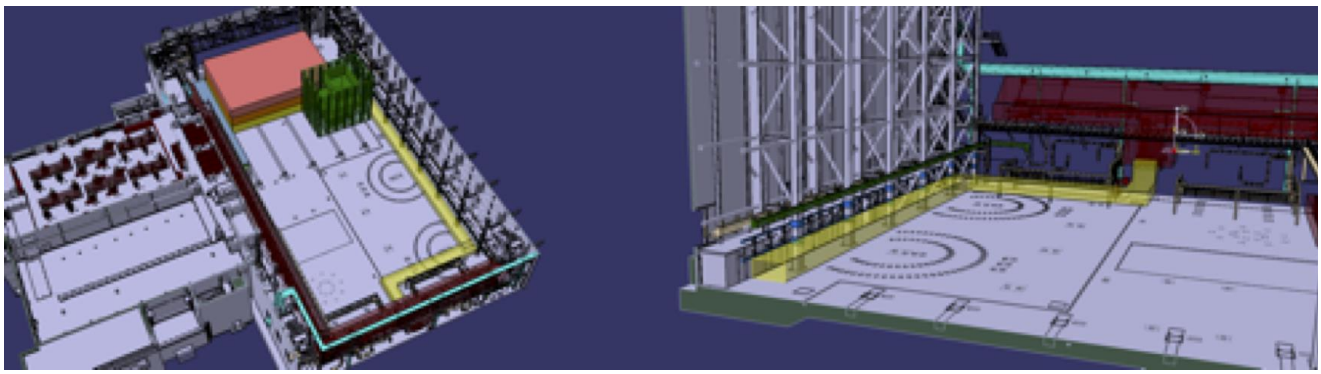

Figure G-9: (Left) Space reservations for the EC upgrade located in the back of the Assembly Hall with the required space for 12 HVPS zones (2 levels), 21 RF sources (1 level) and associated TL. (Right) The routing of the TL would follow the west side of the building and be connected directly to the 24 entries of the EL.

G.4.1.2 Schedule of the 20 MW upgrade of the ECRH system

There are multiple procurement options as well as introduction of new technologies that could simplify the schedule. However, the approach taken herein assumes the following:

- The design of the upgrade is made well in advance and is available prior to the decision date (T0);

- The site infrastructure is installed starting at T0 and requires 18 months. This includes modifications to buildings, cooling water (CCWS), Pulsed Power and Steady State Electrical Networks (PPEN and SSEN), etc.;
- The procurement and manufacturing of the first sets of HVPS and gyrotrons occur during the 18 months of site preparation;
- A single supplier provides the 12 HVPS sets and their delivery proceeds at a rate of 3 sets/year and an installation of two months. Thus, the full 12 HVPS are installed in 4.25 years;
- Two gyrotron suppliers are used with a combined manufacturing rate of four tubes/year and 6-month installation rate. Overlapping the installation and commissioning activities would limit the 24 gyrotron installation to 6 years. This time period could be reduced pending the experience gained from the baseline set of the first 24 gyrotrons;
- A single supplier is used for the 24 TL requiring 3 years for manufacturing and 1 year for installation;
- Commissioning of the EC system up to the EL and UL entries requires 6 months.

The above is outlined in Figure G-10. The total time from T0 to be ready for commissioning with the plasma is T0 + 6 years. Note that this assumes no interruption of the schedule due to ITER operation, all available resources, two shift operation and pre-existing designs of the infrastructure and EC system upgrade layout.

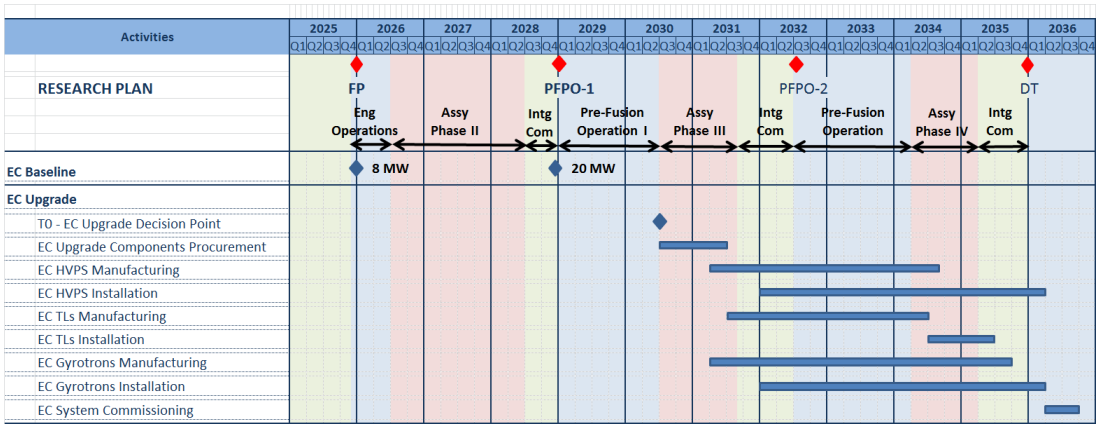

Figure G-10: General schedule of the manufacturing and installation of the ECRH system upgrade of 20 MW (injected).

G.4.2 Upgrade of the ICRF system

The hardware for the ICH&CD system (PBS 51) is spread across building 11, 13 and 15 at the ITER site, as shown in Figure G-11. In building 11, the ICRF system is installed in port cell 13 and 15 at Level 1.

Overall, the ICRF system, including ancillaries, is installed in four buildings:

- The RF Building hosts the HVPS and the RF sources (A);
- The Assembly Hall hosts the main transmission lines (B&D) and the matching system (C);

- The Tokamak Building hosts some transmission lines (E), port cell prematching (F) and antenna (G);
- The Hot Cell Facility hosts the PPTF equipment.

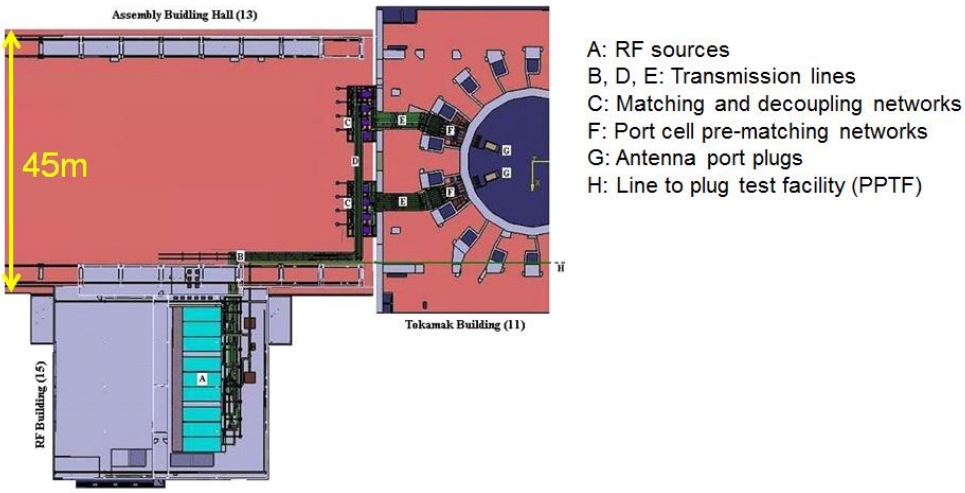

Figure G-11: Layout of ICRF baseline system at the end of construction.

The baseline system has been designed to allow a future upgrade:

- The antenna design is based on electric fields allowing operation up to 45 kV maximum peak RF voltage;
- TL and MS components are designed and tested for power levels corresponding to the upgrade power level.

As a consequence, the implementation of an upgrade of the ICRF system to 40 MW will not require changing or modifying any equipment in the Tokamak Building.

G.4.2.1 Description of the 20 MW upgrade for the ICRF system and its implementation

The upgrade of the ICRF system aims to increase the power coupled to the plasma from the baseline level of 20 MW to 40 MW. All other parameters are unchanged: frequency range, spectra, pulse duration, etc.

The upgrade will involve the following sub-systems:

- *HVPS:* need to procure and install power supplies to feed 8 additional RF sources; no development needed; each unit identical to the ones being developed and tested for the baseline. Switchgear and cables will be needed for connection to PPEN;
- *RF sources:* need to procure and install 8 RF sources; these would be identical to the units developed during construction. A prototype is being tested at present in IPR with successful results;
- *TL:* some components are needed to connect to main transmission lines; these components will be standard components as used in the baseline configuration;

- *RF dummy loads and coaxial switches:* a switching network on RF sources to be installed to allow testing and maintenance of sources; components are identical to the baseline components installed in RF Building;
- *Control system (data acquisition, safety, interlocks):* procurement, software engineering, installation and integration to interface the new equipment with the rest of the system;
- *Cooling system:* The baseline RF power plant uses close to 300 kg/s cooling water from CCWS2A; the upgrade will need a similar quantity; a provision for connection is available in the Assembly Hall that can be used either for an ICRF upgrade or LHCD upgrade;
- *PPEN:* the extension of the ICRF power plant will require the PPEN to supply an additional 50 MW; The connections are already planned in the PPEN network, but additional breakers and distribution will be required;
- *SSEN:* additional distribution required that could be taken from the existing infrastructure used for machine assembly in B13;
- *Building:* the foreseen location of the upgrade is in the Assembly Hall, B13. Different options are shown in PCR-496 [ITER_D_ETLLQC, 2013] and in Figure G-12. The installation of the HVPS and RF sources will require erecting a three level metallic platform in B13, similar to that described for the ECRH upgrade.

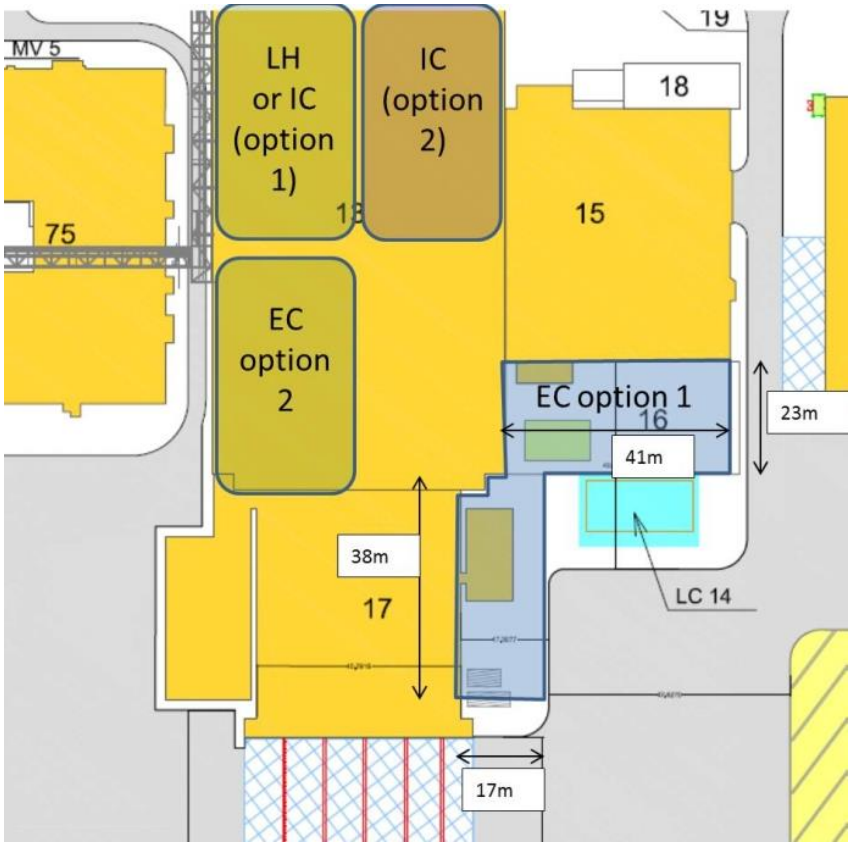

Figure G-12: Proposed location for the ICRF upgrade in North part of the Assembly Hall.

G.4.2.2 Schedule for the 20 MW upgrade of the ICRF system

The schedule driver for the ICRF upgrade is the procurement of the RF sources estimated at 4 years. In parallel, the HVPS, TL and auxiliary equipment can be procured in coherence for a phased installation. Final integration will require 1 year, after delivery of the last RF source.

The total duration must include contract preparation, hence the total time required for the upgrade is in the range of 6 years. Installation and integration takes place during the last three years (platform erection, staged source & HVPS deliveries, etc.).

G.4.3 Neutral Beam Heating Upgrade

The Neutral Beam (NBI) system is spread across buildings 11, 34, and 37, area 30 and 31 at the ITER site. In building 11, the Neutral Beam system is installed in the NB Cell (at L1, L2) and HV Deck room (at L3) while the equipment in building 34, 37 and area 30 consists of NB high voltage power supplies and the SF6 plant is installed in area 31.

The Neutral Beam installation is planned in two stages. The two HNBs and DNB are assembled in Assembly Phases II and III, while a proposal for the installation of the captive components of the 3rd HNB is also under consideration and will be presented to the Change Control Board (CCB) under a specific Project Change Request (PCR). Assembly Phases II and III are separated by the HV tests, which are planned in parallel to the PFPO-1 campaign. The HV tests are an integrated test of the 1 MV HNB and 100 kV DNB power supplies through the transmission line to a spark gap installed on the injector in the NB cell. The installation in the NB cell and the HV deck room at L3 in building 11 will be carried out in two shifts, while for building 34, 37, area 30 and 31 a single shift is utilized.

G.4.3.1 Description of the NBI Upgrade – HNB3

The 3rd HNB injector, HNB3, is one of the proposed upgrades for the heating systems at ITER. The *Project Requirements* [ITER_D_27ZRW8, 2014] prescribe 4 heating and current drive upgrade scenarios to ensure the necessary flexibility for advanced operation regimes in ITER. The *Project Requirements* also state that the ITER design shall not preclude the possibility of accommodating the combination of heating and current drive upgrades, as specified in the Table 4-9 of the *Project Requirements* (PR822-R). Based on these requirements the design of the HNB3 has been considered in the design of the civil structures of the tokamak complex and the interfacing systems needed to allow for this upgrade, when a decision is made on its need.

Unlike the upgrade options for the ICRF and ECRH systems, the HNB3 has strong implications and interfaces with the Tokamak Building (B11). Upgrading the ECRH or ICRF systems would require either an upgrade of the gyrotrons or RF sources, for ECRH or ICRF respectively, and the associated power supplies, which are all located outside of B11. This greatly simplifies the upgrade of these systems and also allows for more flexibility as to when a decision can be made for their implementation.

The HNB3, due to its extensive interfacing and impact in the Tokamak Building, has a time constraint, implying that the decision to install this equipment must be taken within a certain time window. The NBI components are large and heavy components, (an injector is ~1200 t) and many components can only be installed with hands-on access. This restricts the possibility of installation of HNB3 to the pre-nuclear phase. The baseline scenario is that the HNB3, if decided upon, would be installed in Assembly Phase IV (pre-nuclear assembly phase). This installation is time consuming and challenging; many plant systems will need to be dismantled in order to

accommodate the installation of the HNB3 and then these plant systems will be reinstalled upon completion of the HNB3 installation. Another challenge for the HNB3 is that, as for the other injectors, it is installed in the NB Cell. Access to the NB cell is limited and the baseline scenario to install the HNB3 requires dismantling of the West Gallery wall. This means that the NB Cell is opened to the environment following operation with Be components in the tokamak, increasing the risk of Be contamination.

As the Staged Approach was developed, the understanding of the restrictions based on Be contamination evolved further, resulting in the proposal to install the large components of the HNB3 injector, which can only be installed by opening up the NB Cell to the environment prior to operation with Be components in the plasma. This implies that the injector vessels (beam source vessel and beam line vessel) and the passive magnetic shielding around it for HNB3 would be installed through the 'north wall opening' which is a temporary opening used to install the large components of the HNB1&2 prior to PFPO-1. Once these components are installed, the north wall can be closed resulting in confinement of the NB cell from the outside environment. Installing the HNB3 components at the same time ensures that this confinement is maintained for the later stages of the project.

If the large components of the HNB3 were not to be installed at this time, installation through the gallery is still possible; however, discussion with the nuclear regulator would be necessary to ensure that, when considering the restrictions imposed to avoid Be contamination, this possibility would still be realistic. This poses a significant risk to the potential upgrade of the HNB3.

The components of the HNB3 which should be anticipated for installation to ensure the future upgrade of the NB system are detailed in the next section. When this proposed installation is formally accepted by the project, these components will become part of the construction Baseline.

G.4.3.2 Anticipated/captive components of HNB3

The large components of HNB3 are considered captive and it is proposed that they be installed in Assembly Phase II. The components can be easily transported inside the NB cell through the temporary opening in the north wall. ***The HNB3 components will be installed in parallel to DNB, HNB1 & 2 components.*** The NB installation in building 11 will be carried out in two shifts.

The HNB3 captive components to be installed in Assembly Phase II are listed in Table G-2 .

Table G-2 – Captive/ anticipated components of the HNB3

Sr. No.	Description	Location
1	HNB3 Passive Magnetic Shield (PMS) base plates	NB cell
2	HNB3 bottom Active Compensation and Correction Coils (ACCCs) rails and retraction system	NB cell
3	HNB3 PMS (except Top PMS#1 to 4b and High Voltage Bushing (HVB) PMS)	NB cell
4	HNB3 Beam Line Vessel (BLV)	NB cell
5	HNB3 Beam Source Vessel (BSV)	NB cell

G.4.3.3 Schedule for the NBI Upgrade – HNB3

All of the remaining HNB3 components (all except those considered captive and detailed in Table G-2 above) that are required for the installation of a functional 3rd injector are considered as an optional upgrade and a staged approach for installation is outlined in the schedule below.

As the HNBs at ITER will not operate before PFPO-2, a late decision based on their performance in the ITER plasmas will exclude the possibility to have this upgrade in time for the pre-nuclear phase installation, unless nuclear operations are delayed until this upgrade is implemented. However, the performance of the beams will be well understood from the NBTF experiments, at latest by 2026, and therefore a decision point could be considered at that time. Assuming that a decision is made in 2026, the estimated time to complete the procurement of the HNB3 can be seen in the schedule in Figure G-13**:** .

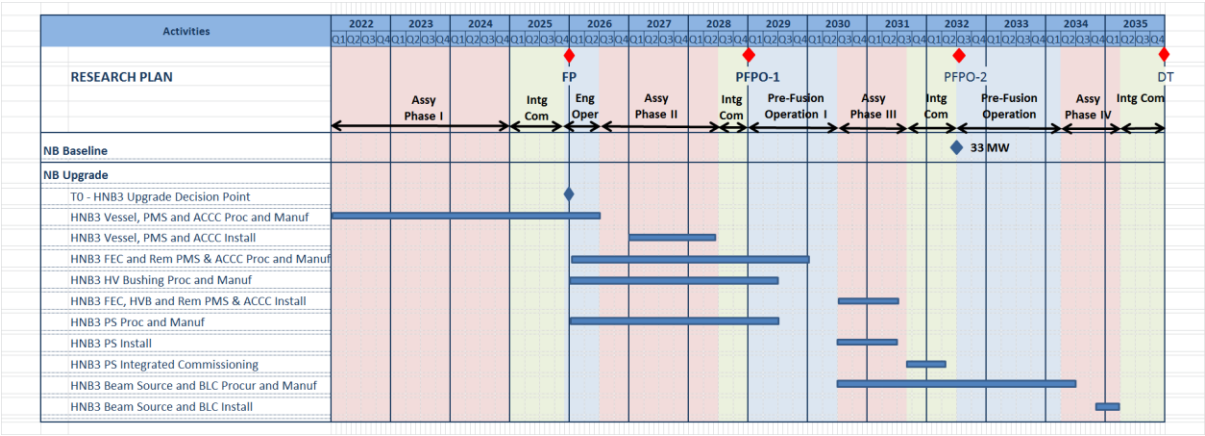

Figure G-13: Schedule of activities for the HNB3 upgrade based on a 2026 decision point.

The latest possible time to make a decision on the HNB3 upgrade, to be ready to install a full HNB3 during the pre-nuclear shutdown, would be during the PFPO-1 plasma operation phase. By this time both the performance of the beams at the NBTF and the performance of the other baseline heating systems will be known, giving insight to determine the most effective upgrade path for the ITER heating systems to ensure a successful implementation of the research program. Should such a decision be made as late as the end of the PFPO-1 phase, it is still possible to install the HNB3 injectors for the DT phase. The corresponding schedule is shown in Figure G-14.

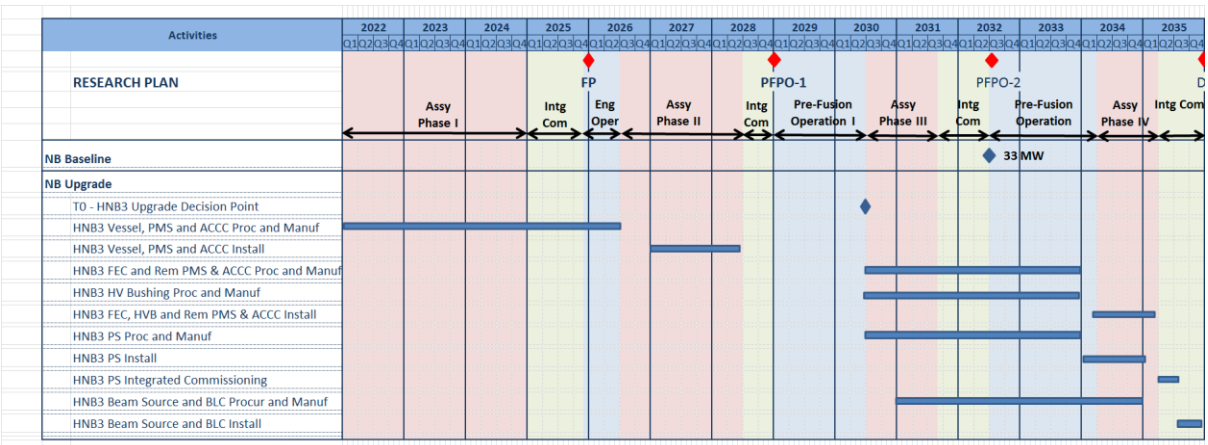

Figure G-14: Schedule of activities for the HNB3 upgrade based on an ‘end of PFPO-1’ decision point.

G.4.4 The ITER Lower Hybrid System (LHCD)

The Lower Hybrid Heating and Current Drive (LHH&CD) system is not included in the ITER construction Baseline. It is, however, considered as an H&CD upgrade scenario for the operational phase. The LHH&CD system is designed to provide off-axis non-inductive current in any plasma scenario and discharge phase. The system is therefore included in the *Project Requirements* as a possible heating and current drive system upgrade. The LHH&CD system is designed to deliver a minimum total Radio Frequency (RF) power of 20 MW. In some upgrade scenarios, the required power level can reach 40 MW. The frequency foreseen is between 3.7 GHz and 5 GHz, with 5 GHz agreed as the reference design frequency. The 3.7 GHz system could be a fall-back solution.

The 20 MW ITER LHH&CD system is composed of the following elements:

- *Wave Launcher:* consists of four modules of radiating elements, arranged in two toroidal and two poloidal rows, located in the ITER vacuum vessel via a port plug; these modules are based on the passive-active multi-junction (PAM) concept;
- *Transmission Lines:* transmit the RF power from the source to the launcher and transmission components following paths of unequal electrical length;
- The Power *Sources* together with their associated *High Voltage Power Supply* (HVPS), auxiliaries and services*:* the operation of the whole system is monitored and co-ordinated by an I&C system under the supervision of the ITER central control system (CODAC).

G.4.4.1 Status of the Lower Hybrid System design development

As this system is not considered part of the construction baseline, the main work has been to ensure that the ITER facility can accommodate such an upgrade, should it be decided to design, construct and install it at a later stage. In preparation for its possible integration, interfaces have been defined, as far as possible, and requirements and interfaces have been documented:

- **System Requirement Definition** [ITER_D_28B384, 2009];
- **Models physical implementation:** space was reserved in the Assembly Hall for the generators and HVPS (Figure G-15); space allocations were reserved in the tokamak south wall for penetrations; embedded plates are defined in the gallery and equatorial port cell 11;
- **Interface definition:** the main interface sheets (with Tokamak Building, Assembly Hall, CCWS, SSEN, etc.) have been developed and approved.

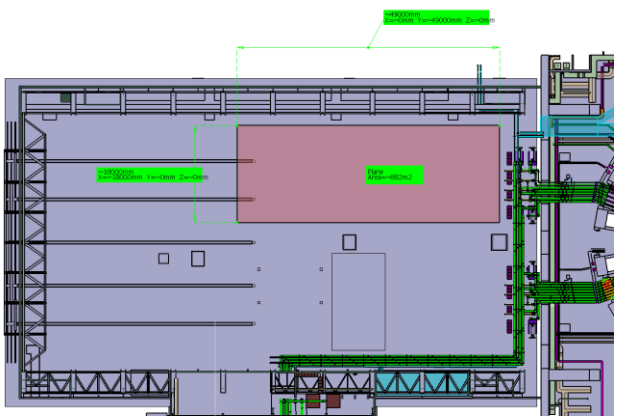

Figure G-15: Space allocation reserved in the Assembly Hall for the LHCD generators, transmitters and power supplies.

In parallel, the design of the system and the associated physics scenarios were reviewed from the initial proposal within a task implemented by EFDA and involving all EU fusion institutions interested in the LHCD system for ITER (WP09-HCD-03-01). The final report of this EFDA task can be found in reference [ITER_D_SN28YH, 2016].

Despite large efforts to develop a klystron at 5 GHz (collaboration KSTAR-TOSHIBA) the tube does not comply with all ITER requirements, in particular, the requirement on the Voltage Standing Wave Ratio (VSWR). Indeed, due to the difficult coupling conditions for H-mode plasmas, the reflected power to the klystron may be high. For that purpose, the tube needs to deliver at least 500 kW at a (high) VSWR of 1.4. The main technical difficulty is linked to the requirement to operate with very high reflected power while ensuring good efficiency [Ho 2011; Park 2013]. The current performance is 500 kW, 600 s at VSWR < 1.2.

The remainder of the components of the LHCD system were also tested, but did not fulfil the full specifications [Hillairet 2012; Hillairet 2015].

A backup solution at 3.7 GHz could potentially be considered:

- *Klystron TH2013C:* CW, 620 kW at VSWR = 1.4, or 750 kW at VSWR = 1; demonstrated successful operation at Tore Supra [Beunas, 2009];
- *PAM launcher:* already tested and currently used on Tore Supra [Ekedahl, 2010; Dumont, 2014];
- *Transmission Line:* CW components currently used on Tore Supra [Goniche, 2014].

In addition, the conceptual launcher design would have to be adapted to the port plug environment, which has changed substantially over the past years, with the implementation of PCR-439 [ITER_D_ETJB4Q, 2014], and the changes that have been made to the bio-shield etc.

G.4.4.2 Lower Hybrid System port allocation and implementation issues

In the *Project Requirements* [ITER_D_27ZRW8, 2014], a number of ports were allocated to the possible upgrade of the LHCD system, namely equatorial port 11, allocated to the launcher for the upgrade scenario #1, ports 11 or 13 for upgrade scenario #2, and ports 13 (or 11) and 14 for upgrade scenario #4. The various upgrade scenarios are described in Table 4-9 of the *Project Requirements*. Note that, in the initial configuration, port 11 is a Diagnostics port, port 13 is an ICRF antenna port and port 14 is an ECRH launcher port.

A number of studies were carried out, from the point of view of integration, and the preferred port allocation was determined to be EP11. At present, the models have implemented in the tokamak construction design for this port only [ITER_D_L9ABVC, 2014]. EP11 was considered the best port due to its proximity to the Assembly Hall, where the transmitters are located, reducing the TL length between the launcher and the transmitters. It should be noted that EP13 and EP15 would also comply with this requirement. However, as the ICRF antennas are currently planned to be installed in EP13 and EP15, the magnetic connection between these systems could create perturbations on the wave propagation from both systems. A conceptual study was also carried out on the possibility to use EP8. This option was ruled out due integration and space reservation issues. Following these studies it was concluded that EP11 was the only viable option for the LHCD system in an upgrade scenario.

In the initial configuration defined in the *Project Requirements*, EP11 is allocated as a Diagnostic port and it is noted in the PR that: "*Note 3: Diagnostics in port EP11 shall be removed for upgrade scenario 1. In case diagnostics necessary for the machine protection and the basic plasma*

operation are located in that port, they will be relocated in another port – or their functions will be fulfilled by another diagnostic system. [PR1666-C]"

In PCR-738 [ITER_D_TL5BR3, 2016] it was finally decided to allocate the EP11 as a Diagnostic port for the diagnostic systems shown in Table G-3.

Table G-3 – Diagnostics located in EP11 as per PCR-738

Diagnostic System	Functional from
55.QB: Eq Port #11 Systems	First Plasma
55.E3: VUV Survey	First Plasma
55.ED: X-Ray Crystal Spec Survey	First Plasma
55.B8: Activation System	PFPO-1
55.G4: Residual Gas Analyzers	PFPO-1
55.E2: H-Alpha (+ visible	PFPO-1
55.EG: Divertor VUV Spectroscopy	PFPO-1
55.E8: Neutral Particle Analyzer	PFPO-2
55.F2: Reflectometer (Main Plasma,	PFPO-2

The fully populated EP11 Port Plug and partly populated Interspace Support Structure (ISS) and Port Cell Support Structure (PCSS) will be installed at First Plasma. The ISS and PCSS contain only components related to functional First Plasma diagnostics. The ISS and PCSS will be removed after the First Plasma campaign and re-assembled to incorporate the components which were not present at First Plasma. The Port Plug may also be removed at this stage, if needed, to give improved access to install in-vessel components. The complete and fully populated Port Plug, ISS and PCSS will thus be installed during Assembly Phase II, ready for PFPO-1 operation. Unless there is a major failure, it is not expected that the EP11 Port Plug, ISS or PCSS should be removed until after DT operations have started.

The decision to allocate this port to Diagnostics plays an important role in the realistic feasibility of implementation of the LHCD upgrade. Other factors have to be also considered for such upgrade in the context of the overall time schedule and a short summary of them is given below.

The projected cost of the LHCD system was developed under the EFDA task [ITER_D_SN28YH, 2016]. In this study the estimated cost for the full system is between €82 million and €87 million. During this task is was also estimated that ~ 9 years, including the conceptual and detailed design phases, R&D, procurement, tests and installation, would be required to implement this upgrade. This timeline was developed prior to understanding the complexity of design and integration into the ITER environment for such a system and could therefore be considered optimistic. The upgrade to include the LHCD system has a time constraint: if the LHCD system is not installed in the pre-nuclear assembly phase then it cannot be installed later. Even though the system can be designed to be maintained by remote handling, installation would require human access in the Tokamak Building. This implies that a decision on the need to implement such a system in ITER would have to be taken by 2021 at the latest. In addition, the allocation of the EP11 to diagnostics systems in the baseline approach means that no suitable port can be made available in this timescale.

The need for such an early decision on the LHCD system, prior to ITER operation, combined with the unavailability of a viable port, raises significant issues concerning the possibility of maintaining

the LHCD option as a viable upgrade path for ITER. To this end a review and assessment of the H&CD needs for the development of the ITER long-pulse and steady-state scenarios has been conducted in parallel with the development of the updated ITER Research Plan. This is described in Appendix E and concludes that upgrades of systems already included in the ITER Baseline (in particular, NBI and ECRH) could provide similar functionalities to those expected from the LHCD system for the steady-state scenario. Indeed, the most challenging feature of the Q = 5 steady-state scenario is the achievement of very high confinement regimes in H-mode at high-q_{95} with $H_{98} \geq 1.6$. This is an essential requirement, which is independent of the H&CD upgrade chosen (i.e. with/without LHCD) to achieve this scenario.

Appendix H: Diagnostic Staging

H.1 Introduction

The diagnostic set on ITER is designed according to the requirements in the SRD-55 [ITER_D_28B39L, 2017] and complemented by the applicable *Project Requirements* (PR) [ITER_D_27ZRW8, 2014].

To assess what parameters are measured and which system is measuring them, one can find the specific parameter and the measurement range along with the diagnostic system that performs that measurement in SRD-55 [ITER_D_28B39L, 2017]. The following is an example of the format for the measurement of the core density profile:

--- [55s1294]

Table MP054 – Measurement Parameter 054. Core n_e shall be delivered with the following specifications [55s1295]

Condition	Range	Time Res.	Spatial Res.	Accuracy
r/a < 0.85	$3\times10^{19} - 3\times10^{20}$ m^{-3}	10 ms	a/30	5 %

The following diagnostic system(s) shall be provided to contribute to meeting this requirement:

- 55.C1 Thomson Scattering (Core) - Primary
- 55.F9 Reflectometer (Main Plasma, HFS) - Primary
- 55.C5 Toroidal Interferometer/Polarimeter - Supplementary
- 55.C6 Poloidal Polarimeter - Supplementary
- 55.F2 Reflectometer (Main Plasma, LFS) - Back-up

Where the word Primary means that the diagnostic is well suited to the measurement. Backup and Supplementary are more limited in what they provide for this measurement. Details of these can be found in the individual Diagnostic Design specific information. In general, all measurements have at least one Primary system to provide them; often, they are dependent on one or more Supplementary contributions for performance and/or a Backup contribution for reliability or availability reasons. All the measurements planned and the corresponding systems can be traced through the SRD-55 [ITER_D_28B39L, 2017] above.

The recent Staged Approach, with four operational phases (including First Plasma), has defined in the project when each system can be available. These will be detailed further below where each phase will be discussed in turn identifying the status of the different systems. For First Plasma, there are some cases where temporary systems are installed to cover the fact that the more advanced system will arrive in phase II. This will be explained below.

H.2 First Plasma Diagnostic Capabilities

For First Plasma, the set of systems that will be available is shown in Table H-1 . It can be seen that these cover mainly the basic systems that are needed for establishing the main parameters of the First Plasma. In this phase the emphasis on measurement capability is for magnetics, plasma breakdown, investment protection (hard X-rays) and density for a plasma with a current of up to 1 MA (presently considered for the Engineering Operations phase after First Plasma).

Table H-1 – First Plasma and Engineering Operations diagnostic systems

PBS	System Name	Comment
55.A0	Magnetics System Electronics & Software	
55.A1	Continuous External Rogowski	
55.A3/A4/A9	Outer Vessel Coils	
55.A5/A6	Steady State Sensors	
55.A7/AD/AE/AI	Flux Loops	
55.AA/AB/AC	Inner Vessel Coils	
55.AF/AG/AH	Diamagnetic Sensors	
55.E2	H-alpha/Vis in EPP12	
55.E3	Vacuum Ultra-Violet Survey	
55.E6	Visible Spectroscopy Reference System (partial)	Temporary version, as port plug not installed
55.ED	X-Ray Crystal Spectrometer	
55.EE	Hard X-ray Monitor	
55.G1.E0	Vis/IR Equatorial in EP16 (temporary)	Only for FP
55.G1	Vis/IR Equatorial in EPP12 (partial)	1 out of 3 views fully working
55.G3.50	Pressure Gauges (temporary)	Temporary for FP
55.GB	Stray ECRH detector	
55.GF	TF Mapping (one-off activity)	Temporary for alignment of the blankets before FP.
55.GL	In-Vessel Lighting	
55.GT	Tokamak Structural Monitoring system	
55.FA	Density Interferometer (partial)	Single channel installed without port plug

A sufficient set of the magnetic sensors will be functionally available; most others will be there either trapped or to benefit from joint commissioning with the PF coils and TF Coils. This phase will include an extensive commissioning phase, in advance, to ensure all the systems are ready. Where not stated otherwise, these systems will be fully installed with the exception of what is called the temporary sub-systems or partially installed systems. These are:

55.E6 Visible Spectroscopy, which will have a single radial channel for visible light observation that will be reconfigured after Phase I.

55.G1.E0 Infrared system, which is a special Infrared system to observe the special ECRH mirror needed for first plasma. This will be removed after FP.

55.G1 Visible/IR system is the conventional system for Vis/IR measurements but only one channel will be functional.

55.GL In-vessel Lighting system is (part of) the in-vessel lighting system to allow visual inspection of the in-vessel surfaces with the cameras of 55.G1

55.G3.50 Pressure gauges will include fast pressure gauges set up close to the back of an empty port plug. These will have a fast time response (better than 100 ms) sufficient for monitoring the breakdown of the plasma.

55.GF Is a temporary system to map the toroidal field to confirm/improve FW alignment.

55.FA Interferometer (DIP), which will have a radial view of a retroreflector on the inner wall and, hence, provide a line averaged density measurement. It will be reconfigured after First Plasma and Engineering Operations.

H.3 Diagnostic Capabilities for PFPO-1 and planned upgrades

As PFPO-1 is a much more demanding phase, the number of systems installed is increased significantly compared to First Plasma. This can be seen in Table H-2. In this table the systems in black are expected to be fully operational after a suitable commissioning phase. In this phase of operations the emphasis on measurement capability is for plasma control, investment protection and basic plasma parameters. Note that, as for the First Plasma systems, the measurement capabilities for each plasma parameter can be found in SRD-55 [ITER_D_28B39L, 2017]. A discussion on the implication of 1.8 T operation for the diagnostic systems available in PFPO-1 can be found in section H.6.

To explain the state of those systems that are not complete for PFPO-1 operation (blue for upgrades and red for enabled systems in Table H-3), a short explanation is provided below:

- **Fibre Optic Current Sensor (55.A8 FOCS)**

The Fibre Optic Current Sensor (FOCS) system will use optical fibres placed around the Vacuum Vessel (VV) to measure the plasma current by means of the Faraday Effect. The optical fibres will be placed inside stainless steel tubes which protect the fibres from mechanical damage and allow fibre replacement. These tubes will be fixed with clamps on the outer VV surface. The tubes themselves will provide the boundary between vacuum and non-vacuum.

The FOCS presents an attractive alternative to other steady-state plasma current diagnostics. Its operation is based on the detection of the Faraday rotation experienced by a polarized light in an optical fibre because of the presence of magnetic field aligned with the fibre axis. The complete sensor requires electronics for the signal processing, but only the sensing fibre is placed in the vicinity of the burning plasma (around the ITER VV) and no front-end electronics, which could be subject to the ITER harsh environment, are required. It was also demonstrated that the radiation-induced absorption levels in radiation hard optical fibres are compatible with the requirements for signal transmission for the full ITER lifetime. The current FOCS design with the optical fibres inserted into stainless steel tubes using a blow-in technique means the sensing head can be easily replaced in case of degradation due to service conditions or development of an improved sensing technology. Furthermore, the optical fibre which is used for the FOCS allows, in principle, distributed high-resolution measurements of other parameters, e.g. temperature, strain, or radiation dose. A distributed magnetic field measurement using the FOCS structure also seems possible. The FOCS installation can potentially host other systems, for example an activation wire for neutron dosimetry.

The system is enabled only: Components up to the cryostat (Figure H-1) will be installed but not functionally tested. Fibre bundles through the building penetration will also be installed. Fibre joints

within port cells and diagnostic hall may or may not be installed depending on cabling schedule and funds. The remainder of the system (bundles in the port cell, polarimetric system in the diagnostic hall) will be installed if funded.

- **In Vessel calibration (55.BV)-(PFPO1-PFPO2-FPO)**

The total neutron yield (Y_n) measurement is the direct measurement of fusion power and it has to be provided by neutron diagnostics with an accuracy of 10% and 1 ms time resolution. This is a strict requirement as it relates to knowing the fusion power generated in ITER. To ensure these requirements the neutron diagnostics have to be calibrated and a strategy has been developed. It consists of three different stages – (a) first is the partial in-vessel neutron calibration campaign with limited toroidal/poloidal scan performed before PFPO-1, (b) second is the full toroidal and poloidal scan at 2.5 MeV neutron energy performed before PFPO-2 and (c) the third is again full scan but at 14 MeV neutron energy performed before FPO. The objective of these campaigns is the comparison of the experimental data/sensitivities with the neutron transport modelling, determining the calibration factors and verifying of the ITER neutronics model.

In the In-vessel neutron calibration campaigns, a neutron source (Californium-252 or DD/DT sealed neutron generators) will be moved inside the vacuum vessel in different toroidal and poloidal positions irradiating the most sensitive detectors (55.B4 NFM in EQ#1, 55.B8 NAS- Neutron Activation System in Upp 18 and 55.BC DNFM- Divertor Neutron Flux Monitor in Lower Port 2, Divertor cassette 3). Investigation is going on the possible use of RH transportation systems or by a manually handled system (pneumatic piping, train transporter or staging) to perform these movements.

In the near future, the technical specification will be defined for neutron sources (Californium-252) and, in particular, for sealed neutron DD/DT generators.

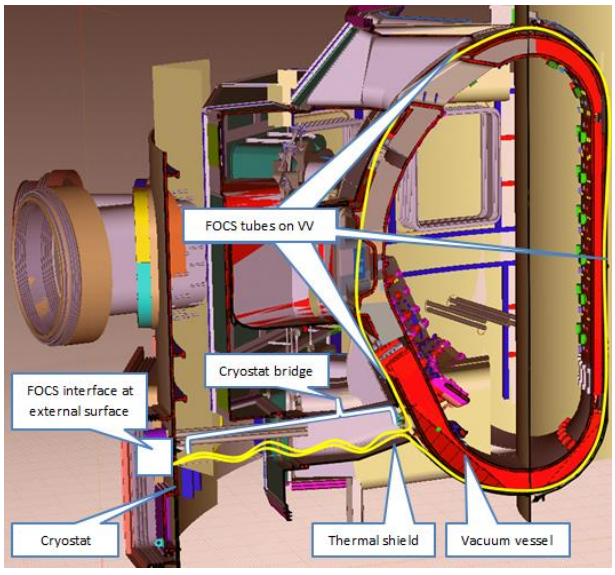

Figure H-1: Overview of the FOCS integration in ITER

- **Neutron Storage Area (55.BT)**

The radiation sources for neutron detector testing and In-Vessel neutron calibrations as well the fission chambers (FC) of the 55.BX Neutron diagnostics need a storage area on the ITER site. The neutron diagnostics (55.BC DNFM, 55.B4 NFM, 55.B1 RNC, 55.B2 VNC, 55.B3 MFC) contain

fission chambers (with different amounts of Uranium-235 and Uranium-238) and will be delivered to ITER starting in the 2020s from Japan Domestic Agency (JA-DA), Russia Domestic Agency (RF-DA), China Domestic Agency (CN-DA) and EU Domestic Agency (EU-DA). The fission chambers have to be stored at ITER site before they are assembled/ installed in the machine. The diagnostics will also use radioactive sources such as α–, γ– and neutron sources for calibration, to perform site acceptance test and functional tests.

Meetings have been held with Facilities and Logistics Management division and safety and security officers within the IO. The storage location has to ensure safety and security of the fissile and radioactive material under normal and off-normal conditions, and has to be inside the ITER INB zone. The IO has to make a declaration to the ASN in order to have Uranium-235 on site and request authorization to ASN for radiation sources on site. The Domestic Agencies will also have to apply for an Export Licence to their respective governments and the whole life cycle of the fission chambers has to be known including the activities in the storage area.

Currently, a storage area has been enabled in the baseline. A layout is being designed representing the necessary required storage for fission chambers and radiation sources. In the storage facility there will be a dedicated area for performing the functional tests of the detectors by using very low yield radiation sources.

- **H-alpha and Visible Spectroscopy (55.E2)**

The H-alpha and Visible Spectroscopy diagnostic on ITER shall consist of 4 optical channels located in several port plugs: two channels in EPP#11, one channel EPP#12 and one channel in UPP#2. The wide field of view (FOV) channels located in EPPs (two channels in EPP#11 and one in EPP#12) shall be aimed to observe the whole poloidal section of ITER FW (at least half a Blanket Module wide in toroidal direction). The EPP#11 channels shall cover the inner wall and top part of the chamber, whereas EPP#12 channel shall cover most of the ITER FW outer part (BM#10-BM#18). The approximate FW areas to be observed by EPP channels are shown in Figure H-2.

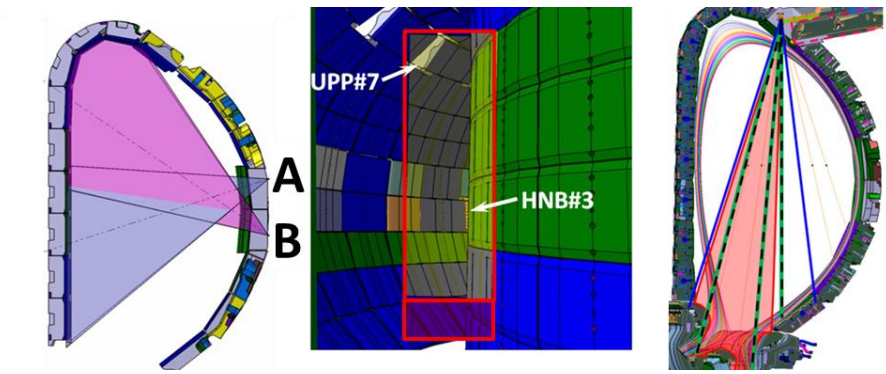

Figure H-2: Fields of views of H-alpha and Visible Spectroscopy.

Strong impurity emission from wall materials (e.g. Be) can indicate excessive levels of interaction between the plasma and the wall and indicate regions of potential erosion and redeposition of material leading to consequent tritium retention and dust production. Therefore the need of Be imaging was identified instead of the currently specified integral measurements. For the same reason imaging of the D and T influx was requested.

The design of the diagnostic allows for imaging, however this option is not in the baseline and thus needs to be an upgrade. Extra cameras are needed to realize this; the optical resolution of the system is about 15 mm on the inner wall and 45mm on the outer wall.

- **Divertor Impurity Monitor (55.E4)**

The baseline for the Divertor Impurity Monitor (DIM) system has 6 views x 70 sightlines per view. This system allows the diagnostic to perform the Machine Protection role of measuring the impurity emission. In this configuration, roughly half of the sightlines are populated with detectors and spectrometers. To improve the spatial resolution for the ion temperature measurement (from approximately 40 mm to approximately 20 mm), more spectrometers are required. Note that the formal requirement is actually 50 mm (along leg) x 3 mm (across leg). Achieving 3 mm is very challenging even after data unfolding, but populating all the sightlines would be significant step closer to the objective and this is included as an upgrade.

- **Radial X-ray System (55.E7)**

The radial X-ray system comprises of in-port and ex-port detectors. In the original plan, it was assumed that the initial non-nuclear detectors would be replaced by nuclear detectors before the start of the DT phase. However, the current plan is that the port plugs will only be removed from the machine and opened at the end of the First Plasma Phase (just before PFPO-1). This means that the detectors need to be developed more quickly than previously planned. As a result of the configuration workshop, funds have been put aside for the development of these detectors and we have worked with the DA involved to reorganize the planning. This work will need to be completed by the time the port plug (EQ12) comes out for complete assembly after the first plasma campaign.

- **Density Interferometer Polarimeter (55.FA)**

The Density Interferometer Polarimeter (DIP in Eq port 8) is of the dispersion interferometer type and will comprise of two channels. One which goes radially inwards and one which goes tangentially from Equatorial port 8 to Equatorial port 3. The tangential chord supports the polarimeter. Following the basic single channel radial installation in the First Plasma phase, the system will be reconfigured and expanded to its planned capacity. In this case, all of the components in port 8 will be installed and roughly half the back-end. In the current planning, the budget for the completion of this system will be available in the operational phase and thus is an upgrade. Note that the TIP (Toroidal Interferometer Polarimeter) in Equatorial 9 is also planned to come on line at this stage. These systems will operate independently.

- **Flow Monitor (55.GE)**

The ITER boundary coherence imaging (CI) system, or simply ‘flow monitor’, is an advanced imaging system for detailed measurement of the impurity ion flows and temperatures in the ITER plasma boundary and divertor. These measurements are essential for benchmarking models of edge and divertor transport. Moreover, the layered co-deposition of beryllium and isotopes of hydrogen in the ITER divertor is a safety issue because of possible tritium retention and the production of dust. A measurement of ion flows between the inner wall and the inner divertor baffle, combined with erosion/deposition measurements and Langmuir probe measurements at the inner baffle will allow validation of Be migration models. Validated models will provide a predictive capability for divertor performance and control in ITER and future fusion devices. The schematic of the ITER flow monitor is shown in Figure H-3. The diagnostic consists of an optical system with a front-end mirror system located inside one of the ITER port plugs and extending through interspace to the port cell which contains the processing optics and CCD camera. The flow monitor is planned for installation in equatorial port 8. A scoping study for the ITER CI flow monitor has been performed and thus this system is currently enabled.

- **Core Thomson Scattering (55.C1)**

The system will bet set up initially with a single well established laser (1064 nm). This will typically have a frequency of between 20 and 50 Hz. The second or further lasers to make up to 100 Hz will come in PFPO-2.

This system will guarantee electron temperature measurements to about 25 keV within specification. For higher temperatures as in the requirements (up to 40 keV), several additional measures are being considered. One is an additional longer wavelength (1320 nm) laser and the other is to use polarization scattering on the conventional laser. Both methods use the same transmission chain.

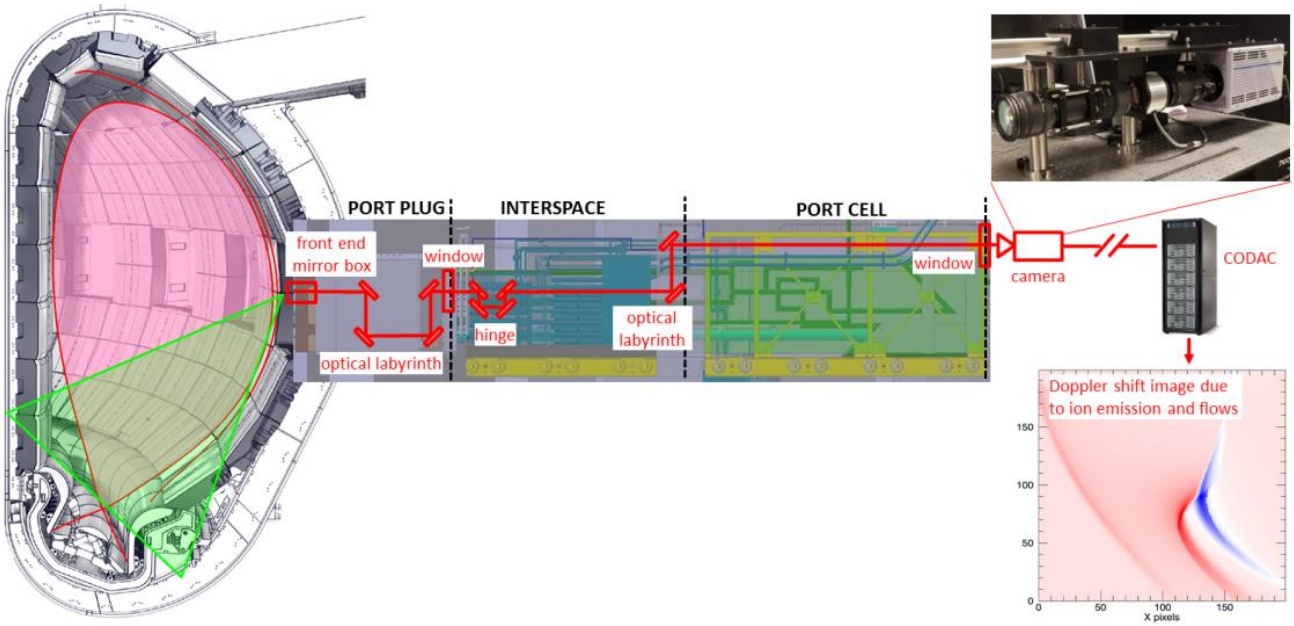

Figure H-3: Outline of the Divertor Flow Monitor.

- **Residual Gas Analyzer (55.G4)**

The Residual Gas Analyzer (RGA) (see Figure H-4) measures the neutral gas composition in a divertor port and an equatorial port during plasma operation. The 2 RGA subsystems are being procured by the US-DA and are planned for this phase. Only vacuum flanges are delivered for the First Plasma to blank-off the RGA sampling points.

Each subsystem comprises a sampling pipe which feeds gas from the primary vacuum at the port to an analysis chamber located in the port cell. In the divertor port the RGA is only able to achieve the required response time, 1 s, when there is a gas flow to the divertor cryopump; typically these pumps are on for only 50% of the plasma discharge. The upgrade of the RGA beyond the scope of the PA with the US-DA consists of a further 2 RGA systems at 2 other divertor port locations, so that continuous monitoring of the divertor is possible with suitable phasing for cryopumps.

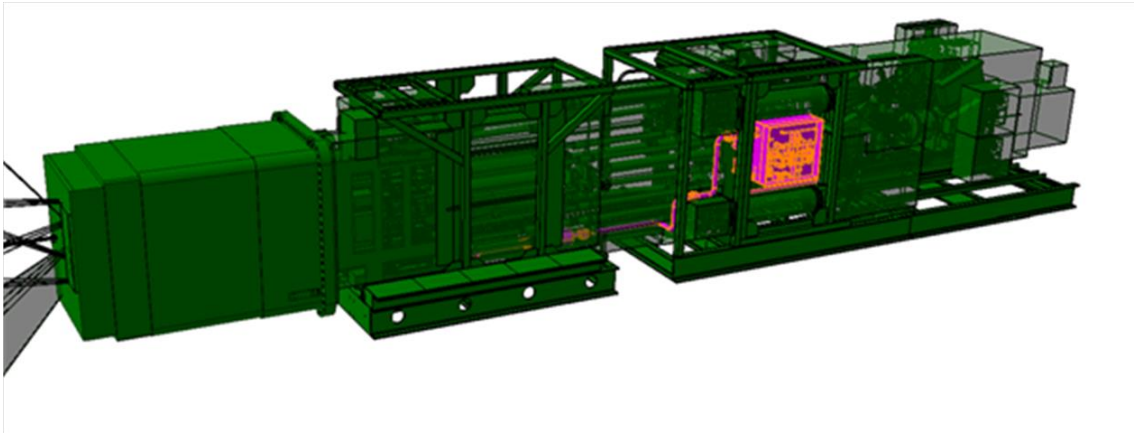

Figure H-4: RGA integrated into the Equatorial 11 Port Cell Support Structure.

Table H-2 – Diagnostic systems available for PFPO-1 (in addition to those for First Plasma)

PBS	System Name	Comment
55.A8	Fibre Optic Current Sensor	Captive part installed
55.AJ	High Frequency Sensors	
55.AL/AO	Divertor Coils	
55.AM	Divertor Shunts	
55.AN/AP	Divertor & Blanket Rogowski Coils	
55.B3	Microfission Chambers	
55.B4	Neutron Flux Monitor Systems	
55.B8	Neutron Activation System	
55.BC	Divertor Neutron Flux Monitors	
55.BV	Neutron Calibration (2.5 MeV) [Partial]	Simple calibration test planned here
55.BT	Neutron Facility Area	
55.C1	Core Plasma Thomson Scattering (partial)	1 laser installed in this phase
55.C5	Toroidal Interferometer polarimeter (TIP and measures line integrated Density in EQ9)	
55.D1	Bolometry System	
55.E2	H-Alpha Visible	Some cameras missing at this stage.
55.E4	Divertor Impurity Monitor	Some spectrometers missing at this stage.
55.E5	Core Imaging X-ray Spectrometer	
55.E6	Visible Spectroscopy Reference System	
55.E7	Radial X-Ray Camera	Edge Detectors still under development
55.EG	VUV Divertor	
55.EH	Vacuum Ultra-Violet Edge	

55.EI	X-Ray Crystal Spectroscopy Edge	
55.F1	Electron Cyclotron Emission	
55.FA	DIP (density-EQ8)	All front-ends will be installed.
55.G1	Vis/IR Eq Ports (remainder of system)	
55.G2	Thermocouples (divertor)	
55.G3	Pressure Gauges	
55.G4	Residual Gas Analyzers	2 channels installed
55.G6	Divertor IR Thermography	
55.G7	Langmuir Probes	
55.GA	Vis/IR Upper Ports	
55.GD	First Wall Samples	
55.GE	Flow Monitor	Captive parts installed
55.GG	Calorimetry (for testing with aux. heating inputs)	

H.4 Diagnostic Capabilities for PFPO-2 and planned upgrades

By PFPO-2, a strong diagnostic set will be established with many systems already in operation since PFPO-1. In this phase, the emphasis on measurement capability is for plasma control, investment protection and basic plasma parameters. The diagnostic set added or upgraded in this phase is shown in Table H-3 . Note that, as for the First Plasma systems, the measurement capabilities for each plasma parameter can be found in SRD-55 [ITER_D_28B39L, 2017]. A discussion on the implication of 1.8 T operation for the diagnostic systems available in PFPO-2 can be found in section H.6. From an operation perspective, this is a much more demanding phase, as it is the phase in which 15 MA/5.3 T plasmas will first be achieved (see section 2.5.5.11) and all systems will be expected to be highly performing in preparation for the transition to D/DT operation. This includes, in particular, the systems that are brought into routine operation in this phase. Note that many of these PFPO-2 systems will already be installed in PFPO-1. For them basic commissioning will be attempted, where possible, using PFPO-1 plasmas.

To explain the state of those systems that are not complete for PFPO-2 operation (blue for upgrades and red for enabled systems in Table H-3), a short explanation is provided below:

- **Edge Thomson Scattering (55.C2)**

The edge Thomson scattering will have most of its components installed in PFPO-1. This will allow it to come in to operation reliably in PFPO-2 with the possibility to commission it in the second half of PFPO-1, if opportunities are available. If this is possible, then this diagnostic can play a role in measuring the edge profiles for the 1.8 T campaign; this is of great interest for the characterization of the H-mode pedestal plasmas in 5 MA/1.8 T plasmas in PFPO-1 (see section 2.5.4.9). The system was originally designed with a spatial range of measurement of $0.85 < r/a < 1.0$. To allow an overlap with the core Thomson Scattering, the viewing range is being extended to $0.8 < r/a < 1.03$. This will also allow having measurements for a wider range of plasma shapes/positions. Therefore, the system is currently being designed with this capability, which is included as an upgrade. The main items of the upgrade are the additional fibres and back-end electronics for the new channels.

- **Poloidal Polarimeter (PoPola) (55.C6)**

The PoPola system measures the plasma current profile by measuring the change in the polarization properties of a fast infrared (FIR) laser beam traversing the plasma, due to the magnetic field. Tomographic reconstruction on an array of laser chords spanning the plasma yields the 1-D q-profile. As with all tomography techniques, increasing the number of chords increases accuracy and reduces errors. The baseline PoPola system has 10 chords, and 'enables' an additional 3 chords by providing front-end (in-vessel) components. The back-end (optics relay, lasers and detectors) for the 3 additional chords is considered an upgrade. As shown in Figure H-5, the average error across the profile is reduced with these additional 3 chords and, therefore, this upgrade is adopted in the diagnostic plan.

- **High Temperature Thomson Scattering (55.C8)**

Accessing the highest temperatures expected in ITER (up to 40 keV) put strong demands on the Thomson Scattering measurement technique. This comes about because at temperatures above 25 to 30 keV, the spectrum is very much shifted towards the blue spectrum. At these wavelengths, there are some issues related to background lines and general detectability of the signals. If the core system can solve these issues (see 55.C1 for details), then this system will not be needed. A decision on this system will need to be taken in the next two years and work is ongoing to support this decision. It should be noted that integration of this option is complex.

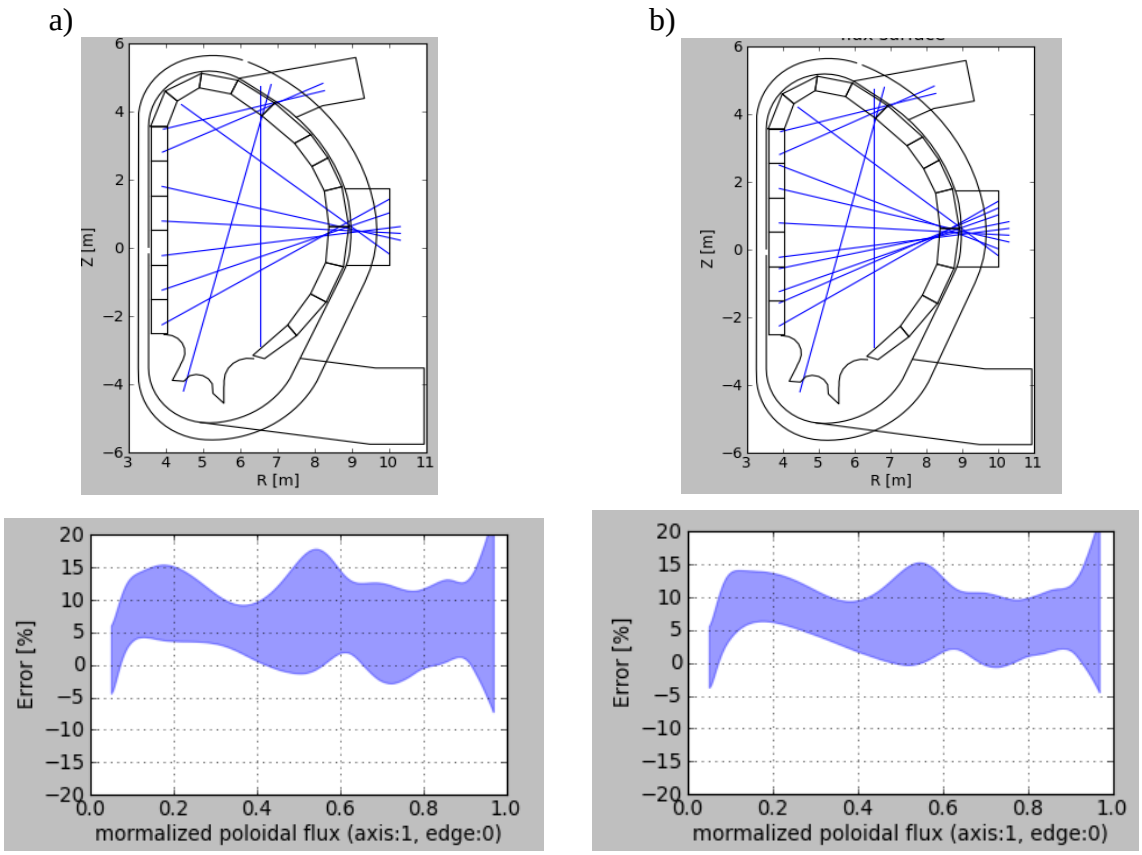

Figure H-5: a) 10 PoPola chord layout and q reconstruction errors, b) 13 chord PoPola layout and q reconstruction errors. Average error across the profile are reduced from ~15% to <10%.

- **Laser Induced Fluorescence (55.EA)**

The LIF (Laser Induced Fluorescence) diagnostic is intended to support the measurement of the helium density in the divertor. This system is currently enabled and is sharing the front-end with the Divertor Thomson Scattering system. Interfaces are preserved for this system.

- **Motional Stark Effect (55.EB)**

The MSE (Motional Stark Effect) diagnostic measures the local magnetic field strength and direction based on the wavelength split and polarization of the Stark split line emission of neutral beam atoms. From these measurements the plasma current profile (q-profile) is derived.

The baseline MSE system on ITER has one view on Heating Neutral Beam 1 (HNB1) from equatorial port 1 (EPP1), measuring the plasma centre, and one view on HNB2 from EPP3, measuring the plasma edge (see Figure H-6). Because the injection direction of the HNBs can be varied between an on-axis (HNB passing through the plasma centre) and an off-axis position (HNB passing below the plasma centre), no measurement of the q-profile can be provided in the plasma centre when HNB1 is aimed off-axis. This is problematic because the main aim of off-axis HNB operation is to create flat or reversed q-profiles, which are difficult to determine experimentally without an on-axis q-profile measurement.

As a solution, the front-end of the MSE diagnostic has been modified to include a view on the diagnostic neutral beam (DNB) from EPP3 (see Figure H-6). Although the DNB has a more limited duty cycle and lower signal levels than the HNBs, it is always aimed on-axis. This leads to following MSE capabilities for different modes of HNB operation:

- HNB1 on-axis & HNB2 off-axis — Full (core & edge) coverage by the MSE system. Core is covered twice (HNB1 and DNB), allowing to commission the DNB view which will have a lower signal.
- HNB1 off-axis & HNB2 off-axis — Full (core & edge) coverage by the MSE system. Core is covered by the DNB view.
- HNB1 on-axis & HNB2 on-axis — Core MSE coverage, but no edge coverage. Acceptable because the edge q-profile is well covered by magnetics and polarimeter.
- HNB1 off-axis & HNB2 on-axis — Core MSE coverage by DNB view, but no edge coverage. This HNB configuration is, in principle, identical to HNB1 on-axis and HNB2 off-axis, which has the best MSE coverage.

The baseline MSE does include the front-end (in-vacuum) optics for the DNB view, but an upgrade is required for the (in-air) back-end; this includes optical fibres (most critical, as they have to be installed no later than Assembly Phase II before PFPO-1), detector systems and instrumentation and control (I&C).

- **BES fluctuations and Escaping Alpha FICX (55.EC)**

Beam Emission Spectroscopy (BES) fluctuation measurements are used in many tokamaks to study both MHD and turbulence, typically using a 2-D array coverage that allows identifying radial and poloidal correlation lengths, E×B velocities and shearing. Especially in the pedestal region, BES fluctuations are of interest in the study of the L-H transition and ELM characteristics.

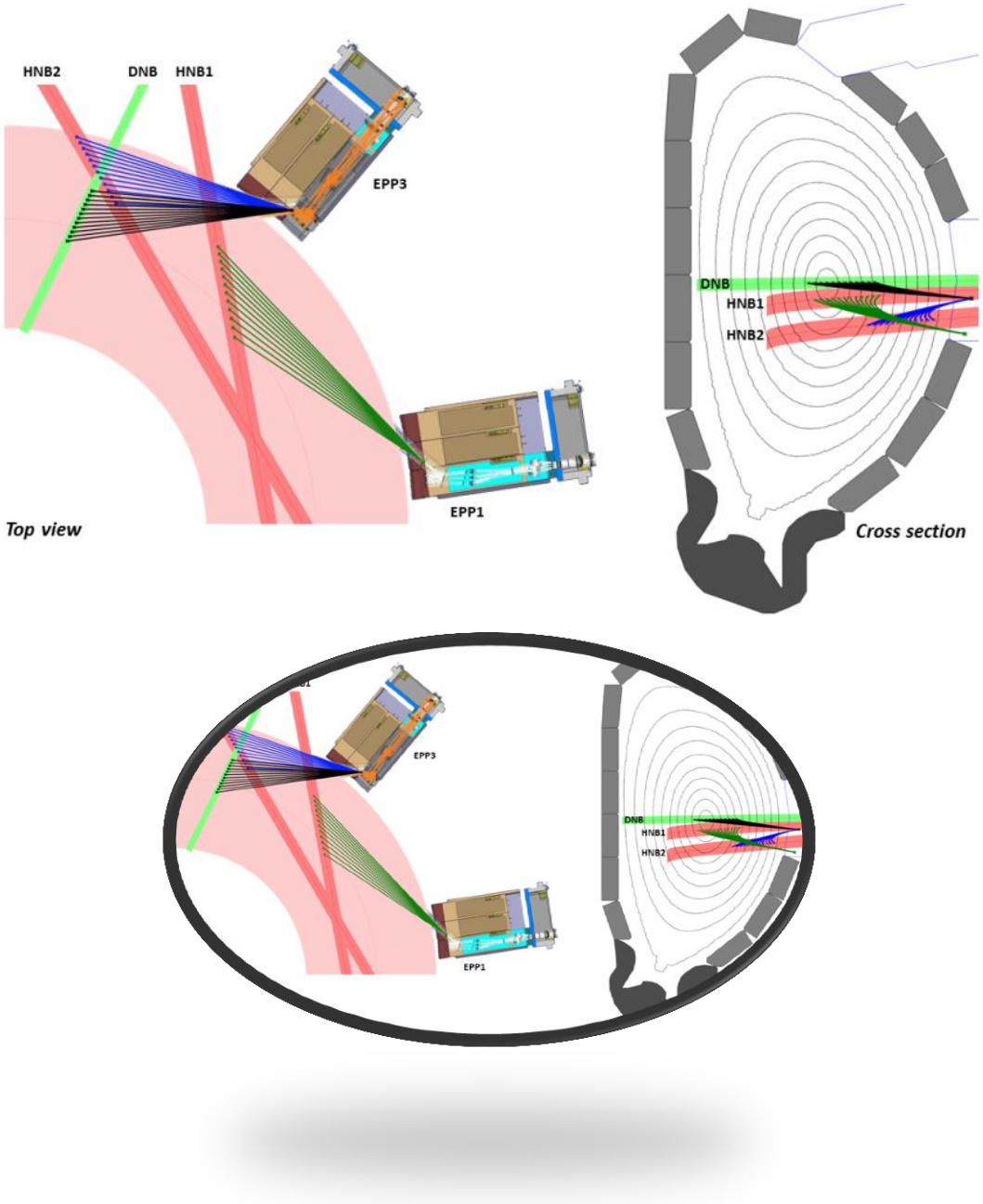

Figure H-6: Top-view and cross section view of the MSE sightlines. The baseline MSE system covers the on-axis HNB1 from EPP1 (core measurement) – green – and the off-axis HNB2 from EPP3 (edge measurement) - blue. It also includes the front-end optics (in-vacuum mirrors) for the DNB view – black – but not the optical fibres nor the back-end detection system and I&C.

Fast α-particles escaping the plasma before thermalizing are a concern, because they create an extra heat load on the walls and they reduce the self-heating of the plasma. Measuring/monitoring them is, however, quite challenging. Fast Ion Charge Exchange (FICX[7]) is predicted to have a substantial signal from the pedestal region upon interaction with HNB2 for escaping-α fractions down to 10%.

[7] FICX is in current tokamaks mainly used to study fast neutral beam particles and therefore named FIDA (Fast Ion D-Alpha). In ITER, however, the main fast ions of interest would the α-particles, rather than the D from the beams, hence the use of the more general term Fast Ion Charge Exchange or FICX.

This diagnostic would monitor the quantity of escaping α-particles and also yield information about the energy distribution of the escaping α's.

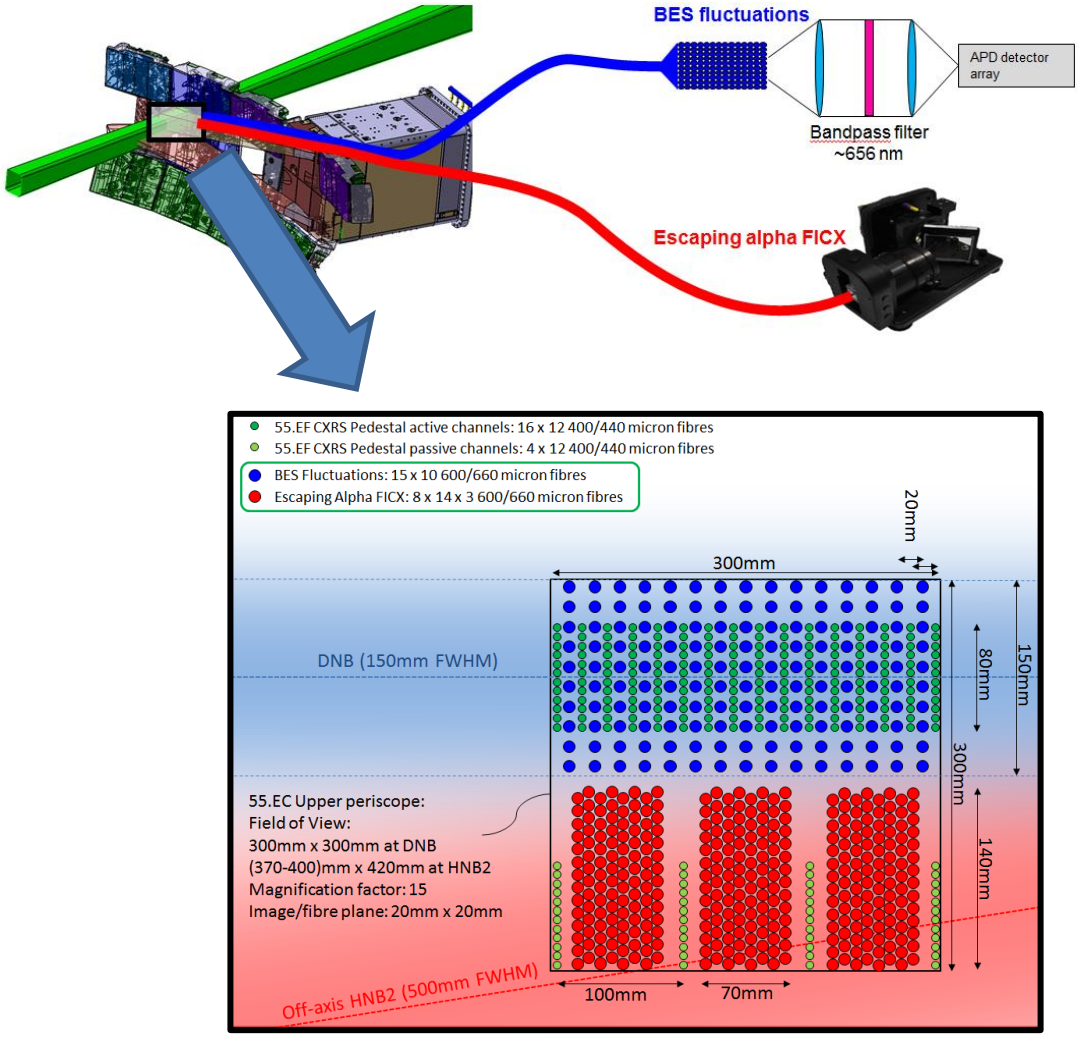

Figure H-7: Sketch of the proposed upgrade that would allow both BES fluctuation and escaping-α FICX measurements. The front-end (in-vacuum) optics already form part of the CXRS Edge system. The upgrade would involve the installation of dedicated optical fibres, back-end detection systems and I&C. The inset gives an overview of the proposed usage of the CXRS Edge image plane, whereby a 15 by 10 array of BES fibres (blue) would be interleaved between the on-axis (active) CXRS channels (dark green) and 3 FICX channels (red) would be interleaved between the off-axis (passive) CXRS channels (light green).

Neither BES fluctuations nor FICX measurements currently form part of the ITER baseline. However, the neutral beams (DNB and HNB2) are already covered in the pedestal area, with adequate spatial resolution, by the CXRS (Charge Exchange Recombination Spectroscopy) Edge system. Therefore, an upgrade to enable BES fluctuation and escaping-α FICX measurements would only involve the (in-air) back-end: this includes optical fibres (most critical as they have to be installed no later than Assembly Phase II before PFPO-1), detector systems and I&C. Figure H-7 shows a sketch of the proposed system, whereby a 15 (radial) by 10 (vertical) array of BES channels is interleaved between the on-axis (active) CXRS channels and 3 FICX channels (that require more fibres to collect more light than standard CXRS channels) are interleaved between the 4 off-axis (passive) CXRS channels. In the diagnostic area the BES fibres would be connected to a

fast, filtered detector array, whereas the FICX fibres would be connected to off-the-shelf high-étendue spectrometers.

Table H-3 – Diagnostic systems available for PFPO-2 (in addition to those for First Plasma and PFPO-1)

PBS	System Name	Comment
55.BV	Neutron Calibration (2.5 MeV)	
55.C1	Core Plasma Thomson Scattering (full)	
55.C2	Edge Thomson Scattering	r/a from 0.85 to 1.0 available
55.C4	Divertor Thomson Scattering	
55.C6	Poloidal Polarimeter	10 channels available
55.C8	High Temperature Thomson Scattering	Still to be decided if this is needed as the Core system may be able to handle the high electron temperature
55.E1	Charge Exchange RS Core	Requires diagnostic neutral beam to be operational
55.E8	Neutral Particle Analyzers	
55.EA	Laser-Induced Fluorescence	Enabled and used Divertor Thomson Scattering front-end
55.EB	Motional Stark Effect	Requires heating neutral beams. Requires extra components and diagnostic neutral beam to measure when heating beam is off-axis.
55.EC	Charge Exchange RS Edge	Requires diagnostic neutron beam. Requires extra components to add measurements of fluctuations and escaping α's.
55.EF	Charge Exchange RS Pedestal	
55.F2	Reflectometry Low Field Side	
55.F3	Plasma Position Reflectometry	
55.F9	Reflectometry High Field Side	
55.G8	Erosion Monitor	
55.G9	Dust Monitor	
55.GG	Calorimetry	
55.GC	Tritium Monitor	Commission in PFPO-2 and obtain first results

H.5 Diagnostic Capabilities for FPO and planned upgrades

By FPO, many diagnostics will be established with many systems already in operation since First Plasma, PFPO-1 and PFPO-2. In this phase the emphasis on measurement capability is for fusion power production and burning plasma physics. The diagnostic set added or upgraded in this phase is shown in Table H-4 . It can be seen that the systems still to be implemented are those that are more specifically related to DT measurements. All these systems are currently having their interfaces defined and the basic system is designed. Most of these systems will undergo a Conceptual Design Review) CDR in the near future year with the exception of the CTS which has already been completed.

- **Radial Gamma Ray Spectrometer (55.B7)**

The Radial Gamma-Ray Spectrometer (RGRS) is a multiple detector, multiple lines-of-sight spectrometer optimized for photons in the energy range up to 17 MeV.

During fusion discharges in ITER, a series of energetic gamma-ray lines are expected, of which the most interesting ones are at 3.21 and 4.44 MeV (from α-Be reactions) and 17 MeV (from D-T reactions). These gamma lines are expected to be used as a sensitive diagnostic for the confined α-particle distribution inside the plasma volume and, secondarily, to evaluate the fusion reaction rate. The confined α-density profile may be inferred from the measured intensity of the 4.44 MeV gamma ray emission from the $^{9}Be(\alpha,n\gamma)^{12}C$ reaction. By measuring this emission along several lines of sight, the profile can be obtained through standard inversion algorithms. Moreover, RGRS is expected to have a prominent role in the diagnosis of runaway electrons (REs), particularly while they are in plasma (before hitting the wall); their maximum energy and other important parameters can be derived from the gamma measurements.

In order to exploit the potential of such a diagnostic, it is necessary to measure: i) the intensity (count rate), ii) the spectrum and iii) the distribution of the emitted photons, and all with an adequate time resolution in order to follow the plasma evolution. To this aim, a multiple lines-of-sight spectrometer has been designed, which matches the requested goals of energy resolution, efficiency and counting rate capabilities; the latter are needed to follow the time evolution of rapid phenomena in plasma discharges. The multiple lines-of-sight approach allows the reconstruction of the emission profile inside the plasma volume through a tomographic reconstruction approach.

The main components of a single RGRS detector are: i) the $LaBr_3$ scintillator crystal, ii) the photomultiplier tube (PMT), and iii) the magnetic shielding for the PMT. The detector assemblies for RGRS are designed to give support for the detectors while also being a component of the magnetic shielding. These are made of two main parts: a detector container/magnetic shield and an assembly support. The RGRS will perform gamma-ray measurements along a view of the collimated channels of the ITER Radial Neutron Camera (RNC) by the design of a suitable set of detectors, collimators and attenuators. This system is currently enabled and a CDR is expected in the near future.

- **Lost Alpha Monitor (55.B9)**

In ITER, the fusion reactions and the use of neutral beam and ion cyclotron heating systems will generate fast ions. Fast ions can be expelled from core region to the plasma edge by magnetohydrodynamic (MHD) perturbations. Fast ion loss can adversely affect confinement and plasma heating and can lead to localized heat load on the plasma-facing components.

The fast ion loss detector (FILD) (see Figure H-8) is one of the most widely used diagnostics for measuring fast ions in the plasma edge. FILD provides the measurement of the fast ion energy and the velocity pitch with time response up to the Alfvénic frequency, which allows extracting important information about the underlying fast ion loss processes. FILDs are installed in all major tokamaks and this diagnostic has been identified as a priority fast ion diagnostic for ITER by the ITPA Energetic Particle Topical Group [ITER_D_UFAXKQ, 2017].

A scoping study for the ITER FILD, slated for installation in equatorial port 8, is currently being performed. The conceptual design consists of a reciprocating system containing a probe head equipped with a scintillator (combined with an array of the Faraday cups) and an optical system transferring the signal from the scintillator to an array of photomultipliers and to a CCD camera.

In addition to the FILD, a lost-α monitor system has been proposed for installation under the divertor dome. This system will consist of an array of Faraday cups and will complement FILD measurements by measuring marginally trapped fast ions in continuous data acquisition mode.

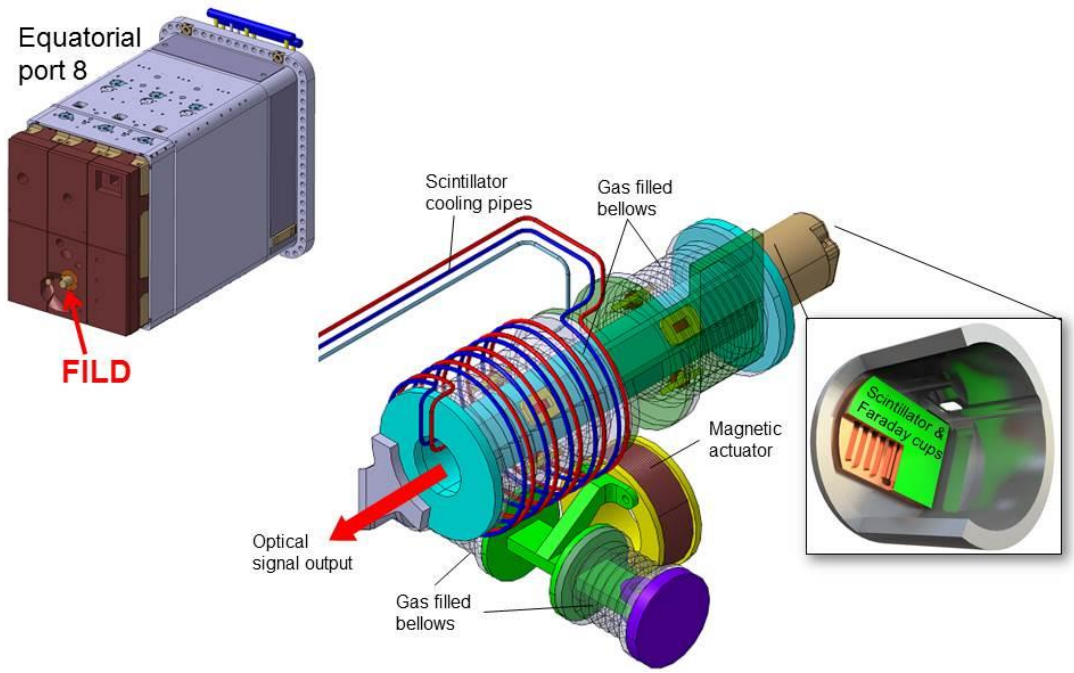

Figure H-8: FILD system outline as conceived for Equatorial 8.

- **High Resolution Neutron Spectrometer (55.BB)**

The High Resolution Neutron Spectrometer (HRNS) is dedicated to measure time-resolved neutron spectra for both DD and DT plasmas, providing mainly the determination of the fuel ion ratio in the plasma core for a wide range of ITER operational scenarios in fusion power (neutron yield) including spectroscopy measurements in the initial deuterium phase. The supplementary functions of HRNS are to provide information on the ion temperature, confined α-particles and fast ions. HRNS is a one-channel collimator system and is able to perform neutron measurements providing line-integrated data, where the record signal is an integral over local plasma conditions along the instrument's line-of-sight (LOS). The HRNS will be installed is in the Equatorial Port Cell #1 behind the RGRS and the RNC.

The HRNS system provides a dedicated measurement of the 14 MeV neutron emission from ITER DT plasmas and also of the 2.45 MeV emission in the initial phase of D operations. A suitable

2.45 MeV spectrometer is an important part of the HRNS system, which can provide important information during scenario development and testing of the heating systems in D. In addition, due to the long pulses and good confinement properties of ITER D H-mode plasmas, the tritium inventory in D plasmas may be sufficiently high to provide a good opportunity for testing and tuning all of ITER's 14 MeV neutron diagnostics by the burn-up of the T produced.

The neutron spectrometers should provide measurements of n_T/n_D with high time resolution (100 ms) and a measurement uncertainty of 20%. Fulfilling these requirements cannot be achieved with a single neutron spectrometer. Most neutron spectrometers have a dynamic range of 3 to 7 due to detection efficiency and/or count rate capability limits, set by random background and/or pile-up. This implies that the HRNS system needs to be built up of a number of different spectrometer techniques. For high performance plasmas generating a high neutron flux at the HRNS position, spectrometers based on the thin-foil proton recoil technique is preferred. For the medium range of neutron fluxes two spectrometer types can be used: back scattering time-of-flight and diamond detectors. For low n_T/n_D levels and pure D plasmas the only option is a conventional ToF system. The HRNS is an enabled system and is planned to undergo a CDR in the near future.

- **Vertical Gamma Ray Spectrometer (55.BD)**

The Vertical Gamma Ray Spectrometer (VGRS) system is currently foreseen to fit in the upper port in the place of the Vertical Neutron Camera (VNC). This system is enabled and the ability to install it is maintained by defining its interfaces. Currently in ITER, it is not possible to have both the VNC and the VGRS together due to space limitations, thus the priority has been given to developing the VNC in the first instance. Note also that background development is needed to provide a reliable system for the vertical views.

- **Tangential Neutron Spectrometer (55.BE)**

The Tangential Neutron Spectrometer (TNS) is a diamond-detector-based spectrometer with tangential lines of sight dedicated to studies of fast ion behaviour, in particular of the redistribution of fast ions in kinetic and real spaces arising from the presence of MHD instabilities, such as fishbones, sawteeth, NTMs and Alfvén Eigenmodes.

In ITER, in addition to heating, NBI will be used for current drive (NBCD). Fast NBI ions can drive Toroidal Alfvén Eigenmodes (TAE) leading to their redistribution. These processes affect the profile of the NBCD leading to a deviation from that predicted in their absence. A multi-lines-of-sight tangential spectrometer that can study the fast ion distribution function will measure this change in fast ion distribution and associated NBCD profile. Tangential measurements will be interpreted in combination with data from other existing radial diagnostics in order to reconstruct the 3-dimensional distribution function. The TNS, based on diamond detectors, could measure fast charge-exchange atoms directly (if operational in PFPO-2) and will provide collimated spectra of DT neutrons in the nuclear phase of ITER.

The measurement timescales of the proposed diamond-based neutron spectrometer would allow the determination of the fast ion distribution function in the presence of MHD events such as sawteeth, fishbones, NTMs and TAE modes. The TNS observes ITER's plasma with three chords that cross i) plasma core, ii) ¼ of minor radius and iii) ½ of minor radius. Three detector modules, consisting of different sensitivity diamond detectors will be installed in the central drawer of equatorial port 8.

- **Collective Thomson Scattering (55.C7)**

The CTS is implemented in Equatorial port 12. Currently, the front-end of this system is being designed as part of an EU-DA package and is progressing well. The back-end interfaces are being enabled and finalization of the design will be carried out once the funds become available.

Table H-4 – Diagnostic systems available for FPO (in addition to those for First Plasma, PFPO-1 and PFPO-2)

PBS	System Name	Comment
55.B1	Radial Neutron Camera	
55.B2	Vertical Neutron Camera	
55.B7	Radial Gamma Ray Spectrometer	Captive parts installed
55.B9	Lost Alpha Monitor	Captive parts installed
55.BB	High Resolution Neutron Spectrometer	Captive parts installed
55.BD	Vertical Gamma Ray Spectrometer	Captive parts installed
55.BE	Tangential Neutron Spectrometer	Design Being Developed
55.BV	Neutron Calibration (14 MeV)	
55.C7	Collective Thomson Scattering	Captive parts installed
55.GC	Tritium Monitor	

H.6 Impact of 1.8 T operation on diagnostic systems and specific upgrades required

The ITER Research Plan considers operation at 1.8 T to access the H-mode in PFPO-1 (section 2.5.4.9) and to further explore it in PFPO-2 (section 2.5.5.7). This has an impact on the ability of the diagnostic systems to meet their measurement requirements. Corrective measures can be taken and the associated cost impact is being evaluated. It is also noted that the ECRH system may operate at a lower frequency (between 104 and 110 GHz) besides the nominal frequency (170 GHz). Therefore, diagnostic systems will have to be protected from ECRH stray radiation at both frequencies if this ECRH option is adopted. In this section we highlight the main diagnostic systems which are impacted by this operation and describe the upgrades that would be required. In general, with the exception of some microwave systems, there is no plan to modify the hardware requirements for the diagnostic systems. This implies that, in general, a compromise has to be reached between measurement accuracy and time resolution for some of the plasma parameters to be measured during 1.8 T operation.

H.6.1 Model plasmas used for the evaluations

To evaluate the impact of 1.8 T operation on the diagnostic systems, the following plasma conditions have been considered

- 5 MA/1.8 T H-mode He scenario with 20 MW of ECRH: [ITER_D_TP3QQA, 2016] and associated DINA output [ITER_D_TMT985, 2016];
- METIS and ASTRA simulations for helium H-modes and hydrogen L-mode plasmas (see Appedix F).

During the flat-top period, the electron densities are in the range of (1-2)×10^{19} m^{-3} while the electron temperature can have peak values higher than 10 keV in these plasmas. Work is on-going to evaluate the performance of the diagnostic systems and to determine the required upgrades. The status of this work is summarized below.

H.6.2 Implications of 1.8 T operation on diagnostic systems

H.6.2.1 ECE (55.F1)

The low frequency radiometer can be used for measurement of the plasma temperature, providing high quality measurements in the pedestal region. However, an upgrade to the back-end is required to provide measurements of the 2nd harmonic X-mode, as detailed in [ITER_D_TXQ5E8, 2016]. Note that this diagnostic is available from PFPO-1.

H.6.2.2 Core Thomson scattering (55.C1)

The Core Thomson Scattering system is available in PFPO-1. The minimum density to be measured by this diagnostic according to SRD-55 [ITER_D_28B39L, 2017] is 3×10^{19} m^{-3} and the baseline temporal resolution is 10 ms (100 Hz) and for PFPO-1, one laser (between 20 and 50 Hz) is currently expected to be delivered. For lower plasma densities than the baseline, such as those for 5 MA/1.8 T operation, measurements are possible by integrating the data over several laser pulses. Assuming that the system is delivered with a 20 Hz laser, then for a reduced density of 1×10^{19} m^{-3}, the integration would be approximately 3-4 times longer (classically 3, but 4 to account for detector noise). This would mean that the signal would be provided on a 200 ms basis rather than with 50 ms. If the 50 Hz laser option is deployed in PFPO-1, then the density measurement at 1×10^{19} m^{-3} would have a correspondingly higher time resolution.

H.6.2.3 Edge Thomson scattering (55.C2)

The edge Thomson scattering (ETS) is available in PFPO-2 although there is a plan to implement it and commission it earlier as described above. If this is possible, then the basic edge electron profile measurements can be available towards the end of PFPO-1. According to the current baseline, the ETS is capable of measuring the electron density within 5×10^{18} - 3×10^{20} m^{-3}. The temporal resolution is 10 ms (100 Hz) assuming the full laser capacity is installed. For lower density measurement, relaxation of the temporal resolution for signal integration is needed as for the core TS. For instance, the temporal resolution would be > 50 ms to measure electron density close to 1×10^{18} m^{-3}. Any further low density measurement would be impractical because of thermal noise in the electronics.

H.6.2.4 LFS-Reflectometer (edge density profiles) (55.F2)

In the current configuration, most of the pedestal would be missed for 1.8 T operation. A mitigation measure would be to install a new back-end in the diagnostic building covering the Q-band (33-50 GHz). The frequency multiplexer should also be adapted. Transmission lines can work with some degraded performance. Note that this diagnostic would only be available from PFPO-2.

H.6.2.5 Plasma Position Reflectometer (gap control) (55.F3)

For this system, there is no significant impact. This system uses O-mode in its baseline and does not rely on the magnetic field. Low density means that its performance might be slightly degraded. Note that this diagnostic would only be available from PFPO-2.

H.6.2.6. HFS Reflectometer (core profile) (55.F9)

To keep a baseline radial coverage, the frequency capability should be lowered by adding a Ku-band 12-18 GHz. A new back-end frequency multiplexer would be required. The transmission lines and vacuum windows are likely to limit the performance of the system; this needs further detailed study. Note that this diagnostic would only be available from PFPO-2.

H.6.2.7 CIXS (X-ray core spectrometer to measure the core Ion Temperature) (55.E5)

Tungsten emission in the 1.8 T discharges would potentially be challenging to measure due to the potentially low W concentrations. This could jeopardize the ion temperature measurement in PFPO-1, which are key because the expected high T_e/T_i ratios in these plasmas. Note that the other diagnostic for ion temperature measurements (CXRS) is not yet available in PFPO-1. As a mitigation, the premixing of 0.001% Xe with the fuelling gas is proposed and has been requested to be included in the gas introduction system (leading to $n_{Xe}/n_e = 10^{-5}$ in the plasma), which, according to modelling, should allow the measurement requirements to be met. Note that this diagnostic is available from PFPO-1.

H.6.2.8 XRCS (X-ray Crystal Spectroscopy Edge- to Measure the Edge Ion Temperature) (55.EI)

The 55.EI XRCS spectrometer is one of four XRCS subsystems that together measure the ITER core and edge plasmas. Its primary goal is to measure ion temperature and plasma rotation profiles in the outer plasma. Poloidal profiles of the plasma at r/a > 0.9 are imaged via a spherical crystal located outside of an upper port, onto a 2-D X-ray detector. It is optimized for very high spectral resolution in a narrow band around wavelengths 0.2 - 0.5 nm interval, chosen to contain representative line emission from the main impurities. This system is important for the PFPO-1 phase, as there will be no other edge ion temperature measurement. The impact of 1.8 T in this diagnostic measurement would be through the level of impurities in the 5 MA/1.8 T H-mode plasmas.

H.6.2.9 TIP Interferometer (55.C5)

No major signal or accuracy degradation is expected for the interferometry measurement. Polarimetry measurement is likely not to be available at these densities. Interferometry fringe jumps would therefore need to be corrected without the help of polarimetry. This is not expected to be a major issue as the densities are low. Note that this diagnostic will be available from PFPO-1.

H.6.2.10 DIP Density Interferometer/Polarimeter (55.FA)

No major signal or accuracy degradation is expected for interferometry measurement. Polarimetry measurement is likely to be not available at these densities. This is not expected to be a major issue as the densities are low. Note that this diagnostic will be available from PFPO-1.

H.6.2.11 MSE Measurement (55.EB)

No impact on hardware and minimal impact on performance are expected. The Doppler shift changes as well as the Stark splitting with 5 MA/ 1.8 T but changes are smaller than the changes expected when going from H-beams (PFPO-2) to D-beams (FPO) and are therefore covered in the design. Note that this diagnostic would only be available from PFPO-2.

H.6.3 ECRH stray radiation protection

All microwave diagnostics have been designed to be protected from 170 GHz stray radiation (and 60 GHz from CTS). They need to be protected from ~ 105 GHz radiation if ECRH heating at this frequency is to be considered for 1.8 T operation. These protection features will make use of: pin switches, notch filters, band-stop filters and stray radiation detectors with active feedback to the ECRH heating:

- **55.F1-ECE**: New filters have to be developed and integrated in the system.
- **55.F2-LFS-Reflectometer**: All the strategy for stray radiation protection has to be changed to include the 105 GHz range. Back-end protection is mostly done in the diagnostic building but vacuum windows are mainly protected by the customized grated mitre bend in the port plug. It is unlikely that it will be possible to change these components for 1.8 T operations. A strategy should be agreed to avoid 105 GHz ECRH stray radiation arriving around Eq. Port#11.
- **55.F3-Plasma Position Reflectometer**: New filters have to be developed and integrated in the system.
- **55.F9-HFS Reflectometer**: New filters have to be developed and integrated in the system.
- **55.NW-Vacuum windows**: In a generic approach, it is planned to protect vacuum windows by coating the inner surfaces of the in-port plug optical paths at risk of stray ECRH radiation with a microwave absorber layer. This coating is optimized for 170 GHz absorption. Its efficiency at 105 GHz should be assessed.

H.7. Conclusions

An explanation of the measurement systems available for each phase of operation in the Staged Approach with an emphasis on the missing components (upgrades to improve baseline diagnostics and to enable diagnostics) has been provided in this Appendix. This shows that a basic diagnostic set is available for First Plasma. Subsequent plasma phases will add diagnostics in line with what is required for the development of the ITER Research Plan. The systems that need further improvement (upgrades) or development (enabled) have been described along with the items that are missing. In the current planning, the budget for these systems is expected to be available for the operational phase. Some budgets for critical system development have already been provided to allow interfaces and other critical aspects to be prepared, in advance, for these diagnostic systems. In some cases, the planning is reasonable as many of the missing items are back-ends and can be delivered quickly. In most cases, a delay in availability of the funding to provide the upgrade or build the enabled diagnostic will cause an increased risk for the systems' availability with the required performance (e.g. lower performance for the upgrades or no measurement capability for the enabled systems).

The second aspect discussed in this Appendix is the ability to measure parameters in 1.8 T plasma operation and with, possibly, some level of ECRH heating at lower frequency (104-110 GHz). In this case, the main impacted systems have been studied to give an indication of how they can address the 1.8 T operation. The general conclusion is that with small adjustments to some systems and, in some cases, increasing the time resolution of the measurements, the 1.8 T plasmas will be reasonably well diagnosed. Note that the Edge Thomson scattering is currently planned for PFPO-2 but it is expected to be installed in PFPO-1 and commissioned during this phase. Currently, the reflectometers which can measure edge density profiles are expected to be installed in PFPO-2, but

these could also be accelerated to make measurements if it is deemed appropriate. A decision on this could be made on the timescale of the PCR that will implement the 1.8 T operation, which is presently in preparation.

Appendix I: Tritium Availability

ITER will procure tritium for the DT experimental program from external civilian sources. The total mass of tritium which will be consumed to achieve the mission goal of producing an average neutron wall loading of 0.3 $MW.yr.m^{-2}$ laid down in the *Project Specification* [ITER_D_2DY7NG, 2010] is ~ 14.5 kg. In addition, a site inventory of several kg must be maintained for the efficient operation of the Fuel Cycle systems, and to account for tritium retained in, e.g., plasma-facing components. The ITER project will not start using tritium on-site until the tritium commissioning of the Tritium Plant commences (currently foreseen in 2033) and the ITER experimental program will start to consume significant amounts of tritium from 2036 onwards. To achieve the neutron wall loading target on a timescale commensurate with the lifetime of the ITER Agreement implies a burn rate of approximately 1 $kg.yr^{-1}$ for ~ 15 years following 2036. The question arises, therefore, as to whether the global civilian tritium inventory during the period 2036 – 2050 will be sufficient to meet the needs of the project.

Most of the tritium within the civilian stockpile is produced by fission reactors using heavy water as a moderator, commonly referred to as CANDU reactors. Such reactors are in operation for power production in Canada, Korea, Romania, India, China and Argentina. However, only Canada and Korea are known to extract significant tritium from their reactors which could be exploited 'commercially', and Romania has plans to do so. Estimates are available for the present stockpile and the current rate of tritium production in the Canadian and Korean fission programs. However, estimating the long-term tritium inventory from these sources involves several uncertainties, since at least some of these reactors will be decommissioned sometime in the next decade and Canada, which is currently the world's major producer of 'commercial' tritium, appears to have no plans to build further CANDU reactors (though it is proposed to refurbish at least some of the CANDU reactors to extend their operating life). Future estimates of the global tritium inventory, therefore, indicate that a maximum inventory is likely to be reached in the late 2020s (see Figure I-1 and Figure **I-2**), with the inventory declining thereafter as the loss of tritium by radioactive decay (tritium has a half-life of 12.3 years) exceeds the production rate.

Based on internal estimates of the current tritium inventory and production rates in Canada and Korea, as well as the expected lifetime of the CANDU-type reactors, an estimate of the evolution of the civilian tritium inventory over the next 35 years has been developed with and without ITER consumption. The results for 2 different assumptions concerning the ITER tritium consumption rate are shown in Figures Figure **I-1** and Figure **I-2**. The profile of tritium consumption used in these calculations is based on the report [Loarte, 2016-1], which was developed to provide an estimate of the profile of fusion power production over an extended ITER DT program satisfying the neutron wall loading mission goal. The analysis was carried out for the prevailing assumptions on the experimental program, in particular that ITER operations would be organized on a 3-shift basis with a 25% burn duty cycle. This led to an estimate of annual tritium consumption (averaged over a 2-year operational campaign with 8 months of scheduled shutdown/maintenance) of ~ 1.2 kg. Figure I-1 shows the evolution of the estimated global tritium inventory when this consumption rate is included, starting in 2038 (it is assumed that during 2036 – 2037 DT campaign a nominal amount of ~100 g of tritium will be consumed). These figures include the need to build sufficient ITER tritium inventory for proper operation of the Fuel Cycle systems and the return of this tritium to the world market at the conclusion of DT operations.

Due to guidance received from the ITER Members on the expected budget for the Operation Phase, it has been proposed, for the present, to plan ITER DT operations on a 2-shift pattern. This reduces

the annual neutron production by approximately 25% and, in consequence, reduces the annual tritium consumption by a similar amount, to ~ 0.9 kg.yr^{-1}. To achieve the lifetime wall loading therefore requires an extension of the DT campaign to ~ 18 years (including the DT campaign of 2036 – 2037), as opposed to 14 years in the case of 3-shift operation. The estimated evolution of the tritium inventory under these assumptions is illustrated in Figure I-2.

Overall, the conclusion from the analysis shown in Figures Figure **I-1** and Figure **I-2** is that the present estimates of global tritium inventory are (just) sufficient for the ITER DT program to meet the neutron wall loading mission goal, if it assumed that there is no other major consumer of tritium during the next 35 years. A somewhat more extensive survey and analysis of the global tritium production and future inventory in the context of the tritium requirements to start-up a Demo reactor was reported recently by [Kovari, 2018]. The results presented indicate a somewhat higher maximum inventory being reached in the 2020's (the maximum Canadian inventory is estimated to correspond roughly to the 'global' maximum shown in Figures Figure **I-1** and Figure **I-2**). This suggests that the analysis presented here may err on the conservative side, which is positive from the perspective of ITER's future tritium requirements.

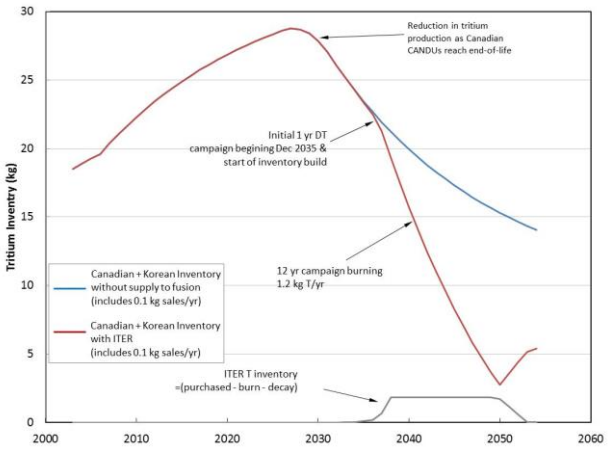

Figure I-1: Predicted evolution of 'global' tritium inventory assuming an ITER DT program achieving an average neutron wall loading of 0.3 MW.yr.m^{-2} over ~12 years in 3-shift operation.

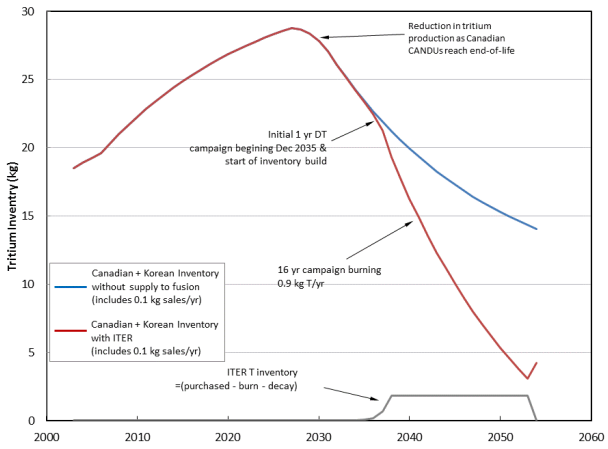

Figure I-2: Predicted evolution of 'global' tritium inventory assuming an ITER DT program achieving an average neutron wall loading of 0.3 MW.yr.m^{-2} over ~16 years in 2-shift operation.

Appendix J: Research Plan Risk Register

The RAMI analysis provides an estimate of the overall availability of the ITER tokamak and its ancillary systems for experimental studies, and establishes a framework within which a time schedule for the development of the experimental program can be assembled. This time schedule is predicated on several assumptions about the efficiency of the experimental program, i.e. its ability to meet the key milestones in the progress towards the $Q \geq 10$ goal, and about fusion plasma physics at the ITER scale: essentially that the physics of plasmas at the ITER scale follows the predictions formulated using the physics basis derived from current tokamak experiments. The rate of progress actually maintained in the experimental program and the level of fusion performance which can be achieved are therefore subject to a variety of uncertainties, and these give rise to risks of delays in the program or of failure to meet the principal mission goals within the timescale desired (or even of failure to meet them at all).

A Risk Assessment has therefore been assembled which identifies the top risks to the scientific program associated with possible limitations in experimental techniques or deviations in plasma behaviour from that predicted. These risks, the potential consequences for the operations time schedule towards DD/DT operation (targeted for late 2035 within the Staged Approach) and for the achievable fusion performance in terms of the long-pulse $Q \geq 10$ mission, together with the possible mitigation measures which could be implemented, are summarized in the appended table. The focus in this analysis has been on factors related to experimental techniques and to plasma physics, and no attempt has been made to assess the implications of limitations in the installed hardware, which is dealt with in the RAMI analysis and in the *Project Risk and Opportunity Register*.

	Risk	Research Plan Implications	Mitigation
1	**Inadequate Disruption Mitigation:** (i) DMS has inadequate performance, in mitigating heat loads or runaway electrons; (ii) consequences of DMS use excessive (e.g. first wall melting, long down time); (iii) inadequate prediction capabilities.	Several potential consequences for Research Plan: (i) limitations in maximum current and fusion power; (ii) more frequent shutdowns to replace in-vessel components; (iii) excessive number of uncontrolled disruptions leading to loss of operational time and slower progress in scientific program.	Focussed R&D on DMS-related experiments in present devices and development of validated models is essential to allow appropriate extrapolation of requirements to ITER. This can also contribute to development of improved disruption predictive capability. Possible mitigating measures related to ITER operation: (i) install flexible DMS (incorporating more than one of present options) to provide greater ability to tune system to ITER plasmas and to respond to present uncertainties; (ii) more cautious approach to scenario development, likely to lead to delays in program; (iii) additional time allocated to R&D on DMS in ITER program and implementation of upgrades, leading to delays in program; (iv) limitations on plasma current and fusion power, with possible consequences for mission goals.
2	**H-mode power threshold at high end of uncertainty range:** (a) in H/He phase (b) in D phase	Potential consequences: (a) inability to achieve H-mode in H/He plasmas (b) access to H-mode only in restricted range at low values of plasma current/ field	Further R&D on H-mode power threshold in current program and its link to confinement quality is an essential prerequisite for ensuring that ITER can take the necessary measures in advance of operation. If uncertainties remain large, possible mitigation measures are: (a.i) prepare increase in baseline H&CD capability in advance of or during operation (latter implies delays); (a.ii) accept risk of proceeding to D operation without H-mode experience and develop H-mode under these conditions – potential delay due to more cautious rate of progress and/or need to replace damaged PFCs. (b.i) prepare for DT operation in D plasmas at low current and field – implies increased risk in DT phase (b.ii) increase H&CD power – possibly implies

	(c) in DT phase	(c) baseline H&CD allows access to H-mode over limited range of current and field	delays unless decision taken before ITER operation. (c.i) increase H&CD power and accept possible limitation of Q < 8 with shorter pulse length due to higher power operation; higher power operation could also be more demanding for detached divertor operation.
3	**Inadequate ELM mitigation schemes:** (i) RMP coils do not have planned mitigation effect, or operate over restricted range in q_{95}, or cause unacceptable braking of plasma (lowers locked mode threshold); (ii) vertical control system not capable of triggering ELMs, even at low plasma current	ITER is equipped with at 27 ELM control coils but the uncertainties in extrapolation to ITER remain large and this risk must be addressed: (i) complete failure of ELM control coils to mitigate type-I ELMs (or achieve mitigation without unacceptable consequences) would necessitate upgrade of the pellet system for pellet pacing or development of an alternative operation scenario or R&D in ITER itself to explore alternative methods of ELM mitigation; (ii) operation over a restricted range in q_{95} would necessitate a focus on the fixed-q_{95} approach to the development of the 15MA scenario; this issue raises potentially serious issues for the hybrid and steady-state scenarios, which operate at higher q_{95} and might imply the need to develop operation in an alternative ELM scenario;	R&D involving multiple devices and several alternative ELM mitigation techniques can reduce the uncertainties in extrapolating to ITER, particularly if successful models of the mitigation processes are developed. Research should continue to identify and understand alternatives to the 'established' techniques. Possible mitigating measures related to ITER operation and their implications include: (i) upgrade of the pellet system to provide ELM control capability with acceptable fuelling/fuel throughput; (ii) development of an alternative operating scenario, which would imply delays in the program as time would have to be invested in exploring alternative scenarios in ITER and might ultimately imply operation at reduced Q; (ii) Development of alternative ELM mitigation methods within the ITER program, which would imply delays due to program time required, and possibly due to the need to install upgrades; (iii) limitations in the applicable range in q_{95}, B_t or n_e, would have consequences for the other main operating scenarios and might lead to delays in the program as alternative approaches were explored.

4	**Inadequate vertical stability control:** (i) unacceptable level of noise in diagnostics for VS; (ii) failure of in-vessel coils;	Limitations in the vertical stabilization capability could result in program delays, since plasma elongation would likely be limited, restricting the development of the baseline scenario until solutions were identified and implemented: (i) an unacceptable level of noise in the VS diagnostics, where there are significant uncertainties, would likely limit the usable elongation and the pulse length due to overheating of in-vessel coils and AC losses in superconducting coils; (ii) failure of the in-vessel coils would necessitate the implementation of the foreseen backup option (VS1 + VS2) and an alternative approach to the 15MA scenario development; the former, in particular, would result in delays to the program.	(i) Further R&D to characterize the level of noise in VS systems in existing devices and to identify the principal sources will allow ITER to plan in advance measures to limit the level of noise in the VS system. If such measures are inadequate, the consequence is likely to be a shorter allowable pulse length and, *in extremis*, restrictions on the plasma elongation and therefore current and Q. The program might also suffer delays as a result of less robust operation. (ii) implementation of the VS1 + VS2 backup option, while delaying the program, would, in principle, allow the baseline 15MA scenario to be maintained. R&D to date has given confidence that techniques for the control of the plasma inductance during the pulse can be used to limit excursions in the stability margin; nevertheless further research, particularly in relation to the controlled exit from the H-mode and current ramp-down is desirable to strengthen confidence on the capability for achieving the required fusion performance and pulse length. In addition, development of high current operation in L-mode might be more constrained, requiring a more measured development program during the non-active phase.

5	**Lack of reliable high power heating during non-active phase of program:**	Poor performance from one or more of the heating systems is more likely to occur early in the program, i.e. during the non-active phase, and would have more severe consequences; the most severe consequence would be an inability to achieve an H-mode under any conditions, implying both (i) the need for the immediate implementation of a H&CD upgrade program and (ii) either delay in the non-active phase program, or deferral of the H-mode program to the deuterium phase.	The extensive R&D program foreseen for ITER H&CD systems and the various design changes incorporated during the Design Review are already significant mitigation measures; nevertheless, progress in the research program remains heavily dependent on reliable high power operation of the H&CD systems; further mitigation measures in the event that reliability is an issue early in the program would include: (i) an immediate upgrade program for one or more H&CD systems, which would nevertheless require several years and likely delay the transition to DT operation; (ii) accept risk of proceeding to D operation without H-mode experience and develop H-mode under these conditions – potential delay due to limitations in non-active operation and need to perform required program after start of nuclear operation. (iii) prepare for DT operation in D plasmas at low current and field – implies increased risk in DT phase. A combination of (ii) and (iii) in parallel with the implementation of (i) might allow a higher risk path to DT operation with minimal delay relative to the proposed schedule.

6	**Unacceptable 'divertor' performance with tungsten PFCs:**	Any failure to reach the level of divertor performance required can delay the program as alternative regimes are sought and might necessitate more frequent divertor PFC replacement:	An expanding program of R&D on the use of high-Z PFCs is being implemented in both the major fusion devices and in laboratory facilities which will greatly improve the understanding of tungsten a high heat flux PFC and of the transport and possible accumulation of tungsten in the divertor, SOL and core plasmas. It is essential that the level and scope of the ongoing R&D be maintained. Nevertheless, given the uncertainties in, e.g., transport physics and the scale of the extrapolation to ITER, e.g., in transient thermal loads, it is inevitable that the use of tungsten for high heat flux components will have an experimental aspect, involving issues which will need to be addressed during ITER operation
	(i) impurity seeding to produce radiative divertor leads to excessive core impurity contamination;	(i) limitation of the capability to establish a radiating divertor with acceptable core impurity contamination will likely limit the Q which can be achieved and possibly shorten the maximum burn if accumulation occurs throughout the pulse;	(i) high power core electron heating, which dominates in ITER might be adequate to limit the impurity concentration and prevent accumulation; if not, and if the problem is limited to the level of seeded impurities required for operation with tungsten, this would result in program delays as techniques are developed to limit core contamination.
	(ii) tungsten concentration in the plasma core is unacceptably high, even with high power core electron heating;	(ii) a high, but stable, tungsten concentration would limit the Q and shorten the burn duration; accumulation would likely cause termination of the pulse, making the scenario untenable as a route to high-Q operation;	(ii) research program would have to be implemented within the Research Plan to optimize core and divertor plasma scenarios to minimize tungsten contamination of core plasma – additional research activities would delay program to achievement of high fusion power and high-Q;
	(iii) mitigation of thermal transients is inadequate to prevent enhanced erosion rates and reduced lifetime;	(iii) inadequate mitigation of thermal transients will inevitably delay the program until a satisfactory solution is found, or delays and costs will accumulate due to more frequent replacement of the divertor;	(iii) additional program time might be required to improve mitigation techniques for thermal transients; more frequent replacement of the divertor would be necessary, implying delays and additional cost;
	(iv) reliable plasma start-up cannot be achieved due to high-sputtering rates in initial low density plasma;	(iv) failure to achieve reliable plasma start-up would either delay the program, while a more limited, but acceptable, window for the start-up was developed; this could have implications for control and for the development of more advanced scenarios if it limited the scope for heating and current drive during the	(iv) R&D in existing devices can contribute to preparations for a suitable start-up scenario, but dedicated experimental work will be required in ITER to develop a regime which is appropriate to the ITER plasma parameters; success would lead to a rapid development of suitable scenarios to meet the

		current ramp-up;	ITER mission, but if difficulties with impurity generation are encountered, it will cause delays in the program and possibly limit the flexibility of operation; subsequent development of hybrid and steady-state scenarios would also be affected;
	(v) partial melting of W-targets limits power handling capability and prevents satisfactory high power operation.	(v) if partial melting of the tungsten target cannot be avoided, it is likely to lead to a delay in the program either to replace areas of the divertor PFCs (if these are infrequent events), or to develop improvements in operational strategies.	(v) the cause of the localized melting would influence the possible mitigation measures: inadequate mitigation of thermal loads would imply either improvements in the mitigation techniques, or if this were unsuccessful (see Risks 1 and 3) more frequent replacement of the affected areas; if the melting were caused by failure of the divertor detachment control, additional program time would be required to develop more robust control of the divertor plasma parameters.
	(vi) operation with helium plasmas could lead to enhanced erosion or to small scale damage to tungsten PFC surface, leading to shortening of PFC lifetime and possible limitation of stationary power-handling.	(vi) this could lead to need, e.g., for extensive replacement of tungsten PFCs before nuclear phase operations (implying additional cost) and/or limitations on divertor PFC power handling capability; alternatively, a decision not to carry out experiments with helium would mean that H-mode and ELM control experiments may not be attempted until deuterium phase, implying a probable delay in experimental program.	(vi) Further R&D in present program will be required to quantify how serious such effects will be and the implications for ITER operation; if substantial helium impact on surface morphology of tungsten PFCs is confirmed, leading to significantly increased erosion rate, and if hydrogen H-modes are not possible in PFPO, the delay of H-mode experiments to deuterium phase would appear to be only solution at present; overall delay in experimental program would then have to be analyzed.
	(vii) Recrystallization of tungsten in the high heat flux area of the divertor increases the risk of macro-crack formation	(yii) this would result in a lowering of the allowable heat fluxes in the divertor and possibly a restriction in the ITER high-Q operational domain (in terms of power and pulse length) or the need to operate with a more deeply detached divertor most likely increasing the disruption risks.	(vii) an operational budget will be defined for the divertor to account for the fact that tungsten recrystallization is a time and temperature-dependent effect. This will define how long the divertor can be operated at a given heat flux density and ensure a tracking of its integrity. R&D is planned to study in details the recrystallization kinetics of the material to be used for the ITER divertor.

7	**Level of toroidal field ripple degrades plasma performance:**	Potential consequences:	Significant R&D in this area is in progress, though a quantitative basis for extrapolation to prediction of confinement effects in ITER has not yet been established; DIII-D experiments with a TBM mock-

			up have shed additional light on these effects and the role of localized field perturbation and allow an improved specification for the TBM configuration so as to reduce any deleterious effects; a key issue in ITER would be to show unambiguously that any shortfall in confinement is due to ripple effects;
	(i) residual TF ripple after installation of ferritic inserts (~0.6% in non-regular sectors) leads to degradation of energy and particle confinement;	(i) reduction of energy confinement would imply a risk that Q=10 could not be achieved in 15MA reference scenario;	(i) if TF ripple is beyond the level at which significant confinement effects are manifested, little can be done in mitigation without removing the blanket modules to attach ferritic material to the vacuum vessel wall, at considerable delay to the program; a more productive approach would be to seek an optimized equilibrium which minimizes the influence of TF ripple on confinement; alternatively, options for scenarios with enhanced confinement could be explored; both approaches would require additional program time;
	(ii) localized ripple due to TBMs either degrades plasma confinement or causes plasma braking and/or error field growth.	(ii) localized ripple might degrade confinement as in (i), while plasma braking and localized error fields could give rise to locked modes reducing reliability of operation.	(ii) the availability of dummy port plugs and non-ferromagnetic TBMs would allow the TBMs to be withdrawn for some period to permit the program towards DT operation to proceed; apart from any loss of time in identifying the deleterious effects and in replacing the TBMs, the impact on the physics program could be limited; however, this would constitute a significant setback for the TBM Program, with potentially long delays unless alternative mitigation techniques were identified; (iii) At least a part of the error field and plasma braking effects due to TBMs can be corrected using the error field correction coils (and possibly, ELM control coils).
8	**Lack of plasma rotation leads to degradation of plasma performance:**	Potential consequences:	R&D is ongoing in present experiments to improve understanding of intrinsic rotation and momentum transport in tokamak plasmas, but it is a long-standing issue in fusion research; there is a strong

			physics basis for the influence of error fields and rotation is clearly an important aspect of this problem, but the quantitative influence remains uncertain. Continuing R&D in this area will be important for improving ITER's capability to deal with error fields, but the change in scale which ITER brings may also reveal new insights or issues.
	(i) intrinsic rotation of ITER plasmas is inadequate to achieve confinement quality consistent with H=1;	(i) reduction of energy confinement would imply a risk that Q=10 could not be achieved in 15MA reference scenario;	(i) there is limited scope for increasing torque in ITER (e.g. the installation of the 3rd HNB); if low rotation is identified as an issue, some mitigation may be possible by accurate correction of residual error fields using both internal (ELM control coils) and external (correction coil) saddle coil systems – the major impact on the schedule might be associated with the time needed for accurate measurement and correction of error fields; if the plasma rotation remains inadequate after careful correction of error fields, the installation of a low (~100 keV) positive ion beam would provide a possible solution, but this would imply a significant delay to the program to procure and install such a system before the tokamak environment became active.
	(ii) low intrinsic rotation makes ITER plasmas particularly sensitive to error fields, either due to assembly tolerances or distribution of magnetic material, leading to growth of locked modes and higher than expected disruptivity.	(ii) additional program time might be required to analyze error field sources and improve level of correction to allow more reliable operation at q_{95}=3;.most severe consequence could be restriction in maximum current (lowest q_{95}), limiting fusion performance.	(ii) ITER is equipped with a significant error field correction capability via an array of 18 external saddle coils – the quality of correction might well depend on the time dedicated to determining the magnitude and distribution of error fields, and additional time, including the use of dynamic detection techniques, could be allocated if required; the internal ELM control coils could provide additional correction capability, at least on an experimental basis, to determine whether the external correction set is adequate; any upgrade in this area would imply a significant delay in the program. (iii) Error field and plasma braking effects due to TBMs can be partially corrected using the error field correction coils (and, possibly, ELM control coils).

9	**High levels of tritium retention require more frequent tritium removal procedures than foreseen:**		
	(i) tritium retention rate in Be/W environment is higher than anticipated due to tritium retention via Be-codeposition.	(i) Research program is slowed by need for frequent vessel conditioning for tritium recovery.	(i) if Be-codeposition dominates the tritium retention rate, a longer-term solution would involve replacing Be first wall surfaces with tungsten, initially in regions not in contact with plasma (i.e. exposed only to neutrals) to test that plasma performance is not degraded by the presence of tungsten on the first wall; increasing areas of the wall could be replaced over time – at least in the medium-term, until the Q=10 mission were accomplished, program delays due to tritium recovery (assuming suitable techniques have been developed) might be more acceptable than delays involved in exchanging first wall materials.
	(ii) Efficiency of the baseline T-removal strategy (baking of first wall at 240^{o}C and divertor at 350^{o}C) is too low for efficient tritium recovery on thick beryllium co-deposits	(ii) very frequent and/or long bake-outs would be necessary, which is penalizing for the machine duty cycle	(ii) R&D is ongoing to refine the understanding of T trapping in Be co-deposits. In addition, several methods are being investigated in the fusion community for alternative T-removal techniques. Performing divertor baking experiments early during PFPO operations will allow checking the fuel removal efficiency and confirm whether additional techniques would be required.
	(iii) Significant tritiated ammonia formation during nitrogen seeding in the divertor, contributing to the tritium retention on divertor cryopumps	(iii) Ammonia is efficiently trapped on the active charcoal used in the divertor cryopumps and requires an elevated regeneration temperature for its release (similar to water-like gases) which is very time-consuming.	(iii) Significant R&D is ongoing in current fusion devices and laboratory to understand where ammonia is formed in the divertor and predict how much would be formed in ITER.

10	**Incompatibility of core plasma requirements for Q=10 with radiative divertor operation and Q = 5 long-pulse/steady-state scenarios:**	Since the divertor peak heat load is limited to 10MWm^{-2} in long-pulse operation due to technological constraints, fusion power, and probably Q would have to be reduced, to allow operation at an acceptable radiation fraction, until a suitable alternative operating regime is identified; the minimum consequence would be a delay to the program. In addition the Q=10 and Q=5 missions would also be at risk unless an alternative operating regime is established.	While many aspects of radiative divertor operation are investigated in existing devices, it is only at the ITER scale that the particular combination of edge and core parameters required for high-Q burning plasma operation can be established and investigated: it is likely, therefore, that mitigation measures would need to be developed in ITER: (i) development of an alternative operating scenario would imply delays in the program as time would have to be invested in exploring options for alternative scenarios in ITER; this issue might ultimately imply operation at reduced fusion power and Q;
	(i) pedestal temperature requirements for acceptable core energy confinement incompatible with edge density for radiative divertor operation;	(i) A high pedestal temperature and pressure are essential to the achievement of the long-pulse Q =5 scenarios, therefore this puts at risk these scenarios most likely preventing the achievement of the steady-state goal.	(ii) exploration of possible alternative radiating impurities might allow an optimum balance to minimize degradation of fusion performance;
	(ii) excessive core radiation prevents access to H=1 H-mode operation;	(ii) H > 1 is essential for the Q = 5 long-pulse and steady-state scenarios. This would limit Q and/or pulse length in these scenarios	(iii) any change in, e.g., divertor geometry contemplated to counteract this issue would imply a delay to the program in order to design, fabricate and explore operation in a new divertor configuration; program time would be required to establish any influence of divertor geometry;
	(iii) divertor asymmetries excessive at required radiation fraction, preventing stable operation;		
	(iv) degradation of core confinement in reference ELMy H-mode associated with use of all-metal PFCs		(iv) may need to develop alternative plasma scenario, for Q =10 resulting in delay to program.
			(v) The Q = 5 long-pulse goal could be achieved with normal inductive H-mode plasmas with I_p = 13 - 15 MA if H ~ 1.

11	**Inability to achieve densities near Greenwald value required for Q = 10 and Q = 5 long-pulse/steady-state:**	Several potential consequences for Research Plan:	While more emphasis is required in existing R&D program on fuelling and particle transport, the significant change of scale and parameters in ITER implies that fuelling behaviour, in particular, may be qualitatively different, with gas fuelling ineffective, at least for hydrogenic species. In this respect ITER is accessing a new regime. Possible mitigating measures for this risk in ITER operation:
	(i) Gas fuelling does not allow adequate density to be achieved in helium plasmas to permit adequate heating e.g. NB shine-through, ICRF coupling resistance) or acceptable H-mode behaviour;	(i) strategy of using helium H-modes to prepare scenarios and ELM mitigation techniques in advance of deuterium operation would not be viable;	(i) if helium gas fuelling ineffective, more emphasis on development of scenarios in hydrogen, where pellet injection available would be required; if hydrogen H-modes are not viable, accept risk of proceeding to D operation without H-mode experience and develop H-mode under these conditions – potential delay due to time required for relevant experimental studies to D phase.
	(ii) fuelling throughput does not allow required densities to be achieved in DT for Q = 10 and Q=5 scenarios;	(ii) reduced fusion performance due to lower density in high-Q scenarios;	(ii) maximum fuelling throughput can be doubled for shorter pulse durations without upgrades, possibly allowing Q=10 mission to be maintained with shorter burn duration but not the Q = 5 long-pulse/steady-state goals; expanding the tritium plant to increase throughput would be a costly and lengthy mitigation measure;
	(iii) existing technology is unable to fuel plasma adequately in DT for Q = 10 and Q = 5 scenarios.	(iii) reduced fusion performance due to lower density in high-Q scenario.	(iii) pursue options for more effective core fuelling – burning plasma physics could be explored at lower Q and in various scenarios while necessary concepts are developed; Overall, inefficient fuelling would be a significant challenge to the development of magnetic fusion energy.
12	**Inadequate particle control to sustain high-Q plasma scenarios and Q = 5 long-pulse/steady-state scenarios:**	Several potential consequences for Research Plan:	Current experiments have generally been able to maintain adequate particle control for the pulse lengths and plasma conditions which can be accessed, and therefore this issue is likely to be associated with the specific parameters of the ITER plasma, implying that investigation and mitigation measures will have to be developed in ITER:

	(i) divertor detaches at much lower neutral pressure than expected, degrading core energy confinement and helium exhaust capability;	(i) required core density for Q ~10 and Q ~ 5 operation cannot be sustained;	(i) present expectations are based on modelling using a limited pumping capability (the pumps are throttled to reduce pumping speed – a further factor of 2-4 is available), so that first mitigation measure would be simply to take advantage of the full pumping capability; if this proved inadequate, the number of cryopumps would have to be increased, implying upgrades and a reorganization of the divertor port allocation; this effect should be observed early enough in the experimental program that mitigation measures could be developed in a timely fashion, minimizing delays to the DT program – the later it is encountered, the more serious the delay and consequences for the high-Q mission;
	(ii) divertor helium enrichment lower than expected, requiring higher particle throughput to maintain required exhaust rate;	(ii) sustainable burn duration in high-Q conditions might be significantly shortened;	(ii) as in (i) headroom in pumping capability is available before the number of cryopumps would have to be increased; the possibility of doubling the fuelling throughput in short pulse operation could also be exploited; delays to the program would be incurred in developing the scenario, but upgrades may be avoidable;
	(iii) particle recycling properties of PFCs change substantially at confinement transitions or due to high power, long-pulse operation, overwhelming capability of exhaust systems and resulting in loss of density control and reduction of plasma temperature and current drive efficiency	(iii) high-Q burn conditions cannot be maintained an/or long-pulse capability is lost due to lower current drive.;	(iii) as in (i) headroom in pumping capability is available before the number of cryopumps would have to be increased; the possibility of doubling the fuelling throughput in short pulse operation could also be exploited; delays to the program would be incurred in developing the scenario, but once again upgrades may be avoidable; Overall, inefficient particle exhaust would be a significant challenge to development of fusion energy, but modelling suggests that ITER has some headroom in this respect before any upgrades to the installed capacity are required.

13	**NBI current drive efficiency lower than expected due to fast ion losses by interactions with Alfvén Eigenmodes**	Several potential consequences for Research Plan: (i) Cannot produce or sustain j(r) profile required for high/full non-inductive operation (ii) Pulse length for long-pulse Q ~5 goal would be difficult to achieve (iii) Steady-state Q ~5 goal may not be possible	 (i) Improve fast ion diagnostic measurements in PFPO-2 (when NBCD will be measured) to: - assess magnitude of ion loss, and consequences for CD, and. - to develop control/mitigation schemes (e.g. with ECRH) as soon as possible ii) Q ~ 5, 1000s goal can be achieved by inductive plasmas I_p = 13 - 15 MA. (iii) Upgrades of H&CD will need to be reconsidered to increase NBCD (if schemes in PFPO-2 are successful) in addition to those for the Q ~ 5 steady-state scenario itself.
14	**Inadequate core MHD control (NTM, RWM)**	Several potential consequences for Research Plan: (i) Impact on driven current and pulse duration for long-pulse scenarios; (ii) If more ECRH is required for NTM control less ECRH power for CD in long-pulse scenarios would be available thus decreasing pulse length and performance; (iii) If RWM cannot be controlled then β_N will be limited preventing the achievement of Q ~ 5 in long-pulse scenarios.	 (i) Additional CD capabilities would need to be installed. This should recover the pulse length but may decrease the achievable Q under 5; (ii) More ECCD would need to be installed. This should recover the scenario β_N but may decrease the achievable Q under 5; (iii) Implement/improve RWM control capability or/and install 3rd HNB to increase input torque and plasma rotation.